

**Overcoming the Limitations of  
Diastereomeric Crystallisation of Chiral Amines**

Maria Hiu Tung Kwan

Submitted in accordance with the requirements for the degree of  
Doctor of Philosophy

The University of Leeds

School of Chemistry

April 2018

The candidate confirms that the work submitted is her own, except where work which has formed part of jointly-authored publications has been included. The contribution of the candidate and the other authors to this work has been explicitly indicated below. The candidate confirms that appropriate credit has been given within the thesis where reference has been made to the work of others.

References for jointly-authored publications:

1. M. R. Chapman, M. H. T. Kwan, G. King, K. E. Jolley, M. Hussain, S. Hussain, I. E. Salama, C. G. Niño, L. A. Thompson, M. E. Bayana, A. D. Clayton, B. N. Nguyen, N. J. Turner, N. Kapur, A. J. Blacker, 'Simple and versatile laboratory scale CSTR for multiphasic continuous-flow chemistry and long residence times', *Org. Process Res. Dev.*, 2017, **21**, 1294-1301.

The work about continuous diastereomeric crystallisation reported within the publication is presented in Chapter 3 of this thesis, which was performed by the candidate with the assistance from M. Hussain. The design and construction of the reactor was performed by N. Kapur and A. J. Blacker. Other work reported in this publication was conducted by other authors.

2. M. H. T. Kwan, J. Breen, M. Bowden, L. Conway, M. F. Jones, R. Munday, T. Screen and A. J. Blacker, 'Increasing Chiral Purity and Yield of Amines by Diastereomeric Crystal Resolution, Continuous Racemisation and Recycle', *Angew. Chem. Int. Ed.*, 2018, *manuscript under review*.

The work described in this manuscript is presented in Chapter 3 of this thesis. Most of the data curation in the research was conducted by the candidate. The immobilised SCRAM catalyst was provided by T. Screen. J. Breen and L. Conway were contributing investigators of the project. Project administration and funding acquisition were carried out by other authors.

This copy has been supplied on the understanding that it is copyright material and that no quotation from the thesis may be published without proper acknowledgement.

The right of Maria Hiu Tung Kwan to be identified as Author of this work has been asserted by her in accordance with the Copyright, Designs and Patents Act 1988.

© 2018 The University of Leeds and Maria Hiu Tung Kwan

## Acknowledgements

First of all, I would like to thank my academic supervisor at Leeds, Prof. John Blacker, who has given me the opportunity to work on this interesting and exciting project, and provided me with support and guidance throughout my PhD. I would also like to thank Prof. Steve Marsden and Dr. Bao Nguyen for their invaluable discussion and advice on the project.

I would like to thank the University of Leeds, EPSRC and AstraZeneca for their funding and in particular, AstraZeneca for their CASE studentship and providing me the opportunity to work in their Macclesfield site for a three-month placement. I would like to give my special thanks to my industrial supervisor, Dr. Rachel Munday, for arranging the placement and helping me during my time at AZ; Drs. Mike Nunn and Coleen Robinson for their assistance in using the Amigo workstation; Dr. Fiona Bell for training me on the chiral supercritical fluid chromatography; Dr. Helen Wheatcroft for her knowledge on crystallisation and Dr. Martin Jones for his insights and ideas on the project. I would also like to thank Drs. Tom Screen and Ben Crossley from Yorkshire Process Technology for preparing and sending over the immobilised SCRAM catalysts; and Dr. Wim Klooster from the UK National Crystallography Service, University of Southampton, for his help in acquiring the single crystal structure data for one of the small-size crystals which we had struggled to analyse in Leeds.

I would like to thank Dr. Chris Pask, Martin Huscroft and Simon Barrett for their help in X-ray crystallography, chiral HPLC and NMR in Leeds, especially Chris and Martin who always analysed my samples and gave me feedback very promptly; and Tom Howell, for his help in acquiring the DSC and TGA data.

I would like to thank my master students Gina, Adil and Caitlin, with special thanks to Caitlin who developed the proton/ deuterium exchange methodology in determining chiral amine racemisation. I would also like to thank all my colleagues in the IPRD: Dr. Mary Bayana for maintaining every equipment in the lab and shared your knowledge and experiences with us; Drs. Jess Breen, Katie Jolley, Will Reynolds, Mike Chapman, James McManus and Alastair Baker for running the lab and giving valuable advices and help at all times; Lisa, Nick, Chris Hones,



Yuhan, Adam, Chris Horbs and Ilias for all the lovely moments throughout the years; and Nisha, Calum, Connor, Chris Holt and Fernando for bringing so much fun to the lab towards the end of my PhD.

I would like to thank my other chemistry friends in the department, Joan, Anjo, Charlene and Cecilia for their friendship and being around during both joyful and hard times in my PhD. I would also like to thank my flatmate, Cigdem, who had also been writing up her thesis for her PhD in civil engineering, for her company and sharing her feeling (and food) with me.

Last but not least, I would like to thank my dear family and friends back in Hong Kong for their love and endless support throughout my time in the UK. I would not be able to make this through without them.

Finally, I would like to dedicate this work to Miss Sharon Fung, a kind and loving biology teacher and career adviser in my high school, who passed away in 2014 just before I started my PhD.

## Abstract

Chiral amines are important building blocks in pharmaceutical compounds. Being able to synthesise chiral amines in high yield and enantiopurity is highly desirable due to the different physiological activities exhibited by the opposite enantiomers. Classical resolution using chiral acids has been the main strategy in preparing enantiopure amines at industrial scale, however the processes often lead to high waste and intrinsically low yields.

To overcome the limitations of classical resolution of chiral amines, the research presented in this work has focused on the development of a resolution-racemisation-recycle ( $R^3$ ) process which couples diastereomeric crystallisation and catalytic racemisation of the undesired enantiomer in the mother liquor. The crystallisation was carried out in batch in a continuous-stirred tank reactor (CSTR) whilst the racemisation was carried out in flow with a packed-bed reactor (PBR) containing the racemisation SCRAM catalyst which was immobilised on a Wang resin support, enabling it to be recycled up to 130 times. The two steps were separated but linked with tubing and a pump to yield a continuous recirculation process. Unlike traditional approaches in asymmetric transformations in which the resolution and *in-situ* racemisation are carried out in one pot, the  $R^3$  process allows each step to be operated independently under its optimum conditions.

The success of the  $R^3$  process depends strongly upon the rate of racemisation, the absolute, and difference in, solubility of the diastereomeric salts, the rates of growth and dissolution of the less soluble and more soluble diastereomers respectively. The system was tested with primary, secondary and tertiary amines with up to 50-times improved resolvability observed. For one secondary amine, a 96% diastereopurity and 78% yield gave a resolvability of 1.5 compared to the classical resolution of 0.11. The  $R^3$  processes of the primary and tertiary amines were less successful, mainly due to the formation of undesired by-products. Racemisation of the amine substrates were studied with homogeneous and immobilised SCRAM catalysts to better understand the reaction kinetics and mechanism. A series of iron- and copper-based metal compounds were also screened in an attempt to search for low-cost alternatives of amine racemisation catalysts.

## Content

<b>Acknowledgements</b> .....	<b>iii</b>
<b>Abstract</b> .....	<b>v</b>
<b>Content</b> .....	<b>vi</b>
<b>Abbreviations</b> .....	<b>xi</b>
<b>1. Introduction</b> .....	<b>1</b>
1.1. Importance of chiral amines .....	1
1.2. Synthetic methodologies of chiral amines .....	3
1.2.1. Chiral Pool .....	3
1.2.2. Asymmetric synthesis .....	4
1.2.3. Resolution .....	8
1.3. Racemisation of chiral amines .....	18
1.3.1 Racemisation methods of chiral amines .....	19
1.3.2. Mechanism of chiral amine racemisation by SCRAM catalyst <b>64</b> ..	29
1.4. De-racemisation .....	30
1.4.1. Dynamic Kinetic Resolution (DKR) .....	32
1.4.2. Crystallisation-Induced Diastereomeric Transformation (CIDT) .....	35
1.4.3. The Viedma ripening technique .....	37
1.4.4. Diastereomeric resolution recycle .....	38
1.5. Continuous processing .....	41
1.5.1. Flow reactors .....	41
1.5.2. Merits and limitations of flow .....	44
1.5.3. Catalyst immobilisation .....	45
1.6. Research objectives .....	49
<b>2. Racemisation of chiral amines</b> .....	<b>50</b>
2.1 Introduction .....	50
2.2 Racemisation in batch .....	51
2.2.1 <i>N</i> -Methyl- $\alpha$ -methylbenzylamine <b>39</b> .....	51
2.2.2 <i>N</i> -Isopropyl- $\alpha$ -methylbenzylamine <b>101</b> .....	68
2.2.3 $\alpha$ -Methylbenzylamine <b>42</b> .....	69
2.2.4 <i>N,N</i> -Dimethyl- $\alpha$ -methylbenzylamine <b>46</b> .....	70
2.2.5 6,7-Dimethoxy-1-methyl-1,2,3,4-tetrahydroisoquinoline <b>9</b> .....	71
2.2.6 2-Methylpiperidine <b>103</b> .....	73
2.3 Racemisation in flow .....	76

2.3.1	Synthesis of immobilised SCRAM <b>92</b> .....	76
2.3.2	Experimental set-up.....	77
2.3.3	Flow racemisation of chiral amines.....	78
2.4	Attempted reactivation of immobilised SCRAM <b>92</b> .....	81
2.4.1	Reactivation of immobilised SCRAM <b>92</b> by hydroiodic acid.....	82
2.4.2	Proton NMR titration of methylamine-bound SCRAM <b>64</b> with hydroiodic acid.....	85
2.5	Rapid screening methodology for determining chiral amine racemisation.....	89
2.5.1	Background.....	89
2.5.2	Methodology and results.....	91
2.5.3	Proposed mechanism.....	101
2.5.4	Limitations.....	102
2.6	Conclusion.....	103
<b>3.</b>	<b>Resolution-Racemisation-Recycle (R<sup>3</sup>).....</b>	<b>105</b>
3.1	Introduction.....	105
3.2	Experimental set-up.....	106
3.3	R <sup>3</sup> processes for different chiral amine substrates using ( <i>S</i> )-mandelic acid <b>34</b> as resolving agent.....	109
3.3.1	6,7-Dimethoxy-1-methyl-1,2,3,4-tetrahydroisoquinoline <b>9</b> .....	110
3.3.2	2-Methylpiperidine <b>103</b> .....	123
3.3.3	<i>N</i> -Methyl- $\alpha$ -methylbenzylamine <b>39</b> .....	128
3.3.4	<i>N</i> -Isopropyl- $\alpha$ -methylbenzylamine <b>101</b> .....	132
3.3.5	$\alpha$ -Methylbenzylamine <b>42</b> .....	136
3.4	Diacid as a resolving agent for diastereomeric transformation of chiral amines.....	140
3.4.1	Resolution of <i>N</i> -Methyl- $\alpha$ -methylbenzylamine <b>39</b> with di- <i>p</i> -toluoyl-D-tartaric acid <b>32</b> in batch.....	140
3.4.2	R <sup>3</sup> process of <i>N</i> -Methyl- $\alpha$ -methylbenzylamine <b>39</b> with di- <i>p</i> -toluoyl-D-tartaric acid <b>32</b> .....	149
3.4.3	<i>N,N</i> -Dimethyl- $\alpha$ -methylbenzylamine <b>46</b> .....	153
3.5	Conclusion and future work.....	156
<b>4.</b>	<b>Alternative racemisation catalysts for chiral amines.....</b>	<b>160</b>
4.1	Introduction.....	160
4.2	Screening of iron- and copper-based metal compounds.....	162

4.3	Racemisation of chiral amines by triiron dodecacarbonyl (Compound E).....	164
4.4	Attempted racemisation/ transfer dehydrogenation of ( <i>R</i> )- 6,7-Dimethoxy-1-methyl-1,2,3,4-tetrahydroisoquinoline 9 by copper(II) acetate (Compound K) .....	168
4.5	Conclusion and future work .....	170
<b>5.</b>	<b>Conclusion.....</b>	<b>172</b>
5.1	Summary.....	172
5.2	Future Work .....	175
<b>6.</b>	<b>Experimental.....</b>	<b>177</b>
6.0	General .....	177
6.0.1	Chemicals and analytical methods.....	177
6.0.2	GC calibrations .....	179
6.0.3	Chromatograms of racemic and optically pure materials .....	184
6.0.4	<sup>1</sup> H NMR spectra of diastereopure salts of chiral amines.....	194
6.1	Synthesis of starting materials and reference compounds .....	197
6.2	Racemisation of chiral amines .....	221
6.2.1.	General procedures for racemisation in batch .....	221
6.2.2.	General procedures for the racemisation of ( <i>S</i> )- <b>39</b> (0.5 M) in batch with spiking of ( <i>S</i> )- <b>39</b> .....	223
6.2.3.	Racemisation of ( <i>S</i> )- <b>39</b> (0.5 M) in batch with spiking of methylamine (2 equiv. with respect to iridium) .....	223
6.2.4.	NMR titration of SCRAM <b>64</b> with methylamine.....	224
6.2.5.	General procedures for racemisation in flow.....	225
6.2.6.	General procedures for reactivation of immobilised SCRAM <b>92</b> with hydroiodic acid.....	232
6.2.7.	Catalyst activity check of immobilised SCRAM <b>92</b> <i>via</i> the racemisation of ( <i>S</i> )- <b>103</b> in flow.....	232
6.2.8.	Deactivation of immobilised SCRAM <b>92</b> with methylamine in flow.....	233
6.2.9.	NMR titration of methylamine-bound SCRAM <b>64</b> with hydroiodic acid.....	233
6.2.10.	General procedures for deuterium/ proton exchange of chiral amines by <i>d</i> <sub>8</sub> -isopropyl alcohol.....	234
6.2.11.	Attempted racemisation of Rasagiline ( <i>R</i> )- <b>109</b> by microwave.....	234

6.3	Resolution-Racemisation-Recycle ( $R^3$ ) .....	234
6.3.1.	Diastereomeric resolution of chiral amines .....	234
6.3.2.	General procedures for the diastereomeric resolution of 6,7-dimethoxy-1-methyl-1,2,3,4-tetrahydroisoquinoline <b>9</b> with ( <i>S</i> )-mandelic acid <b>34</b> in flow.....	238
6.3.3.	Crystal solubility measurement .....	239
6.3.4.	DSC and TGA measurements for the diastereomeric salts of <b>39</b> with ( <i>S,S</i> )- <b>32</b> .....	242
6.3.5.	General procedures for one-pot resolution-racemisation process reaction of <i>N</i> -methyl- $\alpha$ -methylbenzylamine <b>39</b> with di- <i>p</i> -toluoyl-D-tartaric acid ( <i>S,S</i> )- <b>32</b> .....	242
6.3.6.	Resolution-Racemisation-Recycle ( $R^3$ ) processes of chiral amines.....	243
6.3.7.	Attempted racemisation of ( <i>S</i> )- <b>34</b> .....	253
6.3.8.	Attempted racemisation of triethylammonium ( <i>S</i> )-mandelate <b>34</b> .....	254
6.3.9.	Catalyst activity check of immobilised SCRAM <b>92</b> after the $R^3$ processes of <b>9</b> via the racemisation of ( <i>S</i> )- <b>9</b> in flow.....	254
6.4	Alternative racemisation catalysts for chiral amines .....	255
6.4.1.	Racemisation catalyst screening.....	255
6.4.2.	Racemisation of chiral amines by catalyst <b>E</b> .....	255
6.4.3.	Attempted racemisation/ transfer dehydrogenation of <b>9</b> by catalyst <b>K</b> .....	257
<b>7.</b>	<b>Reference</b> .....	<b>259</b>
<b>8.</b>	<b>Appendix</b> .....	<b>269</b>
8.1.	Proton NMR titration of homogeneous SCRAM <b>64</b> with methylamine in $d_6$ -DMSO (Section 2.2.1(b)) .....	269
8.2.	Proton NMR titration of methylamine-bound iridium complexes with hydroiodic acid in $d_6$ -DMSO (Section 2.4.2) .....	273
8.3.	Proton NMR spectra for the determination of chiral amine racemisation via proton/ deuterium exchange in the presence of SCRAM <b>64</b> (Section 2.5.2(b)).....	275
8.4.	Addition of ( <i>S</i> )-mandelic acid <b>34</b> during the $R^3$ processes of <b>9</b> (Table 3.3).....	280
8.5.	X-ray crystal structure data .....	284

8.6. Calculations of turnover number of $\text{Fe}_3(\text{CO})_{12}$ (Compound <b>E</b> ) in the racemisation of ( <i>R</i> )- <b>9</b> (Fig. 4.3) .....	299
---	-----

## Abbreviations

Ac	Acetyl
ATH	Asymmetric Transfer Hydrogenation
BOC	<i>tert</i> -Butyloxycarbonyl
CIAT	Crystallisation Induced Asymmetric Transformation
CIDT	Crystallisation Induced Diastereomeric Transformation
CIET	Crystallisation Induced Enantiomeric Transformation
Cp*	Pentamethylcyclopentadienyl
CSTR	Continuous Stirred Tank Reactor
de	Diastereomeric excess
DKR	Dynamic Kinetic Resolution
DPEN	Diphenylethylenediamine
DTR	Dynamic Thermodynamic Resolution
DME	Dimethoxyethane
DMSO	Dimethyl sulfoxide
ee	Enantiomeric excess
EIB	Ethyl isobutyrate
Equiv.	Equivalence
Et	Ethyl
GC	Gas Chromatography
GCMS	Gas Chromatography Mass Spectrometry
h	Hour
HPLC	High Performance Liquid Chromatography
HRMS	High Resolution Mass Spectrometry
ICP	Inductively coupled plasma
I.D.	Interior diameter
<i>i</i> Pr	Isopropyl
Me	Methyl
min	Minute
ML	Mother liquor
MTBE	Methyl <i>tert</i> -butyl ether
NCS	National Crystallography Service
NMR	Nuclear Magnetic Resonance
O.D.	Outside diameter



pK <sub>a</sub>	-log[K <sub>a</sub> ]
PBR	Packed-bed reactor
PMHS	Polymethylhydrosiloxanes
PTFE	Polytetrafluoroethylene
R <sup>3</sup>	Resolution-Racemisation-Recycle
<i>rac</i>	Racemic
r.t.	Room temperature
RV	Reactor volume
SFC	Supercritical Fluid Chromatography
t	Time
t <sub>1/2</sub>	Half-life
t <sub>R</sub>	Retention time
t <sub>Res</sub>	Residence time
TBAT	Tetrabutylammonium difluorotriphenylsilicate
Ts	Tosyl
v/v	Volume by volume
w/v	Weight by volume
w/w	Weight by weight
XRD	X-ray diffraction

# 1. Introduction

## 1.1. Importance of chiral amines

Chiral amines have widespread importance in the pharmaceutical, agrochemical and fine chemical industries.<sup>1-5</sup> Many therapeutic drugs are either amines or contain functional groups derived from amines (Fig. 1.1).<sup>6</sup> It is due to their ability to interact with biological molecules such as DNA and proteins by hydrogen bonding and electrostatic interactions when they protonate or deprotonate.

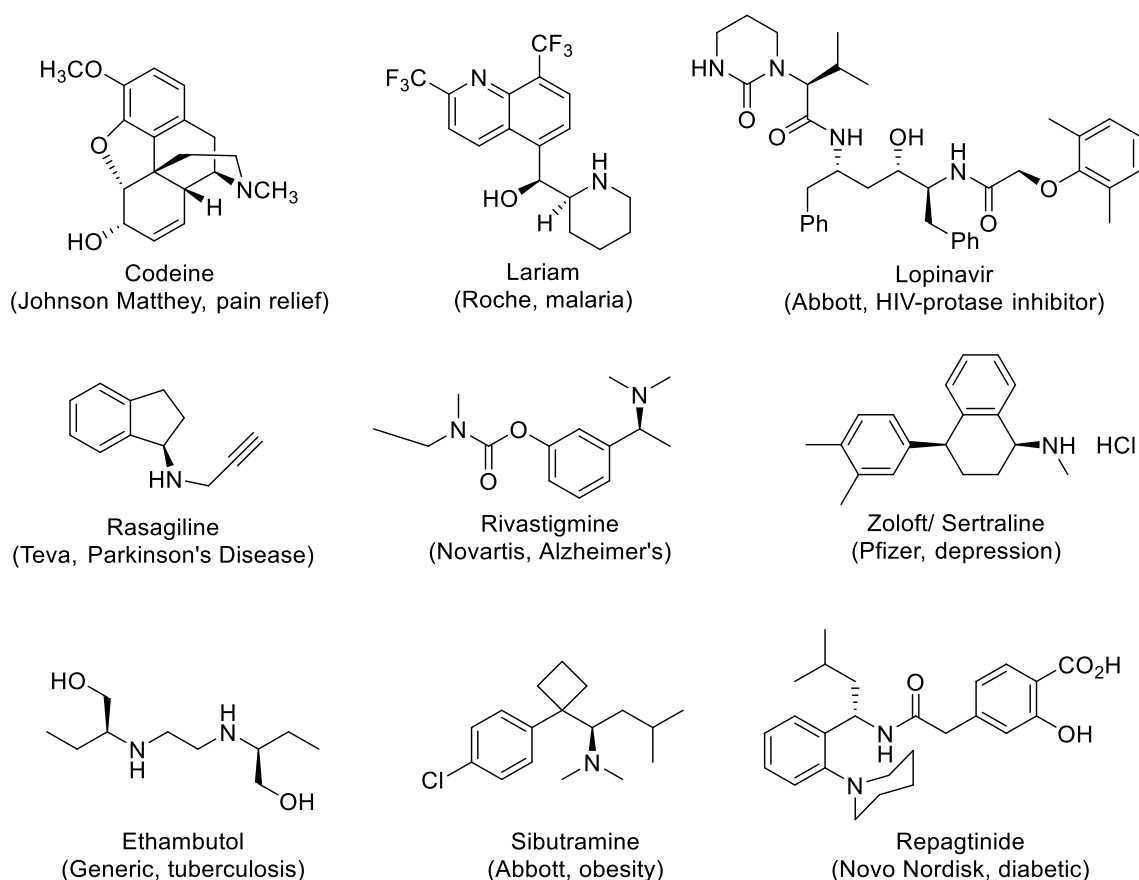
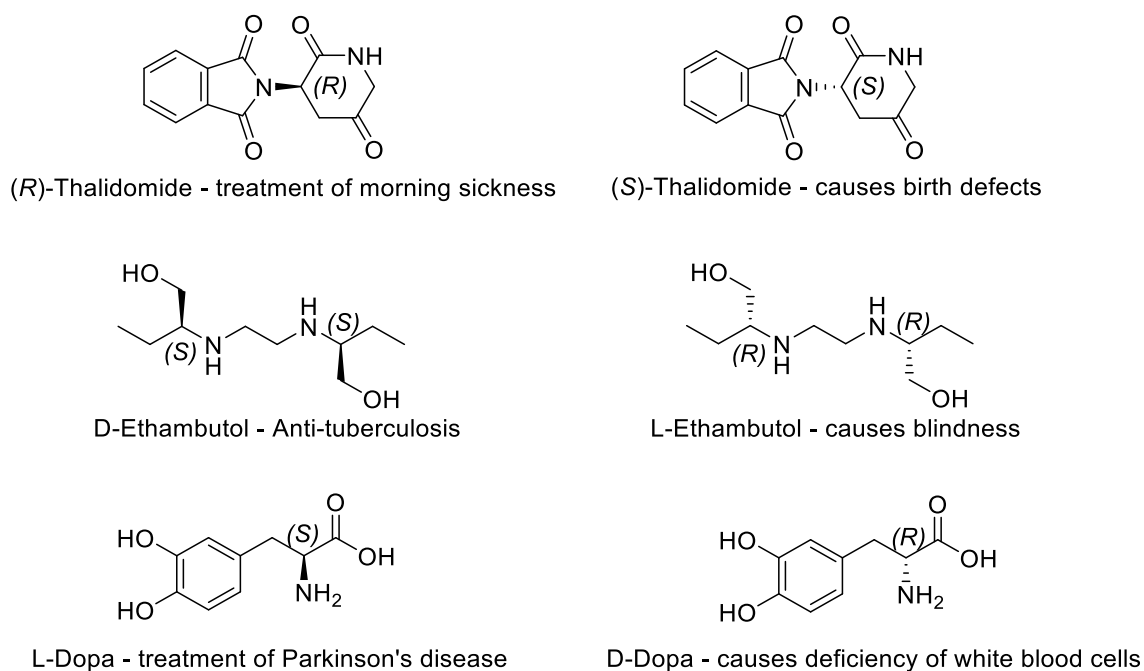


Fig. 1.1 Examples of pharmaceutical drugs containing chiral amine functionalities

Thermodynamically, (*R*)- and (*S*)-enantiomers of a chiral molecule are equally likely to exist. However most chiral molecules in living organisms are over-expressed in one enantiomeric form.<sup>7-9</sup> This implies that two enantiomers of a chiral compound can interact differently with the biological system. This phenomenon is particularly important in pharmaceutical development. Different therapeutic effects were observed for many chiral drugs. A few examples containing chiral amine functionalities are shown in Fig. 1.2.<sup>10</sup>



*Fig. 1.2 Examples of chiral pharmaceutical compounds exhibiting different physiological effects with different enantiomers*

In 1992, policy regarding single enantiomer drugs was published by the U.S. Food and Drug Administration (FDA), which stated the need for the evaluation of pharmacokinetics and toxicity profiles of individual enantiomers and the racemic mixture of a chiral drug, manufacturing control over stereoisomer impurities, full characterisation of individual enantiomers and their composition in the final drug product.<sup>11-13</sup> Although some chiral drugs are still administered as racemate, an increasing proportion of single enantiomer drugs are introduced into the market.<sup>9, 11, 14</sup> 'Chiral switches', which exploit the single enantiomers of existing racemic drugs are one of the important features in drug development portfolios.<sup>14</sup> Being able to synthesise both enantiomers at high enantiopurity is therefore crucial for both safety and efficacy studies and the manufacturing of a chiral drug product.

There are three main approaches in accessing enantiopure amines: the utilisation of 'chiral pool' as the building block which refers to inexpensive and readily available enantiomerically pure materials such as carbohydrates and amino acids;<sup>9</sup> asymmetric syntheses which use chiral catalysts, ligands and auxiliaries to introduce asymmetry to prochiral starting materials; and resolution, which corresponds to the separation of a racemic mixture of the chiral compound

obtained from a non-enantioselective process (Fig. 1.3). These methodologies will be discussed briefly in the following sections, highlighting the problems encountered in each of them.<sup>15</sup>

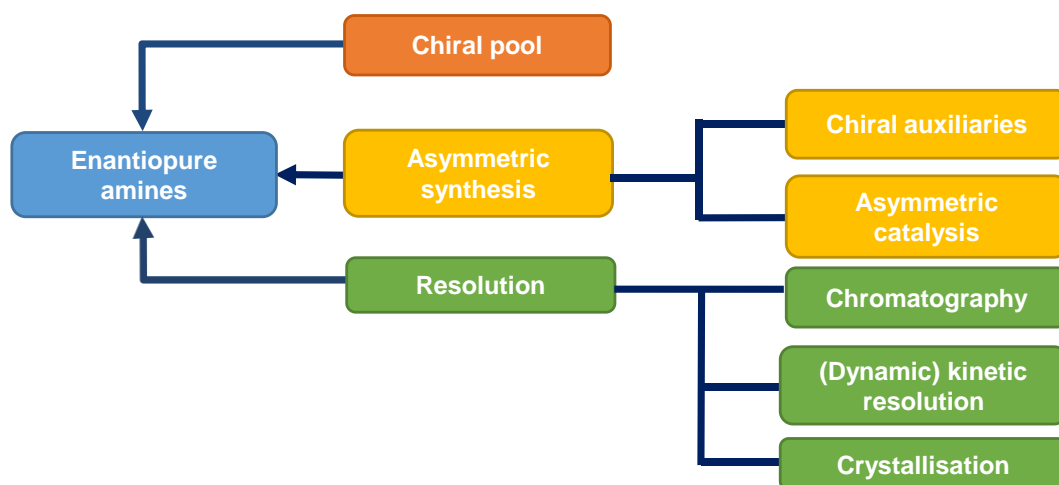
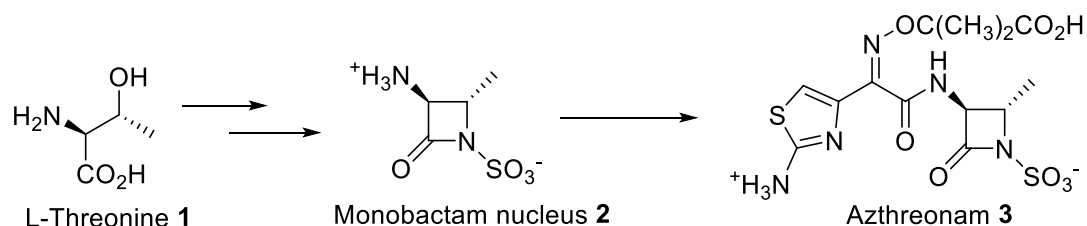


Fig. 1.3 Approaches towards enantiopure chiral amines

## 1.2. Synthetic methodologies of chiral amines

### 1.2.1. Chiral Pool

Chemical modifications of readily available naturally-occurring enantiopure materials from the chiral pool represent the most straightforward approach in accessing a single enantiomer.<sup>16, 17</sup> Commonly used chiral pool materials include  $\alpha$ -amino acids, hydroxyacids, carbohydrates, terpenes and alkaloids.<sup>9, 16-18</sup> The enantiopurity of the naturally-occurring chiral compounds is normally 100% and their stereogenic centres are directly transferred to the products.<sup>17, 19</sup> They are also non-toxic and at reasonable prices.<sup>18</sup> This approach is especially suitable if the target product resembles (part of) the structure of the chiral pool materials. One of the examples was the synthesis of monobactam antibiotic Azthreonam **3** from L-threonine **1** via monobactam nucleus **2** developed by Bristol-Myers Squibb (Scheme 1.1).<sup>20, 21</sup>



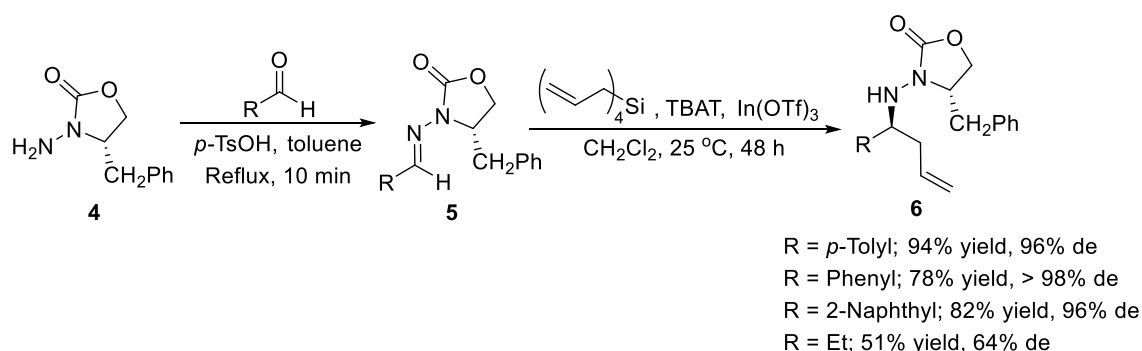
Scheme 1.1 Synthesis of Azthreonam **3** from L-threonine **1** via monobactam nucleus **2**

Enantiopure materials from the chiral pool can also be used as auxiliaries and chiral ligands in asymmetric catalysis and may be recovered and recycled after the synthetic process.<sup>9, 22</sup> Although the chiral pool approach is useful to introduce a chiral centre into the target molecule, usually, only one of the enantiomers is available, while the other has to be synthesised which may be more expensive than the naturally-occurring counterpart.<sup>18</sup> The number of possible transformations that the molecule can undergo may be limited and the synthesis can be complex, lengthy and require various functional group protections.<sup>15, 16</sup> Since the stereogenic centre is often introduced early in the process, detailed analyses are required in each subsequent step to ensure no erosion of enantiopurity occurs.<sup>16</sup>

## 1.2.2. Asymmetric synthesis

### (a) Chiral auxiliaries

Stereogenic centres can be introduced into a molecule by attaching a chiral auxiliary to the prochiral starting material. Nucleophilic addition of an imine bearing a chiral auxiliary can be used to generate enantioenriched  $\alpha$ -branched chiral amines.<sup>6, 19, 23-25</sup> The asymmetric indium (III) triflate-mediated allylation of hydrazones **5** was demonstrated using Friestad's auxiliary **4** to prepare diastereoenriched **6** (Scheme 1.2).<sup>6, 19</sup> Higher diastereoselectivity can be achieved with aryl-substituted aldehydes compared to alkyl-substituted aldehydes. The auxiliary can be removed using samarium diiodide to yield the enantioenriched product.



*Scheme 1.2 Diastereoselective allylation of hydrazone 5 by Friestad's auxiliary 4*

One of the advantages of this approach is that the stereochemistry can be predicted.<sup>17</sup> The resulting adducts are diastereomers which have different

physical properties and therefore can be purified easily if the reaction is not 100% stereoselective.<sup>26</sup> However extra steps are required to attach and remove the auxiliaries. The reaction conditions for removing the auxiliary needs to be carefully chosen to ensure that the stereopurity of the product is maintained. Some enantiopure auxiliaries are readily available from chiral pool but some may require synthesis and resolution prior to use.<sup>9, 15, 22, 26</sup> Since a full equivalence of chiral auxiliary is needed, efficient recovering and recycling of the auxiliaries are essential to make this synthetic approach more economical.<sup>17</sup>

## (b) Asymmetric catalysis

To circumvent the use of stoichiometric amount of chiral-inducing agents, asymmetric catalysis represents an alternative to introduce a stereogenic centre to a prochiral molecule.<sup>17</sup> The commonly employed catalysts include chiral ligand-derived metal complexes, chiral organocatalysts and biocatalysts. Chiral transition metal complexes are widely used in the asymmetric reduction of imines to generate chiral secondary amines.<sup>27</sup> Noyori's type ruthenium complexes **7** with chiral *N*-sulfonylated diamine ligands were used successfully in catalysing the asymmetric transfer hydrogenation (ATH) of cyclic imines such as **8**, using formic acid/ triethylamine as the hydrogen source (Fig. 1.4, Scheme 1.3).<sup>28, 29</sup>

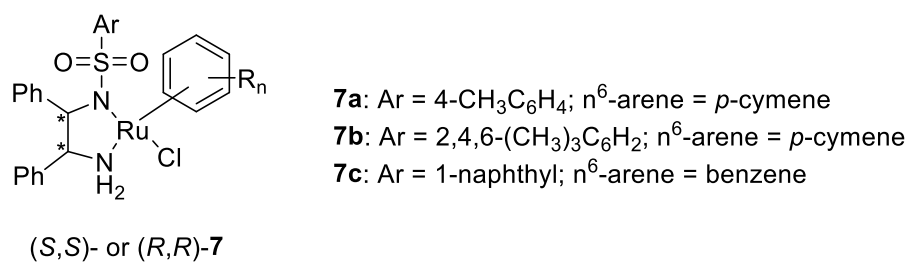
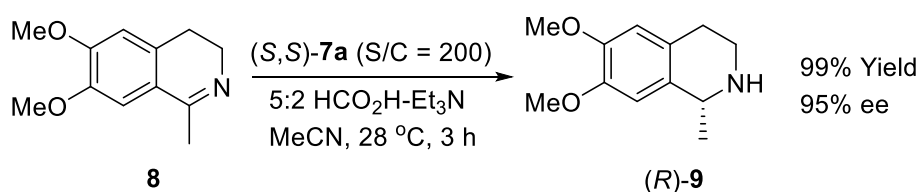
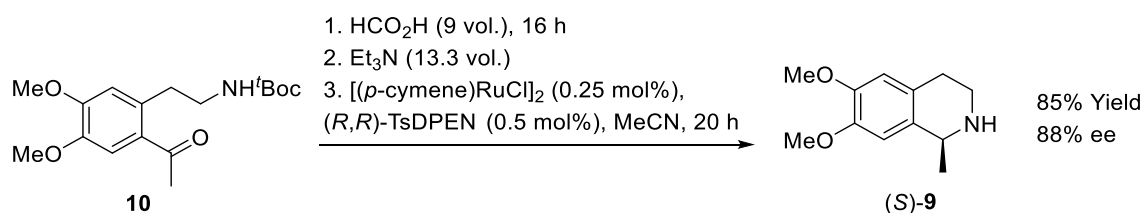


Fig. 1.4 Noyori's catalyst



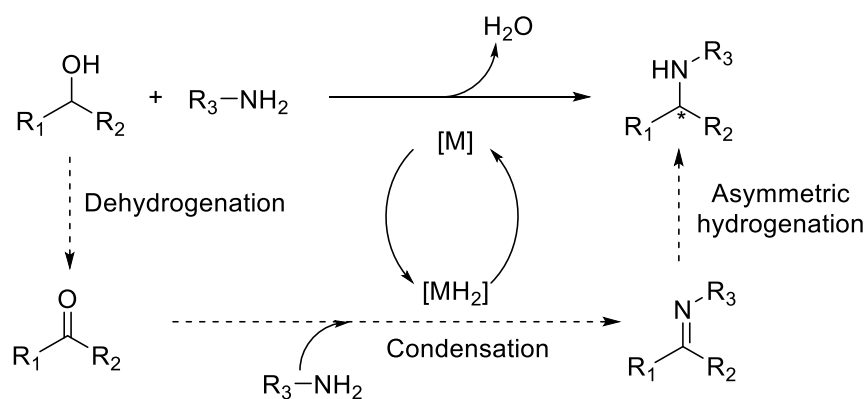
Scheme 1.3 Synthesis of (*R*)-**9** via ATH of imine **8**. S/C refers to the molar ratio of substrate/catalyst

Direct asymmetric reductive amination of ketones is also used to synthesise enantiopure amines in which the imines are formed *in-situ* without isolation.<sup>4</sup> (*S*)-**9** can be synthesised directly from BOC-protected amino-ketone **10** using (*p*-cymene) ruthenium(II) chloride dimer and (*1R,2R*)-TsDPEN in one pot (Scheme 1.4). However the efficiency and enantioselectivity are lower compared to the ATH of imine **8** (Scheme 1.3).<sup>30</sup>

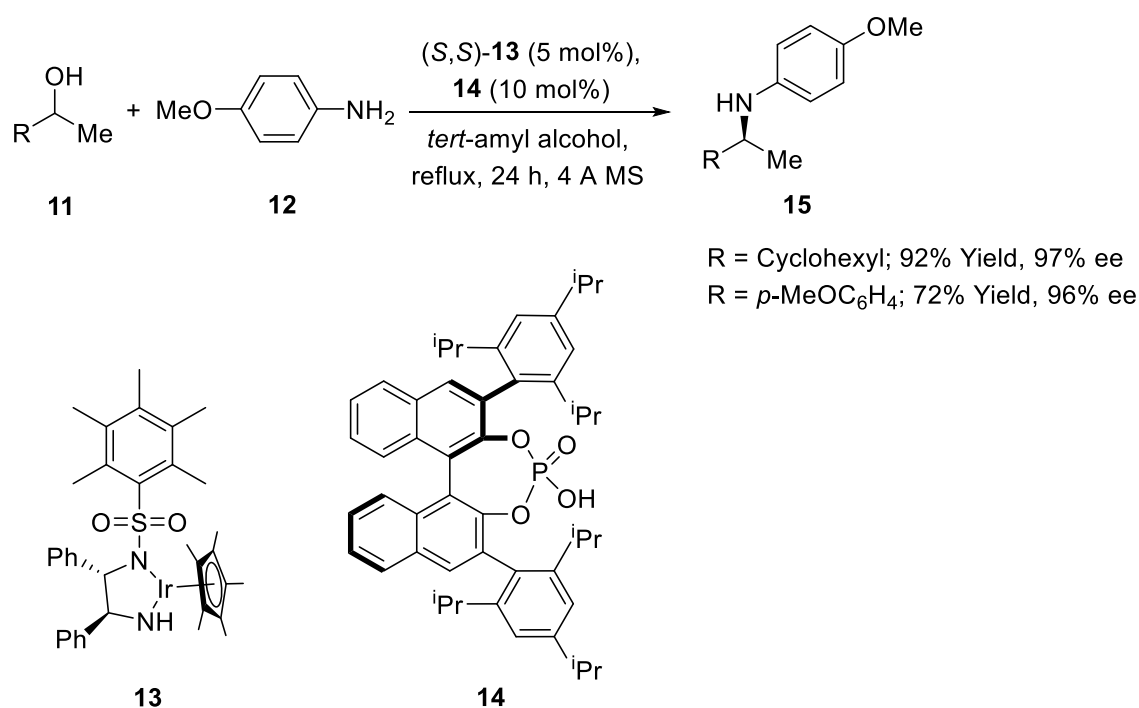


**Scheme 1.4** Synthesis of (*S*)-**9** via asymmetric reductive amination of amino-ketone **10** using [(*p*-cymene)RuCl]<sub>2</sub> and (*R,R*)-TsDPEN

A closely related reaction, the amination of alcohols by borrowing hydrogen methodology, is a well-known atom-efficient and green approach in synthesising amines.<sup>5</sup> It starts with dehydrogenation of the alcohol (primary or secondary) to make the corresponding carbonyl compound which condenses to imine with the amine. The alcohol acts as the hydrogen donor which reduces the imine into amine, with water as the only by-product (Scheme 1.5).<sup>5, 31-35</sup> No additional reductant such as hydrogen gas is required. In 2014, Zhao et al. reported the use of iridium catalyst (*S,S*)-**13** and chiral acid **14** in the asymmetric amination of a variety of aryl and aliphatic alcohols **11** with aniline derivatives such as **12** in the synthesis of secondary amines **15**.<sup>5</sup> An example is shown in Scheme 1.6. Although relatively high yields and ee's were achieved, high loadings of catalyst (5 mol%) and ligand (10 mol%) were required.



Scheme 1.5 Borrowing hydrogen methodology in chiral amine synthesis from the corresponding alcohol



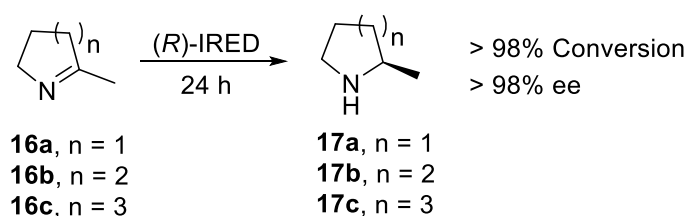
Scheme 1.6 Selected examples of enantioselective amination of alcohols using Ir catalyst **13** and acid **14** by Zhao et al.

In spite of the remarkable success in the development of ligands and catalysts in asymmetric synthesis, their industrial implementations are limited.<sup>36, 37</sup> The high costs of metals and chiral ligands mean that their high turn-over and efficient recycling are essential for an economical process especially at large scale. However it is very difficult to achieve this for homogeneous systems.<sup>38</sup> Another problem with homogeneous catalysis is the product contamination by metal leaching which is of much concern in the pharmaceutical industries.<sup>36</sup> This leads to the development of heterogeneous catalytic systems which include



immobilisation of metal catalysts onto solid supports, allowing their easy separation from the products and their subsequent reuse. This will be further discussed in Section 1.5.3.

Another widely developed field of asymmetric catalysis in the synthesis of chiral amines is the use of enzymes. Turner et al. reported the use of (*R*)-imine reductase [(*R*)-IRED], which was over-expressed from *Streptomyces* sp. GF3587 in *Escherichia coli* to create a recombinant whole-cell biocatalyst for the asymmetric reduction of prochiral cyclic imines.<sup>39</sup> An example is shown in Scheme 1.7.



*Scheme 1.7 Synthesis of chiral cyclic amine 17a to 17c by asymmetric reduction of 16a to 16c by (R)-IRED*

Other commonly used enzymes include transaminases which catalyse the transfer of an amine group to a carbonyl compound such as ketone;<sup>6</sup> and the combination of alcohol dehydrogenase (ADH) and amine dehydrogenase (AmDH) for hydrogen-borrowing cascade reactions discussed above.<sup>40</sup> Although enzymes have become popular in asymmetric synthesis of chiral amines, their sensitivity to temperature and solvent remain major drawbacks. Enzymes are relatively substrate-specific and hence enzyme engineering may be required to widen the substrate scope. This increases the cost and time spent in developing enzymes with optimum activity.

### 1.2.3. Resolution

In spite of the advances that have been made in the development of asymmetric synthesis, resolution, which separates racemic mixtures, remains the most common method to obtain enantiopure compounds at industrial scale, due to its relatively low cost and ease of operation.<sup>41, 42</sup> However, since the desired enantiomers constitute only 50% of the racemate, resolution approaches suffer

from the intrinsic drawback of low yield.<sup>1, 15, 17, 43</sup> The problem can be overcome by recycling the unwanted enantiomers *via* racemisation which will theoretically produce the desired enantiomer in 100% yield and 100% enantiopurity. This methodology will be discussed in more detail in Section 1.4. There are three main strategies for resolution, they are chromatography, kinetic resolution and crystallisation, which will be discussed below.

### **(a) Chromatography**

Much effort has been made in developing enantioselective chromatographic methods to separate racemates for enantiopurity analysis and the preparation of enantioenriched material. One of the major approaches in chromatographic resolution is based on enantioselective interactions of the racemates with chiral stationary phases. Commonly used chiral stationary phases (CSPs) in preparative chiral high performance liquid chromatography (HPLC) are polysaccharide-based and are shown in Table 1.1.<sup>15, 44, 45</sup> Other examples of chiral selectors include cyclodextrins (CDs) and chiral crown ethers.<sup>46-49</sup> They are covalently linked or strongly adsorbed physically onto the chromatographic support such as porous silica. When the enantiomers are eluted through the chiral column with achiral mobile phases, diastereomeric complexes are formed which are retained differently by the stationary phase, allowing resolution to occur.<sup>15</sup>

For sufficient separation of enantiomers, a long column of CSP is needed which increases the cost of the process. As with non-chiral preparative HPLC, the other major drawback is the use of large amount of solvents which poses disposal problems, especially in large scale processes. These led to the development of simulated moving bed (SMB) chromatography. It is operated in a continuous mode which increases the productivity of high-purity products with reduced use of CSPs and mobile phases compared to traditional batch elution chromatography.<sup>50, 51</sup> The optimum combination of CSP and mobile phase for a specific enantioseparation problem is still mainly based on screening a set of available CSPs with various mobile phases, although much progress has been made to better understand the underlying principles of chiral recognitions.<sup>15, 52</sup> Therefore, much time and cost are involved in method development.

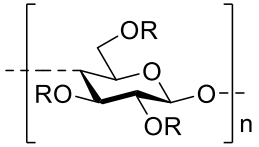
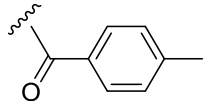
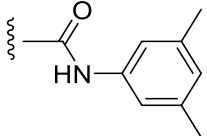
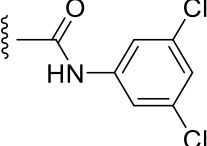
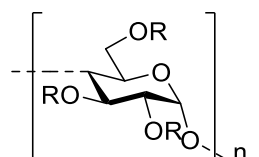
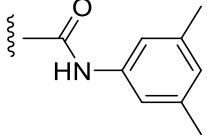
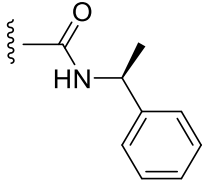
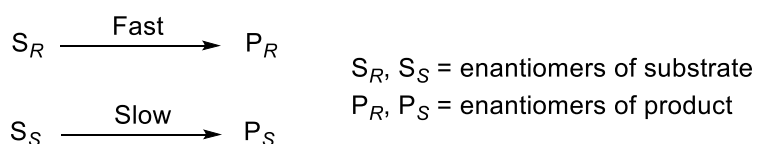
Backbone	Substituent R	Tradename
		Chiralcel OJ
		Chiralcel OD
		Chiralpak IC
		Chiralpak AD
		Chiralpak AS-V

Table 1.1 Examples of polysaccharide-based chiral selectors used as the stationary phases in chiral chromatography

### (b) Kinetic resolution

Kinetic resolution (KR) is defined as a process where two enantiomers of a racemic mixture are transformed into products at different rates, when reacting with a chiral reagent or a chiral catalyst (Scheme 1.8).<sup>42, 53, 54</sup> An efficient KR leads to complete transformation of one of the enantiomers while the other enantiomer remains unchanged, allowing the recovery of both of them in high yield (close to 50% of each enantiomer) and high enantiopurity (close to 100%). Whilst asymmetric synthesis involves product selectivity, KR involves substrate selectivity.<sup>9</sup> The selectivity of a KR process can be quantified by selectivity factor,  $s$  (or the  $E$  value), based on the  $ee$  of the substrate or the product and the conversion (Eqn. 1.1 and 1.2).



Scheme 1.8 A classical KR process

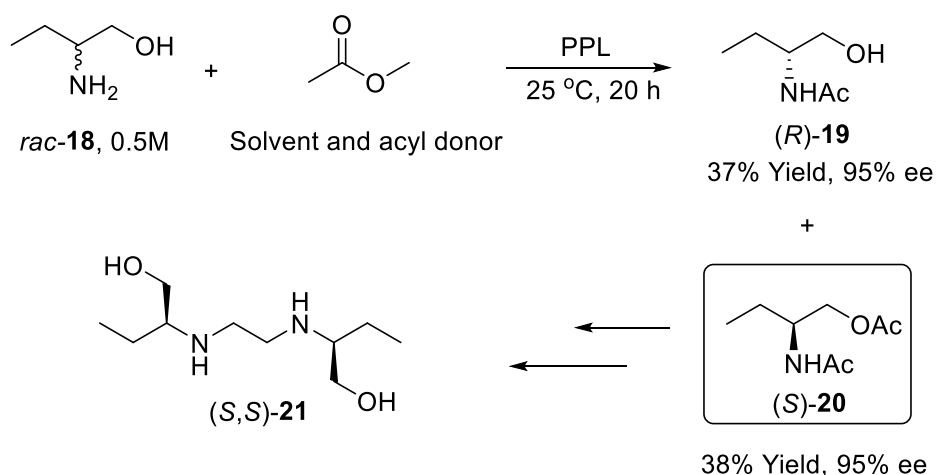
$$E_S = \frac{\ln [(1 - C)(1 - ee_S)]}{\ln [(1 - C)(1 + ee_S)]} \quad (\text{Eqn. 1.1})$$

$$E_P = \frac{\ln [1 - C(1 + ee_P)]}{\ln [1 - C(1 - ee_P)]} \quad (\text{Eqn. 1.2})$$

Where C is the conversion,  $ee_S$  and  $ee_P$  are the ee of the recovered substrate and that of the product respectively.

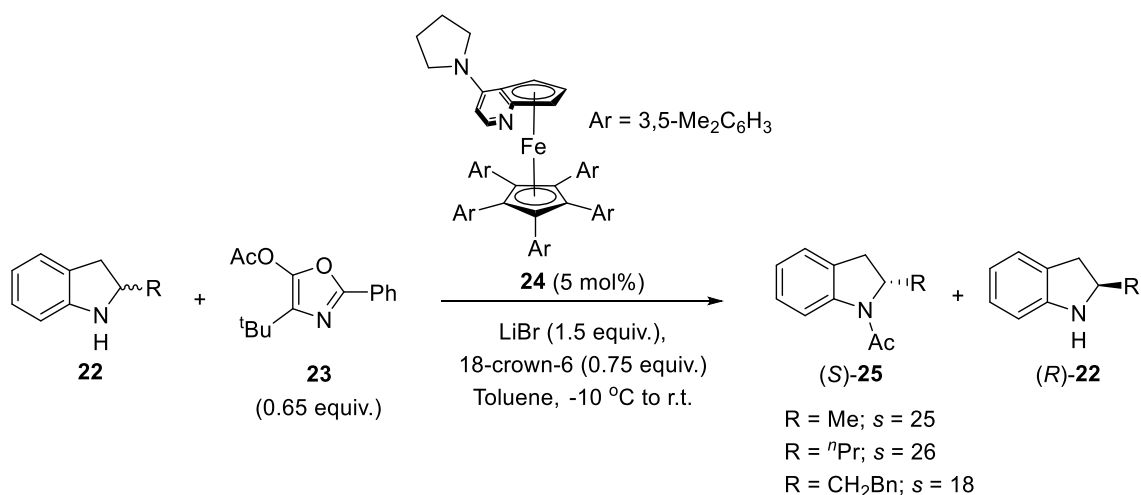
Biocatalysts are most widely employed chiral catalysts in KR and its variants such as dynamic kinetic resolution (DKR).<sup>55-57</sup> A wide range of commercially available enzymes such as hydrolases, transferases and redox enzymes can be used.<sup>53</sup> Enzymatic processes can often be carried out under mild conditions and avoid the need of heavy metal reagents, providing an environmentally benign alternative to chemical methods.<sup>9, 53, 58</sup> Some enzymes have been found to operate in organic solvents, though at reduced rates which increases the substrate scope and the types of possible reactions that can be carried out with enzymes.<sup>53, 57, 59</sup>

Lipases are commonly used in the resolution of amino-alcohols and amines due to their stability, broad substrate range and non-requirement of co-factors, compatibility with organic solvents and the mild reaction conditions required.<sup>60</sup> An early example was reported for the resolution of racemic 2-aminobutan-1-ol **18**.<sup>57</sup> This is a precursor of D-ethambutol **21** used in the treatment of tuberculosis. The resolution of *rac*-**18** was achieved by porcine pancreatic lipase (PPL) which catalyses the enantioselective amide formation and esterification of (*S*)-**18** with methyl acetate as both the acyl donor and solvent, to give (*S*)-**20** with 95% ee; whilst PPL can only acetylate the amino group of (*R*)-**18** to form (*R*)-**19** without transforming the hydroxyl group (Scheme 1.9). (*S*)-**20** can then be separated from (*R*)-**19** and hydrolysed to the desired enantiomer of **21**.



Scheme 1.9 Kinetic resolution of *rac*-**18** by PPL

Whilst enzymes have been extensively used in KR (and DKR) processes, the use of non-enzymatic chiral catalysts have become more popular in recent years.<sup>42, 61</sup> It is more challenging to develop non-enzymatic KR processes for amines than other classes of chiral compounds such as alcohols. This is mainly because of the high nucleophilicity of the amines. The rate of reaction between the amine and the derivatising agent can be competitive with the catalytic rate, resulting in low enantioselectivity.<sup>42</sup> One of the solutions to this problem is to use a less active electrophile, such as *O*-acylated azlactone **23** which was employed as an acylating agent in the KR of indolines **22** in the presence of a chiral iron catalyst **24**. A selectivity factor of up to 26 was achieved (Scheme 1.10).<sup>62</sup>



Scheme 1.10 Non-enzymatic KR of indolines **22** with **23** and chiral iron catalyst **24**

Although KR processes have been widely applied in the synthesis of enantiomerically pure amines, the limited yield that can be achieved leads to the

development of a dynamic system involving *in-situ* racemisation of the unconverted enantiomer which will be discussed further in Section 1.4. Whilst the slower reacting enantiomer can be obtained at high ee by carrying out the reaction to the appropriate conversion, the ee of the product starts to decline as the faster reacting enantiomer is depleted since it is more difficult for the chiral catalyst to bind to the correct enantiomer in the system. A high ee product can only be obtained with reasonable conversion in a simple KR if the E value is high (> 100) (Fig. 1.5).<sup>9, 63</sup> Separation of the product and the unreacted substrates is required which can be difficult and may require additional purification steps. If the desired enantiomer is transformed into the product, an additional step such as hydrolysis may be required to convert the product back to the substrate. This is also true for DKR processes.

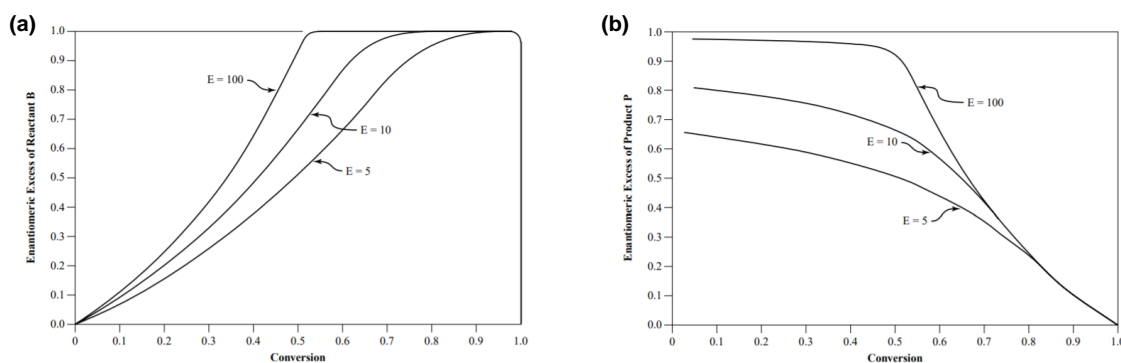


Fig. 1.5 Dependence of ee of (a) remaining substrate; (b) product on the conversion for various E values<sup>64</sup>

### (c) Crystallisation

Crystallisation remains one of the most important and commonly used resolution methods for the synthesis of enantiopure compounds due to their simplicity and robustness.<sup>9</sup> Crystallisation can also be employed to purify the product chemically which makes it more attractive.<sup>65</sup> Depending upon the unit cell symmetry, crystal-forming racemate can be divided into three types. The first type is called conglomerate, which refers to a 1:1 mechanical mixture of crystals of pure (*S*)- and (*R*)-enantiomers. This crystal form accounts for about 5 to 10% of all crystalline racemates. The second type is racemic compound, in which both enantiomers are present in individual crystals in 1:1 ratio arranged in an ordered manner. This is the most common type of crystal form which accounts for 90 to 95% of all crystalline racemates. Finally less than 1% of racemates crystallise as

a pseudo-racemate or solid solution, in which both enantiomers are present in the condensed phase in a non-ordered fashion (Fig. 1.6).<sup>7, 9, 66-68</sup> These different crystal forms can be distinguished by their melting point diagrams (Fig. 1.7).<sup>7, 9, 68</sup>

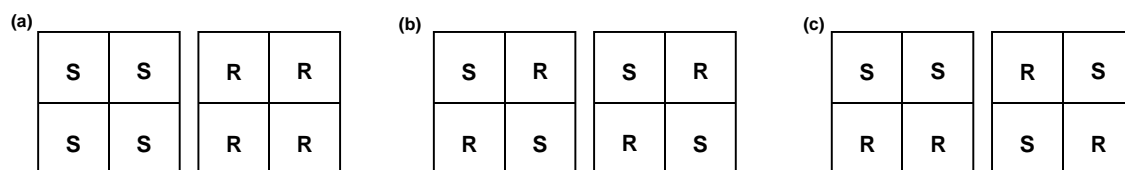


Fig. 1.6 Different crystal structures exhibited by racemates. (a) Conglomerates; (b) racemic compounds; (c) pseudo racemates (solid solutions)

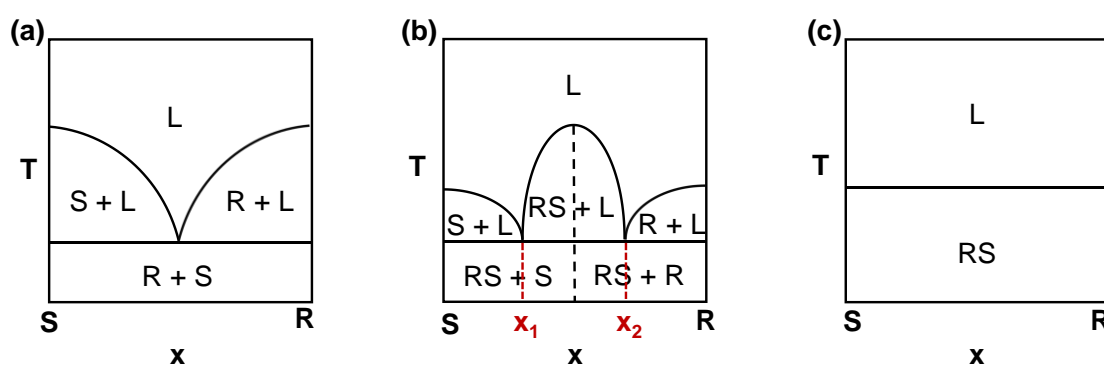
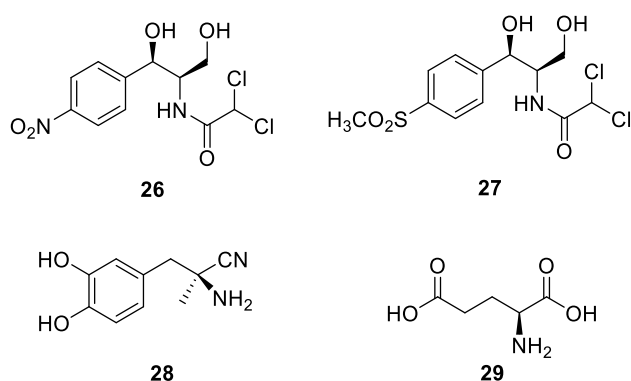


Fig. 1.7 Binary melt phase diagrams of enantiomer mixtures forming (a) conglomerate; (b) racemic compound and (c) solid solution. R, S, RS and L correspond to solid R-enantiomer phase, solid S-enantiomer phase, solid phase for racemic compound RS or solid solution RS, and liquid phase respectively. T is temperature and x is mole fraction of the mixture

In a conglomerate, pure crystalline enantiomer compounds R and S have the highest melting point. The melting point decreases with decreasing enantiomer purity since each enantiomer acts as an impurity so lowering the melting temperature of the other. It reaches a minimum (eutectic temperature) when the mixture constitutes 1:1 ratio of R- and S-enantiomer crystals ( $x = 0.5$ ) (Fig. 1.7(a)). In a racemic compound, slightly decreasing the enantiopurity decreases the melting point of the system to a minimum ( $x = x_1$  or  $x_2$ ) then increases again towards the 1:1 mixture. This is because for the enantiomeric composition between  $x_1$  and  $x_2$ , the racemic compound RS is more stable than the pure R- or S-enantiomer (Fig. 1.7(b)). For a solid solution, the melting temperature remains the same with the enantiomeric composition (Fig. 1.7(c)).

### (i) Direct crystallisation

Racemates which exist as conglomerates can be resolved by direct crystallisation of the enantiomers, without the need of any chiral auxiliary or the formation of diastereomers.<sup>15</sup> There are two approaches of direct crystallisation which are preferential crystallisation (or entrainment) and simultaneous crystallisation. In preferential crystallisation, homochiral crystal seeds of one of the enantiomers are added to a supersaturated solution of the racemate which increases the crystal growth rate of that enantiomer. This creates a difference in crystal growth rates of the two enantiomers, leading to their separation. Consecutive seeding of enantiomerically pure crystals of the opposite enantiomers allows both enantiomers to be crystallised out separately. This method has been applied in smaller scales in batch and is used in the production of some broad-spectrum antibiotics such as chloramphenicol **26** and thiamphenicol **27** (Fig. 1.8). In simultaneous crystallisation, both enantiomers crystallised out from the supersaturated solution of the racemate separately and simultaneously in two separate but linked chambers, each is seeded with the crystals of the respective enantiomers. This approach can be used in a larger scales in both batch and continuous modes,<sup>69</sup> and has been used in the production of an  $\alpha$ -methyl-L-dopa intermediate **28** by Merck (> 100 tonnes/ year) and L-glutamic acid **29** by Ajinomoto (13,000 tonnes/ year in 10 years) (Fig. 1.18).<sup>9, 15, 70</sup>



*Fig. 1.8 Examples of compounds synthesised via direct crystallisation of their racemates by entrainment (**26** and **27**) and simultaneous crystallisation (**28** and **29**)*

### (ii) Classical resolution

Whilst resolution by direct crystallisation is relatively simple, it is restricted to conglomerates which account for < 10% of all crystalline racemates. The majority



of crystal-forming racemates exist as racemic compound. They cannot be resolved by direct crystallisation since both enantiomers are present in each unit cell of the crystal. Instead they are resolved by diastereomeric crystallisation which is also called classical resolution. This involves the derivatisation of the racemate by an enantiopure chiral reagent to form a mixture of diastereomers. This resolution method is of great importance to the synthesis of enantiopure chiral amines on industrial scale.<sup>1, 2, 43, 71</sup> By reacting the racemic, basic chiral amine with a suitable enantiopure chiral acid, a pair of diastereomeric salts is formed with different solubility and therefore, allowing their separation by crystallisation.<sup>9, 15, 72, 73</sup> Some commonly employed chiral acids in the resolution of chiral amines are shown in Fig. 1.9. After the resolution process, the desired enantiopure amine can be recovered by simple acid-base extraction.

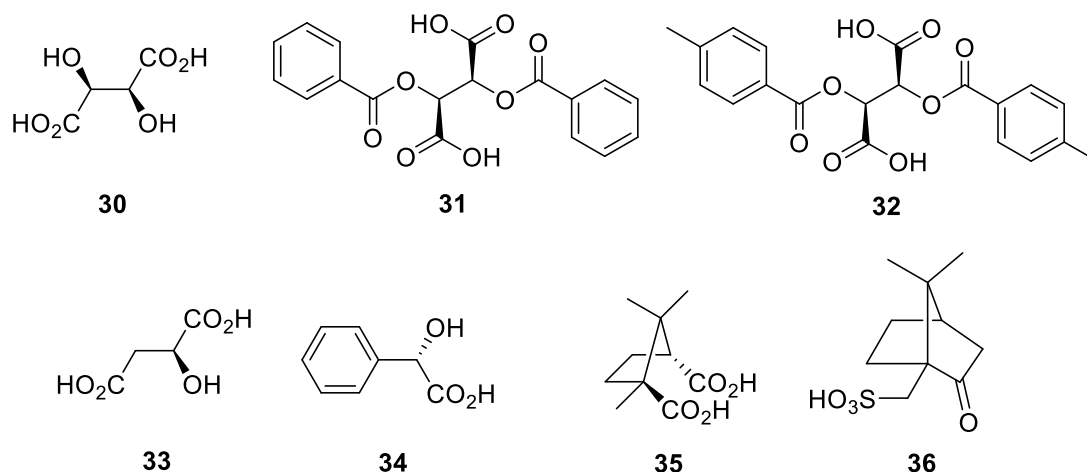
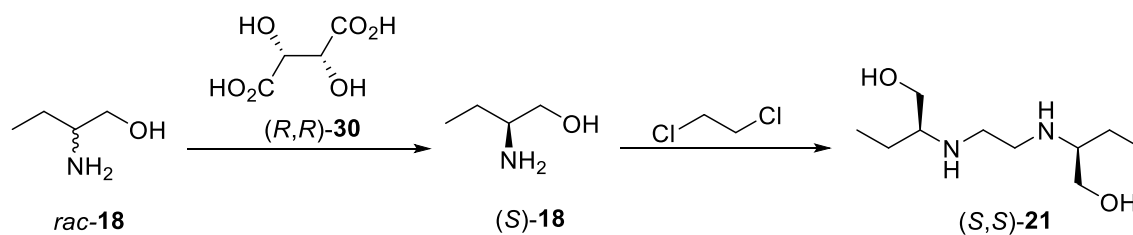


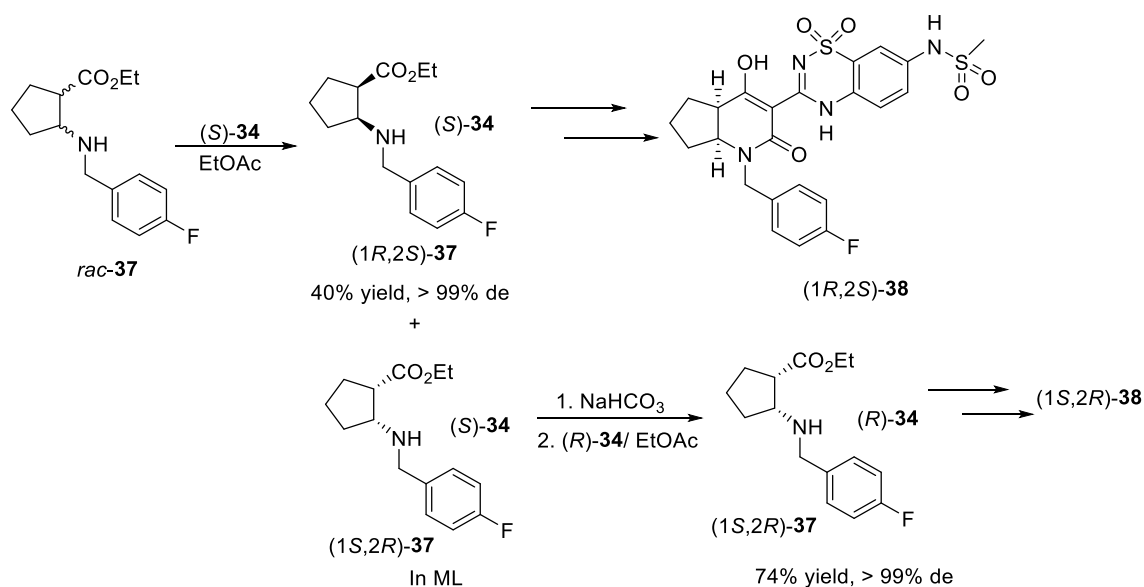
*Fig. 1.9 Examples of commonly used chiral acids for the diastereomeric resolution of chiral amines: Tartaric acid **30**, dibenzyl tartaric acid **31**, di-p-toluyol tartaric acid **32**, malic acid **33**, mandelic acid **34**, camphoric acid **35**, camphorsulfonic acid **36**. Only one of the enantiomers was shown for each acid*

2-Aminobutan-1-ol **18**, the precursor of ethambutol **21**, which was discussed in Section 1.2.3(b) for its kinetic resolution by lipase, was industrially produced by diastereomeric crystallisation using (*R,R*)-tartaric acid **30** (Scheme 1.11).<sup>9, 74, 75</sup>



Scheme 1.11 Industrial synthesis of ethambutol **21** via diastereomeric crystallisation of *rac*-**18** with (*S,S*)-**30**

A chronic hepatitis C virus (HCV) NS5B polymerase inhibitor **38** can be prepared via the resolution of intermediate ethyl ester **37** using (*S*)-mandelic acid **34**. The active diastereomer (*1R,2S*)-**37** was isolated as the salt of (*S*)-**34** in 40% yield and 99% de after single recrystallisation (Scheme 1.12). In order to fully understand the biological activity of the compound, the opposite diastereomer (*1S,2R*)-**37** was also synthesised by precipitating the free-base of the mother liquor (ML) by (*R*)-**34**, resulting in 99% de of (*1S,2R*)-**37**.<sup>76, 77</sup>



Scheme 1.12 Synthesis of both enantiomers of **38** via the diastereomeric resolution of *rac*-**37** by (*S*)-**34**, followed by the precipitation of the opposite enantiomer with (*R*)-**34**

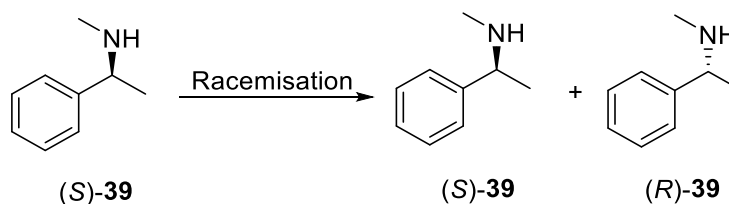
In classical resolution, extra steps and costs are needed to introduce the chiral resolving agent and recover the amine, although the chiral acids (or the resolving agent in general) can sometimes be recovered and recycled to reduce waste. As with all other resolution processes, the yield never exceeds 50% for each of the enantiomers. Usually only one of the enantiomers is desired while the other may

be of little or no use, lowering the efficiency of the process and leads to large waste stream. This is particularly problematic if the resolution is performed with expensive or synthetically challenging products. The problem can be overcome if the enantioenriched mixture can spontaneously or catalytically racemise after the resolution, increasing the yield and efficiency of the process. This leads to the concept of Crystallisation-Induced Diastereomeric Transformation (CIDT) and Crystallisation-Induced Asymmetric Transformation (CIAT). It is important to note that there have been a few ambiguities in defining the above terms.<sup>66</sup> CIDT refers to the coupling process of diastereomeric crystallisation and *in-situ* racemisation; while CIAT refers to the direct crystallisation of conglomerate accompanied by *in-situ* racemisation. This work will focus on CIDT and will be covered in more detail in Section 1.4. The background of racemisation needs to be discussed first.

### 1.3. Racemisation of chiral amines

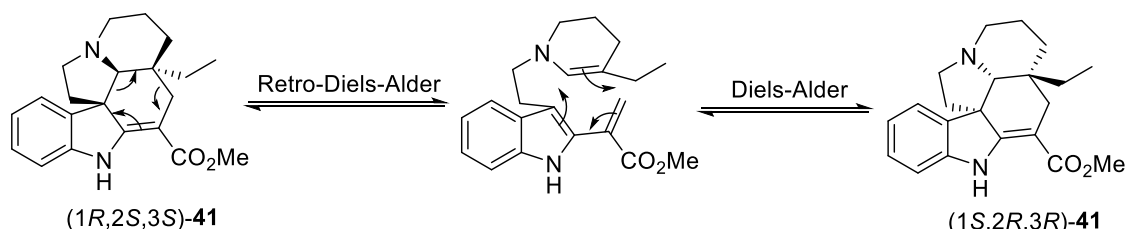
As discussed in Section 1.2.3, resolution is the most commonly employed method in obtaining enantiomerically pure compounds. However the process suffers from the generation of large quantities of unwanted isomers and limited yield of the desired products.<sup>78</sup> In order to minimise the environmental and economical drawbacks from resolution processes, it is highly desirable to recycle the waste enantiomers by racemisation, which can be subject to resolution again.

Racemisation is defined as the irreversible formation of a racemate, which is an equimolar mixture of both enantiomers, from a pure enantiomer (or an enantioenriched mixture), leading to complete loss of optical activity. For a molecule possessing more than one chiral centre, inversion of one of them is called epimerisation, which does not lead to total loss of optical activity.<sup>79</sup> Examples are shown in Scheme 1.13 and Scheme 1.14.



Scheme 1.13 Racemisation of (S)-N-methyl- $\alpha$ -methylbenzylamine **39**

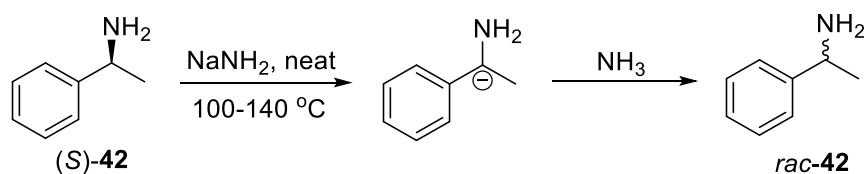




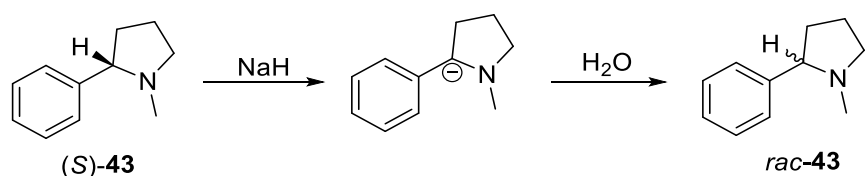
Scheme 1.15 Thermal racemisation of vincadifformine **41**

### (b) Base-catalysed racemisation

Amines such as  $\alpha$ -methylbenzylamine **42** and nicotine **43** can be racemised in the presence of strong base *via* the formation of a planar carbanion (Scheme 1.16 and Scheme 1.17).<sup>78, 82, 83</sup> The method requires an acidic proton at the chiral centre, or the use of a strong base which is incompatible with molecules containing base-sensitive functional groups. However it is often used for the racemisation of amino acids.<sup>79</sup>



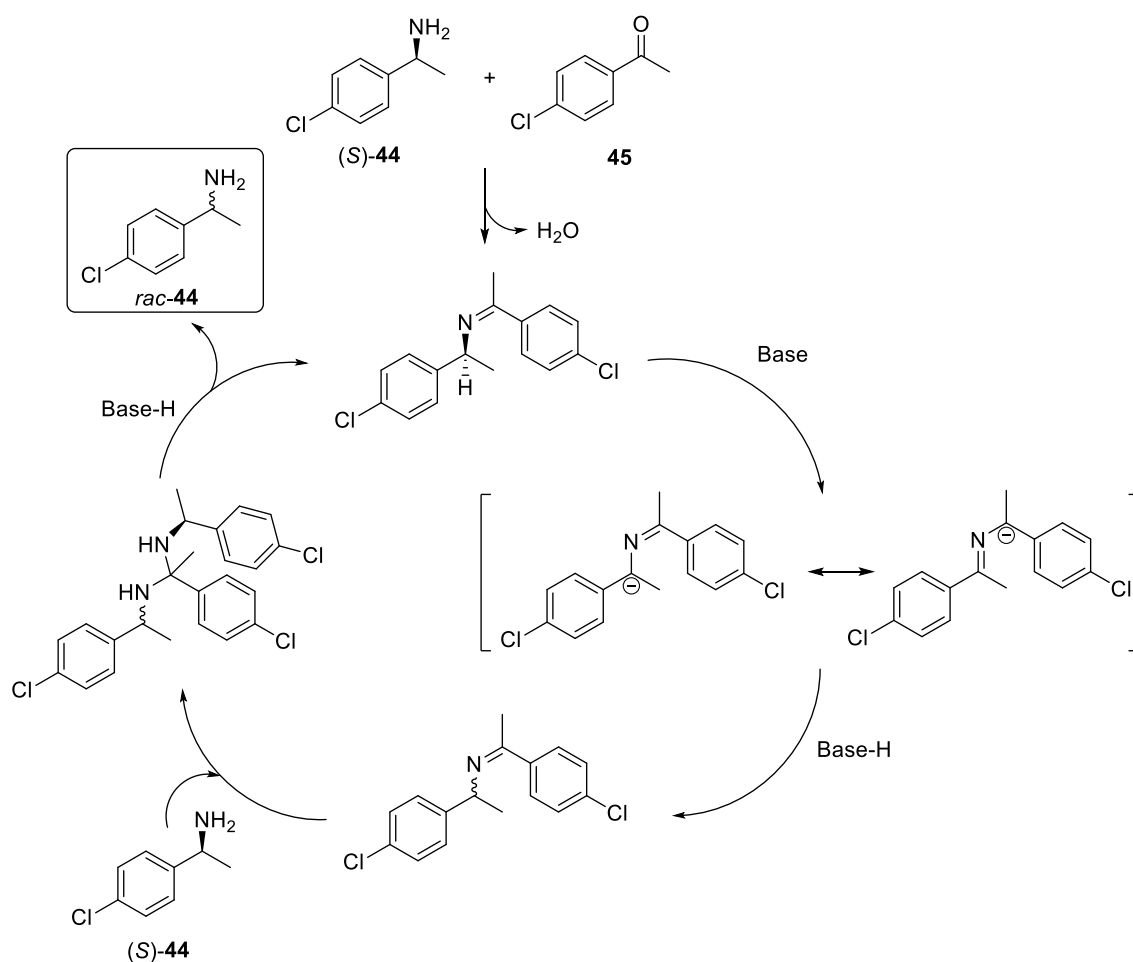
Scheme 1.16 Base-catalysed racemisation of (S)-**42**



Scheme 1.17 Based-catalysed racemisation of nicotine **43**

### (c) Racemisation *via* Schiff base formation

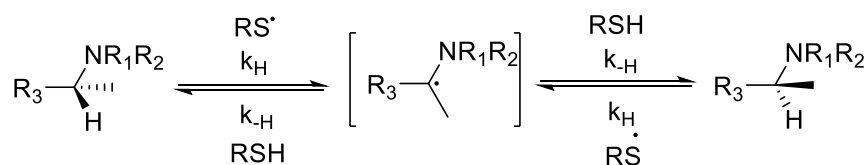
The  $pK_a$  of the proton at the chiral centre of an amine can be lowered by the formation of Schiff base using catalytic amount of aldehyde/ ketone which can then effect racemisation in the presence of a weak base. This is an important method for the racemisation of amino acids and their derivatives, while it is less common for amines. Ditrich published a patent on the racemisation of optically active primary aryl amines such as (S)-1-(4-chlorophenyl)ethylamine **44** using ketone **45** (Scheme 1.18).<sup>84</sup>



Scheme 1.18 Racemisation of (S)-44 via formation of Schiff base with ketone 45

#### (d) Racemisation via radical formation and redox processes

The methods mentioned above are relatively substrate-specific and require amines to have considerable stability towards harsh racemisation conditions such as high temperature and the presence of strong base, or require the presence of an acidic proton at the stereocentre. Therefore applications are fairly limited. Racemisation using enzymes such as racemases are also common. However they are usually employed for amino acids and their derivatives.<sup>79, 83</sup> For chiral amines, racemisation was generally carried out through radical or oxidation-reduction mechanisms.<sup>79</sup> Escoubet et al. demonstrated the ability of sulfur-based radicals to racemise both benzylic and aliphatic amines.<sup>85-87</sup> The process involves reversible hydrogen abstraction at the chiral centre (Scheme 1.19). Thiols are known to be good hydrogen donors.<sup>88</sup> On the other hand, thiyl radicals are electrophilic which are able to abstract hydrogen from electron-rich C-H bonds.<sup>89</sup>



Scheme 1.19 Reversible hydrogen transfer between thiol and C $\alpha$ -H of the amine

Some examples of chiral amine racemisation from Escoubet using different thiols were selected and presented in Fig. 1.10 and Table 1.2.

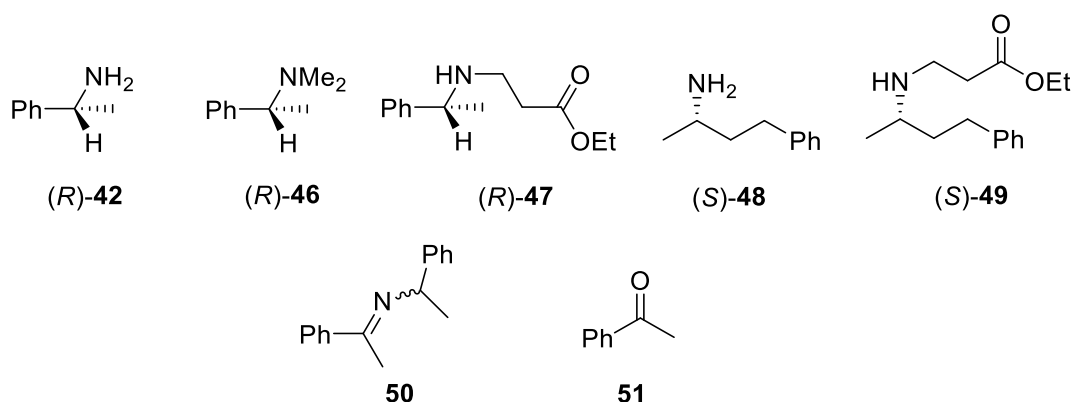


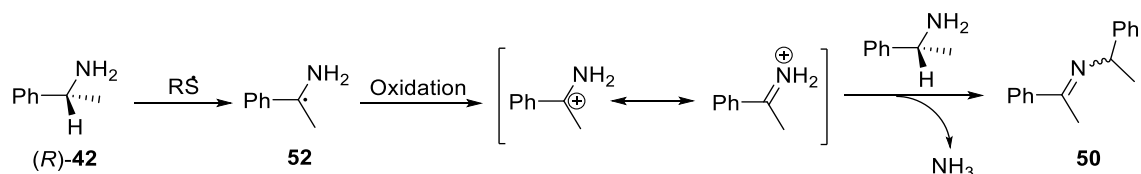
Fig. 1.10 Examples of chiral amines (**42**, **46** to **49**) racemised by thiols as demonstrated by Escoubet et al. and the by-products formed (**50** and **51**)<sup>85, 86</sup>

Entry	Amine <sup>[a]</sup>	RSH (equiv.)	t (h)	Isolated yield (%)	ee (%)	By-product (%)
1	<b>42</b>	PhSH (0.2)	6	30	76	<b>50</b> (20)
2	<b>42</b>	PhSH (1.2)	6	50	40	<b>50</b> (17)
3	<b>46</b>	PhSH (1.2)	6	70	4	<b>51</b> (10)
4	<b>47</b>	TolSH (1.2)	7	70	0	-
5	<b>48</b>	MeOCOCH <sub>2</sub> SH (1.2)	2	67	0	-
6	<b>49</b>	<i>n</i> -OctSH (1.2)	6	70	4	-

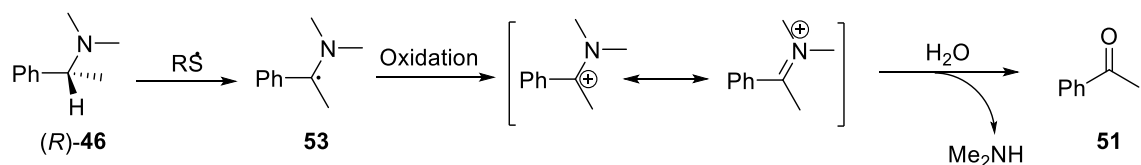
Table 1.2 Racemisation results of amines **42**, **46** to **49** using thiols as demonstrated by Escoubet et al. <sup>[a]</sup>[Amine] = 60 to 67 mM<sup>85, 86</sup>

This method is less suitable for primary amines such as **42**. The corresponding carbon-centred radical **52** is particularly susceptible to oxidation which leads to the formation of **50** via dimerisation (Table 1.2, entries 1 and 2; Scheme 1.20). Stoichiometric amounts of thiol are required to reduce the lifetime of **52** and avoids its oxidation (Table 1.2, entries 2 and 5). Oxidation of carbon-centred

radicals formed from non-primary amines such as **46** can also occur and can hydrolyse to form acetophenone **51** (Table 1.2, entry 3; Scheme 1.21).



Scheme 1.20 Formation of **50** from **42** via oxidation of intermediate radical **52** and subsequent dimerisation

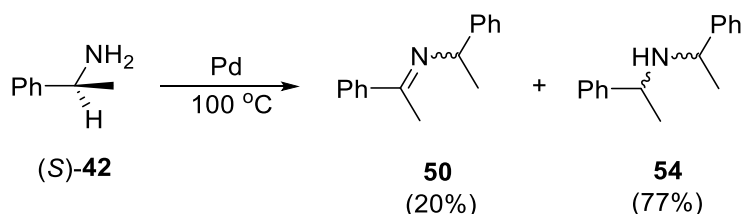


Scheme 1.21 Formation of **51** from **46** via oxidation of intermediate radical **53** and subsequent hydrolysis

Both stabilised (Table 1.2, entries 1 to 4) and unstabilised thiyl radicals (Table 1.2, entries 5 and 6) were able to racemise various aliphatic and benzylic amines. However the choice of a suitable thiol is crucial and is based on the bond strengths of C-H and S-H bonds. They should match such that both forward and backward hydrogen transfer proceed at reasonable rates without forming undesired side-products such as **50** and **51**.<sup>85</sup>

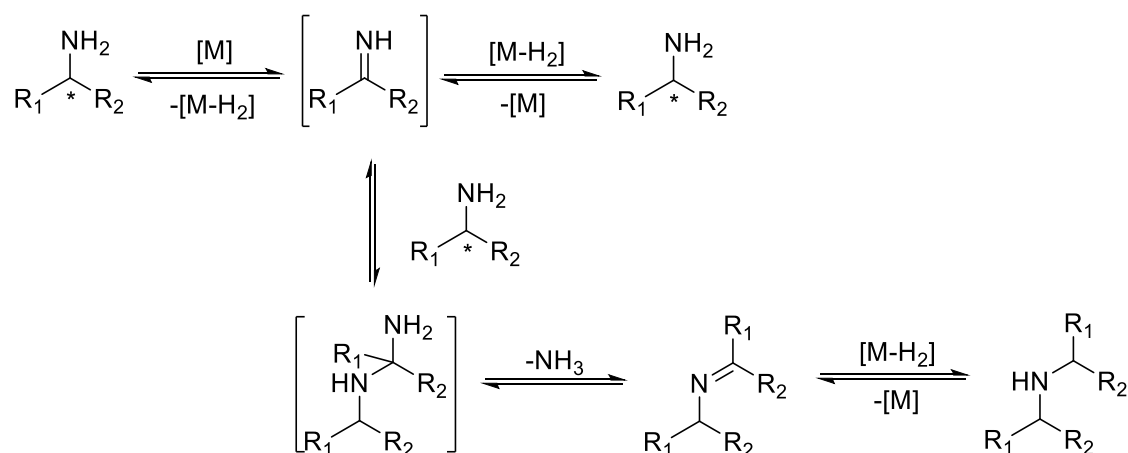
The use of transition metal catalysts is by far the most important method in the racemisation of chiral amines. It is achieved by oxidation/ dehydrogenation of the amine to the imine, which is reduced/ hydrogenated back to the amine non-stereoselectively. In 1983, Murahashi et al. reported the activity of palladium towards the racemisation of (*S*)-**42** when he studied the synthesis of unsymmetrical amines *via* alkyl group exchange reaction between primary and secondary amines.<sup>90</sup> When (*S*)-**42** was heated in the presence of palladium black at 100 °C, imine **50** (which was also observed in the racemisation of (*S*)-**42** by thiol as discussed previously) and dimer **54** were observed with 6.6% and 1.7% optical activity respectively (Scheme 1.22).





Scheme 1.22 Formation of **50** and **54** from (S)-**42** in the presence of Pd

The formation of by-products **50** and **54** is especially pronounced in the racemisation of primary amines. With no electron-releasing alkyl substituents attached to the nitrogen, the imine intermediate formed after dehydrogenation of the amine is more electrophilic and less sterically hindered and therefore, it is more susceptible to the attack of another amine substrate (Scheme 1.23).

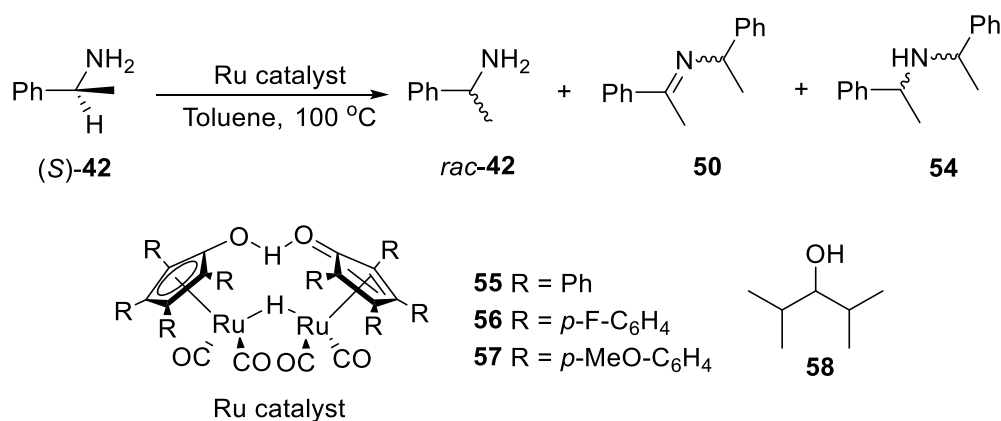


Scheme 1.23 General mechanism of the racemisation of primary amines and the dimerisation side-reaction. [M] = metal complex catalyst

Jacobs et al. used palladium with inorganic support such as barium sulfate, barium carbonate and calcium carbonate in the presence of hydrogen to racemise benzylic amines and to increase the selectivity by suppressing the formation of dimeric products.<sup>91</sup> The reaction was performed at 70 °C which was relatively mild and could also be used to combine with enzymatic resolution. However it is limited to benzylic amines and is only suitable for substrates without any reducible functional groups.

Bäckvall et al. reported the racemisation of chiral amines by ruthenium-cyclopentadienone complex **55** (Shvo's catalyst) and its derivatives **56** and **57** after realising the potential of **55** in catalysing transfer hydrogenation of imines to

amines and transfer dehydrogenation of amines to imines, which are the key steps in the racemisation of amines.<sup>92-96</sup> The system was applicable to both benzylic and aliphatic amines. Bäckvall had demonstrated the use of various approaches in reducing the formation of dimeric products for primary amines such as **42** (Scheme 1.24; Table 1.3). In using the original Shvo's catalyst **55**, lowering the concentration of (*S*)-**42** can reduce the chance of condensation of the imine with **42** (Table 1.3, entries 1 to 3). The addition of ammonia can shift the equilibrium from the dimers to the imines (Scheme 1.23; Table 1.3, entry 4). Adding a hydrogen donor such as 2,4-dimethyl-3-pentanol **58** can facilitate the transfer hydrogenation of the imine back to amine **42** (Table 1.3, entry 5).



Scheme 1.24 Racemisation of (*S*)-**42** and formation of dimeric side products **50** and **54** with Ru catalysts **55** to **57**

Entry	Catalyst (mol %)	Additives (equiv.)	[( <i>S</i> )- <b>42</b> ] (M)	t (h)	ee (%)	<b>42</b> (%)	<b>50</b> (%)	<b>54</b> (%)
1	<b>55</b> (5)	-	1	48	0	5	12	29
2	<b>55</b> (5)	-	0.25	48	6	84	5	11
3	<b>55</b> (5)	-	0.125	48	3	91	3	6
4	<b>55</b> (5)	NH <sub>3</sub> (1)	0.25	48	2	98	< 1	< 1
5	<b>55</b> (5)	<b>58</b> (0.5)	0.25	48	2	98	< 1	< 1
6	<b>55</b> (4)	-	0.25	24	53	82	N.R. <sup>[a]</sup>	N.R. <sup>[a]</sup>
7	<b>56</b> (4)	-	0.25	24	36	25	N.R. <sup>[a]</sup>	N.R. <sup>[a]</sup>
8	<b>57</b> (4)	-	0.25	24	55	95	N.R. <sup>[a]</sup>	N.R. <sup>[a]</sup>

Table 1.3 Racemisation results of (*S*)-**42** by **55** to **57** demonstrated by Bäckvall.<sup>95, 96</sup>

<sup>[a]</sup>Concentrations of **50** and **54** were not reported

The racemisation of (*S*)-**42** was also tested with different variants of **55**. By using electron-withdrawing catalyst **56** with fluorine substituents, a lower ee was achieved compared to **55**. However the selectivity was much lower (Table 1.3, entry 7). The ruthenium centre of **56** is more electron-deficient and therefore facilitates the dehydrogenation of the amine substrate. On the other hand, this slows down the hydrogenation of the imine intermediate and increases its lifetime, which leads to more side reactions. With electron-donating catalyst **57**, having a methoxy substituent, its catalytic activity is lower than that of **56** and is similar to that of **55**, but with the highest selectivity (Table 1.3, entry 8). Since the ruthenium centre in **57** is more electron-rich, this slows down the dehydrogenation of the amine; however this speeds up the hydrogenation of the imine intermediate, reducing its lifetime and hence, less side-reactions occur.<sup>96</sup>

Various primary and secondary benzylic amines were racemised by using 5 mol% of **55** at 110 °C in the presence of alcohol **58** (0.5 equiv.).<sup>95</sup> Some examples of the amine substrates are shown in Fig. 1.11 and their racemisation results are summarised in Table 1.4.

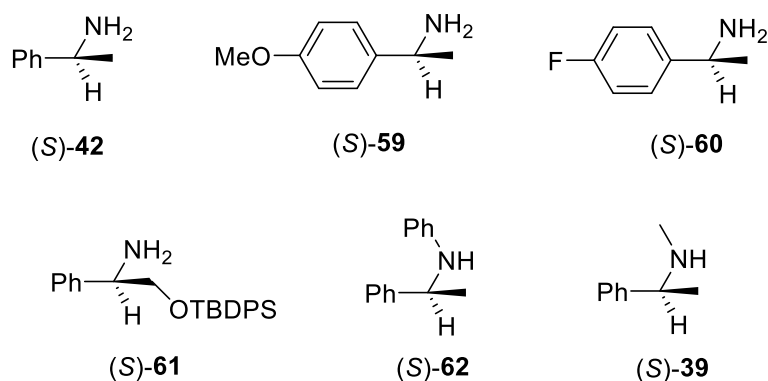


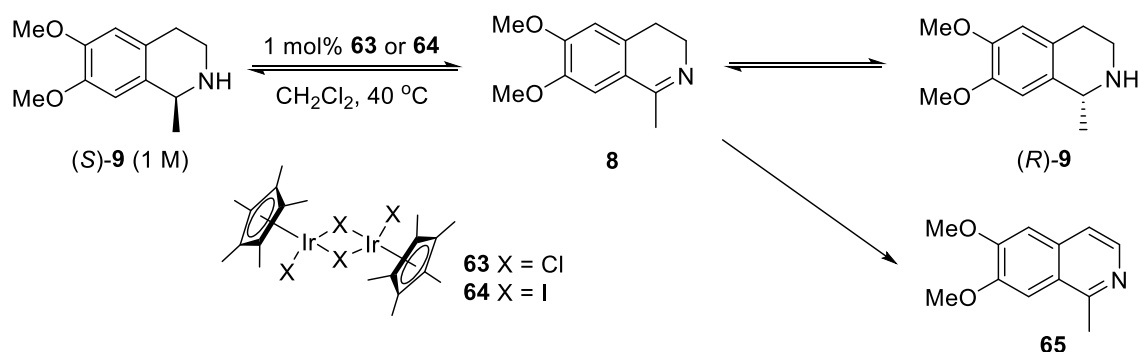
Fig. 1.11 Examples of chiral amines (**39**, **42**, **59** to **62**) racemised by **55** as demonstrated by Bäckvall et al.

Entry	Amine <sup>[a]</sup>	t (h)	Amine (%)	ee (%)
1	<b>42</b>	24	98	3
2	<b>59</b>	9	98	3
3	<b>60</b>	24	95	2
4	<b>61</b>	48	> 95	57
5	<b>62</b>	24	98	1
6	<b>39</b>	1	> 99	0

Table 1.4 Racemisation results of (*S*)-**39**, **42**, **59** to **62** by Shvo's catalyst **55** (5 mol%) in the presence of **58** (0.5 equiv.) at 110 °C in toluene. <sup>[a]</sup>Concentration of amine = 0.125 M

Primary benzylic amines with electron-donating and electron-withdrawing substituents can be racemised with minimal side products formed (Table 1.4, entries 2 and 3). Secondary amine **39** can racemise completely within one hour (Table 1.4, entry 6). Racemisation slowed down dramatically with substrates having bulky substituents (Table 1.4, entries 4 and 5).

In addition to ruthenium-based catalysts, Blacker et al. demonstrated the use of pentamethylcyclopentadienyliridium (III) iodide dimer (SCRAM) **64** in the racemisation of primary, secondary and tertiary chiral amines in relatively mild conditions (40 to 90 °C; 0.1 to 1 mol% catalyst).<sup>1</sup> Initially pentamethylcyclopentadienyliridium (III) chloride dimer **63** was tested in the racemisation of (*S*)-6,7-dimethoxy-1-methyl-1,2,3,4-tetrahydroisoquinoline **9** (Scheme 1.25).



Scheme 1.25 Racemisation of (*S*)-**9** by catalysts **63** and **64**

Although the racemisation of (*S*)-**9** was observed, a significant amount of the dehydrogenated side-products **8** and **65** were formed with some other

unidentified impurities. Since the rate of racemisation and the lifetime of intermediate imine **8** depend on the binding interaction between the substrate and the iridium centre, and the tendency for the catalyst to donate or accept a hydride ion, this can be modified by changing the ligand on the catalyst. Therefore potassium iodide was added into the reaction mixture to form **64** *in-situ*, which resulted in 120-fold increase in the rate of racemisation of (S)-**9** and a significant reduction of **8** and **65** formed. The use of isolated iodo-catalyst **64** led to similar results.<sup>1</sup> These indicate the importance of the halide ligand in the catalytic activity of pentamethylcyclopentadienyliridium (III) complexes towards racemisation of amines.

Catalyst **64** was further tested in the racemisation of other chiral amine substrates (Fig. 1.12 and Table 1.5).<sup>1</sup> Both secondary and tertiary amines were racemised successfully by **64** (Table 1.5, entries 1 to 4, 7 to 9). Cyclic amines tend to racemise at higher rates and this may be due to the more stable imine intermediate formed (Table 1.5, entries 1 to 3). For amines with more than one heteroatom such as **68**, it can act as a bidentate ligand and binds to the iridium which reduced the activity of the catalyst (Table 1.5, entry 4). Significant dimer formation with negligible racemisation was again observed for primary amines (Table 1.5, entries 5 and 6). Amines with less bulky and more electron-donating substituents were found to racemise at higher rates (Table 1.5, entries 1 and 8). These can be due to the stronger binding between the iridium centre and the substrates which allows dehydrogenation of the substrates to occur.

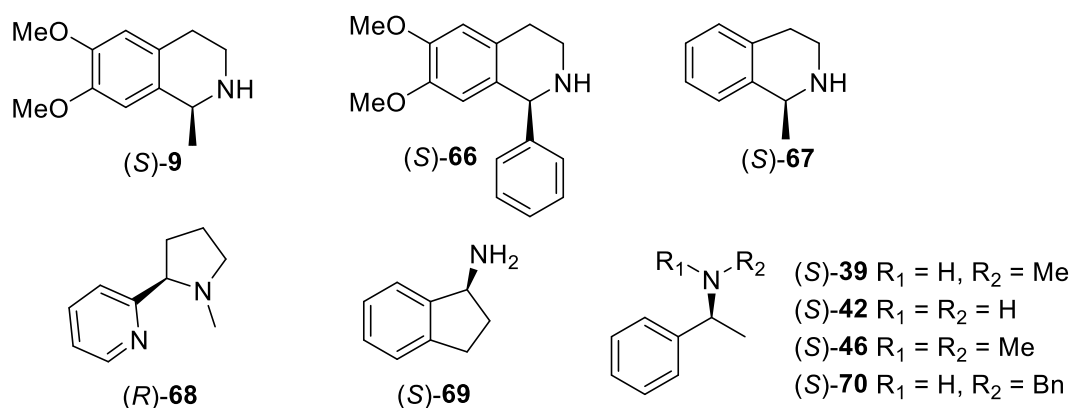


Fig. 1.12 Examples of chiral amines racemised by catalyst **64** demonstrated by Blacker *et al.*

Entry	Amine	T (°C)	Loading of <b>64</b> (mol%)	Racemisation $t_{1/2}$ (min)
1	(S)- <b>9</b>	40	0.2	45
2	(S)- <b>66</b>	80	0.5	180
3	(S)- <b>67</b>	40	0.2	220
4	(R)- <b>68</b>	80	1	> 7200
5	(S)- <b>69</b>	80	1	Dimeric impurities
6	(S)- <b>42</b>	80	1	Dimeric impurities
7	(S)- <b>46</b>	90	1	1250
8	(S)- <b>39</b>	80	1	45
9	(S)- <b>70</b>	80	1	250

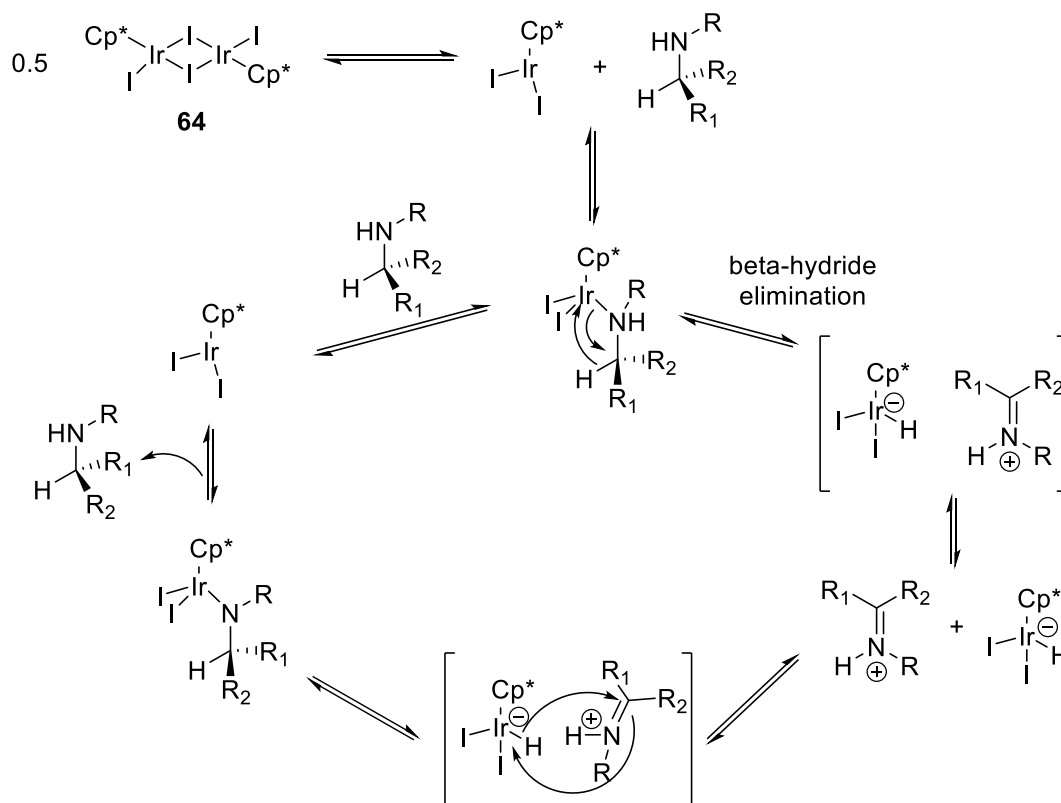
Table 1.5 Racemisation results of chiral amines by SCRAM catalyst **64**

Although transition metal catalysts such as **64** are relatively active towards the racemisation of a wide variety of amines, these catalysts are expensive. Therefore their reuse and recycle after the reaction are highly desirable. However this is often difficult to achieve for homogeneous systems. In this work, the activity of **64** will be further studied. Its immobilisation which allows its efficient recycle will also be discussed.

### 1.3.2. Mechanism of chiral amine racemisation by SCRAM catalyst **64**

Chiral amine racemisation involves hydrogen transfer reactions between the amine substrate and the metal catalyst. Stirling et al. recently proposed a mechanism for amine racemisation by catalyst **64** (Scheme 1.26).<sup>97</sup> It was assumed that initial complex formation between the iridium dimer and the amine substrate was required to initiate the racemisation reaction. The Ir-amine complex was observed at low temperature (-40 °C) in which the binding constant increases with less sterically hindered substrate such as **42**, in comparison to **39**. However, under normal racemisation reaction conditions in which a higher temperature is usually required, the binding is not strong and only a small fraction of **64** can be converted to the Ir-amine complex. Hydride transfer between the coordinated amine to the iridium is the rate-limiting step based on the primary kinetic isotopic effect observed for **9** (1-H) and **9** (1-D). An ion pair is formed between the diiodo-iridium hydride complex which carries a negative charge with the positively charged iminium ion. A cross-over experiment with isotopically labelled amines was carried out by Stirling which showed that the iminium/ imine intermediate

formed can dissociate from the iridium complex. Upon its re-association, hydride is transferred from the iridium back to the imine.



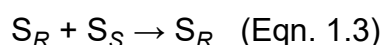
*Scheme 1.26 Plausible mechanism of chiral amine racemisation by SCRAM 64 proposed by Stirling et al. A generic secondary amine was shown as an example. Cp\* = pentamethylcyclopentadienyl*

The proposal of the formation of imine/ iminium intermediate upon hydride transfer from the amine to the iridium and the re-addition of hydride to the imine/ iminium can potentially be used as an indication to determine if an amine substrate can be racemised under certain reaction conditions. This can be achieved by using either a deuterium-labelled substrate, or deuterium donor such as  $d_8$ -isopropyl alcohol, without the need to carry out the actual racemisation reaction with the enantio-enriched material and subsequent chiral analysis. This has been investigated in this project and will be addressed in Section 2.5.

#### 1.4. De-racemisation

As discussed in previous sections, although the resolution of racemates remains one of the major methods for the preparation of enantiopure compounds, the

theoretical yield of the desired enantiomer can never exceed 50%. Considerable effort has been made to overcome this limitation by developing processes which convert a racemate into the desired, single stereoisomer in a concurrent fashion in which the formation of the undesired stereoisomer can be totally avoided.<sup>98</sup> This is known as 'de-racemisation'. This term was originally defined as the opposite of racemisation ('de' means *the opposite of*) which implied the transformation of two enantiomers into one single enantiomer of the same compound (Eqn. 1.3).



Where  $S_R$  and  $S_S$  are the *R*- and *S*-enantiomer of the substrate.

Whilst the enthalpy change of this process is negligible,<sup>79</sup> decrease in entropy means that this is energetically unfavourable. Faber had re-defined the term 'de-racemisation' as any processes during which a racemate is converted into a non-racemic product in 100% theoretical yield without intermediate separation of materials (Eqn 1.4).<sup>98</sup> The unfavourable entropy change can possibly be covered by the enthalpy of the reaction. Product  $P_R$  is a closely related derivative of the substrate. In the case of chiral amine, the product can be diastereomeric salts, amides and carbamates.



Where  $P_R$  is the single enantiomer of the product.

De-racemisation can be achieved by re-racemisation and repeated resolution. Upon the resolution of a racemic mixture in which the desired enantiomer is transformed into the product, the unconverted, undesired enantiomer is racemised to a 1:1 mixture of both enantiomers which is subject to resolution again (Fig. 1.13).<sup>63</sup> Theoretically, an infinite number of cycles is needed for complete transformation of the racemate into the single stereoisomer of the product. Actually the yield of the product can reach above 96% after only 5 cycles and > 99% after 7 cycles, assuming complete racemisation occurs in each cycle and no loss of starting material or products. Some commonly employed de-



racemisation methods in synthesising enantiopure amines utilising repeated resolution and re-racemisation will be discussed below.

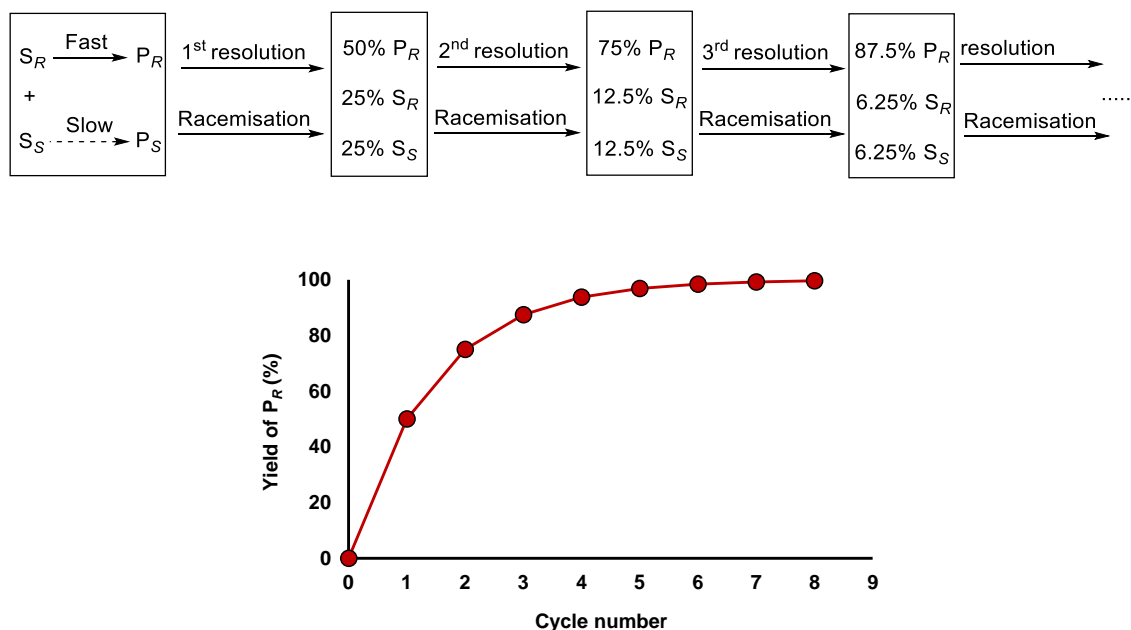


Fig. 1.13 Overall yield of product after repeated resolution and re-racemisation

#### 1.4.1. Dynamic Kinetic Resolution (DKR)

Kinetic resolution is based on the different reaction rates of two enantiomers in forming the products by chiral catalyst. In order to achieve high enantiopurity, KR are often stopped before the conversion reaches 50%, further lowering the productivity of the process.<sup>63, 99</sup> To circumvent this, KR is combined with *in-situ* racemisation of the slower-reacting enantiomer in one single operation which is known as dynamic (kinetic) resolution (DKR) (Fig. 1.14(a)).

For a successful DKR, the rate differences of the enantioselective process of  $R$ - and  $S$ -enantiomers of the substrates need to be large enough, i.e.  $k_R \gg k_S$ . This indicates a highly selective kinetic resolution process. The  $E$  value is typically  $\geq 20$ . In addition, the rate of racemisation must be higher (or at least equal) to the rate of the faster-reacting enantiomer, i.e.  $k_{rac} \geq k_R$ . This ensures that the racemisation step is fast enough to replenish the reacted  $S_R$  and therefore  $S_S$  is not in excess at any time, allowing the enantioselective reagent to react solely with  $S_R$ . Unlike a kinetic resolution where the ee of the product reaches its maximum at the start of the reaction and then declines when the faster-reacting enantiomer starts to deplete, this depletion does not occur in a DKR process and

ee of the product is no longer a function of the conversion, but remains constant throughout (Fig. 1.14(b)).

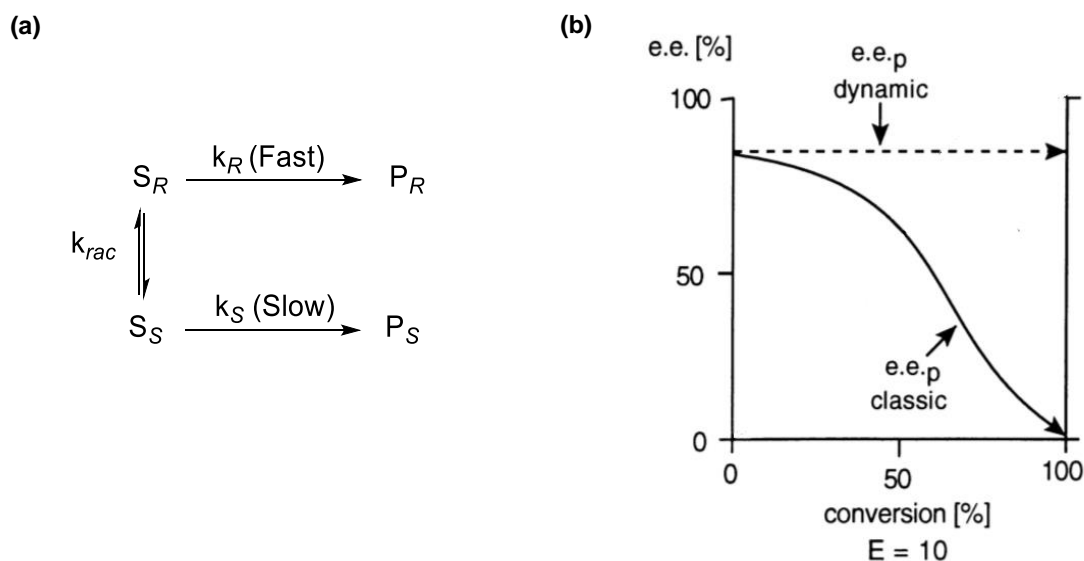
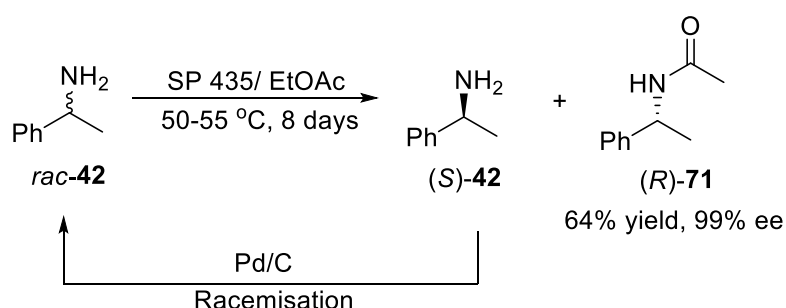


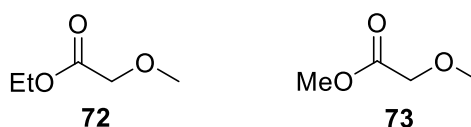
Fig. 1.14 DKR of a racemate. (a) Dynamic equilibration of  $S_R$  and  $S_S$ ;  $k_R$  and  $k_S$  are the rate constants of the enantioselective processes;  $k_{rac}$  is the racemisation rate constant. (b) Comparison of ee profiles of the product ( $P_R$ ) in DKR and KR<sup>63</sup>

Enzymes are very commonly used in DKR due to their high stereoselectivity. The first DKR process in the synthesis of chiral amine was reported by Reetz et al. in 1996.<sup>1, 100</sup> Racemic **42** (1 mmol scale) was resolved by lipase *Candida antarctica* (NOVOZYM SP435®) via enantioselective *N*-acylation with ethyl acetate as the acyl donor. The undesired (*S*)-**42** was recycled using Pd/ C. Enantiopure (*R*)-*N*-acetyl-*N*-methyl- $\alpha$ -methylbenzylamine **71** was produced in 99% ee and 64% yield after 8 days (Scheme 1.27).

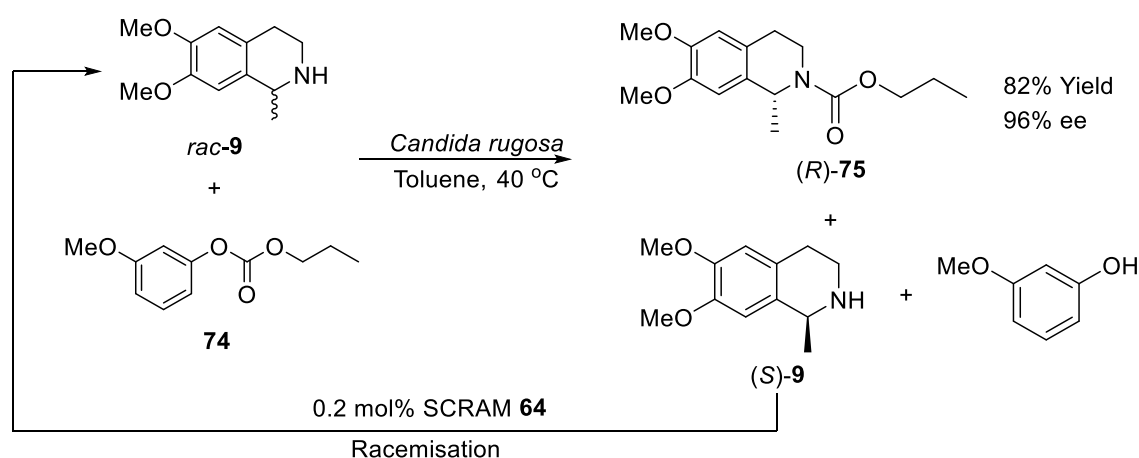


Scheme 1.27 DKR of *rac*-**42**

Bäckvall et al. had reported the DKR of *rac*-**42** in larger scales using alkyl methoxyacetates **72** and **73** as alternative acyl donors, *Candida antarctica* lipase B (CALB) as the enzyme for the KR and Shvo's catalyst derivative **57** (1.25 mol%) as the racemisation catalyst in the presence of alcohol **58** as the hydrogen donor. Possibly due to the higher thermal stability of the enzyme, a higher temperature (100 °C) was used. Acylated (*R*)-**42** was produced in 90% yield with 97% ee (10 mmol scale) and 83% yield with 98% ee (45 mmol scale) by using **72** and **73** as the acyl donor respectively after 72 hours.<sup>101</sup> Bäckvall also reported the DKR processes of a wide range of aliphatic and benzylic primary amines using **55** and **57** as the racemisation catalysts and isopropyl acetate as the acyl donor, achieving  $\geq 70\%$  yield and  $\geq 93\%$  ee of the amide.<sup>102</sup>



The formation of amides from the resolution often require harsh conditions to hydrolyse in order to recover the enantiopure amine.<sup>103</sup> This limits the application of DKR on substrates with sensitive functional groups. Blacker et al. reported the DKR of *rac*-**9** by using 3-methoxyphenyl propyl carbonate **74** as the acyl donor and SCRAM **64** (0.2 mol%) as the racemisation catalyst on a cyclic secondary amine **9**. The process was carried out on a 3 g scale and 82% yield of (*R*)-**75** in 96% ee was achieved after 23 hours (Scheme 1.28).<sup>1, 2</sup>



Scheme 1.28 DKR of *rac*-**9** using acyl donor **74**

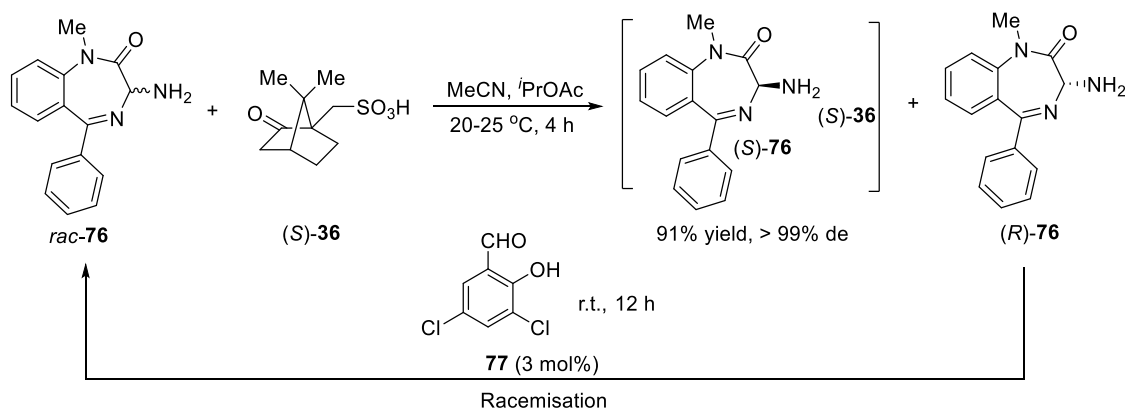
Ideally both resolution and racemisation in a DKR process should be performed under the same conditions. However, racemisation usually requires relatively harsh conditions such as high temperature which may not be compatible with the enzyme used in the resolution step, although some enzymes are still stable at elevated temperature such as CALB, which is the lipase enzyme used in the resolution of *rac*-**42** and other primary amines as demonstrated by Bäckvall. Compromise is often needed between the racemisation and resolution. Being able to carry out the racemisation reaction under mild conditions is beneficial for a successful and efficient DKR.

#### 1.4.2. Crystallisation-Induced Diastereomeric Transformation (CIDT)

Although enzymatic DKR has been widely used in the synthesis of enantiomerically pure amines, restrictions on the reaction conditions that can be employed due to its limited stability remain the major problems, as discussed in Section 1.2.2(b). Therefore in practice, there is still a significant barrier to widespread adoption of enzymatic DKR. On the other hand, diastereomeric crystallisation is easy to operate, can be highly stereoselective and economical, and direct isolation of the desired product in preference to other by-products in the reaction by filtration means that product purification is relatively simple and straightforward.<sup>99, 104</sup> When a racemic mixture of a chiral amine reacts with an enantiopure chiral acid, a pair of diastereomeric salts is formed which can be separated by crystallisation due to their different solubility. Once-through yields of > 50% are feasible if the uncrystallised, undesired diastereomeric salt in the ML undergoes catalysed or spontaneous racemisation. This is known as crystallisation-induced diastereomeric crystallisation (CIDT) or crystallisation-induced dynamic resolution (CIDR). Unlike DKR which depends on different rates of the enantioselective process of two enantiomers, CIDT is thermodynamically controlled. It can also be referred to as dynamic thermodynamic resolution (DTR).<sup>78</sup>

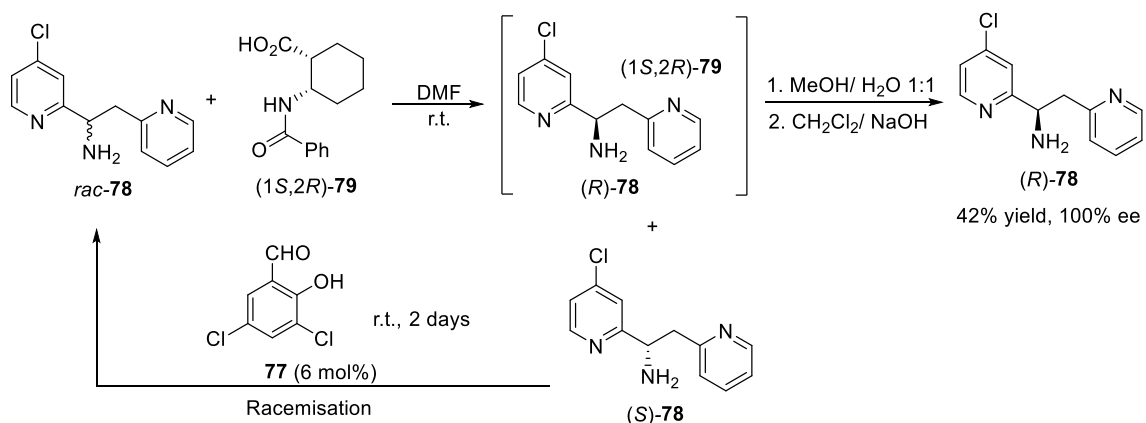
Merck reported the synthesis of a potent antagonist of the gastrointestinal hormone cholecystokin (CCK) which involved diastereomeric resolution of racemic aminodiazepinone **76** by (1*S*)-(+)-10-camphorsulfonic acid **36**.<sup>105</sup> The less soluble (*S*)-**76**-(*S*)-**36** was crystallised in 91% yield and 99.5% de. The undesired (*R*)-**76** was racemised using catalytic amount of 3,5-

dichlorosalicylaldehyde **77** (Scheme 1.29). A Schiff base was formed between (*R*)-**76** and **77** *in-situ* which has a low pK<sub>a</sub> proton at the chiral centre of **76** and is able to undergo racemisation at ambient temperature *via* a similar mechanism shown in Scheme 1.18.



Scheme 1.29 CIDT process for the synthesis of enantiopure (*S*)-**76** using (*S*)-**36** as the resolving chiral acid and aldehyde **77** as the racemisation catalyst

A similar process was reported by Negi et al. in the synthesis of (*2R*)-1-(4-chloro-2-pyridyl)-2-(2-pyridyl)ethylamine **78**, a key intermediate for their target compounds in the field of cardiovascular therapy.<sup>106</sup> Enantiopure chiral acid **79** was used to resolve *rac*-**78**, whilst **77** (6 mol%) was used to racemise the undesired (*S*)-**78** in the ML (Scheme 1.30). Enantiopure (*R*)-**78** was obtained in 42% yield after three recrystallisation of (*R*)-**78**-(*1S,2R*)-**79** and subsequent acid-base extraction by sodium hydroxide solution, which is higher than the yield achieved in the classical resolution (29%) by more than 10%.



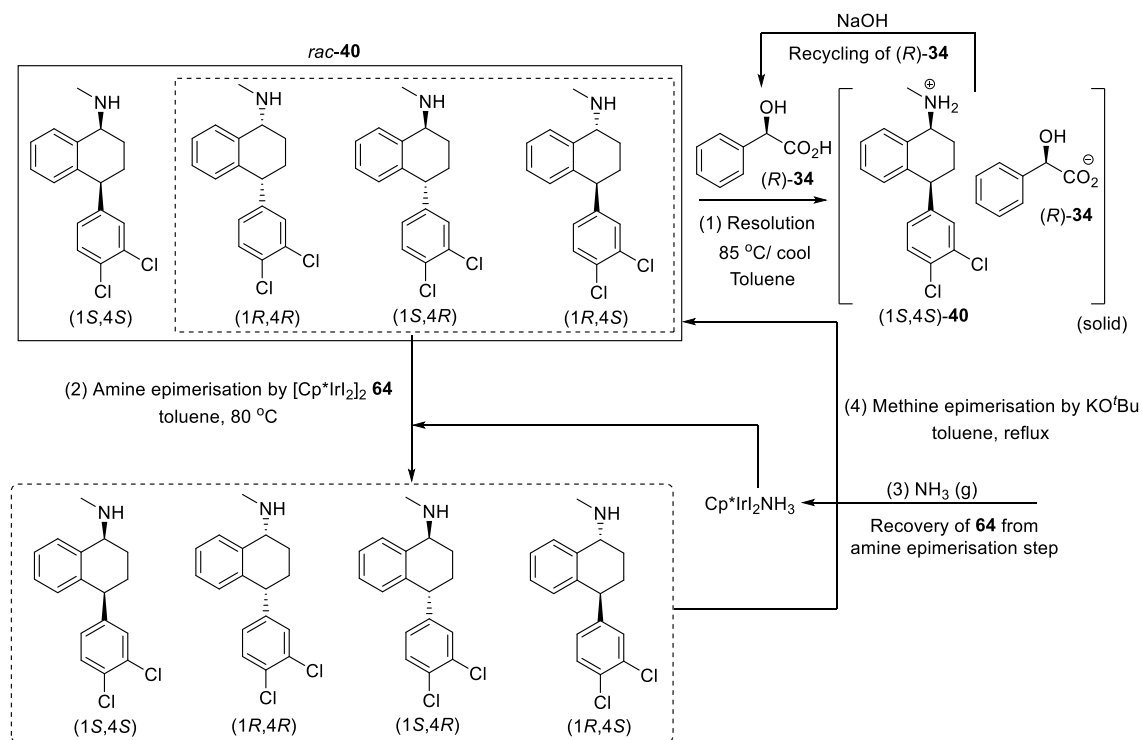
Scheme 1.30 CIDT process for the synthesis of enantiopure (*R*)-**78** using (*1S,2R*)-**79** as the resolving chiral acid and aldehyde **77** as the racemisation catalyst

### 1.4.3. The Viedma ripening technique

Racemic compounds which can crystallise as conglomerates and spontaneously racemise in solution can be transformed into enantiopure state *via* crystallisation-induced enantiomeric transformation (CIET) or crystallisation-induced asymmetric transformation (CIAT). It is also called total spontaneous resolution.<sup>78</sup> Viedma et al. used sodium chlorate, which forms chiral crystals whilst being intrinsically achiral in solution, to demonstrate the emergence of solid state homochirality by intensively grinding a supersaturated solution of sodium chlorate containing crystals of both chiral forms using glass beads.<sup>107, 108</sup> The technique is known as Viedma ripening. Noorduin et al. extended Viedma ripening to intrinsically chiral molecules such as imine **80**, which racemises readily in solution in the presence of a strong base such as 1,8-Diazabicyclo[5.4.0]undec-7-ene (DBU) (Scheme 1.31).<sup>109</sup> Upon crystallisation of one of the enantiomers (which is in small excess at the beginning of the process), the ML is enriched with the enantiomer opposite to the one enriched in the solid phase and is racemised to produce more of the enantiomer which is enriched in the solid phase. The attrition by glass beads continuously break down the crystals into smaller fragments which dissolve and grow onto larger crystals of the same handedness.<sup>7</sup> Complete de-racemisation is eventually observed. Unlike diastereomeric resolution, no chiral acids are required for resolving conglomerates and therefore no subsequent free-basing procedures and recycling of resolving agents are needed.<sup>78</sup> However the scope of Viedma ripening is still limited since conglomerate-forming crystalline chiral compound is required which only accounts for < 10% of all crystalline racemates. Although various amino acid derivatives and some other pharmaceutically-relevant compounds such as Naproxen and Clopidogrel intermediate can undergo this attrition-induced de-racemisation,<sup>110-112</sup> the process has not been employed on industrial scale.<sup>7</sup>



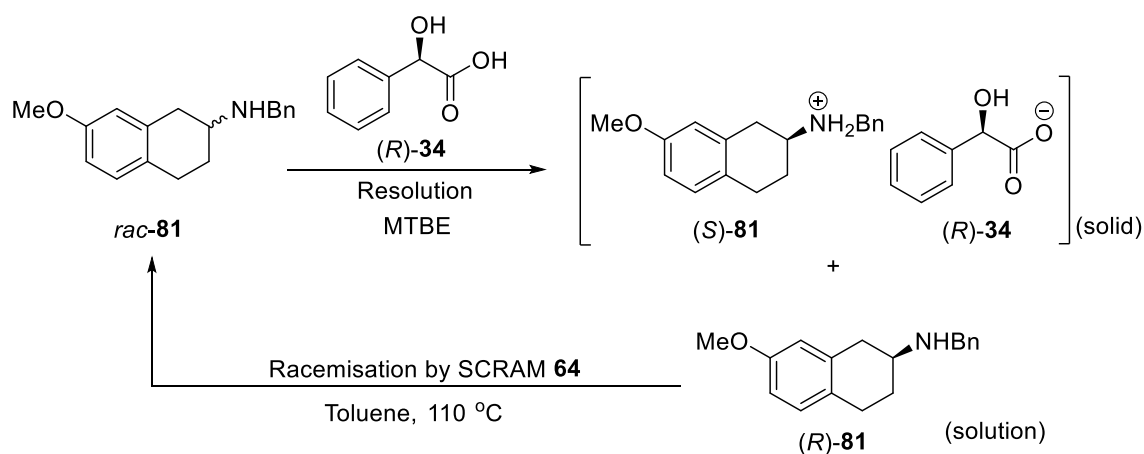
Blacker et al. reported the synthesis of Sertraline **40**, the active pharmaceutical ingredient (API) of an anti-depressant Zoloft from Pfizer, by diastereomeric resolution and waste isomer racemisation.<sup>43</sup> The process started with the resolution of racemic sertraline diastereomers using (*R*)-mandelic acid **34** in which (*R*)-**34** salt of (1*S*,4*S*)-**40** was selectively crystallised and was filtered. (*R*)-**34** was recycled by treating the crystals with sodium hydroxide and was further processed into the hydrochloric acid salt of (1*S*,4*S*)-**40**. The ML containing the waste isomers was free-based and fresh *rac*-**40** was charged. 1-(*N*-methyl)amino chiral centre of **40** was epimerised by SCRAM **64** (0.1 mol%). The catalyst was partially recovered by bubbling gaseous ammonia into the system to form an insoluble ammonio complex which was added back into the reaction mixture in the next cycle. The benzylic chiral centre was epimerised by potassium *tert*-butoxide and the racemised reaction mixture was subjected to resolution again (Scheme 1.32). Toluene was used as the single solvent throughout the process. The process was carried out on 260 g scale of *rac*-**40** and diastereopure enriched crystals of (1*S*,4*S*)-**40**-(*R*)-**34** were obtained in 80 to 98% yield (based on the equivalence of **34** added) with  $\geq 92\%$  de in each cycle.



Scheme 1.32 A simplified scheme showing the semi-continuous resolution-racemisation process for the synthesis of Sertraline **40**



In an unpublished work by the Blacker group, a similar procedure was employed in synthesising (*S*)-7-methoxy-1,2,3,4-tetrahydronaphthalen-2-amine **81**, which is a key fragment in a  $\beta$ -adrenoreceptor antagonist drug candidate from Sanofi-Aventis.<sup>78</sup> The resolution of *rac*-**81** was carried out using (*R*)-**34** (0.5 equiv.) in *tert*-butyl methyl ether. The crystalline products were filtered and the ML containing the undesired (*R*)-**81** was free-based and racemised with SCRAM **64** (0.3 mol%) at 110 °C in the same solvent (Scheme 1.33). The catalyst was precipitated, filtered, screened and reused. An overall yield of 49% was achieved over four cycles without optimisation (based on the amount of *rac*-**81** added) which was higher than the single-step resolution (30%). The ee of (*S*)-**81** from each cycle was about 80 to 90%.



Scheme 1.33 Resolution-racemisation approach in the synthesis of (*S*)-**81**

The two examples demonstrated above required only one single solvent and so avoiding the need of solvent-swap. However it is not uncommon that racemisation and crystallisation require different solvents. Although the used catalyst **64** could be precipitated from the reaction, removed, and recycled, its recyclability was unlikely to be high and complete removal of residual metal from the reaction was difficult to achieve. As discussed earlier, it is highly desirable to separate resolution and racemisation. However it is possible to link them together to generate a continuous process.<sup>78</sup> The concept of designing a crystallisation-based resolution process with continuous recirculation of ML over a heterogeneous racemisation catalyst was first speculated by Sheldon and it will be the main focus of this work.<sup>9</sup>

## 1.5. Continuous processing

### 1.5.1. Flow reactors

Attempts to reduce the number of intermediate isolation and purifications, the need for automation and efficient scale up of synthetic processes has driven industries to develop continuous flow techniques. Different types of flow reactors have been developed recently to accommodate different reaction types.

One of the most simple and commonly used continuous flow reactor is the tubular reactor consisting of a stainless steel tube, which can be heated by aluminium heating block or thermostatic bath, with one or more feeds at the inlet where the reagents are pumped through the tube using a suitable pump. If more than one reagent feeds are used, the feeds and the stainless steel tube are linked by a T-mixer to ensure the reagents are mixed before the reaction starts. The product was collected at the other end of the tube (Fig. 1.15).<sup>113</sup> The tube can be packed with solid-supported reagent or catalyst which enables them to be recycled more easily.

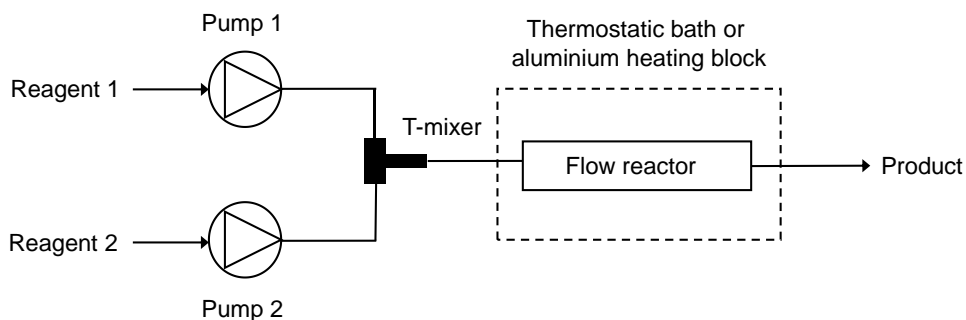


Fig. 1.15 Schematic of a continuous flow tubular reactor system

For multiphasic reactions, no or improper mixing of reagents in ordinary tubular reactors resulted in segmented or density-separated flows (Fig. 1.16).<sup>114</sup> This can be overcome by using tubular reactors with built-in static mixer. However they require high flow rates and are not suitable for solid-forming reactions.



Fig. 1.16 Improper mixing of biphasic reaction in tubular reactors. (a) Segmented flow; (b) density-separated flow

Multiphase reactions in flow involving slurries can be accommodated using cascade continuous stirred tank reactors (CSTRs).<sup>114</sup> With increasing number of CSTRs connected, the system tends to perform as a well-mixed plug-flow reactor.<sup>115</sup> However the conventional cascade CSTRs are often complex, expensive and oversized, which is not suitable for small scale reactions (Fig. 1.17).<sup>116</sup>

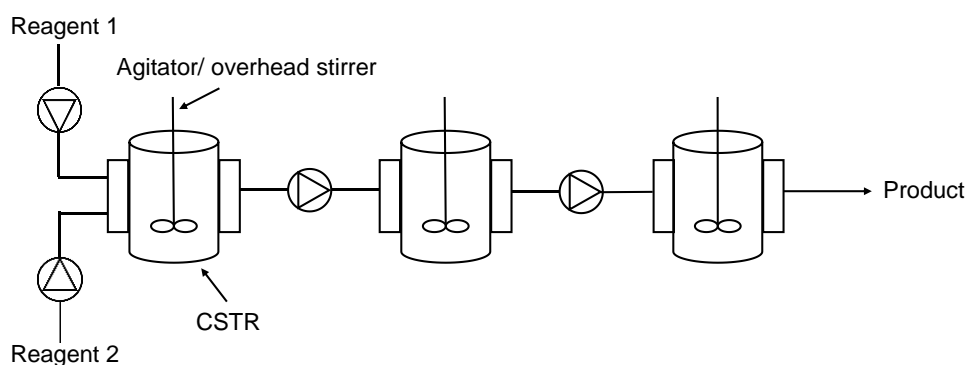


*Fig. 1.17 Schematic for a conventional cascade CSTR*

Solid-forming reactions such as crystallisations have been reported using continuous oscillatory baffled crystalliser (COBC) which was shown to provide high fluid mixing. The reactor consists of a glass tube with periodically spaced baffles perpendicular to the flow of the fluid that is oscillated using a diaphragm with movement generated by a motor placed at one end of the reactor (Fig. 1.18).<sup>115, 117, 118</sup> The interaction between the flow and the baffles leads to the generation and cessation of eddies which create vigorous axial and radial motion of the fluid in each inter-baffle zone, which can be considered as a perfectly mixed CSTR and hence the entire reactor behaves as a large number of CSTRs in series that exhibit plug-flow characteristics.<sup>119</sup> However, the size of the reactor is relatively large (litre scale) with complicated construction which may not be suitable for lab-scale flow reactions.

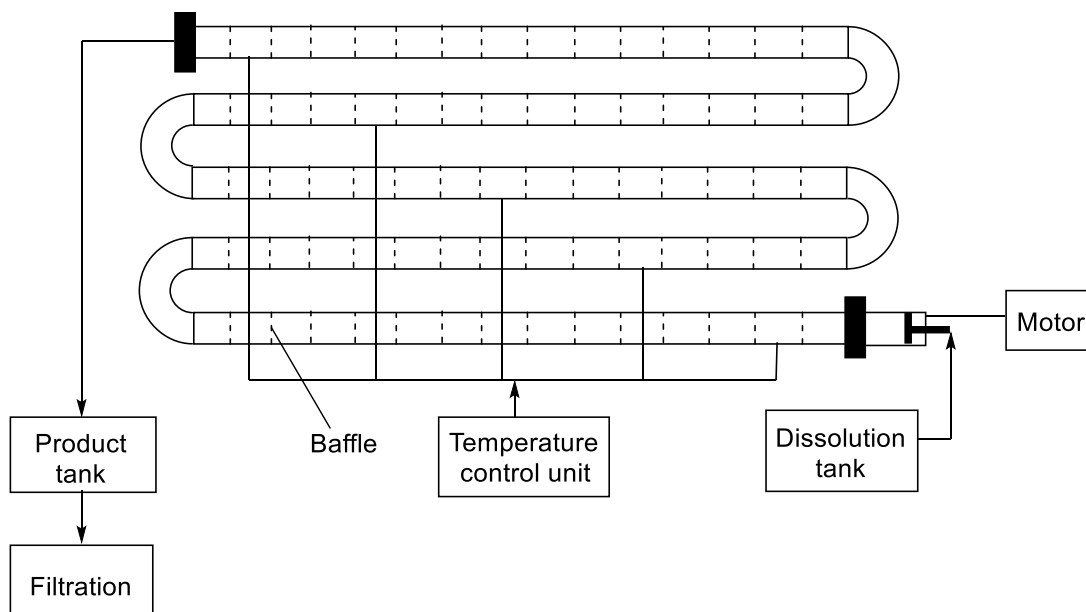


Fig. 1.18 Schematic for a continuous oscillatory baffled crystalliser (COBC)

AMTech had developed the Coflore<sup>®</sup> reactors, which are multistage CSTRs consisting of a series of loose-fitting polymer inserts that provide mixing when the entire reactor was shaken. Different configurations are available which allow reactions of different scales to be carried out (Fig. 1.19).<sup>120</sup>

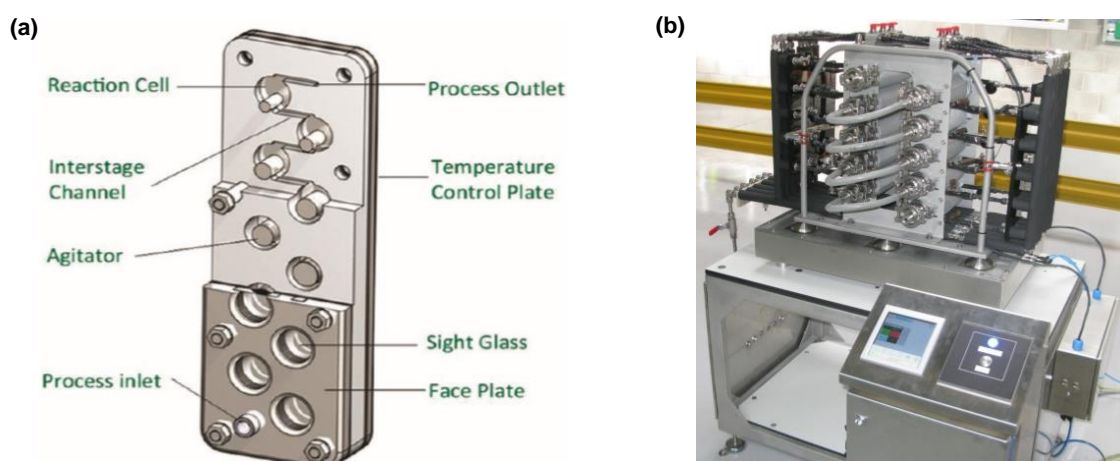


Fig. 1.19 Coflore<sup>®</sup> reactors from AMTech. (a) Schematic for the Agitated Cell Reactor (ACR) with capacities from 10 to 100 mL, reaction times from 10 s to 10 h; (b) Agitator Tube Reactor (ATR) with capacities from 1 to 10 L, reaction times from 10 s to > 10 h (The photo was provided by AMTech)

In addition to the Coflore<sup>®</sup>, Blacker et al. reported a miniaturised cascade CSTR (the 'Freactor') with relatively inexpensive and simple design (Fig. 1.20). Each CSTR has a volume of about 2 mL and therefore, much less materials are

required. They are connected using PTFE ferrules and tubing and are placed onto a stirrer motor or a hot plate.<sup>114</sup> The stirrer bar in each Freactor allows the content to be mixed. A similar design was reported by Jensen et al.<sup>121</sup> Reactions with residence times ( $t_{Res}$ ) ranging from two minutes to three hours were tested and can be used for multiphase reactions involving gas, liquid and solid.<sup>114</sup>

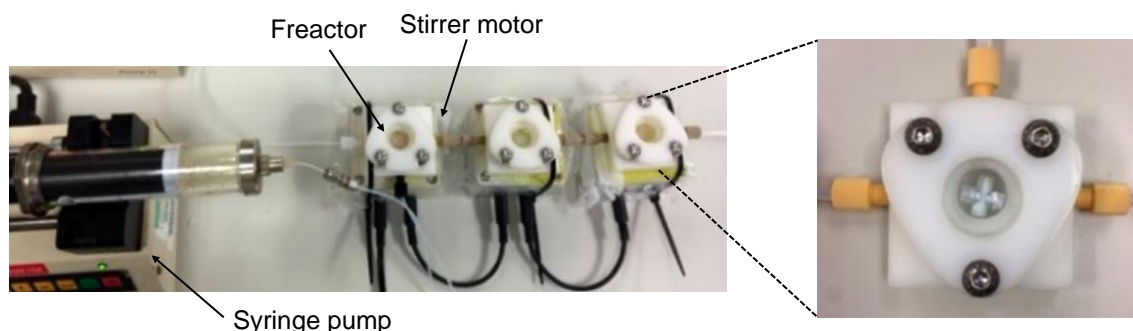


Fig. 1.20 A three-stage Freactor system developed by Blacker et al.

### 1.5.2. Merits and limitations of flow

Carrying out chemical transformations in flow at lab and/ or industrial scales have attracted much interest in recent years. One of the major advantages of using flow reactors over batch ones is the better mixing and heat transfer due to their large surface area to volume ratio, which allows reactions to be carried out at high temperature, high pressure and increased concentrations.<sup>37, 122, 123</sup> Unlike a batch system, where the reaction is changing over time, steady-state can be achieved in flow, resulting in product consistency and minimised impurity accumulation. By assembling a line of reactors, multistep reactions can be performed with direct transfer of unstable intermediates, with no isolation or purification of materials between two steps.<sup>124</sup> Online and inline analysis tools can be integrated into the flow system, enabling process automation and optimisation.<sup>37, 125</sup> One of the other most important benefits in employing flow is the ease of recycling precious catalysts and reagents in the case of heterogeneous reactions with minimum manipulation.<sup>124</sup>

Despite the potential advantages and opportunities offered by using flow, there are problems and limitations which need to be encountered. In achieving steady-state, large amount of materials are often required and any products formed before the steady-state is reached may go into the waste stream.<sup>123</sup> Unlike a

batch process where various probing devices can be used to analyse the reactions *in-situ*, this is currently more difficult in flow reactors due to their small sizes. Technical problems such as leaks and blockages are sometimes observed, especially in multiphasic reactions which require more complicated engineering design of the reactors.

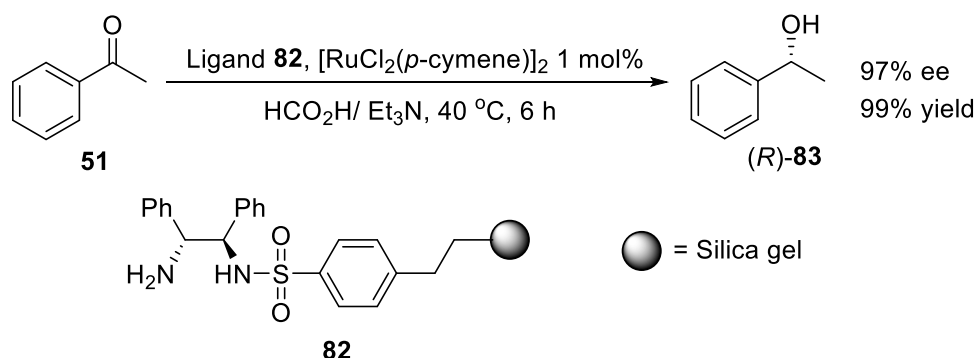
In this work, racemisation of chiral amines in flow will be studied and discussed in more detail in Chapter 2, which utilised a packed-bed reactor (PBR) with SCRAM catalyst **64** immobilised onto a solid support. The major driving force in using flow in racemisation reaction is the ease of recycling the expensive iridium catalyst and minimising product contamination. Besides, the PBR can be readily coupled with the batch crystallisation reactor to generate a continuous recycle process with minimum engineering required. In addition to racemisation, continuous crystallisation in flow was also attempted in the Freactors and will be briefly addressed in Chapter 3.

### 1.5.3. Catalyst immobilisation

In general, homogeneous metal-based catalysts can only be used once due to the difficulty in recovering them from the reaction mixture. Although the recovery of homogeneous SCRAM **64** during the resolution-racemisation process of Sertraline **40** had been made possible *via* the formation of an insoluble ammonio-iridium complex, which released the active catalytic species when it was heated,<sup>43</sup> the number of reuses is not likely to be high and rapid drop in catalytic activity can be readily observed in subsequent reactions. Difficulties in removing any residual metal from the products also raises much concern.<sup>38</sup> Covalent immobilisation of metal catalysts onto solid supports, such as silica and organic polymers, represents one of the best solutions to the above problems. An ideal immobilised catalyst should exhibit catalytic activity and selectivity comparable to its homogeneous counterpart, be easily recovered from the reaction mixture without metal leaching, and can be recycled in many runs without significant loss of activity and selectivity.<sup>36</sup> However reduced catalytic activity and enantioselectivity are often observed when homogeneous chiral catalysts are immobilised.<sup>4, 6, 29, 36, 126-128</sup> In heterogeneous catalysis, the substrate molecules need to diffuse through the porous structure of the supporting matrix in order to reach the active site of the catalyst, contributing to the reduced activity

observed.<sup>36, 129</sup> The geometry of the catalyst is crucial in directing the stereochemistry of the product. It can be unintentionally disturbed upon immobilisation through the interaction between the catalyst and the solid support, leading to reduced enantioselectivity.<sup>36</sup> Despite the plethora of work done to date, development of suitable immobilisation strategies for homogeneous metal catalysts remains a challenge.

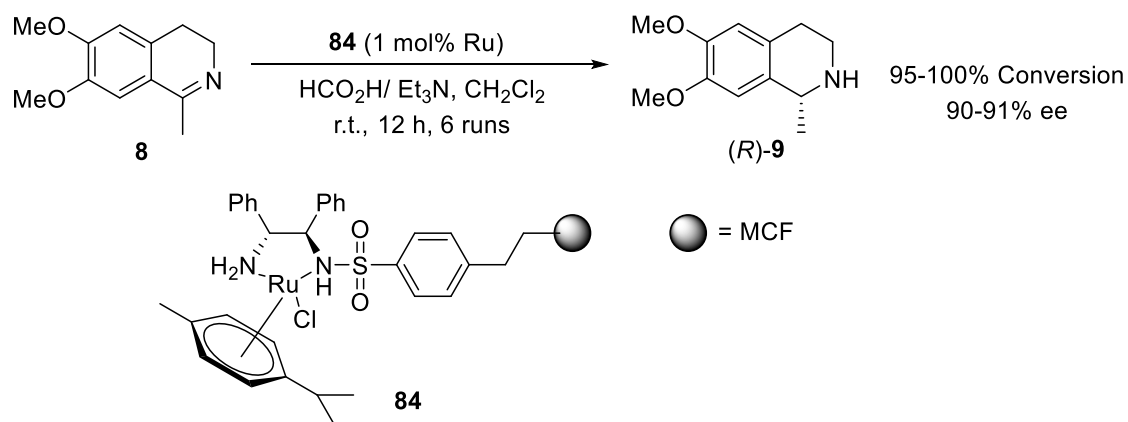
Ruthenium complexes with (*R,R*) or (*S,S*)-TsDPEN ligand reported by Noyori et al. are the most well-known catalysts employed in the ATH reactions of ketones and imines.<sup>28, 29, 130-132</sup> Their immobilisations have been widely studied to try and simplify their separation from the reaction mixture and allow efficient recovery and reuse of expensive and toxic catalysts.<sup>36, 38, 130, 132-134</sup> Liu et al. reported the immobilisation of TsDPEN ligand onto a silica support and the utilisation of the immobilised Ru-TsDPEN complex, which was formed *in-situ*, in the ATH of acetophenone **51** in formic acid/ trimethylamine mixture (Scheme 1.34).<sup>133</sup> (*R*)-1-phenylethanol **83** was synthesised in 99% yield at 97% ee after 6 hours and Ru-**82** could be reused up to 5 times with the enantioselectivity maintained, and only a slight drop in yield, although the reaction time was much longer (94% in 44 hours in run 5).



Scheme 1.34 ATH of **51** using silica-supported Ru-TsDPEN complex

Ying et al. reported the immobilisation of Ru-TsDPEN onto siliceous mesocellular foam (MCF).<sup>132</sup> The main advantage of MCF is its uniform and ultralarge pore size (20 to 50 nm) which allows the immobilisation of large catalytic complexes within the pores without steric hindrance, and can facilitate mass transfer of the substrates. The MCF-supported Ru-TsDPEN catalyst **84** successfully reduced imine **8** to amine **9** and had been recycled for 6 runs, achieving 95 to 100%

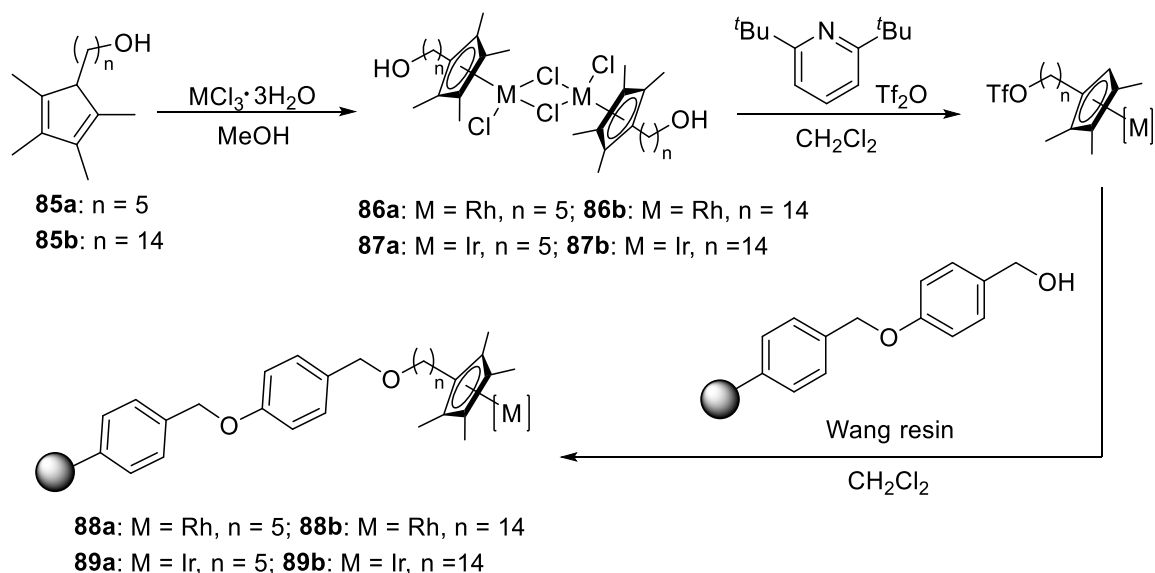
conversion and 90 to 91% ee (Scheme 1.35). It was found that 2 to 5 ppm of ruthenium was leached into the reaction after each run. Elemental analysis showed a total of 17% loss of ruthenium and 7% loss of ligand after 6 runs.



Scheme 1.35 ATH of imine **8** using MCF-supported Ru-TsDPEN catalyst

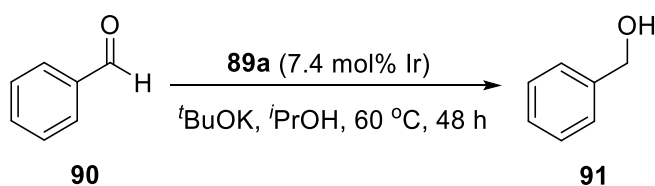
Catalyst recyclability is one of the major driving forces in the development of immobilised catalysts. From the examples discussed above, catalyst recycling studies have been reported but they all showed a decline in catalytic activity in about 3 to 10 runs. ICP analysis showed a loss of ruthenium into the solution phase. This is likely due to the immobilisation *via* bidentate TsDPEN ligand. The resulting coordination between the metal and ligand are not strong enough, causing the metal to leach from the catalyst matrices. Blacker et al. reported the immobilisation of a series of hydroxyl-tethered Cp\*-iridium/ rhodium dichloride complexes onto Wang resin *via* the  $\eta^5$ -Cp\* ligand **85** (Scheme 1.36).<sup>38</sup> This allows a stronger coordination of the metal to the ligand and the support, minimising the problem of leaching and hence increasing the potential for recycling.





Scheme 1.36 Immobilisation of hydroxyl-tethered dimers **86a**, **86b**, **87a** and **87b** onto a Wang resin

Immobilised catalyst **88** and **89** were tested against the transfer hydrogenation of benzaldehyde **90** to benzyl alcohol **91**, and **89a** was found to be the most active catalyst and showed the highest recyclability, achieving 98% conversion in 24 hours at 60 °C when fresh and > 87% conversion in the first 15 runs (Scheme 1.37). From 16 to 26 runs, the activity of **89a** decreased gradually (80% conversion after 48 hours in run 26). ICP analysis of recovered resin showed minimal leaching of iridium from the immobilised catalyst. The observed decrease in the catalytic activity might possibly due to catalyst decomposition and/ or loss of resin in the decantation step.



Scheme 1.37 Benzaldehyde reduction by **89a**

In batch, the immobilised catalysts can be isolated from the reaction by filtration or decantation. However, this can result in physical losses of the catalysts, hence the productivity in the subsequent reactions may gradually decrease. The recycling of catalysts can be made easier by carrying out the reaction in flow. The insoluble catalyst remains in the reactor when the reaction mixture is pumped through. The catalyst can be readily washed by flushing solvent across and new

reagents/ substrates can then be pumped through the catalyst again. The reported success of homogeneous Shvo's catalyst **55** and SCRAM **64** in the racemisation of amines indicates the potential of using their immobilised versions in flow.

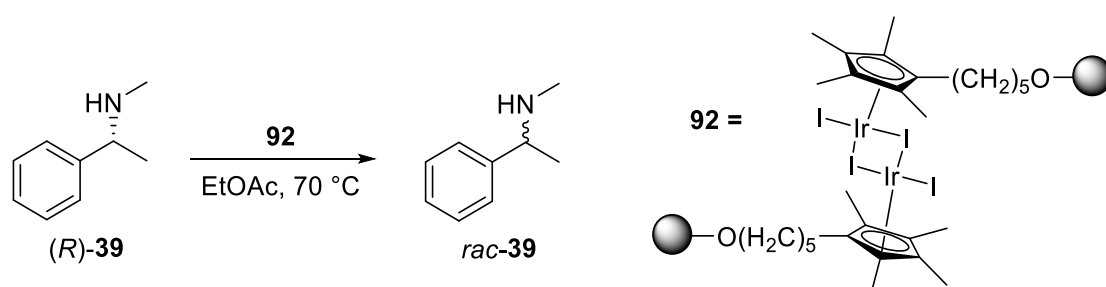
## 1.6. Research objectives

The aim of this research is to develop a novel process in synthesising enantiopure chiral amines which couples diastereomeric crystallisation in batch with racemisation of the ML in flow to yield a continuous resolution-racemisation-recycle ( $R^3$ ) process. Various primary, secondary and tertiary chiral amines were chosen and tested in the  $R^3$  system. Racemisation of the amines in batch and flow using homogeneous and immobilised SCRAM catalysts respectively were first studied in Chapter 2 to better understand the kinetics and mechanism of the racemisation reaction, as well as the deactivation mechanism of the catalyst. A novel and rapid method based on proton/ deuterium exchange was developed to determine the racemisation of chiral amines under a particular set of reaction conditions using  $^1\text{H}$  NMR spectroscopy, which avoided the need of enantio-enriched material and the development of chiral analytical methods. In Chapter 3, diastereomeric resolution of the chosen amine substrates with enantiomerically pure acids (*S*)-mandelic acid and di-*p*-toluoyl-*D*-tartaric acid were investigated and combined with the racemisation of the ML in flow. The two steps operated in separate reactors but were linked *via* external tubing. The batch resolution and the  $R^3$  process for each substrate were compared to understand the merits and limitations of the  $R^3$  process. Due to the high cost of iridium, and other commonly employed transition metals in the racemisation of chiral amines, a series of copper- and iron-based metal salts and complexes were screened and tested against racemisation reaction in order to search for cheaper alternatives of racemisation catalysts, which will be discussed in Chapter 4.

## 2. Racemisation of chiral amines

### 2.1 Introduction

Recycling of the undesired enantiomer in a resolution by racemisation and recirculation of the racemised material can increase the yield and efficiency of the resolution process. One of the racemisation strategies of chiral amines is the reversible transformation between amine and imine *via* oxidation-reduction reactions using transition metal catalysts such as palladium, ruthenium and iridium.<sup>1, 90-92, 95</sup> The use of SCRAM catalyst **64** has been widely studied and its application in the diastereomeric transformation to enantiomerically pure amine has also been demonstrated.<sup>43</sup> Homogeneous SCRAM catalyst **64** and its chloro-analogue **63** have previously been immobilised onto a Wang resin support.<sup>38, 43, 135</sup> In an unpublished work, the supported SCRAM catalyst **92** was employed by J. Breen to improve its recyclability and reusability in the racemisation of (*R*)-**39** in batch (Scheme 2.1). Although the catalyst could be reused, its activity dropped significantly after the first run (Fig. 2.1).



Scheme 2.1 Racemisation of (*R*)-**39** using immobilised SCRAM **92** in batch

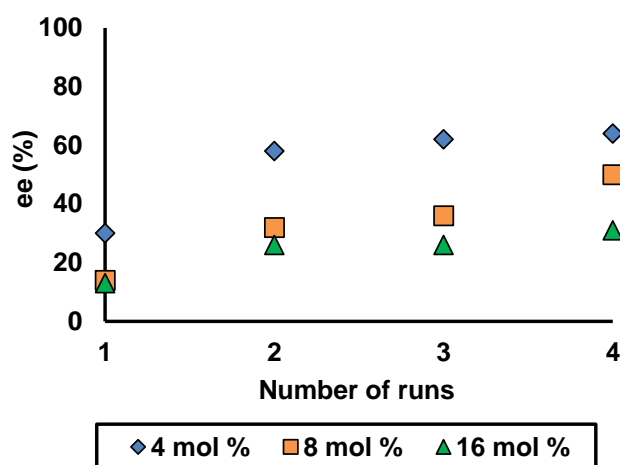


Fig. 2.1 ee of **39** from four consecutive racemisation reactions using the same catalyst **92** in batch, with 4 to 16 mol% Ir loading. Data was provided by J. Breen

Immobilisation of SCRAM **64** allows the catalyst to be used in flow and can be recycled much more easily without frequent manipulation. The racemisation of (*R*)-**39** was carried out in flow with an average drop of 9% ee after one pass through the reactor and the catalyst was used for 25 runs with minimum loss in activity (Fig. 2.2).

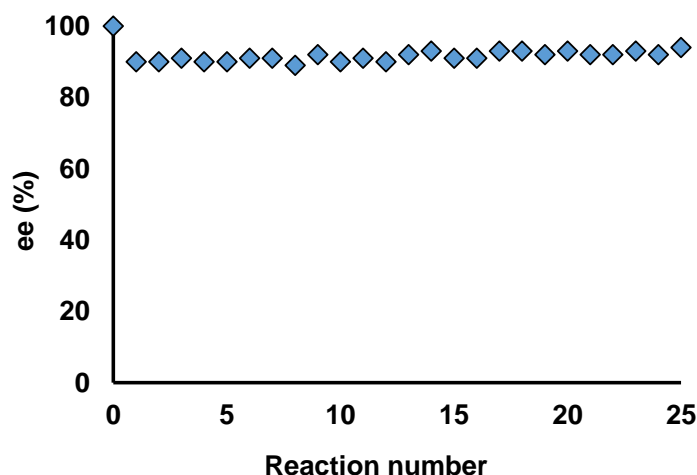


Fig. 2.2 Racemisation of (*R*)-**39** in continuous flow using immobilised SCRAM catalyst **92** (10 mol%) in EtOAc. [**39**] = 74 mM,  $t_{Res}$  = 7.5 min,  $T$  = 75 °C. The same catalyst was used for 25 reactions. Data was provided by J. Breen

The aim of this work was to further investigate the racemisation of various different chiral amines using homogeneous SCRAM **64** and immobilised SCRAM **92** in batch and flow respectively to obtain suitable racemisation conditions that could be used to couple with the diastereomeric crystallisation process (Chapter 3). Kinetic and mechanistic studies will be carried out to better understand the limitation and deactivation pathways of the catalyst.

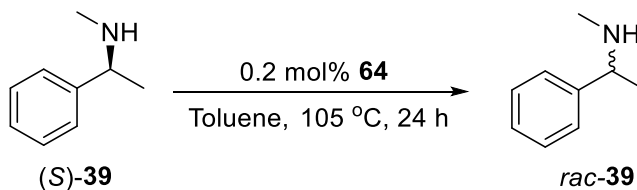
## 2.2 Racemisation in batch

### 2.2.1 *N*-Methyl- $\alpha$ -methylbenzylamine **39**

#### (a) Kinetics

Racemisation of *N*-methyl- $\alpha$ -methylbenzylamine **39** was previously reported by Blacker et al. using 1 mol% homogeneous SCRAM **64** in toluene, with a half-life of 45 minutes at 80 °C.<sup>1</sup> To gain a better understanding of the reaction, it was carried out at various concentrations from 0.1 to 2 M. The catalyst loading was lowered to 0.2 mol% whilst the temperature was increased to 105 °C (Scheme

2.2, Fig. 2.3). The ee of **39** was monitored by chiral GC, after derivatisation with trifluoroacetic anhydride.



Scheme 2.2 Racemisation of *(S)*-**39** with SCRAM **64** (0.2 mol%) in toluene at 105 °C

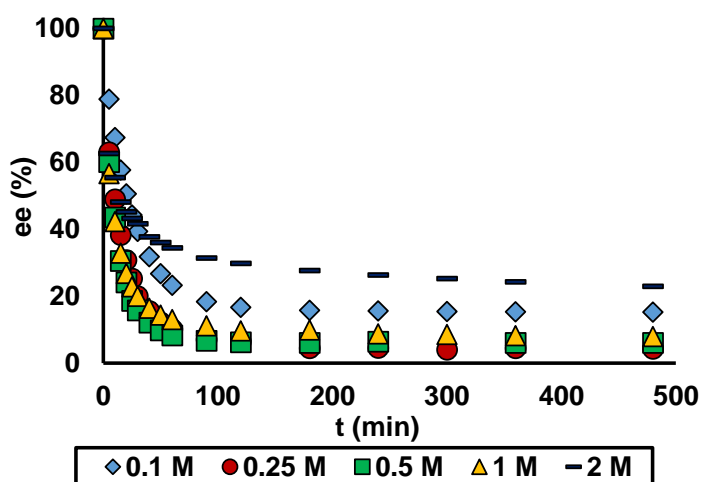
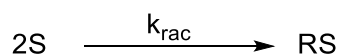


Fig. 2.3 Profiles of ee for the racemisation of *(S)*-**39** at various concentrations with **64** (0.2 mol%) in toluene at 105 °C. Only the data for  $t = 0$  to 480 min was shown

Racemisation can be described as the formation of a scalemic mixture from an optically enriched one which follows first-order kinetics (Eqn. 2.1).<sup>79</sup>



$$\ln \left( \frac{[S]_0}{[S]_t} \right) = k_{\text{rac}} t \quad (\text{Eqn. 2.1})$$

Where  $[S]_0$  and  $[S]_t$  is the concentration of *(S)*-**39** at time = 0, and  $[S]_t$  is the concentration of *(S)*-**39** in the system at time  $t$  excluding that in the RS complex and was calculated based on the ee of the system (Eqn. 2.2);  $k_{\text{rac}}$  is the racemisation rate constant.

$$[S]_t = [S]_0 \times \left[ \frac{\left(50 + \frac{ee}{2}\right)}{100} \right] \quad (\text{Eqn. 2.2})$$

Since,

$$[S]_0 - [S]_t = 2[RS]_t \quad (\text{Eqn. 2.3})$$

$$[RS]_t = [R]_t \quad (\text{Eqn. 2.4})$$

Where  $[RS]_t$  and  $[R]_t$  are the concentration of the racemate and (*R*)-**39** at time  $t$  respectively, therefore by substituting Eqn. 2.3 and 2.4 into Eqn. 2.1,

$$\ln\left(\frac{[S]_0}{[S]_0 - 2[R]_t}\right) = k_{\text{rac}}t \quad (\text{Eqn. 2.5})$$

The value of  $k_{\text{rac}}$  was determined by plotting Eqn. 2.5 where  $k_{\text{rac}}$  is the slope of the graph, assuming that the total concentration of **39** remained constant and no conversion to any side products occurred (Fig. 2.4).

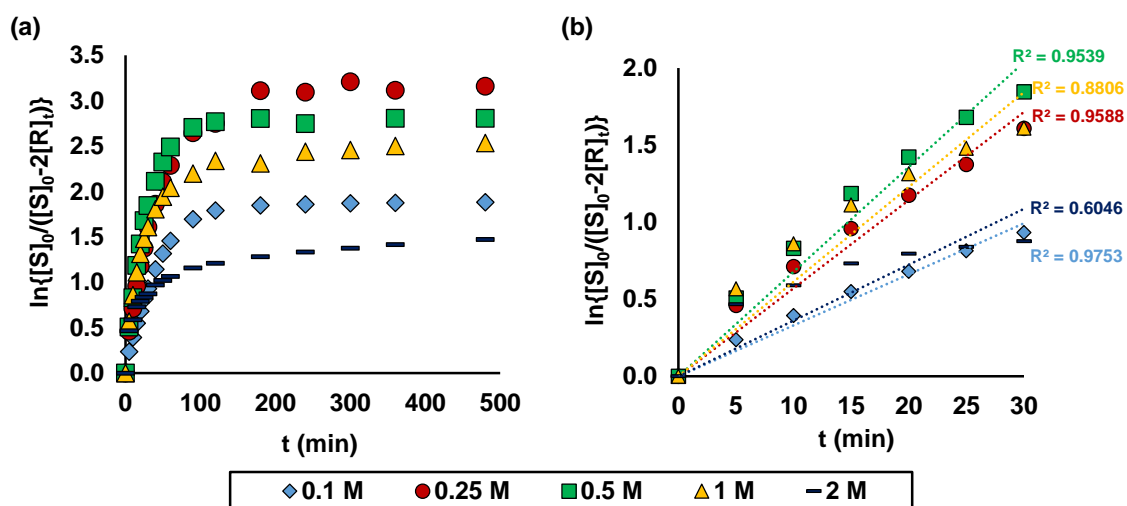


Fig. 2.4 Plots of  $\ln \{[S]_0/([S]_0 - 2[R]_t)\}$  against time for the racemisation of (*S*)-**39** by **64** (0.2 mol%) at various concentrations, assuming no conversion of **39**. (a)  $t = 0$  to 480 min. (b)  $t = 0$  to 30 min, showing the trend lines with the corresponding  $R^2$  values

To be noted is that the total amine concentration remains almost constant making the reaction zero order in the amine, but first order in the (*S*)-enantiomer. Initial racemisation rates were determined to allow comparison of the same catalyst

concentration (time = 0 and 5 minutes in this case). It was deduced from this and later data that in this reaction, the catalyst deactivation was occurring. The values are summarised in Table 2.1.

Entry	[(S)-39] (M)	$k_{rac}$ (min <sup>-1</sup> )	Calc. $t_{1/2}$ (min) <sup>[a]</sup>	Act. $t_{1/2}$ (min) <sup>[b]</sup>	ee (24 h) (%) <sup>[c]</sup>	51 (24 h) (%) <sup>[d]</sup>
1	0.1	0.047	15	20	14	0.5
2	0.25	0.092	8	10	4	0.4
3	0.5	0.102	7	5-10	6	0
4	1	0.114	6	5-10	7	0.6
5	2	0.094	7	15	14	1.8

Table 2.1 Rate constants, half-lives, ee of **39** and the amount of acetophenone **51** formed for the racemisation of (S)-**39** at various concentration with 0.2 mol% **64** at 105 °C in toluene. <sup>[a]</sup>Values calculated by Eqn. 2.6. <sup>[b]</sup>Values obtained from the ee profiles (Fig. 2.3). <sup>[c]</sup>ee was determined by chiral GC after derivatisation by trifluoroacetic anhydride. <sup>[d]</sup>Amount of **51** was determined by GC

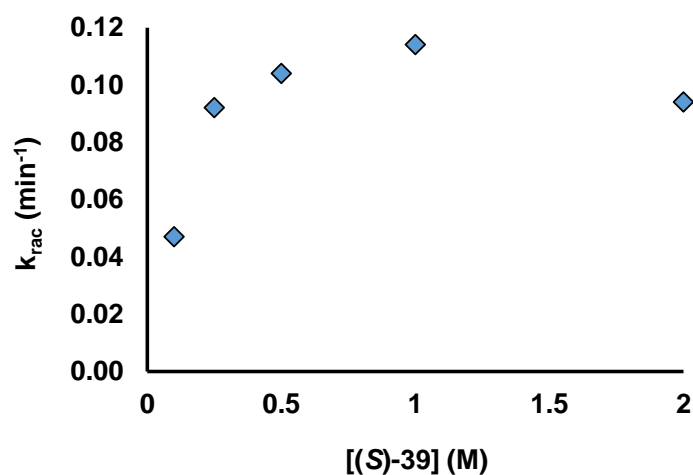


Fig. 2.5 Racemisation rate constants  $k_{rac}$  at different concentration of (S)-**39**

The initial rate increased with increasing concentration of **39** from 0.1 to 1 M. However the increase was not linear and slowed down after 0.25 M (Fig. 2.5). No further increase in the reaction rate was observed when the concentration of **39** increased to 2 M. Most of the kinetic plots of  $\ln \{[S]_t / ([S]_0 - 2[R]_t)\}$  against time remained linear for  $\leq 30$  minutes and then levelled off (Fig. 2.4(a)). A trend line was drawn through the data points from time 0 to 30 minutes for each concentration to compare their deviation from linearity (Fig. 2.4(b)). At 1 and 2 M,

the trend lines were less linear with  $R^2 < 0.9$ , and that at 2 M showed the largest deviation from linearity ( $R^2 \sim 0.6$ ). The half-lives of the reactions were calculated using Eqn. 2.6 and were compared to the values obtained directly from the graph (Table 2.1). The actual half-life of the 2 M reaction was much longer than the calculated value (Table 2.1, entry 5).

$$t_{1/2} = \frac{\ln 2}{k_{\text{rac}}} \quad (\text{Eqn. 2.6})$$

The non-linear time plots shown in Fig. 2.4 and the differences observed between the actual and calculated half-lives indicated that the racemisation reaction deviates from the first-order model which becomes more significant with increasing amine concentration. This might be due to the catalyst deactivation or alternatively, the formation of higher order complexes. A further surprising observation that corroborates these hypotheses is that the ee of **39** which stopped decreasing after 3 to 8 hours and failed to completely racemise at all of the concentrations evaluated. In order to test the deactivation of the catalyst, the reaction at 0.5 M was spiked with more (S)-**39** (0.5 equiv.) after 24 hours and no further racemisation was observed, indicating that the catalyst was fully deactivated (Fig. 2.6).

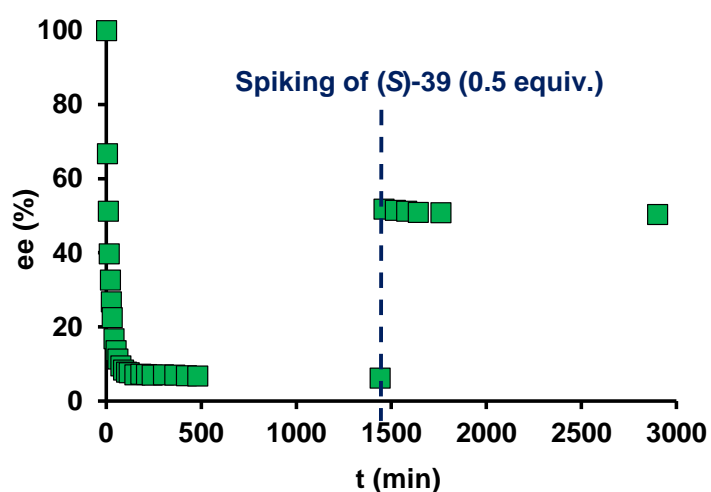
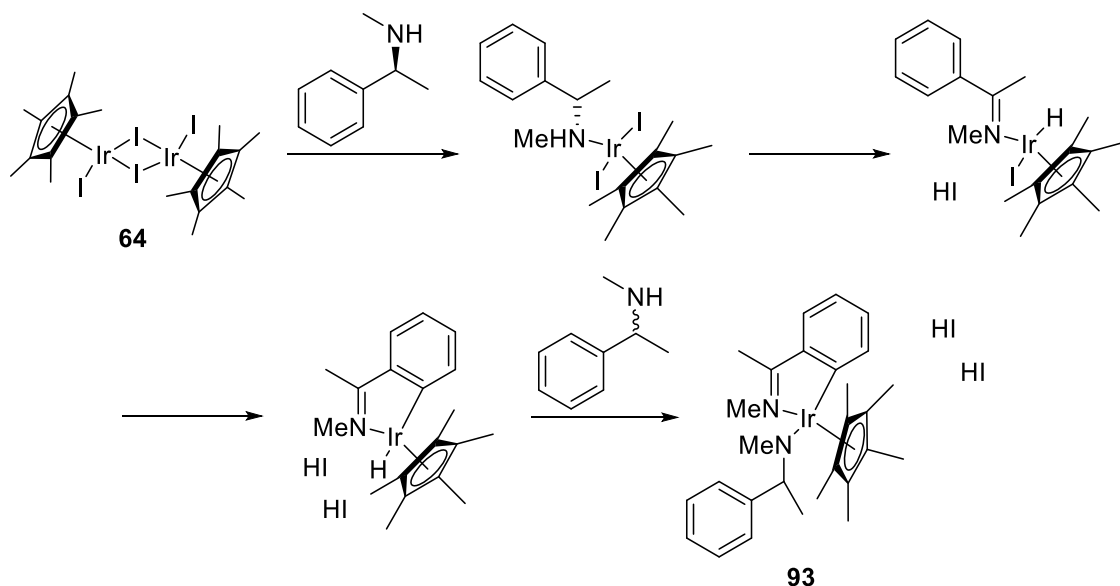


Fig. 2.6 Racemisation reaction of (S)-**39** (0.5 M) with spiking of (S)-**39** (0.5 equiv.) after 24 h

One of the plausible catalyst deactivation pathways was proposed by Blacker et al., where a carbon-metalated species **93** was formed from SCRAM **64** via C-H

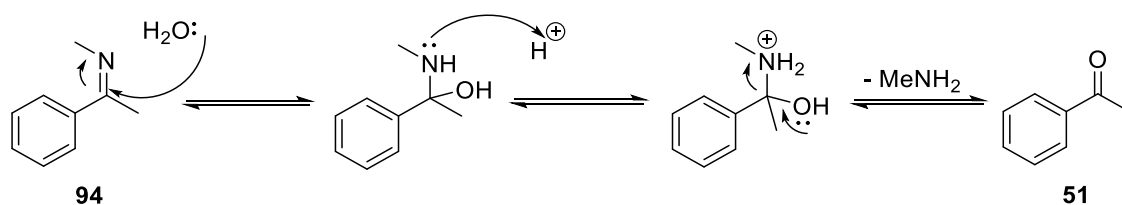


activation of the substrate and the structure was characterised previously by mass spectrometry,  $^1\text{H}$  and  $^{13}\text{C}$  NMR spectroscopy (Scheme 2.3).<sup>43</sup> Since the iridium is coordinatively saturated, oxidation of **39** at the iridium centre is not possible and subsequent racemisation cannot proceed. Complex **93** is more likely to form at higher reaction concentration. At higher concentration of 2 M, the catalyst might degrade early in the reaction, leading to significant deviation from the first-order model.



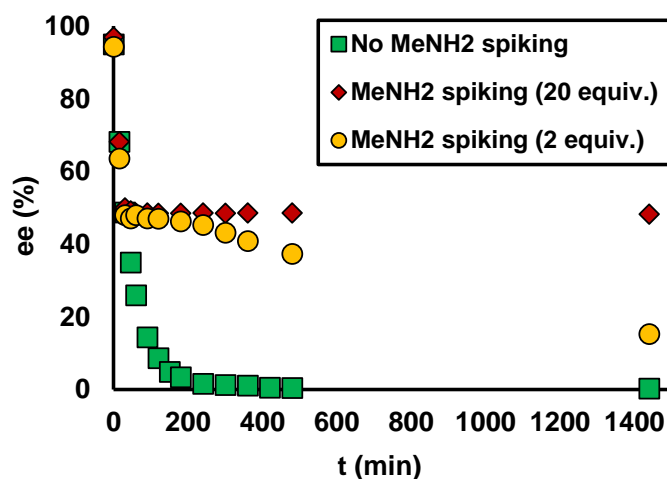
Scheme 2.3 Plausible deactivation pathway of **64** – Transformation of **64** into **93**

Another plausible deactivation mechanism of **64** is its binding with methylamine, which is the by-product from the hydrolysis of imine **94**, an intermediate formed during the racemisation of **39** (Scheme 2.4).



Scheme 2.4 Formation of **51** from the hydrolysis of **94**

To investigate the effect of methylamine on the racemisation of (*S*)-**39**, both 2 and 20 equiv. (with respect to iridium) were spiked into the reaction in tetrahydrofuran at 60 °C after 30 minutes, which is approximately one reaction half-life (Fig. 2.7).



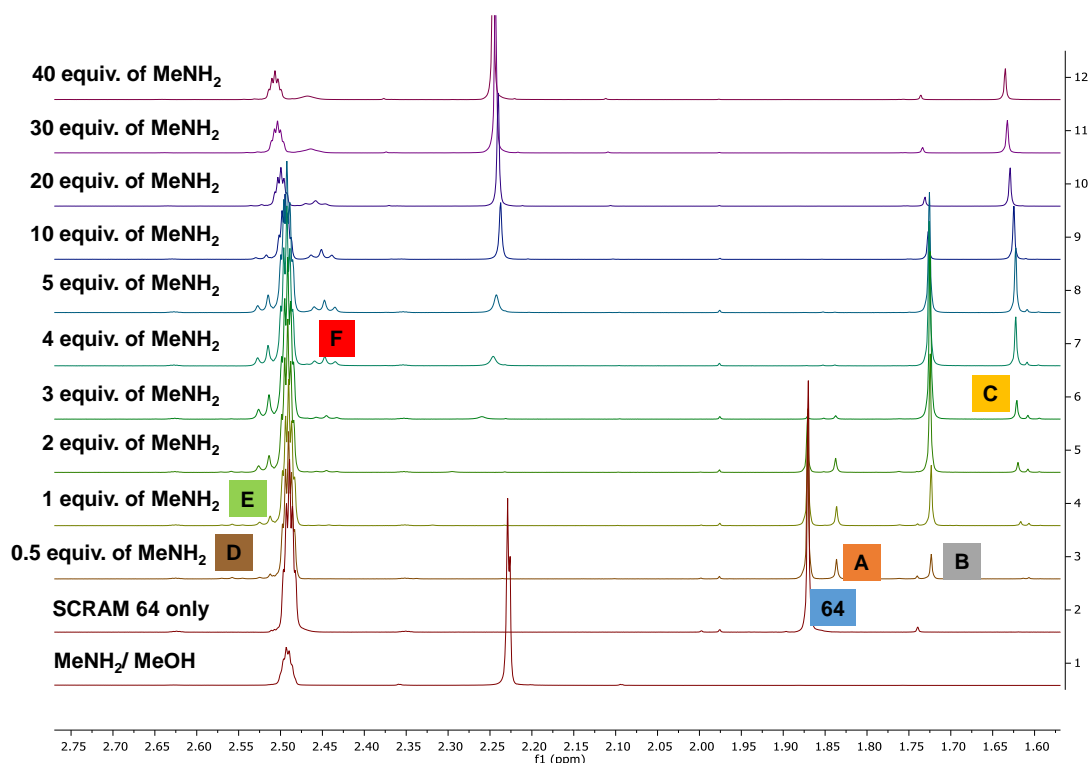


Fig. 2.8  $^1\text{H}$  NMR titration of **64** with  $\text{MeNH}_2$  (2 M in  $\text{MeOH}$ ) in  $d_6$ -DMSO. Benzene was added as the internal standard (7.35 ppm, not shown above)

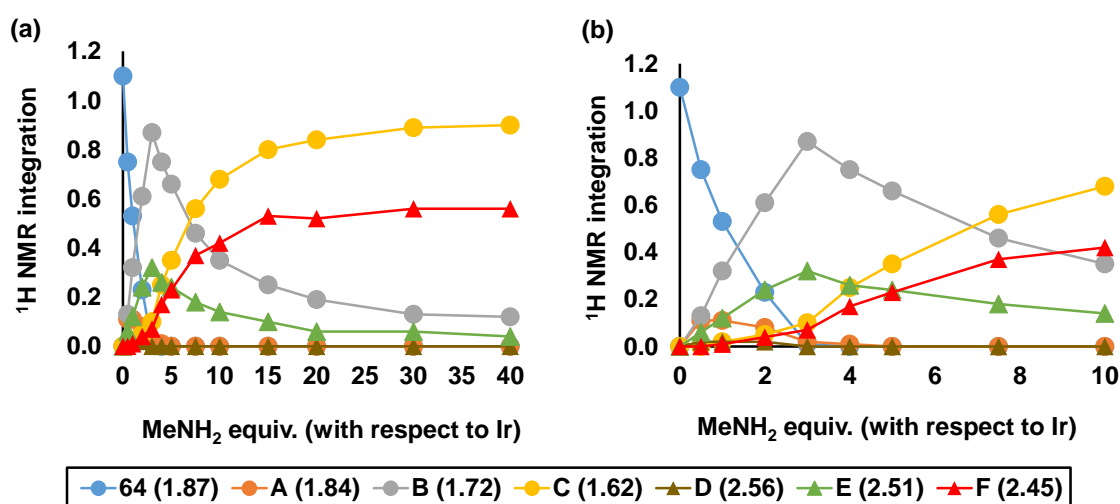


Fig. 2.9  $^1\text{H}$  NMR Integrations of  $\text{CH}_3\text{-Cp}^*$  and coordinated  $\text{CH}_3\text{-NH}_2$  in the titration reaction of  $\text{CH}_3\text{NH}_2$  into **64** in  $d_6$ -DMSO. All integrations were based on benzene which was added as the internal standard. (a) 0 to 40 equiv. of  $\text{MeNH}_2$ ; (b) Zoom-in version of (a) showing 0 to 10 equiv. of  $\text{MeNH}_2$

The methyl group on the  $\text{Cp}^*$  ligand of **64** appears at 1.87 ppm as a singlet. When methylamine was added, the intensity of the peak at 1.87 ppm decreased whilst new singlet peaks at 1.84, 1.72 and 1.62 ppm started to emerge. Eventually the

signal at 1.87 ppm disappeared, followed by that at 1.84 ppm. The singlet at 1.72 reached a maximum when 3 equiv. of methylamine was added and then decreased while that at 1.62 ppm continued to increase until 30 equiv. of methylamine was added. The total integrations of the signals at 1.87, 1.84, 1.72 and 1.62 ppm were calculated based on the integration of the benzene peak and was found to be 26 to 28 which was close to the total number of Cp\* protons of **64** (30), indicating that the newly formed signals at 1.84, 1.72 and 1.62 ppm correspond to Cp\* protons in different iridium species (Section 1, Table 8.2).

Identification of the methyl peaks of the coordinated methylamine was also attempted. Upon binding to the iridium centre, the methyl signals of the methylamine shifted downfield from 2.24 ppm to 2.56, 2.51 and 2.45 ppm. The multiplicity of the signal also changed from a singlet for the free methylamine, to triplets occurring as a result of coupling of the methyl group to the NH<sub>2</sub> which is not observed in free methylamine due to rapid proton exchange. The different triplets correspond to different Ir-NH<sub>2</sub>CH<sub>3</sub> species formed and the increasing and decreasing trends of the methylamine signals correlated to those of the methyl signals of the Cp\* (Fig. 2.9). The number of methylamine coordinated to the iridium in each species was determined by the integration ratio of the methyl signals of Cp\* and the corresponding coordinated methylamine (Table 2.2).

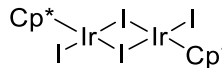
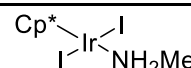
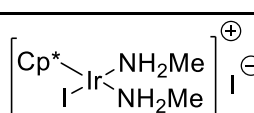
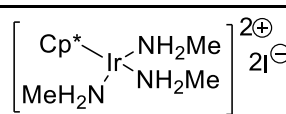
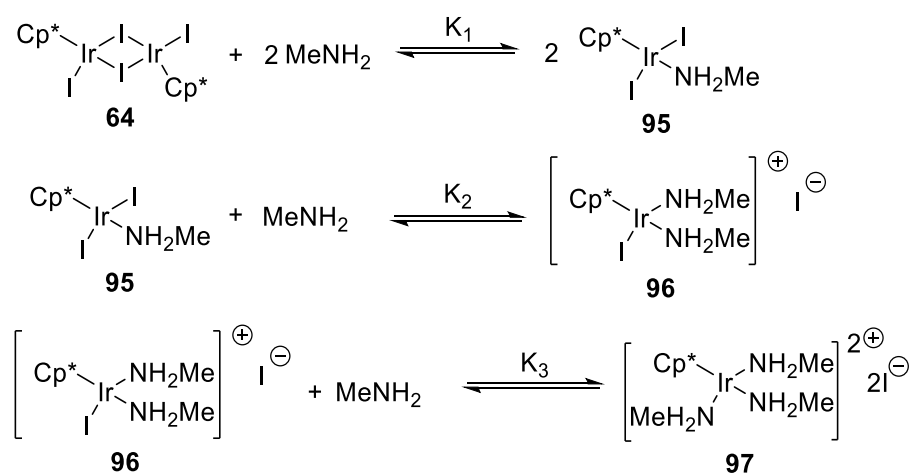
Entry	Cp* shift (ppm)	Correlated CH <sub>3</sub> NH <sub>2</sub> shift (ppm)	Cp*/ CH <sub>3</sub> NH <sub>2</sub> <sup>[a]</sup>	No. of CH <sub>3</sub> NH <sub>2</sub> protons <sup>[b]</sup>	Proposed structure
1	1.87 (64)	NA	NA	NA	 <b>64</b>
2	1.84 (A)	2.56 (D)	5	3	 <b>95</b>
3	1.72 (B)	2.51 (E)	2.6	5.8	 <b>96</b>
4	1.62 (C)	2.45 (F)	1.6	9.4	 <b>97</b>

Table 2.2 Correlation between <sup>1</sup>H NMR signals of CH<sub>3</sub>-Cp\* and coordinated CH<sub>3</sub>NH<sub>2</sub> and proposed structures of the corresponding Ir-species. <sup>[a]</sup>Average ratio of the integrations of CH<sub>3</sub>-Cp\* and coordinated CH<sub>3</sub>NH<sub>2</sub> signals. <sup>[b]</sup>Calculated as 15/ average integration ratio of CH<sub>3</sub>-Cp\*/ CH<sub>3</sub>NH<sub>2</sub> signals

Three different methylamine-bound iridium species were suspected to have formed during the titration experiment. The singlet signal at 1.84 ppm corresponds to the monomeric complex with one methylamine coordinated to the iridium, which is indicated from the ratio of the integrations of the signals of Cp\* and the corresponding bound CH<sub>3</sub>NH<sub>2</sub> (Table 2.2, entry 2). Similarly the signals at 1.72 and 1.62 ppm correspond to the complexes with two and three methylamines bound to the iridium centre respectively (Table 2.2, entries 3 and 4). Isolation of each complex was attempted without success. The crude product contained a mixture of **64**, **95**, **96** and **97** which might imply that the four iridium-species were in equilibrium (Scheme 2.5).



Scheme 2.5 Equilibrium between **64**, **95**, **96** and **97** in the titration of **64** with MeNH<sub>2</sub>

The observed equilibrium constants, K<sub>1</sub> to K<sub>3</sub>, were calculated at 3 equiv. of methylamine, where all of the iridium species, dimer **64**, **95**, **96** and **97** were present. Their integrations were converted to concentrations based on the concentration of the internal standard, benzene and were shown in Table 2.3.

Species	Concentration (mM)
<b>64</b>	0.063
<b>95</b>	0.251
<b>96</b>	10.934
<b>97</b>	1.257
Free MeNH <sub>2</sub>	2.555

Table 2.3 Concentration of different Ir species and free MeNH<sub>2</sub> when 3 equiv. of MeNH<sub>2</sub> was added

$$K_1 = \frac{[\mathbf{95}]^2}{[\mathbf{64}] \times [\text{MeNH}_2]^2} = 0.16 \text{ mM}^{-1}$$

$$K_2 = \frac{[\mathbf{96}]}{[\mathbf{95}] \times [\text{MeNH}_2]} = 17.31 \text{ mM}^{-1}$$

$$K_3 = \frac{[\mathbf{97}]}{[\mathbf{96}] \times [\text{MeNH}_2]} = 0.046 \text{ mM}^{-1}$$

The calculated values of K<sub>1</sub> to K<sub>3</sub> represent potential equilibrium constants of the equilibrium processes shown in Scheme 2.5. It indicates that under this particular

set of conditions, the equilibrium lies mainly towards the di-substituted methylamine-iridium complex **96**; while the formation of tri-substituted methylamine-iridium complex **97** is energetically less favoured due to steric hindrance. And although **95** is the least sterically demanding, the dissociation of **64** requires certain amount of activation energy which results in a relatively small equilibrium constant.

### (c) Racemisation by Shvo's catalyst **55**

The racemisation reaction of (*S*)-**39** was repeated using Shvo's catalyst **55**, which has also been reported for the racemisation of both chiral amines and alcohols. Under the same conditions as **64**, complete racemisation was observed after 8 hours using **55**, although the reaction was slower (Fig. 2.10).

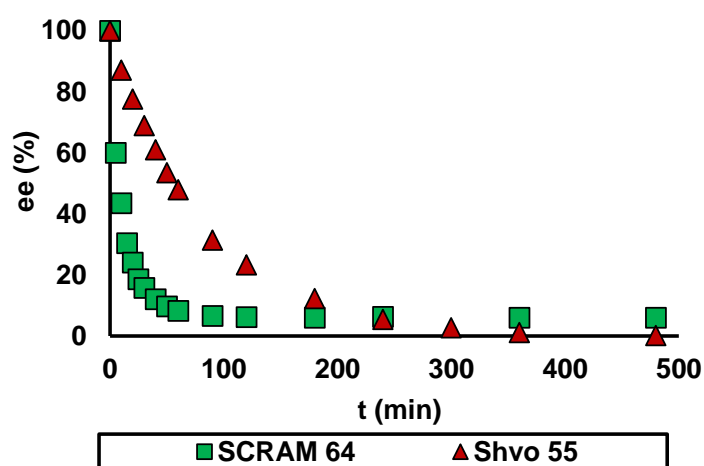


Fig. 2.10 Profiles of ee for the racemisation of (*S*)-**39** with SCRAM **64** and Shvo's catalyst **55** (0.2 mol%) in toluene at 105 °C. Only the data for  $t = 0$  to 480 min was shown

The kinetic plot of Eqn. 2.5 for the racemisation of (*S*)-**39** by **55** is shown in Fig. 2.11. The plot was close to linearity with  $R^2 > 0.99$ , assuming no conversion of **39**.  $k_{\text{rac}}$  was calculated to be  $0.014 \text{ min}^{-1}$  from time 0 to 480 min, corresponding to a half-life of 50 minutes, which was close the actual value (50 to 60 minutes). This showed that no significant degradation of **55** occurred and the catalyst remained active throughout the reaction.

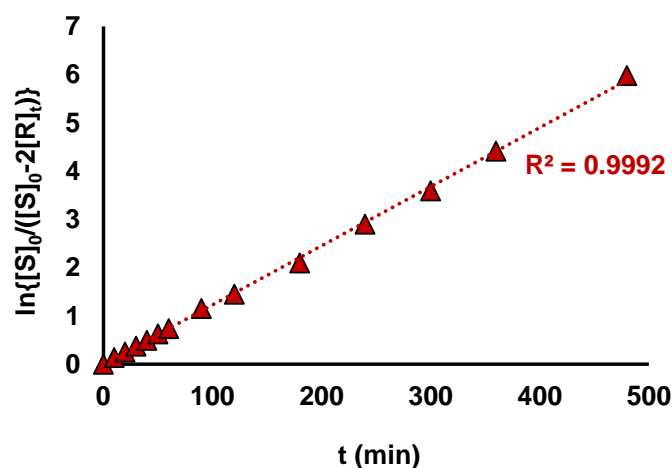


Fig. 2.11 Plot of  $\ln \{[S]_0/([S]_0 - 2[R]_t)\}$  against time for the racemisation of (S)-**39** by **55** (0.2 mol%), assuming no conversion of **39**. The trend line and the  $R^2$  value were shown

In order to further investigate the activity of **55**, the racemisation reaction was repeated, which was spiked twice with more (S)-**39** after the reaction was completed (Fig. 2.12(a)). Complete racemisation was still observed after the first spiking and the catalyst still showed activity after the second spiking, although the reaction slowed down after each spiking. The racemisation rate constants and the corresponding theoretical half-lives were determined from their  $\ln\{[S]_0/([S]_0 - 2[R]_t)\}$  versus time plots (Fig. 2.12(b), Table 2.4).

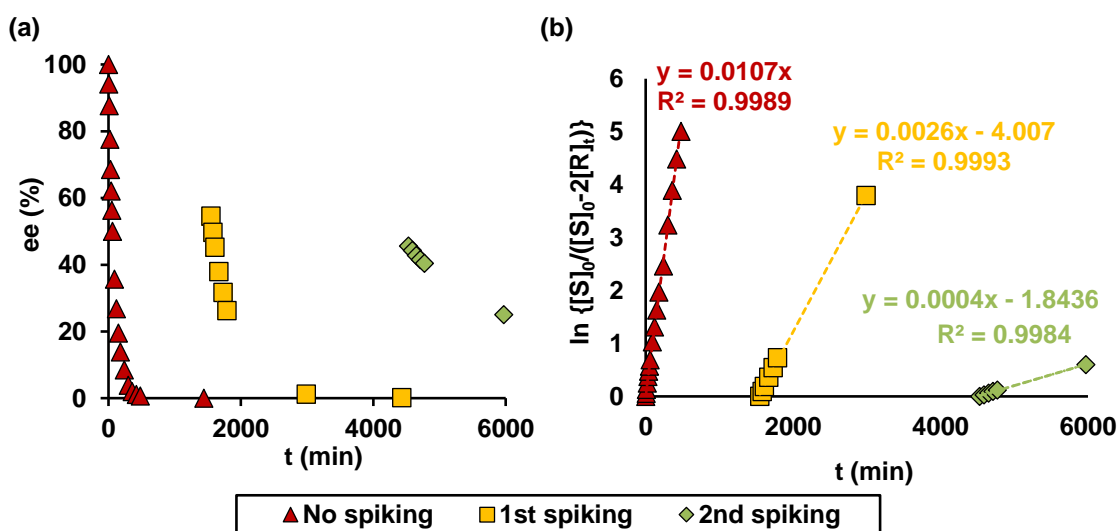
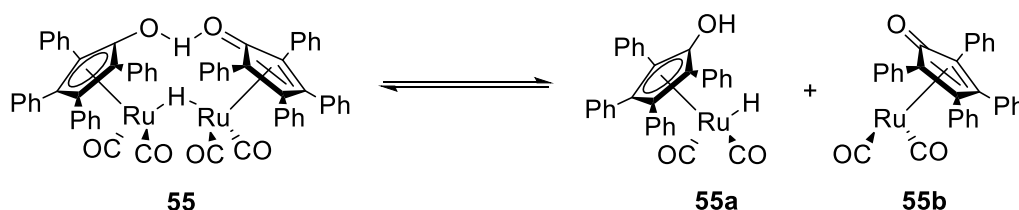


Fig. 2.12 Racemisation of (S)-**39** (0.5 M) by Shvo's catalyst **55** (0.2 mol%) with spiking of (S)-**39** (0.5 equiv.) after 25 and 76 hours. (a) ee profiles; (b) Plots of  $\ln\{[S]_0/([S]_0 - 2[R]_t)\}$  against time. The trend lines, their respective equations and  $R^2$  values were shown



Entry	Spiking	$k_{\text{rac}}$ ( $\text{min}^{-1}$ )	Calc. $t_{1/2}$ (min)	Act. $t_{1/2}$ (min)
1	None	0.011	63	60
2	1st	0.0026	267	240
3	2nd	0.0004	1733	> 1440

Table 2.4 Rate constants and half-lives for the racemisation of (S)-**39** by Shvo's catalyst **55** before and after spiking of (S)-**39**



Scheme 2.6 Dissociation of Shvo's catalyst **55**

The racemisation data suggested that **55** has a lower catalytic activity than **64**. However it is more robust, which can be used for a considerably longer time. Based on the reported proposed mechanism of amine racemisation by **55**, dissociation of **55** gives **55a** and **55b**, where **55b** has a vacant site for the amine to bind (Scheme 2.6).<sup>95</sup> The ruthenium centre at **55b** is at zero oxidation state which is much lower than that of iridium of **64** (+III). Also **55b** is more hindered than the monomer from **64** due to more bulky ligands. Therefore the binding of the amine substrate to **55b** is more difficult, leading to slower reaction. However if the catalyst deactivation of **64** goes through the C-H activation pathway as discussed in Section 2.2.1(a) (Scheme 2.3), the formation of any carbon-metalated species similar to **93** is less likely to occur. Unfortunately to date, an immobilised version of **55** has not been reported, preventing its use in fixed-bed continuous flow processes.

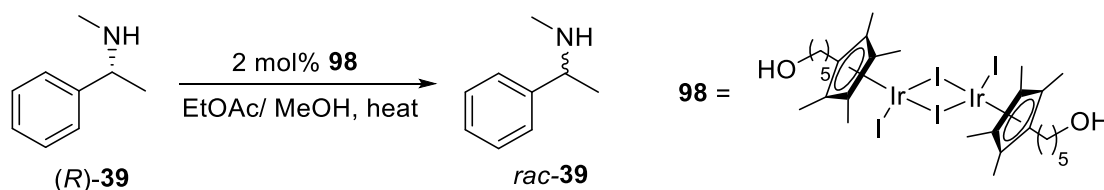
#### (d) Solvent effect – alcohol as co-solvent in racemisation

Previous studies showed that solvents with increasing polarity slow down the racemisation reaction of **39** (Table 2.5).<sup>136</sup>

Reaction solvent	<b>39</b> (%)	ee (%)
Dimethylformamide	97.6	99.2
Toluene	93.7	29
Dimethylacetamide	93.9	93.1
Chlorobenzene	87.3	50.2
1,4-Dioxane	93.4	74.6
Pyridine	98.9	99.6
Dimethyl sulfoxide	98.1	100
4-Methyl-2-Pentanone	79.2	55.8

Table 2.5 Racemisation study of **39** using different solvents

Racemisation of **39** had previously been investigated by J. Breen using C<sub>5</sub>-hydroxy-tethered SCRAM **98** in ethyl acetate by varying the amount of methanol and found that the presence of methanol inhibited the reaction (Scheme 2.5, Table 2.6).



Scheme 2.7 Racemisation of (*R*)-**39** (12 mM) using **98** (2 mol%) in EtOAc/ MeOH

MeOH (% by volume)	ee (%)
0	0
7	9
17	17
23	25
29	60
33	100

Table 2.6 Effect of MeOH in the racemisation of (*R*)-**39** by SCRAM **98** (results by J. Breen)

In the development of a Resolution-Racemisation-Recycle (R<sup>3</sup>) process, it is crucial to find a solvent system which is compatible with both racemisation and resolution. For diastereomeric crystallisation, it often requires the use of alcohols

as the main/ co-solvent. In order to further understand the effect of different alcohols to the racemisation reaction, racemisation of (S)-**39** was carried out in ethyl acetate/ alcohol (20% by volume) using SCRAM **64** (1 mol%). Methanol, ethanol and isopropyl alcohol were studied (Fig. 2.13, Table 2.7).

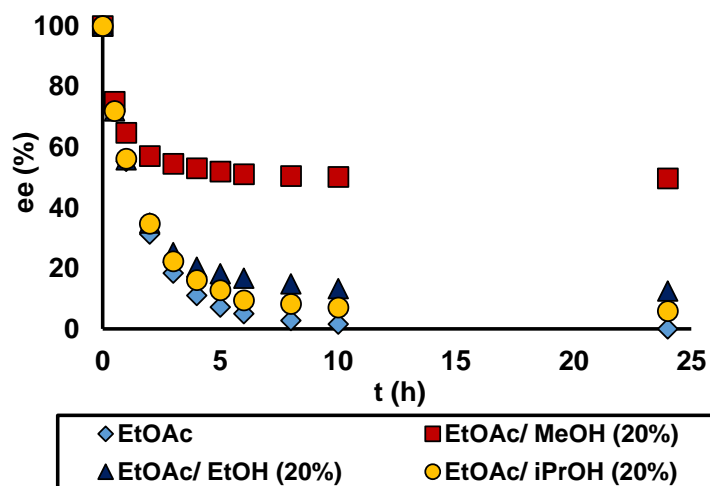


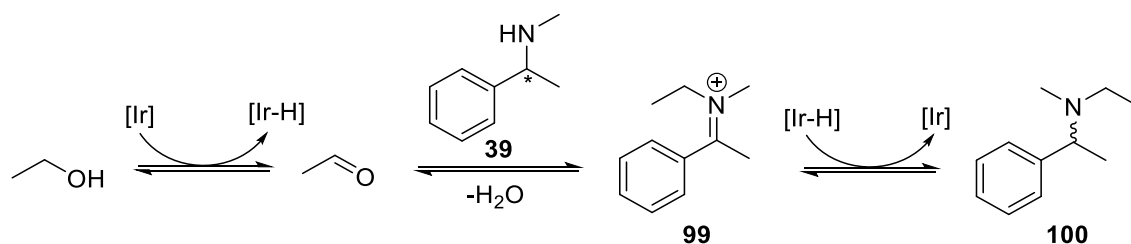
Fig. 2.13 Profiles of ee for the racemisation of (S)-**39** (0.5 M) in EtOAc/ alcohol (20% by volume) with SCRAM **64** (1 mol%) at 60 °C

Entry	Alcohol (20% v/v)	$k_{rac}$ ( $h^{-1}$ ) <sup>[b]</sup>	Calc. $t_{1/2}$ (h) <sup>[c]</sup>	Act. $t_{1/2}$ (h) <sup>[d]</sup>	ee (24 h) (%) <sup>[e]</sup>	<b>39</b> (24 h) (%) <sup>[f]</sup>
1	None	0.639	1.1	1-2	0	93
2	MeOH	0.536	1.3	8	50	98
3	EtOH	0.658	1.1	1-2	13	57
4	iPrOH	0.659	1.1	1-2	6	93

Table 2.7 Rate constants, half-lives, ee and [**39**] after 24 h for the racemisation of (S)-**39** in EtOAc/ alcohol with 1 mol% **64** at 60 °C. <sup>[a]</sup>Values calculated by Eqn. 2.5 using first two data points, assuming no conversion of **39**. <sup>[b]</sup>Values calculated by Eqn. 2.6. <sup>[c]</sup>Values obtained from the ee profiles (Fig. 2.13). <sup>[d]</sup>ee was determined by chiral GC after derivatisation by trifluoroacetic anhydride. <sup>[e]</sup>**39** (%) was determined by GC

A control reaction for the racemisation was performed in pure ethyl acetate for comparison (Table 2.7, entry 1). Methanol has the largest impact on the racemisation of (S)-**39** (Table 2.7, entry 2). The initial rate of the reaction was lower and the reaction seems to slow down and started to level-off after about 3 hours (Fig. 2.13). The large deviation of the calculated half-life from the actual value suggested possible catalyst deactivation. One possibility is the oxidation of

methanol to form formaldehyde, which might be toxic to the catalyst or the amine substrate; another possibility is the coordination of the alcohol to the metal centre, blocking the coordination site. The use of ethanol and isopropyl alcohol as the co-solvent led to similar initial rates of racemisation as the reaction using only ethyl acetate (Table 2.7, entries 3 and 4). However, for ethanol, significant conversion of > 40% of **39** was observed (Table 2.7, entry 3). The new species formed had a similar retention time in the GC as the imine **94**, however it had a *m/z* value of 163 in the GCMS which is different from that of **94** (*m/z* 133). Also the <sup>1</sup>H and <sup>13</sup>C NMR spectra did not show the presence of **94** in the crude reaction mixture. Instead an additional set of signals with comparable chemical shifts with **39** and tertiary amine, *N,N*-dimethyl- $\alpha$ -methylbenzylamine **46** were found, indicating that the newly formed species was not **94**, but a compound possessing similar chemical structure as **39** and **46**. It was suggested that an *N*-alkylated product, **100**, might have formed *via* a borrowing hydrogen mechanism (Scheme 2.8), in which ethanol was first oxidised by **64** to give acetaldehyde, which coupled with **39** to form an iminium intermediate **99** with elimination of water, followed by transfer hydrogenation to generate **100**. However the retention times of the unknown product and **46** were significantly different which was not expected since they have very similar structures. As the unknown product was not isolated, its identity could not be fully confirmed.



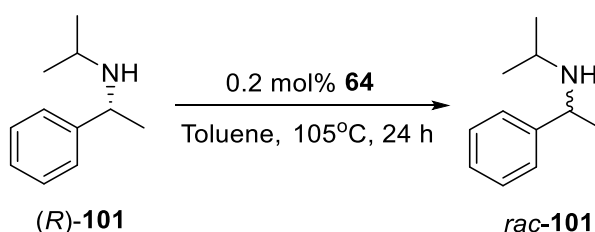
Scheme 2.8 Plausible formation of **100** via *N*-alkylation of **39** with EtOH

For isopropyl alcohol, the reaction proceeded at a similar initial rate as that in ethyl acetate without significant formation of impurities. This might be because acetone formed upon the oxidation of isopropyl alcohol might be too bulky for **39** to attack, avoiding the *N*-alkylation reaction. However, the reaction started to slow down slightly after about three hours which might indicate a drop in the activity of **64**. Complete racemisation could not be achieved after 24 hours, unlike the case in ethyl acetate. Since isopropyl alcohol can act as an efficient hydrogen donor

which can also turn over the catalyst, this may have affected the activity towards **39**.

### 2.2.2 *N*-Isopropyl- $\alpha$ -methylbenzylamine **101**

*N*-isopropyl- $\alpha$ -methylbenzylamine **101** is an analogue of **39** which has an isopropyl group attached to the nitrogen. The racemisation of (*R*)-**101** was carried out in batch in toluene at 105 °C using SCRAM **64** (0.2 mol%) (Scheme 2.9). The reaction was slower than that of **39** with initial rate constant of 0.022 min<sup>-1</sup> and a half-life of about 32 minutes (calculated, versus actual = 30-45 minutes). However complete racemisation was observed after 8 hours (Fig. 2.14).



Scheme 2.9 Racemisation of (*S*)-**101** (0.5 M) with **64** (0.2 mol%) in toluene at 105 °C

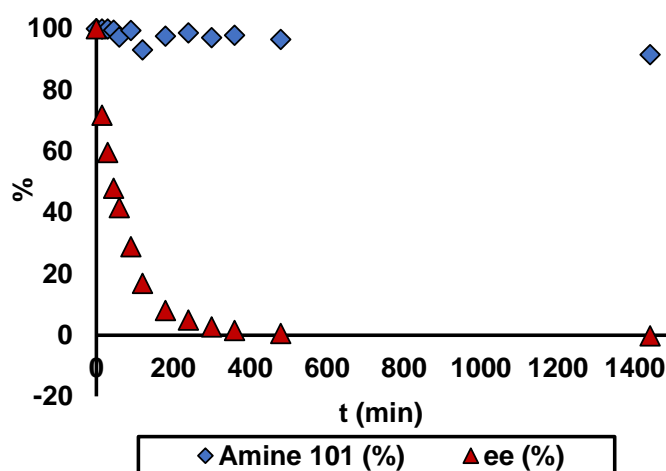
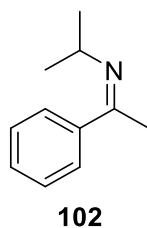


Fig. 2.14 Reaction profile for the racemisation of (*R*)-**101** (0.5 M) with **64** (0.2 mol%) in toluene at 105 °C

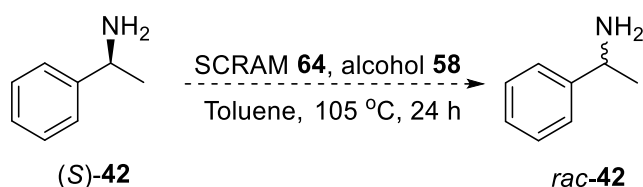
Since **101** is more sterically hindered than **39**, it is more difficult for it to bind to the iridium centre of **64**, slowing down the reaction. However the deactivation of **64** via the C-H activation pathway as shown in Scheme 2.3 is less likely to occur. The intermediate imine **102** is also more hindered for the attack by water to generate **51** and isopropylamine, and isopropylamine is more bulky than

methylamine and is more difficult to bind to **64**. Therefore **64** maintains its activity and the ee of **101** is able to reach 0%.



### 2.2.3 $\alpha$ -Methylbenzylamine **42**

Racemisation of enantiopure **42** has been reported in the literature.<sup>1, 85, 90, 91, 95, 96, 101-103</sup> Since **42** is a primary amine with no substituents at the nitrogen except hydrogen, it is considerably less sterically demanding than **39** or **101**. The lack of any electron-releasing alkyl substituents at the nitrogen make the intermediate imine more electrophilic to nucleophilic attack by surrounding molecules of **42**. As a result, various dimer products are readily formed (Scheme 1.23). Bäckvall et al. reported the use of 2,4-dimethylpentan-3-ol **58** as an effective hydrogen donor to suppress the formation of dimers in the racemisation of (*S*)-**42** at low concentration (0.25 M) with Shvo's catalyst **55** (5 mol%).<sup>95</sup> Similar procedures were attempted using SCRAM **64** as the catalyst (Scheme 2.10, Fig. 2.15).



Scheme 2.10 Attempted racemisation of (*S*)-**42** using **64** with and without **58** in toluene at 105 °C

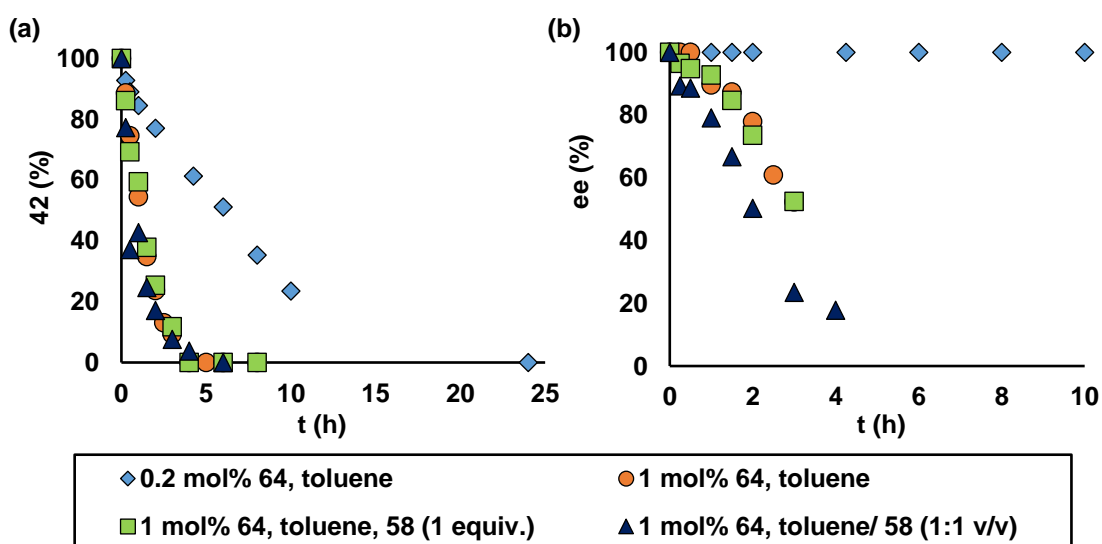
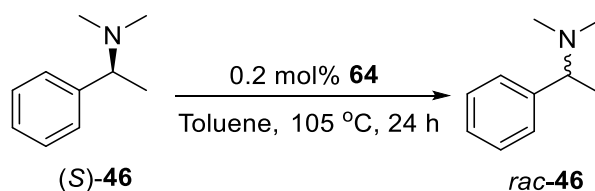


Fig. 2.15 Reaction profiles for the racemisation of (S)-**42** using SCRAM **64** with and without alcohol **58** in toluene at 105 °C. (a) Concentration of **42** (%), determined by GC with *n*-decane as internal standard. (b) ee of **42**, determined by chiral HPLC after derivatisation with benzoyl chloride in the presence of triethylamine

Control experiments were first carried out without alcohol **58**. With 0.2 mol% of SCRAM **64**, a gradual drop in the concentration of **42** in the reaction was observed due to the formation of dimers and no racemisation of **42** occurred. A higher loading of 1 mol% of **64** was used. A much faster dimerisation was observed alongside with the racemisation of **42** from 100% to 61% after three hours. To try suppressing the dimerisation, 1 equiv. of **58** was added, which led only to a similar rate of conversion and racemisation of **42**. Increasing the amount of **58** by using it as a co-solvent with toluene in 1:1 (v/v), the racemisation of **42** was faster and reached 18% ee after four hours. However no improvement was observed in reducing the formation of dimers. This indicated that SCRAM **64** is less suitable for the racemisation of **42** compared to Shvo's catalyst **55** under similar conditions.

#### 2.2.4 *N,N*-Dimethyl- $\alpha$ -methylbenzylamine **46**

Racemisation of **46** was previously reported by Blacker et al.<sup>1</sup> At 0.2 M, the reaction proceeded with a half-life of 21 hours with 1 mol% SCRAM **64** at 90 °C in toluene. In order to compare the results with amines **39** and **101**, the racemisation was carried out at a higher concentration of 0.5 M in toluene at 105 °C, with only 0.2 mol% **64** (Scheme 2.11, Fig. 2.16).



Scheme 2.11 Racemisation of (S)-**46** (0.5 M) using **64** (0.2 mol%) in toluene at 105 °C

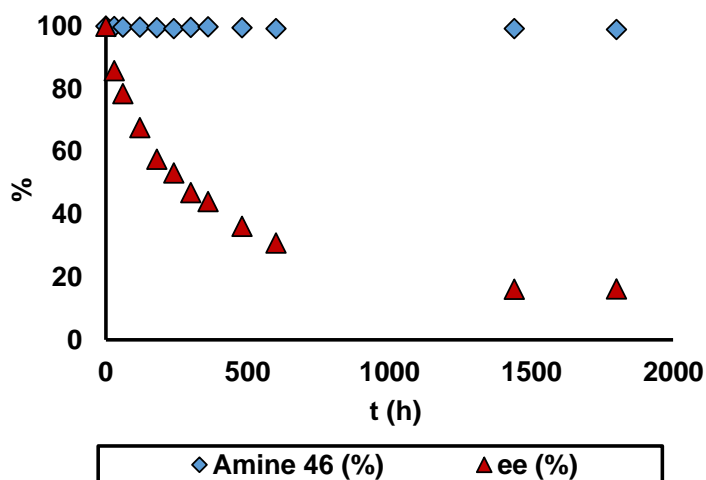


Fig. 2.16 Reaction profile for the racemisation of (S)-**46** using SCRAM **64** (0.2 mol%) in toluene at 105 °C. The ee of **46** was measured by free-basing the sample with  $\text{Na}_2\text{CO}_3$  (aq), derivatised by (S)-mandelic acid **34** and analysed by  $^1\text{H}$  NMR ( $\text{CDCl}_3$ , 500 MHz)

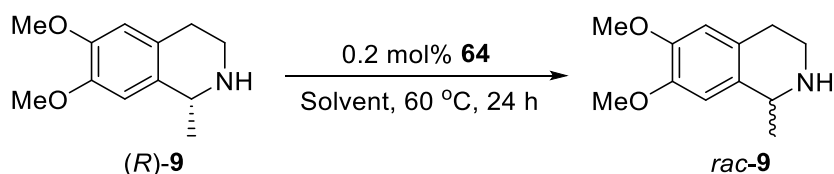
The racemisation of **46** had a half-life of about 4 hours, without significant formation of impurities. It was much slower compared to either amines **39** or **101**, which is due to its bulky tertiary amine structure, hindering binding to the iridium centre. The lack of a NH proton on **46** may affect the energy of formation of the intermediate iridium-quaternary iminium complex/ transition state. The racemisation rate constant of the reaction was calculated to be  $0.304 \text{ h}^{-1}$  ( $0.005 \text{ min}^{-1}$ ) with a half-life of 2.3 hours, based on first-order model (Eqn. 2.5 and 2.6), whilst the actual half-life is between 4 to 5 hours. Deviation of the calculated and actual half-lives suggested possible degradation of **64**. This is also reflected from the ee profile which reached a plateau at 16% after 24 hours.

### 2.2.5 6,7-Dimethoxy-1-methyl-1,2,3,4-tetrahydroisoquinoline **9**

The racemisation of enantiopure **9** was reported by Blacker et al. with **39** and **46**.<sup>1</sup> The reaction was very fast with a half-life of 45 minutes at 40 °C in dichloromethane, with only 0.2 mol% loading of SCRAM **64**. Diastereomeric resolution of *rac*-**9** had previously been carried out by Shi et al. using ethyl



acetate/ isopropyl alcohol mixture as the solvent system, which will be further discussed in Chapter 3.<sup>137</sup> As discussed in Section 2.2.1(d), the use of alcohol can have a negative impact on the rate of racemisation of **39**. However, since the racemisation of **9** is much faster, the reaction was also attempted using ethyl acetate/ alcohol mixtures to investigate the effect of solvent polarity (Scheme 2.12, Fig. 2.17). The reaction was also carried out in toluene for comparison.



Scheme 2.12 Racemisation of *(R)*-**9** (0.1 M) using SCRAM **64** (0.2 mol%) at 60 °C

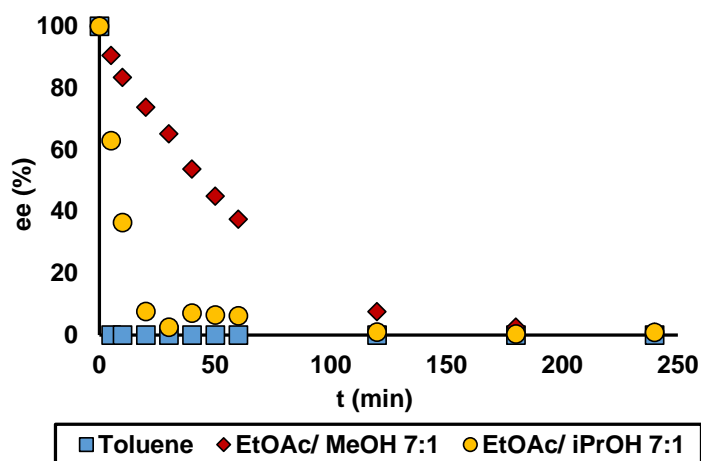


Fig. 2.17 Profiles of ee for the racemisation of *(R)*-**9** (0.1 M) using SCRAM **64** (0.2 mol%) at 60 °C in various solvent. Only  $t = 0$  to 240 min was shown

The racemisation of *(R)*-**9** was completed within 5 minutes in toluene, with 0.2 mol% of **64** (Fig. 2.17). When the solvent was changed to ethyl acetate/ alcohol mixtures, the racemisation slowed down. The initial rate was lower with longer half-lives (both calculated and actual) when methanol was used compared to isopropyl alcohol, which is also the case for the racemisation of *(S)*-**39** (Table 2.8, entries 2 and 3). However, unlike **39**, complete racemisation was still observed for **9** after 4 hours. In toluene, a higher conversion of **9** to imine **8** and isoquinoline **65** was observed which was slightly lower in the presence of methanol or isopropyl alcohol. Being a hydrogen donor, isopropyl alcohol can reduce **8** and **65** back to **9**. Methanol is less likely to act as a hydrogen donor and the lower

concentrations of **8** and **65** may be explained by the slower turnover of the catalyst.<sup>138</sup>

Entry	Solvent	$k_{\text{rac}}$ ( $\text{min}^{-1}$ ) <sup>[a]</sup>	Calc. $t_{1/2}$ (min) <sup>[b]</sup>	Act. $t_{1/2}$ (min) <sup>[c]</sup>	<b>9</b> (%) <sup>[d]</sup>	<b>8</b> (%) <sup>[d]</sup>	<b>65</b> (%) <sup>[d]</sup>
1	Toluene	N.D. <sup>[e]</sup>	N.D. <sup>[e]</sup>	< 5	83	4	7
2	EtOAc/ MeOH 7:1 (v/v)	0.02	35	40-50	96	3	3
3	EtOAc/ <sup>t</sup> PrOH 7:1 (v/v)	0.093	7.5	5-10	95	4	4

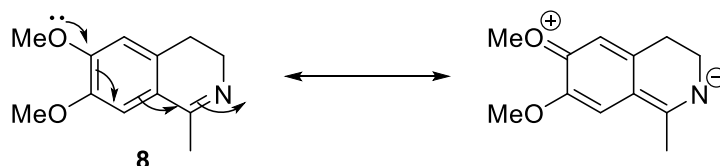
Table 2.8 Rate constants, half-lives and concentrations of **9**, imine **8** and isoquinoline **65** for the racemisation of (*R*)-**9** using SCRAM **64** (0.2 mol%) at 60 °C in various solvent.

<sup>[a]</sup> Values calculated by Eqn. 2.5 using first two data points, assuming no conversion of **9**.

<sup>[b]</sup> Values calculated by Eqn. 2.6. <sup>[c]</sup> Values obtained from the ee profiles (Fig. 2.17).

<sup>[d]</sup> Values after 8 h, determined by GC. <sup>[e]</sup> Not determined

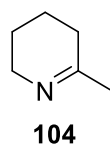
Racemisation of **9** is fast compared to amines **39**, **101** and **46**. This could be due to the more stable cyclic imine intermediate **8**. Its stability is further enhanced by the methoxy substituents on the aromatic ring (Scheme 2.13).



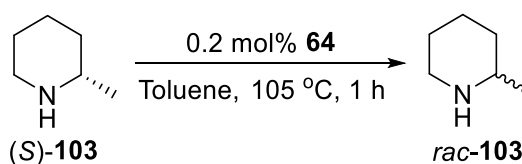
Scheme 2.13 Stabilisation of imine **8** by its conjugation with the aromatic ring and the MeO substituents

### 2.2.6 2-Methylpiperidine **103**

2-Methylpiperidine **103** is also a secondary cyclic amine but is non-benzylic. The intermediate imine **104** is not stabilised by any conjugation, although the methyl group at the chiral centre can stabilise the C=N by inductive effect, making it less electrophilic. So it might be expected that enantiopure **103** is racemised more easily than acyclic amines such as **39** or **101**, but slower than **9**.



The racemisation of (*S*)-**103** was first carried out in toluene at 105 °C with 0.2 mol% **64** (Scheme 2.14, Fig. 2.18). The reaction was completed in 30 minutes with a half-life of < 5 minutes (calculated as 4 minutes). Although it is slower than the racemisation of **9**, it is faster than acyclic amines **39** and **101**.



Scheme 2.14 Racemisation of (*S*)-**103** (0.5 M) using **64** (0.2 mol%) in toluene at 105 °C

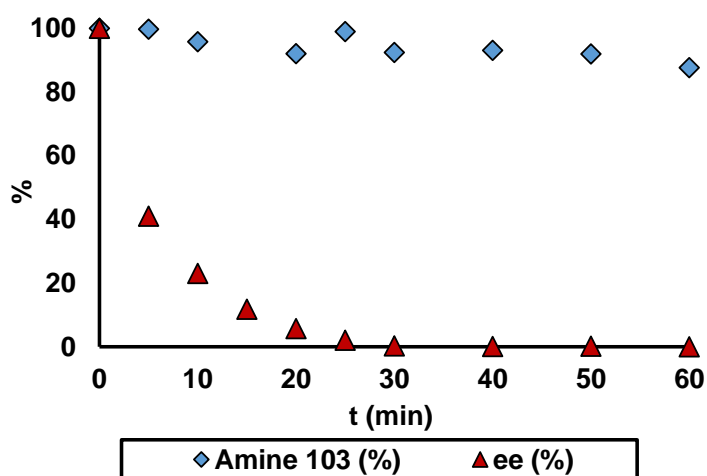


Fig. 2.18 Reaction profile for the racemisation of (*S*)-**103** (0.5 M) using SCRAM **64** (0.2 mol%) in toluene at 105 °C

The diastereomeric resolution of *rac*-**103**, which will be discussed in Chapter 3, showed that a relatively high resolvability could be achieved with methyl-*tert*-butyl ether/ alcohol mixture and isopropyl acetate as the solvents. Therefore the racemisation of (*S*)-**103** was also carried out in methyl-*tert*-butyl ether and isopropyl acetate (Fig. 2.19). Their initial rates, half-lives and final ee were compared in different solvents in Table 2.9.

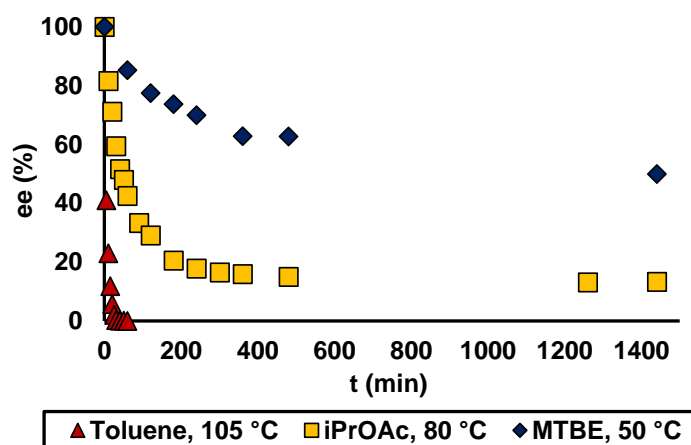


Fig. 2.19 Profiles of ee for the racemisation of (S)-**103** (0.5 M) using **64** (0.2 mol%) in toluene at 105 °C, *i*PrOAc at 80 °C and MTBE at 50 °C

Entry	Solvent	T (°C)	$k_{\text{rac}}$ ( $\text{min}^{-1}$ ) <sup>[a]</sup>	Calc. $t_{1/2}$ (min) <sup>[b]</sup>	Act. $t_{1/2}$ (min) <sup>[c]</sup>	Final ee (%) [t (h)]
1	Toluene	105	0.18	4	< 5	0 [0.5]
2	<i>i</i> PrOAc	80	0.02	34	40	13 [24]
3	MTBE	50	N.D. <sup>[d]</sup>	N.D. <sup>[d]</sup>	≤ 1440	50 [24]

Table 2.9 Rate constants, half-lives and the final ee for the racemisation of (S)-**103** using SCRAM **64** (0.2 mol%) under different conditions. <sup>[a]</sup>Values calculated by Eqn. 2.5 using the first two data points, assuming no conversion of **103**. <sup>[b]</sup>Values calculated by Eqn. 2.6. <sup>[c]</sup>Values obtained from the ee profiles (Fig. 2.18 and Fig. 2.19). <sup>[d]</sup>Not determined

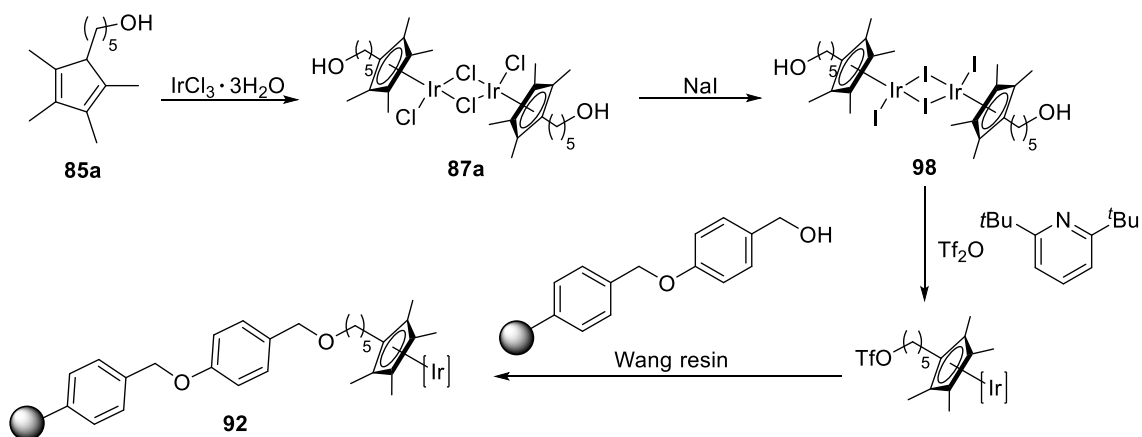
The racemisation was about 10 times faster in toluene than in isopropyl acetate, not only because of the higher temperature, but possibly also due to the lower polarity of toluene which favours the reaction. With isopropyl acetate, the racemisation of **103** did not reach zero ee. This could be due to catalyst deactivation. However, since the racemisation of **103** goes through cyclic imine **104**, its hydrolysis into the corresponding amino-ketone is improbable. Any deactivation may be more likely to go *via* the formation of Ir-**103** complexes but the exact mechanism involved is not yet known. The use of methyl *tert*-butyl ether led to much slower racemisation due to its low boiling point which limits the temperature of the reaction.

## 2.3 Racemisation in flow

Although the homogeneous SCRAM catalyst **64** was able to racemise a broad range of chiral amines, the catalyst was difficult to reuse/ recycle. To increase its recyclability, **64** was immobilised onto a Wang resin support. The immobilised version of SCRAM, **92**, can be reused in a batch reaction by either filtration, or decanting the reaction mixture with subsequent washing of the catalyst. However, this can cause physical losses which reduces the effectiveness of the next reaction(s). Catalyst **92** can be used in flow, where it is packed into a reactor and the reaction mixture can be pumped through the catalyst. Since the catalyst is insoluble in the reaction solvent, the catalyst will stay intact in the reactor, assuming no leaching or reaction-specific catalyst deactivation occurs. Much less manipulation is required to recycle the catalyst and therefore minimising any physical losses. A further advantage is that after steady state is reached, any change in catalyst can be observed simply, and reaction optimisation can be achieved more quickly.

### 2.3.1 Synthesis of immobilised SCRAM **92**

Immobilised SCRAM **92** was synthesised and provided by Yorkshire Process Technology (Scheme 2.15). The iridium dimer **87a** was prepared by heating iridium trichloride trihydrate with functionalised pentamethylcyclopentadiene (Cp\*) ligand **85a**, followed by halide exchange with sodium iodide, forming **98**. Triflated **98** was then reacted with polystyrene-supported Wang resin to give **92**.<sup>135</sup>



Scheme 2.15 Synthesis of immobilised SCRAM **92**

### 2.3.2 Experimental set-up

The schematic of the flow racemisation set-up was shown in Fig. 2.20. It consists of a packed-bed reactor (PBR) which is a stainless steel HPLC column (3 or 4 mL) packed with a mixture of **92** and sand. The amount of iridium being loaded onto the PBR was calculated based on the ICP value of each batch of **92** (Eqn. 2.7) and was relative to the total amount of amine pumped through the reactor throughout the experiment.

$$\text{Ir loading (mol\%)} = \frac{\left[ \frac{m_{92} \times \text{ICP (\% w/w)}}{M_{\text{Ir}}} \right]}{n_{\text{Amine}}} \quad (\text{Eqn. 2.7})$$

Where  $m_{92}$  is the mass of **92**,  $n_{\text{amine}}$  is the total number of moles of the chiral amine pumped across the PBR,  $M_{\text{Ir}}$  is the atomic mass of iridium which is 192.

The column was heated inside an aluminium heating block by either a stirrer hot plate (Configuration A, Fig. 2.20(a)) or nickel heating cartridges that were electrically-controlled (Configuration B, Fig. 2.20(b)).

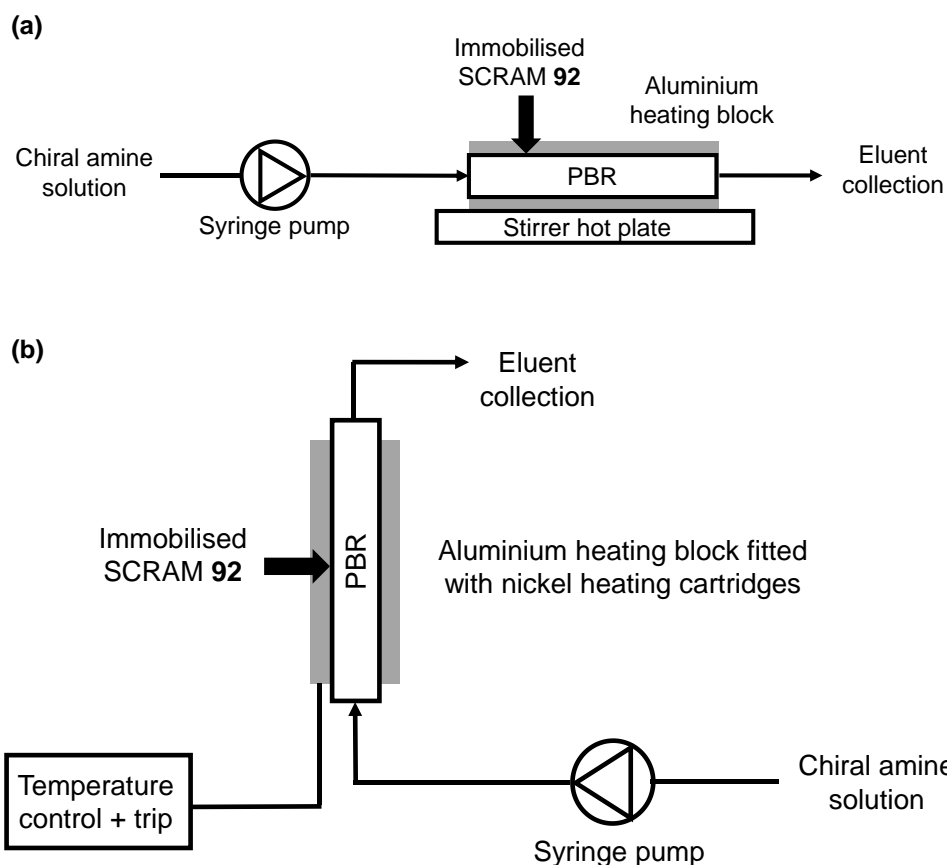


Fig. 2.20 Flow racemisation set-up. (a) Configuration A: PBR (3 mL) was heated in an aluminium block by a stirrer hot plate. (b) Configuration B: PBR (4 mL) was heated in an aluminium block by electrically-controlled nickel heating cartridges

The inlet of the PBR was connected to a syringe pump *via* PTFE tubing (1/16" O.D., 1/32" I.D.), which pumps the chiral amine solution through the PBR at a specific flow rate. Eluent containing the racemised product was collected at the outlet of the PBR in reactor volumes (RV). The residence time,  $t_{\text{Res}}$ , is defined as the time spent by the reactants in the reactor, which can be calculated as,

$$t_{\text{Res}} \text{ (min)} = \frac{\text{RV (mL)}}{\text{Flow rate (mL min}^{-1}\text{)}} \quad (\text{Eqn. 2.8})$$

Where RV is the volume of the reactor (PBR).

### 2.3.3 Flow racemisation of chiral amines

Racemisation of the same amines as discussed in Section 2.2 were tested in flow using the set-up in Fig. 2.20 except primary amine **42** (Table 2.10). A total of five fractions (each fraction corresponds to one RV) were collected in each reaction

and the conversion and ee of each fraction was monitored by GC and chiral GC (or chiral HPLC) respectively. The average ee of the substrate after one pass through the PBR was calculated across RV2 to RV5, where the reaction was in steady state. An example is shown in Fig. 2.21 for the racemisation of (S)-**39** in flow. The rate of racemisation in flow was approximated by the average drop in ee after one pass through the catalyst divided by  $t_{Res}$ .

Entry	Amine	[Amine] (mM)	Solvent <sup>[a]</sup>	Ir loading (mol%) <sup>[b]</sup>	T (°C)	$t_{Res}$ (min)	Drop in ee after one pass (%) [min <sup>-1</sup> ] <sup>[c]</sup>
1 <sup>[d]</sup>	(S)- <b>39</b>	100	<sup>i</sup> PrOAc	5	80	40	42 [1.1] <sup>[e]</sup>
2 <sup>[f]</sup>	(S)- <b>39</b>	100	EtOAc/ MeOH 8:2	5	73	12	14 [1.2]
3 <sup>[d]</sup>	(R)- <b>101</b>	50	EIB <sup>[g]</sup>	10	80	80	14 [0.2]
4 <sup>[d]</sup>	(S)- <b>46</b>	50	<sup>i</sup> PrOAc/ <sup>i</sup> PrOH 7:3	10	80	80	11 [0.14]
5 <sup>[d]</sup>	(S)- <b>46</b>	50	<sup>i</sup> PrOAc/ <sup>i</sup> PrOH 7:3	10	80	120	16 [0.13]
6 <sup>[f]</sup>	(S)- <b>9</b>	62	EtOAc/ MeOH 7:1	10	60	6	83 [13.8]
7 <sup>[f]</sup>	(R/S)- <b>9</b> - (S)- <b>34</b>	64 <sup>[h]</sup>	EtOAc/ MeOH 7:1	10	60	6	26 [4.3] <sup>[i]</sup>
8 <sup>[d]</sup>	(S)- <b>103</b>	80	MTBE/ <sup>i</sup> PrOH 95:5	5	50	12	0 [0]
9 <sup>[d]</sup>	(S)- <b>103</b>	100	<sup>i</sup> PrOAc	5	80	16	79 [4.9]

Table 2.10 Results for the racemisation of various chiral amines in flow. <sup>[a]</sup>Ratios referred to volume ratios. <sup>[b]</sup>Relative to the total amount of amine pumped through the catalyst. <sup>[c]</sup>An average value was taken from RV2 to RV5 or from RV3 to RV5. Values in bracket correspond to the average drop in ee per minute, assuming the rate of racemisation was constant. <sup>[d]</sup>Configuration B was used. <sup>[e]</sup>Initial ee of (S)-**39** was 86%. <sup>[f]</sup>Configuration A was used. <sup>[g]</sup>Ethyl isobutyrate. <sup>[h]</sup>The concentration of **9** was calculated by <sup>1</sup>H NMR with an external standard (trimethylsilane). <sup>[i]</sup>Initial ee of ML was 38%



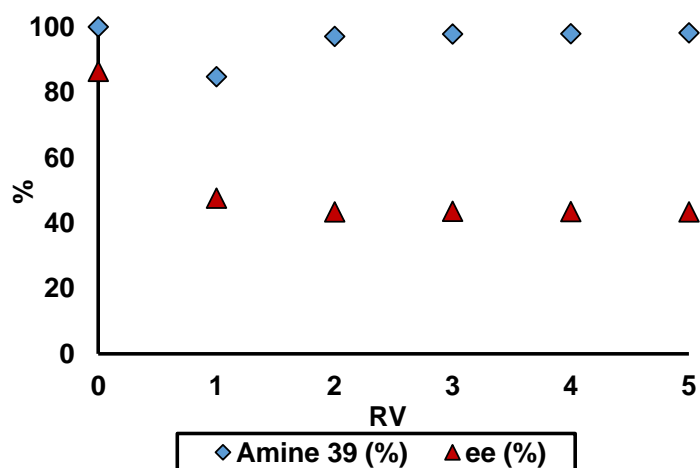


Fig. 2.21 The ee profile for the racemisation of (S)-**39** in flow in *i*PrOAc at 80 °C with 5 mol% loading of **92** (Table 2.10, entry 1)

Using a longer  $t_{\text{Res}}$  led to a bigger drop in ee (Table 2.10, entries 1 and 2; 4 and 5). In the case of (S)-**39**, the use of less polar solvent (isopropyl acetate) and slightly higher temperature did not have a significant impact on the rate of racemisation (Table 2.10, entries 1 and 2). With higher loading of **92** and longer  $t_{\text{Res}}$ , (R)-**101** and (S)-**46** showed racemisation but were slower compared that of (S)-**39** (Table 2.10, entries 3 to 5). It is partly due to their more sterically hindered structures, which is also observed in batch, and possibly the lower concentrations used. As shown in batch, the racemisation of **9** was very fast compared to the other substrates tested. In flow, (S)-**9** was successfully racemised by over 80% in 6 minutes (Table 2.10, entry 6). The mother liquor (ML) from the diastereomeric resolution of *rac*-**9** with (S)-mandelic acid **34** was also racemised without removal of the acid (Table 2.10, entry 7). The slower racemisation rate of the ML compared to enantiopure **9** may be explained by the weaker binding of the substrate to iridium due to protonation at the nitrogen of **9** by **34**. The lower starting ee of the ML compared to enantiopure substrate also led to smaller drop in ee. Racemisation of (S)-**103** did not occur in flow in methyl *tert*-butyl ether/isopropyl alcohol mixture (Table 2.10, entry 8). It is likely to be due to the lower temperature and short  $t_{\text{Res}}$  used; whilst in batch, (S)-**103** racemised by 50% in 24 hours in methyl *tert*-butyl ether at the same temperature. By switching the solvent to isopropyl acetate which has a higher boiling point, a higher temperature can be used and (S)-**103** was racemised by nearly 80% in 16 minutes (Table 2.10, entry 9). Some of the solvent systems used in the flow racemisation study were also found to be the solvent of choice for the diastereomeric resolution of

the corresponding racemic substrate, which will be discussed further in Chapter 3.

## 2.4 Attempted reactivation of immobilised SCRAM 92

As part of a collaborative project with our group, Syngenta studied the deactivation of immobilised catalyst **92** by monitoring the racemisation of (S)-**39** in continuous flow for 10 days (Fig. 2.22). The approximate rate of deactivation was about 6.5% per day under the employed reaction conditions.

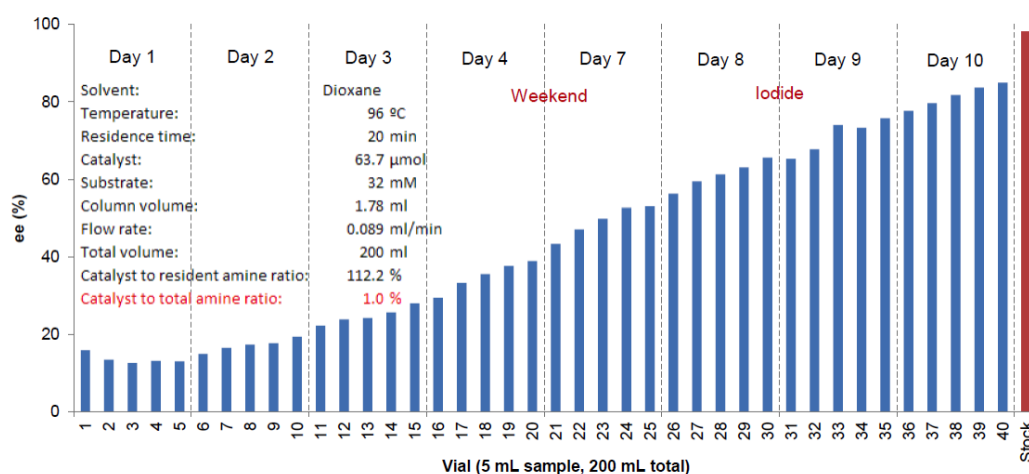
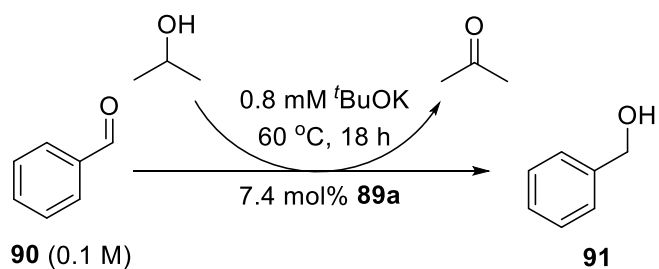


Fig. 2.22 Deactivation study of **92** via continuous flow racemisation of (S)-**39**. Data was provided by L. Conway from Syngenta

As discussed in Section 2.2.1, one of the plausible mechanisms for the deactivation of homogeneous SCRAM **64** is the binding of small amines to the iridium centre such as methylamine, which is one of the by-products from the hydrolysis of imine **94** formed from the racemisation of **39**. Spiking excess methylamine into the racemisation of **39** led to the inhibition of the reaction, whilst the titration of **64** with methylamine showed the formation of various Ir-MeNH<sub>2</sub> species **95** to **97** and the disappearance of **64** in the presence of excess methylamine. Nguyen et al. previously reported the deactivation of immobilised [Cp\*IrCl<sub>2</sub>]<sub>2</sub> **89a**, the chloro-version of **92**, after repeated use in the transfer hydrogenation of benzaldehyde **90** in batch using isopropyl alcohol in the presence of potassium *tert*-butoxide as the base (Scheme 2.16).<sup>139</sup>

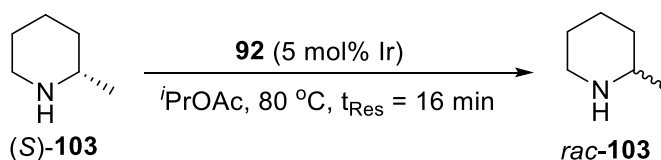


Scheme 2.16 Catalytic transfer hydrogenation of benzaldehyde **90** by isopropyl alcohol using **89a** as the pre-catalyst in batch

Alkoxide ions from both the added base and deprotonated isopropyl alcohol bind to the iridium centre and replace all the chloride ions. The strong Ir-OR bonds do not allow the substrate to bind, preventing the catalyst from turning over. Temporary reactivation was achieved by stirring the **89a** with 1 M hydrochloric acid, which protonated the bound alkoxide ligands that can dissociate more readily, allowing the substrate to bind again. In an analogous fashion, methylamine can replace the iodide ligands in homogeneous SCRAM **64**/immobilised catalyst **92** easily and the bound methylamine can be difficult to dissociate from the iridium due to its small size, hindering the binding of any incoming substrates. A similar strategy of reactivating **92** was attempted using hydroiodic acid, which should protonate the bound amines, making them more labile and allow the iodide ions to bind back to the iridium. The iodide is important to the catalytic activity of **64**/ **92** as shown from the racemisation of (*S*)-**9** by  $[\text{Cp}^*\text{IrCl}_2]_2$  **63** which led to 12 times slower reaction with increased concentrations of imine **8** and isoquinoline **65**.<sup>1</sup>

#### 2.4.1 Reactivation of immobilised SCRAM **92** by hydroiodic acid

Reactivation of **92** was studied using the catalyst that was previously used in the Resolution-Racemisation-Recycle ( $R^3$ ) process of **101** which will be discussed in detail in Chapter 3. Its activity was assessed *via* the racemisation of (*S*)-**103** in flow (Scheme 2.17). The average ee of **103** after one pass through the catalyst was 64% which was significantly lower than that of a fresh batch (21%).



Scheme 2.17 Racemisation of (S)-**103** in flow to assess the activity of **92**

In the R<sup>3</sup> process of **101**, about 13% of acetophenone **51** was observed, indicating the hydrolysis of the intermediate imine **102**, which also generated isopropylamine as the by-product. Although it is more bulky compared to methylamine, it can also bind to the iridium, reducing the activity of the catalyst similar to the case for methylamine.

Reactivation of the partially deactivated **92** was attempted with relatively mild conditions, in which the catalyst/ sand mixture (27 mg mL<sup>-1</sup> of **92**) was stirred in aqueous hydroiodic acid solution (0.1 M) at room temperature for two hours. The reaction was carried out in batch since hydroiodic acid can corrode the stainless steel column. After the reaction, the slurry was washed with isopropyl alcohol/ water mixture and decanted. The washing process was repeated until pH of the decant became neutral. The solid was further washed with isopropyl alcohol and dried in the vacuum oven. The treated **92**/ sand mixture was reloaded into the stainless column and its activity was checked by performing the racemisation of (S)-**103** in flow. The ee of **103** decreased to an average of 46% which indicated an increase in the catalytic activity of **92** (Fig. 2.23). The reactivation procedure was repeated with the same batch of **92** with more concentrated hydroiodic acid and was treated for a longer time. The results are shown in Fig. 2.23.

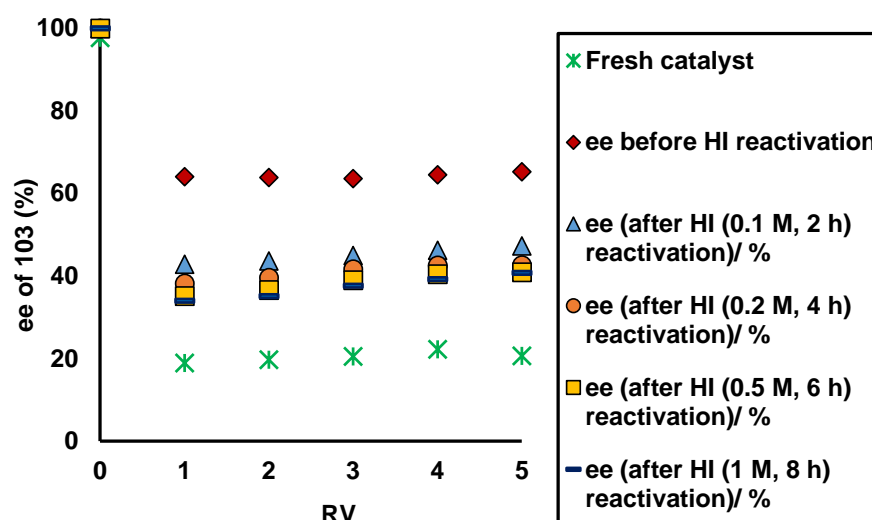
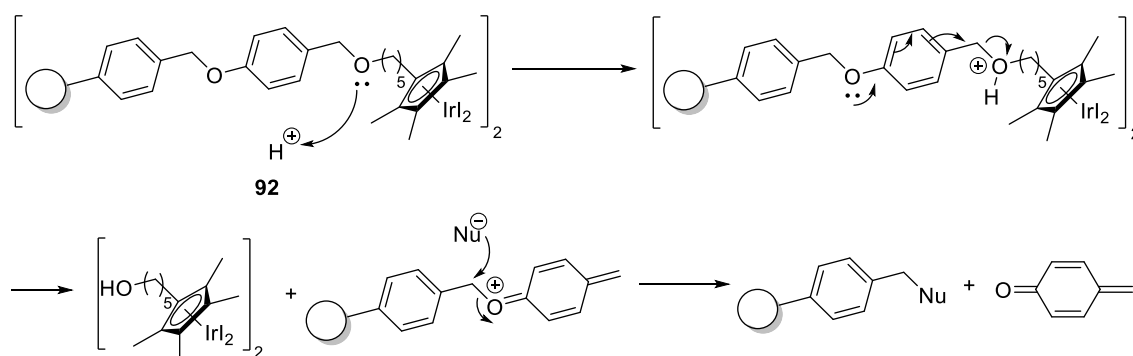


Fig. 2.23 Catalytic activity of partially deactivated **92** after treatment with various concentrations of HI (aq)

Further treatment of **92** with higher concentrations of hydroiodic acid only led to slight increase in its activity. When the column was heated up to 80 °C during the equilibration with isopropyl acetate before carrying out the racemisation of (S)-**103**, the eluent was yellow in colour which became colourless again when more solvent was pumped through. This indicated that the iridium might have leached from the support. Although acid can aid the removal of amine ligands from the catalyst, treatment of **92** with strong acid can also cleave the tether of **92** (Scheme 2.18). The ICP of **92** was not checked after the reactivation procedures, therefore the extent of leaching, if any, could not be quantified.



Scheme 2.18 Plausible mechanism of iridium leaching from **92** in the presence of acid

The reactivation procedures were repeated using immobilised catalyst **92** that was fully depleted. This was prepared by pumping an isopropyl acetate solution of methylamine (0.2 M) through an old batch of **92** at 80 °C with  $t_{Res}$  of 6.7 hours

for about 4 days. The average ee of amine **103** after one pass was 82% (from 100%), so it still showed some activity. The catalyst was stirred in hydroiodic acid (1 M) for 8 hours, then overnight. The racemisation profiles of (*S*)-**103** are shown in Fig. 2.24.

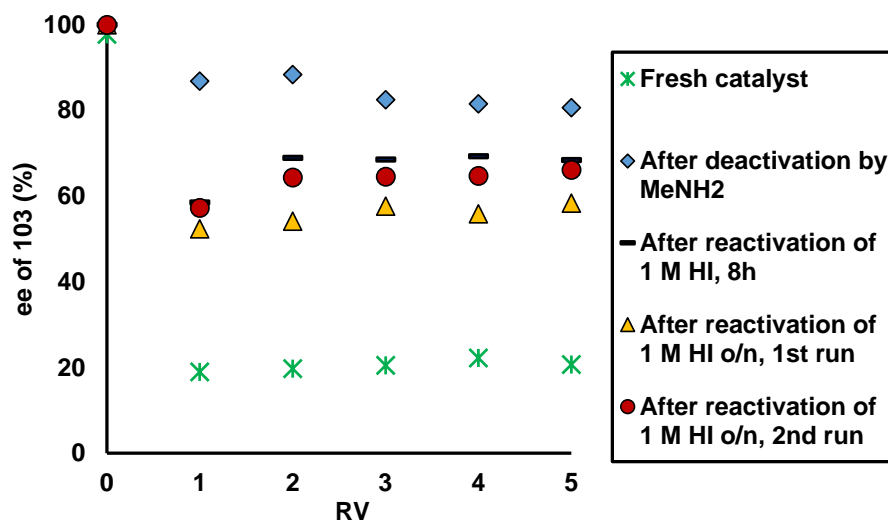


Fig. 2.24 Catalytic activity of 'fully deactivated' **92** after treatment with 1 M HI (aq)

The average ee of amine **103** decreased from 82% to 69%, showing some catalyst reactivation. Increasing the time the catalyst was stirred with hydroiodic acid from 8 hours to overnight led to further decrease of ee from 100% to 57%. However, the activity of catalyst **92** fell when the racemisation of (*S*)-**103** was repeated, where the ee of amine **103** was increased to 65% rather than 57%. Iridium might have started to leach upon prolonged treatment with hydroiodic acid.

#### 2.4.2 Proton NMR titration of methylamine-bound SCRAM **64** with hydroiodic acid

In order to understand the reactivation of immobilised catalyst **92** with hydroiodic acid, initial titration experiments were done with methylamine-bound **64**. The homogeneous SCRAM **64** was first treated with 20 equiv. of methylamine (in methanol, 2 M) in *d*<sub>6</sub>-DMSO, then aqueous hydroiodic acid (1.5 M) was added and the sample was analysed by <sup>1</sup>H NMR spectroscopy (Fig. 2.25). The integrated Cp\* and CH<sub>3</sub>NH<sub>2</sub> peaks were plotted against the equivalences of hydroiodic acid (Fig. 2.26).

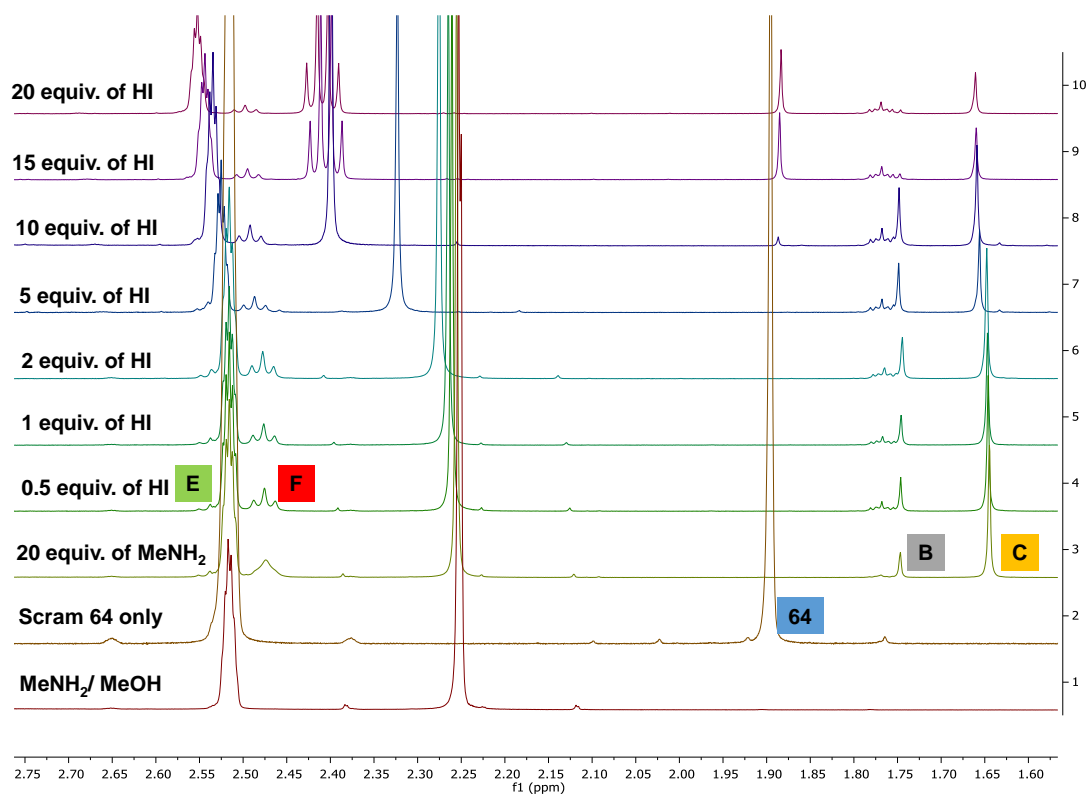


Fig. 2.25  $^1\text{H}$  NMR titration of  $\text{MeNH}_2$ -bound **64** with HI (1.5 M) in  $d_6$ -DMSO.  $\text{MeNH}_2/\text{MeOH}$  (2 M, 20 equiv. with respect to Ir) was added to **64** prior to the addition of HI. Benzene was added as the internal standard (7.38 ppm, not shown above)

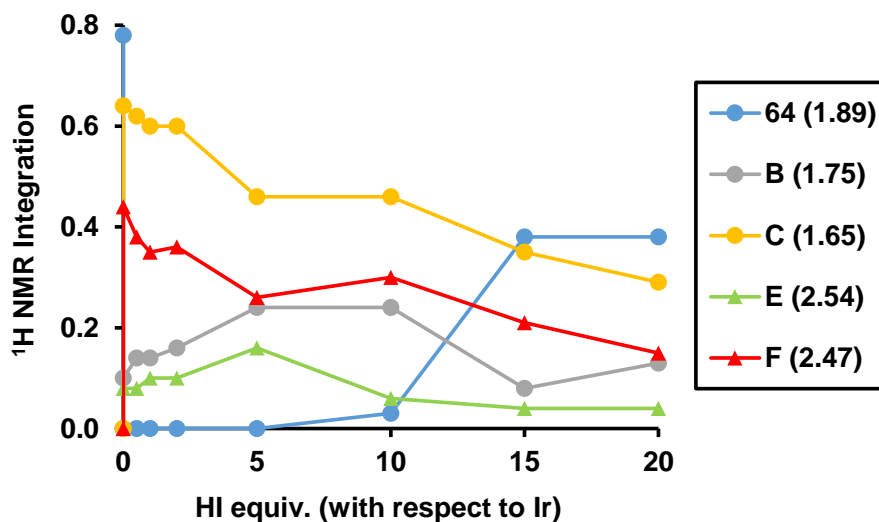
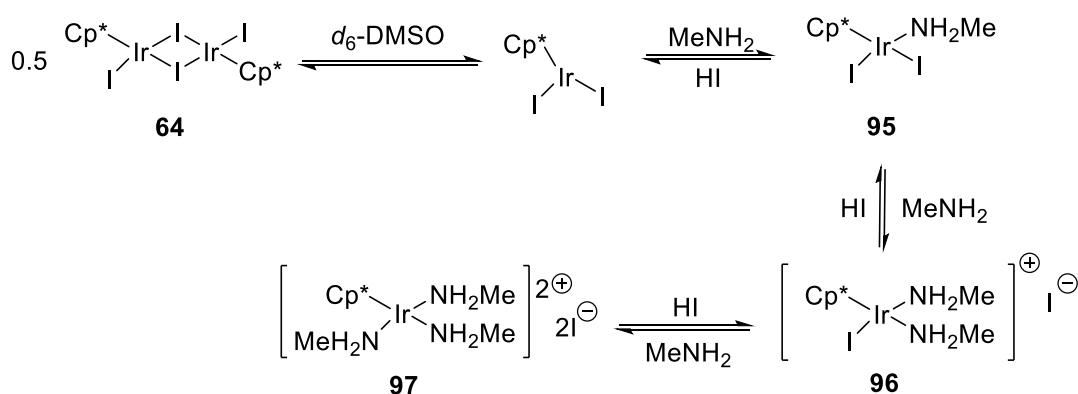


Fig. 2.26  $^1\text{H}$  NMR Integrations of  $\text{CH}_3\text{-Cp}^*$  and coordinated  $\text{CH}_3\text{-NH}_2$  in the titration reaction of HI (aq) into **64** in  $d_6$ -DMSO. All integrations were based on benzene which was added as the internal standard. **B** and **C** correspond to the  $\text{Cp}^*$  protons of di-substituted Ir- $\text{MeNH}_2$  species **96** and tri-substituted Ir- $\text{MeNH}_2$  species **97** respectively; **E** and **F** correspond to the methyl protons of the bound  $\text{CH}_3\text{NH}_2$  of **96** and **97** respectively

As shown in Section 2.2.1(b), the addition of excess methylamine to **64** led to the formation of di- and tri-methylamine-bound iridium species (**96** and **97** respectively), whilst **64** and the mono-substituted species **95** disappeared completely. When aqueous hydroiodic acid was added to the sample, the singlet signal corresponding to **97** (1.65 ppm) started to decrease whilst that of **96** (1.75 ppm) increased. These changes were accompanied by a fall and an increase in the integrations of the bound- $\text{CH}_3\text{NH}_2$  signals at 2.47 and 2.54 ppm respectively. After 10 equiv. of hydroiodic acid was added, a singlet at 1.89 ppm was observed which became more intense when more acid was added. However, the  $\text{CH}_3\text{NH}_2$  signal corresponding to mono-methylamine-bound species **95** was not observed. Also the titration experiment of **64** with methylamine showed that the concentration of species **95** remained low and did not accumulate in the system (Fig. 2.8 and Fig. 2.9). Therefore, it was suggested that the signal at 1.89 ppm corresponded to the dimer **64**. The addition of hydroiodic acid protonated the bound-methylamine, causing it to dissociate from the iridium to regenerate the less/ non-substituted species (Scheme 2.19).



Scheme 2.19 Interconversion of **64**, **95**, **96** and **97** in the presence of  $\text{MeNH}_2$  and  $\text{HI}$

We would like to determine which of the species **95**, **96** and **97** were active and inactive in racemisation. The concentration changes of the species were determined with excess methylamine and hydroiodic acid (Table 2.11). Based on the NMR titration experiments with the homogeneous catalyst **64** in excess methylamine, about 14% of **96** and 86% of **97** were formed, whilst no **64** or **95** was observed.



Species	Concentration (based on <sup>1</sup> H NMR integration, %)	
	MeNH <sub>2</sub> (20 equiv.)	HI (20 equiv.)
<b>64</b>	0	31
<b>95</b>	0	0
<b>96</b>	14	21
<b>97</b>	86	48

Table 2.11 Concentrations of **64**, **95**, **96** and **97** after addition of excess MeNH<sub>2</sub> and excess HI in the <sup>1</sup>H NMR titration experiment of **64**, calculated based on the integrations of NMR signals

When three methylamine are bound to the iridium, the species **97** formed is unlikely to be active towards racemisation. Furthermore, as there is no **64** or **95** was observed, the only species left is **96**. Since it has one iodide ligand that might be displaced by the incoming substrate, it could be responsible for any remaining activity.

We now sought to relate the activity of the homogeneous catalyst **64** to that of immobilised catalyst **92**. The activities of immobilised catalyst **92** before and after reactivation were expressed in terms of the conversion of (*S*)-**103** to (*R*)-**103** (Table 2.12).

Entry	Catalyst <b>92</b> batch	ee of ( <i>S</i> )- <b>103</b> (%)	( <i>S</i> )- <b>103</b> (%) <sup>[a]</sup>	Catalytic activity (Conversion of ( <i>S</i> )- to ( <i>R</i> )- <b>103</b> ) (%) <sup>[b]</sup>
1	Fresh	21	61	39
2	Deactivated with excess MeNH <sub>2</sub>	82	91	9
3	Reactivated with excess HI	57	79	21

Table 2.12 Catalytic activity of **92** before and after reactivation, expressed in terms of the conversion of (*S*)-**103** to (*R*)-**103** during racemisation. <sup>[a]</sup>Calculated as 50 + (ee/2).

<sup>[b]</sup>Catalytic activity = 100 – [(*S*)-**103**] (%)

When excess methylamine solution was pumped through immobilised catalyst **92**, its activity decreased from 39% (when it was fresh) to 9% (Table 2.12, entries 1 and 2). However, the catalyst still showed some activity, which indicated that the resulting species could still turnover. After reactivation of **92** with excess

hydroiodic acid, its activity increased from 9% to 21% (Table 2.12, entry 3), which could be due to the regeneration of **92** (or its monomer) and the immobilised equivalences of **96** from **97**. Only about 12% reactivation was observed, compared to about 52% reactivation of homogeneous catalyst **64**, as inferred from the NMR titration results of **64** (Table 2.11, the sum of [**64**] and [**96**]). This discrepancy might be explained by the nature and activity of species **64** and **92**. Immobilisation of **64** to the resin has a significant impact on the interaction between the catalyst and the amine, the ease of protonation of the methylamine and its ease of dissociation. Also, iridium might have leached from **92** after prolonged treatment with hydroiodic acid (as shown from the decline in activity in the second run of racemisation of (*S*)-**103** after overnight treatment of **92** with 1 M hydroiodic acid (Fig. 2.24)), so the increase in activity by excess hydroiodic acid was lower than expected.

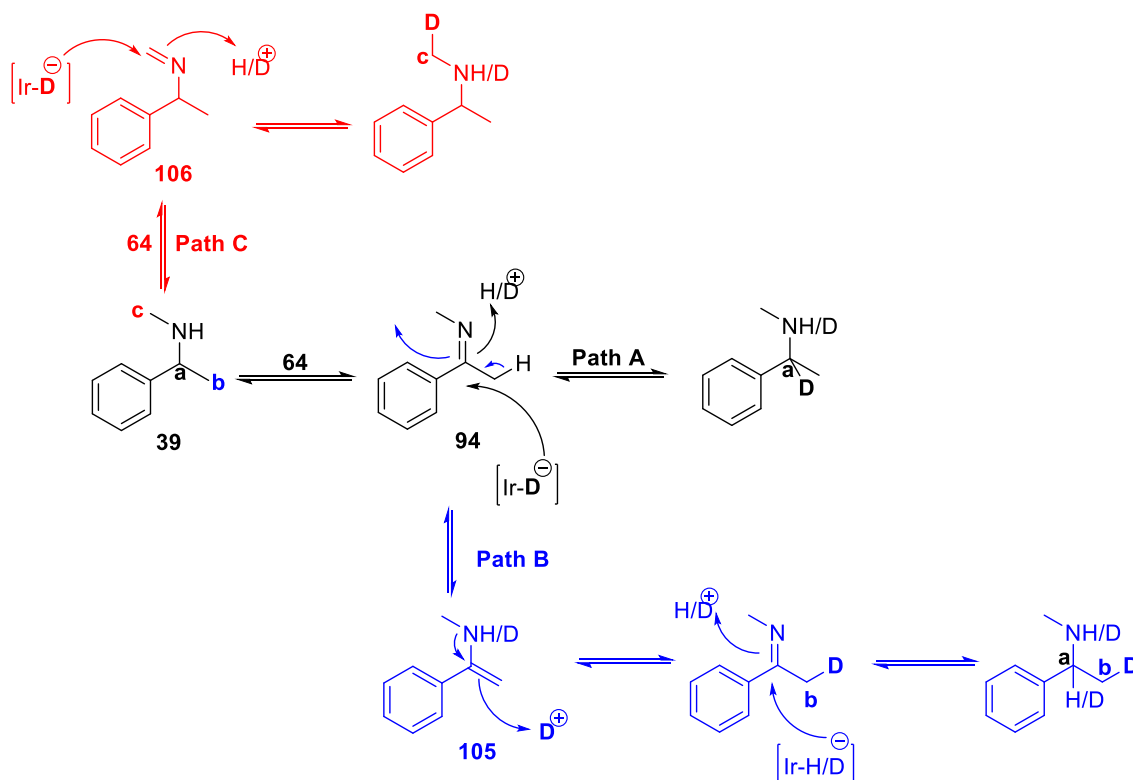
## 2.5 Rapid screening methodology for determining chiral amine racemisation

### 2.5.1 Background

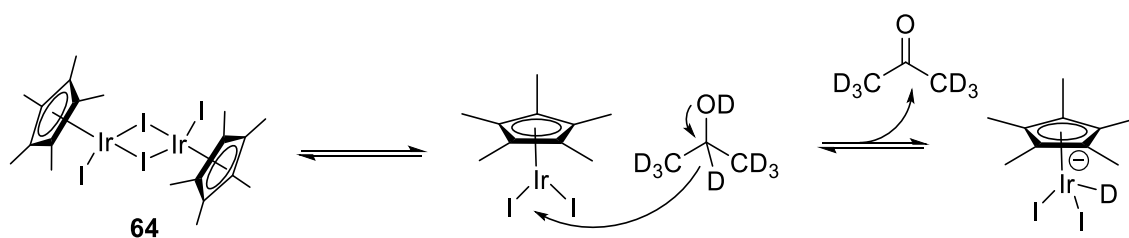
The traditional method in determining whether a chiral amine can be racemised under certain conditions is to carry out the racemisation reaction and analyse the ee of the amine. However this method requires enantiopure/ enantio-enriched material which can be expensive and/ or difficult to synthesise. Besides, analytical methods such as chiral GC, HPLC or NMR are needed to monitor the reaction but the development of these can be time-consuming and costly. Therefore, a more rapid and low cost procedure is highly desirable and a deuterium-labelling method was evaluated. Part of this work was carried out by an MChem student (Caitlin Davies). In addition to this, a deuterium/ proton exchange reaction of amine **39** in the presence of **64** and *d*<sub>8</sub>-isopropyl alcohol was studied by Syngenta as part of a collaborative project with our group.

The aim of the method was to correlate the replacement of the  $\alpha$ -hydrogen by deuterium into the amine with racemisation. One of the advantages of this method is that either the racemate or the enantiopure substrate can be used, depending on their availability. It was proposed that racemisation of **39** proceeds *via* the formation of imine **94** (Scheme 2.20). Deuterium incorporation can occur at

position **a**, if imine **94** is reduced by an iridium-deuteride species (Path A). The iridium-deuteride species can only be formed by oxidation of *d*<sub>8</sub>-isopropyl alcohol by **64** (Scheme 2.21). It can be inferred that because oxidation of the non-deuterated amine by **64** only results in iridium-hydride complex, to show deuterium incorporation at position **a**, the imine has to be de-coordinated from this complex and coordinate with an iridium-deuteride species, assuming no Ir-D and Ir-H exchange occurs. This provides important mechanistic information that the imine can de-coordinate from the iridium centre. Imine **94** can also tautomerise into enamine **105** to deuterate at position **b** (Path B). Reaction of a deuteron with the enamine is required, and the deuteron can come from *d*<sub>8</sub>-isopropyl alcohol, O-D. Deuterium incorporation at either positions **a** or **b** indicate the racemisation of **39**. Another alternative imine **106** can be formed by isomerisation of **94** or by direct oxidation of **39** by **64**, and deuteration can also occur at position **c** (Path C). However the formation of **106** does not indicate the racemisation of **39**. By locating the position of deuteration in the molecule, one can determine whether the amine can be racemised under the employed conditions.



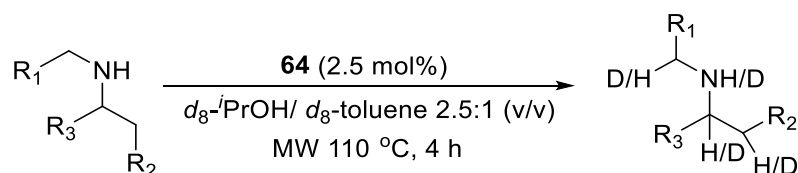
Scheme 2.20 Possible pathways of deuterium incorporation of **39**



Scheme 2.21 Formation of Ir-D complex from **64** via oxidation of  $d_8$ -*i*PrOD

## 2.5.2 Methodology and results

A deuteration procedure was developed by C. Davies in which 1 M of chiral amine was dissolved into a mixture of  $d_8$ -isopropyl alcohol/  $d_8$ -toluene (2.5:1 by volume) with 2.5 mol% **64**.<sup>140</sup> The reaction mixture was heated to 110 °C under pressure for 4 hours by microwave (Scheme 2.22).

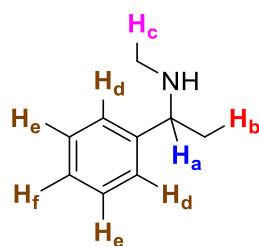


Scheme 2.22 General deuteration procedures of chiral amines by  $d_8$ -*i*PrOD

Proton/ deuterium exchange can be readily observed by  $^1\text{H}$  NMR spectroscopy since any deuterium incorporation leads to a decrease in integration of the corresponding signal. The reaction was sampled for  $^1\text{H}$  NMR analysis after each hour of heating. However, it is important to note that this method can only provide a qualitative indication on whether an amine can be racemised. During racemisation, the imine/ enamine can also pick up a hydride/ proton which does not result in any changes in the NMR integrations. Therefore, the rate of change of the NMR integrations due to deuterium incorporation does not quantitatively relate to the rate nor extent of racemisation.

### (a) *N*-Methyl- $\alpha$ -methylbenzylamine **39**

The deuteration procedure described in Scheme 2.22 was first tested with **39**. The  $^1\text{H}$  NMR spectra before and after heating are shown in Fig. 2.27.<sup>140</sup>



**39**

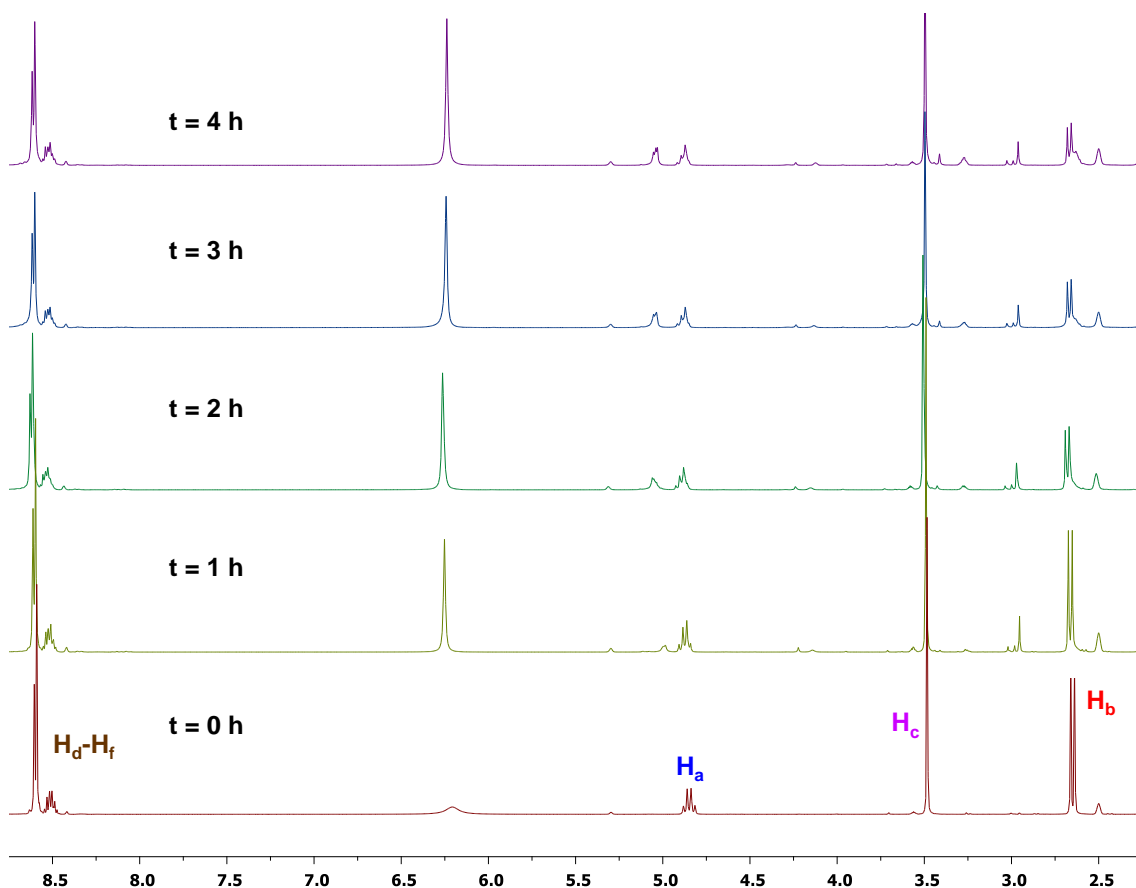


Fig. 2.27 <sup>1</sup>H NMR spectra for the H/ D exchange reaction of **39** with *d*<sub>8</sub>-*i*PrOD in the presence of **64**. The spectra were measured with a *d*<sub>6</sub>-DMSO insert<sup>140</sup>

The broad singlet at about 6.3 ppm was believed to be the OH of deuterated isopropyl alcohol (*d*<sub>7</sub>-*i*PrOH). A similar signal was present in all experiments with different amine substrates, including **46** which is a tertiary amine lacking an NH proton (Fig. 8.4). At t = 0, the amount of *d*<sub>7</sub>-*i*PrOH in the reaction mixture was minimal. When it was turning over the catalyst, proton-deuterium exchange occurred with the NH of the substrate, leading to increased concentration of *d*<sub>7</sub>-*i*PrOH, therefore the signal became more intense. Since no change in multiplicity was observed in H<sub>d</sub> to H<sub>f</sub>, there was no proton/ deuterium exchange occurred in the aromatic region and therefore, they were used as a reference for integrating

other signals and no internal standard was added to the reaction mixture (Fig. 2.28).

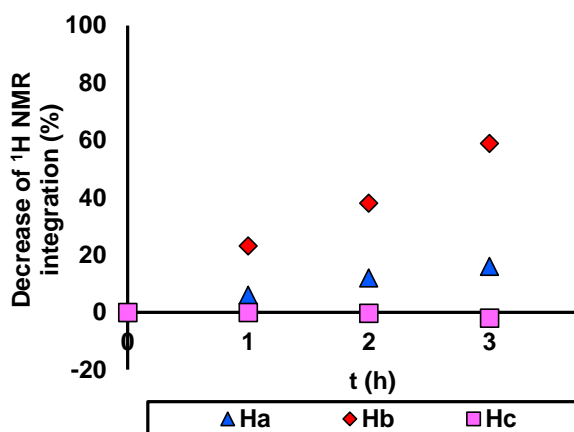


Fig. 2.28 Percentage drop in  $^1\text{H}$  NMR integrations of  $\text{H}_a$  to  $\text{H}_c$  of **39** with time (h).  $\text{H}_d$  to  $\text{H}_f$  were used as reference and integrated to be 5.00 in every sample, assuming no H/ D exchange occurred at the aromatic region.  $\text{H}_d$ ,  $\text{H}_e$  and  $\text{H}_f$  were not shown

The most significant change in integration was observed for  $\text{H}_b$  which dropped by 70% after 4 hours, indicating that deuterium incorporation occurred most rapidly at position **b** resulting from the formation of enamine **105**.  $\text{H}_a$  also showed a drop in integration by 21%, therefore deuterium incorporation also occurred at position **a**. This implies that most of the imine **94** remains coordinated to the iridium-hydride complex while only some de-coordinates from it and binds to another iridium complex possessing a deuteride. On the other hand, the integration of  $\text{H}_c$  stayed virtually constant throughout the reaction and no deuterium/ proton exchange happened at position **c**. The oxidation of an *N*-methyl is energetically unfavourable. Furthermore, since the C=N bond in imine **106** is not conjugated to the aromatic ring, it is thermodynamically less stable than **94** and therefore not formed.

### (b) Other substrates

The proton/ deuterium exchange reaction was further used to assess the deuterium incorporation pattern of various chiral amines and determine their ability to racemise by **64** under the applied conditions (Fig. 2.29).

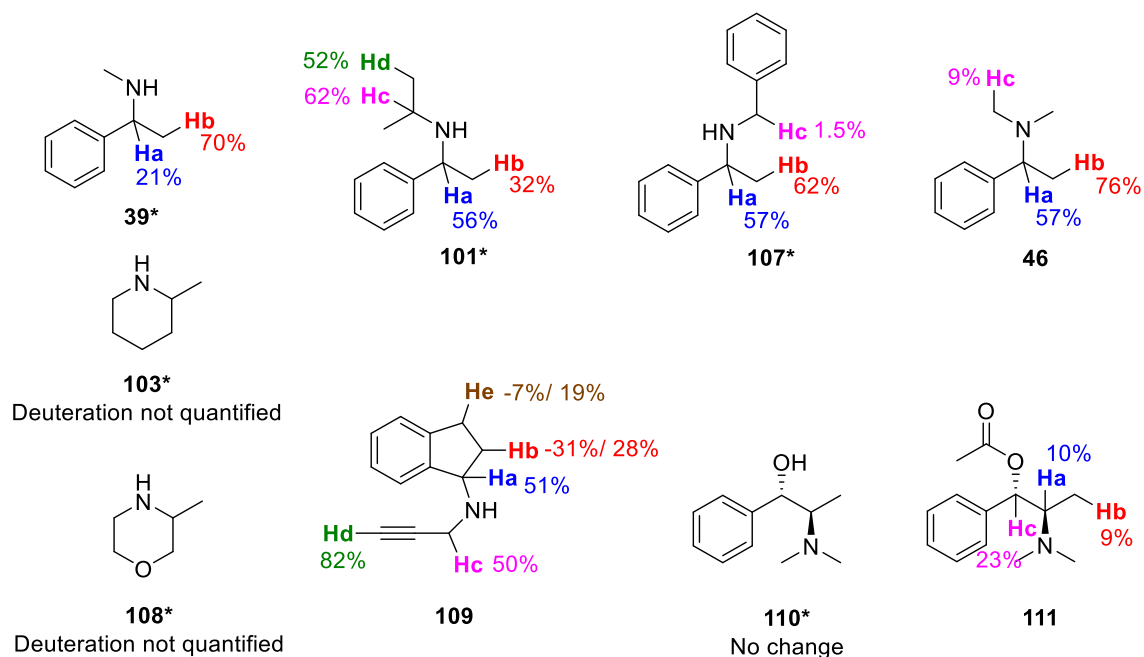
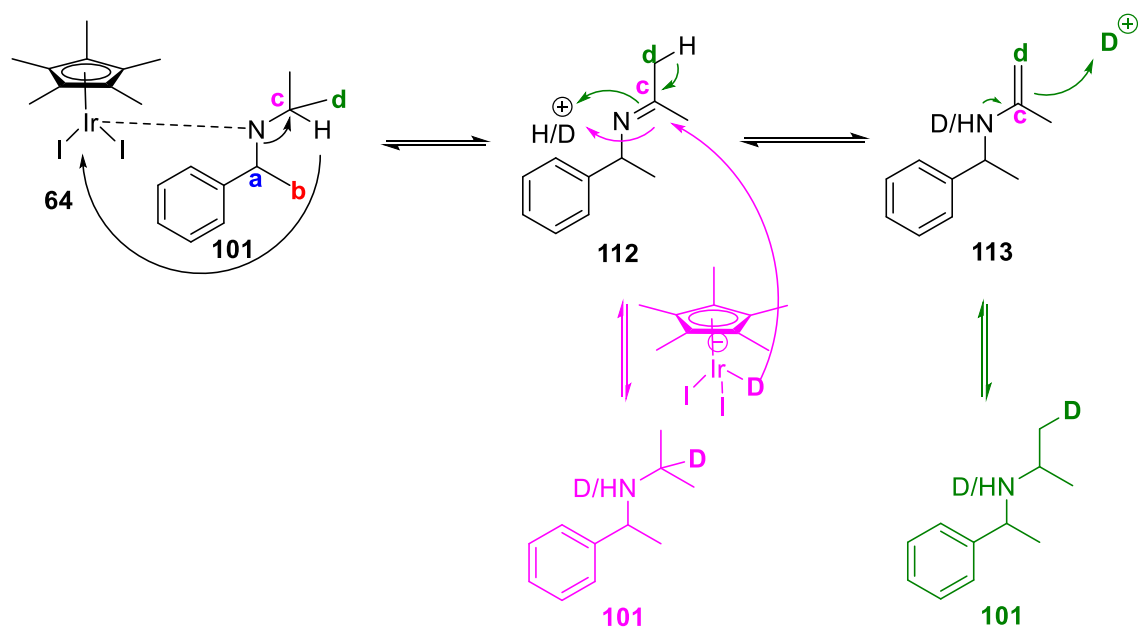


Fig. 2.29 D-incorporation pattern of various substrates. The percentages of deuteration were determined by  $^1\text{H}$  NMR. \*Results were obtained by C. Davies

### (i) Benzylic acyclic amines **101**, **107** and **46**

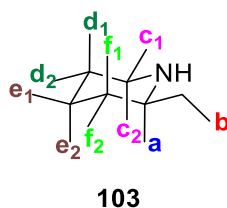
Amines **101**, **107** and **46** were structurally similar to **39**. All showed deuteration at positions **a** and **b**, indicating the formation of the corresponding imine and enamine which are responsible for their racemisation. However, the degree of deuteration at position **a** is higher (> 55%) than that of **39**. This may be because they have more bulky structures than **39**, and their imine intermediates cannot bind to the iridium-hydride complex as strongly, and are more likely to de-coordinate and interact with an iridium-deuteride species. Substrate **101** also showed a high degree of deuteration at position **c**, which is much less significant for **107** and **46**, and was not observed for **39**. This implies the occurrence of dehydrogenation of **101** at the isopropyl group at position **c**. Imine **112** is formed which is more stable compare to those formed from position **c** in **39**, **107** or **46**, due to the presence of two electron-donating methyl substituents adjacent to the C=N bond (Scheme 2.23). Tautomerisation of **112** into enamine **113** led to proton/deuterium exchange at position **d**.



Scheme 2.23 Formation of imine **112** and enamine **113** which accounts for the D-incorporation at positions **c** and **d** of **101** respectively

## (ii) Non-benzylic cyclic amines **103** and **108**

Non-benzylic cyclic secondary amines **103** and **108** were also tested using this procedure. The <sup>1</sup>H NMR spectra of 2-methylpiperidine **103** were shown in Fig. 2.30. The signals of different protons are relatively close to one another in the region of 2.7 to 1.9 ppm. They also become broader and less resolved upon proton/ deuterium exchange, resulting in much less reliable integrations.





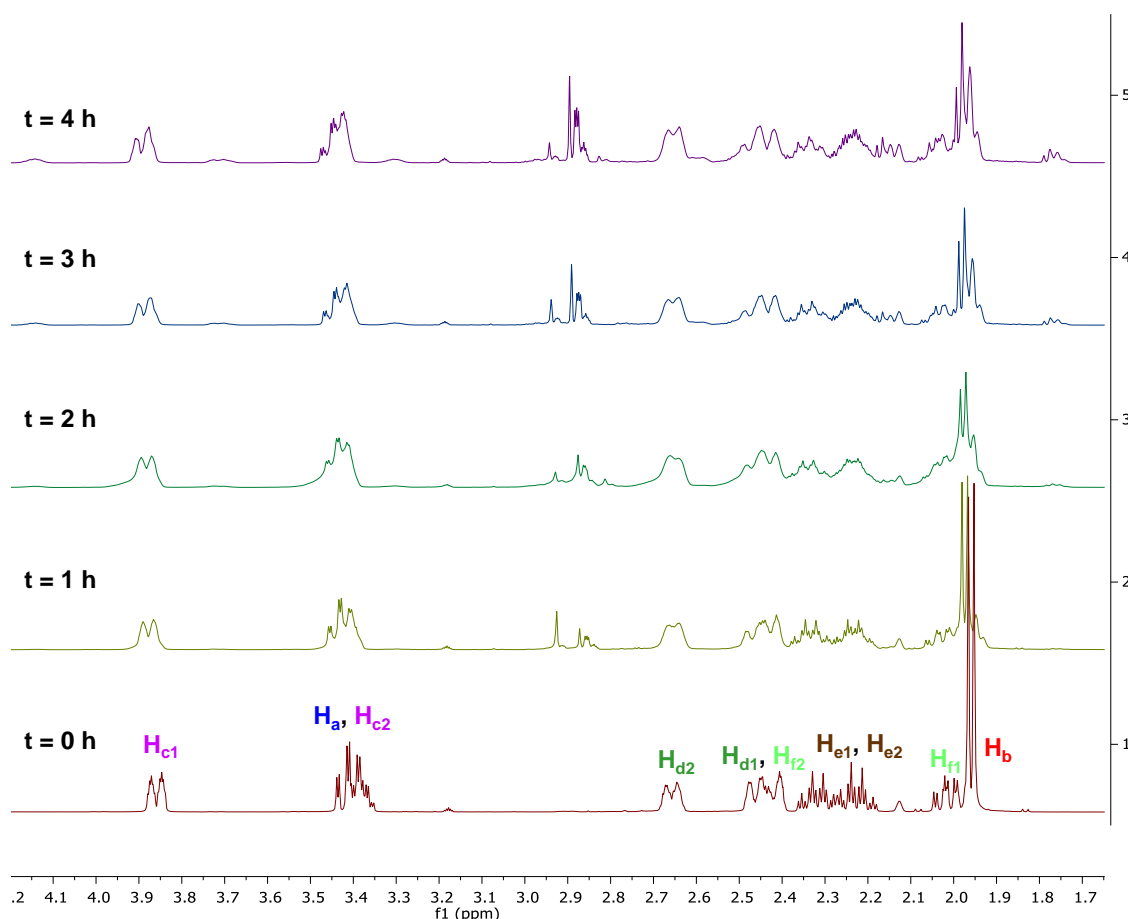
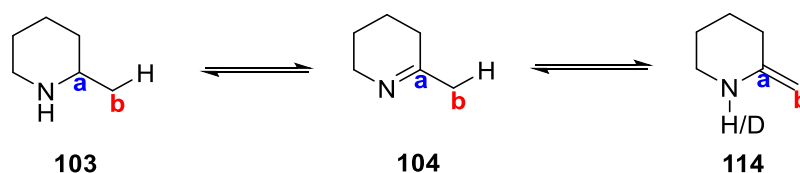


Fig. 2.30  $^1\text{H}$  NMR spectra for the H/ D exchange reaction of **103** with  $d_8$ -iPrOD in the presence of **64**<sup>140</sup>

Based on the visual inspection of the spectra, there was a significant decrease in the integration of the methyl group signal ( $\text{H}_b$ ), indicating possible deuterium incorporation of the corresponding enamine **114** (Scheme 2.24). Under the reaction conditions, amine **103** can be racemised, which is apparent from the racemisation reactions of **103** discussed in Sections 2.2.6 and 2.3.3.



Scheme 2.24 Formation of imine **104** from **103** and its tautomerisation to enamine **114**

For 3-methylmorpholine **108**, the proton signals are better separated than those of **103** (Fig. 2.31). However overlapping of signals is still observed and the lack

of a suitable internal standard also made the quantitative comparison of integrations difficult.

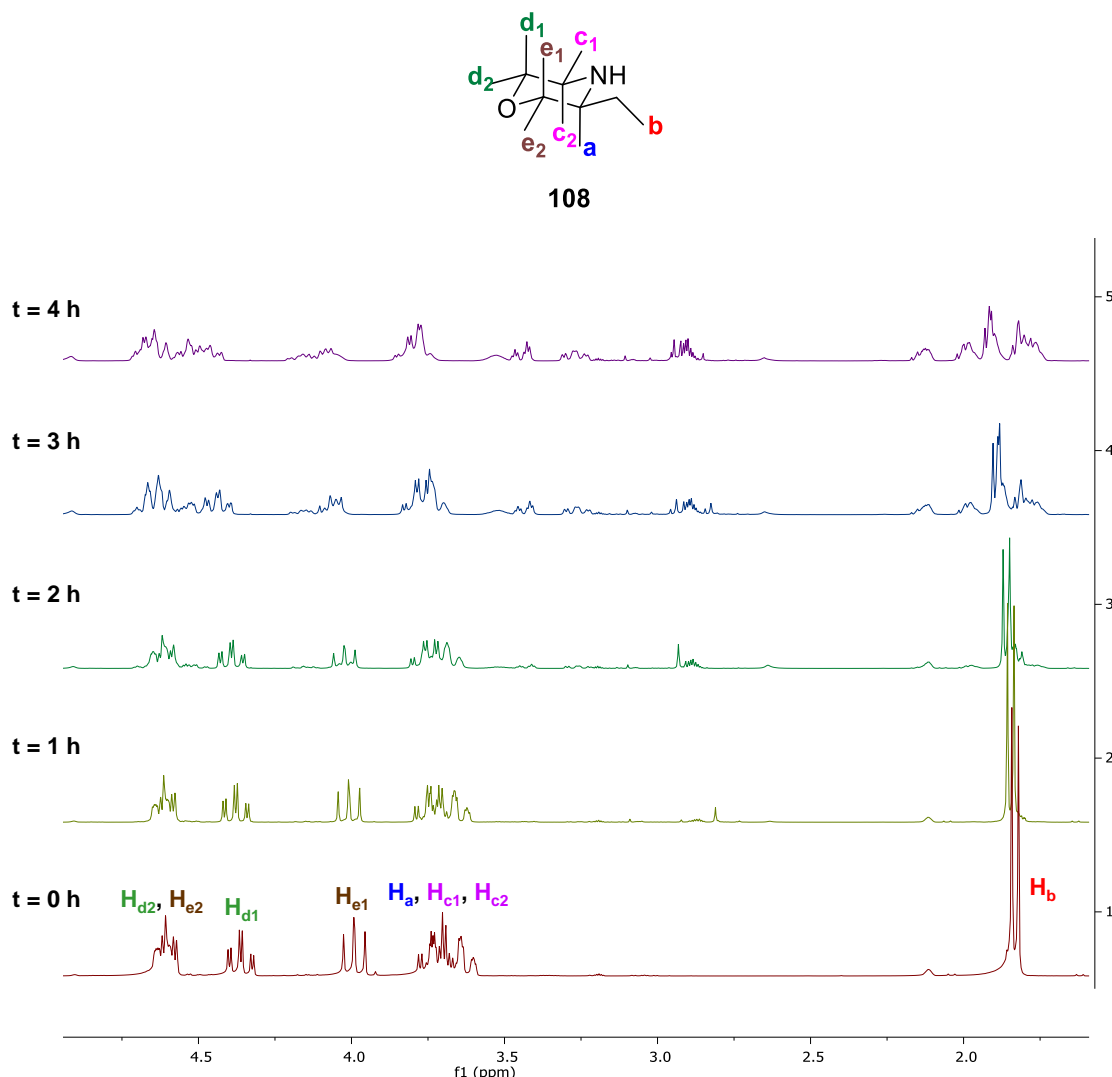
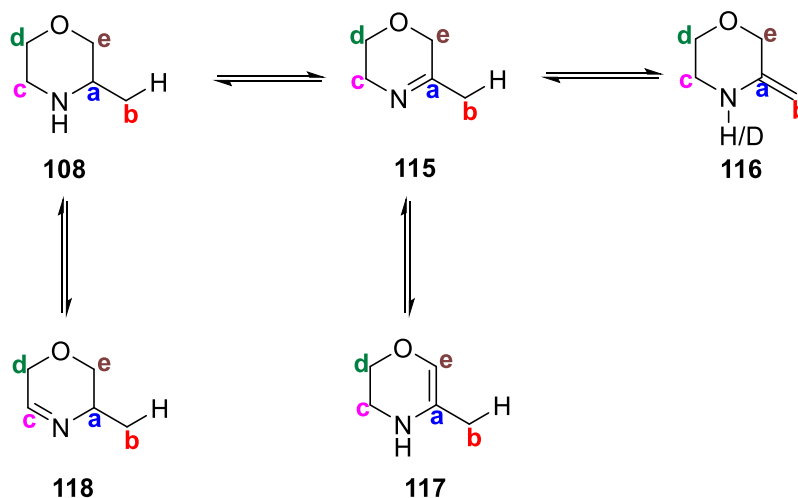


Fig. 2.31  $^1\text{H}$  NMR spectra for the H/ D exchange reaction of **108** with  $d_8$ -*i*PrOD in the presence of **64**<sup>140</sup>

Nevertheless, visual inspection of the spectra showed a significant decrease in the integration of the methyl signal ( $H_b$ ) which indicated its deuteration due to the formation of enamine **116** from imine **115**, similar to that of **103** (Scheme 2.25). Therefore amine **108** can likely be racemised by SCRAM **64** under these conditions. The multiplet at 3.69 ppm corresponds to the NCH protons  $H_a$ ,  $H_{c1}$  and  $H_{c2}$  which showed a decrease in integration visually. Due to the overlap of signals of these protons, it was difficult to confirm exactly which proton was exchanged. However imine **115** was more stable and more likely to form than imine **118**,  $H_a$  was more readily exchanged with the deuteride. The dd signal at

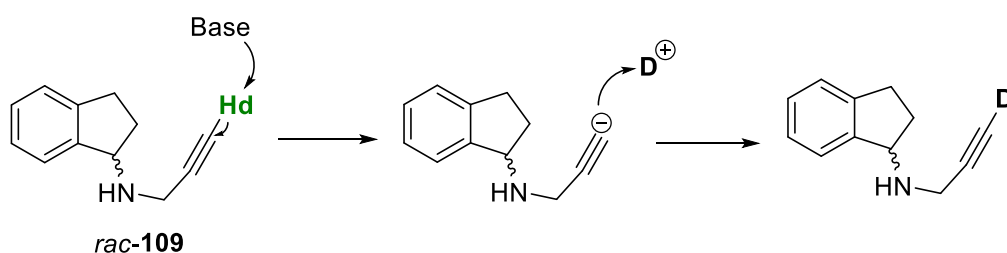
3.98 ppm correspond to one of the OCH protons ( $H_{e1}$ ) which also showed a drop in integration. This may indicate the formation of enamine **117** from imine **115**.



Scheme 2.25 Formation of imines **115** and **118** from **108** and tautomerism of **115**

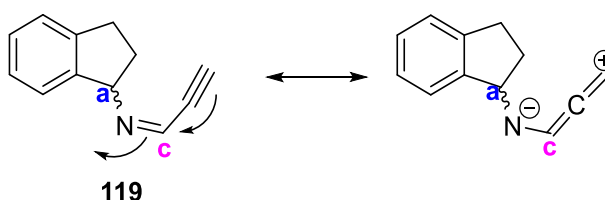
### (iii) Rasagiline (*R*)-**109**

Rasagiline, (*R*)-**109** is an irreversible inhibitor of monoamine oxidase-B used to treat Parkinson diseases.<sup>141, 142</sup> It is interesting to test if (*R*)-**109** can be racemised using SCRAM **64**, which will allow the use of resolution-racemisation-recycle ( $R^3$ ) methodology for its synthesis. Using the proton/ deuterium exchange procedure on *rac*-**109**, deuteration was observed mainly at position **d** since  $H_d$  is the most acidic proton which exchanges readily with any deuterium in the system (Scheme 2.24).



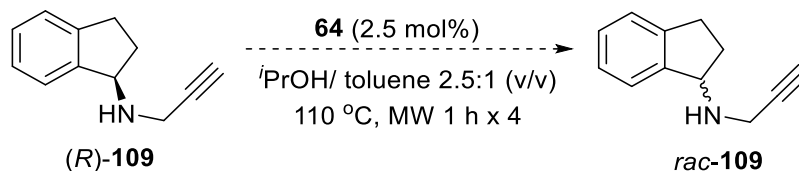
Scheme 2.26 H/ D exchange at position **d** of **109**

Positions **a** and **c** were also found to deuterate by about 50%. Imine **119** formed from **c** is relatively stable due to its conjugation with the alkyne group, resulting in deuterium incorporation at **c** (Scheme 2.27). However it does not correspond to any racemisation of **109**.



Scheme 2.27 Stabilisation of imine **119** via conjugation with the adjacent alkyne group

On the other hand, deuteration at **a** may indicate the possibility of racemisation under the employed conditions. For positions **b** and **e**, the two protons at each position showed both an increase and decrease in integrations. It was unclear where deuteration took place. To confirm if **109** can be racemised by **64**, a batch racemisation was attempted using the same conditions as the proton/ deuterium exchange experiment, with the use of non-deuterated solvents (Scheme 2.28).



Scheme 2.28 Attempted racemisation of *(R)*-**109** in batch using **64** (2.5 mol%) in *i*PrOH/ toluene (2.5:1 by volume) in 110 °C by microwave heating

No racemisation was observed after 4 hours. However the concentration of **109** decreased to only 27% which indicated the formation of side-products (Fig. 2.32). The impurities could not be identified from GC/ GCMS. From this, it was suspected that the decrease in integrations of some of the proton signals might be due to formation of the side products instead of deuterium incorporation. On the other hand, some of the newly formed peaks in the NMR may also overlap with other signals, resulting in an increase in integrations which makes the NMR interpretation more difficult.

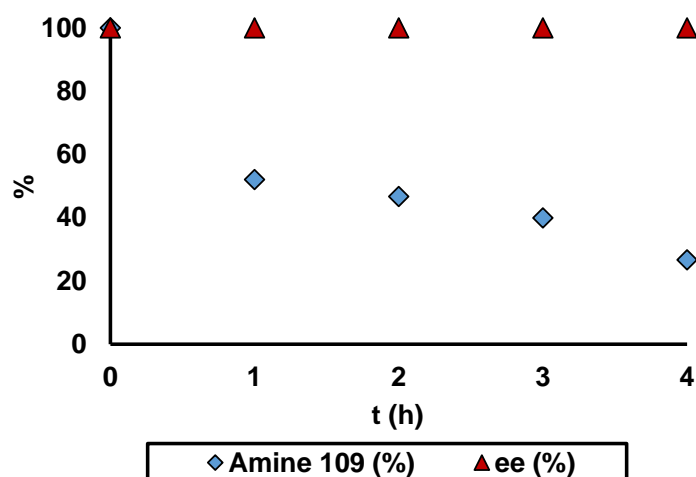
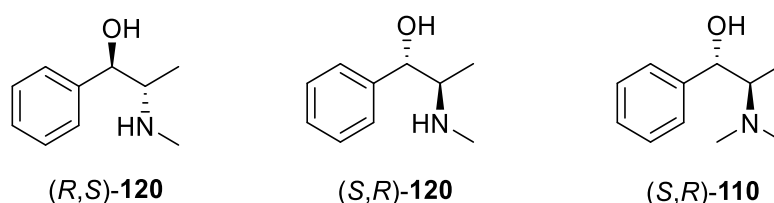


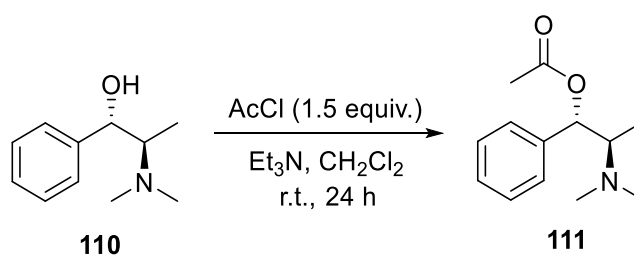
Fig. 2.32 Reaction profile of the attempted racemisation of (*R*)-**109** using **64** (2.5 mol%) in *i*PrOH/ toluene (2.5:1 by volume) at 110 °C by microwave heating

#### (iv) Ephedrine and derivatives

Ephedrine (*R,S*)-**120** and pseudoephedrine (*S,R*)-**120** are bronchodilators and prevent low blood pressure.<sup>143</sup> They are diastereomeric amino-alcohols and may be useful to understand if the amino group can be racemised by **64** in the presence of the hydroxyl group. The proton/ deuterium exchange experiment was carried out on the *N*-methyl derivative of **120**, (*1S,2R*)-*N*-methylephedrine **110**, and was found to have no change in the integrations of the <sup>1</sup>H NMR signals. The substrate **110** can act as a bidentate ligand in asymmetric transfer hydrogenation, in which both the hydroxyl and amino groups coordinate to the iridium centre, deactivating the catalyst towards racemisation.<sup>144</sup>

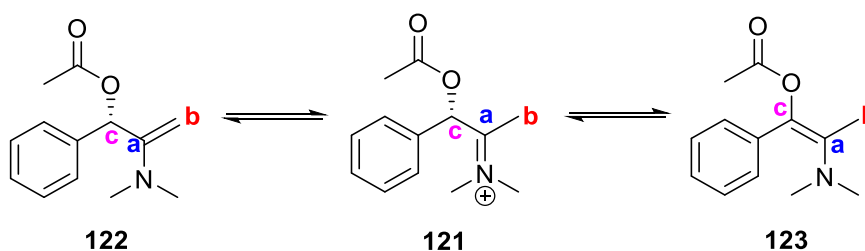


To block the hydroxyl group and prevent it from binding to the iridium, (*S,R*)-**110** was acetylated at the hydroxyl group, converting it into **111** (Scheme 2.29). The proton/ deuterium experiment was repeated and was heated in the microwave for 6 hours.



Scheme 2.29 Synthesis of **111** via acetylation of the hydroxyl group of **110**

The proton signals at positions **a**, **b** and **c** showed a decrease in integrations. However the changes in NMR integrations were relatively small, the degree of deuteration was only about 10%. Since **111** is non-benzylic, imine **121** formed from the dehydrogenation at position **a** was not stabilised. Besides, the presence of the electron-withdrawing ester group may destabilise the C=N bond and its formation is less favoured. Enamines **122** and **123** are formed upon the tautomerisation of imine **121** (Scheme 2.30). Enamine **123** is much more stable than **122** due to the neighbouring benzyl group. A higher level of deuteration was observed at position **c** (23%) than position **b** (9%). The overall result indicated that **111** may be able to epimerise at both the amino and acetylated hydroxyl chiral centres by **64** under similar reaction conditions. However the actual racemisation experiment is needed to confirm this.

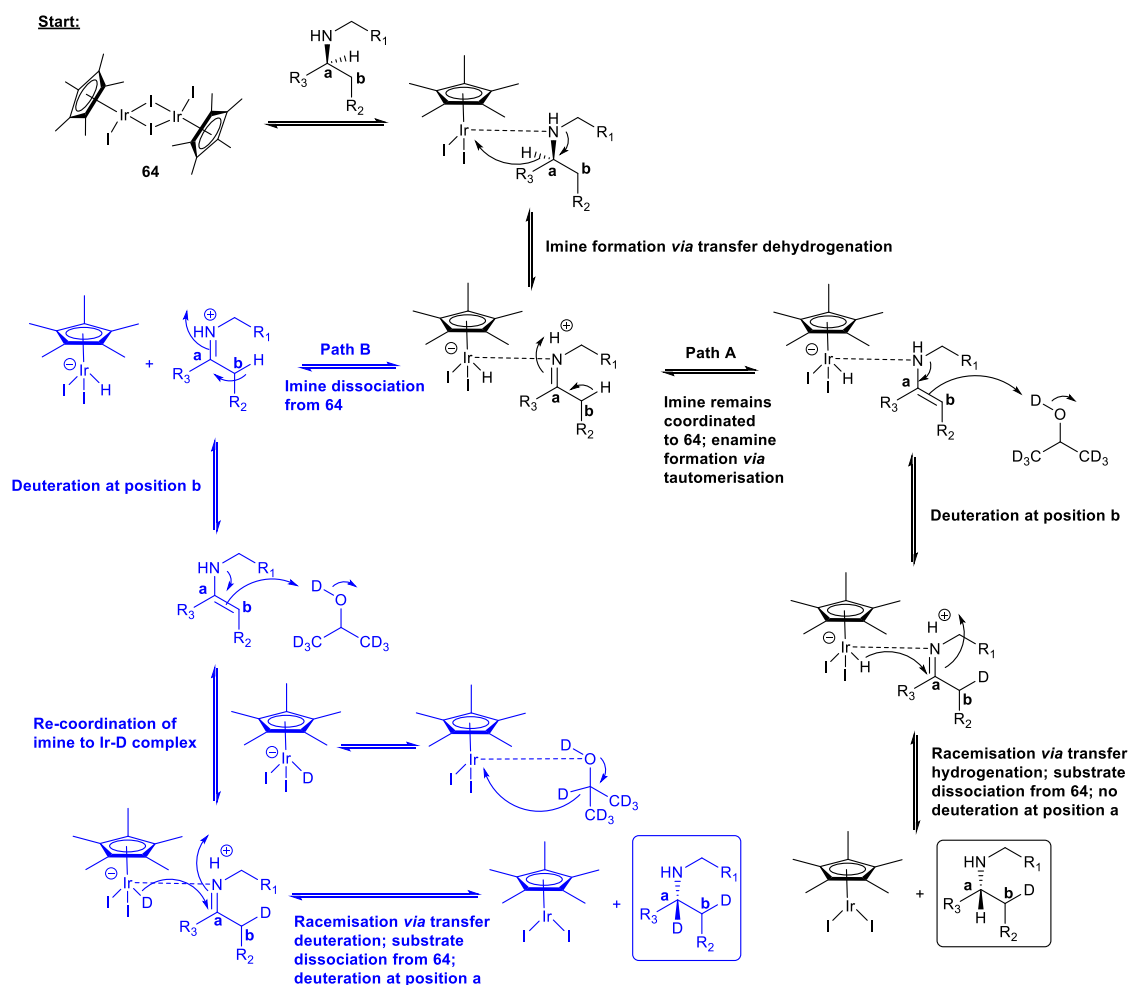


Scheme 2.30 Tautomerisation of imine **121**

### 2.5.3 Proposed mechanism

The  $^1\text{H}$  NMR proton/ deuterium exchange method for determining the racemisation of chiral amines confirmed the formation of an imine as the intermediate during racemisation. The imine can remain coordinated or de-coordinated from the iridium centre of the catalyst, which may depend on the size of the imine/ amine substrate. The imine also tautomerises into the enamine. The mechanism leading to deuterium incorporation at positions **a** and **b** are

summarised in Scheme 2.31, which also corresponds to the plausible mechanism of racemisation.



*Scheme 2.31 Plausible mechanism of H/ D exchange at positions **a** and **b** of a chiral amine in the presence of **64**. A generic structure of an enantiomerically pure amine was shown to illustrate its racemisation via the same pathways. Pathway A led to deuteration at position **b**; pathway B led to deuteration at both positions **a** and **b***

## 2.5.4 Limitations

The newly developed deuteration procedure provides a rapid method to determine if a chiral amine can be racemised by homogeneous SCRAM **64** (and potentially by immobilised SCRAM **92**) without the need to carry out the actual racemisation which requires enantio-enriched material and a chiral analytical method. However upon deuteration, both chemical shifts and multiplicities of the signals will change which can affect the accuracy in determining their integrals. Conversion of the substrate to unknown side-products can also result in the change of integrations, leading to misinterpretations of the spectra. For more

complicated structures, overlapping of signals of both substrate and product are readily observed, which makes the assignment and integrations of individual signals difficult. Another problem is that there is no correlation of the rates of deuteration and racemisation. This is because  $^1\text{H}$  NMR spectroscopy can only detect the deuteride/ deuterium incorporating into the substrate, while the incorporation of hydride/ proton into the imine/ enamine cannot be observed. Therefore this method can only be used qualitatively. It can also be challenging to find an internal standard whose signals do not overlap with any of the substrate peaks, is non-volatile, can withstand the reaction conditions, and is chemically inert towards any hydrogen transfer/ C-H activation by **64**, further limiting its use in quantitative analysis.

## 2.6 Conclusion

The racemisation of various chiral amines was carried out in batch using homogeneous catalyst **64**. The effect of varying concentration was studied for the racemisation of amine **39** and the reaction rate was found to increase from 0.1 M to 1 M but eventually dropped when the concentration of **39** increased further. With 0.2 mol% of **64**, complete racemisation was not observed for **39** in toluene at 105 °C. Deactivation of **64** might have occurred *via* the formation of C-H activation complex **93** with **39**, and/ or the coordination of methylamine, a by-product from the hydrolysis of imine **94**, to the iridium centre of **64**, forming iridium-methylamine complexes which inhibit the binding of **39**. The binding interaction of methylamine with **64** was studied using a  $^1\text{H}$  NMR titration experiment and the mono-, di- and tri-methylamine-bound iridium complexes were observed, in which the tri-methylamine-bound complex was believed to be the major species that stopped **64** from turning over. The racemisation of **39** was also carried out in ethyl acetate with different alcohols as co-solvent, and it was found that methanol reduced the activity of **64** more significantly than ethanol or isopropyl alcohol. Racemisation of other bulky substrates **101** and **46** proceeded more slowly than **39** due to more hindered interaction with **64**. Racemisation of primary amine **42** mainly led to formation of dimers with minimal racemisation. Cyclic secondary amines **103** and **9** were successfully racemised by **64** and proceeded at much higher rates than acyclic amines, probably due to the more stable imine intermediates formed.



Racemisation of **39**, **101**, **46**, **9** and **103** were also carried out in flow using immobilised SCRAM **92**. The catalyst was packed in a HPLC column and the substrate solution was pumped through the reactor at elevated temperature to effect racemisation. The extent of racemisation can be increased by increasing the  $t_{Res}$  of the reaction which depends on the flow rate (and reactor volume). The de-activated **92** was found to regain its activity by about 12% after re-activation by hydroiodic acid which protonate and remove some of the bound-methylamine from the iridium.

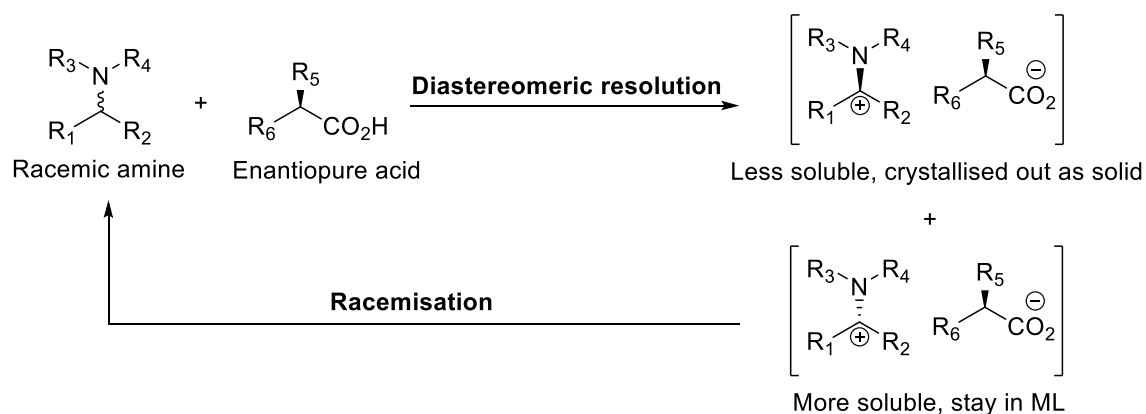
A non-quantitative method was developed to determine the racemisation of chiral amines by locating the positions of deuteration of the molecule using  $^1H$  NMR spectroscopy, which does not need the use of enantio-enriched substrates or a chiral analytical method for determining the ee. This procedure also confirmed the formation of imine and enamine as the intermediate during racemisation which can remain bound or de-coordinate from the catalyst before converting back to the amine. However, deuterium incorporation causes changes in chemical shifts and multiplicities, and the overlapping of signals of the substrates and formation of side products make the spectral interpretations difficult. To further confirm the positions of deuteration, if any, deuterium NMR may be used which shows only deuterium signals. On the other hand, substrates deuterated at various positions may have to be prepared that can be used as references in both proton and deuterium NMRs.

### 3. Resolution-Racemisation-Recycle (R<sup>3</sup>)

#### 3.1 Introduction

The maximum theoretical yield of the desired enantiomer from a resolution process is only 50%. The yield is often compromised further when attempting to increase the enantiopurity of the product.<sup>9, 63</sup> As discussed in chapters 1 and 2, the undesired enantiomer in the resolution can be recycled by racemisation which produces a racemate that can be subjected to resolution again. By repeating the resolution-racemisation processes, the desired enantiomer can be synthesised in theoretical yield of 100%.

Crystallisation-Induced Diastereomeric Transformation (CIDT) is one of the widely employed strategies in the asymmetric transformation of chiral amines by combining diastereomeric crystallisation with racemisation in one pot to obtain the desired enantiomer in high yield and ee (Scheme 3.1).<sup>66</sup>



*Scheme 3.1 CIDT process. The less soluble diastereomer crystallises from solution whilst the more soluble diastereomer resides in the ML which undergoes in-situ racemisation*

The undesired enantiomer in the mother liquor (ML) can be racemised *via* Schiff base formation in the presence of catalytic amount of an aldehyde.<sup>66</sup> The configuration is lost either by the formation of an anion or 1,3-isomerisation of the imine. However the method has limited scope since it requires the amine to have an acidic proton at the chiral centre. Alternatively, transition metal catalysts such as SCRAM catalyst **64**, Shvo's catalyst **55**, Pd/ C, Pd/ inorganic salt such as barium sulfate have been used in the racemisation of chiral amines. These

catalysts do not rely on low pK<sub>a</sub> protons and can potentially widen the scope of the CIDT process. In developing a one-pot procedure, the compatibility of both reactions have to be considered. Racemisation by transition metal catalysts often requires high temperature which also causes dissolution of the crystals. The metal residues from the catalyst can affect the crystallisation and contaminate the product. Therefore an alternative design of a CIDT-type process is necessary.

The aim of this work is to develop a Resolution-Racemisation-Recycle (R<sup>3</sup>) process by combining diastereomeric crystallisation and SCRAM **64**-catalysed racemisation. The results of racemisation of chiral amines using **64** was discussed in Chapter 2; the work demonstrated that **64** could be immobilised onto a Wang resin support and used in continuous flow. The racemisation substrate in the R<sup>3</sup> process is the ML from the diastereomeric crystallisation containing enantio-enriched chiral amine that was pumped through a packed-bed reactor (PBR) containing the immobilised SCRAM catalyst **92**. This enables the racemisation to be carried out independently from the crystallisation, allowing each process to be operated under its optimum conditions. The continuous stirred tank reactor (CSTR) for crystallisation and the racemisation PBR were linked *via* a pump and tubing to yield a continuous, recirculation process. The process was used to investigate the syntheses of a series of chiral amines (Fig. 3.1). Limitations and learning from the system are also discussed in this chapter.

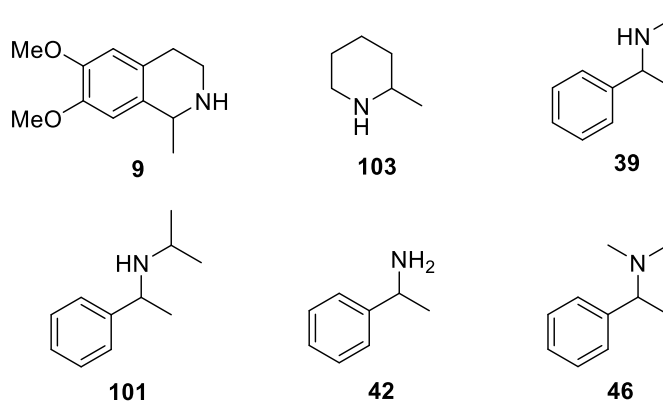


Fig. 3.1 Chiral amines tested on the R<sup>3</sup> system

## 3.2 Experimental set-up

The experimental set-up consisted of two parts, diastereomeric crystallisation in batch and racemisation in flow (Fig. 3.2(a)). The crystallisation was carried out in

a glass CSTR (50 mL). The CSTR was fitted to a PTFE lid with three ports (3 mm O.D.) (Fig. 3.3(a)). The racemic amine, resolving acid (0.5 to 0.98 equiv.) and reaction solvent (20 mL) were added into the CSTR. An inline filter/ frit (40  $\mu$ m pore sizes) was held inside the CSTR which allowed only the ML to leave the CSTR. It was connected to the inlet of a HPLC pump (Knauer PS4.1 or Jasco pump) *via* one of the ports with PTFE and marprene tubing (Fig. 3.3(b)). The outlet of the pump was connected to the inlet of the PBR (4 mL), which is a stainless steel HPLC column packed with **92** to allow racemisation to occur when the ML was pumped through. Two configurations were used during the development of the R<sup>3</sup> process. Initially the PBR was heated with a stirrer hot plate (Fig. 3.2(a)), however the heating was uneven and suboptimal. An improved design employing an aluminium block containing nickel heating cartridges was then used which were electrically controlled, where more efficient heating and better temperature control of the PBR was achieved (Fig. 3.2(b)). The outlet from the PBR was fed into the CSTR *via* one of the ports using PTFE tubing (1/16" O.D., 1/32" I.D.). For experiments that required slow addition of the resolving acid, an additional syringe pump was connected to the CSTR *via* one of the ports for adding the acid solution into the crystallisation mixture.

The total reactor volume of the system (RV) was determined by pumping a known volume of reaction solvent from a beaker through the whole set-up until the CSTR was filled with 20 mL of solvent. RV equals the difference in the original and the remaining volumes of the solvent in the beaker, which were 25 mL and 28.5 mL in using Knauer PS4.1 and Jasco pumps respectively.

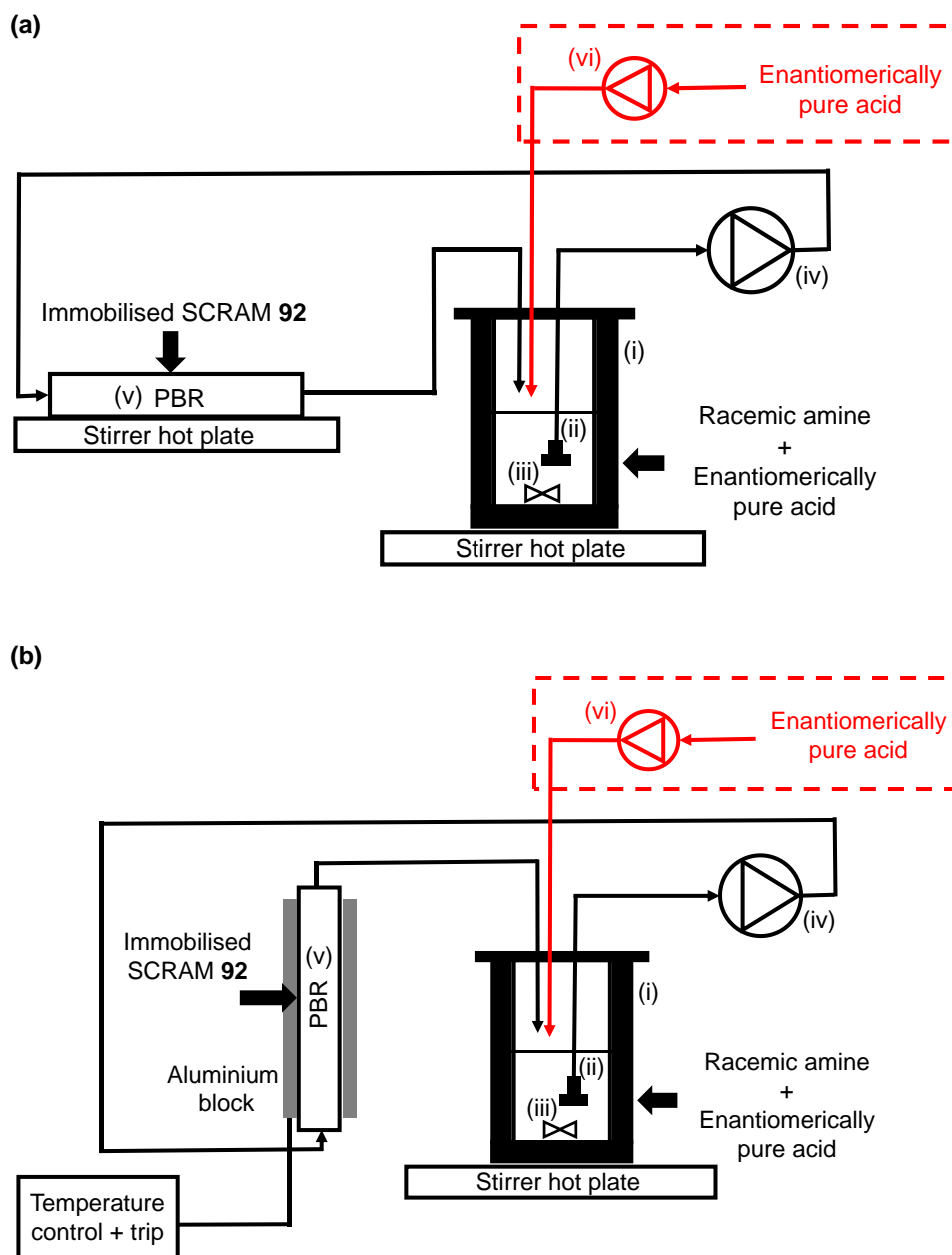


Fig. 3.2 Schematic of the two configurations used in the  $R^3$  process. (i) CSTR (50 mL), (ii) Frit, (iii) Magnetic stirrer, (iv) HPLC pump (Knauer PS4.1 or Jasco pump), (v) PBR packed with immobilised SCRAM 92, (vi) Syringe pump for acid addition. (a) PBR was heated by a stirrer hot plate. (b) PBR was heated by electrically controlled nickel heating cartridges

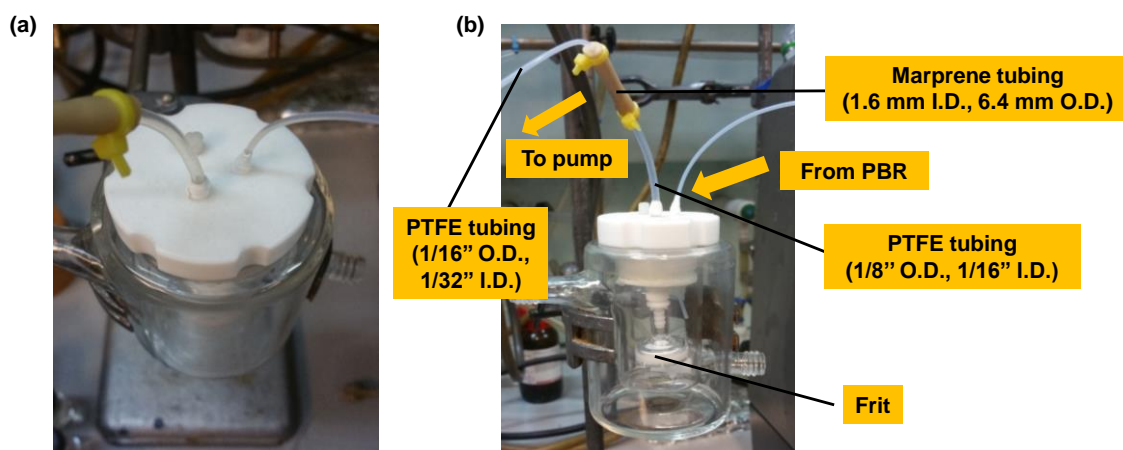


Fig. 3.3 The glass CSTR used in the diastereomeric crystallisation of the  $R^3$  process. (a) PTFE lid fitted to the CSTR with three ports. (b) The frit and PTFE tubing fitted via the ports on the lid

In the  $R^3$  process, the racemic amine and the resolving acid were stirred inside the CSTR. After the crystals were formed, the ML which was enriched with the more soluble diastereomer (corresponded to the undesired enantiomer of the amine) was pumped out from the CSTR at a designated flow rate, which passed through the PBR containing the immobilised **92** where the ML was racemised and then returned to the CSTR. The desired enantiomer was formed in the PBR as the ML was racemised. The racemised ML was introduced into the crystalliser, allowing further resolution with the resolving acid and precipitation of the desired diastereomer.

### 3.3 $R^3$ processes for different chiral amine substrates using (S)-mandelic acid **34** as resolving agent

Diastereomeric resolution of various racemic chiral amines were studied to obtain suitable conditions which could be combined with the racemisation in flow to develop the  $R^3$  process. The yields of all resolutions reported in this work were calculated using Eqn. 3.1. The equation is a function of the quantity of amines in the system irrespective of the amount of chiral acids charged, assuming the stoichiometry of the amine and acid in the salts remain constant under the conditions employed.

$$\text{Yield} = \frac{m_{\text{crystals}}}{\left(\frac{n_{\text{amine}}}{r} \times M_{\text{salt}}\right)} \times 100\% \quad (\text{Eqn. 3.1})$$

Where  $m_{\text{crystals}}$  is the mass of crystals obtained from the resolution;  $n_{\text{amine}}$  is the number of moles of amine in the system;  $r$  is the ratio of amine: acid in the salt;  $M_{\text{salt}}$  is the molar mass of the salt formed.

For diastereomeric resolutions, especially in non-dynamic systems (with no racemisation of the ML), product with high de often gives low yield and vice versa. While yield and de are both important, it is very difficult to compare different processes based on two quantities. Therefore a single quantitative term called resolvability ( $S$ ) was introduced which combines both yield and de. It can be used to measure the efficiency of a diastereomeric resolution (Eqn. 3.2).<sup>145</sup>

$$S = 2 \times \text{Yield} \times \text{de} \quad (\text{Eqn. 3.2})$$

For a simple resolution, where the undesired diastereomer is not recycled, the maximum de and yield of the product are 100% and 50% respectively. Therefore the maximum value of  $S$  is 1; whilst a dynamic resolution can theoretically lead to 100% de and 100% yield and therefore its  $S$  has a maximum value of 2.

Based on Eqn. 3.2, two processes having the same value of  $S$  may have very different yield and de. For example, a diastereomeric resolution leading to product with 100% de and 50% yield has the same resolvability as that with 50% de and 100% yield. This term has to be used in caution and the information on both yield and de of the resolution process have to be known to draw any definite conclusions. Nevertheless, the term enables comparison of different resolution processes.

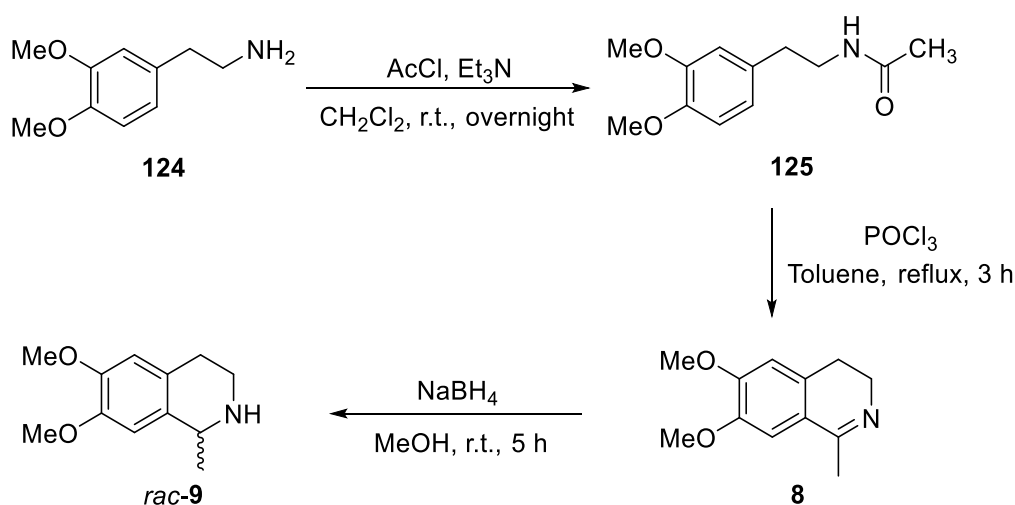
### 3.3.1 6,7-Dimethoxy-1-methyl-1,2,3,4-tetrahydroisoquinoline **9**

#### (a) Diastereomeric crystallisation in batch

Enantiopure amine **9** has been readily racemised by both homogeneous SCRAM **64** and immobilised SCRAM **92** in batch and flow, as shown in Sections 2.2.5 and 2.3.3 and by Blacker et al.<sup>1</sup> The diastereomeric resolution of *rac*-**9** was also

reported by Shi et al. which used (*S*)-mandelic acid **34** as the resolving acid.<sup>137</sup> With some preliminary knowledge regarding both racemisation and resolution, **9** was chosen to be the model substrate in the development of the R<sup>3</sup> process.

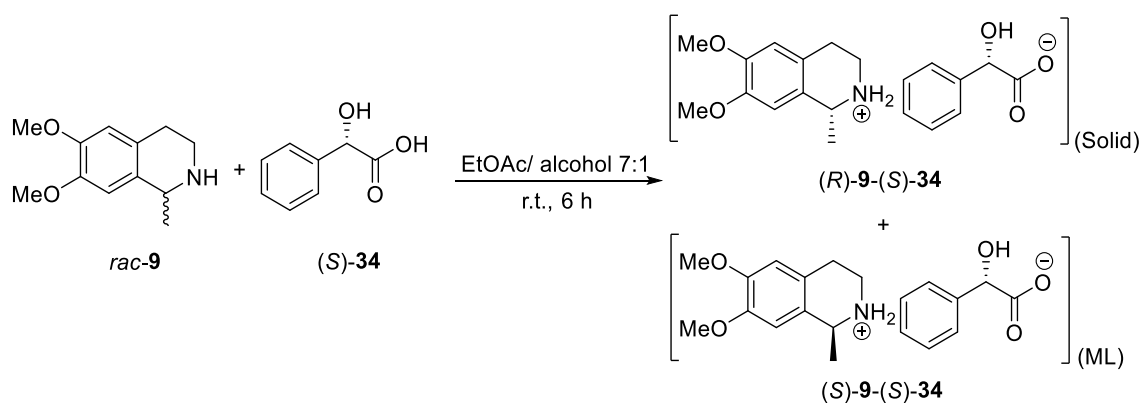
Racemic **9** was synthesised from 3,4-dimethoxyphenethylamine **124**, which was first acetylated to acetamide **125**, followed by Bischler-Napieralski cyclisation to form imine **8**. Subsequent reduction of imine **8** using excess sodium borohydride gave *rac*-**9** (Scheme 3.2).<sup>137</sup>



Scheme 3.2 Synthesis of *rac*-**9** from amine **124**

The diastereomeric resolution of *rac*-**9** was previously reported using 0.5 equiv. of (*S*)-**34** and stirred under reflux in ethyl acetate/ isopropyl alcohol 5:1. The resulting crystals were purified by suspending them under reflux in ethyl acetate/ isopropyl alcohol 7:1. The diastereopure (*R*)-**9**-(*S*)-**34** was obtained in 41% yield (based on **9**) with > 98% de.<sup>137</sup> The conditions were further investigated at ambient temperature without heating/ reflux and without purification (Scheme 3.3, Table 3.1).





Scheme 3.3 Diastereomeric resolution of *rac-9* by (*S*)-**34** at room temperature

Entry	Alcohol	( <i>S</i> )- <b>34</b> (equiv.)	Yield (%) <sup>[a]</sup>	de (%) <sup>[b]</sup>	S
1 <sup>[c]</sup>	MeOH	0.5	28	98	0.549
2 <sup>[c]</sup>	EtOH	0.5	30	95	0.570
3 <sup>[c]</sup>	<sup>i</sup> PrOH	0.5	34	86	0.585
4	MeOH	1	59	27	0.319
5	EtOH	1	74	14	0.207
6	<sup>i</sup> PrOH	1	80	7	0.112

Table 3.1 Condition screening of diastereomeric crystallisation of *rac-9* with (*S*)-**34** at room temperature in ethyl acetate/ alcohol 7:1 (v/v). <sup>[a]</sup>Seed was excluded from the yield calculation. <sup>[b]</sup>De was determined by <sup>1</sup>H NMR (in CDCl<sub>3</sub>, 500 MHz). <sup>[c]</sup>The reaction was seeded with (*R*)-**9**-(*S*)-**34** (5% w/w)

A suitable solvent system was determined by changing the alcohol co-solvent. With the same amount of (*S*)-**34** added, the use of methanol led to higher de but lower yield compared to the other solvent systems (Table 3.1, entries 1 and 4); whilst the use of isopropyl alcohol resulted in lower de and higher yield (Table 3.1, entries 3 and 6). With the use of 0.5 equiv. of (*S*)-**34**, crystals of higher de were obtained, leading to higher resolvability (Table 3.1, entries 1 to 3). Although the yields were higher when (*S*)-**34** was increased to 1 equiv., the significant drop in de led to much lower resolvability (Table 3.1, entries 4 to 6). One of the possible reasons behind the dramatic changes in the de and yield of the crystals upon changing the alcohol from methanol to ethanol and isopropyl alcohol especially with 1 equiv of (*S*)-**34** is the absolute solubility of (*R*)-**9**-(*S*)-**34** and (*S*)-**9**-(*S*)-**34** which decreases considerably from ethyl acetate/ methanol to ethyl acetate/

isopropyl alcohol 7:1 (v/v) (Fig. 3.4). More of both salts are likely to crystallise out from solution, leading to lower de and higher yield.

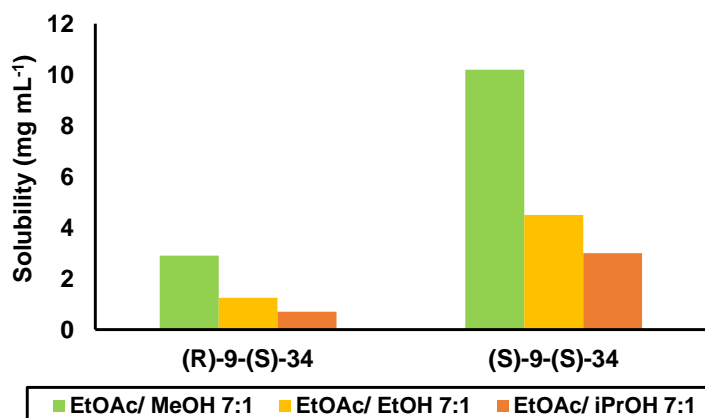


Fig. 3.4 Solubility of (R)-9-(S)-**34** and (S)-9-(S)-**34** in EtOAc/ alcohol 7:1 (v/v) at r.t.

### (b) Diastereomeric crystallisation in flow

The diastereomeric resolution of *rac*-**9** with (S)-**34** was also carried out in continuous flow using cascade CSTRs called Freactors (Fig. 3.5).<sup>114</sup> Each Freactor is a 1.8 mL CSTR fitted with a magnetic stirrer which provides effective mixing of reagents. The Freactors can be connected in series using HPLC 1/8" O.D. ferrules and tube fittings. Previous studies showed that the Freactor(s) display plug-flow characteristics up to a  $t_{Res}$  of three hours and are capable of performing multiphasic reactions.<sup>114</sup> The diastereomeric crystallisation of **9** by mixing (S)-**34** and *rac*-**9** was found to be successful in this system, showing its remarkable ability in handling solids generated within a reaction.

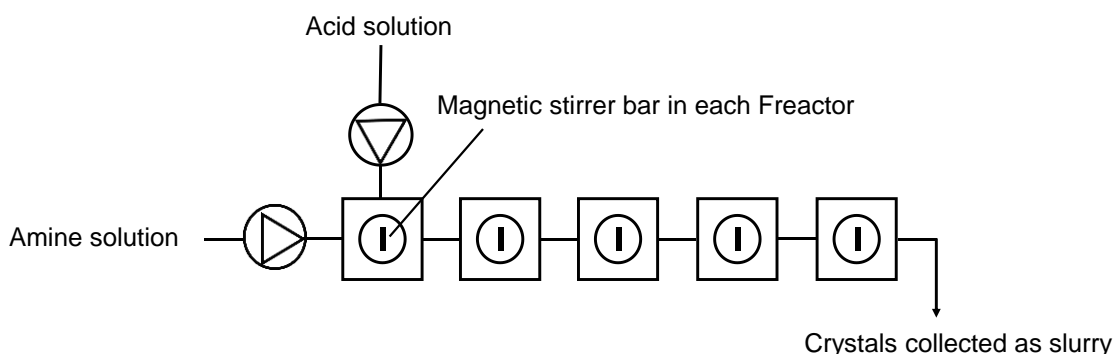


Fig. 3.5 Schematic of the experimental set-up for diastereomeric crystallisation in flow by connecting five Freactors in series (1.8 mL volume each) using PTFE tubing (1/8" O.D., 1/16" I.D.)

Based on the results of diastereomeric crystallisation of **9** with (*S*)-**34** in batch, ethyl acetate/ methanol 7:1 was chosen to be the solvent system in flow and only 0.5 equiv. of (*S*)-**34** was used. The effects of  $t_{\text{Res}}$  on the yield and de of the crystals were investigated by varying the flow rate and the total volume of the system (reactor volume, RV) (Table 3.2).

Entry	No. of reactors	RV (mL)	Flow rate (mL min <sup>-1</sup> )	$t_{\text{Res}}$ (min)	Yield (%)	de (%) <sup>[a]</sup>	S
1	5	10	5	2	23	86	0.396
2 <sup>[b]</sup>	3	1.2	0.5	2.5	14	91	0.255
3	2	4	0.5	8	19	88	0.334
4	5	10	1	10	24	87	0.418
5	5	10	0.5	20	24	91	0.437
6	5	10	0.25	40	19	91	0.346

Table 3.2 Variation of RV and flow rate in the diastereomeric crystallisation of **9** with (*S*)-**34** in flow using Freactors. <sup>[a]</sup>De was determined by <sup>1</sup>H NMR (in CDCl<sub>3</sub>, 500 MHz). <sup>[b]</sup>The Freactors were not fully filled and contained air bubbles

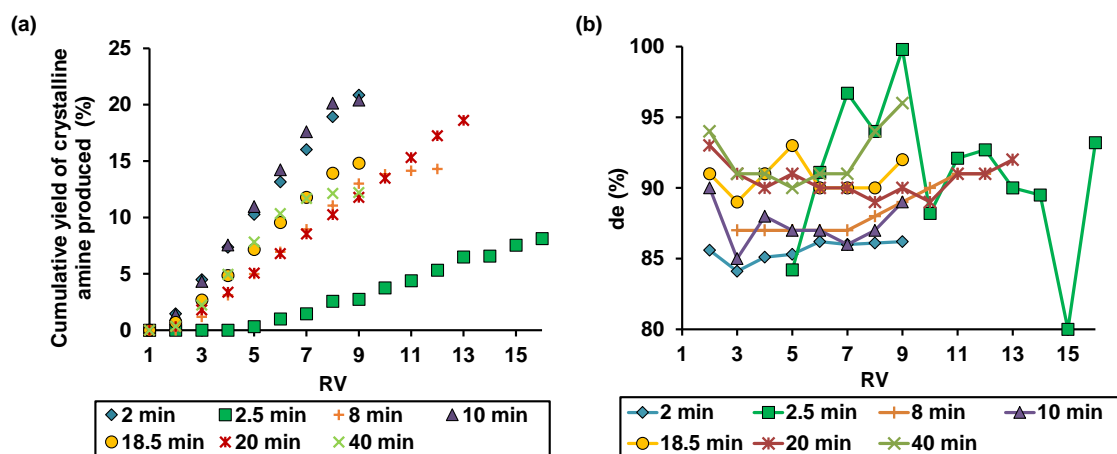


Fig. 3.6 Diastereomeric crystallisation of **9** with (*S*)-**34** in flow. (a) Cumulative yield of crystals formed; (b) De of the crystals collected from each RV, measured by <sup>1</sup>H NMR (CDCl<sub>3</sub>, 500 MHz)

One of the benefits of continuous flow methods in chemical processing is the ability to achieve steady state which minimises the variations of reaction outcomes. With  $t_{\text{Res}}$  of 2.5 minutes where the system contained air bubbles (Table 3.2, entry 2), steady state could not be achieved which led to fluctuation of the

yield as reflected by the cumulative yield plot being less smooth than the others (Fig. 3.6(a)). The  $d_e$  of the crystals was also found to be less consistent across the RVs (Fig. 3.6(b)). Properly filling the Freactors ensured no air bubbles in the system, leading to more consistent flow throughout the crystallisation.

With the same RV (Table 3.2, entries 1, 4 to 6), crystals were formed more quickly when flow rate was increased, as shown from the higher yield of solids in RV 2 (Fig. 3.6). This showed the importance of initial mixing to the reaction rate. The overall yield (including the washing) was virtually unaffected by the flow rate. At  $t_{Res}$  40 minutes, the system started to block relatively quickly and was not able to reach steady state, which may explain the slightly lower yield compared to the other systems. With shorter  $t_{Res}$  of 2 and 10 minutes (Table 3.2, entries 1 and 4), lower  $d_e$  of the crystals was observed compared to those obtained at longer  $t_{Res}$  (Table 3.2, entries 5 and 6).

One of the main problems with micro-reactors is their gradual blockage when crystallisation proceeds. At  $t_{Res}$  2, 10 and 40 minutes, the reactors started to get blocked at RVs 9, 8 and 7 respectively. At  $t_{Res}$  20 minutes, however, no blockage was observed for 12 RVs (Fig. 3.6(a)). Significant amount of solid was found to accumulate in the first reactor and may account for the blockages. The solids at the bottom of the reactor were not able to enter into the suspension and started to stick together to form large agglomerates, eventually blocking the reactor. Agglomeration is more likely to happen especially in reactive crystallisations such as amine-acid neutralisations due to the high supersaturation levels present upon precipitate formation.<sup>146</sup> It may also be facilitated by electrostatic charges built up on the particles.

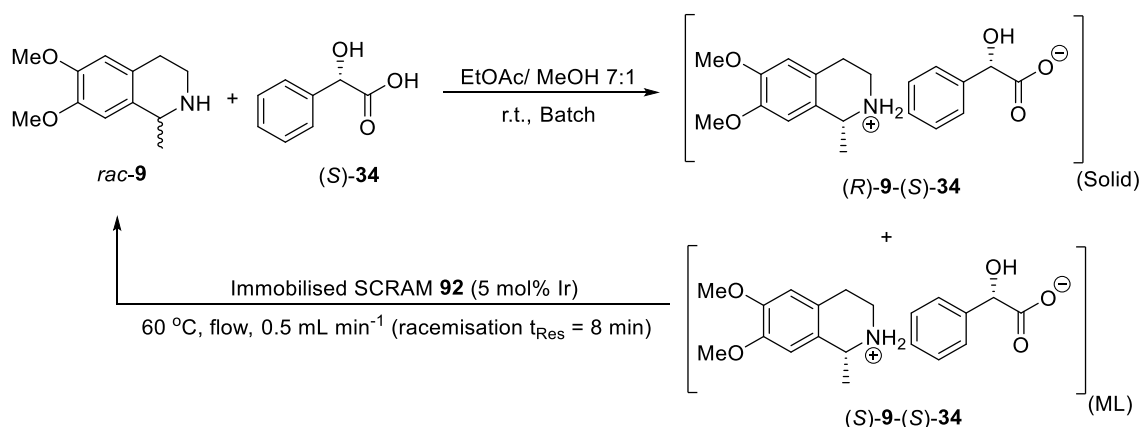
In addition to varying flow rate,  $t_{Res}$  was varied by changing the volume, i.e. the number of reactors. With only two reactors flowing (4 mL) at  $0.5 \text{ mL min}^{-1}$  ( $t_{Res} = 8$  minutes), a slight drop in yield and  $d_e$  were observed (Table 3.2, entry 3). Blockage occurred from RV10. The reason was unclear as no blockage was found with 5 reactors at the same flow rate.

Diastereomeric resolution of *rac*-**9** with (*S*)-**34** in continuous flow showed a slightly lower resolvability compared to that carried out in batch but with much

shorter crystallisation times (2 to 40 minutes) compared to 6 hours in batch. The lower de crystals containing less (*R*)-**9**-(*S*)-**34** and/ or more (*S*)-**9**-(*S*)-**34** may be formed as the kinetic product at the start of the crystallisation process. Upon prolonged stirring of the reaction mixture, the most thermodynamically stable product will be formed, in which more (*R*)-**9**-(*S*)-**34** (the less soluble solid) crystallises out where more (*S*)-**9**-(*S*)-**34** (the more soluble solid) dissolves, leading to higher de of the final crystal product. A shorter diastereomeric crystallisation of **9** with (*S*)-**34** was previously carried out in batch for 2 hours in ethyl acetate/ methanol 7:1 (v/v) which also led to a lower de of only 83%.

### (c) R<sup>3</sup> process of amine **9** with (*S*)-**34**

Since a higher resolvability of *rac*-**9** with (*S*)-**34** was achieved in ethyl acetate/ methanol 7:1, and this solvent system has been used in the racemisation of enantiopure **9** using both homogeneous SCRAM **64** and immobilised SCRAM **92**, it was initially chosen as the solvent system for the R<sup>3</sup> process of **9** (Scheme 3.4).



Scheme 3.4 R<sup>3</sup> process of **9**. t<sub>Res</sub> for the whole cycle = 25 mL/ 0.5 mL min<sup>-1</sup> = 50 min

At the start of this work, it was believed that acids might have an inhibitory effect on the racemisation, as shown by J. Breen during the racemisation of (*S*)-**39** by C<sub>5</sub>-hydroxy-tethered SCRAM **98** in the presence of (*S,S*)-**32** (Fig. 3.7). Acids would be expected to affect Ir-N coordination of the amine, imine or iminium, react with hydride to produce hydrogen, and coordinate to the iridium as a carboxylate ligand, as occurs with formate.<sup>147</sup>

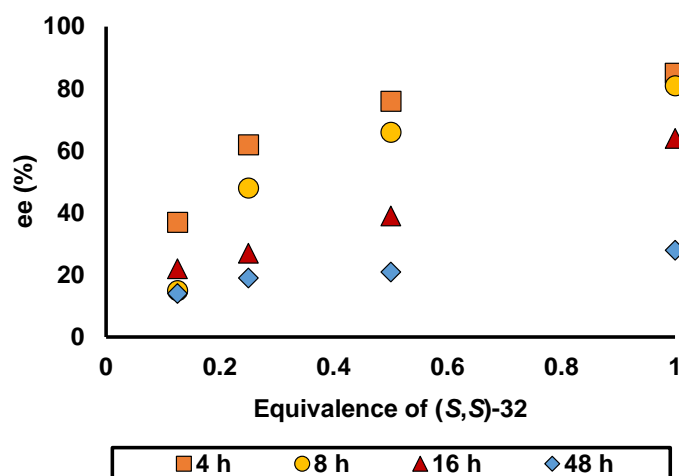


Fig. 3.7 Profiles of ee for the racemisation of (*R*)-**39** in the presence of (*S,S*)-**32** by SCRAM **98** in EtOAc/ MeOH (17% by volume) (results by J. Breen)

During the early stage of R<sup>3</sup> process development, the amount of (*S*)-**34** was kept at its minimum concentration to ensure the system was as basic as possible. At the start of the diastereomeric crystallisation, only 0.5 equiv. of (*S*)-**34** was added which reacted with half of the amount of *rac*-**9**. The remaining 0.5 equiv. of (*S*)-**34** was added slowly into the CSTR by a syringe pump (Fig. 3.2(a)). Its rate of addition was based on the approximate drop in ee of the ML after each pass through the catalyst. This corresponds to the amount of (*R*)-**9** formed from (*S*)-**9** after each cycle. As (*R*)-**9**-(*S*)-**34** crystallised preferentially due to its lower solubility, the total amount of **9** in the system decreased after each cycle, therefore the rate of acid addition was reduced accordingly. The assumptions and approximations of the addition rate of (*S*)-**34** are described in Section 8.4. The ML was pumped through the system at 0.5 mL min<sup>-1</sup> which equated to a t<sub>Res</sub> of 8 minutes and 50 minutes for racemisation and one recycle of the R<sup>3</sup> process respectively. The first attempt of R<sup>3</sup> process of **9** is shown in Fig. 3.8. The ML was recirculated for 17 cycles corresponding to a process time of 14 hours. The overall process cycle time is calculated as the product of t<sub>Res</sub> (one whole cycle) and the number of times recirculated (Eqn. 3.3).

$$\text{Process time} = t_{\text{Res}}(\text{whole cycle}) \times \text{no. of cycles} \quad (\text{Eqn. 3.3})$$

Samples were taken from the reaction solution in order to determine the concentrations of amine **9**, imine **8** and isoquinoline **65** in the ML by GC. Chiral HPLC was also used to determine the ee of the ML and de of the crystals from

each sample. The total yield of the crystals obtained at the end of the process included those from each sample and was calculated using Eqn. 3.1.

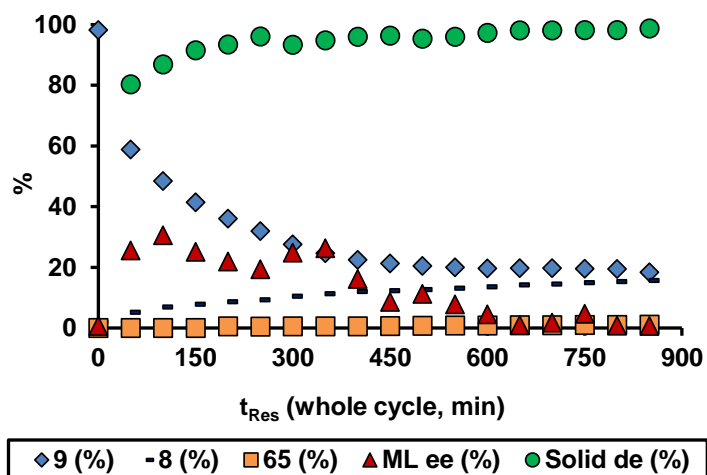


Fig. 3.8 The first attempt of  $R^3$  process of **9** with (*S*)-**34** in EtOAc/ MeOH 7:1 (v/v) (Table 3.3, entry 1). A total of 0.92 equiv. of (*S*)-**34** was added

The concentration of **9** decreased for about 8 cycles and eventually levelled-off. The amine was transformed with (*S*)-**34** into crystals and impurities such as imine **8** and isoquinoline **65**. These latter compounds were formed, presumably, by loss of hydrogen as a result of acid quenching of the Ir-H catalytic intermediate. The concentration of **9** did not reach zero since some of the diastereomeric salts remained in solution, as defined by their solubility. Interestingly, the de of the crystals gradually increased from 80 to 99% and their overall yield was 55% (including the crystals isolated during reaction sampling), resulting in an S value of 1.09 (Table 3.3, entry 1). This showed a significant improvement over the batch resolution-only process (Table 3.1, entries 1 and 4).

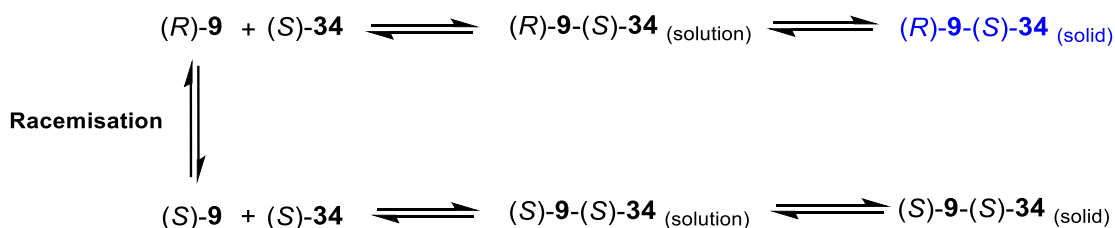
Entry		1	2	3	4 <sup>[a]</sup>
Reaction conditions	Alcohol <sup>[b]</sup>	MeOH	MeOH	<sup>i</sup> PrOH	MeOH
	Average acid addition rate during recirculation (mg min <sup>-1</sup> ) <sup>[c]</sup>	0.22	0.43	0.63	0.63
	No. of cycles	17	11	8	8
	Process time (h)	14.2	9.2	6.7	6.7
Results	Initial crystal de (%)	N.D. <sup>[d]</sup>	76	65	76
	Final crystal de (%)	99	99	96	97
	Yield (%)	55	52	65	33
	<b>9</b> in ML (%)	18	15	9	66
	<b>8</b> in ML (%)	16	13	5	0.8
	<b>65</b> in ML (%)	1	1.4	0.5	1.2
	ML ee (%)	0.6	3	69	55
	S	1.089	1.030	1.248	0.640

Table 3.3 R<sup>3</sup> process of **9** with slow addition of (S)-**34**. <sup>[a]</sup>Formic acid (1 equiv.) was added into the crystallisation. <sup>[b]</sup>All solvent system contained ethyl acetate/ alcohol 7:1 (v/v). <sup>[c]</sup>Average addition rate of (S)-**34** was calculated by summation of the rates of all cycles divided by the number of cycles in which **34** was added (Section 8.4). <sup>[d]</sup>Not determined

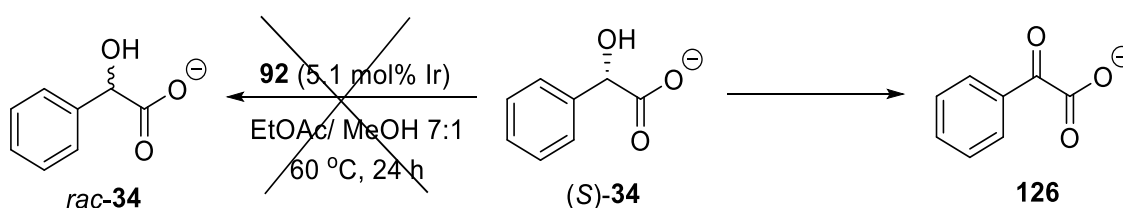
In the R<sup>3</sup> process, there are six species in equilibrium (Scheme 3.5). During racemisation of the ML, amine (*R*)-**9** was formed from (*S*)-**9**, and with the acid (S)-**34**, the least soluble diastereomeric salt crystallised as a solid. As the concentration of (*R*)-**9** in solution decreased, racemisation allowed the equilibrium to shift from (*S*)-**9** towards (*R*)-**9**. Any (*S*)-**9**-(*S*)-**34** which was formed initially as a solid started to dissolve to form the desired, less soluble (*R*)-**9**-(*S*)-**34** (solid), increasing both the yield and diastereopurity of the crystals. In this regard, neither optimisation of the racemisation, nor the resolution was necessary, as the process was driven by the system's thermodynamics. Any difference in solubility of the diastereomeric salts will create an excess of one of the enantiomers/ diastereomers in the ML. If the ML can be racemised, the equilibrium will eventually shift towards the less soluble diastereomeric salt. Mandelic acid (S)-**34** or the mandelate ion is unlikely to racemise under the conditions employed for the R<sup>3</sup>. Control experiments were carried out in batch using **92** and no racemisation was observed. However, phenylglyoxylate ion **126** was formed in the case of triethylammonium (S)-**34**, indicating that **34** is able to



dehydrogenate at the chiral centre, but subsequent reduction does not occur (Scheme 3.6, Fig. 3.9).



Scheme 3.5 Equilibrium between (*R*)-**9**, (*S*)-**9** and their salts of (*S*)-**34** in solution and solid states. (*R*)-**9**-(*S*)-**34** was the less soluble diastereomer (highlighted in blue)



Scheme 3.6 Formation of phenylglyoxylate ion **126** from (*S*)-mandelate **34** in the presence of **92** without racemisation

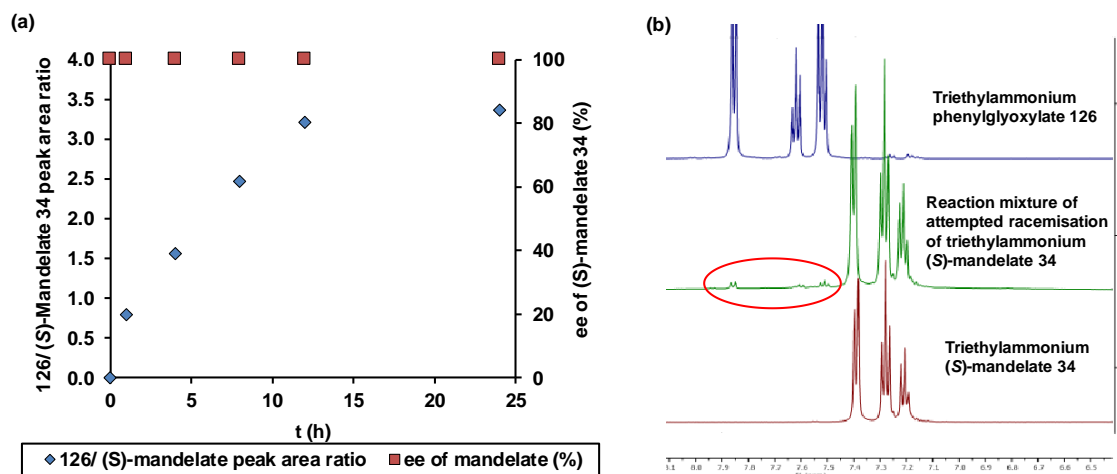


Fig. 3.9 Attempted racemisation of Et<sub>3</sub>N-(*S*)-**34** with **92**. (a) Reaction profile showing constant ee and HPLC peak area ratio of **126** and mandelate; (b) <sup>1</sup>H NMR spectra showing the formation Et<sub>3</sub>N-**126**

Following the success of the first attempt of the recycle, different conditions were evaluated to further optimise the R<sup>3</sup> process (Table 3.3, entries 2 to 4). During the first attempt, (*S*)-**34** was added slowly throughout the process which required 17 cycles to add 0.92 equiv. of (*S*)-**34** into the reaction. This corresponded to 14

hours of process time. In order to improve the efficiency, higher addition rate was used which did not cause significant change in the de and only a slight decline in the yield of the crystals was observed (Table 3.3, entry 2). Although the resolvability of the R<sup>3</sup> system were significantly improved over the batch resolution with much higher product de (Table 3.3, entries 1 and 2; Table 3.1, entries 1 and 4), the yields of the R<sup>3</sup> processes were still low ( $\leq 55\%$ ) due to the loss of **9** to impurities imine **8** and isoquinoline **65**. In this regard, isopropyl alcohol was used as a co-solvent instead of methanol, as this could act as a hydrogen donor to reduce **8** and **65** *in-situ* back to **9** (Table 3.3, entry 3). This led to an increase in isolated yield to 65% with only small decrease in de. Formic acid was tested as an alternative hydrogen donor and was successful in reducing the levels of **8** and **65**, but changed the pH of the system, affecting the solubilities of both (*R*)-**9**-(*S*)-**34** and (*S*)-**9**-(*S*)-**34**, and causing a drop in yield (Table 3.3, entry 4).

Despite the concerns over the system acidity, it was shown that increasing the rate of (*S*)-**34** addition had no significant impact on the yield or de of the crystals. It was decided that instead of adding (*S*)-**34** slowly, it might be added at the start of the process (Table 3.4). The system was kept slightly basic with small excess of free amine present by adding less than 1 equiv. of (*S*)-**34** (0.9 to 0.98 equiv.) to initiate the racemisation reaction (Scheme 3.5).<sup>9</sup> Adding acid at the beginning did not affect the resolution nor the racemisation reactions when methanol was used as the co-solvent, as shown by the similar yields and de of the products as previous experiments (Table 3.4, entries 1 and 2). When isopropanol was used, a lower de was observed after 12 cycles (Table 3.4, entry 3). When the process was run for 30 cycles, a higher de (96%) was observed with a yield of 78% and resolvability of 1.5 (Table 3.4, entry 5; Fig. 3.10). High de (97%) could also be achieved after 12 cycles by using a mixture of methanol/ isopropyl alcohol (8:2 by volume) as co-solvent instead of pure isopropyl alcohol (Table 3.4, entry 4).

Entry		1 <sup>[a]</sup>	2	3	4	5	6 <sup>[b]</sup>
Reaction conditions	Alcohol <sup>[c]</sup>	MeOH	MeOH	<i>i</i> PrOH	MeOH/ <i>i</i> PrOH (20%)	<i>i</i> PrOH	<i>i</i> PrOH
	No. of cycles	8	12	12	12	30	12
	Process time (h)	6.7	10	10	10	25	10
Results	Initial crystal de (%)	76	76	43	67	50	41
	Final crystal de (%)	98	99	72	97	96	60
	Yield (%)	62	63	72	68	78	75
	<b>9</b> in ML (%)	16	11	10	13	4	8
	<b>8</b> in ML (%)	10	3.5	4	6	2	1.3
	<b>65</b> in ML (%)	0.3	3	0.2	0.5	0.3	0.2
	ML ee (%)	18	10	64	14	6	81
	S	1.215	1.247	1.037	1.319	1.498	0.900

Table 3.4 R<sup>3</sup> process of **9** with 0.98 equiv. of (S)-**34** added at the beginning of the process with no further addition of acid. <sup>[a]</sup>0.9 equiv. of (S)-**34** was added. <sup>[b]</sup>The PBR was electrically heated in an aluminium block. <sup>[c]</sup>All solvent system contained ethyl acetate/ alcohol 7:1 (v/v)

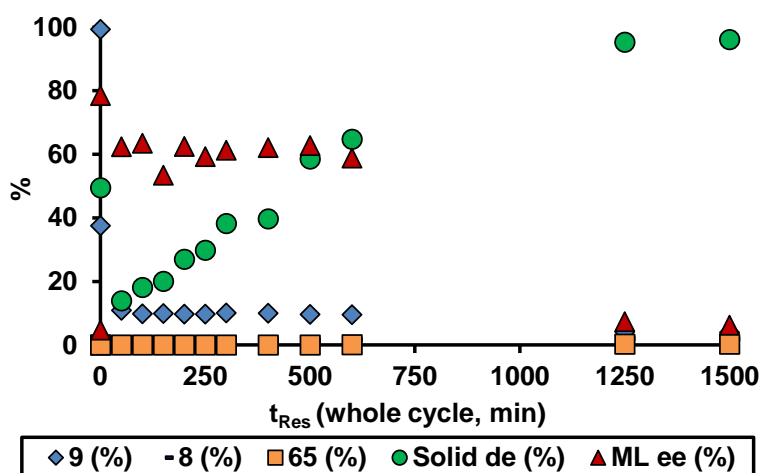


Fig. 3.10 R<sup>3</sup> process of **9** with (S)-**34** in EtOAc/*i*PrOH 7:1 (v/v) (Table 3.4, entry 5). The process was run for 30 cycles (25 h)

In the R<sup>3</sup> processes listed in Table 3.3 and Table 3.4 (entries 1 to 5), the flow racemisation reactions were carried out at approximately 60 °C by heating the column on a stirrer hot plate. For a better temperature control and more uniform

heating, the column was inserted into an aluminium block with two thermocouples attached and was electrically heated to 60 °C (Fig. 3.2(b)). The R<sup>3</sup> process of **9** was repeated in ethyl acetate/ isopropanol using the modified set-up (Table 3.4, entry 6). A similar yield but lower de were observed as compared to the original set-up (Table 3.4, entry 3). This might be explained by the repeated use of the same catalyst and deactivation might have started to occur.

In the R<sup>3</sup> processes of **9** described, the same catalyst **92** was reused after each reaction without unloading from the PBR. The catalyst was recycled for a total of 130 times (108 hours of reuse). In order to assess its activity, a racemisation of (S)-**9** was carried out in flow. The eluent collected was re-introduced into the PBR five times. The ee of **9** was monitored, which dropped gradually from 100% to 47% after five passes through the catalyst respectively, indicating that the 130-times used **92** still showed activity (Fig. 3.11). As discussed in Section 2.3.3, racemisation of (S)-**9** in flow at 60 °C using fresh **92** with t<sub>Res</sub> of 6 minutes resulted in a drop of ee from 100 to 17% after one pass. This showed that the catalyst was about 8 times less active after 130 uses. The cause of deactivation might be the coordination of amine to the iridium with C-H insertion to generate a Ir-C<sub>arom</sub> complex, as discussed in Section 2.2.1.

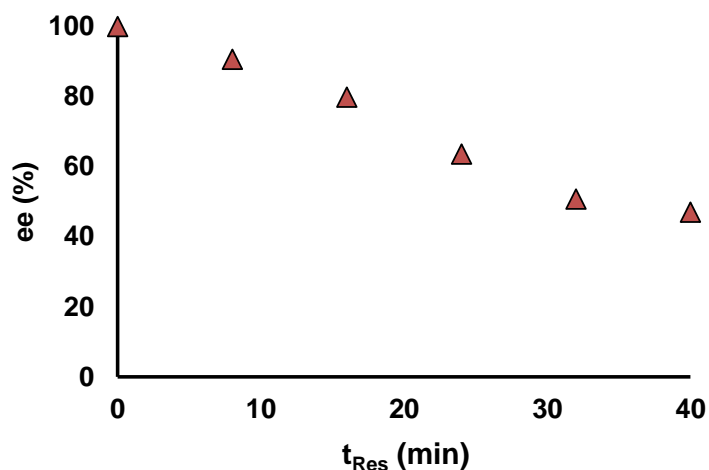
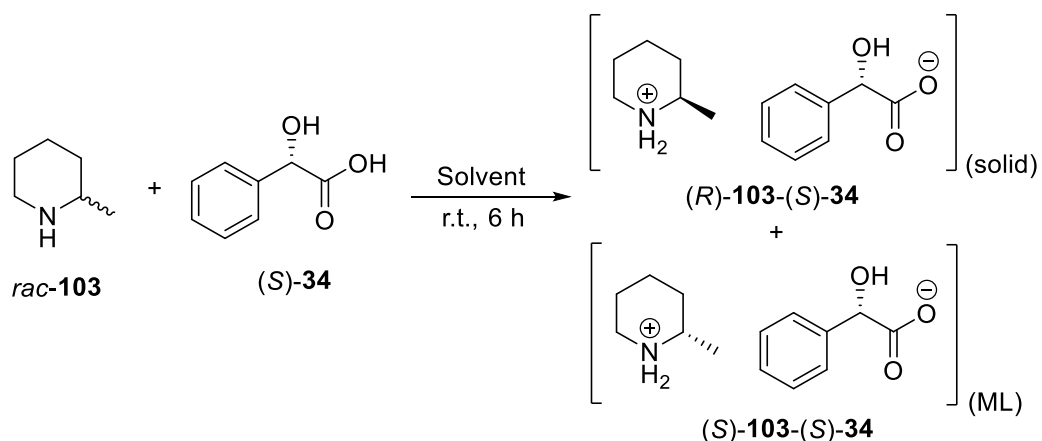


Fig. 3.11 Activity check of immobilised SCRAM **92** after 130 uses in the R<sup>3</sup> process of **9**, via the racemisation of (S)-**9** in flow at 60 °C in EtOAc/ MeOH 7:1 (by volume); Ir loading = 10 mol%

### 3.3.2 2-Methylpiperidine **103**

Piperidine derivatives form part of the alkaloid group and can be found in plant and animal kingdoms.<sup>148, 149</sup> They are also building blocks of many drugs and fine

chemicals.<sup>150</sup> The resolution of a simple piperidine derivative, 2-methylpiperidine **103**, by enantiopure **34** was reported using mainly diethyl ether as the solvent which is too low boiling to be useful in racemisation reactions.<sup>149, 151</sup> Therefore other solvents with higher boiling points were screened (Scheme 3.7, Table 3.5).



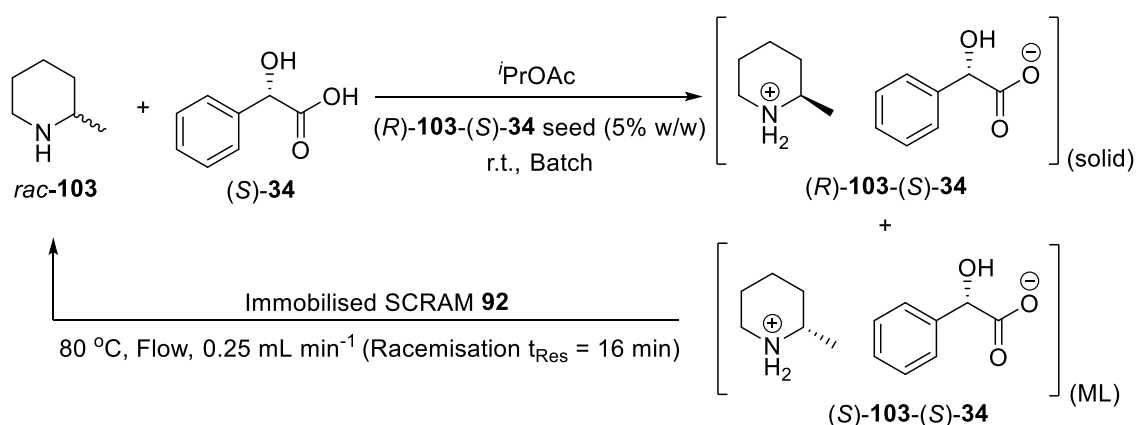
Scheme 3.7 Diastereomeric resolution of *rac*-**103** by (*S*)-**34**

Entry	[ <b>103</b> ] (M)	Solvent	Seeded? <sup>[a]</sup>	Yield (%) <sup>[b]</sup>	De (%) <sup>[c]</sup>	S
1	0.14	MTBE	No	78	3	0.047
2	0.14	MTBE/ MeOH (4% by volume)	No	29	87	0.505
3	0.14	MTBE/ <i>i</i> PrOH (5% by volume)	No	35	83	0.581
4 <sup>[d]</sup>	0.28	DME	No	11	91	0.200
5 <sup>[d]</sup>	0.28	EtOAc	No	24	82	0.394
6 <sup>[d]</sup>	0.14	<i>i</i> PrOAc	No	22	87	0.383
7	0.14	<i>i</i> PrOAc	Yes	26	85	0.442
8	0.25	<i>i</i> PrOAc	Yes	48	27	0.259
9	0.35	<i>i</i> PrOAc	Yes	53	20	0.212

Table 3.5 Condition screen of diastereomeric resolution of *rac*-**103** with (*S*)-**34**. <sup>[a]</sup>(*R*)-**103**-(*S*)-**34** (5% w/w) was used as the seed. <sup>[b]</sup>Seeds were not included in yield calculations. <sup>[c]</sup>De were determined by <sup>1</sup>H NMR (in CDCl<sub>3</sub>, 500 MHz). <sup>[d]</sup>Crystals precipitated from solution after ≥ 1 h

Methyl *tert*-butyl ether (MTBE) was first used which is a less volatile ether solvent than diethyl ether (Table 3.5, entry 1). Virtually no resolution was observed. Therefore an alcohol was added as a co-solvent which led to improved resolvability (Table 3.5, entries 2 and 3). However the boiling point of MTBE was

still relatively low. Racemisation of (*S*)-**103** in MTBE at 50 °C in batch was slow with a half-life of  $\leq 24$  hours (Section 2.2.6). In addition, the MTBE-containing systems require an alcohol for resolution to occur which can slow down the racemisation of ML. Dimethoxyethane (DME) and ethyl acetate require a higher concentration of **103** and a long stirring time for crystals to precipitate, indicating a slow nucleation (Table 3.5, entries 4 and 5). The highest de was observed using DME but the yield was very low (Table 3.5, entry 4). Crystallisation in isopropyl acetate was also slow although it can be carried out at 0.14 M (Table 3.5, entry 6). The system was seeded with diastereopure (*R*)-**103**-(*S*)-**34** to speed up the nucleation step (Table 3.5, entry 7). The resolutions were repeated at higher concentrations but the resolvability of the systems dropped significantly (Table 3.5, entries 8 and 9). Isopropyl acetate allows the racemisation of (*S*)-**103** to proceed at higher temperature (80 °C) at reasonable rates in both batch and flow, as discussed in Sections 2.2.6 and 2.3.3. Therefore it was chosen to be the solvent for the R<sup>3</sup> process development of **103** (Scheme 3.8).



Scheme 3.8 R<sup>3</sup> process of **103**. The  $t_{Res}$  for the whole cycle =  $28.5 \text{ mL} / 0.25 \text{ mL min}^{-1} = 114 \text{ min}$

Development of the R<sup>3</sup> process for amine **9** showed that the amount of acid **34** in the system did not have any impact upon its performance, therefore 0.9 equiv. of (*S*)-**34** was added with amine **103** at the start of the process, without adding more during the ML recirculation. Since the rate of racemisation of **103** is lower than that of **9**, a longer  $t_{Res}$  (16 minutes) was employed, using a flow rate of 0.25 mL min<sup>-1</sup>. This made the recirculation of the whole volume longer ( $t_{Res} = 114$  minutes). The crystallisation was seeded with diastereopure (*R*)-**103**-(*S*)-**34** (5% w/w) to

encourage crystal growth from the start. The conditions and the results for the R<sup>3</sup> processes of **103** were shown in Table 3.6.

Entry		1	2	3
Reaction conditions	[ <b>103</b> ] (M)	0.14	0.25	0.35
	Ir loading (mol%)	7	4	2.8
	No. of cycles	6	12	16
	Process time (h)	10	22.8	30.4
Results	Initial crystal de (%) <sup>[a]</sup>	70	62	73
	Final crystal de (%) <sup>[a]</sup>	90	90	89
	Yield (%) <sup>[b]</sup>	26	44	52
	<b>103</b> in ML (%) <sup>[c]</sup>	47	39	22
	ML ee (%) <sup>[d]</sup>	16	9	26
	S	0.468	0.792	0.926
Activity of <b>92</b>	Average ee of <b>103</b> (%) <sup>[e]</sup>	20	34	42

Table 3.6 Experimental conditions attempted for the R<sup>3</sup> process of **103** with 0.9 equiv. of (S)-**34** added at the beginning of the process with no further addition of acid. <sup>[a]</sup>De was determined by <sup>1</sup>H NMR (CDCl<sub>3</sub>, 500 MHz). <sup>[b]</sup>Crystals from each sample were included while the seeds were excluded from yield calculation. <sup>[c]</sup>Amount of **103** was determined by GC after free-based with Na<sub>2</sub>CO<sub>3</sub> (aq). <sup>[d]</sup>ee of **103** in ML was determined by chiral GC after derivatisation with acetic anhydride <sup>[e]</sup>After one pass through the catalyst

A concentration of 0.14 M of **103** was used, as it gave the highest resolvability of those tested in isopropyl acetate (Table 3.6, entry 1). An increased loading of **92** (7 mol% Ir) was used to increase the rate of racemisation. Under these conditions, the overall yield of the process was only 28% which was similar to the resolution-only process (Table 3.5, entry 7). Gratifyingly, the de of the crystals increased very slowly from 70% to 90% after 6 cycles (Fig. 3.12(a)). Since the amount of **103** in the ML did not change significantly over time whilst its ee was decreasing gradually, this indicated that the ML was slowly racemising and the concentration of (R)-**103** was increasing in the system. However the amount of solid formed was low, as it stayed in the ML without precipitating out as the mandelate salt. This may be due to the slow growth rate of the less soluble (R)-**103**-(S)-**34**.

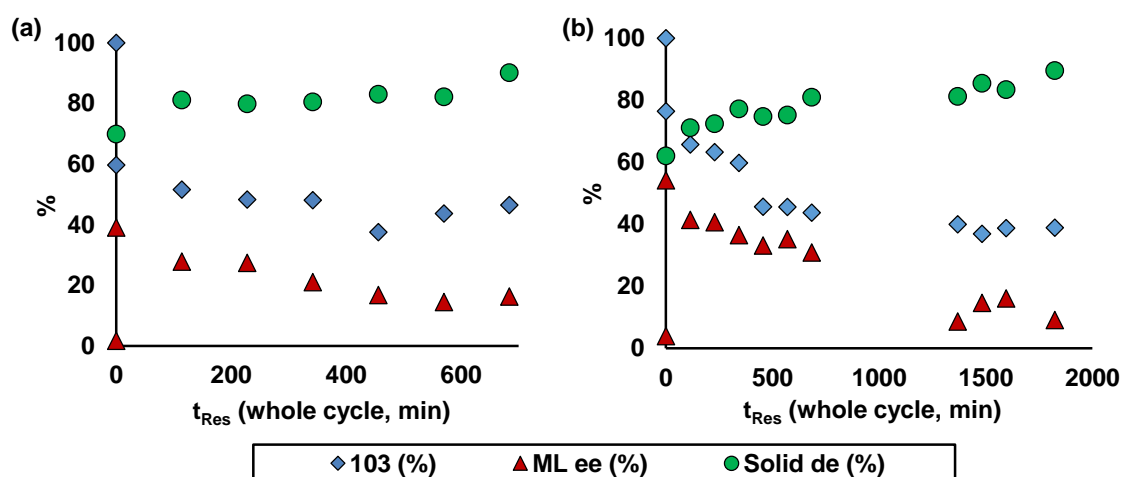


Fig. 3.12 The  $R^3$  processes of **103** at different concentration of **103** and process time. (a) 0.14 M, 6 cycles; (b) 0.25 M, 16 cycles

The concentration of **103** in the crystallisation was increased to 0.25 M with increased process time of 16 cycles (Table 3.6, entry 2; Fig. 3.12(b)). Whilst the de of the crystals fluctuated, a gradual increase from 62% to 90% was observed. The concentration of **103** in the ML slowly decreased from 72% to 39%. Whilst the isolated yield was better than the first attempt. It was still below 50% so the concentration was increased further to 0.35 M (Table 3.6, entry 3). In this case the yield increased to 52%, with similar de of 89%. This also indicate that the rate of nucleation/ growth of the less soluble diastereomer might be rate-limiting.

After each repeated reaction, the activity of the used **92** was assessed by the racemisation of (*S*)-**103** in flow (Fig. 3.13, Table 3.6). With fresh catalyst, the ee decreased from 100% to an average of 21% with 5 mol% iridium loading at 80 °C with  $t_{Res}$  of 16 minutes. Catalytic activity started to drop after the second and third  $R^3$  processes (Table 3.6, entries 2 and 3) which resulted in an average ee of 33 and 41% respectively over the five RVs collected.



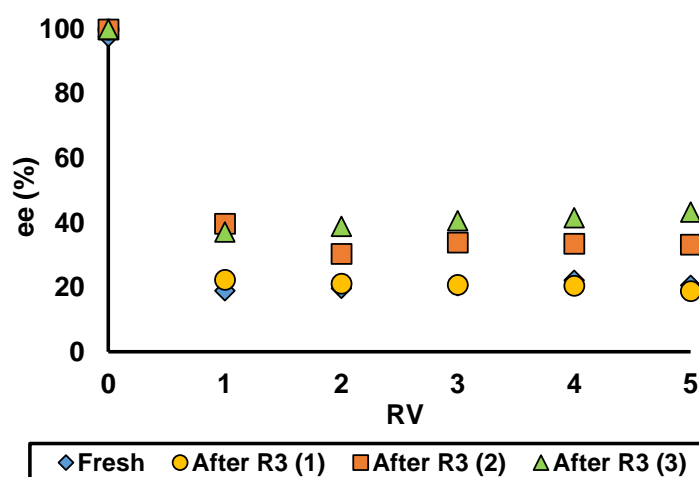
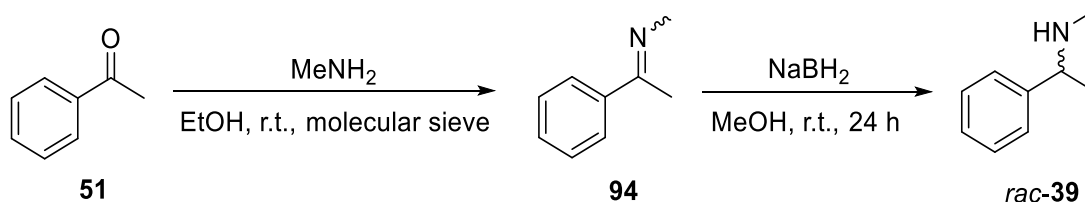


Fig. 3.13 Activity check of **92** after each  $R^3$  process of **103**, via the racemisation of (*S*)-**103** in flow at 80 °C in *i*PrOAc;  $t_{Res}$  = 16 min; *I*r loading = 5 mol%

In the batch resolutions, an increasing concentration of **103** led to a drop in resolvability due to the significant fall in diastereopurity (Table 3.5, entries 7 to 9). The best resolution gave a resolvability of 0.44. In the  $R^3$  process, higher concentration led to faster crystal growth, improving both the yield and de of the product, and increased the resolvability of the system to 0.93.

### 3.3.3 *N*-Methyl- $\alpha$ -methylbenzylamine **39**

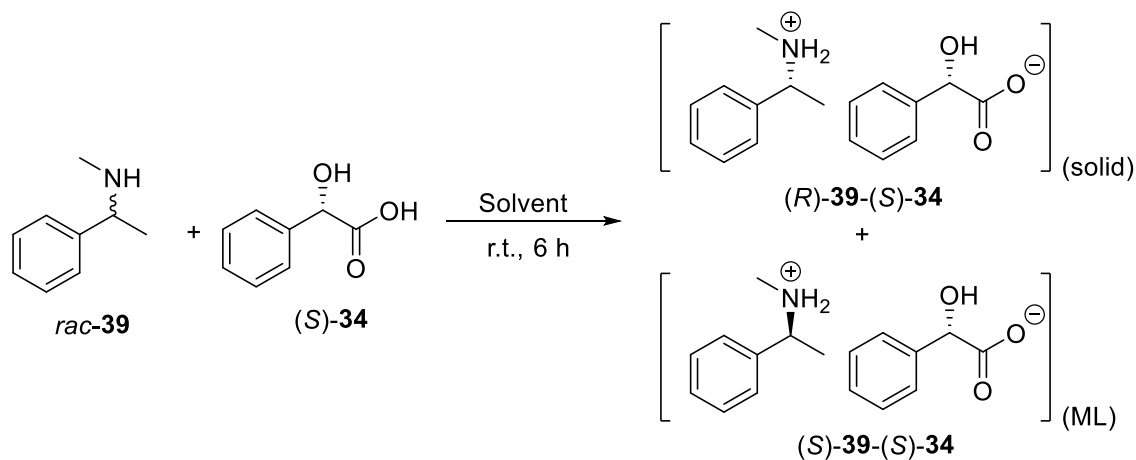
*N*-Methyl- $\alpha$ -methylbenzylamine **39** was used as a model substrate for the study of amine racemisation by homogeneous SCRAM **64**, as discussed in Section 2.2.1. However the diastereomeric resolution of **39** has not been previously reported in literature. Synthesis of *rac*-**39** was carried out *via* reductive amination of **51** by methylamine and sodium borohydride (Scheme 3.9).



Scheme 3.9 Synthesis of *rac*-**39**

Diastereomeric resolution of *rac*-**39** had been studied previously in the group by screening various chiral acid resolving agents. In particular, the use of di-*p*-toluoyl-tartaric diacid (*S,S*)-**32** in the resolution and CIDT of **39** were studied in depth by Y. Patel.<sup>152</sup> This system will be investigated further in Section 3.4. In the

meantime, acid (*S*)-**34** was used and a brief solvent screen was carried out (Scheme 3.10, Table 3.7).



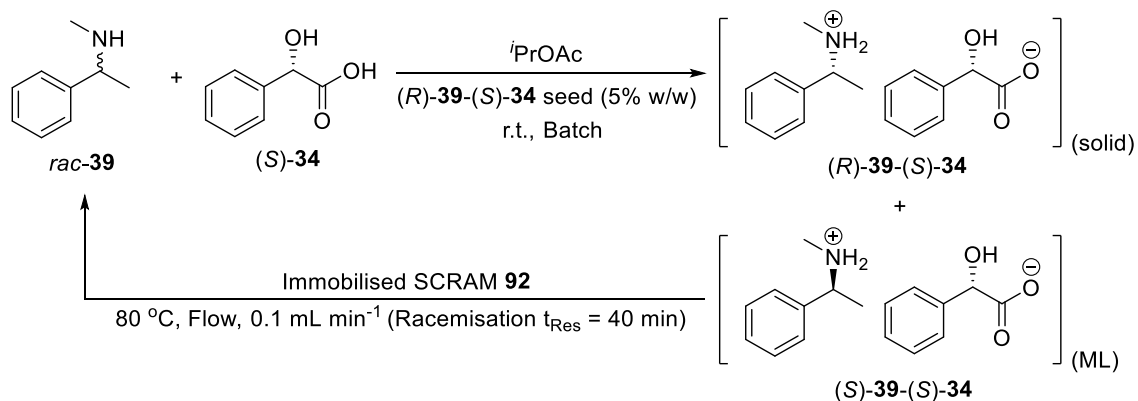
Scheme 3.10 Diastereomeric resolution of *rac*-**39** by (*S*)-**34**

Entry	Solvent	Seeded? <sup>[a]</sup>	Yield (%) <sup>[b]</sup>	De (%) <sup>[c]</sup>	S
1	EIB <sup>[d]</sup>	No	60	24	0.288
2 <sup>[e]</sup>	EIB <sup>[d]</sup>	No	67	18	0.241
3	EIB <sup>[d]</sup> / <i>i</i> PrOH (5%)	Yes	49	35	0.343
4	EIB <sup>[d]</sup> / <i>i</i> PrOH (10%)	Yes	35	47	0.329
5	<i>i</i> PrOAc	Yes	49	37	0.363
6 <sup>[e][f]</sup>	<i>i</i> PrOAc	Yes	56	30	0.336

Table 3.7 Solvent screen of diastereomeric crystallisation of **39** (0.2 M) with (*S*)-**34** (1 equiv.). <sup>[a]</sup>(*R*)-**39**-(*S*)-**34** (5% w/w) was used as the seed. <sup>[b]</sup>Seeds were not included in yield calculations. <sup>[c]</sup>De were determined by <sup>1</sup>H NMR (in CDCl<sub>3</sub>, 500 MHz). <sup>[d]</sup>Ethyl isobutyrate. <sup>[e]</sup>[**39**] = 0.3 M. <sup>[f]</sup>Alcohol **58** (1 equiv. with respect to **39**) was added

Ethyl isobutyrate (EIB) was tested in the resolution of **39** with (*S*)-**34** without seeding. Only a de of 24% was achieved (Table 3.7, entry 1). Increasing the concentration of **39** from 0.2 M to 0.3 M led to lower resolvability (Table 3.7, entry 2), whilst the addition of isopropyl alcohol co-solvent improved the resolvability (Table 3.7, entries 3 and 4). The crystallisations were also seeded with diastereopure (*R*)-**39**-(*S*)-**34** to speed up the nucleation. Isopropyl acetate gave slightly higher resolvability compared to the ethyl isobutyrate/ isopropyl alcohol systems (Table 3.7, entry 5), though the de was still quite low.

The R<sup>3</sup> process of **39** with (S)-**34** was attempted using isopropyl acetate (Scheme 3.11). With slower racemisation of **39** compared to **9** and **103**, the flow rate of the process was lowered to 0.1 mL min<sup>-1</sup>. By using the Jasco pump, the t<sub>Res</sub> for the racemisation and the whole process were about 40 and 285 minutes (4.75 hours) respectively.



Scheme 3.11 R<sup>3</sup> process of **39**. t<sub>Res</sub> for the whole cycle = 28.5 mL / 0.1 mL min<sup>-1</sup> = 285 min (4.75 h)

At 0.2 M of **39** with 0.9 equiv. of (S)-**34** added at the start of the process, de of the crystals increased very slowly from 37% to 60% over 40 cycles (190 hours). A higher crystal de was achieved compared to the batch resolution, but there was no improvement in the overall resolvability for the R<sup>3</sup> process due to the decrease in yield (Table 3.8, entry 1; Fig. 3.14(a)). One of the possible reasons was the formation of methylamine from the hydrolysis of acetophenone **51**, which can deactivate **92**, as discussed in Sections 2.2.1 and 2.4.1, lowering the efficiency of the process. Another cause might be the low rate of precipitation of the less soluble solid (R)-**39**-(S)-**34** due to its high absolute solubility (See Section 6.3.3), further limiting the yield of the product.

Entry		1	2 <sup>[a]</sup>
Reaction conditions	[ <b>39</b> ] (M)	0.2	0.3
	Ir loading (mol%)	3.8	3
	Crystallisation T (°C)	r.t.	12
	No. of cycles	40	70
	Process time (h)	190	333
Results	Initial crystal de (%) <sup>[b]</sup>	37	20
	Final crystal de (%) <sup>[b]</sup>	60	43
	Yield (%) <sup>[c]</sup>	30	53
	<b>39</b> in ML (%) <sup>[d]</sup>	50	24
	<b>51</b> in ML (%) <sup>[d]</sup>	14	14
	ML ee (%) <sup>[e]</sup>	3	-4
	S	0.36	0.46
Activity of <b>92</b>	Average ee of <b>103</b> (%) <sup>[f]</sup>	77	77

Table 3.8 Experimental conditions attempted for the R<sup>3</sup> process of **39**. <sup>[a]</sup>Alcohol **58** (1 equiv.) was added into the crystallisation mixture at the start. <sup>[b]</sup>De was determined by <sup>1</sup>H NMR (CDCl<sub>3</sub>, 500 MHz). <sup>[c]</sup>Crystals from each sample were included while the seeds were excluded from the yield calculation. <sup>[d]</sup>Amount of **39** and **51** from the ML were determined by GC after free-based with Na<sub>2</sub>CO<sub>3</sub> (aq). <sup>[e]</sup>ee was determined by chiral GC after derivatisation with acetic anhydride. <sup>[f]</sup>After one pass through the catalyst

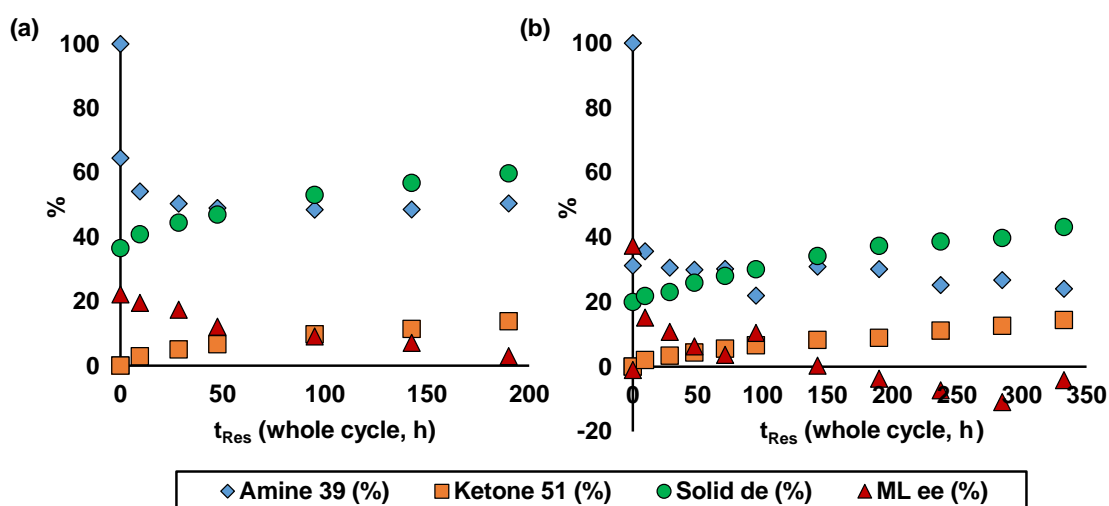


Fig. 3.14 R<sup>3</sup> processes of **39** with (*S*)-**34** at different concentration of **39** and process time. (a) 0.2 M, 40 cycles (190 h); (b) 0.3 M, 1 equiv. of **58**, 70 cycles (333 h)

The R<sup>3</sup> process of **39** was attempted at 0.3 M concentration at resolution temperature of 12 °C in order to increase the rate of crystal growth (Table 3.8,

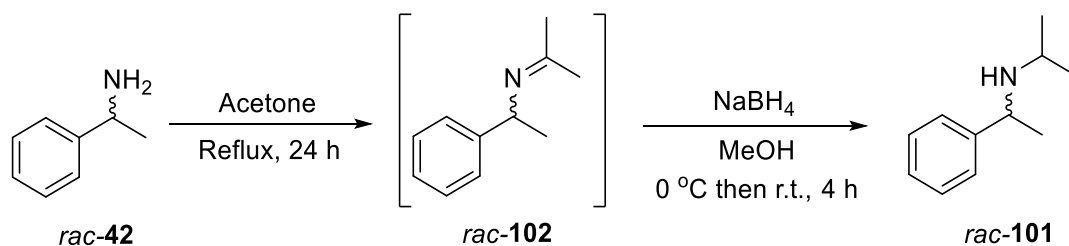
entry 2; Fig. 3.14(b)). The solvent was degassed and dried over molecular sieves to remove any water in the system and minimise the hydrolysis of the imine intermediate. Alcohol **58** (1 equiv.) was also added into the crystallisation which acted as a hydrogen donor to reduce any imine back to **39**. The slurry in the CSTR was stirred for 1 hour before starting recirculation of the ML to allow the system to reach equilibrium.

The higher concentration of **39** and lower resolution temperature led to an increased yield, compared to the first attempt. On the other hand, the initial de of the crystals was lower, indeed less than the batch reaction (Fig. 3.14(b)). Similar to the case at 0.2 M, the de of the crystals increased gradually during the process, from 20% to 43% over 70 cycles (333 h), i.e. higher than the batch resolution, with resolvability increased from 0.34 to 0.46 (Table 3.7, entry 6). About 9% of **51** was still formed after 40 cycles, less than the first attempt (14%). Unlike **9** and **103**, the concentration of **39** remained relatively constant throughout both R<sup>3</sup> processes with de increasing over time. Overall the results are relatively poor, and a different resolving agent was tested (Section 3.4.2).

The catalyst activity was again assessed by carrying out the racemisation of (*S*)-**103** in flow (Table 3.8). In both cases, ee of **103** dropped from 100% to an average of 77% after one pass through the catalyst, which was much higher than that of fresh catalyst (21%). This indicated a significant loss of activity of the catalysts and could be the result of the formation of methylamine and the carbon-metalated complex as discussed in Section 2.2.1(a) which hindered the racemisation reaction.

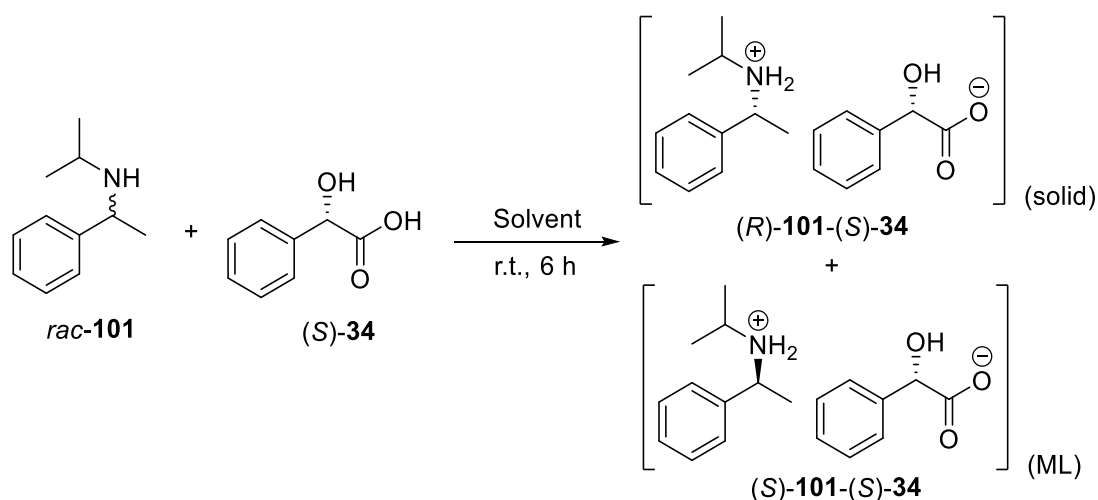
### 3.3.4 *N*-Isopropyl- $\alpha$ -methylbenzylamine **101**

*N*-Isopropyl- $\alpha$ -methylbenzylamine **101** is an analogue of **39** with the *N*-substituent being a more bulky isopropyl group. Racemic **101** was synthesised by reacting *rac*-**42** with acetone to form an intermediate racemic imine **102**, which was then reduced non-stereoselectively by sodium borohydride (Scheme 3.12).



Scheme 3.12 Synthesis of *rac-101*

The diastereomeric resolution of *rac-101* by (*S*)-**34** was carried out in three different solvents and similar resolvability was observed with similar yields and *de* (Scheme 3.13, Table 3.9).



Scheme 3.13 Diastereomeric resolution of *rac-101* by (*S*)-**34**

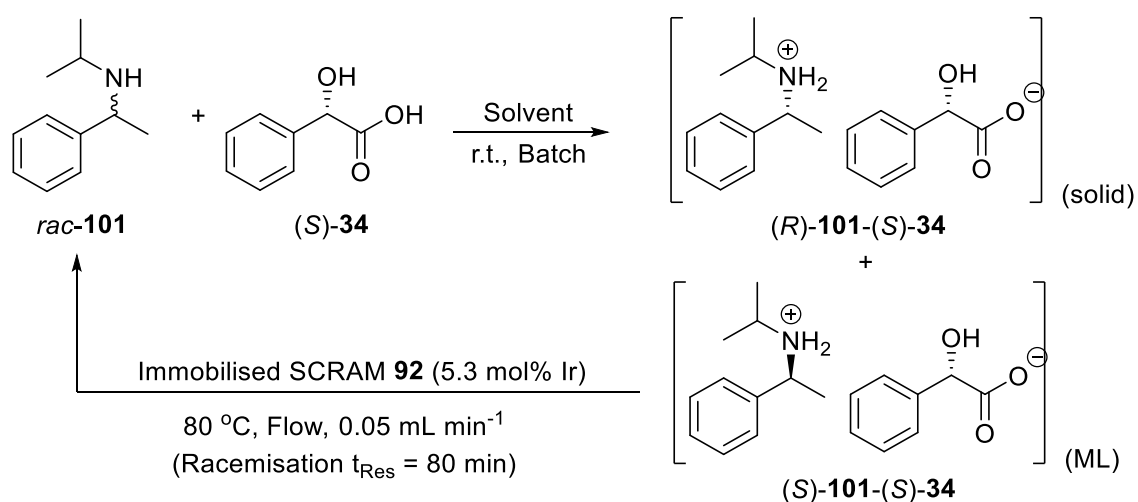
Entry	Solvent	Yield (%)	De (%) <sup>[a]</sup>	S
1	<i>i</i> PrOAc	48	67	0.643
2	<i>t</i> BuOAc	49	63	0.617
3	EIB <sup>[b]</sup>	48	70	0.672

Table 3.9 Solvent screen for diastereomeric crystallisation of *rac-101* (0.1 M) with (*S*)-**34** (1 equiv.). <sup>[a]</sup>De were determined by <sup>1</sup>H NMR (in CDCl<sub>3</sub>, 500 MHz). <sup>[b]</sup>Ethyl isobutyrate

The yields from the resolutions of **101** by (*S*)-**34** were nearly 50% with *de*s of 60 to 70%, leading to much higher resolvability of the system (> 0.6) compared to the resolutions of **39** by (*S*)-**34** (> 0.3). The solubility of the diastereopure crystals of (*R*)/ (*S*)-**39**-(*S*)-**34** and (*R*)/ (*S*)-**101**-(*S*)-**34** were determined in isopropyl acetate and ethyl isobutyrate respectively and the solubility difference between (*R*)- and (*S*)-**101**-(*S*)-**34** was much higher than that between (*R*)- and (*S*)-**39**-(*S*)-

**34** (See Section 6.3.3). In addition, no seeding was required for the diastereomeric resolution of **101** by (S)-**34** as the crystals formed quickly. This result indicates that the nitrogen substituent has a significant impact upon packing within the crystal structure, and the rate of both nucleation and crystal growth.

With the more bulky substituent at the nitrogen atom in **101**, the racemisation by SCRAM **64/ 92** is much slower than that of **39**, as shown by their racemisation half-life in the homogeneous batch systems and the  $t_{Res}$  required in flow (Sections 2.2.2 and 2.3.3). Therefore, in developing the  $R^3$  process of **101**, the same low flow rate of  $0.05 \text{ mL min}^{-1}$  was used as that in the flow racemisation study. The  $t_{Res}$  for the racemisation and the whole process were 80 minutes and 9.5 hours respectively with the use of Jasco pump (Scheme 3.14). The conditions and results for the  $R^3$  processes of **101** were summarised in Table 3.10.



Scheme 3.14  $R^3$  process of **101**.  $t_{Res}$  for the whole cycle =  $28.5 \text{ mL} / 0.05 \text{ mL min}^{-1} = 570 \text{ min}$  (9.5 h)

Entry		1	2	3
Reaction conditions	Solvent	EIB <sup>[a]</sup>	<sup>i</sup> PrOAc	EIB <sup>[a]</sup>
	Equiv. of (S)- <b>34</b> added at the start	0.9	0.9	0.98
	No. of cycles	11	20	30
	Process time (h)	105	190	285
Results	Initial crystal de (%) <sup>[b]</sup>	39	57	64
	Final crystal de (%) <sup>[b]</sup>	85	83	89
	Yield (%) <sup>[c]</sup>	56	58	62
	<b>101</b> in ML (%) <sup>[d]</sup>	18	17	5
	<b>51</b> in ML (%) <sup>[d]</sup>	9	13	15
	ML ee (%) <sup>[e]</sup>	N.D. <sup>[f]</sup>	34	17
	S	0.95	0.96	1.1
Activity of <b>92</b>	Average ee of <b>103</b> (%) <sup>[g]</sup>	53	64	51

Table 3.10 Experimental conditions attempted for the R<sup>3</sup> process of **101**. <sup>[a]</sup>Ethyl isobutyrate. <sup>[b]</sup>De was determined by <sup>1</sup>H NMR (CDCl<sub>3</sub>, 500 MHz). <sup>[c]</sup>Crystals from each sample were included in the yield calculation. <sup>[d]</sup>Amount of **101** and **51** from ML was determined by GC after free-based with Na<sub>2</sub>CO<sub>3</sub> (aq). <sup>[e]</sup>ee was determined by chiral GC after derivatisation with trifluoroacetic anhydride. <sup>[f]</sup>Not determined. <sup>[g]</sup>After one pass through the catalyst

Resolvability of the R<sup>3</sup> systems increased over the resolution-only processes, with improvement on both yield and de. Switching solvent between ethyl isobutyrate and isopropyl acetate, increasing the number of recirculation cycles and charging more (S)-**34** at the start of the process did not result in significant improvement in the results. The third attempt of the R<sup>3</sup> process of **101** was illustrated in Fig. 3.15 (Table 3.10, entry 3). Increasing the process time increased the amount of **51** formed in the reaction. The R<sup>3</sup> processes of **101** were more successful than those of **39**, mainly due to the larger solubility difference of diastereomers of **101**, the higher rates of dissolution of the more soluble (S)-**101**-(S)-**34** and precipitation of (R)-**101**-(S)-**34**, which outweigh the slower racemisation of the ML.



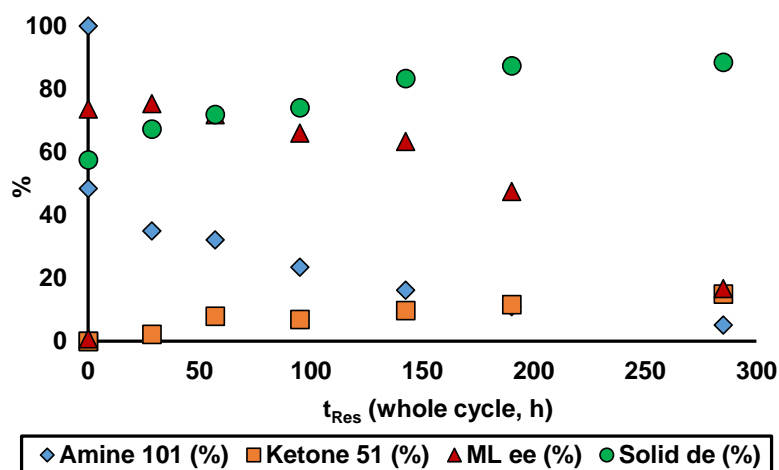
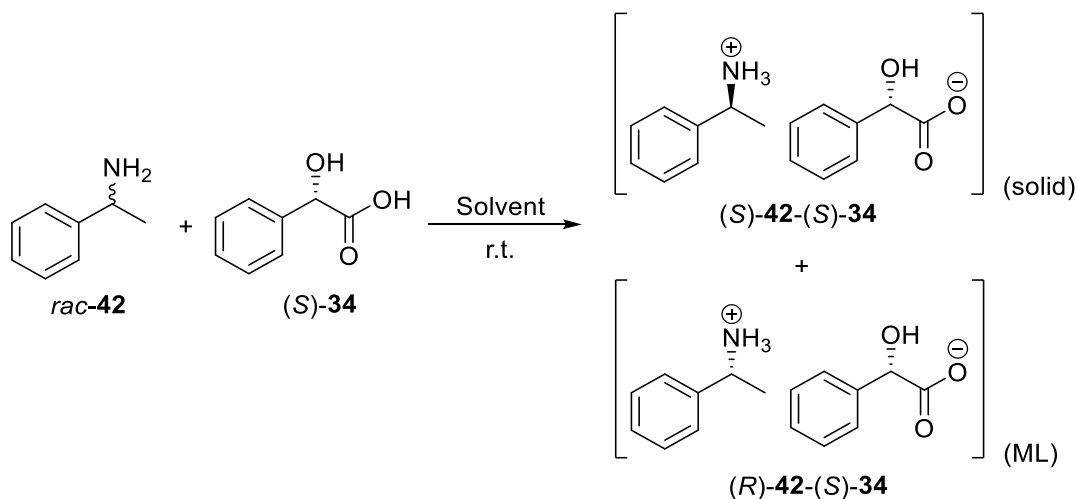


Fig. 3.15  $R^3$  process of **101** with 0.98 equiv. of (*S*)-**34** added at the start of the process (Table 3.10, entry 3)

### 3.3.5 $\alpha$ -Methylbenzylamine **42**

$\alpha$ -Methylbenzylamine **42** is a primary amine which has been used as a resolving agent for racemic chiral acids such as **34**.<sup>153, 154</sup> Therefore, the resolution of *rac*-**42** was tested with (*S*)-**34** and a various solvent systems were screened (Scheme 3.15, Table 3.11).



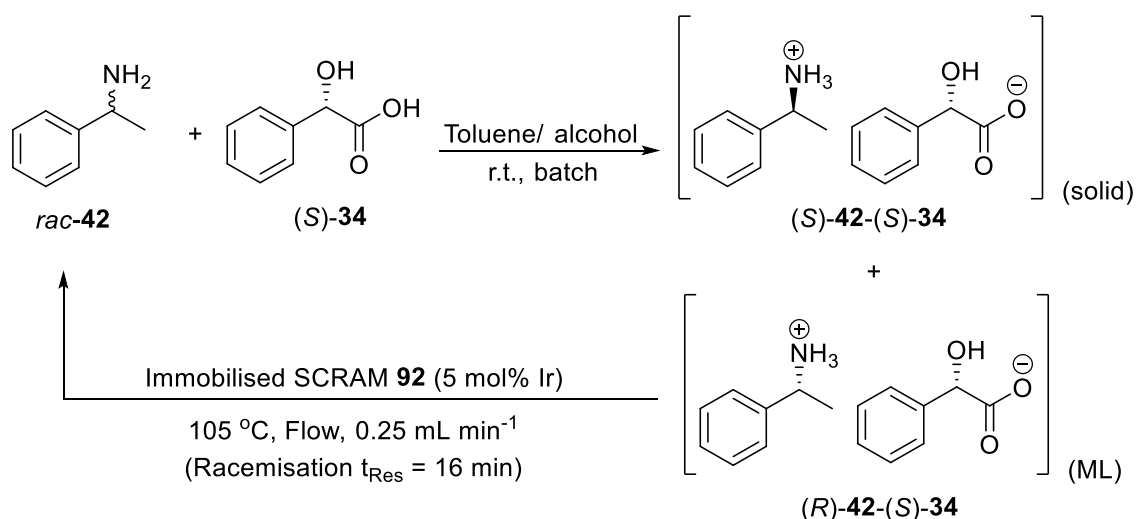
Scheme 3.15 Diastereomeric resolution of *rac*-**42** by (*S*)-**34**

Entry	[42] (M)	Solvent	De (%) <sup>[a]</sup>	Yield (%)	S
1	0.28	EtOH	96	18	0.346
2	0.14	<sup>i</sup> PrOH	92	37	0.681
3	0.14	Toluene/ MeOH (10%)	94	31	0.583
4	0.14	Toluene/ MeOH (5%)	86	41	0.705
5	0.14	Toluene/ <sup>i</sup> PrOH (20%)	81	46	0.745
6	0.14	Toluene/ <sup>i</sup> PrOH (10%)	13	85	0.221

Table 3.11 Solvent screen for diastereomeric crystallisation of rac-**42** with (S)-**34** (1 equiv.) at r.t. <sup>[a]</sup>De of crystals were determined as the ee of the free amine by chiral HPLC, after free-based with Na<sub>2</sub>CO<sub>3</sub> (aq) and derivatised with benzoyl chloride in the presence of triethylamine

The resolution was first attempted using ethanol which had been reported in the literature for studying the separability of the diastereomeric salts formed between acid **34** and amine **42** (Table 3.11, entry 1).<sup>153</sup> A high de of 96% was achieved but the yield was only 18% even at a higher concentration compared to the use of other solvents. With the use of isopropyl alcohol at a lower concentration, the resolvability of the system was better compared to that using ethanol due to higher yield with minimal drop in de (Table 3.11, entry 2). Since the use of polar solvents such as pure alcohols can inhibit racemisation by SCRAM **64**, solvent systems with lower polarity such as toluene/ alcohol mixtures were used (Table 3.11, entries 3 to 5). Resolution using methanol as co-solvent led to higher de but lower yield than using isopropyl alcohol (Table 3.11, entries 3 and 4). Reducing the amount of isopropyl alcohol from 20 to 10% resulted in a significant drop in the resolvability of **42** by (S)-**34**.

The R<sup>3</sup> process of **42** was developed using the Knauer PS4.1 pump and a flow rate of 0.25 mL min<sup>-1</sup> was employed. The t<sub>Res</sub> of racemisation and the whole process were 16 and 100 minutes respectively (Scheme 3.16). In both R<sup>3</sup> processes, the ML was recirculated for 6 cycles. The total process time was 10 hours.



Scheme 3.16  $R^3$  process of **42**. The  $t_{\text{Res}}$  for the whole cycle = 25 mL / 0.25 mL min<sup>-1</sup> = 100 min (1.7 h)

Entry		1	2
Reaction conditions	Solvent	Toluene/ MeOH (5%)	Toluene/ <sup>i</sup> PrOH (20%)
	Initial crystal de (%) <sup>[a]</sup>	87	79
Results	Final crystal de (%) <sup>[a]</sup>	83	93
	Yield (%) <sup>[b]</sup>	42	29
	<b>42</b> in ML (%) <sup>[c]</sup>	14	12
	Dimers in ML (%) <sup>[c]</sup>	29	28
	<b>101</b> in ML (%) <sup>[c]</sup>	N.A.	22
	ML ee (%) <sup>[a]</sup>	45	4
	S	0.7	0.54

Table 3.12 Experimental conditions attempted for the  $R^3$  process of **42**. (S)-**34** (0.8 equiv.) was added at the start of the process. No. of cycles = 6. Total process time = 600 min (10 h). <sup>[a]</sup>De of crystals and ee of ML were determined as the ee of the free amine by chiral HPLC after free-based with Na<sub>2</sub>CO<sub>3</sub> (aq) and derivatisation with benzoyl chloride in the presence of triethylamine. <sup>[b]</sup>Crystals from each sample were included in the calculation of yield. <sup>[c]</sup>Amount of **42**, dimers and amine **101** were determined by GC after free-based the samples

As discussed in Section 2.2.3, the major problem of the racemisation of primary amines such as **42** is the formation of various dimer impurities (Scheme 1.23). In the  $R^3$  process, it was hoped that the low concentration of **42** in the ML after crystallisation could reduce the formation of dimers. However, significant dimer

formation was still observed (Table 3.12). Using methanol as co-solvent did not result in any improvement in either yield or de compare to the resolution-only process (Table 3.12, entry 1; Fig. 3.16).

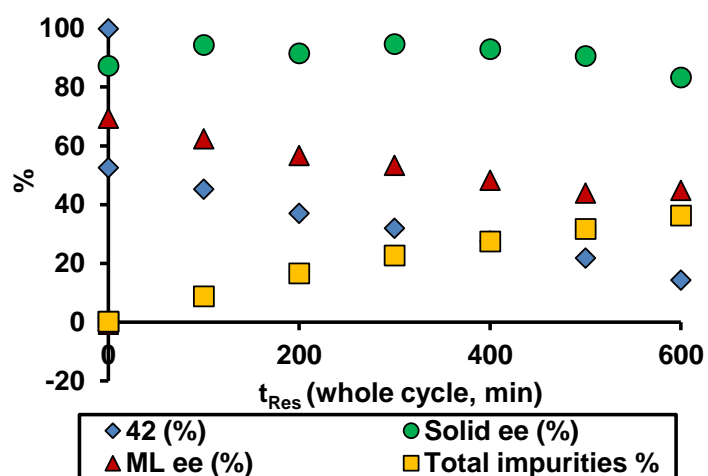
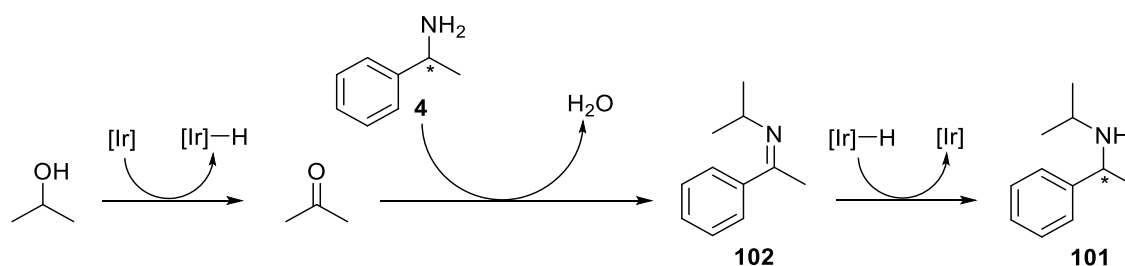


Fig. 3.16 R<sup>3</sup> process of **42** with 0.8 equiv. of (S)-**34** added at the start of the process (Table 3.12, entry 1)

Although isopropyl alcohol can act as a hydrogen donor which may reduce dimer formation, it can also react with **42** to form amine **101** via borrowing hydrogen mechanism (Scheme 3.17),<sup>32</sup> further lowering the yield and the overall resolvability, though the de of the product was found to increase over the batch resolution-only process (Table 3.12, entry 2).



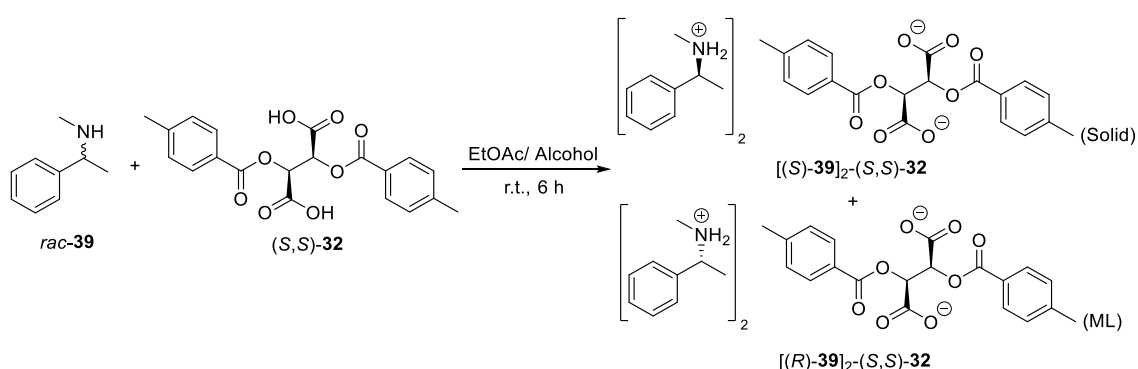
Scheme 3.17 Formation of **101** from **42** in the presence of **92** (and **64**)

The R<sup>3</sup> processes of **42** were less successful compared to other substrates mainly due to significant by-product formation during racemisation. Alternative (immobilised) catalysts that can mitigate the problem are needed to develop an efficient R<sup>3</sup> process of **42**, or primary amines in general.

### 3.4 Diacid as a resolving agent for diastereomeric transformation of chiral amines

#### 3.4.1 Resolution of *N*-Methyl- $\alpha$ -methylbenzylamine **39** with di-*p*-toluoyl-*D*-tartaric acid **32** in batch

Resolution of *N*-Methyl- $\alpha$ -methylbenzylamine **39** using (*S*)-**34** was discussed in Section 3.3.3. The resolvability achieved in batch resolution was only 0.36 in isopropyl acetate and could only be improved slightly to 0.46 by applying the R<sup>3</sup> process (Table 3.8, entry 2). Therefore, an alternative chiral acid, (*S,S*)-**32** was used as the resolving acid (Scheme 3.18).



Scheme 3.18 Diastereomeric resolution of **39** with (*S,S*)-**32**

Entry	Alcohol (%) <sup>[a]</sup>	[ <b>39</b> ] (M)	( <i>S,S</i> )- <b>32</b> (Equiv.)	Yield (%)	de (%) <sup>[b]</sup>	S
1	MeOH (20)	0.14	0.5	27	84	0.43
2	MeOH (15)	0.14	0.5	79	3	0.10
3	MeOH (10)	0.14	0.5	79	4	0.13
4	MeOH (20)	0.07	0.5	21	88	0.37
5	MeOH (20)	0.21	0.5	73	5	0.07
6	MeOH (20)	0.14	0.25	19	90	0.34
7	MeOH (20)	0.14	0.125	8	91	0.15
8	MeOH (20)	0.21	0.25	22	86	0.38
9	<sup>i</sup> PrOH (20)	0.21	0.25	36	54	0.39
10	<sup>i</sup> PrOH (20)	0.21	0.5	84	1.6	0.03

Table 3.13 Condition screen of diastereomeric resolution of *rac*-**39** with (*S,S*)-**32** at r.t.

<sup>[a]</sup>Volume ratio. <sup>[b]</sup>De was determined as the ee of the free amine by chiral GC after derivatisation with trifluoroacetic anhydride

Screening of conditions was initially performed at room temperature by varying the solvent system, concentration of amine **39** and the equivalence of acid (*S,S*)-**32** (Table 3.13). With 0.5 equiv. of **32**, neutral diastereomeric salts containing two amines and one acid are formed, as determined by <sup>1</sup>H NMR spectroscopy. The use of 20% v/v methanol solution gave a much better de than either 10% or 15% concentrations of methanol, leading to higher resolvability (Table 3.13, entry 1). It is surprising that such a small change of in the concentration of methanol has a drastic effect on the resolvability (Table 3.13, entries 2 and 3). An increase in de but lower yield was observed when a lower concentration of **39** was used; whilst increasing the concentration of **39** reduced the resolvability of the system significantly (Table 3.13, entries 4 and 5). A higher de was also achieved with less resolving acid (Table 3.13, entries 6 to 8). Using 20% (v/v) methanol at 0.21 M and halving **32** to 0.25 equiv. greatly increased the de of the product and significantly improved the system resolvability (Table 3.13, entries 5 and 8). A similar trend was observed when 20% (v/v) isopropyl alcohol was used, in which the resolvability dropped drastically when **32** was increased from 0.25 to 0.5 equiv. (Table 3.13, entries 9 and 10). The use of isopropyl alcohol led to higher yield but lower de compared to the resolution using methanol as co-solvent, with similar overall resolvability (Table 3.13, entries 5, 8 to 10). As with the concentration of methanol and isopropyl alcohol, the system is also remarkably sensitive to the acid: amine stoichiometry. This will be investigated in the following study.

Before developing the R<sup>3</sup> process of **39** with (*S,S*)-**32**, one-pot recycle reactions were carried out by stirring *rac*-**39** and (*S,S*)-**32** with soluble SCRAM **64** and Shvo's catalyst **55** in ethyl acetate with 20% (v/v) methanol (Fig. 3.17). The reactions were performed at room temperature with supersaturation, ensuring a slurry of the crystals remained in solution. Racemisations are usually carried out at elevated temperatures, so at ambient temperature the diastereomeric transformation was very slow. Under these conditions, the optical excesses and concentration of **39** remained constant for about 25 hours. De of the crystals was about 75% whilst ee of the ML was 40%. However after 30 hours a sudden fall in the crystal de to < 5% was observed, which is much lower than that of the batch resolution process (Table 3.13, entry 1). The concentration of **39** in solution decreased and the amine ee in the ML fell to about 16%.

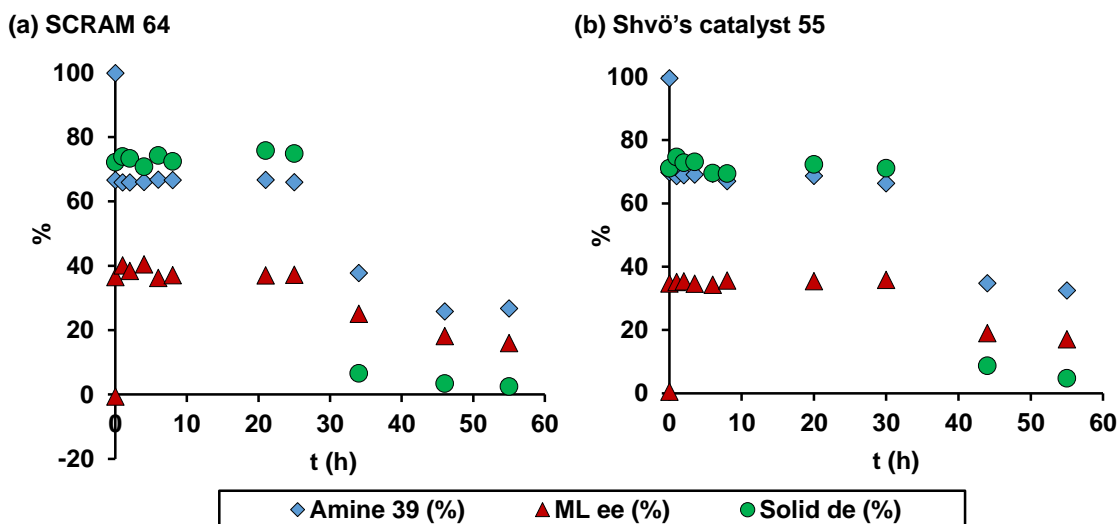


Fig. 3.17 One-pot recycle reactions of **39** with (*S,S*)-**32** in the presence of homogeneous racemisation catalysts at room temperature in EtOAc/ MeOH (20% v/v). (a) SCRAM **64**; (b) Shvö's catalyst **55**

To investigate any effect of the catalysts in the resolution of **39** with (*S,S*)-**32**, a simple batch crystallisation reaction was carried out without them at 25 °C with controlled temperature and stirring (Fig. 3.18). After initially forming crystals of about 80% de, after about 5 hours, the de fell rapidly, as did the solution concentration of the amine and the ML ee. The drop in de is not a result of the racemisation catalysts.

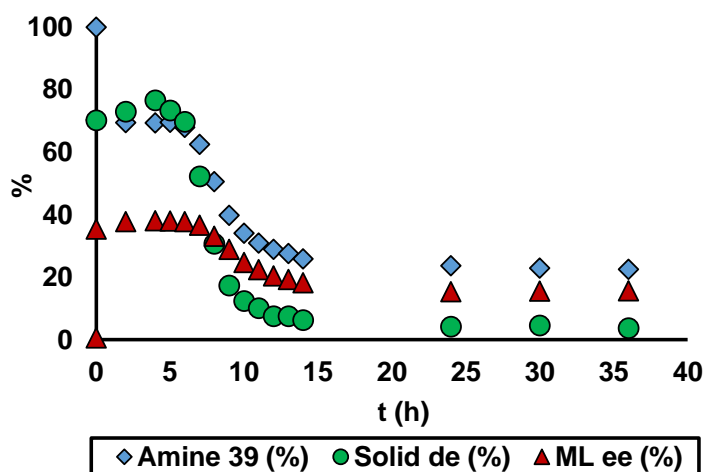


Fig. 3.18 Diastereomeric resolution of *rac*-**39** with (*S,S*)-**32** at 25 °C, 400 rpm stirring, with no racemisation catalysts

The low de crystals, obtained at 25 °C, were analysed by differential scanning calorimetry (DSC) and thermogravimetric analysis (TGA) and the results were

compared with those of the pure diastereomers and a 1:1 mixture of the pure diastereomers (Fig. 3.19). The peaks on the DSC graph correspond to the melting points of each species (Fig. 3.19(a)). The different melting temperatures observed for the low de crystals and the 1:1 mixture of diastereomers indicated that they are different entities. TGA showed a drop in mass of all species at about 130 to 150 °C (Fig. 3.19(b)). It was likely to be thermal decomposition instead of solvent loss from the crystals due to the relatively high temperatures at which the drop of mass occurred.

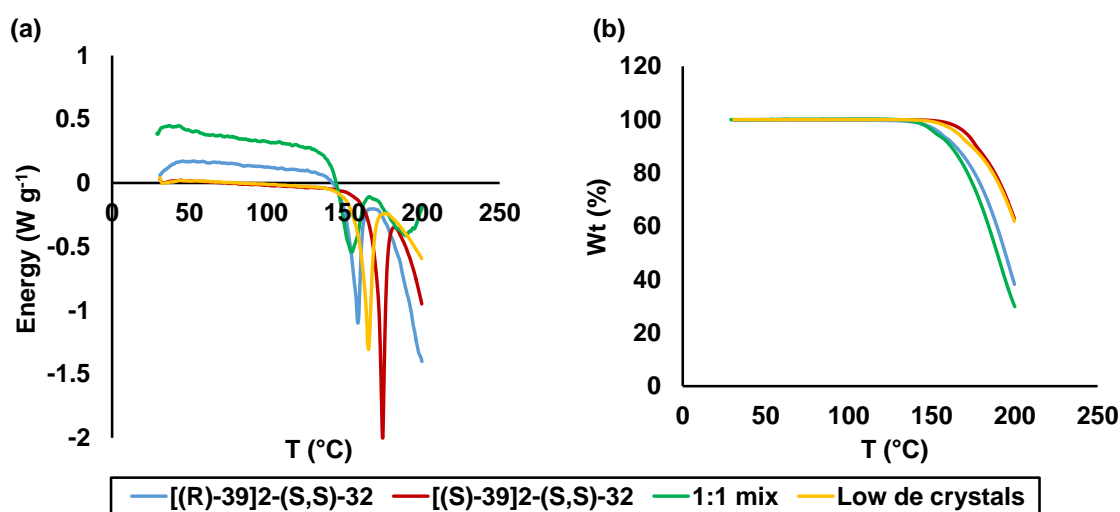


Fig. 3.19 Thermal analysis of  $[(R)\text{-39}]_2\text{-(S,S)-32}$ ,  $[(S)\text{-39}]_2\text{-(S,S)-32}$ , 1:1 mixture of  $[(S)\text{-39}]_2\text{-(S,S)-32}$  and  $[(R)\text{-39}]_2\text{-(S,S)-32}$  (1:1 mix) and crystals with low de from diastereomeric resolution of **39** with (S,S)-**32** at 25 °C by (a) DSC; (b) TGA. The measurements were carried out by T. Howell from School of Chemical and Process Engineering, University of Leeds

Since the fall in crystal diastereopurity was not a result of the formation of a mixture of pure diastereomers (e.g. by tartrate racemisation/ epimerisation), it indicated a switch in crystal form. The formation of solvate was ruled-out from the TGA. So it was suspected that an exchange of amine enantiomers was occurring to go from  $[(S)\text{-39}]_2\text{-(S,S)-32}$  and  $[(R)\text{-39}]_2\text{-(S,S)-32}$  (with the former in excess), to a 'racemic' diamine salt which contains both (R)-**39** and (S)-**39**, i.e. (S)-**39**-(S,S)-**32**-(R)-**39** (Fig. 3.20). The working hypothesis is that the diastereopure diamine salts are kinetic products which are formed first, whilst the racemic diamine salt is initially formed below its critical concentration, and remains in solution. With prolonged stirring, (R)-**39** and (S)-**39** exchange between the



solution and solid phases and cause the concentration of (S)-**39**-(S,S)-**32**-(R)-**39** to increase and eventually reach its critical concentration, where crystallisation of the more thermodynamically favoured ‘racemic’ diamine salt occurs.

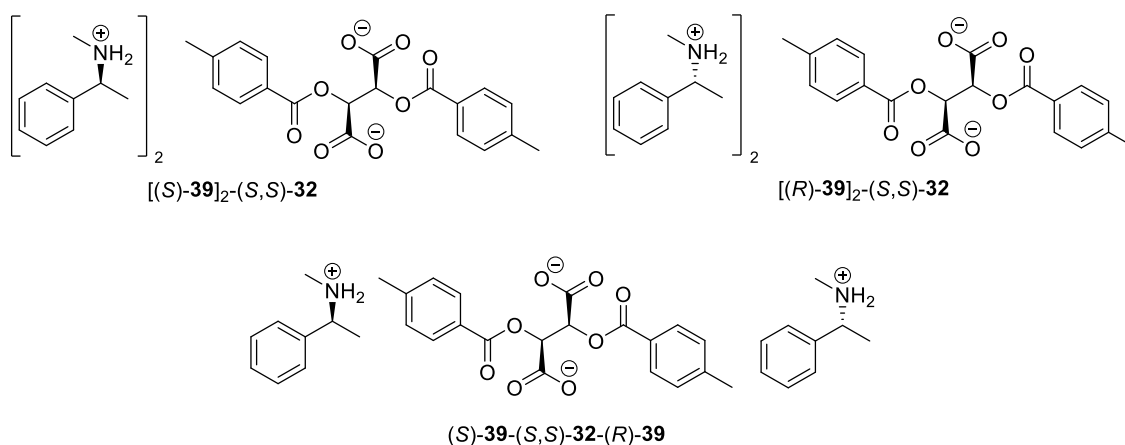


Fig. 3.20 Structures of diastereopure di-toluoyl-D-tartrate salts of **39** and racemic diamine salt containing both (R)-**39** and (S)-**39**

The hypothesis was further verified with X-ray analysis of the crystals. Powder X-ray diffraction (XRD) data were collected for  $[(S)\text{-}39]_2\text{-}(S,S)\text{-}32$ ,  $[(R)\text{-}39]_2\text{-}(S,S)\text{-}32$ , 1:1 mixture of  $[(S)\text{-}39]_2\text{-}(S,S)\text{-}32$  and  $[(R)\text{-}39]_2\text{-}(S,S)\text{-}32$  and the low-de crystals obtained from the batch resolution at 25 °C (Fig. 3.21(a) to (d)). The XRD spectrum of the low-de crystals was different from that of the diastereopure salts, and their 1:1 mixture, indicating they were different species. Initially, the small size of the low-de crystals precluded diffraction, but with the help of the National Crystallography Service (NCS) from University of Southampton, a single crystal X-ray structure was obtained which showed a racemic 2:1 salt of **39** and (S,S)-**32** containing one (R)-**39** and one (S)-**39** (Fig. 3.22(a)). The powder XRD data predicted from the single crystal X-ray structure resembles that collected from the actual crystals (Fig. 3.21(e)). The single crystal X-ray structures of the diastereopure (S,S)-**32** salts of **39** were also shown in Fig. 3.22(b) and (c).

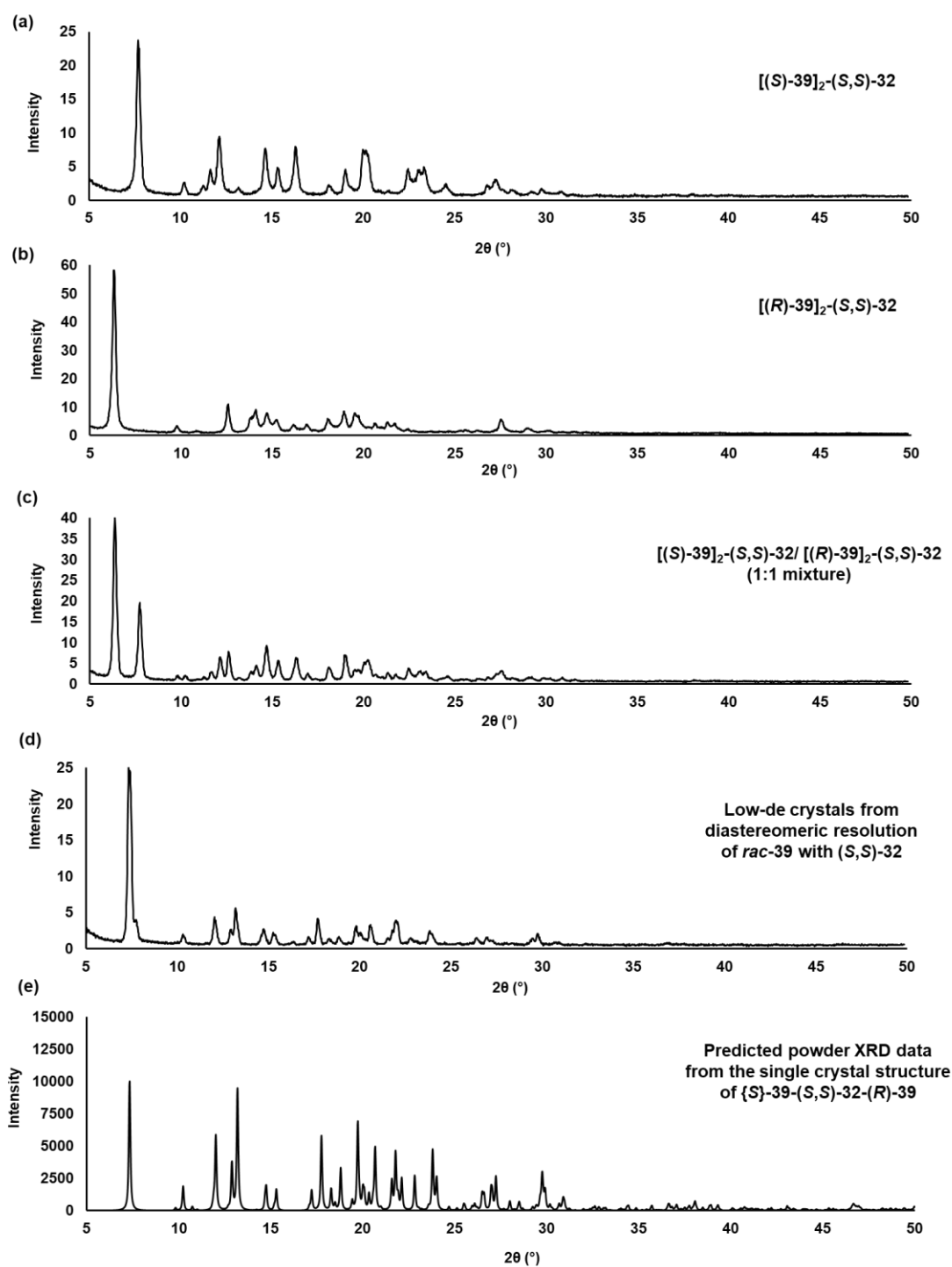


Fig. 3.21 Powder XRD data of (a)  $[(S)\text{-}39]_2\text{-(S,S)\text{-}32}$ ; (b)  $[(R)\text{-}39]_2\text{-(S,S)\text{-}32}$ ; (c) 1:1 mixture of  $[(S)\text{-}39]_2\text{-(S,S)\text{-}32}$  and  $[(R)\text{-}39]_2\text{-(S,S)\text{-}32}$ ; (d) Low-de crystals from diastereomeric resolution of  $\text{rac}\text{-}39$  with  $(S,S)\text{-}32$ ; (e) XRD data predicted from the single crystal structure of  $(S)\text{-}39\text{-(S,S)\text{-}32}\text{-(R)\text{-}39}$  (Fig. 3.22(a))

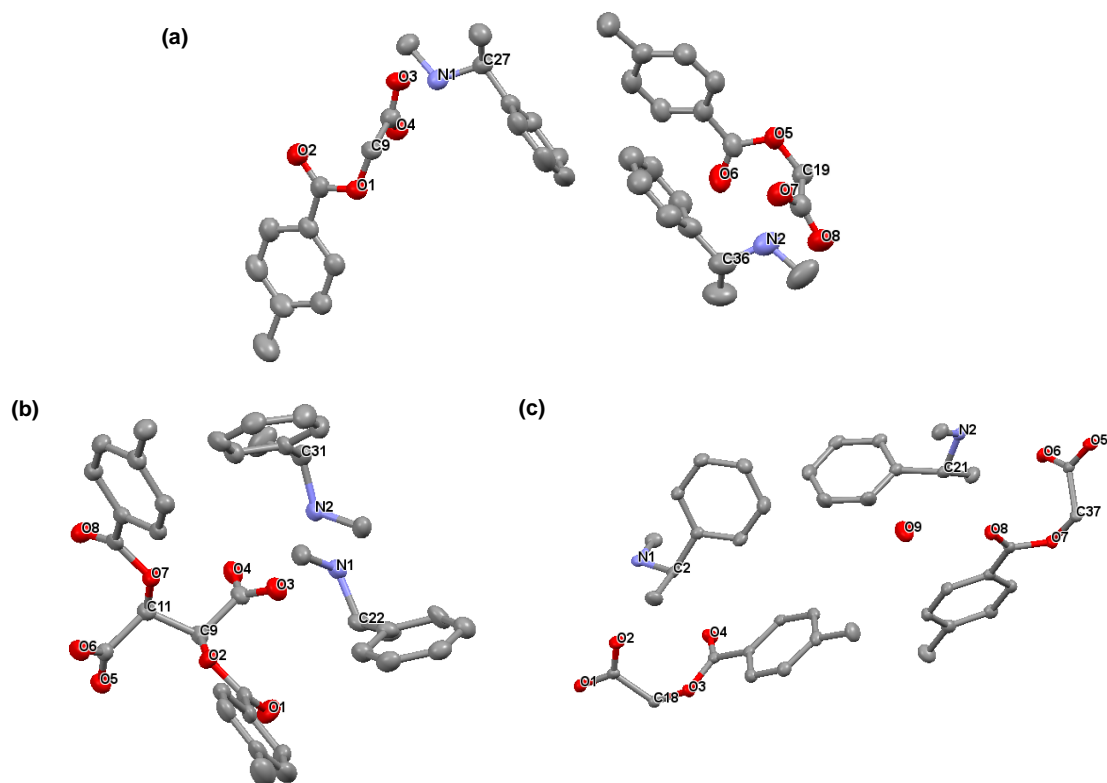


Fig. 3.22 Single crystal structures of (a) low-de crystals obtained from diastereomeric resolution of **39** with **(S,S)-32** showing a stoichiometric ratio of 2:1 of **39/32** and the opposite stereochemistry of the two molecular ions of **39**; (b) Diastereopure  $[(S)\text{-}39]_2\text{-(S,S)-32}$ ; (c) Diastereopure  $[(R)\text{-}39]_2\text{-(S,S)-32}$ . The hydrogen atoms were omitted for clarity. All atoms are displaced as ellipsoid, which are depicted at 50% probability. The chiral carbon, nitrogen and oxygen atoms are numbered. The nitrogen and oxygen atoms are highlighted (blue and red respectively)

The crystals obtained from the diastereomeric resolution of *rac*-**39** with **(S,S)-32** in ethyl acetate/ methanol mixtures were analysed by XRD to further investigate the effect of the amount of methanol in the resolvability of the system (Table 3.13, entries 1 to 3; Fig. 3.23). With 20% (by volume) methanol where the de of the crystals is relatively high (Table 3.13, entry 1), its X-ray diffraction pattern shows a mixture of pure diastereomers with  $[(S)\text{-}39]_2\text{-(S,S)-32}$  in excess (Fig. 3.23(a)). Resolution with both 10 and 15% (by volume) methanol resulted in low de crystals (Table 3.13, entries 2 and 3). However their XRD patterns are different. The crystals obtained from 10% methanol correspond to a mixture of  $[(S)\text{-}39]_2\text{-(S,S)-32}$  and  $[(R)\text{-}39]_2\text{-(S,S)-32}$  (Fig. 3.23(c)); whilst those obtained from 15% methanol correspond to **(S)-39-(S,S)-32-(R)-39** (Fig. 3.23(b)). This explains the drastic drop in de in reducing the amount of methanol from 20 to 15%. With 10% methanol,

both pure diastereomers have very low solubility in the solvent system. After they are formed at the beginning of the resolution, their dissolution and hence the exchange of (*S*)- and (*R*)-**39** between the solid and solution phases is so slow that the concentration of (*S*)-**39**-(*S,S*)-**32**-(*R*)-**39** remains low and not able to nucleate. Therefore the crystals of (*S*)-**39**-(*S,S*)-**32**-(*R*)-**39** was not observed.

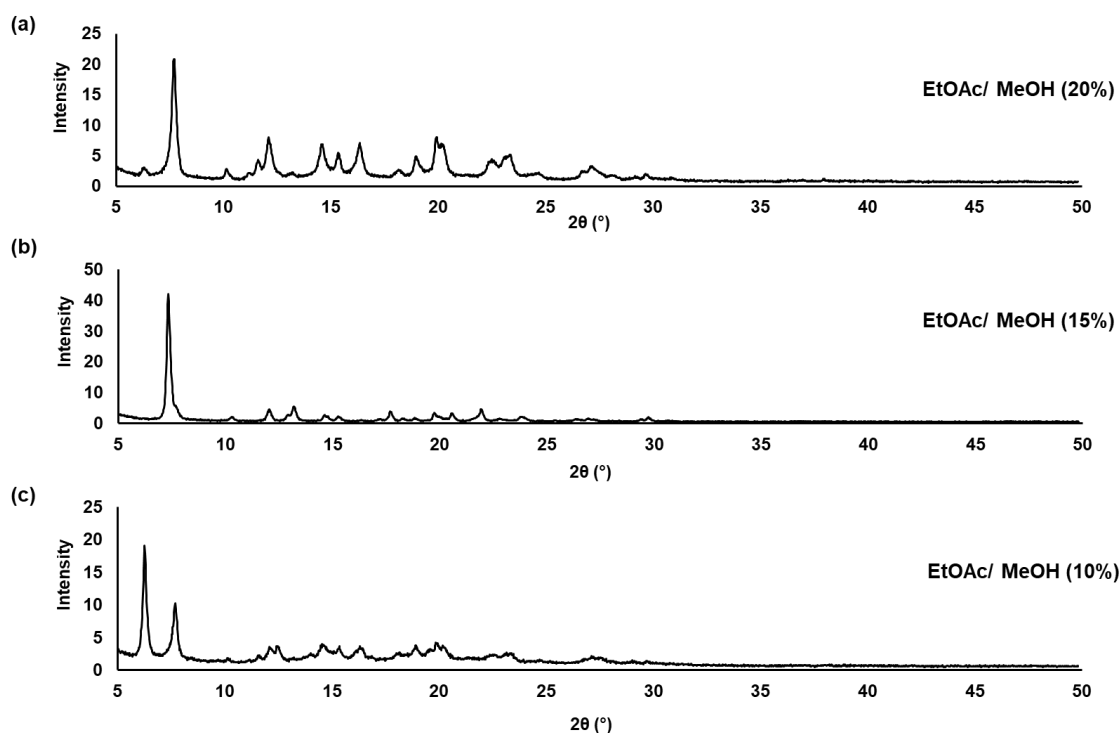


Fig. 3.23 XRD data of the crystals from diastereomeric resolution of **39** with (*S,S*)-**32** in ethyl acetate/ methanol mixture. (a) 20% MeOH; (b) 15% MeOH; (c) 10% MeOH. All percentages are by volume

The switching of crystal forms was further investigated under different experimental conditions (Fig. 3.24). It was found that the rate of switching depends on temperature, concentration of **39** and **32**, stirring speed and the types of seed crystals present. The switching of crystal form occurred later in the process at lower temperatures since (*S*)-**39**-(*S,S*)-**32**-(*R*)-**39** is the thermodynamic product which requires more energy to form (Fig. 3.24(a)). At lower concentrations of **39** and **32**, the concentration of (*S*)-**39**-(*S,S*)-**32**-(*R*)-**39** formed is likely to be below its critical concentration, which avoids it from growing and precipitating out from solution (Fig. 3.24(b) and (c)). When the system was stirred at a higher speed, the switching occurred faster. The crystals were broken down into smaller sizes more quickly, facilitating their dissolution and the

exchange between (*R*)- and (*S*)-**39** in the solid/ solution phases and speeds up the formation of (*S*)-**39**-(*S,S*)-**32**-(*R*)-**39**. Switching of crystal form was still observed without stirring but at a lower rate (Fig. 3.24(d)). Seeding the resolution with pure [(*S*)-**39**]<sub>2</sub>-(*S,S*)-**32** had no observable impact on the crystal switching. However when the system was seeded with (*S*)-**39**-(*S,S*)-**32**-(*R*)-**39**, the switching occurred much faster. The seed provided the nuclei for (*S*)-**39**-(*S,S*)-**32**-(*R*)-**39** to grow, which was indicated by the lower de of the crystals at the start compared to the systems without seeding (Fig. 3.24(e)).

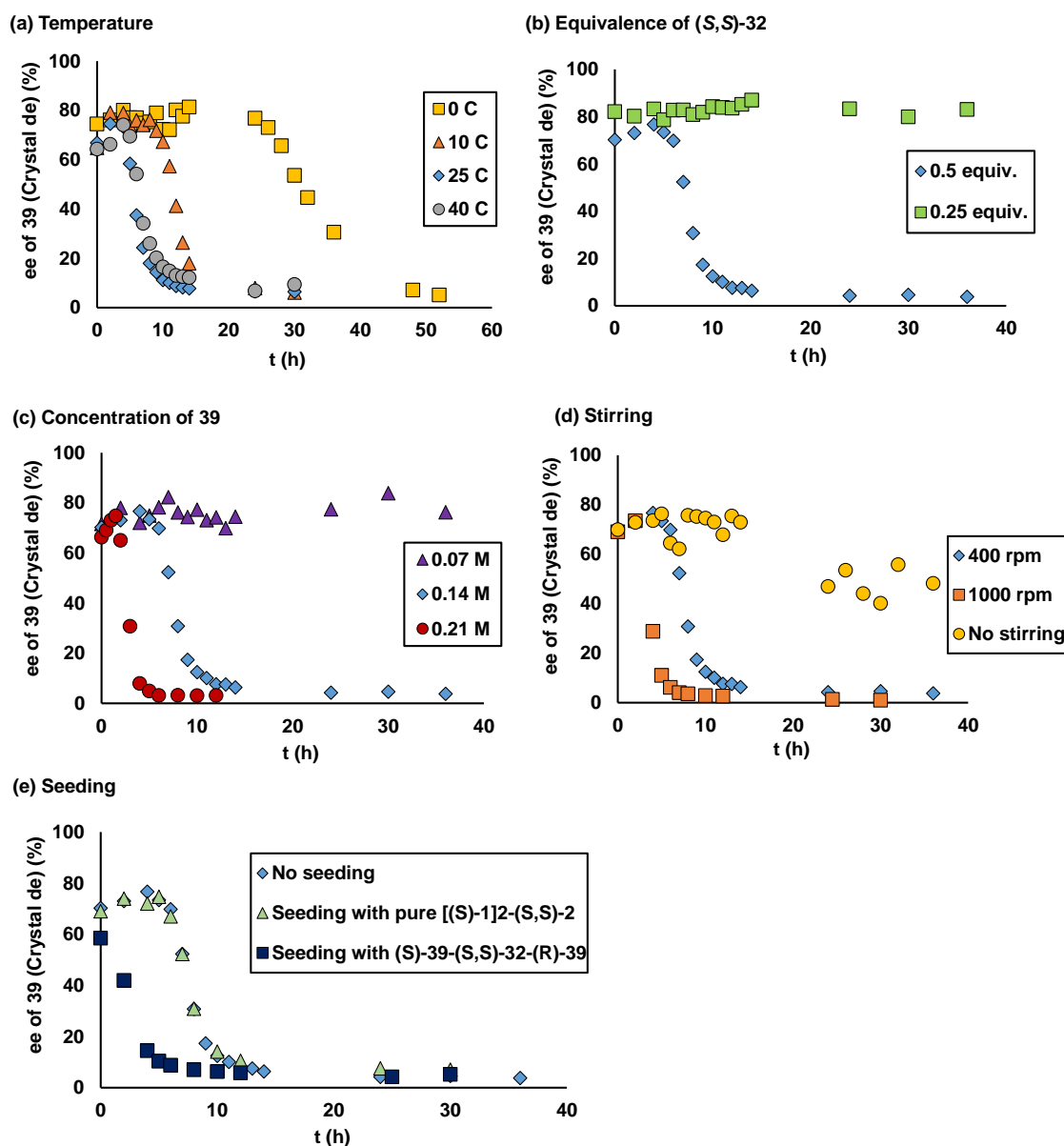
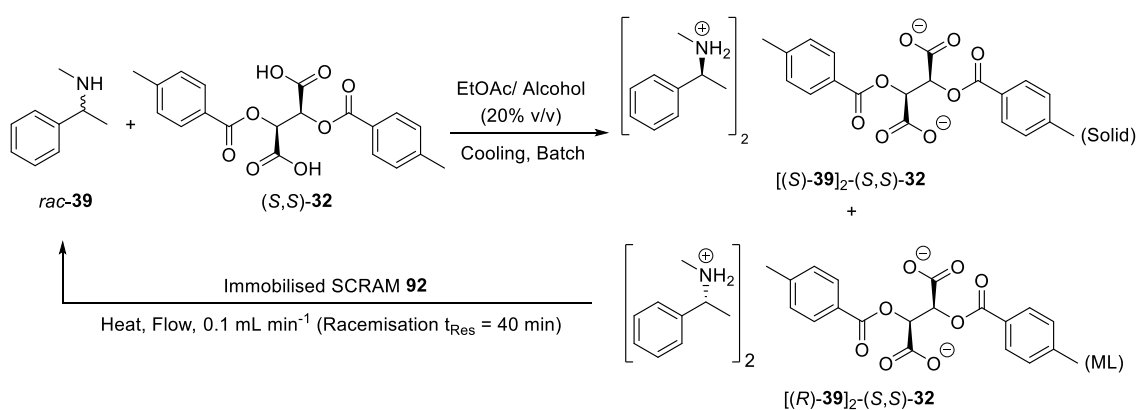


Fig. 3.24 Diastereomeric resolution of *rac*-**39** with (*S,S*)-**32** under different experimental conditions

The changes in the salt form observed here have not been previously reported, but appear to be the opposite to that seen by Viedma in spontaneous deracemisation of conglomerate crystals. In the Viedma ripening process, the system is initially at a thermodynamic minimum, but under racemising conditions and mechanically-induced attrition. The grinding causes the system to be kinetically controlled, with small crystals trying to grow in the supersaturated, racemising system but being continuously broken down. As described by Gibbs-Thompson rule, the small crystals exert a higher supersaturation causing growth to larger ones, eventually leading to the evolution of a single enantiomer.<sup>7, 107, 108, 155, 156</sup>

### 3.4.2 R<sup>3</sup> process of *N*-Methyl- $\alpha$ -methylbenzylamine **39** with di-*p*-toluoyl-*D*-tartaric acid **32**

Enantiomerically pure diacids are common resolving agents for racemic chiral amines.<sup>73</sup> However if the possibility of them forming the racemic neutral diamine salts is general, it might pose a limitation on the R<sup>3</sup> process. The formation of (*S*)-**39**-(*S,S*)-**32**-(*R*)-**39** or the switching from the diastereopure salts is dependent on temperature, stirring, concentration of **39** and the amount of **32** added. It is necessary to take these factors into consideration in developing the R<sup>3</sup> process of **39**, using **32** as the resolving acid (Scheme 3.19). The conditions employed and the results are summarised in Table 3.14.



Scheme 3.19 R<sup>3</sup> process of **39** with (*S,S*)-**32**. *t*<sub>Res</sub> for the whole cycle = 28.5 mL / 0.1 mL min<sup>-1</sup> = 285 min (4.75 h)

Entry		1	2	3	4
Reaction conditions	[ <b>39</b> ] (M)	0.14	0.21	0.21	0.21
	Alcohol <sup>[a]</sup>	MeOH	MeOH	MeOH	iPrOH
	Ir loading (mol%)	5	4	4	4
	Crystallisation T (°C)	0	5	12	12
	Racemisation T (°C)	65	65	65	70
	Acid addition rate during recirculation (mg min <sup>-1</sup> )	0 <sup>[b]</sup>	0 <sup>[b]</sup>	0.1	0.1
	No. of cycles	41	10	25	35
	Process time (h)	195	48	119	166
Results	Initial crystal de (%) <sup>[c]</sup>	68	64	42	63
	Final crystal de (%) <sup>[c]</sup>	91	20	50	86
	Yield (%) <sup>[d]</sup>	20	58	35	78
	<b>39</b> in ML (%)	59	28	41	5
	<b>51</b> in ML (%)	15	3	4.4	0.4
	<b>94</b> in ML (%)	0	3	12	0
	ML ee (%)	4	14	19	20
	S	0.36	0.23	0.35	1.34
<b>Activity of 92</b>	Average ee of (S)- <b>103</b> (%) <sup>[e]</sup>	58	36	N.D. <sup>[f]</sup>	23

Table 3.14 Experimental conditions attempted for the R<sup>3</sup> process of **39** with (S,S)-**32**.

<sup>[a]</sup>All solvent system contained ethyl acetate/ alcohol (20% v/v). <sup>[b]</sup>0.49 equiv. of (S,S)-**32** was added at the start of the process without further addition during the ML recirculation.

<sup>[c]</sup>de of crystals were determined as the ee of the free amine by chiral GC, after free-based with Na<sub>2</sub>CO<sub>3</sub> (aq) and derivatised with trifluoroacetic anhydride. <sup>[d]</sup>Crystals from each sample were included in the calculation of yield. <sup>[e]</sup>After one pass through the catalyst. <sup>[f]</sup>Activity was not determined

To delay the switching of crystal form during the R<sup>3</sup> process, the crystallisation was first carried out at 0 °C (Table 3.14, entry 1). Despite the negative impact of stirring on the resolvability, it is still necessary, since it facilitates dissolution of the more soluble diastereomer ([(*R*)-**39**]<sub>2</sub>-(S,S)-**32**) which allows more (*R*)-**39** to racemise by **92**. The de of the crystals remained high throughout the whole process (Fig. 3.25(a)), however the yield was low (20%). This was partly because of the formation of side product acetophenone **51** from hydrolysis of the intermediate imine **94**. Furthermore, crystallisation of the less soluble [(S)-**39**]<sub>2</sub>-(S,S)-**32** might be slow at the operating concentration. To overcome this, the

concentration of **39** was increased to 0.21 M. Degassed and dried solvents were used and the temperature of crystallisation was also increased to 5 °C to reduce the amount of water condensation in the system and minimise the formation of **51**. Although it was previously shown that a high concentration of **39** is undesirable in the resolution by **32**, with the aid of the racemisation process, the amount of (*R*)-**39** in solution may decrease to a level where the formation of (*S*)-**39**-(*S,S*)-**32**-(*R*)-**39** can be suppressed. However it was observed that the de of the crystals dropped to 20% after 5 cycles (Table 3.14, entry 2; Fig. 3.25(b)), which indicated that the racemisation was not fast enough to remove the excess (*R*)-**39** in the ML.

One strategy to limit the formation of (*S*)-**39**-(*S,S*)-**32**-(*R*)-**39** is to lower the concentration of **32** in the system. An initial quantity of 0.25 equiv. of (*S,S*)-**32** was added, and recirculation continued for 5 cycles. Then an additional 0.25 equiv. of **32** was pumped slowly into the crystalliser at 0.1 mg min<sup>-1</sup> (as a solution). The de of the crystals was maintained at > 80% for 10 cycles after which it started to drop to 50% after 25 cycles (Table 3.14, entry 3; Fig. 3.25(c)). This result indicated that with slow addition of **32**, (*S*)-**39**-(*S,S*)-**32**-(*R*)-**39** is kept below its critical concentration by giving time for (*R*)-**39** to racemise and lowering its concentration. Although the switching behaviour was still observed, the final de of the crystals was higher than that when 0.49 equiv. of **32** was added in one portion (Table 3.14, entry 2), leading to a higher resolvability.

Whilst the formation of acetophenone **51** was minimised using dried solvents, its precursor, imine **94**, was found to accumulate in the system instead (Table 3.14, entry 3). It could be reduced *in-situ* back to **39** using isopropyl alcohol as a hydrogen donor which can also be used as co-solvent (Table 3.14, entry 4). As described above, 0.25 equiv. of (*S,S*)-**32** was added and stirred for one hour to reach equilibrium before recirculation of the ML started. After two cycles, the de of the crystals increased from 63% to 79%, while the amount of **39** decreased from 52 to 41% and the ee of the ML from 60% to 40% (Fig. 3.25(d)). Both the de and the yield of crystals (based on the concentration of **39** in the ML) were significantly higher than the batch resolution process (Table 3.13, entry 9). The ML were recirculated for 7 cycles (33 hours) and an additional 0.25 equiv. of (*S,S*)-**32** was pumped into the resolution mixture slowly. The amount of **39**



dropped gradually, while the de of the crystals stayed at about 84%. The ee of the ML started increasing when (S,S)-**32** was added, since more [(S)-**39**]<sub>2</sub>-(S,S)-**32** crystallised out from solution and the crystallisation was faster than ML racemisation. However it slowly decreased after complete addition of **32**, as the racemisation was now faster than that of the precipitation of [(S)-**39**]<sub>2</sub>-(S,S)-**32**. The de of the crystals did not increase above 86% despite further stirring of the system. An overall yield of 78% was achieved, with a resolvability of 1.34 which was 45 times higher than the batch resolution process ( $S = 0.03$ ).

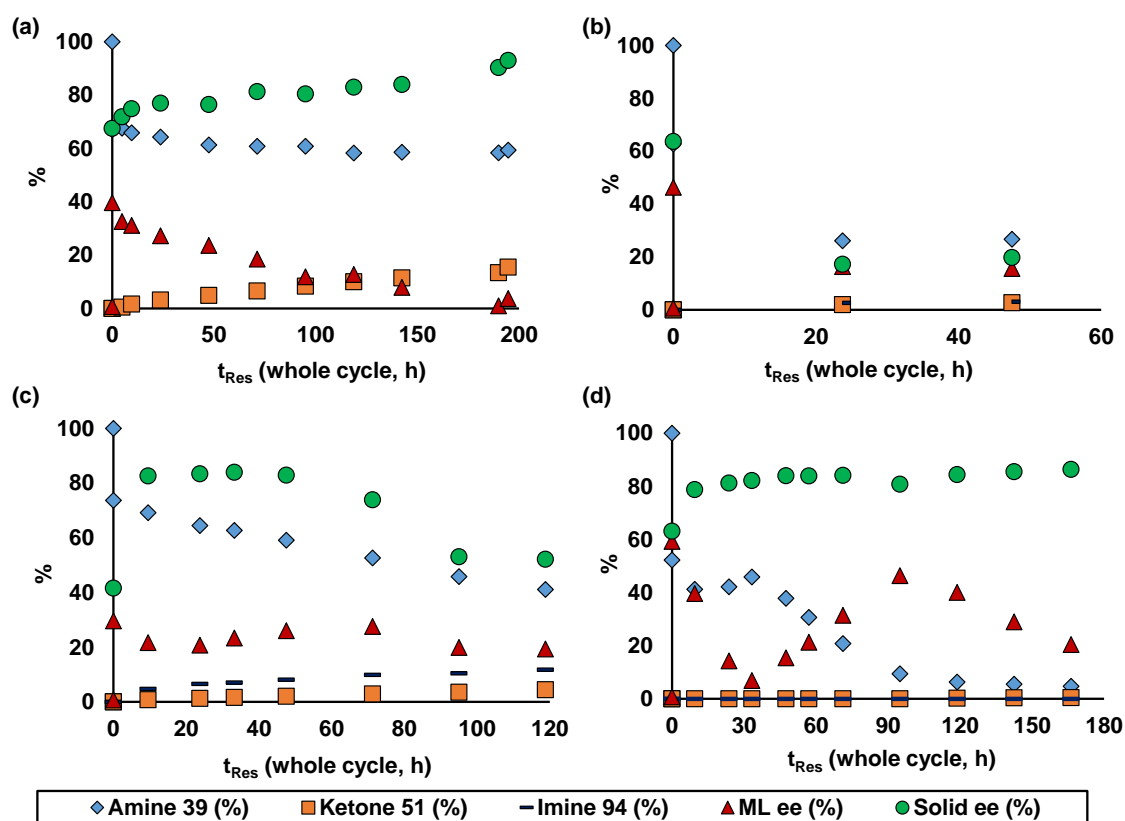


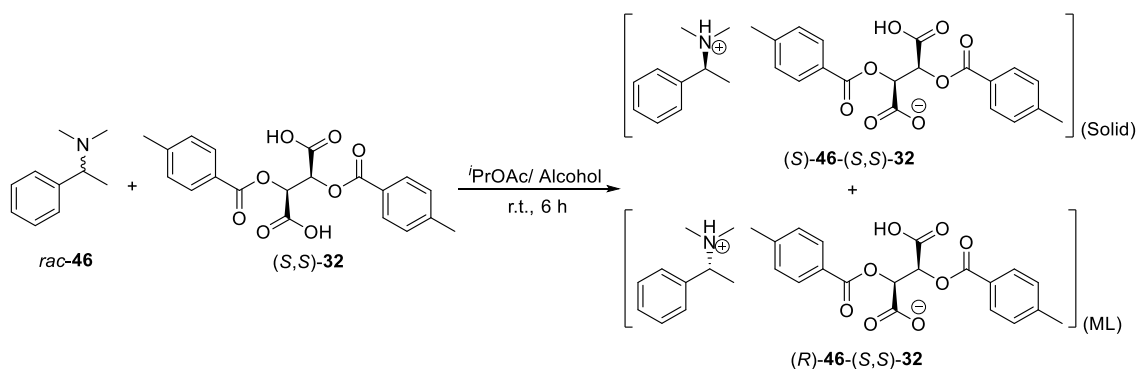
Fig. 3.25 The  $R^3$  processes of **39** with (S,S)-**32** under the conditions described in Table 3.14. (a) Entry 1; (b) Entry 2; (c) Entry 3; (d) Entry 4

Acetophenone **51** was not observed in the process while only a small amount of imine **94** (0.4%) was formed after 35 cycles (166 hours), showing that isopropyl alcohol could efficiently prevent its accumulation. Preventing the formation of **51** had the benefit of stopping the formation of methylamine, avoiding catalyst deactivation. The catalyst activity was checked by the racemisation of (S)-**103** in flow and an average of 23% ee was achieved after one pass through the catalyst with  $t_{Res}$  of 16 minutes at 80 °C, which was very similar to that of fresh **92**.

The high de and yield achieved indicated that (S)-**39**-(S,S)-**32**-(R)-**39** was not formed. In comparison with the previous R<sup>3</sup> process of **39** with **32** (Table 3.14, entry 3), one of the main differences was the use of isopropyl alcohol instead of methanol as the co-solvent. In using isopropyl alcohol, ee of the ML, which was enriched with (R)-**39**, was higher before recirculation than that when methanol was used, which facilitated its racemisation. In addition, isopropyl alcohol had less negative impact on the racemisation of **39** as shown in Section 2.2.1(d), and it allowed a higher racemisation temperature to be used which can increase the racemisation rate further. Therefore (R)-**39** was converted to (S)-**39** more quickly and the concentration of (R)-**39** in the system remained low enough throughout the process. The slow addition of (S,S)-**32** further reduce the concentration of (S)-**39**-(S,S)-**32**-(R)-**39** formed in solution, avoiding its nucleation. Also the absolute solubility of [(S)-**39**]<sub>2</sub>-(S,S)-**32** was lower in ethyl acetate/ isopropyl alcohol than that in ethyl acetate/ methanol which speeded up the rate of precipitation of [(S)-**39**]<sub>2</sub>-(S,S)-**32**. The significant reduction of impurity formation also led to improved yield of the process.

### 3.4.3 N,N-Dimethyl- $\alpha$ -methylbenzylamine **46**

Unlike amine **39**, N,N-dimethyl- $\alpha$ -methylbenzylamine **46** forms an acidic salt with (S,S)-**32**, where the ratio of **46**:**32** is 1:1 when 0.5 or 1 equiv. of (S,S)-**32** was added (Scheme 3.20). This was also shown by the <sup>1</sup>H NMR spectra (Section 6.1.16) and the single crystal structures of the diastereopure salts prepared (Section 8.5). A solvent screen was carried out using isopropyl acetate as the main solvent with the addition of either ethanol or isopropyl alcohol as the co-solvent (Table 3.15).



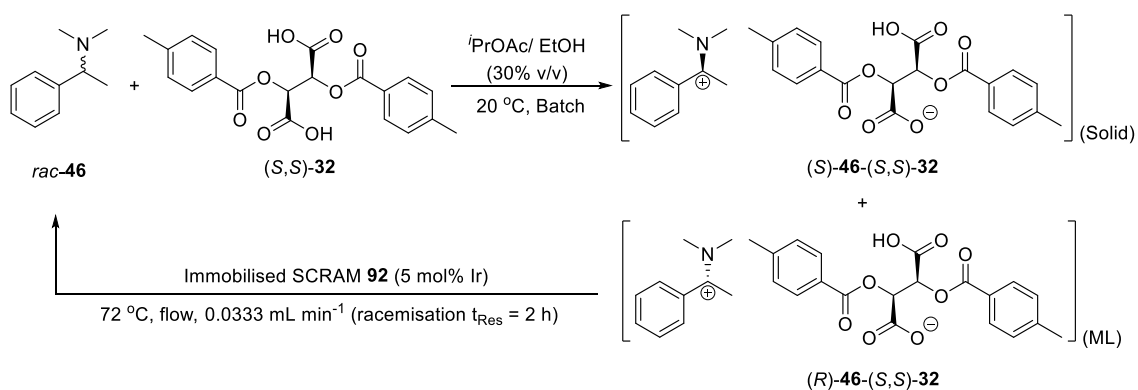
Scheme 3.20 Diastereomeric resolution of **rac-46** with (S,S)-**32**

Entry	Alcohol (% by volume)	[46]/ M	Yield (%)	De (%) <sup>[a]</sup>	S
1 <sup>[b]</sup>	-	0.3	34	52	0.360
2	-	0.14	83	2	0.034
3	<i>i</i> PrOH (10%)	0.14	79	6	0.092
4	<i>i</i> PrOH (30%)	0.14	65	19	0.248
5	EtOH (10%)	0.14	78	7	0.109
6	EtOH (20%)	0.14	53	38	0.399
7	EtOH (30%)	0.14	42	59	0.494
8	EtOH (30%)	0.21	50	45	0.452

Table 3.15 Condition screen of diastereomeric resolution of *rac*-**46** with (*S,S*)-**32** (1 equiv.). <sup>[a]</sup>De was determined as the ee of the free amine by <sup>1</sup>H NMR (CDCl<sub>3</sub>, 500 MHz) after derivatisation with (*S*)-**34**. <sup>[b]</sup>0.5 equiv. of (*S,S*)-**32** was added and stirred for 24 h

Using 0.5 equiv. of (*S,S*)-**32**, a much higher resolvability was achieved at 0.3 M of **46** compared to 0.14 M with 1 equiv. of (*S,S*)-**32** (Table 3.15, entries 1 and 2). The resolvability of the system was improved with ethanol or isopropyl alcohol as co-solvent (Table 3.15, entries 3 to 8). Higher percentage of alcohol gave a higher de of the product, although the yield was lower. Isopropyl acetate/ ethanol 30% (by volume) gave the best resolvability, and increasing the concentration of **46** to 0.21 M reduced the resolvability slightly (Table 3.15, entries 7 and 8).

An R<sup>3</sup> process of **46** was developed as shown in Scheme 3.21. Since the racemisation of **46** in flow was found to be very slow (Section 2.3.3), a long *t*<sub>Res</sub> of two hours and 14.3 hours were employed for the racemisation and the whole process respectively.



Scheme 3.21 R<sup>3</sup> process of **46**. *t*<sub>Res</sub> for the whole cycle = 28.5 mL/ 0.0333 mL min<sup>-1</sup> = 856 min (14.3 h)

Entry		1	2
Reaction conditions	Solvent	<i>i</i> PrOAc/ EtOH (30%)	<i>i</i> PrOAc/ <i>i</i> PrOH (30%)
	Ir loading (mol%)	5	6
	No. of cycles	17	15
	Process time (h)	242	215
Results	De of crystals (%) <sup>[a]</sup>	77	-
	Yield of crystals (%) <sup>[b]</sup>	17	-
	<b>46</b> in ML (%)	86	98
	<b>51</b> in ML (%)	1.3	4
	ML ee (%)	16	N.D. <sup>[c]</sup>
	S	0.262	0
Activity of 92	Average ee of ( <i>S</i> )- <b>103</b> (%)	47	36

Table 3.16 Conditions attempted and results of the  $R^3$  process of **46**. (*S,S*)-**32** (0.9 equiv.) was added at the start of the process. <sup>[a]</sup>De was determined by <sup>1</sup>H NMR (CDCl<sub>3</sub>, 500 MHz) after free-based with Na<sub>2</sub>CO<sub>3</sub> (aq) and derivatised by (*S*)-**34**. <sup>[b]</sup>Crystals from each sample were included in the yield calculation. <sup>[c]</sup>Not determined

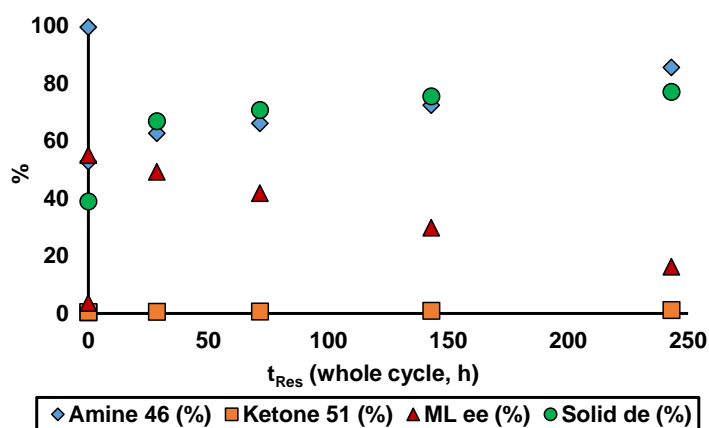
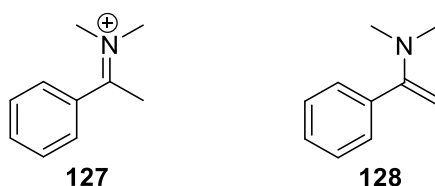


Fig. 3.26 The  $R^3$  processes of **46** with (*S,S*)-**32** under the conditions described in Table 3.16, entry 1

Since **46** and **32** formed a 1:1 acid salt, 0.9 equiv. of (*S,S*)-**32** was added at the beginning of the process. When the recirculation proceeded, a gradual increase in de of the solid was observed. Surprisingly, the amount of **46** in the ML increased slowly, indicating dissolution of the amine salt crystals. The ML ee dropped, indicating that racemisation is occurring (Fig. 3.26). One explanation of this behaviour is that crystallisation of the less soluble (*S*)-**46**-(*S,S*)-**32** is significantly slower than that of the dissolution of the more soluble (*R*)-**46**-(*S,S*)-

**32.** To test this hypothesis, a different solvent was used, with 30% (by volume) isopropyl alcohol in isopropyl acetate, in which the solubility of both (*R*)-**46**-(*S,S*)-**32** and (*S*)-**46**-(*S,S*)-**32** are lower, however no improvement in either de or yield were observed, instead all of the crystals dissolved after 15 cycles of recirculation (Table 3.16, entry 2). There are three possible explanations for this observation. First, epimerisation of (*S,S*)-**32** might have occurred, forming (*S*)-**46**-(*S,R*)-**32** and (*R*)-**46**-(*S,R*)-**32** which are very soluble, leading to complete dissolution. This needs to be further verified by attempting the racemisation/ epimerisation reaction of (*S,S*)-**32** and a non-ammonium salt of (*S,S*)-**32** using catalyst **92** at elevated temperature with analysis using chiral HPLC, <sup>1</sup>H NMR and/ or [α]<sub>D</sub> measurements. Second, the thermodynamic minimum of this system may be controlled by the entropy of the amine salt in solution rather than the enthalpy of the solid, the solution phase of both diastereomers may be the most thermodynamically stable phase which leads to complete dissolution of the solid. A control experiment will be required in which the R<sup>3</sup> process is repeated without the racemisation of ML by **92**. Complete dissolution of solid will still be observed if it is caused by the thermodynamics of the system. Lastly, since iminium ion **127** was formed as the intermediate during racemisation of **46** and it can also tautomerise into the corresponding enamine **128**. Both of them can act as nucleation inhibitors which inhibit the crystallisation of both (*S*)-**46**-(*S,S*)-**32** and (*R*)-**46**-(*S,S*)-**32**. Samples of **127** and **128** can be prepared and added into the crystallisation mixture at the start and/ or during the crystallisation to examine any decline in the yield or complete inhibition of the crystallisation.



### 3.5 Conclusion and future work

Resolution-racemisation-recycle (R<sup>3</sup>) processes have been successfully developed for several secondary amines that couple diastereomeric resolution in a CSTR and continuously recirculating the ML across a fixed-bed racemisation catalyst. The resolution and racemisation are separate but linked with tubing and a pump to allow each reaction to be carried out at their optimal condition. By

applying the R<sup>3</sup> process, screening of the optimised resolution conditions, such as chiral acid and solvent, the equivalence and the concentration of amine, could be avoided as long as the solubility of the diastereomeric salts are different and are low enough to form a solid. The difference in solubility between the diastereomeric salts creates an enantiomeric excess of the amine in the ML, which upon racemisation, replenishes the enantiomer of the amine which forms the less soluble diastereomeric salt. Theoretically, a complete transformation to a single diastereomer will occur. Six different chiral amine substrates, which include primary, secondary (cyclic and acyclic) and tertiary amines were tested with the R<sup>3</sup> system. A summary of the results comparing both the yields and de in the R<sup>3</sup> and batch resolution processes under similar conditions are shown in Fig. 3.27.

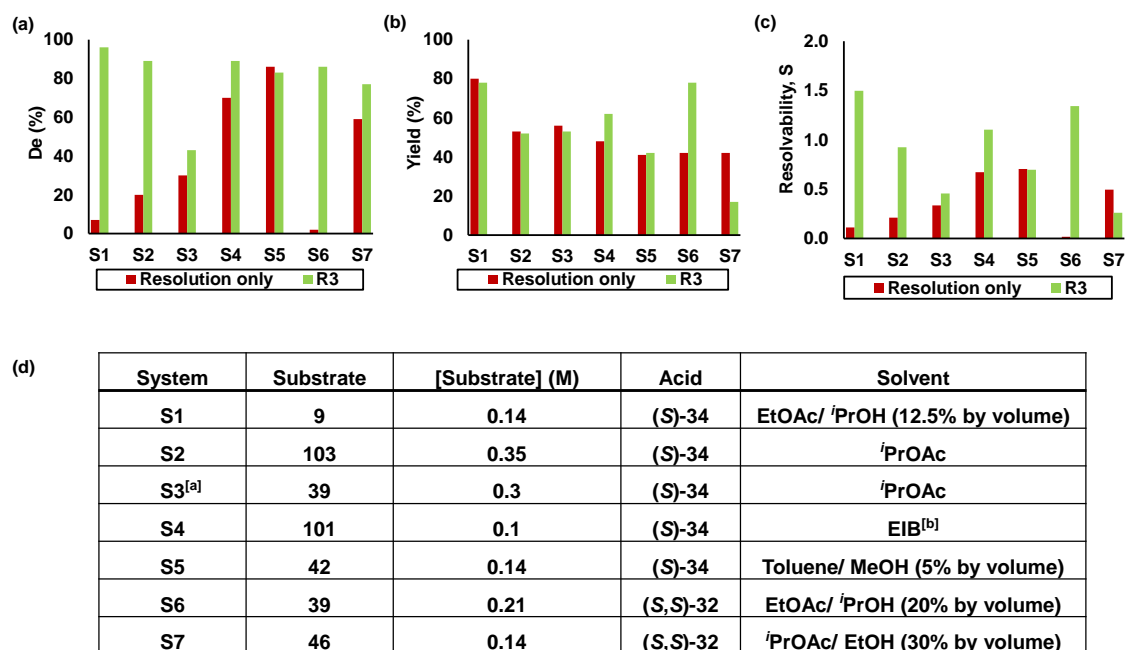


Fig. 3.27 Comparison of selected R<sup>3</sup> and batch resolution-only processes under similar conditions. (a) de; (b) Yield; (c) Resolvability; (d) Conditions of selected R<sup>3</sup> and batch resolution-only processes. <sup>[a]</sup>Alcohol **58** (1 equiv.) was added in the crystallisation mixture. <sup>[b]</sup>Ethyl isobutyrate

For all of the substrates tested, higher de was achieved when using the R<sup>3</sup> process, except for amine **42** which was slightly lower. The most dramatic increase in de was observed for systems S1 and S6 which led to a significant improvement in their resolvability by 13 and 45 times for amines **9** and **39** respectively. Whilst the yields in most of the R<sup>3</sup> processes were similar to those

in the batch resolution processes, that of S4 showed considerable improvement, whilst that in S7 showed a decline in yield.

The efficiency and success of the R<sup>3</sup> process depends strongly on the rate of racemisation, the solubility difference between the diastereomeric salts formed, and their solubility in the selected solvent, the rate of dissolution of the more soluble diastereomeric salt, and the rate of crystallisation of the less soluble one. The rate of racemisation by **92** is limited to the maximum temperature ( $\leq 80$  °C) that can be applied without causing iridium leaching from the catalyst, or breakdown of the polymer support. The maximum yield depends on the solubility of the diastereomeric salts in the solvents used. Increasing the concentration of the system can lead to higher yield. Continuous dissolution and precipitation of the diastereomers and racemisation of the ML causes the de to increase gradually over the course of the process. Formation of by-products such as amine dimers from **42** and ketone **51** from the dehydrogenated precursor also resulted in low yield of their R<sup>3</sup> processes. Suppression of these by-products is important as methylamine and ammonia formed during racemisation of **39** and **42** respectively can deactivate the catalyst.

The use of diacid (*S,S*)-**32** was studied in the resolution of **39** and **46**, which forms neutral and acid salts respectively. In the resolution of **39** with (*S,S*)-**32**, the crystal form switched from pure diastereomeric salts to less soluble racemic (*R*)-**39**-(*S,S*)-**32**-(*S*)-**39** crystal form upon prolonged stirring. This greatly affects the resolvability of the system. The speed at which the switching occurred was increased by seeding with the racemic salt, stirring and increased concentration of the system. In spite of the formation of (*R*)-**39**-(*S,S*)-**32**-(*S*)-**39**, amine **39** was successfully resolved by slow addition of the acid and fast racemisation. These conditions were critical in minimising the concentration of acid and one of the enantiomers of the amine in the system ((*R*)-**39** in this case), to avoid nucleation and precipitation of the racemic salt.

Diastereomeric crystallisation of *rac*-**9** with (*S*)-**34** was carried out in flow using a cascade CSTR system (the Freactors) which were built in-house. Although the system has slightly lower resolvability compared to that of batch due to shorter crystallisation time in flow ( $t_{Res} = 2$  to 40 min), being able to carry out continuous

crystallisation is beneficial since the reaction can reach steady state and produce crystals with more consistent quality. Projects regarding self-optimisation of reactions in flow have been ongoing in the group, in which the flow reactors can incorporate online analysis with a feedback control loop which uses self-optimising algorithm to keep generating new reaction conditions until an optimum is reached.<sup>125</sup> By connecting the Freactors to the self-optimisation system, variables such as yield and de of the crystals can be optimised by changing parameters such as flow rate of each of the amine and acid solution with online (chiral) HPLC analysis.

The work discussed has only covered relatively simple amine substrates containing one chiral centre. In other work in the group, other substrates such as diastereomeric amines, are being tested. The R<sup>3</sup> methodology may also be applied in the asymmetric transformation of chiral carboxylic acids using enantiomerically pure amines as the resolving agents; chiral alcohols which possess an adjacent chiral (or achiral) amino or carboxylic group that can be resolved by a chiral acid or amine respectively are also potential substrates. However, suitable racemisation catalysts need to be identified that show higher activity towards carboxylic acids and/ or alcohols.

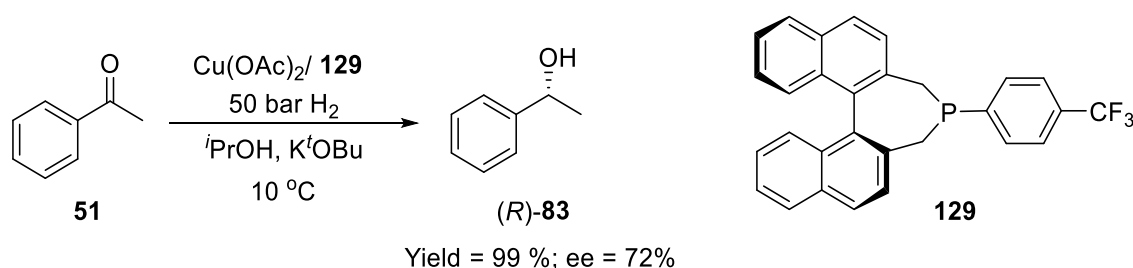
The rate of racemisation and by-product formation during racemisation can pose a limit in developing an efficient R<sup>3</sup> process. Alternative catalysts to SCRAM **64** and **92** are needed that are more active and stable at higher temperature. Shvo's catalyst **55** was found to racemise **42** in the presence of alcohol **58** with minimal formation of dimers, which cannot be achieved with **64** under similar conditions. Immobilisation of **55** onto a solid support may allow it to be applied in flow and overcome the problem of low yield in the R<sup>3</sup> process of **42** and other primary amines. It would be useful to carry out a larger scale R<sup>3</sup> process to demonstrate its scalability and its potential in industrial application. However the cost of the SCRAM catalyst required, as yet precludes this.



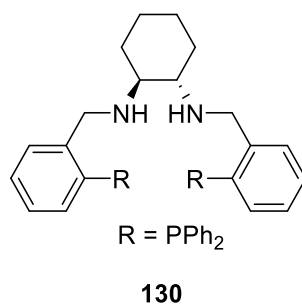
## 4. Alternative racemisation catalysts for chiral amines

### 4.1 Introduction

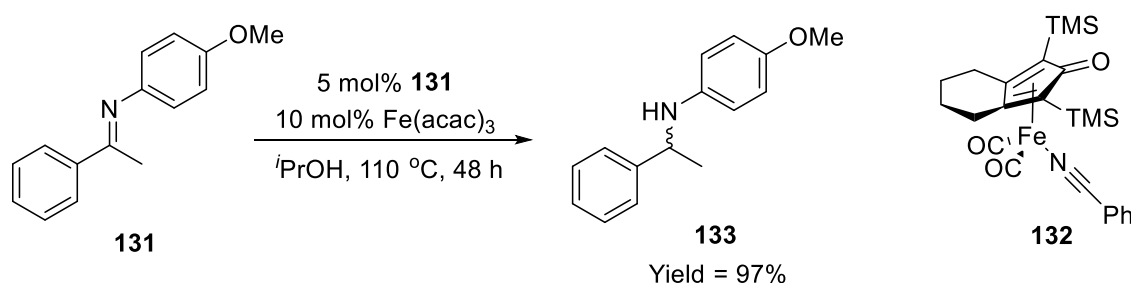
SCRAM catalysts **64** and **92** are iridium-based catalysts used for the racemisation of chiral amines.<sup>1, 2, 43, 78, 135, 157</sup> Other known racemisation catalysts for chiral amines include ruthenium, rhodium and palladium-based complexes.<sup>158</sup> Their limited availability, high prices and significant toxicity have driven the search for cheaper and more environmentally benign alternatives.<sup>158-161</sup> First row transition metals such as iron, cobalt, nickel and copper are cheap, abundant and relatively non-toxic. Catalytic systems have been developed based on copper and iron complexes/ salts in combination with appropriate ligands, bases and various reducing agents in the asymmetric hydrogenation and transfer hydrogenation reactions of ketones.<sup>159, 160, 162</sup> Copper(I) hydride complexes, such as Stryker's reagent ( $[(PPh_3)CuH]_6$ ), has been used to catalyse the reduction of electrophilic double bonds, including  $\alpha,\beta$ -unsaturated compounds in the presence of stoichiometric amount of reducing agents such as silanes and hydrogen gas. The reactions were highly regioselective depending on the reaction conditions.<sup>160, 163-165</sup> Beller et al. reported the asymmetric hydrogenation of acetophenone **51** using copper(II) acetate with monodentate binaphthophosphine ligands such as **129** in the presence of potassium *tert*-butoxide at 50 bar of hydrogen gas to give 99% of the alcohol product (*R*)-**83** with 72% ee (Scheme 4.1).<sup>160</sup> The same ketone substrate was shown to be reduced by an iron carbonyl cluster  $[Et_3NH][HFe_3(CO)_{11}]$  with **130** and potassium hydroxide. However, a lower conversion of 92% with 56% ee were achieved.



Scheme 4.1 Asymmetric hydrogenation of acetophenone **51** by copper(II) acetate with **129** under hydrogen atmosphere

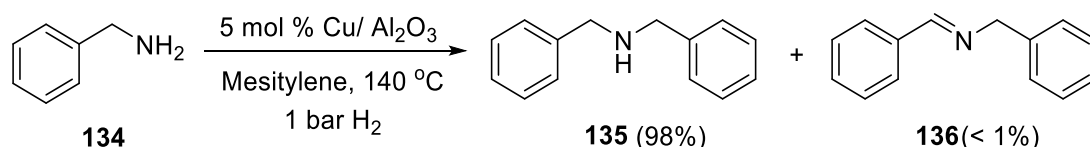


Zhao et al. reported the transfer hydrogenation of various imines by iron complex **132** assisted by Lewis acid using isopropyl alcohol as the hydrogen donor.<sup>158</sup> Imine **131** was reduced to the amine product **133** with 97% yield using iron(III) acetylacetonate (Scheme 4.2).



Scheme 4.2 Transfer hydrogenation of **131** by **132** and iron(III) acetylacetonate<sup>158</sup>

Self-condensation of primary amines such as benzylamine **134** was reported by Mizuno et al. using copper(0) supported onto aluminium oxide (Scheme 4.3),<sup>166</sup> whilst the use of 0.5 mol% copper(I) chloride in air solely gave **136**.<sup>161</sup>

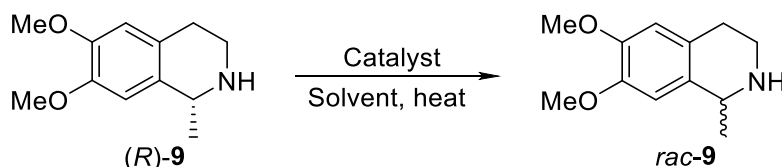


Scheme 4.3 Self condensation of **134** by Cu/ Al<sub>2</sub>O<sub>3</sub> under hydrogen atmosphere<sup>166</sup>

The use of iron- and copper-based compounds in amine oxidations and imine reductions suggested that they can potentially be used in catalysing the racemisation of chiral amines. In this chapter, a series of iron- and copper-based complexes and salts were screened for racemisation using (*R*)-**9** as the major substrate. Compounds which showed the desired racemisation capability and the ability to oxidise the substrate to its imine will be identified.

## 4.2 Screening of iron- and copper-based metal compounds

A series of iron- and copper-based metal salts and complexes **A** to **Q** were screened for their activity in the racemisation of (*R*)-**9** (Scheme 4.4, Table 4.1). The compounds contain metal centre(s) which can achieve various oxidation states; and are either coordinatively unsaturated or contain labile ligands which allow the substrate to bind.



Scheme 4.4 Catalyst screening for the racemisation of (*R*)-**9** in batch

Catalyst	Compound	Average mol% <sup>[a]</sup>	Catalyst	Compound	Average mol% <sup>[a]</sup>
<b>A</b>		12	<b>J</b>		16
<b>B</b>	Fe(OAc) <sub>2</sub>	10	<b>K</b>	Cu(OAc) <sub>2</sub>	40
<b>C</b>		31	<b>L</b>		11
<b>D</b>	FeBr <sub>3</sub>	41	<b>M</b>	CuI	14
<b>E</b>	Fe <sub>3</sub> (CO) <sub>12</sub>	12	<b>N</b>	[(MeCN) <sub>4</sub> Cu] <sup>+</sup> BF <sub>4</sub> <sup>-</sup>	23
<b>F</b>	Fe(OCH <sub>2</sub> CH <sub>3</sub> ) <sub>3</sub>	30	<b>O</b>	[CpCu(PEt <sub>3</sub> )]	13
<b>G</b>	Fe <sub>3</sub> O <sub>4</sub>	28	<b>P</b>	[Cu(NH <sub>3</sub> ) <sub>4</sub> ] <sup>+</sup> SO <sub>4</sub> <sup>-</sup>	23
<b>H</b>		12	<b>Q</b>		11
<b>I</b>	[Cp <sup>+</sup> Fe(CO) <sub>2</sub> ] <sub>2</sub>	13			

Table 4.1 Fe- and Cu-based metal compounds used in the catalyst screening of racemisation of (*R*)-**9**. <sup>[a]</sup>Average amount of compound used (in mol%) over three screening experiments carried out in three different solvents (toluene, PhCl and <sup>i</sup>PrOAc)

The initial screening was carried out inside the glove box using a 48-well plate under nitrogen atmosphere in toluene at 105 °C. Samples were taken after 4 and 22 hours and were analysed by chiral supercritical fluid chromatography (SFC). Under the reaction conditions employed, only **E** was able to racemise (*R*)-**9** from 100 to 73% after 22 hours (Fig. 4.1). The screening was repeated in chlorobenzene and isopropyl acetate (Table 4.2). In chlorobenzene, no racemisation was observed with the use of **E**, further showing the negative effect of solvents with increasing polarity on racemisation (Table 4.2, entry 2). In isopropyl acetate, **E** was able to racemise (*R*)-**9** but to a lower extent compared to the reaction in toluene since lower temperature was used (Table 4.2, entry 3).

The amount of imine formed was also monitored throughout the reaction by imine **8**/ amine **9** peak area ratio (Fig. 4.2). Not much **8** was formed using **E**. Although **K** did not racemise (*R*)-**9**, significant formation of **8** was observed which suggested that **K** can transfer dehydrogenate **9**. Both catalysts **E** and **K** were further studied by closely monitoring the racemisation/ transfer dehydrogenation reaction of **9**. Other amine substrates will also be attempted using **E**.

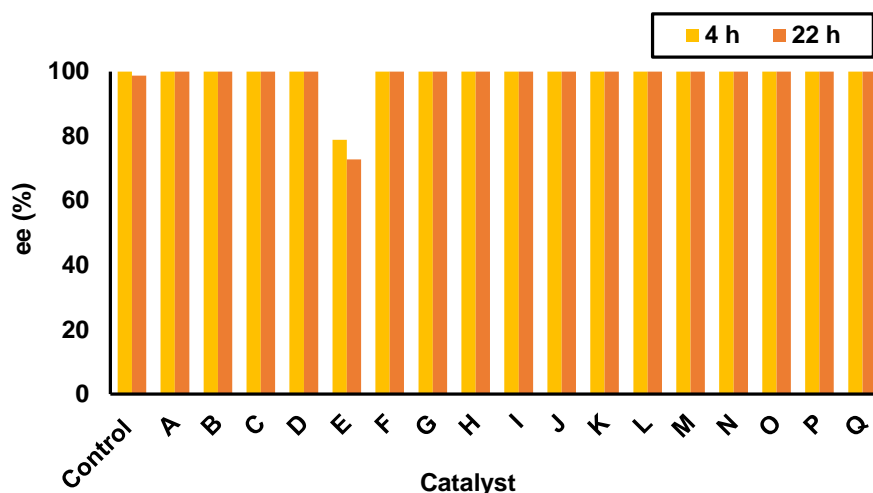


Fig. 4.1 ee of **9** after 4 and 22 h in the catalyst screen at 105 °C in toluene. The reactions were carried out at 50 mM of (*R*)-**9** in a 0.5 mL scale under nitrogen atmosphere inside the glove box. No catalysts were added in the control experiment

Entry	Solvent	T (°C)	ee of <b>9</b> using <b>E</b> (%)
1	Toluene	105	73
2	Chlorobenzene	120	100
3	Isopropyl acetate	80	83

Table 4.2 Racemisation of (*R*)-**9** by **E** in the catalyst screen in different solvents after 22 h (toluene) and 20 h (chlorobenzene and isopropyl acetate)

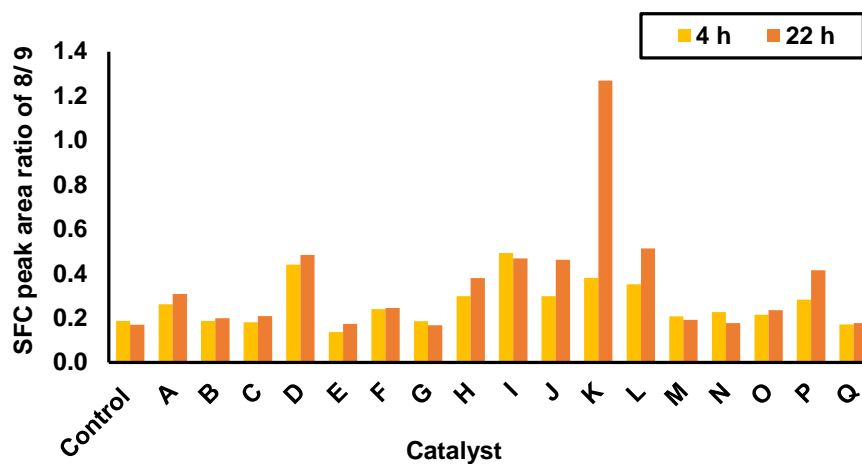


Fig. 4.2 SFC peak area ratio of imine **8**/ amine **9** after 4 and 22 h in the catalyst screen at 105 °C in toluene

### 4.3 Racemisation of chiral amines by triiron dodecacarbonyl (Compound **E**)

Racemisation of (*R*)-**9** was repeated under different conditions using 10 mol% **E** in toluene. The ee of **9** dropped slowly from 100 to 53% after 24 hours when the reaction was carried out inside the glove box under nitrogen atmosphere (Fig. 4.3(a); Table 4.3, entry 1). The amount of imine **8** remained low (< 1%) throughout the reaction. This can be beneficial for substrates such as primary amines where dimeric by-products are formed readily from the reaction between the amine and the imine. The kinetic plot of  $\ln \{[R]_0 / ([R]_0 - 2[S]_t)\}$  against time is non-linear, indicating that the racemisation deviates from first order kinetic model which is likely to be the result of catalyst deactivation (Fig. 4.3(b)). In a separate experiment, more **E** (further 10 mol%) was added after 6 hours when the racemisation slowed down. The reaction rate increased and ee dropped to 25% after 24 hours (Fig. 4.4).

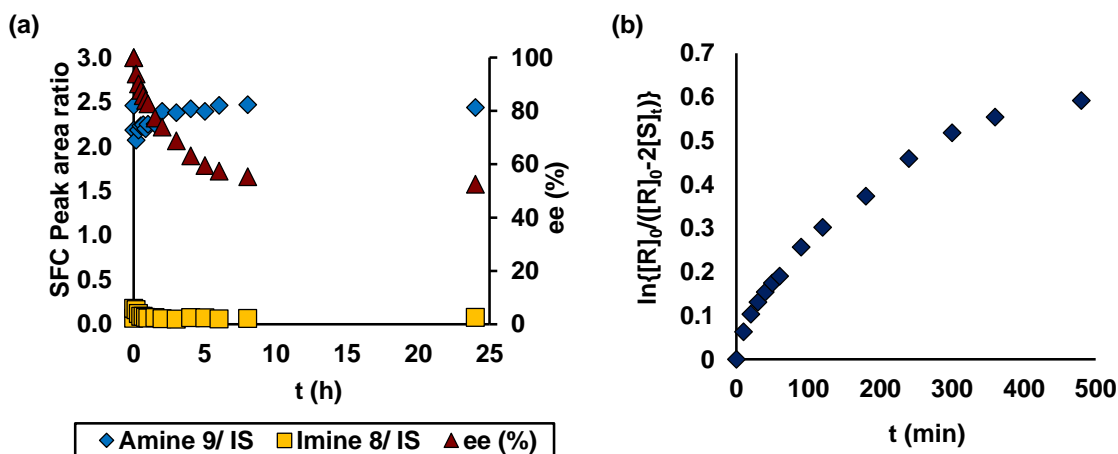


Fig. 4.3(a) Full reaction profile of the racemisation of (R)-9 (0.1 M) by E (10 mol%) carried out inside the glove box. IS = Internal standard (4,4'-di-tert-butylbiphenyl); (b) Plot of  $\ln\{[R]_0/([R]_0 - 2[S]_t)\}$  against time for the racemisation of (R)-9 by E

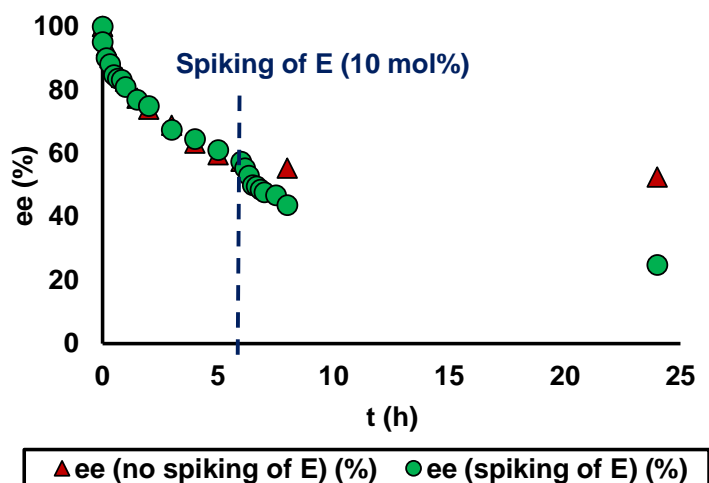


Fig. 4.4 Profiles of ee of (R)-9 (0.1 M) with and without spiking of E after 6 h. Initial loading of E = 10 mol %

When the reaction was carried out in air, the racemisation did not proceed (Fig. 4.5; Table 4.3, entry 3). The reaction was also repeated outside the glove box but under nitrogen. The racemisation stopped after one hour (Fig. 4.5; Table 4.3, entry 2). The insertion of a needle during sampling might have introduced air into the system which destroyed the catalyst, indicating that E is very air-sensitive.

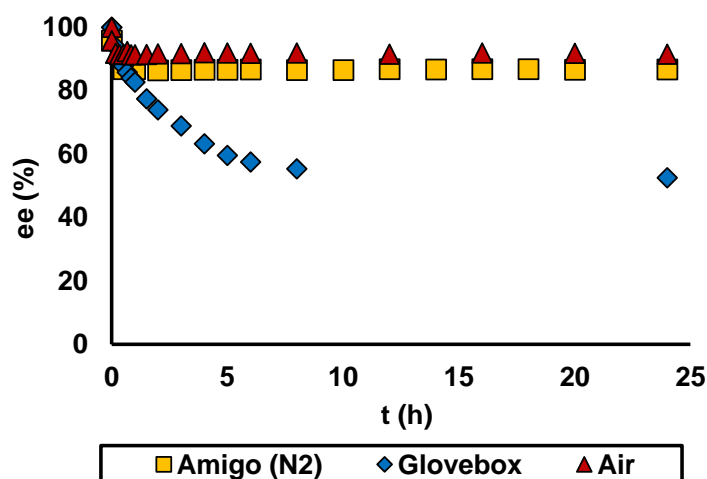


Fig. 4.5 Racemisation of (*R*)-**9** (0.1 M) by **E** (10 mol%) in toluene at 100 °C under different conditions

Entry	Conditions	ee after 1 h (%)	ee after 24 h (%)
1	Nitrogen atmosphere inside glove box	83	53
2	Nitrogen atmosphere outside glove box <sup>[a]</sup>	87	87
3	Air	91	92

Table 4.3 ee of **9** after 1 and 24 h under different reaction conditions. All reactions were carried out at 100 °C in toluene. <sup>[a]</sup>The reaction was carried out in an Amigo reaction tube under nitrogen

To understand the substrate scope of **E**, racemisation of (*S*)-**39**, (*S*)-**103** and (*S*)-**42** were attempted using 10 mol% of **E** (Table 4.4). The reactions mixtures were prepared in sealed ampoule tubes under nitrogen to avoid any air. The reactions were then heated in degassed toluene for 24 hours. (*S*)-**103** was racemised to 58% ee (Table 4.4, entry 1), whilst no racemisation was observed for (*S*)-**39** and (*S*)-**42** (Table 4.4, entries 3 and 4). It showed that **E** was more active towards cyclic secondary amines than acyclic substrates. This can possibly be due to the more stable cyclic imines which are more easily formed during racemisation, allowing enough time for transfer hydrogenation to occur. Although a high loading of **E** is required for the racemisation of (*R*)-**9** and (*S*)-**103** (10 mol% **E**, 30 mol% iron), the turnover numbers were calculated to be 1.5 and 1.4 respectively which are larger than 1 (Section 8.6). Therefore, **E** is still regarded as a catalyst. However, it is much less efficient compared to other commonly used racemisation catalysts such as SCRAM **64** and Shvo's catalyst **55**.

Entry	Substrate	T (°C)	ee after 24 h (%)
1 <sup>[a]</sup>	(S)-Methylpiperidine <b>103</b>	105	58 <sup>[b]</sup>
2 <sup>[a][c]</sup>	(S)-Methylpiperidine <b>103</b>	105	91 <sup>[b]</sup>
3 <sup>[d]</sup>	(S)-N-methyl- $\alpha$ -methylamine <b>39</b>	100	96 <sup>[e]</sup>
4 <sup>[d]</sup>	(S)- $\alpha$ -Methylbenzylamine <b>42</b>	100	100 <sup>[f]</sup>

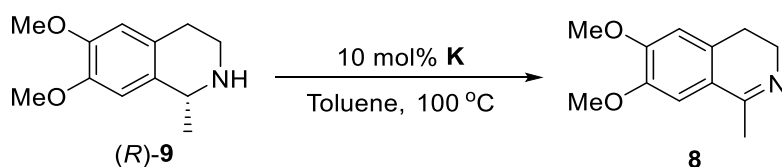
Table 4.4 Attempted racemisation of (S)-**103**, (S)-**39** and (S)-**42** (0.1 M) with **E** (10 mol%). The reactions were heated in sealed ampoule tubes for 24 h outside the glove box. <sup>[a]</sup>Reaction mixtures were prepared in an atmosbag filled with nitrogen. <sup>[b]</sup>Ee was determined by chiral GC after derivatisation with benzoyl chloride. <sup>[c]</sup>Elemental mercury (90 equiv.) was added at the start of the reaction prior to heating. <sup>[d]</sup>Reaction mixtures were prepared in a glovebox under nitrogen atmosphere. <sup>[e]</sup>Ee was determined by chiral GC after derivatisation with trifluoroacetic anhydride. <sup>[f]</sup>Ee was determined by chiral HPLC after derivatisation with triethylamine and benzoyl chloride

Decomposition of **E** to form iron and iron oxide nanoparticles at elevated temperatures had been reported in the literature.<sup>167, 168</sup> In the presence of excess carbon monoxide, **E** can decompose to Fe(CO)<sub>5</sub> at ambient temperature; while in the absence of carbon monoxide, both Fe(CO)<sub>5</sub> and HFe<sub>3</sub>(CO)<sub>11</sub><sup>-</sup> clusters are produced in solvents such as acetonitrile, dimethylformamide, dimethylsulfoxide and tetrahydrofuran.<sup>169</sup> **E** was found to catalyse alkene isomerisation by intramolecular hydrogen shift mechanism, probably *via* the formation of HFe(CO)<sub>3</sub>( $\pi$ -allyl) species.<sup>170, 171</sup> Racemisation of **9** may involve the binding of **9** to the Fe<sub>x</sub>(CO)<sub>y</sub> clusters with subsequent loss of carbon monoxide. Hydride transfer from **9** to iron can lead to the formation of imine and [HFe<sub>x</sub>(CO)<sub>y</sub>] species which can transfer the hydride to the imine to form back **9** non-enantioselectively. On the other hand iron and/ or iron oxide nanoparticles may also be the catalytic species. In order to investigate whether any nanoparticles were involved in the catalysis, a poisoning experiment was carried out by adding elemental mercury (90 equiv.) into the reaction mixture containing both (S)-**103** and 10 mol% of **E** in toluene prior to heating. A control experiment without mercury was carried out at the same time for comparison and the reactions were analysed by chiral GC after being heated to 105 °C for 24 hours (Table 4.4, entries 1 and 2). Much lower activity was observed in the presence of mercury, indicating that nanoparticles might have initially formed in the catalytic cycle, which formed amalgam with mercury and halted the reaction.<sup>172</sup>



#### 4.4 Attempted racemisation/ transfer dehydrogenation of (*R*)-6,7-Dimethoxy-1-methyl-1,2,3,4-tetrahydroisoquinoline **9** by copper(II) acetate (Compound **K**)

Although (*R*)-**9** was not racemised by **K** under the employed conditions during the catalyst screen, a significant amount of imine **8** was formed which suggests that **K** was turning over to dehydrogenate **9** (Scheme 4.5). The reaction was repeated in toluene with 10 mol % **K** and was monitored more closely (Fig. 4.6). Imine **8** was formed at the expense of **9**. The ee of **9** is not shown as it remained at 100%. The reaction was also carried out in 1:1 toluene/ 2,4-dimethyl-3-pentanol **58**. Alcohol **58** was used as a hydrogen donor in the racemisation of (*S*)- $\alpha$ -methylbenzylamine **42** using Shvo's catalyst **55** to suppress the formation of dimeric products.<sup>95</sup> However, with the use of **K**, imine formation was not reduced in the presence of **58** and no racemisation was observed (Fig. 4.6).



Scheme 4.5 Transfer dehydrogenation of (*R*)-**9** by **K**

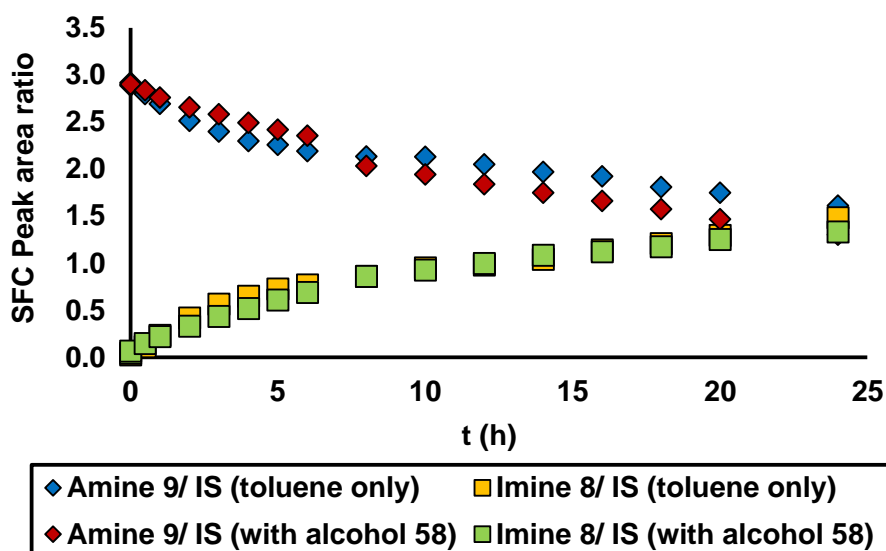


Fig. 4.6 Transfer dehydrogenation of (*R*)-**9** (0.1 M) by **K** (10 mol%) in toluene and toluene/ **58** (1:1). ee of **9** was not shown. IS = Internal standard (4,4'-di-*tert*-butylbiphenyl)

Copper-catalysed enantioselective hydrogenation of ketones had been reported by Beller et al.<sup>160</sup> Compound **K** was employed with monodentate binaphthophosphine ligands under hydrogen atmosphere in the presence of potassium *tert*-butoxide. The main purpose of the ligand is to induce stereoselectivity of the product. In the case of racemisation, the ligand may not be needed. Potentially, a combination of **K** and hydrogen may be sufficient to reduce **8** back to **9**. In addition, silanes can serve as hydrogen donors. Various silanes such as alkylsilanes, phenylsilanes and polymethylhydrosiloxanes (PMHS) had been used to reduce ketones and aldehydes to their respective alcohols.<sup>163, 164</sup> Blackwell et al. reported the use of dimethyl(phenyl)silane to reduce benzaldimines and ketimines to their respective amines.<sup>173</sup> Therefore, different hydrogenating conditions were employed in an attempt to reduce any imine intermediate formed which can lead to racemisation (Table 4.5).

Entry	<b>K</b> (mol%)	T (°C)	Reaction time (h)	Hydride donor (equiv.)	Conversion (%) <sup>[a]</sup>	ee (%) <sup>[b]</sup>
1 <sup>[c]</sup>	10	100	8	-	26	100
2 <sup>[d]</sup>	20	98 <sup>[e]</sup>	8	Hydrogen gas <sup>[f]</sup>	12	100
3	10	165 <sup>[g]</sup>	1	PMHS (1.1)	10	100
4	10	165 <sup>[g]</sup>	1	PhSiH <sub>3</sub> (1.5)	3	95
5	10	165 <sup>[g]</sup>	1	PhMe <sub>2</sub> SiH (4.5)	6	100
6	10	165 <sup>[g]</sup>	1	-	16	100

Table 4.5 Attempted racemisation of (*S*)-**9** (0.1 M) by **K** under different hydrogenating conditions. <sup>[a]</sup>Conversion was determined by GC. <sup>[b]</sup>ee was determined by chiral HPLC. <sup>[c]</sup>The entry corresponds to the reaction presented in Fig. 4.6 in toluene. <sup>[d]</sup>(*R*)-**9** was used. <sup>[e]</sup>By conventional heating. <sup>[f]</sup>A hydrogen balloon was used. <sup>[g]</sup>By microwave heating

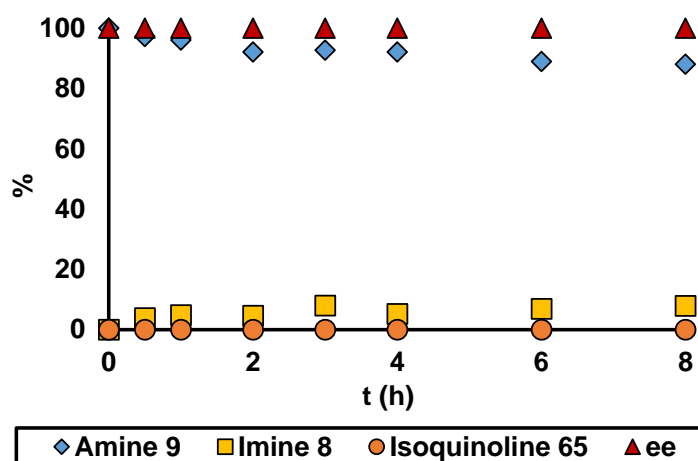


Fig. 4.7 Attempted racemisation of (*R*)-**9** (0.1 M) by **K** (20 mol%) under H<sub>2</sub> atmosphere

Under hydrogen atmosphere, the conversion of **9** was only 12% after 8 hours which is lower than that in the absence of hydrogen, which reached 26% conversion after 8 hours with lower loading of **K** (Table 4.5, entry 2; Fig. 4.7). However no racemisation was observed. The use of silanes were not successful either (Table 4.5, entries 3 to 5). No racemisation occurred except in the case of using phenylsilanes but only 95% ee was achieved which was not satisfactory (Table 4.5, entry 4). The presence of silanes were also found to suppress the formation of **8**. Reactions were also carried out without any additional hydrogen donors under sealed conditions to avoid any loss of hydride in the form of hydrogen but only **8** was formed with no subsequent reduction (Table 4.5, entry 6). It indicated that the Cu-H species are either not formed or it is too unstable to reduce the imine before it decomposes.

## 4.5 Conclusion and future work

A series of iron- and copper-based metal salts and complexes were tested in the racemisation of (*R*)-**9**. Iron carbonyl complex **E** were found to be active towards the racemisation of (*R*)-**9**. However, 10 mol% of **E** is required to racemise (*R*)-**9** from 100 to 53% over 24 h, which is equivalent to 30 mol% of iron. Its low activity makes it less applicable in industrial processes. Besides, **E** is very air-sensitive and can only be used under rigorously inert atmosphere. Any air introduced into the system during sampling is sufficient to inhibit the reaction. The racemisation of (*R*)-**9** by **E** might involve iron nanoparticles which were tested in the presence of mercury in the racemisation of (*S*)-**103** which led to catalyst deactivation.

Among the substrates tested, **E** was only able to racemise (*R*)-**9** and (*S*)-**103** which are cyclic secondary amines whilst acyclic amines such as (*S*)-**39** and (*S*)-**42** were not racemised by **E** under the employed conditions. Transfer dehydrogenation of **9** was observed using **K** but no racemisation was observed under hydrogen atmosphere or in the presence of silanes indicating that the Cu-H species are either not formed or too unstable to reduce imine **8** back to amine **9**.

Further investigation is needed to gain more insight on the mechanism of the transfer (de)hydrogenation reactions by **E** *via* nanoparticle formation to better understand the limitation of the substrate scope and the types of nanoparticles involved. Other metal carbonyl analogues may also be studied. Immobilisation of **E** onto a solid support such as graphite nanofibers may also be made possible which can be applied in flow and increase its recyclability.

## 5. Conclusion

### 5.1 Summary

In this research, a novel resolution-racemisation-recycle ( $R^3$ ) process was developed for the synthesis of chiral amines, by coupling diastereomeric resolution of the racemic amine with catalytic racemisation of the undesired enantiomer in the ML, without any isolation of intermediate. The major drawback of a classical resolution is the limiting yield which can never exceed 50% in obtaining the desired enantiomer. Several approaches have been developed to overcome this intrinsic limitation, including DKR, CIDT and CIAT processes which were discussed in Chapter 1. One of the merits of using the  $R^3$  process over the traditional asymmetric transformation is the segregation of the resolution and racemisation processes, allowing them to operate separately under different conditions and no compromise between the two steps is required. And they are connected together with a flow engineering design, generating a continuous process. The utilisation of flow technology also enables the use of immobilised metal catalysts which can be recycled much more easily, making this process commercially useful and attractive.

Six different chiral amines were selected in the development of the  $R^3$  process, which are 6,7-Dimethoxy-1-methyl-1,2,3,4-tetrahydroisoquinoline **9**, 2-methylpiperidine **103**, *N*-methyl  $\alpha$ -methylbenzylamine **39**, *N*-isopropyl  $\alpha$ -methylbenzylamine **101**,  $\alpha$ -methylbenzylamine **42** and *N,N*-dimethyl  $\alpha$ -methylbenzylamine **46**. Firstly, their racemisation was studied using homogeneous SCRAM in batch, in order to understand the kinetics and mechanism of the reaction. Amine **39** was used as the model substrate and was found to racemise faster compare to other analogous acyclic amines **46** and **101** which are more sterically hindered, but slower compare to cyclic amines **9** and **103** which can be due to the formation of more stable cyclic imine intermediates. Primary amine **42** does not racemise properly, but form various dimeric products. Catalyst deactivation was observed for amines **39** and **46** under the reaction conditions studied, as reflected from incomplete racemisation. One of the possible reasons is the formation of methylamine from imine hydrolysis that can bind to the catalyst and causes deactivation. This was further investigated by  $^1\text{H}$  NMR titration of SCRAM **64** with methylamine. Suspected formation of mono-, di-

and tri-methylamine substituted iridium species **95** to **97** were observed. However, their isolation was not successful to date and their activities could not be tested.

Racemisation in flow was also investigated using a packed-bed reactor which was packed with immobilised SCRAM catalyst **92**. Using immobilised catalyst in flow simplifies the reuse/ recycle of precious metal catalyst. Product contamination with metal residues can also be minimised. Racemisation times, which were controlled by setting different flow rate of the system, were shorter compare to the total reaction time in batch and therefore leading to a smaller degree of racemisation after one pass through the catalyst. However, the amine can be pumped through the catalyst several times to achieve complete racemisation. The reactivation of the used immobilised catalyst was also attempted and found to regain its activity temporarily using hydroiodic acid, which potentially protonates the bound amine (methylamine), facilitating its de-coordination from the iridium centre for substrate to bind again.

A relatively rapid qualitative method was developed to determine if an amine can be racemised under certain conditions, which involved proton-deuterium exchange in the amine substrate in the presence of SCRAM **64** and  $d_8$ -isopropyl alcohol and was monitored by  $^1\text{H}$  NMR. A decrease in the integration of a signal indicates deuterium incorporation at the corresponding position. If this occurs at the chiral centre ( $\alpha$ -position) and/ or the  $\beta$ -position, imine/ enamine must have been formed respectively and the amine can be racemised under the operating conditions. This method can avoid the need of developing chiral analytical methods in the early stage and do not require enantiopure/ enantioenriched materials.

Secondly, diastereomeric crystallisation of the chosen amine substrates was investigated in batch at ambient temperature in general, using (*S*)-mandelic acid **34** and di-*p*-toluyl-*D*-tartaric acid (*S,S*)-**32** as the resolving acid. Solvent and concentration screens were carried out briefly without full optimisation of reaction conditions. Diastereomeric resolution of amine **9** was also carried out in continuous flow using the Freactors with different  $t_{\text{Res}}$ . A slightly lower resolvability was observed due to shorter resolution times compared to batch.

Based on the sub-optimal conditions for the racemisation and diastereomeric resolution of individual chiral amines, both steps were coupled by connecting the batch crystalliser (CSTR) to a Jasco/ HPLC pump which was also connected to the packed-bed racemisation flow reactor containing the immobilised SCRAM **92**. The racemised ML re-entered the crystalliser for further resolution. By using the R<sup>3</sup> process, a higher de was achieved for most substrates, since the ML which is enriched with the (undesired) enantiomer racemises to replenish the (desired) enantiomer which crystallises from solution as the less soluble diastereomeric salt. In theory, no optimisation of individual steps is required, as long as the amine can be racemised by **92** and there is a solubility difference between the diastereomers. However in reality, the efficiency of a R<sup>3</sup> process also depends on the rate of racemisation and the absolute solubilities of the diastereomers. With the use of monoacid (S)-**34**, the R<sup>3</sup> process of **9** showed the biggest improvement in resolvability, a 13-times increase compared to batch resolution alone, achieving a de of 96% and yield of 78% which is much higher than the maximum limit of a classical resolution of 50%. Although amine **39** also showed an increase in de and resolvability when the R<sup>3</sup> process was employed, the results were less satisfactory compared to amines **9**, **101** and **103**. An alternative chiral acid, (S,S)-**32** was used which is a diacid. However, the formation of neutral, racemic salt containing both enantiomers of **39** led to a significant drop in resolvability of the system. By controlling the rate of acid addition, the concentration of the racemic salt in solution was minimised, avoiding its nucleation and subsequent crystallisation, leading to a 45-times improvement in the resolvability compared with batch resolution alone, with a de of 83% and yield of 78%. The R<sup>3</sup> processes of primary amine **42** and tertiary amine **46** with (S)-**34** and (S,S)-**32** respectively were less successful due to the formation of various side-products. The used immobilised SCRAM catalyst was tested after each R<sup>3</sup> processes with either the racemisation of **9** or **103** as the standard reaction. The catalyst could be recycled up to 130 times over 100 hours, and still remained active. However, the catalyst was not analysed for potential leaching. Therefore any decrease in activity could not be quantified.

Lastly, due to the high cost and toxicity of transition metal catalysts, a series of iron- and copper-based salts and complexes were tested for their potential racemisation activity, using (*R*)-**9** as the model compound. It was found that triiron

dodecacarbonyl complex (compound **E**) was active towards the racemisation of (*R*)-**9** and (*S*)-**103**. However, it is very air-sensitive and a high loading of 10 mol% (30 mol% iron) is required to racemise **39** by about 50% after 24 hours. Copper(II) acetate (compound **K**) was found to be able to oxidise **9** to its imine but no subsequent reduction was observed, even in the presence of hydrogen sources such as hydrogen gas and silanes. Therefore SCRAM **64/ 92** and Shvo's catalyst **55** still remained the most promising racemisation catalysts for chiral amines.

## 5.2 Future Work

Detailed mechanistic investigation of chiral amine racemisation is ongoing in our group. Racemisation monitoring by flow NMR has been in progress in the Dynamic Reaction Monitoring (DReaM) facility in the University of Bath with the observation of hydride formation. DFT study may be helpful in understanding the energies of different transition states and provide more evidences on the binding of intermediate imine/ enamine, if any, and if the hydride transfer occurs through outer- or inner-sphere mechanism and how it depends on the substrate itself.

Primary amine racemisation has been problematic due to the formation of dimeric by-products. Whilst SCRAM **64** (and **92**) is not able to eliminate the problem at this stage, the use of Shvo's catalyst **55** under dilute conditions, in the presence of ammonia or a hydrogen donor was previously proven to help minimising the formation of dimers and allow the amine to racemise to a significant extent. Immobilisation of Shvo's catalyst will allow its use in flow and in the R<sup>3</sup> process. This can extend the substrate scope of the R<sup>3</sup> process to primary amines.

The method developed for determining chiral amine racemisation involves proton-deuterium exchange monitored by the disappearance of proton signals in the <sup>1</sup>H NMR spectra. This method can be tested with fully-deuterated substrates instead which produces proton signals upon deuterium-proton exchange, leading to clearer spectra and simplify their assignment. Alternatively, <sup>2</sup>D NMR can also be used as a complimentary approach in monitoring deuterated species formation. Partially deuterated amine substrates will have to be prepared which act as references for the deuterium signals.



Diacids have been commonly used in the resolution of chiral amines. Although the possibility of racemic salt formation as occurred in the case of amine **39** and (*S,S*)-**32** was reported, it had not been studied in detail. In order to generalise this phenomenon, previously failed resolutions using diacids reported in the literature can be investigated. By controlling the crystallisation of the less soluble racemic salt, if any, the scope of the R<sup>3</sup> process can be further extended with the use of a wider range of resolving acids.

Through the collaboration with AstraZeneca, 4 g of iridium(III) chloride trihydrate is available which will be used to synthesise the immobilised SCRAM **92** for a large scale R<sup>3</sup> process. This is an important study as it provides information on the scalability and potential industrial applications of the process. Whilst the substrates chosen for the development of the R<sup>3</sup> process are relatively simple involving cyclic and acyclic benzylic/ non-benzylic amines, other substrate classes including chiral aliphatic amines, carboxylic acids, amino-alcohols, chiral compounds bearing a non-chiral amine/ acid groups, and chiral compounds containing more than one chiral centres can all be tested with the R<sup>3</sup> process. For substrates involving the resolution of carboxylic acids, enantiomerically pure amines can be used as the resolving agent. Development of alternative catalysts may be required for non-amine racemisation.

Although the triiron dodecacarbonyl complex **E** was identified in the catalyst screen for the racemisation of **9** and **103**, understanding of the mechanism is limited at this stage. The involvement of nanoparticles in the catalytic cycle may indicate the potential use of nanoparticles directly in the racemisation and its subsequent immobilisation may also be possible, increasing its stability and recyclability, and allowing its use in flow.

## 6. Experimental

### 6.0 General

#### 6.0.1 Chemicals and analytical methods

Unless otherwise stated, all chemicals were obtained from Sigma-Aldrich, Fisher Scientific, Alfa Aesar or Fluorochem and were used without further purification. Immobilised SCRAM catalyst **92** was obtained from Yorkshire Process Technology and was used without further purification. All solvents used were HPLC grade. All syringe pumps used were Harvard Apparatus Model 11 from Scientific Support. Column chromatographic purifications were performed using Biotage (Isolera™ Spektra One, silica column = RediSep®Rf). Nuclear Magnetic Resonance (NMR) spectra were recorded on Bruker 500 UltraShield™ Spectrometer operating at 500 MHz (<sup>1</sup>H NMR) and 126 MHz (<sup>13</sup>C NMR), or Bruker DX300 Spectrometer operating at 300 MHz (<sup>1</sup>H NMR) and 75 MHz (<sup>13</sup>C NMR), or Bruker ADVANCE III HD-400 Spectrometer operating at 400 MHz (<sup>1</sup>H NMR). The atoms in the compounds are numbered to aid assignment. Liquid Chromatography-Mass Spectrometry (LCMS) was performed on an Agilent Technologies 1200 Series LC system with a C18 column (Phenomenex Luna 5u C18(2), 50 mm × 2 mm × 5 μm) eluted with acetonitrile/ water gradient (15-95% acetonitrile, 0.1% formic acid over 3 minutes) and a Bruker Daltonics HCT®Ultra system equipped with an ion trap MS detector; or a Thermo Ultimate 3000 UHPLC system with a C18 column (Phenomenex Kinetex, 50 mm × 2.1 mm × 2.6 μm) eluted with acetonitrile/ water gradient (2-95% acetonitrile, 0.1% formic acid over 1 minute) and a Bruker Amazon Speed ion trap mass spectrometer. Gas Chromatography-Mass Spectrometer (GCMS) was performed on A HP6890 series GC system with A HP5973 mass selective detector and helium flow gas. High resolution mass spectrometry (HRMS) was performed on a Bruker Maxis Impact Electron Spray Ionisation (ESI) spectrometer. For clarity in the assignment of MS peaks of the amine salts, the cationic and anionic fragments were assigned as **X** and **Y** respectively. Melting points were recorded using Stuart Scientific SMP3 melting point apparatus. Fourier-transform infrared (FT-IR) spectroscopy was recorded using Bruker Platinum-ATR spectrometer. Optical rotations ( $[\alpha]_D$ ) were measured using Polartronic H532 at 589 nm and were calculated as,

$$[\alpha]_D^T = \frac{\text{Rotation} \times 100}{c \times l} \quad (\text{Eqn. 5.1})$$

Where T = temperature; c = concentration of sample in g per 100 mL; l = path length which is the length of the cell in dm (the cell used was 1 dm).

Achiral and chiral gas chromatography (GC) were performed using a HP6890 series GC system, Agilent Technologies 7683 series injector and HP7683 series autosampler, with an FID detector and hydrogen flow gas. Both the GCMS and achiral GC used the HP-5 column (5% phenyl methyl siloxane; 30 m × 0.32 mm × 0.25 μm). Chiral High Performance Liquid Chromatography (HPLC) was performed on an Agilent Technologies 1290 Infinity system or an Agilent 1100 Series system. Chiral SFC was performed on the WATERS Aquity UPC2 system in AstraZeneca.

Single crystal structures were obtained at 120 K on an Agilent SuperNova diffractometer equipped with an Atlas CCD detector and connected to an Oxford Cryostream low temperature device using mirror monochromated Cu K<sub>α</sub> radiation (λ = 1.54184 Å) from a Microfocus X-ray source. The structure was solved by intrinsic phasing SHELXT<sup>174</sup> and refined by a full matrix least squares technique based on F<sup>2</sup> using SHELXL2014.<sup>175</sup> The exception was the single crystal structure of (*R*)-**39**-(*S,S*)-**32**-(*S*)-**39** from UK National Crystallography Service (NCS), which was obtained on a Rigaku 007HF diffractometer equipped with Varimax confocal mirrors and an AFC11 goniometer and HyPix 6000 detector. The crystal was kept at T = 100(1) K during data collection. Using Olex2,<sup>176</sup> the structure was solved with ShelXT structure solution program,<sup>174</sup> using the Intrinsic Phasing solution method. The model was refined with version 2014/7 of ShelXL using Least Squares minimisation.<sup>175</sup> The powder X-ray diffraction (XRD) data were collected using a Bruker AXS D2Phaser diffractometer at room temperature using Cu-K<sub>α</sub> (λ = 1.54184 Å) radiation. Diffraction patterns were recorded with a step size of 0.02° from 5° to 50° (1 s per step). Experimental data was processed using Diffrac.Eva.

The racemisation reactions of (*R*)-**9** by iron complex **E** (Section 5.4.2(a)(ii) and (iii)) and its transfer dehydrogenation by Copper(II) acetate **K** (Section 5.4.3(a))

were carried out in the First Generation Amigo Workstation from Amigochem with automated sampler. These reactions and the racemisation catalyst screening experiments (Section 6.4.1) were carried out in AstraZeneca.

## 6.0.2 GC calibrations

Stock solutions of known concentrations of internal standards, amines **9**, **103**, **39**, **101**, **42**, **46**, imine **8** and acetophenone **51** were prepared (Table 6.1). For each calibration sample, a known volume of the stock solutions of an internal standard (50 mM, 20  $\mu$ L) and the compound of interest were diluted into ethyl acetate to make up 1 mL. The samples were analysed by achiral GC. The calibration curves were produced by plotting the peak area ratio of the compounds to the internal standard against the concentration of the compound (Fig. 6.1 to 6.8).

Compound	[Stock solution] (mM)	Internal standard
( <i>R</i> )- <b>9</b>	81	<i>n</i> -Hexadecane
<i>rac</i> - <b>103</b>	100	<i>n</i> -Decane
( <i>R</i> )- <b>39</b>	100	<i>n</i> -Decane
<i>rac</i> - <b>101</b>	100	<i>n</i> -Decane
<i>rac</i> - <b>42</b>	100	<i>n</i> -Decane
( <i>S</i> )- <b>46</b>	100	<i>n</i> -Decane
Imine <b>8</b>	10	<i>n</i> -Hexadecane
Ketone <b>51</b>	10	<i>n</i> -Decane

Table 6.1 Concentrations of stock solutions and internal standards used in GC calibrations

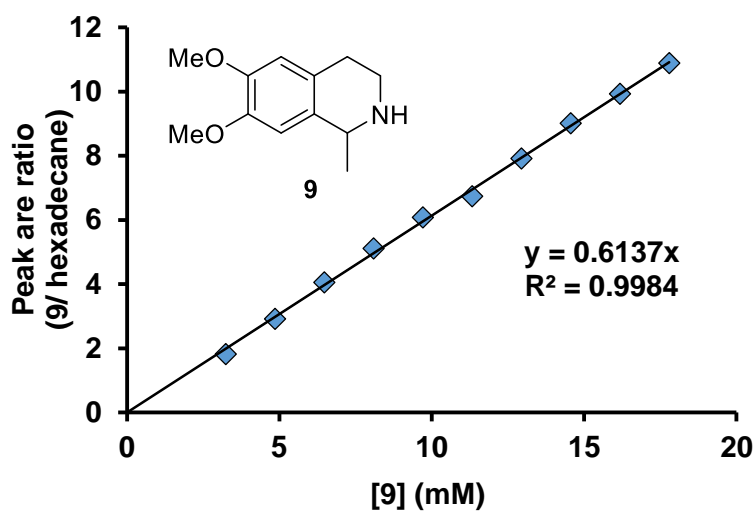


Fig. 6.1 GC calibration for **9**. Method, column = HP-5 (5% phenyl methyl siloxane; 30 m × 0.32 mm × 0.25 μm); oven temperature = 2 °C min<sup>-1</sup> ramped from 150 °C to 180 °C, 10 °C min<sup>-1</sup> ramped to 300 °C; inlet pressure = 10 psi. *t<sub>R</sub>*, n-hexadecane = 2.6 min; **9** = 4.6 min

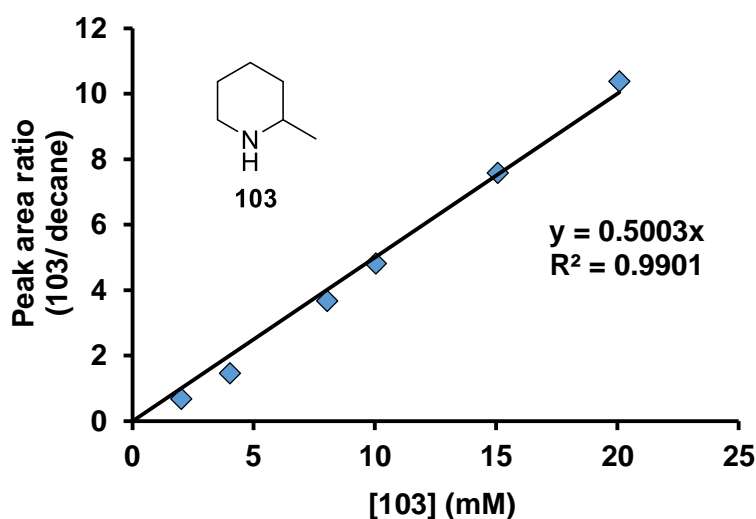


Fig. 6.2 GC calibration for **103**. Method, column = HP-5 (5% phenyl methyl siloxane; 30 m × 0.32 mm × 0.25 μm); oven temperature = 35 °C isothermal for 10 min, 50 °C min<sup>-1</sup> ramped to 300 °C and isothermal for 5 min; inlet pressure = 10 psi. *t<sub>R</sub>*, n-decane = 7.1 min; **103** = 2.1 min

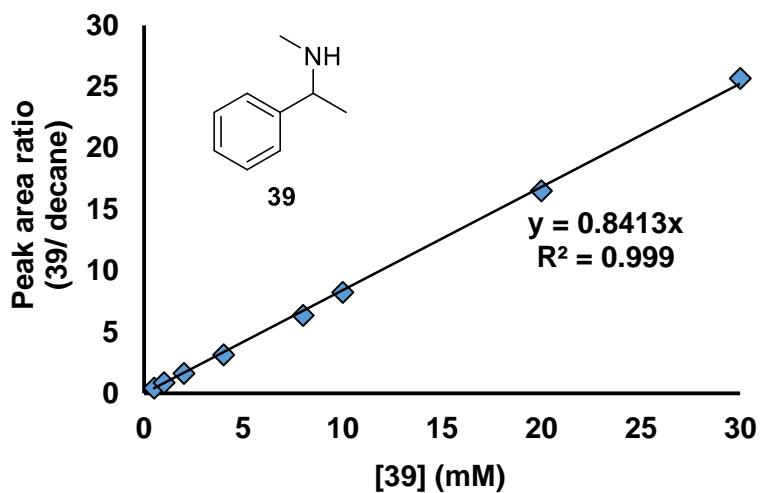


Fig. 6.3 GC calibration for **39**. Method, column = HP-5 (5% phenyl methyl siloxane; 30 m × 0.32 mm × 0.25 μm); oven temperature = 60 °C isothermal for 10 min, 5 °C min<sup>-1</sup> ramped to 100 °C and isothermal for 3 min, then 50 °C min<sup>-1</sup> ramped to 300 °C and isothermal for 5 min; inlet pressure = 10 psi. *t<sub>R</sub>*, decane = 1.9 min; **39** = 2.9 min

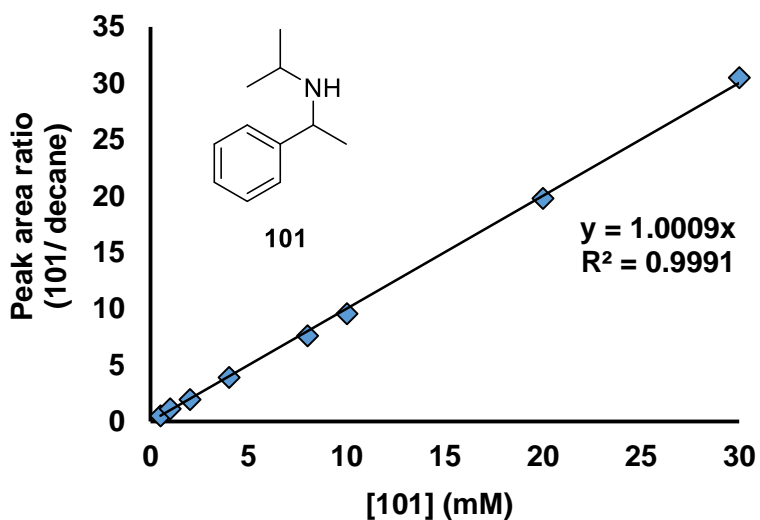


Fig. 6.4 GC calibration for **101**. Method (i), column = HP-5 (5% phenyl methyl siloxane; 30 m × 0.32 mm × 0.25 μm); oven temperature = 60 °C isothermal for 10 min, 5 °C min<sup>-1</sup> ramped to 100 °C and isothermal for 3 min, then 50 °C min<sup>-1</sup> ramped to 300 °C and isothermal for 5 min; inlet pressure = 10 psi. *t<sub>R</sub>*, decane = 1.9 min; **101** = 5.1 min

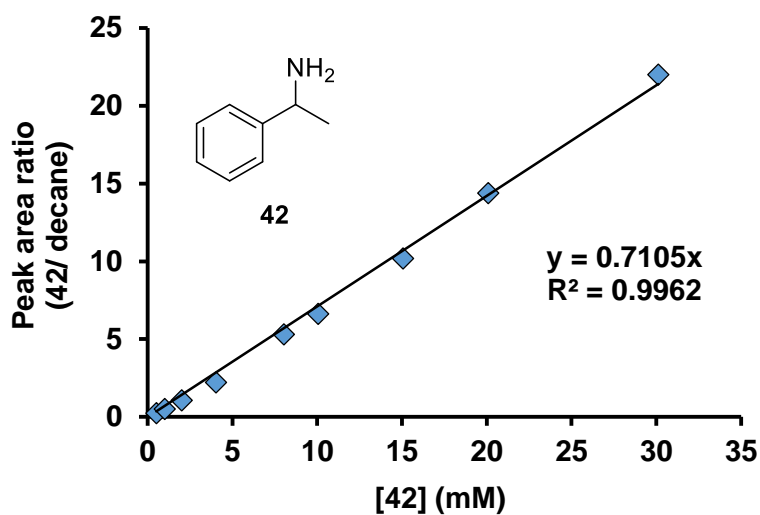


Fig. 6.5 GC calibration for **42**. Method (i), column = HP-5 (5% phenyl methyl siloxane; 30 m × 0.32 mm × 0.25 μm); oven temperature = 60 °C isothermal for 10 min, 5 °C min<sup>-1</sup> ramped to 100 °C and isothermal for 3 min, then 50 °C min<sup>-1</sup> ramped to 300 °C and isothermal for 5 min; inlet pressure = 10 psi.  $t_R$ , decane = 1.9 min; **42** = 2.4 min

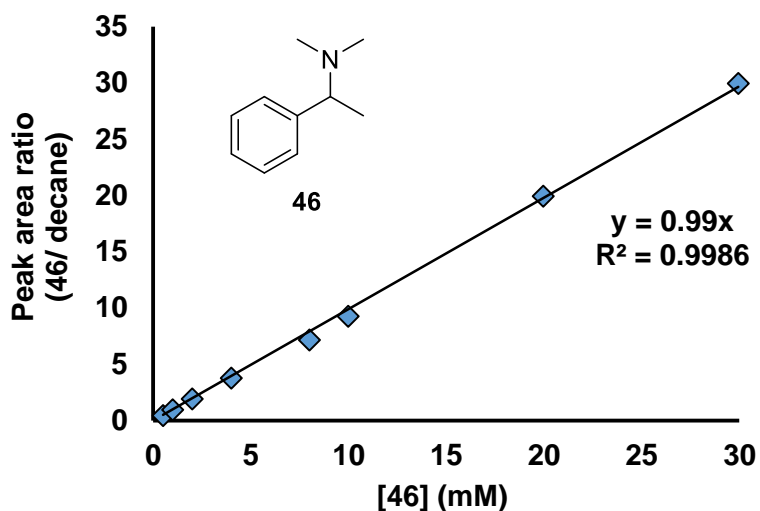


Fig. 6.6 GC calibration for **46**. Method (i), column = HP-5 (5% phenyl methyl siloxane; 30 m × 0.32 mm × 0.25 μm); oven temperature = 50 °C isothermal for 2 min, 4 °C min<sup>-1</sup> ramped to 70 °C and isothermal for 10 min, then 50 °C min<sup>-1</sup> ramped to 300 °C and isothermal for 5 min; inlet pressure = 10 psi.  $t_R$ , decane = 1.5 min; **46** = 2.5 min

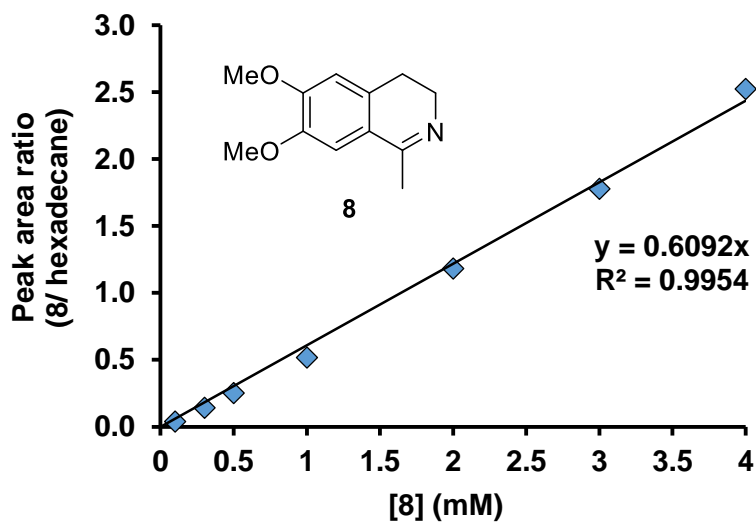


Fig. 6.7 GC calibration for **8**. Method, column = HP-5 (5% phenyl methyl siloxane; 30 m × 0.32 mm × 0.25 μm); oven temperature = 2 °C min<sup>-1</sup> ramped from 150 °C to 180 °C, 10 °C min<sup>-1</sup> ramped to 300 °C; inlet pressure = 10 psi. *t<sub>R</sub>*, n-hexadecane = 2.6 min; **8** = 5.0 min

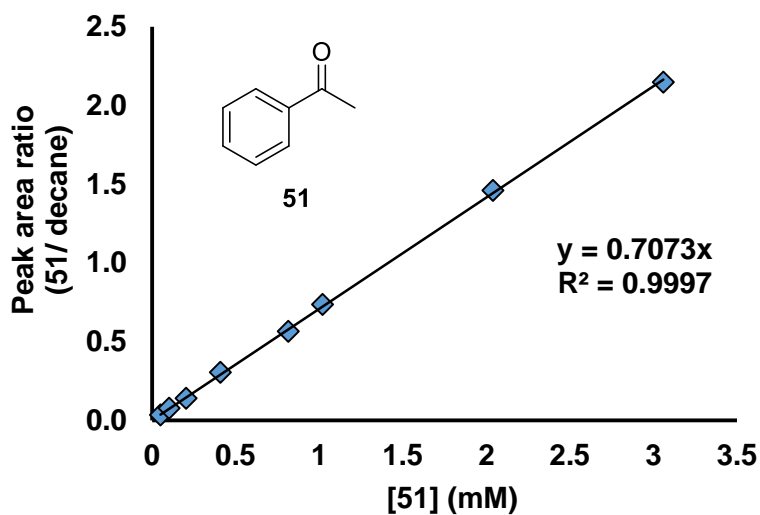


Fig. 6.8 GC calibration for **51**. Method, column = HP-5 (5% phenyl methyl siloxane; 30 m × 0.32 mm × 0.25 μm); oven temperature = 60 °C isothermal for 10 min, 5 °C min<sup>-1</sup> ramped to 100 °C and isothermal for 3 min, then 50 °C min<sup>-1</sup> ramped to 300 °C and isothermal for 5 min; inlet pressure = 10 psi. *t<sub>R</sub>*, decane = 1.9 min; **51** = 2.6 min



### 6.0.3 Chromatograms of racemic and optically pure materials

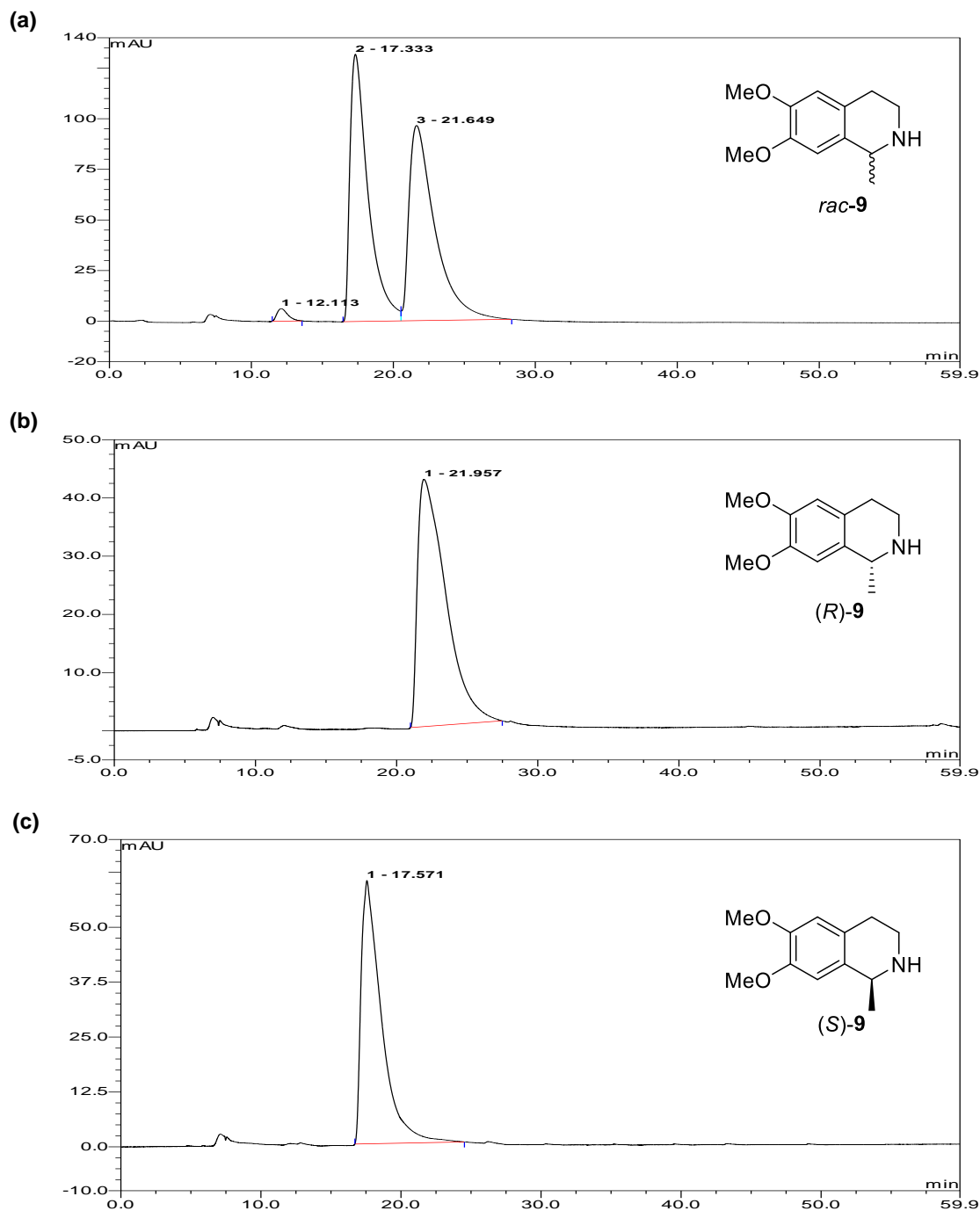


Fig. 6.9 Chiral HPLC traces of **9**. Method; column = Chiralcel® OD-H 250 mm x 4.6 mm x 5  $\mu$ m; hexane/*i*PrOH/*E*<sub>2</sub>NH 80: 20: 0.1 isocratic for 60 min; flow rate = 0.5 mL min<sup>-1</sup>;  $\lambda$  = 280 nm; T = 25 °C. (a) Racemate; (b) (R)-**9** (21.8 min); (c) (S)-**9** (17.3 min)

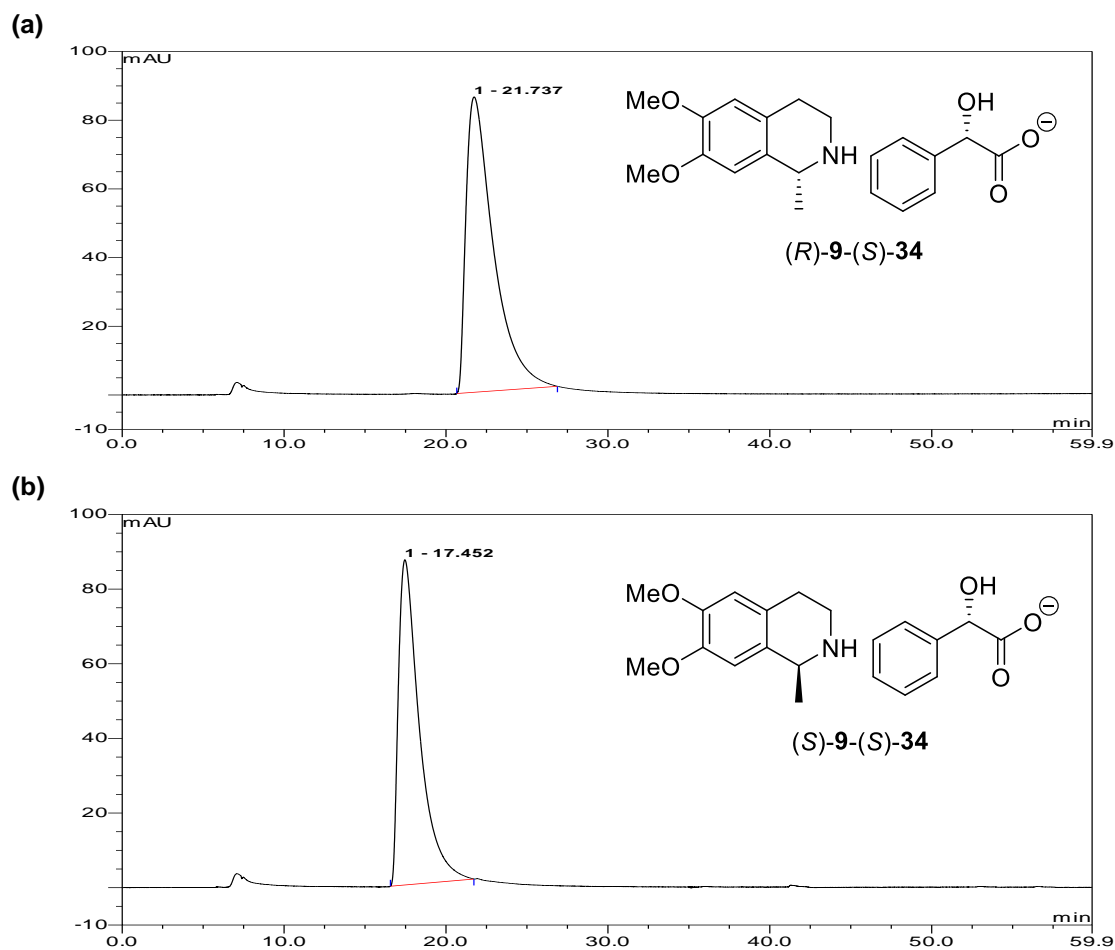


Fig. 6.10 Chiral HPLC traces of (S)-34 salts of enantiopure 9. Method, column = Chiralcel® OD-H 250 mm × 4.6 mm × 5 μm; hexane/ *i*PrOH/ Et<sub>2</sub>NH 80: 20: 0.1 isocratic for 60 min; flow rate = 0.5 mL min<sup>-1</sup>; λ = 280 nm; T = 25 °C. (a) (R)-9-(S)-34 (21.8 min); (b) (S)-9-(S)-34 (17.5 min)

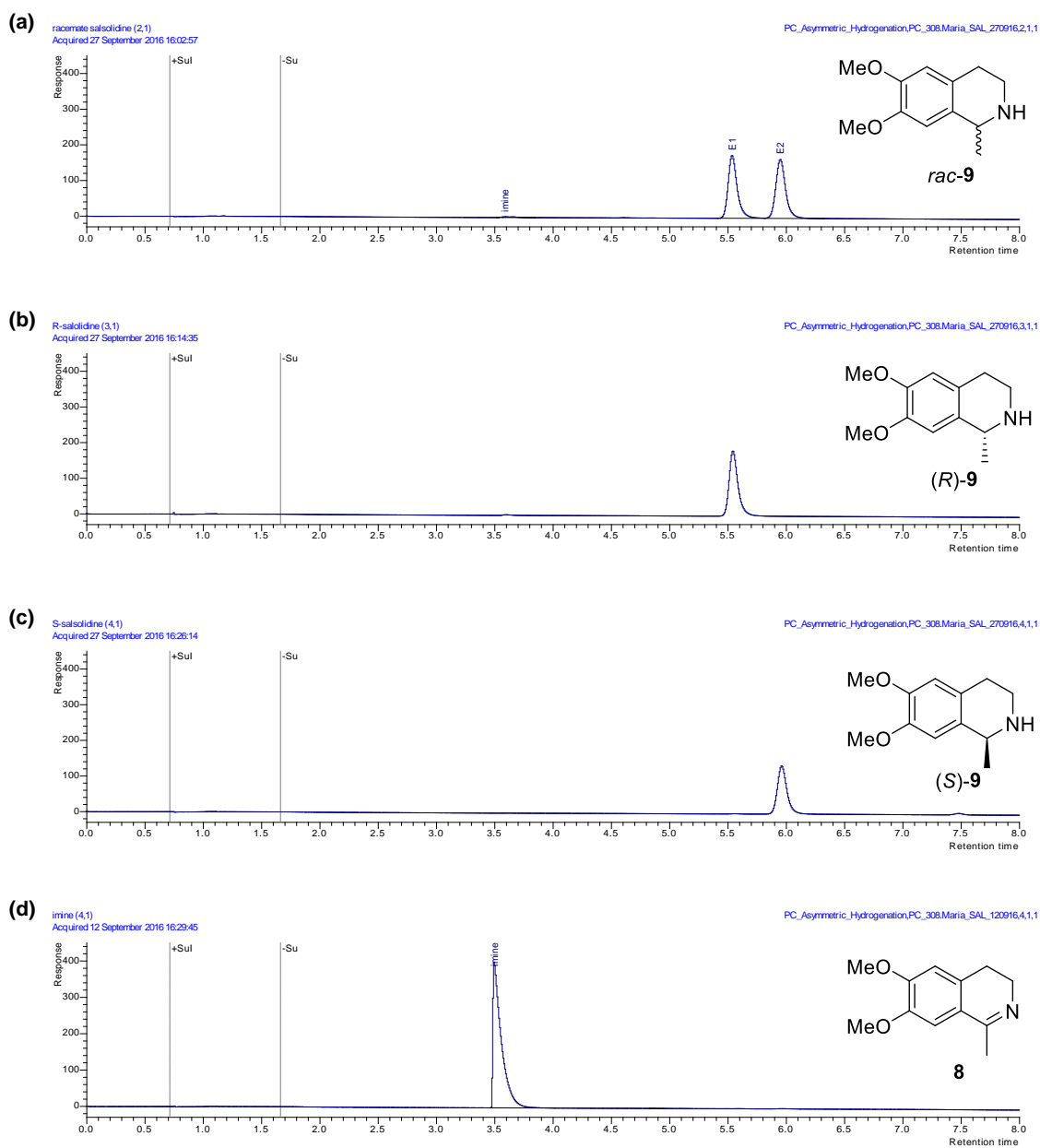


Fig. 6.11 Chiral SFC traces of amine **9** and imine **8**. Method, column = Chiralpak® AD-H 150 mm × 4.6 mm × 3 μm; A = CO<sub>2</sub> (150 bar), B = *i*PrOH/*i*PrNH<sub>2</sub> 99.9:0.1, A/B ramped from 95:5 to 50:50 over 8 min; flow rate = 2.5 mL min<sup>-1</sup>; λ = 280 nm; T = 35 °C. (a) Racemate; (b) (R)-**9** (5.6 min); (c) (S)-**9** (5.9 min); (d) imine **8** (3.5 min)

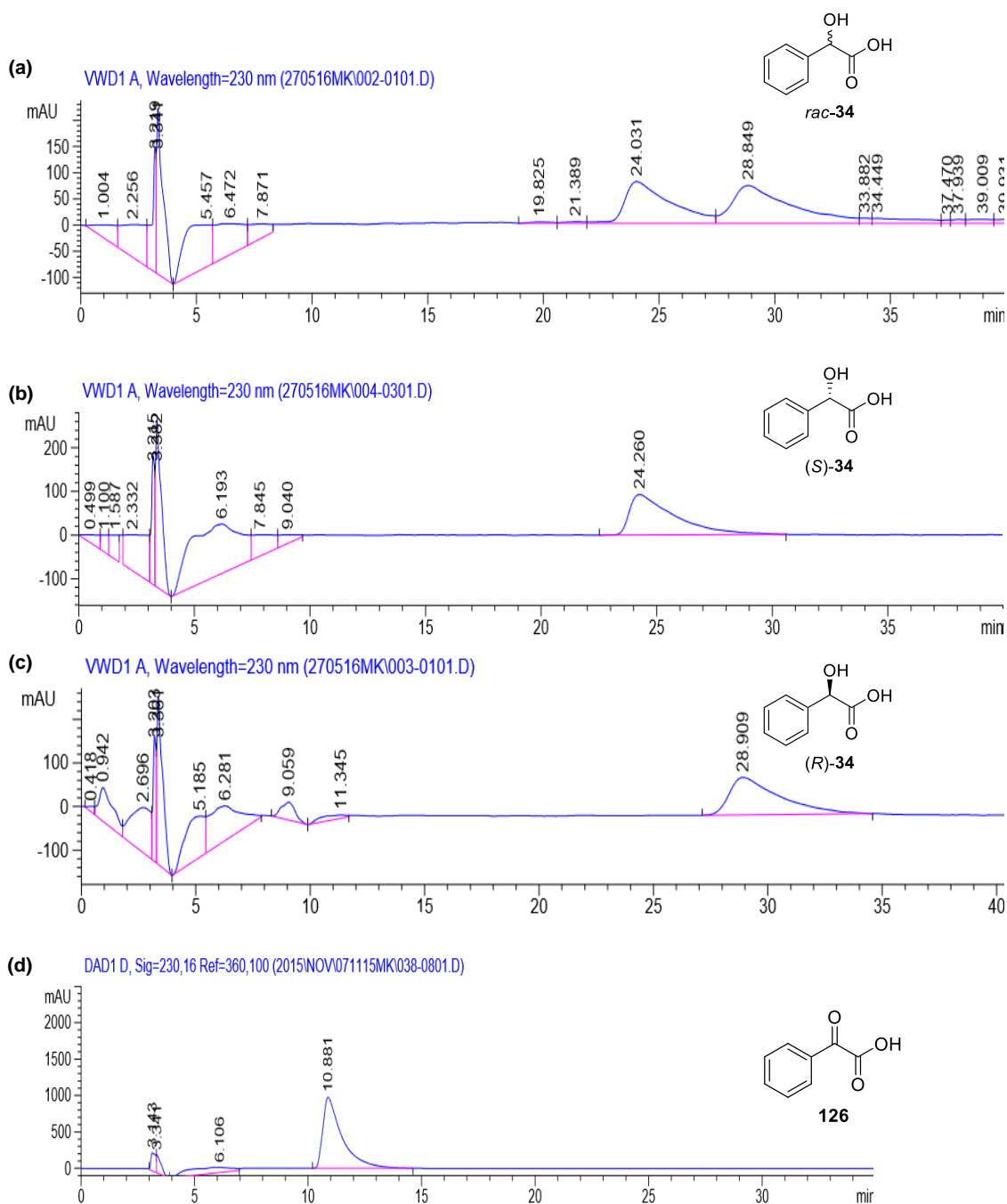
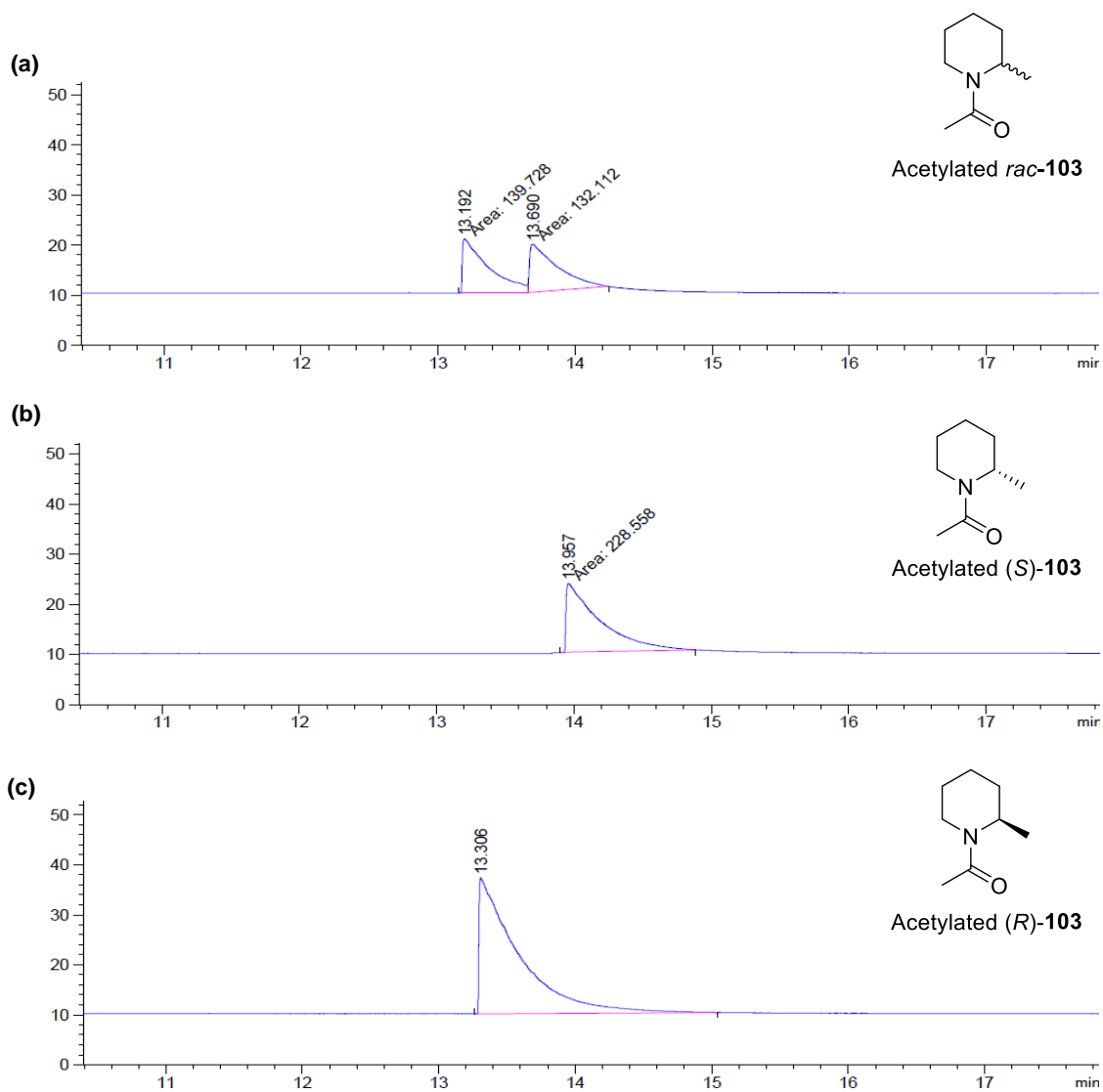
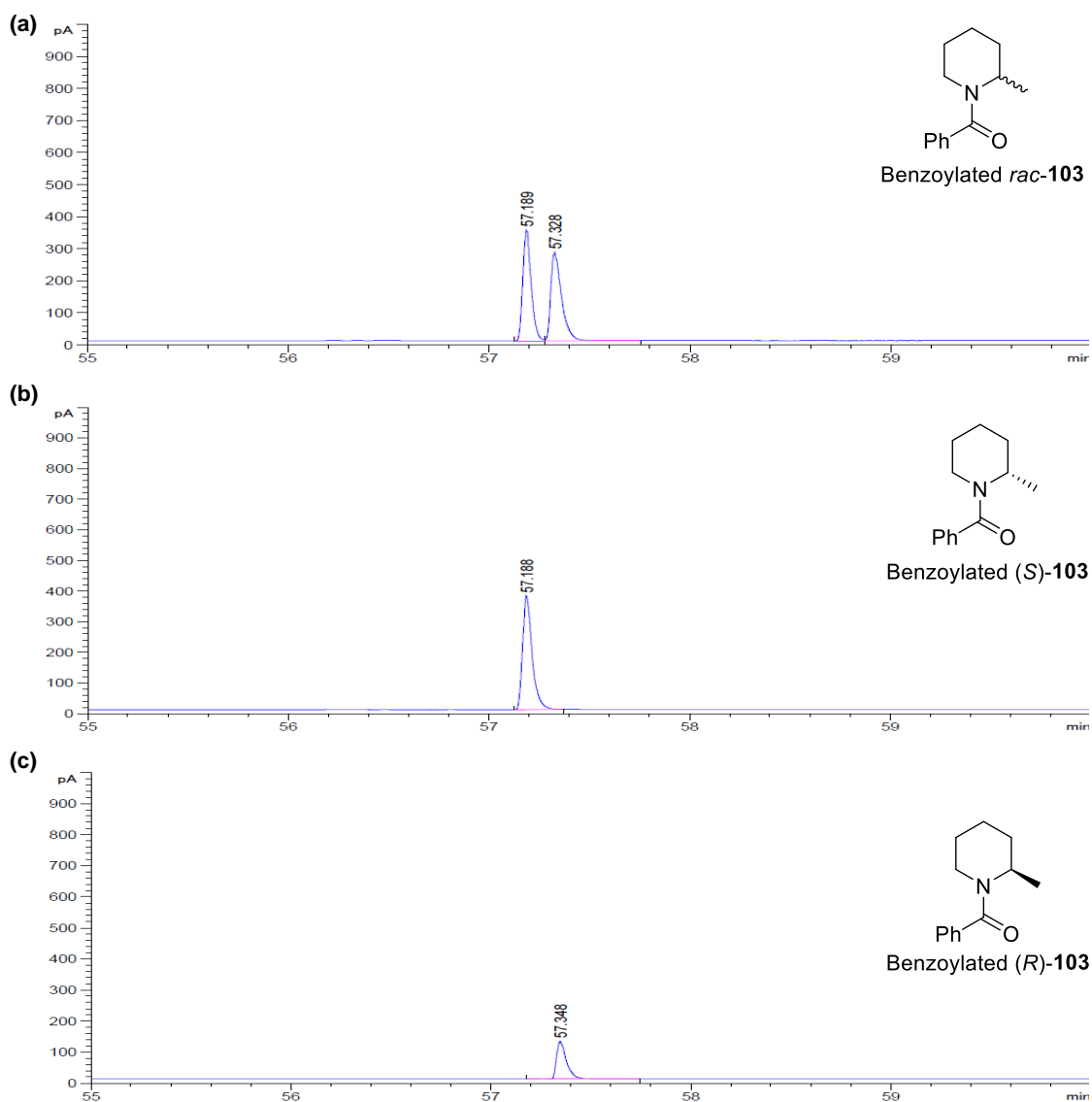


Fig. 6.12 Chiral HPLC traces of acids **34** and **126**. Method, column = Chiralpak® AD-H 250 mm × 4.6 mm × 5 μm; hexane/ *i*PrOH/ CF<sub>3</sub>CO<sub>2</sub>H 95: 5: 0.1 isocratic for 35-40 min; flow rate = 1 mL min<sup>-1</sup>; λ = 230 nm; T = 25 °C. (a) **rac-34**; (b) **(S)-34** (24.3 min); (c) **(R)-34** (28.9 min); (d) **keto-acid 126** (10.9 min)



**Fig. 6.13** Chiral GC traces of acetylated **103**. Method (i), column = CP-CHIRASIL-DEX column (25 m × 0.25 mm × 0.25 μm); oven temperature = 100 °C isothermal for 5 min; 1 °C min<sup>-1</sup> ramped to 120 °C and isothermal for 5 min, 50 °C min<sup>-1</sup> to 200 °C and isothermal for 5 min; inlet pressure = 7.5 psi; samples were derivatized with acetic anhydride before measurements were taken. (a) Acetylated racemate; (b) Acetylated (*S*)-**103** (14.0 min); (c) Acetylated (*R*)-**103** (13.3 min)



**Fig. 6.14** Chiral GC traces of benzoylated **103**. Method (ii), column = CP-CHIRASIL-DEX column (25 m × 0.25 mm × 0.25 μm); oven temperature = 80 °C isothermal for 40 min, 5 °C min<sup>-1</sup> to 180 °C and isothermal for 10 min; inlet pressure = 15 psi; samples were derivatized with benzoyl chloride before measurements were taken. (a) Benzoylated racemate; (b) Benzoylated (S)-**103** (57.2 min); (c) Benzoylated (R)-**103** (57.3 min)

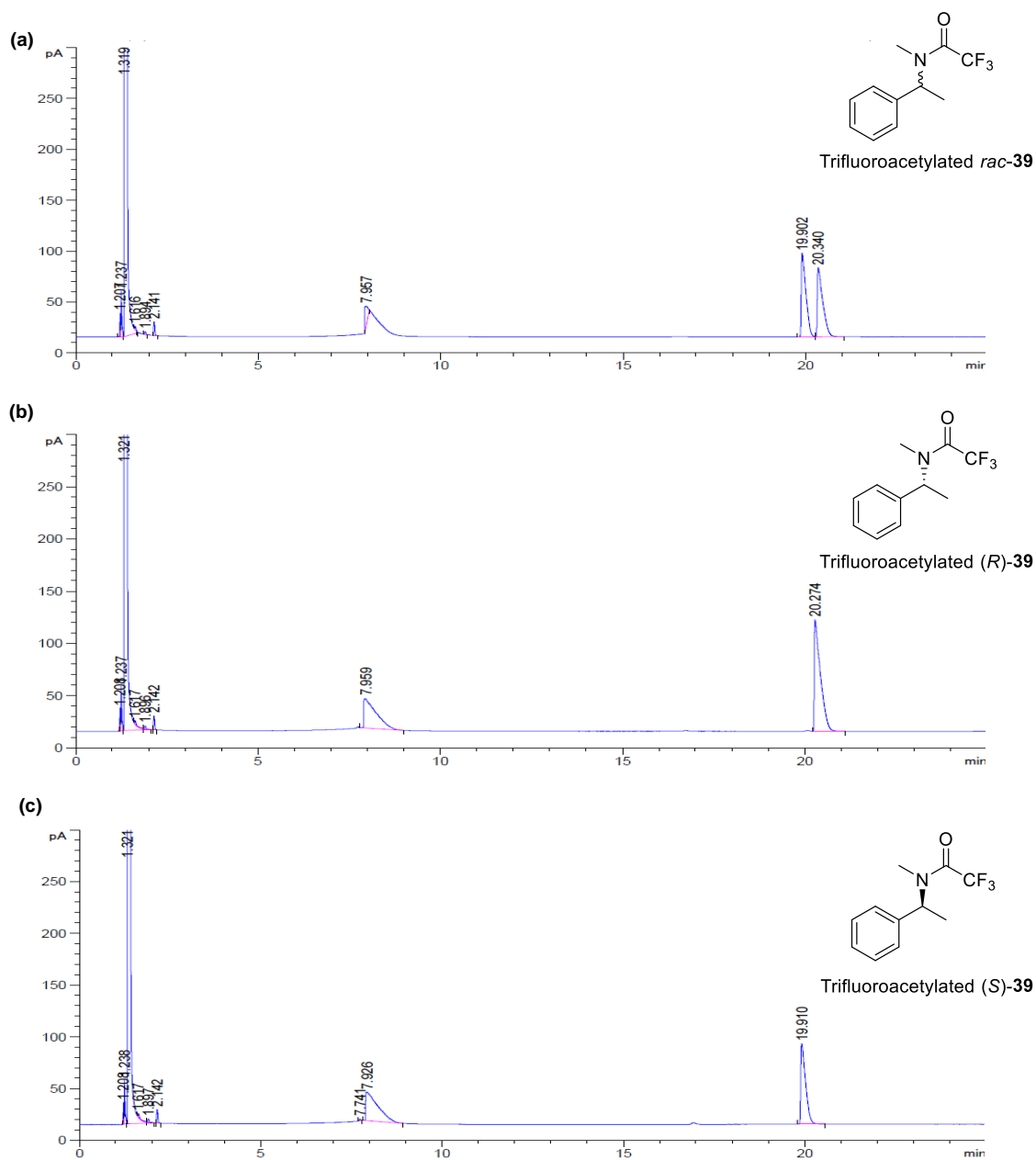


Fig. 6.15 Chiral GC traces of trifluoroacetylated **39**. Method, column = CP-CHIRASIL-DEX column (25 m × 0.25 mm × 0.25 μm); oven temperature = 80 °C isothermal for 4 min, 5 °C min<sup>-1</sup> ramped to 100 °C and isothermal for 30 min; inlet pressure = 7.5 psi. (a) Trifluoroacetylated racemate; (b) Trifluoroacetylated (*R*)-**39** (20.3 min); (c) Trifluoroacetylated (*S*)-**39** (19.9 min)

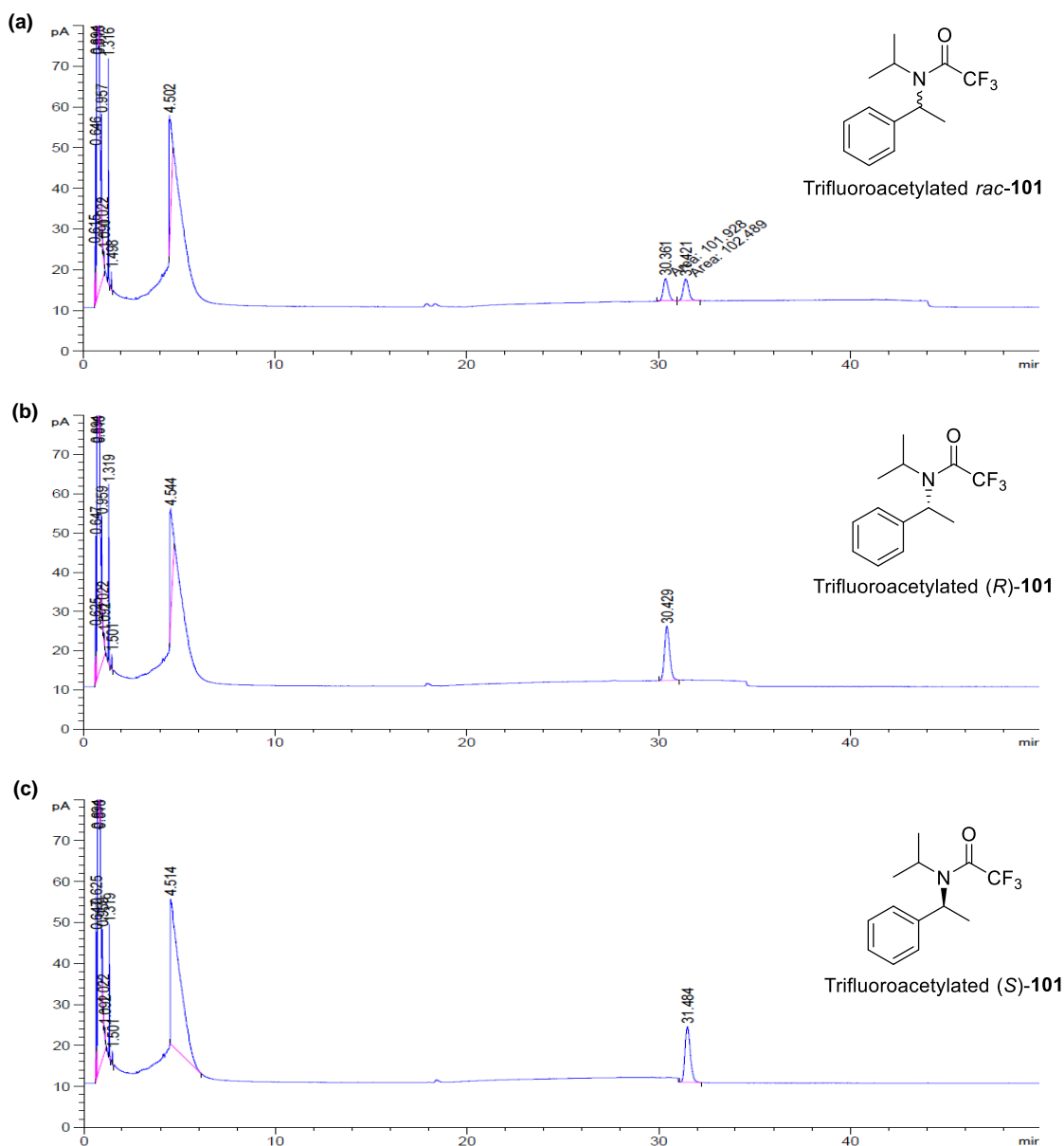


Fig. 6.16 Chiral GC traces of trifluoroacetylated **101**. Method, column = CP-CHIRASIL-DEX column (25 m × 0.25 mm × 0.25 μm); oven temperature = 80 °C isothermal for 60 min, 40 °C min<sup>-1</sup> ramped to 180 °C and isothermal for 10 min; inlet pressure = 15 psi. (a) Trifluoroacetylated racemic **101**; (b) Trifluoroacetylated (*R*)-**101** (30.4 min); (c) Trifluoroacetylated (*S*)-**101** (31.5 min)



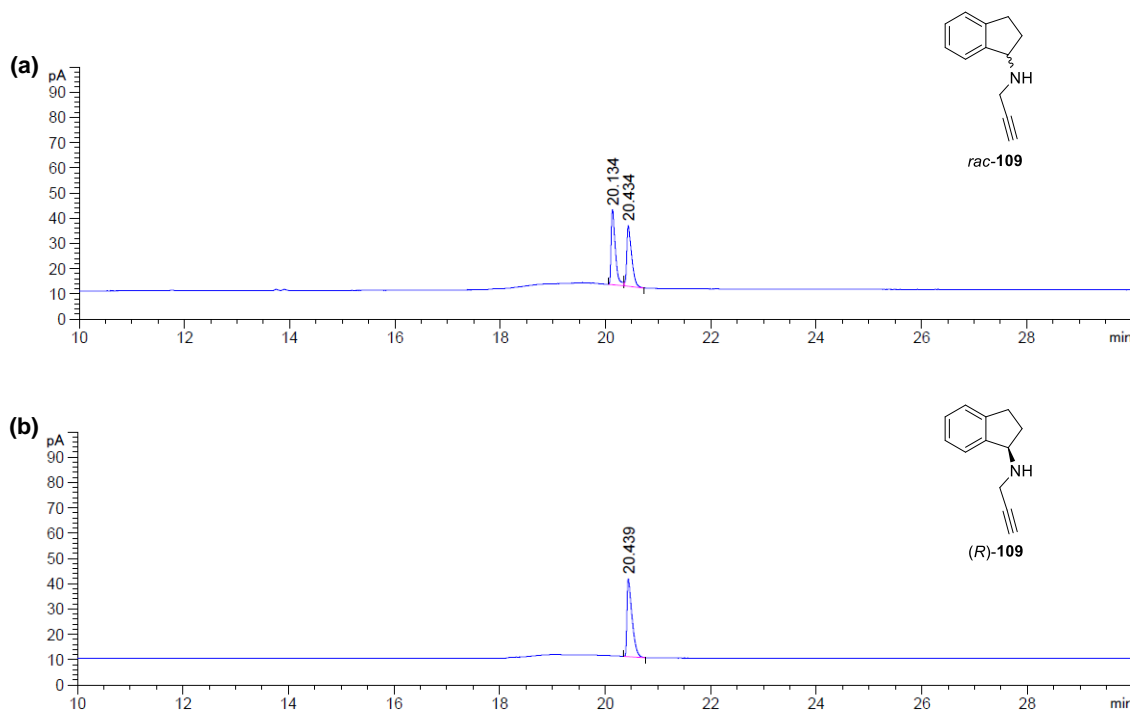
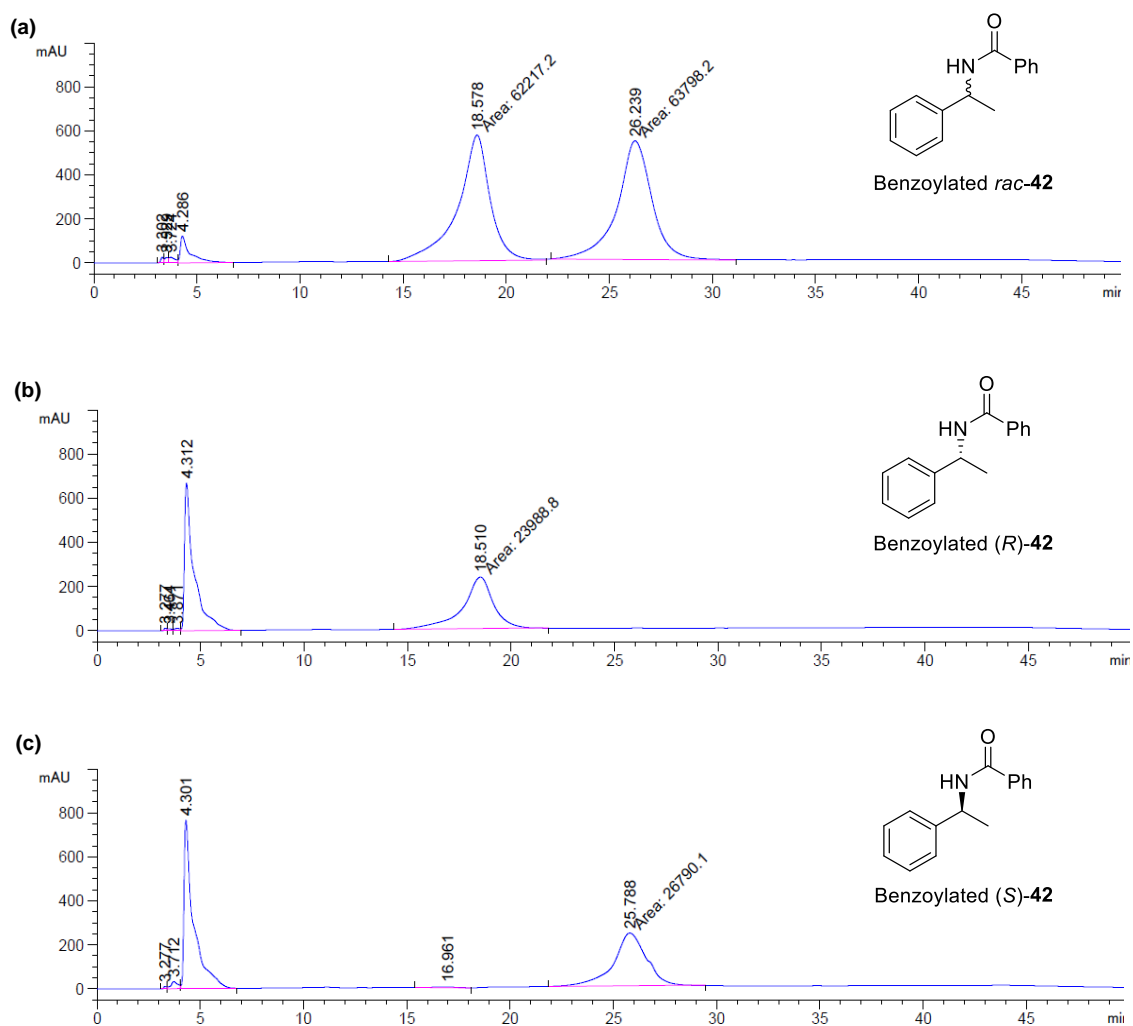


Fig. 6.17 Chiral GC traces of **109**. Method, column = CP-CHIRASIL-DEX column (25 m × 0.25 mm × 0.25 μm); oven temperature = 100 °C isothermal for 5 min, 2 °C min<sup>-1</sup> ramped to 130 °C and isothermal for 10 min, 25 °C min<sup>-1</sup> ramped to 200 °C and isothermal for 3 min; inlet pressure = 7.5 psi. (a) *rac*-**109**; (b) *(R)*-**109** (20.4 min)



**Fig. 6.18** Chiral HPLC traces of benzoylated **42**. Method; column = Chiralpak® AD-H 250 mm × 4.6 mm × 5 μm; hexane/ *i*PrOH ramped from 5% to 10% *i*PrOH over 40 min; flow rate = 1 mL min<sup>-1</sup>; λ = 254 nm; T = 25 °C. (a) Benzoylated racemate; (b) Benzoylated (*R*)-**42** (18.5 min); (c) Benzoylated (*S*)-**42** (25.8 min)

## 6.0.4 $^1\text{H}$ NMR spectra of diastereopure salts of chiral amines

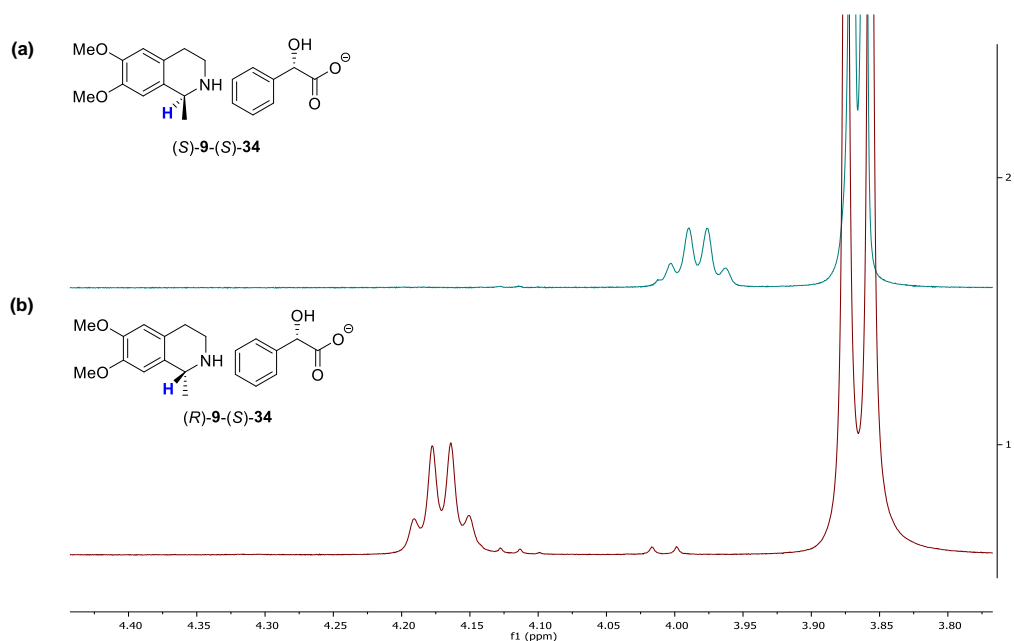


Fig. 6.19  $^1\text{H}$  NMR spectra of (S)-**34** salts of enantiopure **9** recorded in  $\text{CDCl}_3$  (500 MHz, 32 scans, relaxation delay = 2.49 s, acquisition time = 2.1825 min), showing the benzylic CH protons in **7** as a quartet (highlighted in blue). (a) (S)-**9**-(S)-**34**, 3.98 ppm (q,  $J = 6.6$  Hz); (b) (R)-**9**-(S)-**34**, 4.17 ppm (q,  $J = 6.6$  Hz)

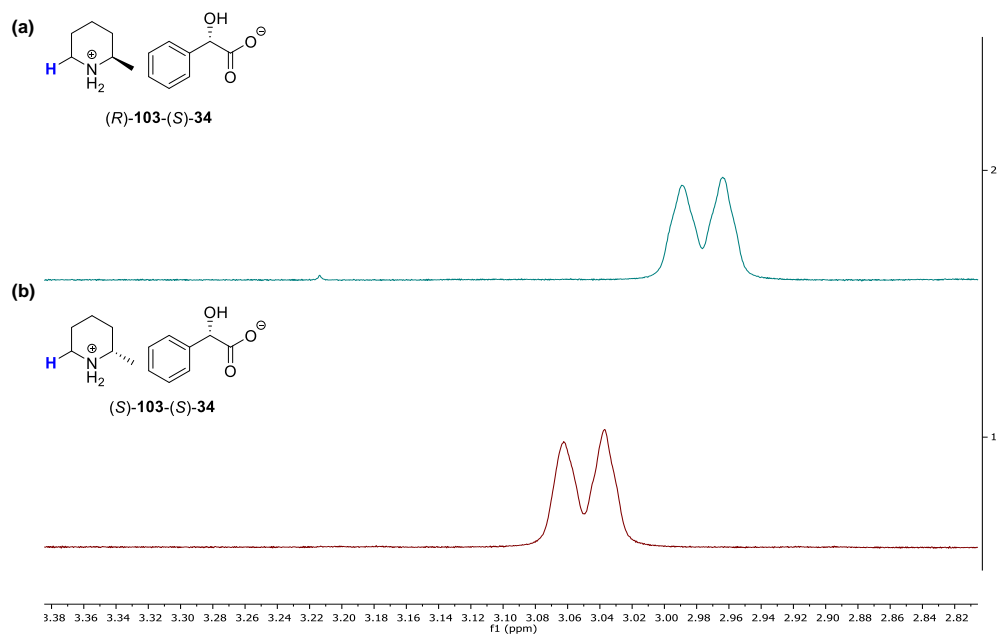


Fig. 6.20  $^1\text{H}$  NMR spectra of (S)-**34** salts of enantiopure **103** recorded in  $\text{CDCl}_3$  (500 MHz, 32 scans, relaxation delay = 2.49 s, acquisition time = 2.1825 min), showing one of the  $\text{CH}_2$  protons adjacent to  $\text{NH}_2$  (highlighted in blue). (a) (R)-**103**-(S)-**34**, 2.98 ppm (d,  $J = 12.5$  Hz); (b) (S)-**103**-(S)-**34**, 3.05 ppm (d,  $J = 12.5$  Hz)

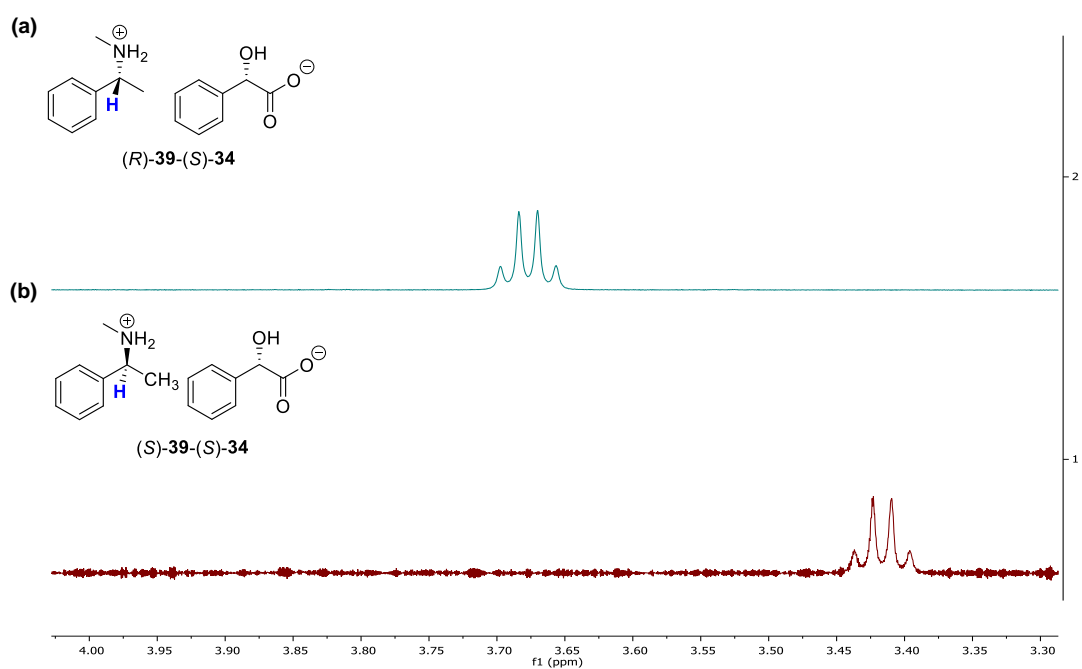


Fig. 6.21  $^1\text{H}$  NMR spectra of  $(S)\text{-}34$  salts of enantiopure **39** recorded in  $\text{CDCl}_3$  (500 MHz, 32 scans, relaxation delay = 2.49 s, acquisition time = 2.1825 min), showing the benzylic  $\text{CH}$  in **39** as a quartet (highlighted in blue). (a)  $(R)\text{-}39\text{-}(S)\text{-}34$ , 3.68 ppm (q,  $J = 6.9$  Hz); (b)  $(S)\text{-}39\text{-}(S)\text{-}34$ , 3.42 ppm (q,  $J = 6.8$  Hz)

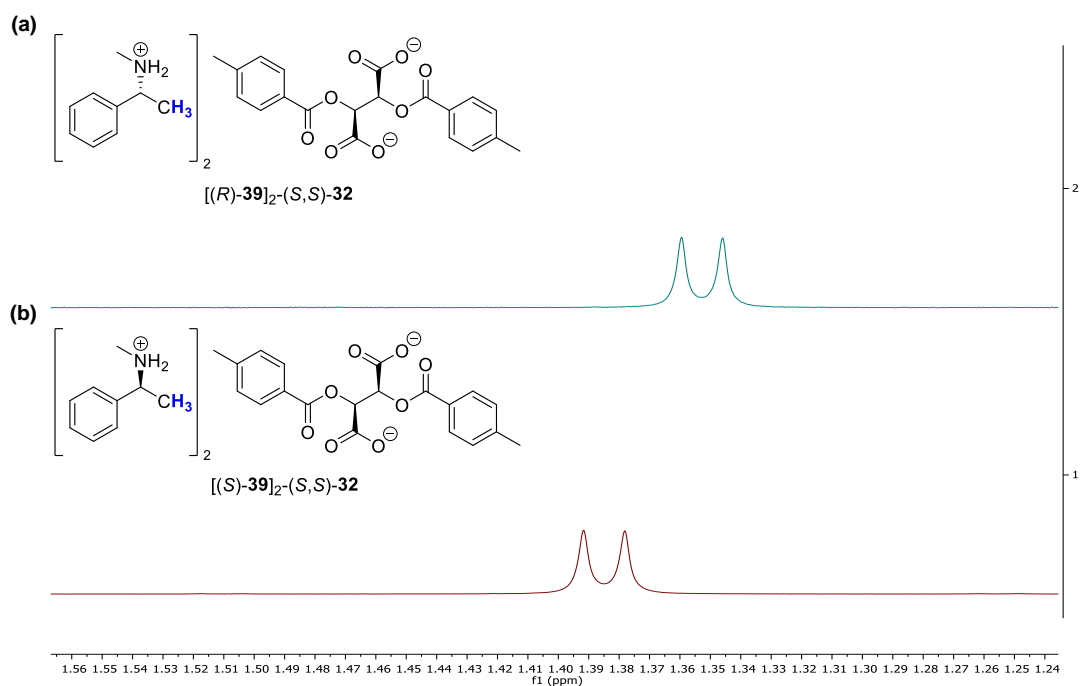


Fig. 6.22  $^1\text{H}$  NMR spectra of  $(S,S)\text{-}32$  salts of enantiopure **39** recorded in  $d_6\text{-DMSO}$  (500 MHz, 32 scans, relaxation delay = 2.49 s, acquisition time = 2.1825 min), showing  $\text{CH}_3$  at the chiral centre in **39** as a doublet (highlighted in blue). (a)  $(R)\text{-}39\text{-}(S,S)\text{-}32$ , 1.35 ppm (d,  $J = 6.8$  Hz); (b)  $(S)\text{-}39\text{-}(S,S)\text{-}32$ , 1.38 ppm (d,  $J = 6.9$  Hz)

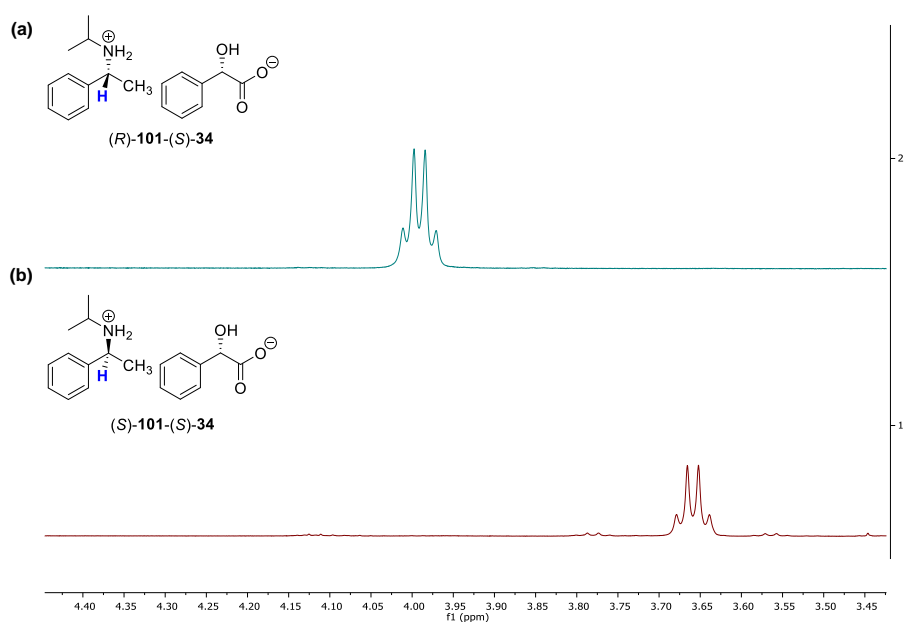


Fig. 6.23  $^1\text{H}$  NMR spectra of  $(S)$ - $34$  salts of enantiopure  $101$  recorded in  $\text{CDCl}_3$  (500 MHz, 32 scans, relaxation delay = 2.49 s, acquisition time = 2.1825 min), showing the benzylic  $\text{CH}$  in  $101$  as a quartet (highlighted in blue). (a)  $(R)$ - $101$ - $(S)$ - $34$ , 3.99 ppm (q,  $J = 6.7$  Hz); (b)  $(S)$ - $101$ - $(S)$ - $34$ , 3.66 ppm (q,  $J = 6.6$  Hz)

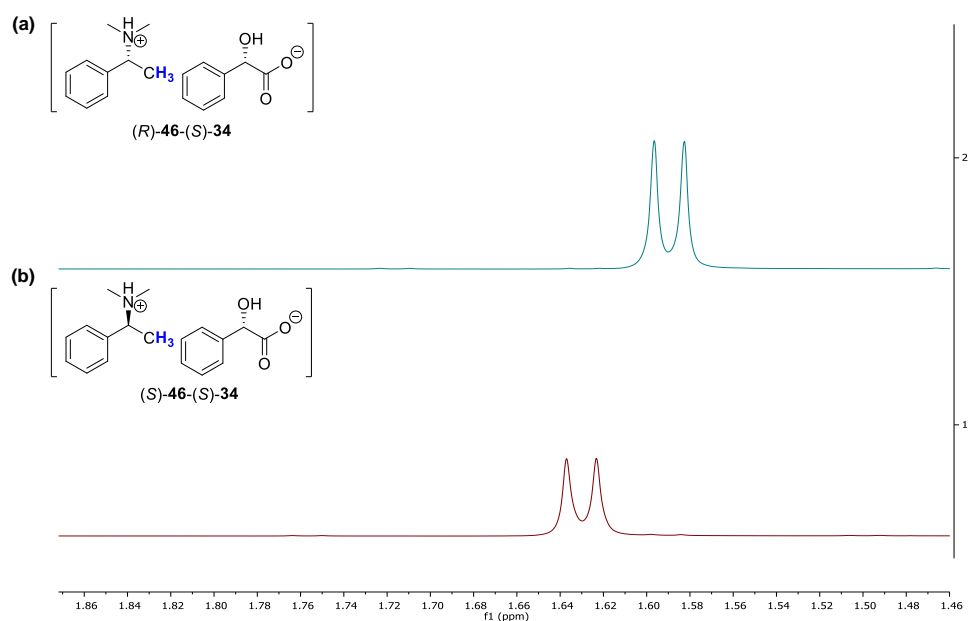
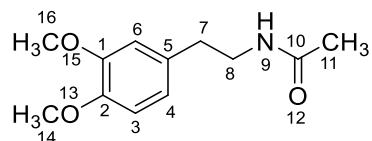


Fig. 6.24  $^1\text{H}$  NMR spectra of  $(S)$ - $34$  salts of enantiopure  $46$  recorded in  $\text{CDCl}_3$  (500 MHz, 64 scans, relaxation delay = 2 s, acquisition time = 3.0672 min), showing  $\text{CH}_3$  at the chiral centre in  $46$  as a doublet (highlighted in blue). It was used to determine the ee of  $46$  in its racemisation and resolution reactions. (a)  $(R)$ - $46$ - $(S)$ - $34$ , 1.59 ppm (d,  $J = 6.8$  Hz); (b)  $(S)$ - $46$ - $(S)$ - $34$ , 1.63 ppm (d,  $J = 6.9$  Hz)

## 6.1 Synthesis of starting materials and reference compounds

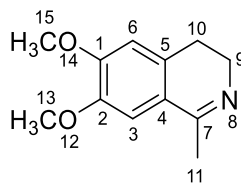
### 6.1.1. *N*-(3,4-Dimethoxyphenethyl)acetamide **125**<sup>177</sup>



3,4-Dimethoxyphenethylamine **124** (97%, 9.9 g, 53.1 mmol) was charged to a mixture of dichloromethane (50 mL) and triethylamine (12 mL, 86.3 mmol) and the mixture was cooled to 0 °C. With stirring, acetyl chloride (5 mL, 70.3 mmol) was charged dropwise to the reaction mixture over 0.5 hour. The pH was checked to ensure the reaction mixture stayed basic. The reaction mixture was warmed to room temperature and stirred overnight. The content was then poured into ice-cold water and was acidified by aqueous hydrochloric acid (1 M). The organic and aqueous layers were separated and the aqueous layer was further extracted with dichloromethane (3 × 50 mL). The combined organic layer was washed with water (100 mL), dried by anhydrous MgSO<sub>4</sub> and filtered. The solvent was removed *in vacuo* to yield a pale yellow solid (12.1 g). The product was recrystallised in hexane/ ethyl acetate 1:1 (v/v) to yield **125** as off-white crystals (9.2 g, 78%).

M.p. 98-100 °C {lit.<sup>177</sup> 100-101 °C};  $\delta_{\text{H}}$  in ppm (500 MHz, CDCl<sub>3</sub>); 6.82 (d,  $J$  = 8.0 Hz, 1H, H-4), 6.74–6.71 (m, 2H, H-3 and H-6), 5.43 (br s, 1H, NH), 3.88 (s, 3H, H-14 or H-16), 3.87 (s, 3H, H-14 or H-16), 3.50 (q,  $J$  = 7.0 Hz, 2H, H-8), 2.76 (t,  $J$  = 7.0 Hz, 2H, H-7), 1.95 (s, 3H, H-11);  $\delta_{\text{C}}$  in ppm (126 MHz, CDCl<sub>3</sub>); 170.0 (C-10), 149.1 (C-1 or C-2), 147.8 (C-1 or C-2), 131.4 (C-5), 120.6 (C-4), 111.9 (C-3 or C-6), 111.4 (C-3 or C-6), 56.0 (C-14 or C-16), 55.9 (C-14 or C-16), 40.8 (C-7), 35.2 (C-8), 23.4 (C-11);  $\nu_{\text{max}}$ / cm<sup>-1</sup>; 3249, 3078, 2992, 2928, 2839, 1632, 1563, 1515, 1471, 1261, 1233. The spectral data correspond to those reported in the literature.<sup>177</sup> HRMS, calculated for C<sub>12</sub>H<sub>18</sub>NO<sub>3</sub><sup>+</sup> [M+H]<sup>+</sup>: 224.128669, found by LCMS, ESI-MS [M+H]<sup>+</sup>: 224.0 {lit.<sup>177</sup> ESI-MS [M+H]<sup>+</sup>: 224.37}.

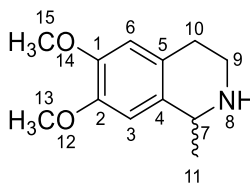
### 6.1.2. 6,7-Dimethoxy-1-methyl-3,4-dihydroisoquinoline **8**<sup>178</sup>



Acetamide **125** (6.0 g, 27.0 mmol) was added to toluene (30 mL, dried over molecular sieve 4 Å, 1-2 mm beads) in a round bottom flask fitted with an air condenser and calcium chloride drying tube. The mixture was warmed to 40 °C. Phosphoryl chloride (6 mL, 64.4 mmol) was charged dropwise into the mixture over 20 minutes. When the addition was complete, the mixture was heated to reflux for 3 hours. The reaction mixture was then cooled to 0 °C for 2 hours. The mixture was decanted and water was charged to the remaining solid at 0 °C. The content was warmed to room temperature and stirred overnight. The reaction mixture was basified by aqueous sodium hydroxide (5 M) and extracted with dichloromethane (4 × 50 mL). The combined organic layer was dried over anhydrous MgSO<sub>4</sub>, filtered and the solvent was removed *in vacuo* to yield **8** as an orange solid (5.4 g, 97%). The product was used in the next step without purification.

M.p. = 103-105 °C {lit.<sup>137</sup> m.p. 108-109 °C}; δ<sub>H</sub> in ppm (500 MHz, CDCl<sub>3</sub>); 6.99 (s, 1H, H-3), 6.69 (s, 1H, H-6), 3.92 (s, 3H, H-13 or H-15), 3.91 (s, 3H, H-13 or H-15), 3.63 (dt, *J* = 7.5 and 1.4 Hz, 2H, H-9), 2.64 (t, *J* = 7.5, 2H, H-10), 2.36 (t, *J* = 1.4 Hz, 3H, H-11); δ<sub>C</sub> in ppm (126 MHz, CDCl<sub>3</sub>); 163.1 (C-7), 150.4 (C-1 or C-2), 147.0 (C-1 or C-2), 130.7 (C-5), 122.0 (C-4), 109.8 (C-6), 108.6 (C-3), 55.8 (C-13 or C-15), 55.5 (C-13 or C-15), 46.6 (C-9), 25.3 (C-10), 22.9 (C-11); ν<sub>max</sub>/ cm<sup>-1</sup>; 2941, 2924, 2837, 1625, 1603, 1571, 1512, 1286, 1272, 1211. The spectral data correspond to those reported in the literatures.<sup>137</sup> HRMS, calculated for C<sub>12</sub>H<sub>16</sub>NO<sub>2</sub><sup>+</sup> [M+H]<sup>+</sup>: 206.118104, found by LCMS, ESI-MS [M+H]<sup>+</sup>: 206.0 {lit.<sup>137</sup> HRMS [M<sup>+</sup>]: 205.1102}.

### 6.1.3. Racemic 6,7-Dimethoxy-1-methyl-1,2,3,4-tetrahydroisoquinoline 9<sup>137</sup>



Imine **8** (4.3 g, 21.0 mmol) was dissolved into methanol (70 mL) and was cooled to 0 °C. Sodium borohydride (4.0 g, 105.5 mmol) was added slowly in portions over 20 minutes. The reaction mixture was stirred at room temperature overnight. The reaction mixture was acidified by aqueous hydrochloric acid (1 M) and then concentrated *in vacuo*. The white solid obtained was basified with aqueous sodium hydroxide (1 M) and extracted with dichloromethane (3 × 100 mL). The combined organic layer was washed with brine (1 × 50 mL) and dried over anhydrous MgSO<sub>4</sub>, filtered and the solvent was removed *in vacuo* to yield a light brown oil. The crude product was purified by column chromatography using Biotage (ethyl acetate/ triethylamine gradient, 95 to 96.5% ethyl acetate by volume); TLC: Silica plate, ethyl acetate/ triethylamine 95:5 (v/v), visualisation by UV (254 nm; R<sub>f</sub> of product = 0.15) to yield *rac*-**9** as a pale yellow oil. Off-white solid was formed overnight (3.7 g, 84 %).

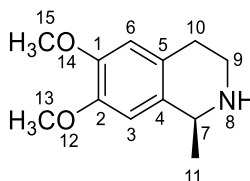
M.p. = 35-38 °C {lit.<sup>137</sup> m.p. 48-49 °C}; δ<sub>H</sub> in ppm (500 MHz, CDCl<sub>3</sub>); 6.63 (s, 1H, H-3), 6.57 (s, 1H, H-6), 4.05 (q, *J* = 6.7 Hz, 1H, H-7), 3.85 (s, 3H, H-13 or H-15), 3.84 (s, 3H, H-13 or H-15), 3.25 (dt, *J* = 13.0 and 5.2 Hz, 1H, H-9), 3.00 (ddd, *J* = 13.0, 8.8 and 4.9 Hz, 1H, H-9), 2.79 (ddd, *J* = 15.9, 8.8 and 5.2 Hz, 1H, H-10), 2.65 (dt, *J* = 15.9 and 4.9 Hz, 1H, H-10), 1.82, (br s, 1H, NH), 1.44 (d, *J* = 6.7 Hz, 3H, H-11); δ<sub>C</sub> in ppm (126 MHz, CDCl<sub>3</sub>); 147.3 (C-2), 147.2 (C-3), 132.6 (C-5), 126.9 (C-4), 111.8 (C-3), 109.1 (C-6), 56.0 (C-13 or C-15), 55.9 (C-13 or C-15), 51.3 (C-7), 41.9 (C-9), 29.6 (C-10), 22.9 (C-11); ν<sub>max</sub>/ cm<sup>-1</sup>; 3311, 2931, 2831, 1609, 1509, 1462, 1404, 1253, 1220. The spectral data correspond to those reported in the literatures.<sup>137</sup> HRMS, calculated for C<sub>12</sub>H<sub>18</sub>NO<sub>2</sub><sup>+</sup> [M+H]<sup>+</sup>: 208.133754, found by LCMS, ESI-MS [M+H]<sup>+</sup> 208.0 {lit.<sup>137</sup> HRMS [M<sup>+</sup>]: 207.1258}.



#### 6.1.4. Enantiopure 6,7-Dimethoxy-1-methyl-1,2,3,4-tetrahydroisoquinoline

**9**<sup>179</sup>

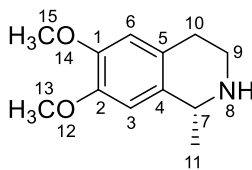
##### (a) (S)-**9**



Formic acid (7.2 mL) was added to acetonitrile (20 mL) under nitrogen and stirred at 0 °C. Triethylamine (10.6 mL) was added slowly to maintain the temperature to below 10 °C. After the addition was complete, the reaction mixture was warmed to room temperature. Ru(*p*-cymene)(*R,R*-TsDPEN) (0.2 g, 0.3 mmol) was dissolved in acetonitrile (25 mL) and added to the formic acid-triethylamine mixture. The content was stirred for 15 minutes. A solution of imine **8** (6.2 g, 30.3 mmol) in acetonitrile (35 mL) was charged to the reaction mixture and was warmed to 30 °C. The reaction was stirred overnight. After the reaction was complete, the reaction mixture was cooled to room temperature and concentrated *in vacuo*. The residue was acidified aqueous hydrochloric acid (2 M) and washed with toluene (2 × 20 mL). The aqueous layer was basified with aqueous sodium hydroxide (5 M) and was extracted with dichloromethane (3 × 50 mL). The combined organic layer was dried with anhydrous MgSO<sub>4</sub>, filtered and the solvent was removed *in vacuo* to give a dark brown oil (ee = 100% by chiral HPLC). The crude product was purified by column chromatography using Biotage (ethyl acetate/ triethylamine gradient, 95-96.5% ethyl acetate by volume); TLC: Silica plate, ethyl acetate/ triethylamine 95:5 (v/v), visualisation by UV (254 nm; R<sub>f</sub> of product = 0.15) to yield (S)-**9** as a pale brown oil (5.4 g, 88%).

[ $\alpha$ ]<sub>D</sub><sup>23</sup> = -54.4° (c 1.10, ethanol) {lit.<sup>137</sup> [ $\alpha$ ]<sub>D</sub><sup>20</sup> = -41.3° (c 1.10, ethanol)}. The spectral and MS data correspond to those reported for *rac*-**9** and in the literature.<sup>180</sup>

(b) (*R*)-**9**

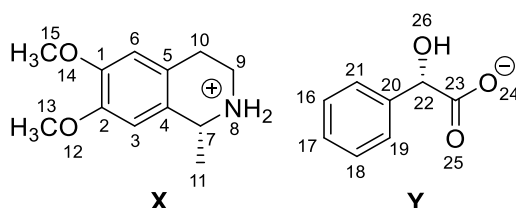


Similar procedures as (*S*)-**9** were employed in the synthesis of (*R*)-**9** with Ru(*p*-cymene)(*S,S*-TsDPEN). Toluene was used instead of dichloromethane in the extraction of product from the aqueous layer during work-up. A pale brown oil (5.7 g, 94%) was obtained with ee of 96% (by chiral HPLC).

$[\alpha]_D^{23} = +52.3^\circ$  (*c* 1.13, ethanol) {lit.<sup>137</sup>  $[\alpha]_D^{20} = +59.7^\circ$  (*c* 1.10, ethanol)}. The spectral and MS data correspond to those reported for *rac*-**9**.

**6.1.5. Diastereopure (*S*)-mandelate salts of 6,7-dimethoxy-1-methyl-1,2,3,4-tetrahydroisoquinoline **9****

(a) (*R*)-**9**-(*S*)-**34**

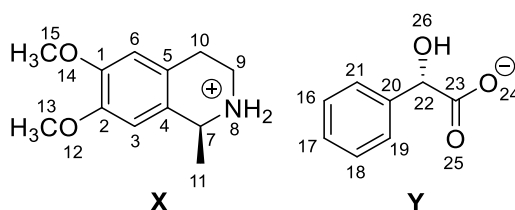


A solution of (*S*)-**34** (0.3 g, 1.9 mmol) in ethyl acetate/ methanol 7:1 (v/v, 2 mL) was added to a solution of (*R*)-**9** (0.4 g, 1.9 mmol) in ethyl acetate/ methanol 7:1 (2 mL). The mixture was heated to reflux. More solvent (ethyl acetate/ methanol 7:1) was added until all solids dissolved. Then stirring was stopped and the heat was switched off. The mixture was cooled to room temperature. The slurry was filtered to give an off-white crystalline solid (0.4 g, 47%) with de 100% (by <sup>1</sup>H NMR in CDCl<sub>3</sub>, 500 MHz). Single crystal structure was obtained by XRD analysis.

M.p. = 172-174 °C;  $[\alpha]_D^{23} = +66.3^\circ$  (*c* 1.10, chloroform);  $\delta_H$  in ppm (500 MHz, CDCl<sub>3</sub>); 7.31-7.23 (m, 2H, H-19 and H-21), 7.20-7.15 (m, 3H, H-16, H-17 and H-18), 6.55 (s, 1H, H-3), 6.48 (s, 1H, H-6), 4.74 (s, 1H, H-22), 4.17 (q, *J* = 6.6 Hz, 1H, H-7), 3.87 (s, 3H, H-13 or H-15), 3.86 (s, 3H, H-13 or H-15), 3.24-3.13 (m, 1H, H-9), 2.95-2.84 (m, 2H, H-9 and H-10), 2.79-2.68 (m, 1H, H-10), 1.41 (d, *J* = 6.6 Hz, 3H, H-11);  $\delta_C$  in ppm (126 MHz, CDCl<sub>3</sub>); 178.8 (C-23), 148.6 (C-2), 148.3

(C-1), 142.1 (C-20), 127.9 (C-16 and C-18), 127.0 (C-17), 126.4 (C-19 and C-21), 125.7 (C-4), 123.6 (C-5), 111.3 (C-3), 108.7 (C-6), 74.4 (C-22), 56.1 (C-13 or C-15), 56.0 (C-13 or C-15), 50.3 (C-7), 38.9 (C-9), 25.3 (C-10), 19.6 (C-11);  $\nu_{\max}/\text{cm}^{-1}$ ; 3188, 3061, 2832, 2757, 2656, 2573, 2525, 2493, 1582, 1518, 1366, 1244, 1211. HRMS, calculated for  $\text{C}_{12}\text{H}_{18}\text{NO}_2^+$   $[\text{M}-\text{Y}]^+$ : 208.133754, found by LCMS, ESI-MS/MS (+)  $[\text{M}-\text{Y}]^+$ : 208.53; HRMS, calculated for  $\text{C}_8\text{H}_7\text{O}_3^-$   $[\text{M}-\text{X}]^-$ : 151.03952; found by LCMS, ESI-MS/MS (-)  $[\text{M}-\text{X}]^-$ : 150.87.

**(b) (S)-9-(S)-34**

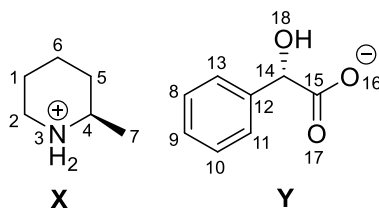


A similar procedure as in Section 5.1.5(a) was used to synthesise (S)-9-(S)-34. Ethyl acetate/ methanol 15:1 was used as the solvent mixture. (S)-9-(S)-34 was isolated as an off-white crystalline solid (0.2 g, 32%) with de 100% (by  $^1\text{H}$  NMR in  $\text{CDCl}_3$ , 500 MHz). Single crystal structure was obtained by XRD analysis.

M.p. = 163-166 °C;  $[\alpha]_{\text{D}}^{23} = +39.6^\circ$  (c 1.10, chloroform);  $\delta_{\text{H}}$  in ppm (500 MHz,  $\text{CDCl}_3$ ); 7.31 (d,  $J = 7.0$  Hz, 2H, H-19 and H-21), 7.24-7.14 (m, 3H, H-16, H-17 and H-18), 6.53 (s, 1H, H-3), 6.47 (s, 1H, H-6), 4.77 (s, 1H, H-22), 3.98 (q,  $J = 6.6$  Hz, 1H, H-7), 3.87 (s, 3H, H-13 or H-15), 3.86 (s, 3H, H-13 or H-15), 3.16 (dt,  $J = 12.5$  and  $5.5$  Hz, 1H, H-9), 2.98 (ddd,  $J = 12.5$ ,  $8.0$  and  $5.5$  Hz, 1H, H-9), 2.85-2.76 (m, 1H, H-10), 2.72 (dt,  $J = 17.0$  and  $5.5$  Hz, H-10), 1.45 (d,  $J = 6.6$  Hz, 3H, H-11);  $\delta_{\text{C}}$  in ppm (126 MHz,  $\text{CDCl}_3$ ); 178.8 (C-23), 148.6 (C-2), 148.3 (C-1), 142.2 (C-20), 128.0 (C-16 and C-18), 127.0 (C-17), 126.5 (C-19 and C-21), 125.6 (C-4), 123.6 (C-5), 111.3 (C-3), 108.7 (C-6), 74.4 (C-22), 56.1 (C-13 or C-15), 55.9 (C-13 or C-15), 50.3 (C-7), 39.0 (C-9), 25.2 (C-10), 19.8 (C-11);  $\nu_{\max}/\text{cm}^{-1}$ ; 3410, 3001, 2836, 2580, 2533, 2410, 1577, 1512, 1360, 1257, 1218; HRMS, calculated for  $\text{C}_{12}\text{H}_{18}\text{NO}_2^+$   $[\text{M}-\text{Y}]^+$ : 208.133754, found by LCMS, ESI-MS/MS (+)  $[\text{M}-\text{Y}]^+$ : 208.06; HRMS, calculated for  $\text{C}_8\text{H}_7\text{O}_3^-$   $[\text{M}-\text{X}]^-$ : 151.03952, found by LCMS, ESI-MS/MS (-)  $[\text{M}-\text{X}]^-$ : 151.03.

### 6.1.6. Diastereopure (S)-mandelate salts of 2-methylpiperidine 103

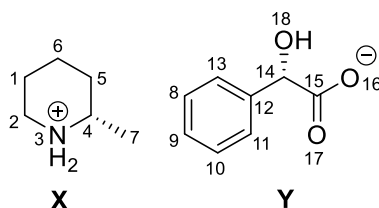
#### (a) (R)-103-(S)-34



(S)-**34** (2.3 g, 15.1 mmol) was added to a solution of *rac*-**103** (1.5 g, 15.1 mmol) in methyl *tert*-butyl ether (MTBE)/ methanol 4% (v/v, 20 mL). The mixture was heated to reflux. More solvent (MTBE/ methanol 4% v/v) was added until all solid dissolved. The mixture was cooled to room temperature and stirred overnight. The slurry was filtered to yield a white solid which was recrystallised from MTBE/ methanol 4% to give a white crystalline solid (0.7 g, 19%) with de 100% (by  $^1\text{H}$  NMR in  $\text{CDCl}_3$ , 500 MHz). Crystals suitable for XRD analysis were grown by slow diffusion of hexane into a saturated solution of (*R*)-**103**-(*S*)-**34** in MTBE/ methanol 4% (v/v).

M.p. = 119-122 °C {lit.<sup>148</sup> m.p. 119 °C};  $[\alpha]_{\text{D}}^{20} = +76.3^\circ$  (c 1.0, chloroform) {lit.<sup>148</sup>  $[\alpha]_{\text{D}}^{22} = +78.0^\circ$  (c 1.0, chloroform)};  $\delta_{\text{H}}$  in ppm (500 MHz,  $\text{CDCl}_3$ );  $\delta$  7.46 (d,  $J = 7.3$  Hz, 2H, H-11 and H-13), 7.28 (t,  $J = 7.3$  Hz, 2H, H-8 and H-10), 7.21 (t,  $J = 7.3$  Hz, 1H, H-9), 4.86 (s, 1H, H-14), 2.98 (d,  $J = 12.5$  Hz, 1H, H-2), 2.70-2.64 (m, 1H, H-4), 2.25-2.20 (m, 1H, H-2), 1.69 (d,  $J = 13.5$  Hz, 1H, H-1), 1.57-1.51 (m, 3H, H-5 and H-6), 1.29-1.19 (m, 1H, H-5), 1.16-1.09 (m, 4H, H-1 and H-7);  $\delta_{\text{C}}$  in ppm (126 MHz,  $\text{CDCl}_3$ ); 178.3 (C-15), 142.6 (C-12), 128.0 (C-8 and C-10), 127.0 (C-9), 126.6 (C-11 and C-13), 74.5 (C-14), 52.3 (C-4), 43.8 (C-2), 30.2 (C-5), 22.5 (C-6), 21.8 (C-1), 19.1 (C-7).  $\nu_{\text{max}}$ /  $\text{cm}^{-1}$ ; 3153, 2696, 2590, 2544, 1593, 1491, 1477, 1444, 1381, 1267. The spectral data correspond to those reported in the literatures.<sup>148, 149</sup> HRMS, calculated for  $\text{C}_6\text{H}_{14}\text{N}^+$  [M-Y]<sup>+</sup>: 100.112624, found by LCMS, ESI-MS/MS (+) [M-Y]<sup>+</sup>: 100.27 {lit.<sup>148</sup> HRMS [M-Y]<sup>+</sup>: 100.1125}; HRMS, calculated for  $\text{C}_8\text{H}_7\text{O}_3^-$  [M-X]<sup>-</sup>: 151.03952, found by LCMS, ESI-MS/MS (-) [M-X]<sup>-</sup>: 151.02.

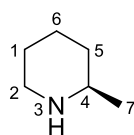
(b) (S)-103-(S)-34



A solution of (S)-**103** (0.50 g, 5.0 mmol) in MTBE (10 mL) and a solution of (S)-**34** (0.77 g, 5.0 mmol) in MTBE (10 mL) were mixed and the slurry was heated to reflux. More *tert*-butyl methyl ether was added (20 mL) followed by methanol until all solid dissolved. The reaction was cooled to r.t. with reduced stirring. After 2 h, the mixture was filtered to give a white fluffy solid (1.0 g, 81 %) with de 100% (by  $^1\text{H}$  NMR in  $\text{CDCl}_3$ , 500 MHz). Crystals suitable for XRD analysis were grown by slow diffusion of hexane into a saturated solution of (S)-**103**-(S)-**34** in MTBE/methanol 4% (v/v).

M.p. = 92-95 °C;  $[\alpha]_{\text{D}}^{20} = +63.9^\circ$  (*c* 1.0,  $\text{CHCl}_3$ );  $\delta_{\text{H}}$  in ppm (500 MHz,  $\text{CDCl}_3$ );  $\delta$  7.46 (d,  $J = 7.6$  Hz, 2H, H-11 and H-13), 7.28 (t,  $J = 7.6$  Hz, 2H, H-8 and H-10), 7.21 (t,  $J = 7.6$  Hz, 1H, H-9), 4.87 (s, 1H, H-14), 3.05 (d,  $J = 12.5$  Hz, 1H, H-2), 2.50 (td,  $J = 12.5$  and 3 Hz, 1H, H-2), 2.44-2.34 (m, 1H, H-4), 1.66 (d,  $J = 10.5$  Hz, 1H, H-6), 1.58 (d,  $J = 14.5$  Hz, 1H, H-5), 1.51 (d,  $J = 14.0$  Hz, 1H, H-1), 1.39-1.16 (m, 3H, H-1, H-5 and H-6), 1.04 (d,  $J = 6.5$  Hz, 3H, H-7);  $\delta_{\text{C}}$  in ppm (126 MHz,  $\text{CDCl}_3$ ); 178.3 (C-15), 142.6 (C-12), 128.0 (C-8 and C-10), 127.0 (C-9), 126.6 (C-11 and C-13), 74.4 (C-14), 52.1 (C-4), 44.0 (C-2), 30.4 (C-5), 22.5 (C-6), 21.7 (C-1), 19.1 (C-7).  $\nu_{\text{max}}$ /  $\text{cm}^{-1}$ ; 3184, 2695, 2582, 2541, 1627, 1574, 1497, 1449, 1382, 1337, 1213. HRMS, calculated for  $\text{C}_6\text{H}_{14}\text{N}^+$  [M-Y] $^+$ : 100.112624, found by LCMS, ESI-MS/MS (+) [M-Y] $^+$ : 100.27; HRMS, calculated for  $\text{C}_8\text{H}_7\text{O}_3^-$  [M-X] $^-$ : 151.03952, found by LCMS, ESI-MS/MS (-) [M-X] $^-$ : 150.97.

6.1.7. (R)-2-Methylpiperidine (R)-103

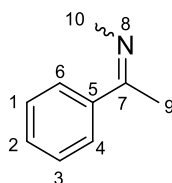


(R)-**103**-(S)-**34** (0.25 g, 0.99 mmol) was dissolved into aqueous ammonia solution (10%, 10 mL) and was extracted with dichloromethane (20 mL). The mixture was separated and the aqueous layer was further extracted with dichloromethane (2

× 10 mL). The combined organic layer was dried with anhydrous MgSO<sub>4</sub>, filtered and the solvent was removed *in vacuo* to yield a pale yellow oil (0.063 g, 63%) with ee 100% (by chiral GC after derivatisation with acetic anhydride).

$[\alpha]_D^{20} = -3.65^\circ$  (c 2.0, methanol) {lit.<sup>181</sup>  $[\alpha]_D^{22} = -8.5^\circ$  (c 0.5, methanol)};  $\delta_H$  in ppm (500 MHz, CDCl<sub>3</sub>);  $\delta$  3.09-3.01 (m, 1H, H-2), 2.64 (td,  $J = 11.8$  and  $3.0$  Hz, 1H, H-2), 2.61-2.55 (m, 1H, H-4), 1.80-1.72 (m, 1H, H-1), 1.62-1.52 (m, 3H, H-1, H-5 and NH), 1.44-1.28 (m, 2H, H-6), 1.12-0.99 (m, 4H, H-5 and H-7);  $\delta_C$  in ppm (300 MHz, CDCl<sub>3</sub>); 52.3 (C-4), 47.1 (C-2), 34.6 (C-5), 26.1 (C-6), 24.3 (C-1), 23.0 (C-7). The spectral data correspond to those for *rac*-**3**.  $\nu_{max}/\text{cm}^{-1}$ ; 3270, 2925, 2854, 2795, 1441, 1375, 1325, 1306. HRMS, calculated for C<sub>6</sub>H<sub>14</sub>N<sup>+</sup> [M+H]<sup>+</sup>: 100.112624, found by LCMS, ESI-MS/MS [M+H]<sup>+</sup>: 100.58 {lit.<sup>182</sup> LCMS [M+H]<sup>+</sup>: 100.1}.

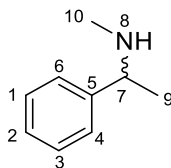
#### 6.1.8. *N*-methyl- $\alpha$ -methylbenzylimine **94**



Acetophenone **51** (10 g, 83.2 mmol) and degassed ethanol (40 mL) were added to a round bottom flask containing molecular sieve (3 Å, 16 g) which was purged with nitrogen, followed by the addition of methylamine solution in ethanol (33 % w/w, 22 mL). The mixture was stirred at room temperature for 48 hours. The reaction was then filtered through celite and was washed with dichloromethane. The solvent was removed *in vacuo* to give a yellow oil (12.5 g) which contained about 10% **51** (by <sup>1</sup>H NMR). The E/Z isomeric ratio of crude product **94** was not determined and was used directly in the next step without further purification.

$\delta_H$  in ppm (500 MHz, CDCl<sub>3</sub>); 7.74 (dd,  $J = 6.5$  and  $3.0$  Hz, 2H, H-4 and H-6), 7.39-7.34 (m, 3H, H-1, H-2 and H-3), 3.34 (s, 3H, H-10), 2.22 (s, 3H, H-9);  $\delta_C$  in ppm (126 MHz, CDCl<sub>3</sub>); 167.1 (C-7), 141.2 (C-5), 129.4 (C-2), 128.2 (C-4 and C-6), 126.4 (C-1 and C-3), 39.5 (C-10), 15.1 (C-9). The spectral data correspond to those reported in the literatures.<sup>183</sup>  $\nu_{max}/\text{cm}^{-1}$ ; 1634, 1578, 1493, 1445, 1396, 1365, 1284.

### 6.1.9. Racemic *N*-methyl- $\alpha$ -methylbenzylamine **39**

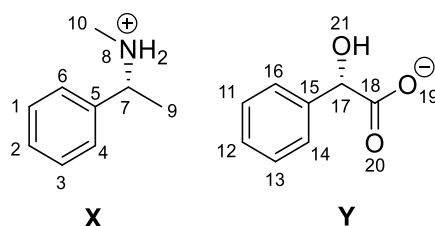


Imine **94** (12.4 g, 93.1 mmol) was dissolved into methanol (200 mL). The mixture was cooled to  $< 0$  °C. Sodium borohydride (18.3 g, 484.5 mmol) was added slowly in portions over 2 hours to maintain the temperature to  $< 10$  °C. After the addition was complete, the reaction mixture was warmed to room temperature. After 24 hours of stirring, the reaction was cooled to 0-5 °C and was acidified by aqueous hydrochloric acid (2 M, 250 mL). The mixture was concentrated *in vacuo* to give a white solid which was basified by aqueous sodium hydroxide (3 M, 200 mL). Dichloromethane (100 mL) was added and the mixture was separated. The aqueous layer was further extracted with dichloromethane (2  $\times$  100 mL). The combined organic layer was dried by anhydrous  $\text{MgSO}_4$ , filtered and the solvent was removed *in vacuo* to give a yellow oil (9.3 g). The crude product was purified by column chromatography using Biotage (ethyl acetate/ triethylamine gradient, 95-96.5% ethyl acetate by volume); TLC: Silica plate, ethyl acetate/ triethylamine 95:5 (v/v), visualisation by UV (254 nm;  $R_f$  of product = 0.33) to yield *rac*-**39** as a pale yellow oil (7.9 g, overall yield from acetophenone **51** = 70%).

$\delta_{\text{H}}$  in ppm (500 MHz,  $\text{CDCl}_3$ ); 7.36-7.26 (m, 4H, H-1, H-3, H-4 and H-6), 7.29-7.24 (m, 1H, H-2), 3.64 (q,  $J = 6.5$  Hz, 1H, H-7), 2.31 (s, 3H, H-10), 1.45 (br s, 1H, NH), 1.35 (d,  $J = 6.5$  Hz, 3H, H-9);  $\delta_{\text{C}}$  in ppm (128 MHz,  $\text{CDCl}_3$ ); 145.4 (C-5), 128.4 (C-1 and C-3), 126.9 (C-2), 126.6 (C-4 and C-6), 60.3 (C-7), 34.5 (C-10), 23.9 (C-9). The spectral data correspond to those reported in the literature.<sup>183</sup>  $\nu_{\text{max}}$ /  $\text{cm}^{-1}$ ; 3284, 3025, 2787, 1603, 1493, 1475, 1449, 1281, 1222. HRMS, calculated for  $\text{C}_9\text{H}_{14}\text{N}^+$   $[\text{M}+\text{H}]^+$ : 136.112624, found by LCMS, ESI-MS  $[\text{M}+\text{H}]^+$ : 136.47 {lit.<sup>183</sup> HRMS (ESI)  $[\text{M}+\text{H}]^+$ : 136.1120}.

### 6.1.10. Diastereopure (*S*)-mandelate salts of *N*-methyl- $\alpha$ -methylbenzylamine **39**

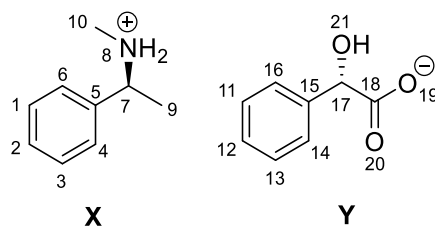
#### (a) (*R*)-**39**-(*S*)-**34**



(*S*)-**34** (0.11 g, 0.74 mmol) was dissolved into ethyl isobutyrate (2 mL) and the solution was added to (*R*)-**39** (0.10 g, 0.74 mmol). The slurry was heated to reflux until all solid dissolved. The mixture was cooled to room temperature with reduced stirring and was filtered to give a white solid which was dried in air overnight (0.17 g, 82%) with *de* = 100% (by  $^1\text{H}$  NMR in  $\text{CDCl}_3$ , 500 MHz). Crystals suitable for XRD analysis were grown by slow diffusion of hexane into a saturated solution of (*R*)-**39**-(*S*)-**34** in isopropyl acetate.

M.p. = 109-111°C;  $[\alpha]_{\text{D}}^{23} = +62.3^\circ$  (*c* 0.49, MeOH);  $\delta_{\text{H}}$  in ppm (500 MHz,  $\text{CDCl}_3$ ); 7.48 (d,  $J = 7.5$  Hz, 2H, H-4 and H-6), 7.32 (m, 5H, H-1, H-2, H-3, H-11 and H-13), 7.24 (m, 3H, H-12, H-14 and H-16), 4.91 (s, 1H, H-17), 3.68 (q,  $J = 6.9$  Hz, 1H, H-7), 1.99 (s, 3H, H-10), 1.46 (d,  $J = 6.9$  Hz, 3H, H-9);  $\delta_{\text{C}}$  in ppm (128 MHz,  $\text{CDCl}_3$ ); 178.5 (C-18), 142.6 (C-5), 136.3 (C-15), 129.2 (C-1 and C-3), 129.1 (C-2), 128.1 (C-11 and C-13), 127.6 (C-14 and C-16), 127.3 (C-12), 126.8 (C-4 and C-6), 74.6 (C-17), 59.1 (C-7), 30.2 (C-10), 19.5 (C-9).  $\nu_{\text{max}}$ /  $\text{cm}^{-1}$ ; 3029, 2698, 2460, 1622, 1556, 1509, 1491, 1453, 1363, 1330, 1302, 1273. HRMS, calculated for  $\text{C}_9\text{H}_{14}\text{N}^+$  [*M*-*Y*] $^+$ : 136.112624, found: 136.1118; calculated for  $\text{C}_8\text{H}_7\text{O}_3$  [*M*-*X*] $^-$ : 151.039520, found: 151.0397.

#### (b) (*S*)-**39**-(*S*)-**34**



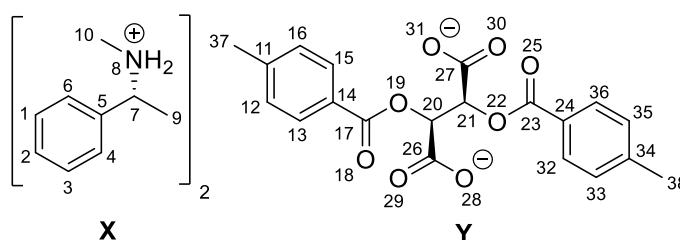


(*S*)-**34** (0.11 g, 0.74 mmol) was dissolved into ethyl isobutyrate (1 mL) and the solution was added to (*S*)-**39** (0.10 g, 0.74 mmol). The mixture was stirred overnight at room temperature for solid to precipitate which was then heated to reflux. After all solid dissolved, the mixture was cooled to room temperature with reduced stirring overnight. The slurry was filtered and the solid collected was dried in air overnight (0.14 g, 67%) with de = 100% (by <sup>1</sup>H NMR in CDCl<sub>3</sub>, 500 MHz). Crystals suitable for XRD analysis were grown by slow diffusion of hexane into a saturated solution of (*S*)-**39**-(*S*)-**34** in isopropyl acetate.

M.p. = 93-94 °C; [α]<sub>D</sub><sup>23</sup> = +37.5° (c 0.50, MeOH); δ<sub>H</sub> in ppm (500 MHz, CDCl<sub>3</sub>); 7.44 (m, H-4 and H-6), 7.36 (m, 3H, H-1, H-2 and H-3), 7.27 (m, 5H, H-11, H-12, H-13, H-14 and H-16), 4.89 (s, 1H, H-17), 3.42 (q, *J* = 6.8 Hz, 1H, H-7), 2.00 (s, 3H, H-10), 1.37 (d, *J* = 6.8 Hz, 3H, H-9); δ<sub>C</sub> in ppm (128 MHz, CDCl<sub>3</sub>); 178.5 (C-18), 142.5 (C-5), 136.5 (C-15), 129.2 (C-1 and C-3), 129.1 (C-2), 128.1 (C-11 and C-13), 127.6 (C-14 and C-16), 127.2 (C-12), 126.8 (C-4 and C-6), 74.6 (C-17), 59.0 (C-7), 30.3 (C-10), 19.9 (C-9). ν<sub>max</sub>/ cm<sup>-1</sup>; 3301, 2706, 2465, 1623, 1578, 1451, 1380, 1359, 1330, 1314, 1279, 1220. HRMS, calculated for C<sub>9</sub>H<sub>14</sub>N<sup>+</sup> [M-Y]<sup>+</sup>: 136.112624, found: 136.1114; calculated for C<sub>8</sub>H<sub>7</sub>O<sub>3</sub> [M-X]<sup>-</sup>: 151.039520, found: 151.0398.

#### 6.1.11. Diastereopure di-*p*-toluoyl-*D*-tartrate salts of *N*-methyl- $\alpha$ -methylbenzylamine **39**

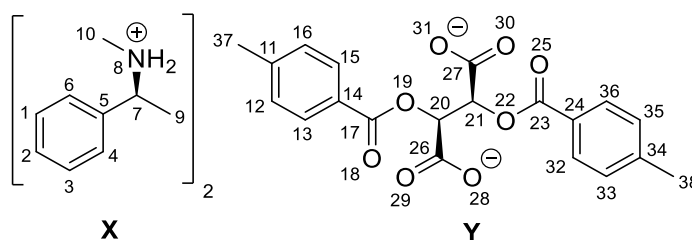
##### (a) [(*R*)-**39**]<sub>2</sub>-(*S,S*)-**32**



(*S,S*)-**32** (72.5 mg, 0.19 mmol) was dissolved into ethyl acetate/ methanol 10:1 (v/v, 2.9 mL) and was added to (*R*)-**39** (50.7 mg, 0.38 mmol). The mixture was stirred at room temperature overnight and then filtered. The solid was dried in air to obtain a white solid (0.1 g, 80%) with de 100% (by <sup>1</sup>H NMR in *d*<sub>6</sub>-DMSO, 500 MHz). Crystals were recrystallised from ethyl acetate/ methanol 9:1 (v/v) for XRD analysis.

M.p. = 160-163 °C;  $[\alpha]_D^{20} = +102.2^\circ$  (*c* 0.11, MeOH);  $\delta_H$  in ppm (500 MHz, *d*<sub>6</sub>-DMSO); 7.86 (d, *J* = 8.0 Hz, 4H, H-4 and H-6), 7.35 (m, 14H, H-1, H-2, H-3, H-12, H-13, H-15, H-16, H-32, H-33, H-35 and H-36), 5.63 (s, 2H, H-20 and H-21), 3.95 (q, *J* = 6.8 Hz, 2H, H-7), 2.37 (s, 6H, H-37 and H-38), 2.23 (s, 6H, H-10), 1.35 (d, *J* = 6.8 Hz, 6H, H-9);  $\delta_C$  in ppm (126 MHz, *d*<sub>6</sub>-DMSO); 169.6 (C-17 and C-23), 165.1 (C-26 and C-27), 143.1 (C-5), 139.1 (C-14 and C-24), 129.3 (C-4 and C-6), 129.0 (C-13, C-15, C-32 and C-36), 128.6 (C-12, C-16, C-33 and C-35), 128.1 (C-2), 127.8 (C-11 and C-34), 127.4 (C-1 and C-3), 74.3 (C-20 and C-21), 57.9 (C-7), 30.7 (C-10), 21.1 (C-37 and C-38), 20.1 (C-8).  $\nu_{max}/\text{cm}^{-1}$ ; 3016, 2878, 1714, 1633, 1611, 1566, 1455, 1371, 1329, 1265. HRMS, calculated for C<sub>9</sub>H<sub>14</sub>N<sup>+</sup> [M-Y]<sup>+</sup>: 136.112624, found: 136.1117; calculated for C<sub>20</sub>H<sub>17</sub>O<sub>8</sub><sup>-</sup> [M-2X+H]<sup>-</sup>: 385.092345, found: 385.0913.

**(b) [(S)-39]<sub>2</sub>-(S,S)-32**

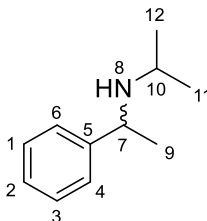


A similar procedure as in Section 5.1.11(a) was used to synthesise [(S)-39]<sub>2</sub>-(S,S)-32 using (S)-39 (50.2 mg, 0.37 mmol). A white solid was obtained (0.1 g, 80%) with de 100% (by <sup>1</sup>H NMR in *d*<sub>6</sub>-DMSO, 500 MHz). Crystals were recrystallised from ethyl acetate/ methanol 9:1 (v/v) for XRD analysis.

M.p. = 179-182 °C;  $[\alpha]_D^{20} = +69.3^\circ$  (*c* 0.12, MeOH);  $\delta_H$  in ppm (500 MHz, *d*<sub>6</sub>-DMSO); 7.90 (d, *J* = 8.5 Hz, 4H, H-4 and H-6), 7.41 (dd, *J* = 7.0 and 1.5 Hz, 4H, H-13, H-15, H-32 and H-36), 7.32 (m, 10H, H-1, H-2, H-3, H-12, H-16, H-33 and H-35), 5.66 (s, 2H, H-20 and H-21), 3.99 (q, *J* = 6.8 Hz, 2H, H-2), 2.38 (s, 6H, H-37 and H-38), 2.20 (s, 6H, H-10), 1.38 (d, *J* = 6.8 Hz, 6H, H-9);  $\delta_C$  in ppm (126 MHz, *d*<sub>6</sub>-DMSO); 169.1 (C-17 and C-23), 165.0 (C-26 and C-27), 143.2 (C-5), 139.6 (C-14 and C-24), 129.3 (C-4 and C-6), 129.0 (C-13, C-15, C-32 and C-36), 128.6 (C-12, C-16, C-33 and C-35), 128.0 (C-2), 127.6 (C-11 and C-34), 127.3 (C-1 and C-3), 73.6 (C-20 and C-21), 58.0 (C-7), 31.0 (C-10), 21.1 (C-37 and C-38), 20.5 (C-8).  $\nu_{max}/\text{cm}^{-1}$ ; 3017, 2870, 1712, 1637, 1612, 1594, 1455, 1371,

1337, 1268; HRMS, calculated for  $C_9H_{14}N^+$   $[M-Y]^+$ : 136.112624, found: 136.1118; calculated for  $C_{20}H_{17}O_8^-$   $[M-2X+H]^-$ : 385.092345, found: 385.0919.

### 6.1.12. Racemic *N*-Isopropyl- $\alpha$ -methylbenzylamine 101

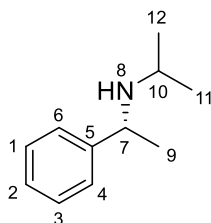


The crude product was prepared by Dr. Lisa Thompson. Acetone (250 mL) was added to *rac*-**42** (10.0 g, 82.5 mmol) and the mixture was heated to reflux. After 24 hours, the reaction was cooled to room temperature and the solvent was removed *in vacuo* to give a yellow oil. Methanol (200 mL) was added and the solution was cooled on ice. Sodium borohydride (5.6 g, 148.0 mmol) was added and the mixture was stirred on ice for 1.5 hours and for a further 2.5 hours at room temperature. The mixture was acidified by aqueous hydrochloric acid (2 M) and the solvent was removed *in vacuo* to give a white solid. Water and dichloromethane were added and the mixture was basified with aqueous sodium hydroxide (1 M). The layers were separated and the organic layer was washed with brine, dried with anhydrous  $MgSO_4$  and the solvent was removed *in vacuo* to give a yellow oil (8.5 g). The crude product was purified by column chromatography using Biotage (ethyl acetate/ triethylamine gradient, 96.3-98.5 % ethyl acetate by volume; TLC: Silica plate, ethyl acetate/ triethylamine 95:5 (v/v), visualisation by UV (254 nm;  $R_f$  of product = 0.49) to yield *rac*-**101** as a pale yellow oil (7.4 g, 55%).

$\delta_H$  in ppm (500 MHz,  $CDCl_3$ ); 7.34-7.30 (m, 4H, H-1, H-3, H-4 and H-6), 7.22 (tt,  $J = 1.8, 7$  Hz, 1H, H-2), 3.88 (q,  $J = 6.5$  Hz, 1H, H-7), 2.62 (hept,  $J = 6.2$  Hz, 1H, H-10), 1.33 (d,  $J = 6.5$  Hz, 3H, H-9), 1.02 (d,  $J = 6.2$  Hz, 3H, H-11 or H-12), 0.99 (d,  $J = 6.2$  Hz, 3H, H-11 or H-12);  $\delta_C$  in ppm (126 MHz,  $CDCl_3$ ); 146.2 (C-5), 128.4 (C-1 and C-3), 126.7 (C-2), 126.5 (C-4 and C-6), 55.1 (C-7), 45.5 (C-10), 24.9 (C-9), 24.1 (C-11 or C-12), 22.2 (C-11 or C-12). The spectral data correspond to those reported in the literature.<sup>184</sup>  $\nu_{max}/cm^{-1}$ ; 2960, 1602, 1492, 1465, 1451, 1367, 1336. HRMS, calculated for  $C_{11}H_{18}N^+$   $[M+H]^+$ : 164.143924, found by LCMS, ESI-MS  $[M+H]^+$ : 164.41 {lit.<sup>184</sup> HRMS (ESI)  $[M+H]^+$ : 164.1434}.

### 6.1.13. Enantiopure *N*-isopropyl- $\alpha$ -methylbenzylamine **101**

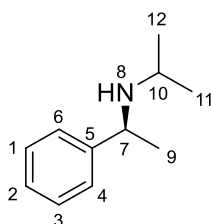
#### (a) (*R*)-*N*-isopropyl- $\alpha$ -methylbenzylamine (*R*)-**101**



Same procedures as the synthesis of *rac*-**101** were applied to synthesise (*R*)-**101** using (*R*)-**42** (2 g, 16.5 mmol).

Yield = 1.8 g (68%); ee = 100% (by chiral GC after derivatisation with trifluoroacetic anhydride).  $[\alpha]_{\text{D}}^{23} = +56.1^\circ$  (c 0.52, chloroform);  $^1\text{H}$  and  $^{13}\text{C}$  NMR, IR and MS data correspond to those reported for the racemate.

#### (b) (*S*)-*N*-isopropyl- $\alpha$ -methylbenzylamine (*S*)-**101**

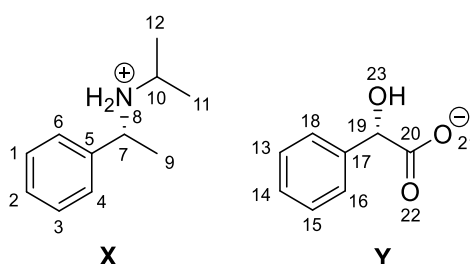


Same procedures as the synthesis of *rac*-**101** were applied to synthesise (*S*)-**101** using (*S*)-**42** (1 g, 8.3 mmol).

Yield = 0.64 g (48%); ee = 98% (by chiral GC after derivatisation with trifluoroacetic anhydride).  $[\alpha]_{\text{D}}^{23} = -61.9^\circ$  (c 0.40, chloroform);  $^1\text{H}$  and  $^{13}\text{C}$  NMR, IR and MS data correspond to those reported for the racemate.

### 6.1.14. Diastereopure (*S*)-mandelate salts of *N*-isopropyl- $\alpha$ -methylbenzylamine **101**

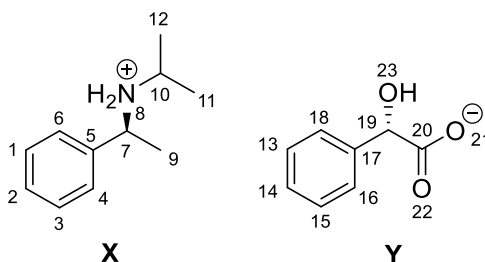
#### (a) (*R*)-**101**-(*S*)-**34**



(*S*)-**34** (0.094 g, 0.62 mmol) and (*R*)-**101** (0.1 g, 0.62 mmol) were dissolved into isopropyl acetate (1.5 mL and 0.5 mL respectively). The two solutions were mixed and more isopropyl acetate (8 mL) was added. The mixture was heated to reflux. Isopropanol was added until all solid dissolved. The mixture was then cooled to room temperature with reduced stirring and was filtered to give a white fluffy solid (0.14 g, 74%) with de = 100% (by  $^1\text{H}$  NMR in  $\text{CDCl}_3$ , 500 MHz). Single crystal structure was obtained by XRD analysis.

M.p. = 169-174 °C;  $[\alpha]_{\text{D}}^{23} = +61.5^\circ$  (c 0.39, methanol);  $\delta_{\text{H}}$  in ppm (500 MHz,  $\text{CDCl}_3$ ); 7.52 (d,  $J = 7.5$  Hz, 2H, H-4 and H-6), 7.32 (m, 7H, H-1, H-2, H-3, H-13, H-15, H-16 and H-18), 7.22 (t,  $J = 7.5$  Hz, 1H, H-14), 4.94 (s, 1H, H-19), 3.99 (q,  $J = 6.6$  Hz, 1H, H-7), 2.72 (hept,  $J = 6.5$  Hz, 1H, H-10), 1.46 (d,  $J = 6.6$  Hz, 3H, H-9), 1.12 (d,  $J = 6.5$  Hz, 3H, H-11 or H-12), 0.96 (d,  $J = 6.5$  Hz, 3H, H-11 or H-12);  $\delta_{\text{C}}$  in ppm (128 MHz,  $\text{CDCl}_3$ ); 177.2 (C-20), 142.4 (C-5), 136.9 (C-17), 129.1 (C-1 and C-3), 128.8 (C-2), 128.0 (C-13 and C-15), 127.7 (C-16 and C-18), 127.1 (C-14), 126.7 (C-4 and C-6), 74.7 (C-19), 55.5 (C-7), 47.2 (C-10), 20.6 (C-11 or C-12), 19.9 (C-11 or C-12), 17.6 (C-9).  $\nu_{\text{max}}/\text{cm}^{-1}$ ; 3040, 2866, 2679, 2461, 1617, 1568, 1518, 1490, 1446, 1364, 1329, 1265, 1217. HRMS, calculated for  $\text{C}_{11}\text{H}_{18}\text{N}^+$   $[\text{M}-\text{Y}]^+$ : 164.143924, found: 164.1429; calculated for  $\text{C}_8\text{H}_7\text{O}_3^-$   $[\text{M}-\text{X}]^-$ : 151.039520, found: 151.0391.

(b) (S)-101-(S)-34

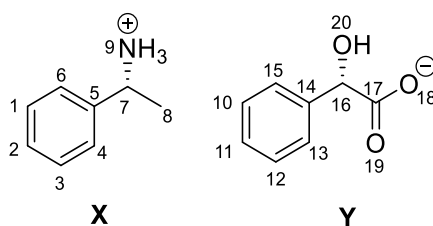


(S)-34 (0.093 g, 0.61mmol) and (S)-101 (0.1 g, 0.61mmol) were dissolved into isopropyl acetate (1.5 mL and 0.5 mL respectively) at room temperature. The two solutions were mixed and was dried *in vacuo* to give a thick oil which solidified upon standing (0.17 g, 90%); de = 100% (by  $^1\text{H}$  NMR in  $\text{CDCl}_3$ , 500 MHz). Single crystal structure was obtained by XRD analysis.

M.p. = 97-102 °C;  $[\alpha]_{\text{D}}^{23} = +36.2^\circ$  (c 0.51, methanol);  $\delta_{\text{H}}$  in ppm (500 MHz,  $\text{CDCl}_3$ ); 7.47 (d, 2H, H-4 and H-6), 7.40 (m, 5H, H-1, H-2, H-3, H-13 and H-15), 7.27 (m, 3H, H-14, H-16 and H-18), 4.97 (s, 1H, H-19), 3.70 (q,  $J = 6.7$  Hz, 1H, H-7), 2.69 (m, 1H, H-10), 1.33 (d,  $J = 6.7$  Hz, 3H, H-9), 1.09 (d,  $J = 6.5$  Hz, 3H, H-11 or H-12), 0.99 (d,  $J = 6.5$  Hz, 3H, H-11 or H-12);  $\delta_{\text{C}}$  in ppm (128 MHz,  $\text{CDCl}_3$ ); 177.3 (C-20), 141.9 (C-5), 136.8 (C-17), 129.2 (C-1 and C-3), 128.9 (C-2), 128.0 (C-13 and C-15), 127.6 (C-16 and C-18), 127.3 (C-14), 126.7 (C-4 and C-6), 74.4 (C-19), 55.4 (C-7), 47.3 (C-10), 20.7 (C-11 or C-12), 19.7 (C-11 or C-12), 17.7 (C-9).  $\nu_{\text{max}}/\text{cm}^{-1}$ ; 3385, 2985, 2716, 2514, 1709, 1625, 1596, 1454, 1390, 1357, 1276, 1214. HRMS, calculated for  $\text{C}_{11}\text{H}_{18}\text{N}^+$   $[\text{M}-\text{Y}]^+$ : 164.143924, found: 164.1429; calculated for  $\text{C}_8\text{H}_7\text{O}_3^-$   $[\text{M}-\text{X}]^-$ : 151.039520, found: 151.0395.

6.1.15. Diastereopure (S)-mandelate salts of  $\alpha$ -methylbenzylamine 42

(a) (R)-42-(S)-34

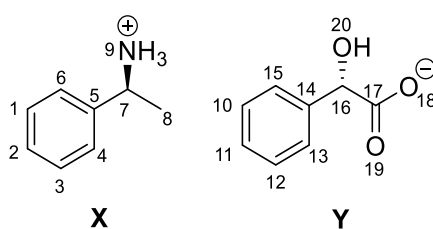


(S)-34 (0.13 g, 0.83 mmol) as dissolved into isopropyl acetate (2 mL) and was added to (R)-42 (0.1 g, 0.83 mmol). The mixture was heated to reflux. Isopropyl acetate/ methanol (10% v/v, 4.4 mL) was added until solid dissolved. Stirring was

stopped. The reaction mixture was cooled to room temperature and filtered to give a white crystalline solid (0.12 g, 52%). Small amount of crystals was dissolved into aqueous sodium carbonate solution (10% w/v, 1 mL) and extracted with ethyl acetate (1 mL). The organic layer was dried with anhydrous MgSO<sub>4</sub>, filtered through a plug of celite and dried *in vacuo*. The residue was re-dissolved into methanol (1 mL). Triethylamine (10 μL) was added followed by benzoyl chloride (5 μL) and the sample was analysed by chiral HPLC to determine the ee of **42** (100%) which corresponds to the de of the crystals. Single crystal structure was obtained by XRD analysis.

M.p. = 108-109 °C;  $[\alpha]_D^{20} = +69.9^\circ$  (c 1.0, water);  $\delta_H$  in ppm (400 MHz, *d*<sub>6</sub>-DMSO); 7.44 (d, *J* = 7.2 Hz, 2H, H-4 and H-6), 7.41-7.29 (m, 5H, H-1, H-2, H-3, H-13 and H-15), 7.23 (t, *J* = 7.3 Hz, 2H, H-10 and H-12), 7.15 (t, *J* = 7.3 Hz, 1H, H-11), 4.53 (s, 1H, H-16), 4.29 (q, *J* = 6.8 Hz, 1H, H-7), 1.42 (d, *J* = 6.8 Hz, 3H, H-8);  $\delta_C$  in ppm (75 MHz, *d*<sub>6</sub>-DMSO); 174.6 (C-17), 144.0 (C-5), 141.5 (C-14), 129.0 (C-1 and C-3), 128.4 (C-2), 127.8 (C-4 and C-6), 127.0 (C-13 and C-15), 126.8 (C-10 and C-12), 126.5 (C-11), 73.8 (C-16), 50.4 (C-7), 22.1 (C-8);  $\nu_{max}$ / cm<sup>-1</sup>; 3434, 2844, 1634, 1574, 1537, 1448, 1378, 1351. HRMS, calculated for C<sub>8</sub>H<sub>12</sub>N<sup>+</sup> [M-Y]<sup>+</sup>: 122.096974, found: 122.0926; calculated for C<sub>8</sub>H<sub>7</sub>O<sub>3</sub><sup>-</sup> [M-X]<sup>-</sup>: 151.039520, found: 151.0399.

**(b) (S)-42-(S)-34**

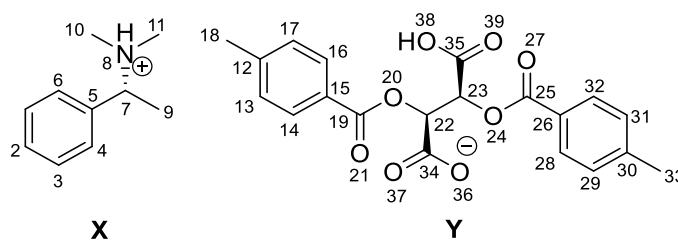


A similar procedure as in Section 5.1.15(a) was used to synthesise (S)-**42**-(S)-**34**. Isopropyl acetate/ methanol (25% v/v, 10 mL) was added to the hot solution of (S)-**42**/ (S)-**34** in isopropyl acetate for complete dissolution of the precipitate. (S)-**42**-(S)-**34** was isolated as a white crystalline solid (0.16 g, 71%) with de = 100% (determined as the ee of **42**). Single crystal structure was obtained by XRD analysis.

M.p. = 172-175 °C;  $[\alpha]_{\text{D}}^{20} = +65.6^{\circ}$  (*c* 1, water);  $\delta_{\text{H}}$  in ppm (400 MHz,  $d_6$ -DMSO); 7.44 (d, *J* = 6.8 Hz, 2H, H-4 and H-6), 7.41-7.29 (m, 5H, H-1, H-2, H-3, H-13 and H-15), 7.24 (t, *J* = 7.3, 7.2 Hz, 2H, H-10 and H-12), 7.16 (t, *J* = 7.3 Hz, 1H, H-11), 4.54 (s, 1H, H-16), 4.28 (q, *J* = 6.8 Hz, 1H, H-7), 1.43 (d, *J* = 6.8 Hz, 3H, H-8);  $\delta_{\text{C}}$  in ppm (75 MHz,  $d_6$ -DMSO); 174.3 (C-17), 143.5 (C-5), 140.8 (C-14), 128.5 (C-1 and C-3), 127.9 (C-2), 127.3 (C-4 and C-6), 126.5 (C-13 and C-15), 126.3 (C-10 and C-12), 126.0 (C-11), 73.3 (C-16), 49.9 (C-7), 21.5 (C-8);  $\nu_{\text{max}}$ /  $\text{cm}^{-1}$ ; 3301, 2915, 1610, 1565, 1530, 1450, 1379. HRMS, calculated for  $\text{C}_8\text{H}_{12}\text{N}^+$   $[\text{M}-\text{Y}]^+$ : 122.096974, found: 122.0931; calculated for  $\text{C}_8\text{H}_7\text{O}_3^-$   $[\text{M}-\text{X}]^-$ : 151.039520, found: 151.0400.

### 6.1.16. Diastereopure di-*p*-toluoyl-*D*-tartrate salts of *N,N*-dimethyl- $\alpha$ -methylbenzylamine **46**

#### (a) (*R*)-**46**-(*S,S*)-**32**



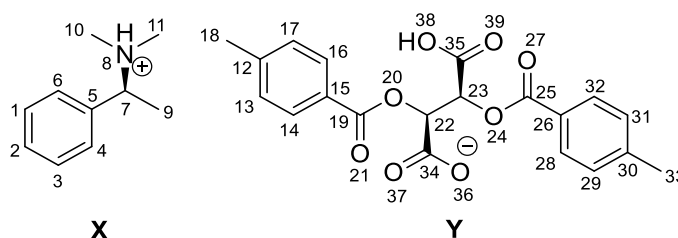
(*S,S*)-**32** (0.26 g, 0.67 mmol) and (*R*)-**46** (99.7 mg, 0.67 mmol) were dissolved into isopropyl acetate (3 mL and 2 mL respectively). The two solutions were mixed and heated to reflux with stirring. More isopropyl acetate (9 mL) was added until all solid dissolved. Stirring was stopped. The reaction mixture was cooled to room temperature and filtered to give a white crystalline solid (0.24 g, 67%). Small amount of crystals was dissolved into aqueous sodium carbonate solution (10% w/v, 1 mL) and extracted with ethyl acetate (1 mL). The organic layer was dried with anhydrous  $\text{MgSO}_4$  and filtered through a plug of celite. A solution of (*S*)-**34** in methanol (21 mg  $\text{mL}^{-1}$ , 100  $\mu\text{L}$ ) was added and the mixture was sonicated, then dried *in vacuo*. The residue was analysed by  $^1\text{H}$  NMR ( $\text{CDCl}_3$ , 500 MHz) to determine the ee of **46** (100%) which corresponds to the de of the crystals. Single crystal structure was obtained by XRD analysis.

M.p. = 129-130 °C;  $[\alpha]_{\text{D}}^{20} = +128.4^{\circ}$  (*c* 0.5, methanol);  $\delta_{\text{H}}$  in ppm (500 MHz,  $d_6$ -DMSO); 7.83 (d, *J* = 8.0 Hz, 4H, H-14, H-16, H-28 and H-32), 7.45-7.39 (m, 2H,



H-4 and H-6), 7.39-7.34 (m, 3H, H-1, H-2 and H-3), 7.31 (d,  $J = 8.0$  Hz, 4H, H-13, H-17, H-29 and H-31), 5.67 (s, 2H, H-22 and H-23), 4.10 (br d,  $J = 7.3$  Hz, 1H, H-7), 2.44 (s, 6H, H-10 and H-11), 2.35 (s, 6H, H-18 and H-39), 1.45 (d,  $J = 7.3$  Hz, H-8);  $\delta_C$  in ppm (75 MHz,  $d_6$ -DMSO); 168.1 (C-19 and C-25), 164.8 (C-33 and C-34), 143.8 (C-15 and C-26), 136.7 (C-5), 129.3 (C-14, C-16, C-28 and C-32), 129.3 (C-13, C-17, C-29 and C-31), 129.1 (C-2), 128.8 (C-5), 128.7 (C-4 and C-6), 128.5 (C-1 and C-3), 126.7 (C-18 and C-39), 72.0 (C-22 and C-23), 64.4 (C-7), 21.2 (C-18 and C-39), 16.8 (C-8);  $\nu_{max}/\text{cm}^{-1}$ : 2984, 2731, 1719, 1680, 1610, 1456, 1406, 1388, 1338, 1265, 1252, 1232. HRMS, calculated for  $\text{C}_{10}\text{H}_{15}\text{N}^+$   $[\text{M}-\text{Y}]^+$ : 150.128274, found: 150.1249; calculated for  $\text{C}_{20}\text{H}_{17}\text{O}_8^-$   $[\text{M}-\text{X}]^-$ : 385.092345, found: 385.0828.

**(b) (S)-46-(S,S)-32**

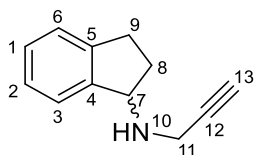


A similar procedure as in Section 5.1.16(a) was used to synthesise (S)-46-(S,S)-32. After more isopropyl acetate was added to the hot solution of (S)-46/ (S,S)-32, isopropyl alcohol (8 mL) was added for the complete dissolution of the precipitate. (S)-46-(S,S)-32 was isolated as a white crystalline solid (0.26 g, 73%) with de = 100% (determined as the ee of 46). Single crystal structure was obtained by XRD analysis.

M.p. = 140-141 °C;  $[\alpha]_D^{20} = +200.2^\circ$  (c 0.5, methanol);  $\delta_H$  in ppm (500 MHz,  $d_6$ -DMSO); 7.84 (d,  $J = 8.0$  Hz, 4H, H-14, H-16, H-28 and H-32), 7.45-7.39 (m, 2H, H-4 and H-6), 7.35 (t,  $J = 3.3$  Hz, 3H, H-1, H-2 and H-3), 7.31 (d,  $J = 8.0$  Hz, 4H, H-13, H-17, H-29 and H-31), 5.68 (s, 2H, H-22 and H-23), 4.13 (q,  $J = 6.7$  Hz, 1H, H-7), 2.43 (s, 6H, H-10 and H-11), 2.36 (s, 6H, H-18 and H-39), 1.47 (d,  $J = 6.7$  Hz, H-8);  $\delta_C$  in ppm (75 MHz,  $d_6$ -DMSO); 168.0 (C-19 and C-25), 164.8 (C-33 and C-34), 143.8 (C-15 and C-26), 136.8 (C-5), 129.3 (C-14, C-16, C-28 and C-32), 129.2 (C-13, C-17, C-29 and C-31), 129.1 (C-2), 128.8 (C-5), 128.6 (C-4 and C-6), 128.5 (C-1 and C-3), 126.7 (C-18 and C-39), 71.9 (C-22 and C-23), 64.3

(C-7), 21.2 (C-18 and C-39), 16.8 (C-8);  $\nu_{\max}/\text{cm}^{-1}$ : 2955, 2701, 1719, 1681, 1611, 1458, 1408, 1325, 1251. HRMS, calculated for  $\text{C}_{10}\text{H}_{15}\text{N}^+$  [M-Y]<sup>+</sup>: 150.128274, found: 150.1248; calculated for  $\text{C}_{20}\text{H}_{17}\text{O}_8^-$  [M-X]<sup>-</sup>: 385.092345, found: 385.0818.

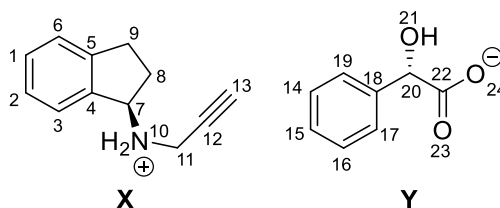
### 6.1.17. Racemic propargyl aminoindan 109



Racemic 1-aminoindan (4.0 g, 29.8 mmol) was dissolved into toluene (15 mL) in a 100 mL three-neck round bottom flask under nitrogen. Aqueous sodium hydroxide solution (1.6 M, 32 mL) was added and the mixture was heated to 40 °C. A solution of propargyl benzenesulfonate (96%, 6.2 g, 30.3 mmol) in toluene (5 mL) was added slowly over one hour. The reaction was stirred at 45 °C for 5 hours. After the reaction was complete, water (20 mL) was added and the mixture was separated. The aqueous layer was further extracted with toluene (2 × 20 mL). The combined organic layer was washed with aqueous sodium hydroxide solution (5 M, 20 mL) followed by water (20 mL). The organic layer was dried with anhydrous  $\text{MgSO}_4$ , filtered and concentrated *in vacuo* to give a brown oil with fine precipitate. Ethyl acetate was added and the crude mixture was filtered. The filtrate was dried *in vacuo* and was purified by column chromatography using Biotage (ethyl acetate/ petroleum 40-60 gradient, 20 to 80% ethyl acetate by volume); TLC: Silica plate, ethyl acetate/ trimethylamine 95:5 (v/v), visualisation by UV (254 nm;  $R_f$  of product = 0.84) to yield the *rac*-**109** as a brown oil (2.8 g, 54%).

$\delta_{\text{H}}$  in ppm (300 MHz,  $\text{CDCl}_3$ ); 7.37-7.27 (m, 1H, H-3), 7.26-7.13 (m, 3H, H-1, H-2 and H-6), 4.39 (t,  $J = 6.2$  Hz, 1H, H-7), 3.49 (t,  $J = 2.4, 1.5$  Hz, 2H, H-11), 3.02 (ddd,  $J = 15.6, 8.7$  and  $6.6$  Hz, 1H, H-9); 2.80 (ddd,  $J = 15.6, 8.7$  and  $6.6$  Hz, 1H, H-9), 2.45-2.30 (m, 1H, H-8), 2.24 (t,  $J = 2.4$  Hz, 1H, H-13), 1.91-1.76 (m, 1H, H-8), 1.62 (br s, NH);  $\delta_{\text{C}}$  in ppm (75 MHz,  $\text{CDCl}_3$ ); 144.5 (C-4), 143.8 (C-5), 127.7 (C-3), 126.3 (C-2), 124.9 (C-1), 124.2 (C-6), 82.5 (C-12), 71.5 (C-13), 61.9 (C-7), 36.2 (C-11), 33.3 (C-8), 30.5 (C-9);  $\nu_{\max}/\text{cm}^{-1}$ : 3290, 3231, 2940, 2851, 2129, 1636, 1558, 1478, 1328. The spectral data correspond to those reported in the literature.<sup>185</sup> HRMS, calculated for  $\text{C}_{12}\text{H}_{14}\text{N}$  [M+H]<sup>+</sup>: 172.112624, found: 172.0679.

### 6.1.18. Diastereopure (*S*)-mandelate salt of Rasagiline (*R*)-109 (for the preparation of pure (*R*)-109)

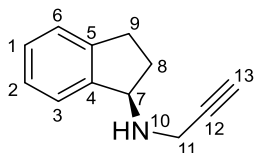


Rasagiline mesylate (1.0 g, 3.7 mmol) was dissolved into aqueous ammonia solution (10%, 20 mL) and aqueous sodium hydroxide solution (4 M, 25 mL). MTBE (40 mL) was added and the mixture was stirred at room temperature. The mixture was separated and the aqueous layer was further extracted with MTBE (2 × 20 mL). The combined organic layer was dried with anhydrous MgSO<sub>4</sub>, filtered and dried *in vacuo* to give a pale yellow oil (0.58 g, 91%, 82% ee). MTBE/methanol (4% v/v) (10 mL) was added to a mixture of crude (*R*)-**109** (0.53 g, 3.1 mmol) and (*S*)-**34** (0.47 g, 3.1 mmol) and was stirred and heated to reflux. More solvent was added until all solid dissolved (30 mL). The mixture was cooled to room temperature with reduced stirring. After about 4 hours, the slurry was filtered to give a white fluffy solid (0.61 g, 61% from crude (*R*)-**109**). A small amount of crystals was dissolved into aqueous sodium carbonate solution (10% w/v, 600 μL) and extracted with ethyl acetate (600 μL). The organic layer was dried with anhydrous MgSO<sub>4</sub> and filtered through a plug of celite. The filtrate was analysed by chiral GC to determine the ee of **109** (100%) which corresponds to the de of the crystals.

M.p. = 108-110 °C;  $[\alpha]_D^{20} = +75.6^\circ$  (c 0.5, ethanol);  $\delta_H$  in ppm (500 MHz, CDCl<sub>3</sub>); 7.37 (d,  $J = 7.0$  Hz, 2H, H-17 and H-19), 7.35-7.18 (m, 6H, H-1, H-2, H-3, H-6, H-14 and H-16), 7.12 (t,  $J = 7.3$  Hz, 1H, H-15), 6.77 (br s, 3H, OH and NH<sub>2</sub><sup>+</sup>), 4.86 (s, 1H, H-20), 4.58 (dd,  $J = 7.5, 3.5$  Hz, 1H, H-7), 3.38 (qd,  $J = 16.8, 2.4$  Hz, 2H, H-11), 3.04 (dt,  $J = 16.0, 8.3$  Hz, 1H, H-9), 2.77 (ddd,  $J = 16.0, 8.3, 4.0$  Hz, 1H, H-9), 2.33 (t,  $J = 2.4$  Hz, 1H, H-13), 2.31-2.20 (m, 1H, H-9), 2.07-1.96 (m, 1H, H-9);  $\delta_C$  in ppm (75 MHz, CDCl<sub>3</sub>); 177.9 (C-22), 144.7 (C-4), 141.0 (C-18), 138.5 (C-5), 129.3 (C-2), 128.1 (C-1), 127.5 (C-15), 126.8 (C-6), 126.6 (C-17 and C-19), 125.3 (C-3), 125.2 (C-14 and C-16), 75.6 (C-13), 73.8 (C-20), 60.9 (C-7), 34.0 (C-11), 30.3 (C-9), 29.7 (C-8);  $\nu_{max}$ / cm<sup>-1</sup>; 3404, 3232, 2133, 1637, 1557,

1453, 1405, 1328, 1312. HRMS, calculated for  $C_{12}H_{14}N^+$   $[M-Y]^+$ : 172.112624, found: 172.1090; calculated for  $C_8H_7O_3^-$   $[M-X]^-$ : 151.039520, found: 151.0406.

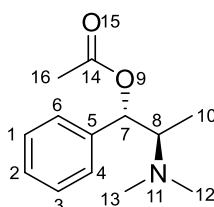
#### 6.1.19. Rasagiline (*R*)-109



(*R*)-**109**-(*S*)-**34** (79.6 mg, 0.25 mmol) was dissolved into aqueous potassium carbonate solution (0.1 M, 20 mL). Dichloromethane (20 mL) was then added and was stirred for about 10 minutes. The mixture was separated and the aqueous layer was further extracted with dichloromethane (2 × 20 mL). The combined organic layer was dried by anhydrous  $MgSO_4$  and filtered. The solvent was removed *in vacuo* to yield (*R*)-**109** as a brown oil (35.6 mg, 85%).

$[\alpha]_D^{20} = +25.4^\circ$  (c 1.0, chloroform) {lit.<sup>185</sup>  $[\alpha]_D^{20} = +17.6^\circ$  (c 1.0, chloroform)}. The spectral and MS data correspond to those reported for *rac*-**109** and from the literature.

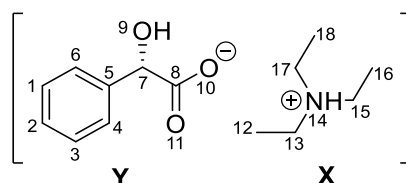
#### 6.1.20. *O*-Acetyl-(1*S*,2*R*)-*N*-methylephedrine **49**



(1*S*,2*R*)-*N*-Methylephedrine **110** (99.8 mg, 0.56 mmol) was dissolved in dichloromethane (3 mL) and the solution was cooled in ice. Triethylamine (156  $\mu$ L) was added followed by acetyl chloride (60  $\mu$ L). The slurry was stirred at room temperature overnight. The reaction mixture was diluted with dichloromethane (5 mL) and basified with aqueous sodium hydroxide solution (1 M, 5 mL) and the mixture was separated. The aqueous layer was further extracted with dichloromethane (2 × 5 mL). The combined organic layer was washed with aqueous sodium hydroxide solution (1 M, 5 mL), dried in anhydrous  $MgSO_4$  and filtered. The solvent was removed *in vacuo* to yield (1*S*,2*R*)-**111** as a brown oil (0.1 g, 81%). The crude product was used without further purification.

$\delta_{\text{H}}$  in ppm (500 MHz,  $\text{CDCl}_3$ ); 7.34-7.29 (m, 2H, H-4 and H-6), 7.29-7.21 (m, 3H, H-1, H-2 and H-3), 5.94 (d, 1H, H-7), 2.90-2.83 (m, 1H, H-8), 2.28 (s, 6H, H-12 and H-13), 2.09 (s, 3H, H-16), 1.05 (d,  $J = 6.5$  Hz, 3H, H-10);  $\delta_{\text{C}}$  in ppm (75 MHz,  $\text{CDCl}_3$ ); 170.0 (C-14), 140.1 (C-5), 128.2 (C-4 and C-6), 127.5 (C-2), 126.3 (C-1 and C-3), 75.5 (C-7), 63.6 (C-8), 41.4 (C-12 and C-13), 21.3 (C-16), 9.5 (C-10);  $\nu_{\text{max}}/\text{cm}^{-1}$ ; 2971, 2939, 2866, 2825, 2779, 1738, 1639, 1453, 1372, 1232. HRMS, calculated for  $\text{C}_{13}\text{H}_{20}\text{NO}_2$   $[\text{M}+\text{H}]^+$ : 222.149404, found: 222.0944.

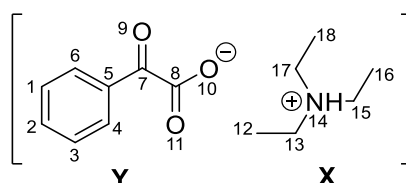
### 6.1.21. Triethylammonium (S)-mandelate **34**



Triethylamine (0.7 mL, 5.0 mmol) and (S)-**34** (0.3 g, 2.0 mmol) were stirred in ethyl acetate (10 mL) at room temperature for 3 hours. The solvent was removed *in vacuo* to yield  $\text{Et}_3\text{N}-(\text{S})$ -**34** as a colourless oil (0.47 g, 94%).

$[\alpha]_{\text{D}}^{20} = +62.1^\circ$  ( $c$  1.0, methanol);  $\delta_{\text{H}}$  in ppm (500 MHz,  $d_6$ -DMSO); 7.39 (d,  $J = 7.3$  Hz, 2H, H-4 and H-6), 7.28 (t,  $J = 7.3$  Hz, 2H, H-1 and H-3), 7.22 (t,  $J = 7.3$  Hz, 1H, H-2), 4.71 (s, 1H, H-7), 2.93 (q,  $J = 7.3$  Hz, 4H, H-13, H-15 and H-17), 1.10 (t,  $J = 7.3$  Hz, 6H, H-12, H-16 and H-18);  $\delta_{\text{C}}$  in ppm (126 MHz,  $d_6$ -DMSO); 174.7 (C-8), 142.5 (C-5), 127.6 (C-1 and C-3), 126.5 (C-2), 126.4 (C-4 and C-6), 73.1 (C-7), 45.1 (C-13, C-15 and C-17), 8.8 (C-12, C-16 and C-18).  $\nu_{\text{max}}/\text{cm}^{-1}$ ; 3324, 2984, 2431, 1732, 1599, 1494, 1478, 1452, 1339. HRMS, calculated for  $\text{C}_6\text{H}_{16}\text{N}^+$   $[\text{M}-\text{Y}]^+$ : 102.128274, found by LCMS, ESI-MS/MS (+)  $[\text{M}-\text{Y}]^+$ : 102.3; HRMS, calculated for  $\text{C}_{16}\text{H}_{14}\text{O}_6\text{Na}^-$   $[\text{M}-\text{X}+\text{Y}+\text{Na}]^-$ : 325.068809, found by LCMS, ESI-MS/MS (-)  $[\text{M}-\text{X}+\text{Y}+\text{Na}]^-$ : 325.1.

### 6.1.22. Triethylammonium phenylglyoxylate **126**



Triethylamine (0.35 mL, 2.5 mmol) and phenylglyoxylic acid (0.15 g, 1.0 mmol) were stirred in ethyl acetate (5 mL) at room temperature overnight. The solvent was removed *in vacuo* to yield Et<sub>3</sub>N-**126** as a thick pale yellow oil (0.24 g, 95%).

$\delta_{\text{H}}$  in ppm (500 MHz, *d*<sub>6</sub>-DMSO): 7.85 (m, 2H, H-4 and H-6), 7.62 (tt, *J* = 7.3 and 1.5 Hz, 1H, H-2), 7.52 (m, 2H, H-1 and H-3), 3.10 (q, *J* = 7.4 Hz, 6H, H-13, H-15 and H-17), 1.21 (t, *J* = 7.4 Hz, 9H, H-12, H-16 and H-18);  $\delta_{\text{C}}$  in ppm (126 MHz, *d*<sub>6</sub>-DMSO): 195.1 (C-7), 169.6 (C-8), 134.1 (C-2), 133.0 (C-5), 128.9 (C-4 and C-6), 128.5 (C-1 and C-3), 45.4 (C-13, C-15 and C-17), 8.5 (C-12, C-16 and C-18).  $\nu_{\text{max}}$ / cm<sup>-1</sup>: 2987, 2639, 2489, 1676, 1594, 1475, 1450, 1398, 1311, 1224. HRMS, calculated for C<sub>6</sub>H<sub>16</sub>N<sup>+</sup> [M-Y]<sup>+</sup>: 102.128274, found by LCMS, ESI-MS/MS (+) [M-Y]<sup>+</sup>: 102.3; HRMS, calculated for C<sub>16</sub>H<sub>10</sub>O<sub>6</sub>Na<sup>-</sup> [M-X+Y+Na]<sup>-</sup>: 321.037509, found by LCMS, ESI-MS/MS (-) [M-X+Y+Na]<sup>-</sup>: 321.1.

## 6.2 Racemisation of chiral amines

### 6.2.1. General procedures for racemisation in batch

The racemisation of (*S*)-**39** (0.5 M) in toluene by SCRAM **64** was described as an example. Catalyst **64** (5.1 mg, 4.4  $\mu$ mol) and a stirrer bar were added into a three-neck round bottom flask and was flushed with nitrogen for 10 minutes. (*S*)-**39** (0.3 g, 2.2 mmol, 323  $\mu$ L) and *n*-decane (31.2 mg, 0.22 mmol, 43  $\mu$ L) were dissolved into toluene (4 mL, dried over molecular sieves). The solution was added to the catalyst. The reaction was stirred and heated to 105 °C for 24 hours. The reaction was sampled (20  $\mu$ L) before heating and during the reaction by diluting the sample into ethyl acetate (980  $\mu$ L). The samples were analysed by GC for conversion and chiral GC for the determination of ee, after derivatisation with trifluoroacetic anhydride (30  $\mu$ L).

A similar procedure was employed for the racemisation of other substrates under designated conditions (Table 6.2). The ee of the samples were determined by either chiral GC, HPLC or <sup>1</sup>H NMR (Table 6.3).

Amine	[Amine] (M)	Catalyst (mol%)	Solvent <sup>[a]</sup>	T (°C)	I.S. (equiv.) <sup>[b]</sup>	Sampling vol. (μL) <sup>[c]</sup>
(S)-39	0.1	64 (0.2)	Toluene	105	0.1	20 <sup>[d]</sup>
(S)-39	0.25	64 (0.2)	Toluene	105	0.1	40
(S)-39	0.5	64 (0.2)	Toluene	105	0.1	20
(S)-39	1	64 (0.2)	Toluene	105	0.1	10
(S)-39	2	64 (0.2)	Toluene	105	0.1	5
(S)-39 <sup>[e]</sup>	0.25	64 (1)	EtOAc	60	0.2	4 <sup>[d]</sup>
(S)-39 <sup>[e]</sup>	0.25	64 (1)	EtOAc/ MeOH (20%)	60	0.2	4 <sup>[d]</sup>
(S)-39 <sup>[e]</sup>	0.25	64 (1)	EtOAc/ EtOH (20%)	60	0.2	4 <sup>[d]</sup>
(S)-39 <sup>[e]</sup>	0.25	64 (1)	EtOAc/ <sup>i</sup> PrOH (20%)	60	0.2	4 <sup>[d]</sup>
(S)-39	0.5	55 (0.2)	Toluene	105	0.5	40
(R)-101	0.5	64 (0.2)	Toluene	105	0.1	20
(S)-46	0.5	64 (0.2)	Toluene	105	0.1	20
(R)-46	0.1	64 (0.2)	Toluene	105	0.5	20 <sup>[f]</sup>
(R)-46	0.1	64 (1)	Toluene	105	0.2	50 <sup>[f]</sup>
(R)-46	0.1	64 (1)	Toluene/ 58 (1.4%)	105	0.2	50 <sup>[f]</sup>
(R)-46	0.1	64 (1)	Toluene/ 58 (50%)	105	0.2	50 <sup>[f]</sup>
(R)-9	0.1	64 (0.2)	Toluene	60	0.1	10 <sup>[f]</sup>
(R)-9	0.1	64 (0.2)	EtOAc/ MeOH (12.5%)	60	0.1	10 <sup>[f]</sup>
(R)-9	0.1	64 (0.2)	EtOAc/ <sup>i</sup> PrOH (12.5%)	60	0.1	10 <sup>[f]</sup>
(S)-103	0.5	64 (0.2)	MTBE	50	NA	20 <sup>[e]</sup>
(S)-103	0.5	64 (0.2)	<sup>i</sup> PrOAc	80	0.1	20 <sup>[f]</sup>
(S)-103	0.5	64 (0.2)	Toluene	105	0.1	20 <sup>[f]</sup>

Table 6.2 Reaction conditions for the racemisation of chiral amines. <sup>[a]</sup>The percent in bracket refers to volume percent. <sup>[b]</sup>Internal standard. *n*-Decane was used for all except (R)-9 which used *n*-hexadecane. <sup>[c]</sup>The samples were diluted to 1 mL by EtOAc. <sup>[d]</sup>The samples were diluted to 200 μL. <sup>[e]</sup>Volume of reaction is 2.2 mL. <sup>[f]</sup>MeOH was used as the diluent. <sup>[g]</sup>MeCN was used as the diluent

Amine	ee Method	Derivatisation of samples ( $\mu\text{L}$ )
<b>39</b>	Chiral GC (Fig. 6.15)	Trifluoroacetic anhydride (30-50)
<b>101</b>	Chiral GC (Fig. 6.16)	Trifluoroacetic anhydride (100)
<b>46</b>	$^1\text{H}$ NMR ( $\text{CDCl}_3$ , 500 MHz) (Fig. 6.24) <sup>[a]</sup>	(S)- <b>34</b> (100) <sup>[b]</sup>
<b>42</b>	Chiral HPLC (Fig. 6.18)	Triethylamine (10) followed by benzoyl chloride (3)
<b>9</b>	Chiral HPLC (Fig. 6.9)	NA
<b>103</b>	Chiral GC (Fig. 6.13 and Fig. 6.14)	Acetic anhydride (10) or benzoyl chloride (10)

Table 6.3 Methods for ee analysis of different amine substrates. <sup>[a]</sup>A solution of (S)-**34** in MeOH ( $21 \text{ mg mL}^{-1}$ ,  $100 \mu\text{L}$ ) was added to the sample, sonicated for 5-10 min and dried in vacuo. The residue was analysed by  $^1\text{H}$  NMR ( $\text{CDCl}_3$ , 500 MHz). <sup>[b]</sup>(S)-**34** was added as a  $21 \text{ mg mL}^{-1}$  solution in MeOH ( $100 \mu\text{L}$ )

### 6.2.2. General procedures for the racemisation of (S)-**39** (0.5 M) in batch with spiking of (S)-**39**

A similar procedure as in Section 1 was employed. After 25 to 26 hours where the racemisation stopped, or reached 0% ee, (S)-**39** (0.5 equiv. with respect to the original amount of (S)-**39** in the reaction) and *n*-decane (0.25 equiv.) were dissolved into toluene and was charged into the reaction mixture at  $105 \text{ }^\circ\text{C}$ . The reaction was sampled immediately after the addition and at specific times. When Shvo's catalyst **55** was used, the same spiking procedure was repeated two times.

### 6.2.3. Racemisation of (S)-**39** (0.5 M) in batch with spiking of methylamine (2 equiv. with respect to iridium)

A similar procedure as in Section 1 was employed. SCRAM **64** (25.8 mg,  $22.2 \mu\text{mol}$ ) and tetrahydrofuran (4 mL) were used and the reaction was heated to  $60 \text{ }^\circ\text{C}$ . After 30 minutes, where ee of **39** reached approximately 50%, methylamine/tetrahydrofuran solution (1.7 M,  $52.2 \mu\text{L}$ ,  $88.7 \mu\text{mol}$ ) was added. The reaction was sampled 15 minutes after the addition and at specific times for 24 hours. The same procedures were repeated for spiking 20 equiv. of methylamine ( $520 \mu\text{L}$ , 0.88 mmol) after 30 minutes from the start of the reaction.



#### 6.2.4. NMR titration of SCRAM 64 with methylamine

Catalyst **64** (3.1 mg, 2.7  $\mu\text{mol}$ , 5.3  $\mu\text{mol}$  iridium) and benzene (9.1 mg, 10  $\mu\text{L}$ , 0.117 mmol) were dissolved into  $d_6$ -dimethylsulfoxide (0.6 mL). The sample was analysed by  $^1\text{H}$  NMR (500 MHz). Methylamine/ methanol solution (2 M) was added as shown in Table 6.4. After each addition, the sample was shaken for 60 seconds and  $^1\text{H}$  NMR was recorded.

Total MeNH <sub>2</sub> (equiv.) <sup>[a]</sup>	Total MeNH <sub>2</sub> ( $\mu\text{mol}$ )	Total vol. of MeNH <sub>2</sub> (in MeOH) ( $\mu\text{L}$ )	Vol. of MeNH <sub>2</sub> (in MeOH) added ( $\mu\text{L}$ )
0	0	0	0
0.5	2.7	1.33	1.33
1	5.3	2.67	1.34
2	10.7	5.33	2.66
3	16.0	8	2.67
4	21.3	10.7	2.7
5	26.7	13.3	2.6
7.5	40.0	20	6.7
10	53.3	26.7	6.7
15	80.0	40	13.3
20	106.7	53.3	13.3
30	160.0	80	26.7
40	213.3	106.7	26.7

Table 6.4 Addition of MeNH<sub>2</sub> (2 M in MeOH) to **64** in  $d_6$ -DMSO (0.6 mL). <sup>[a]</sup>With respect to Ir

## 6.2.5. General procedures for racemisation in flow

### (a) (S)-N, $\alpha$ -Dimethylbenzylamine **39**

#### (i) Configuration A (Fig. 2.20(a) and Fig. 6.25) (Table 2.10, entry 2)

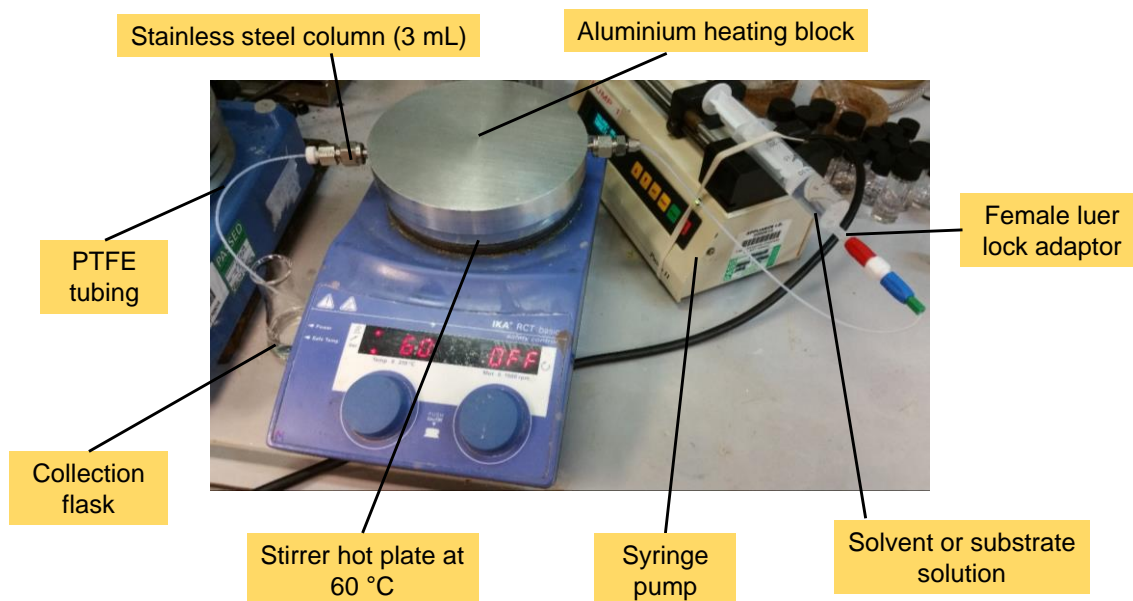


Fig. 6.25 Configuration A for flow racemisation (corresponds to the schematic in Fig. 2.20(a))

The experimental set-up for configuration A was shown in Fig. 6.25. Catalyst **92** (ICP 6.3%, 0.24 g, 79.3  $\mu\text{mol Ir}$ ) was loaded onto an empty stainless HPLC column (3 mL). The column was equilibrated with ethyl acetate/ methanol (20% v/v) at 0.25 mL  $\text{min}^{-1}$  by a syringe pump and was heated to 73  $^{\circ}\text{C}$  by a hot plate. A solution of (S)-**39** (0.21 g, 1.6 mmol) and *n*-decane (10.5 mg, 73.8  $\mu\text{mol}$ ) in ethyl acetate/ methanol (20% v/v) (15 mL) was pumped through the column at 0.25 mL  $\text{min}^{-1}$  ( $t_{\text{Res}} = 12$  minutes) at 73  $^{\circ}\text{C}$ . The eluent was collected in reactor volumes (RV). When all reaction mixture was pumped through, the column was washed with ethyl acetate/ methanol mixture whilst cooling to room temperature. The reaction was sampled before pumping through the column and from the eluent collected. Each sample (200  $\mu\text{L}$ ) was diluted into ethyl acetate (800  $\mu\text{L}$ ) and analysed by GC for determining the conversion of **39** and chiral GC for determining the ee after derivatising the samples with trifluoroacetic anhydride (60  $\mu\text{L}$ ) (Table 6.5).

RV	39 (%)	ee of 39 (%)
0	100	100
1	84	90
2	100	84
3	100	86
4	99	86
5	98	87
Average (RV2-5)	99	86
Drop <sup>[a]</sup>	1	14

Table 6.5 Results for the racemisation of (*S*)-**39** in flow at 73 °C in EtOAc/ MeOH (20% v/v) ( $t_{Res} = 12$  min) using configuration A. <sup>[a]</sup>Drop = RV0 – average (RV2-5)

(ii) Configuration B (Fig. 2.20(b) and Fig. 6.26) (Table 2.10, entry 1)

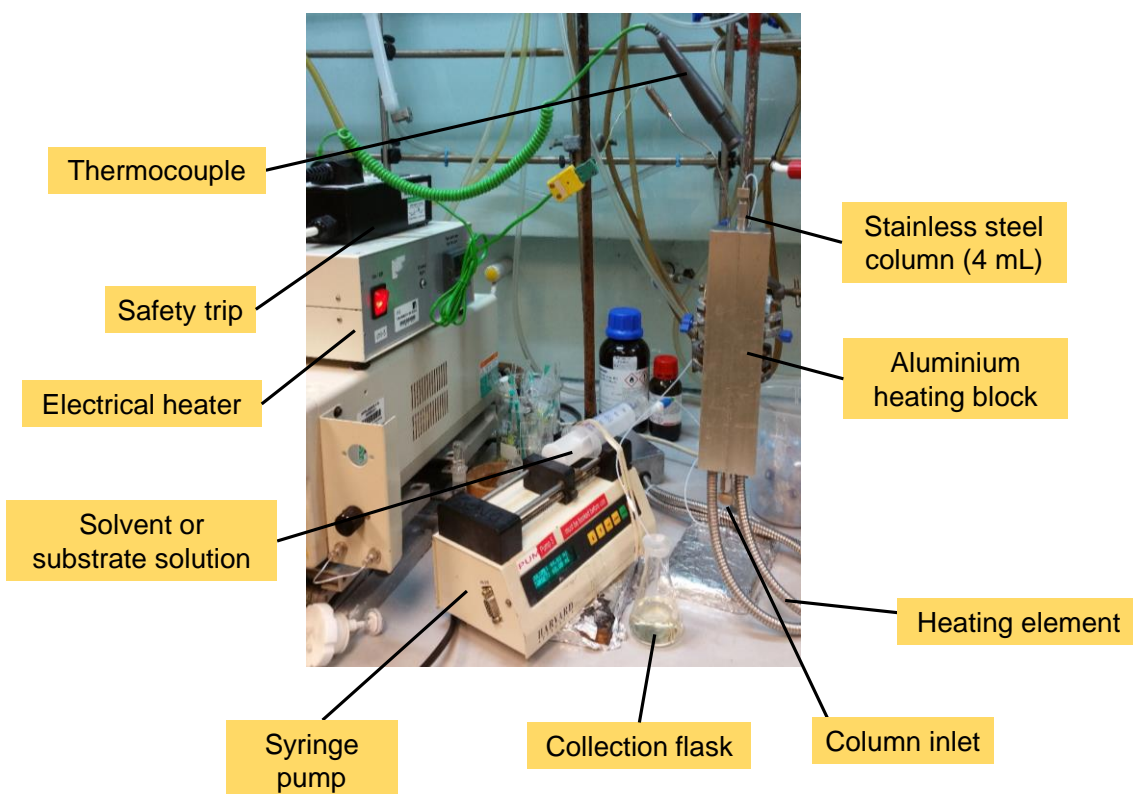


Fig. 6.26 Configuration B for flow racemisation (corresponds to the schematic in Fig. 2.20 (b))

The racemisation of (*S*)-**39** was also carried out in flow using configuration B (Fig. 6.26). A similar procedure as in configuration A was employed. Catalyst **92** (ICP 6.3%, 0.32 g, 0.11 mmol iridium) and sand (5.5 g) were mixed and loaded onto a stainless steel HPLC column (4 mL). The column was equilibrated with isopropyl

acetate. A solution of (*S*)-**39** (0.3 g, 2.1 mmol, ee 86%) and *n*-decane (28.4 mg, 0.2 mmol) in isopropyl acetate (20 mL) was pumped through the catalyst at 80 °C at 0.1 mL min<sup>-1</sup> ( $t_{\text{Res}} = 40$  minutes). The column was flushed with isopropyl alcohol after the reaction whilst cooled to room temperature. Each sample (100  $\mu\text{L}$ ) from each RV was diluted into ethyl acetate (900  $\mu\text{L}$ ) and analysed by GC and chiral GC as described for configuration A (Table 6.6).

RV	39 (%)	ee of 39 (%)
0	100	86
1	85	48
2	97	43
3	98	44
4	98	44
5	98	43
Average (RV2-5)	98	44
Drop <sup>[a]</sup>	2	42

Table 6.6 Results for the racemisation of (*S*)-**39** in flow at 80 °C in <sup>i</sup>PrOAc ( $t_{\text{Res}} = 40$  min) using configuration B. <sup>[a]</sup>Drop = RV0 – average (RV2-5)

**(b) (*R*)-*N*-Isopropyl- $\alpha$ -methylbenzylamine 101 (Table 2.10, entry 3)**

Configuration B was used for the racemisation of (*R*)-**101** in flow. A similar procedure as in Section 5.2.5(a)(ii) was employed. Catalyst **92** (ICP 6.3%, 0.32 g, 0.11 mmol) and sand (5.5 g) were mixed and loaded onto the stainless steel HPLC column (4 mL). The column was equilibrated with ethyl isobutyrate. A solution of (*R*)-**101** (0.17 g, 1 mmol) was dissolved into ethyl isobutyrate (20 mL) was pumped through the catalyst at 80 °C at 0.05 mL min<sup>-1</sup> ( $t_{\text{Res}} = 80$  minutes). Each sample (100  $\mu\text{L}$ ) from each RV was diluted into ethyl acetate (900  $\mu\text{L}$ ) and analysed by chiral GC as described in Section 5.2.5(a) (Table 6.7). Conversion was not measured.

RV	ee of 101 (%)
0	100
1	90
2	86
3	84
4	86
5	87
Average (RV2-5)	86
Drop <sup>[a]</sup>	14

Table 6.7 Results for the racemisation of (S)-**101** in flow at 80 °C in ethyl isobutyrate ( $t_{Res}$  = 80 min) using configuration B. <sup>[a]</sup>Drop = RV0 – average (RV2-5)

**(c) (S)-N,N-Dimethyl- $\alpha$ -methylbenzylamine 46 (Table 2.10, entries 4 and 5)**

Configuration B was used for the racemisation of (S)-**46** in flow. A similar procedure as in Section 5.2.5(a)(ii) was employed. Catalyst **92** (ICP 7.7%, 0.25 g, 0.1 mmol) and sand (5.7 g) were mixed and loaded onto the stainless steel HPLC column (4 mL). The column was equilibrated with isopropyl alcohol then isopropyl acetate/ isopropyl alcohol (30%). A solution of (S)-**46** (0.15 g, 1 mmol) in isopropyl acetate/ isopropyl alcohol (30%) (20 mL) was pumped through the catalyst at 0.05 mL min<sup>-1</sup> ( $t_{Res}$  = 80 minutes) at 80 °C. A methanol solution of (S)-**34** (21 mg mL<sup>-1</sup>, 100  $\mu$ L) was added to each sample (200  $\mu$ L) from each RV. The sample was sonicated and dried *in vacuo* and analysed by <sup>1</sup>H NMR (CDCl<sub>3</sub>, 500 MHz) to determine the ee of **46** (Table 6.8). Conversion was not measured. The reaction was repeated at 33  $\mu$ L min<sup>-1</sup> ( $t_{Res}$  = 120 minutes) (Table 6.8).

RV	ee of 46 (%)	
	t <sub>Res</sub> = 80 min	t <sub>Res</sub> = 120 min
0	100	100
1	100	N.D. <sup>[a]</sup>
2	87	68
3	89	82
4	89	86
5	90	85
Average (RV2-5)	89	84
Drop <sup>[b]</sup>	11	16

Table 6.8 Results for the racemisation of (*S*)-**46** in flow at 80 °C in <sup>1</sup>PrOAc/<sup>1</sup>PrOH (30% by volume) (t<sub>Res</sub> = 80 and 120 min) using configuration B. <sup>[a]</sup>Not determined. <sup>[b]</sup>Drop = RV0 – average (RV2-5)

**(d) (*R*)-6,7-Dimethoxy-1-methyl-1,2,3,4-tetrahydroisoquinoline 9 (Table 2.10, entries 6 and 7)**

Configuration A was used for the racemisation of (*R*)-**9** in flow. A similar procedure as in Section 5.2.5(a)(i) was employed. Catalyst **92** (ICP 7.7%, 0.19 g, 74.8 μmol iridium) and sand (4 g) were mixed and loaded onto the stainless steel HPLC column (3 mL). The column was equilibrated with isopropyl alcohol followed by ethyl acetate/ methanol 7:1. A solution of (*R*)-**9** (0.16 g, 0.75 mmol) and *n*-hexadecane (0.17 g, 0.75 mmol) in ethyl acetate/ methanol 7:1 (v/v, 15 mL) was pumped through the catalyst at 60 °C at 0.5 mL min<sup>-1</sup> (t<sub>Res</sub> = 6 minutes). Each sample (6 μL) from each RV was diluted into methanol (294 μL). The samples were analysed by GC and chiral HPLC for the conversion and ee of **9** respectively (Table 6.9).

RV	9 (%)	8 (%)	65 (%)	ee of 9 (%)
0	100	0	0	100
1	49	20	0	17
2	87	11	0	11
3	90	4	0	14
4	92	5	0	17
5	94	4	0	20
Average (RV3-5)	92	4	0	17
Drop <sup>[a]</sup>	8	NA	NA	83

Table 6.9 Results for the racemisation of (*R*)-**9** in flow at 60 °C in EtOAc/ MeOH 7:1 (v/v) ( $t_{Res} = 6$  min) using configuration A. <sup>[a]</sup>Drop = RV0 – average (RV3-5)

Configuration A was also used for the racemisation of the ML in flow from diastereomeric crystallisation of *rac*-**9** with (*S*)-**34**. A similar procedure as in Section 5.2.5(d) was employed. Catalyst **92** (ICP 7.4%, 0.33 g, 0.13 mmol iridium) was loaded onto the stainless steel HPLC column (3 mL) with no sand. The column was equilibrated with ethyl acetate/ methanol 7:1. *n*-Hexadecane (22.8 mg, 0.11 mmol) was added to the ML from a previous diastereomeric crystallisation of *rac*-**9** in flow (Table 3.2, entry 1, 64 mM from <sup>1</sup>H NMR). The reaction mixture was sampled (200  $\mu$ L) into ethyl acetate (800  $\mu$ L) and basified with aqueous sodium carbonate solution (10% w/v, 1 mL). The top organic layer was removed and analysed by GC and chiral HPLC for the conversion and ee of **9** respectively. The ML solution was pumped through the catalyst at 60°C at 0.5 mL min<sup>-1</sup> ( $t_{Res} = 6$  minutes). The first RV (RV1) was discarded and the remaining eluent (RV2 to 6) was collected into one single flask. It was sampled and analysed as described above (Table 6.10).

RV	9 (%)	8 (%)	65 (%)	ee of 9 (%)
0	99	1	0	37
2-6	93	7	0	11
Drop	6	NA	NA	26

Table 6.10 Results for the racemisation of ML from the diastereomeric crystallisation of *rac*-**9** in flow at 60 °C in EtOAc/ MeOH 7:1 (v/v) ( $t_{Res} = 6$  min) using configuration A. <sup>[a]</sup>Drop = RV0 – average (RV2-6)

**(e) (S)-2-Methylpiperidine 103 (Table 2.10, entries 8 and 9)**

Configuration A was used for the racemisation of (S)-**103** in flow in MTBE/ isopropyl alcohol 95:5 (v/v) at 50 °C (Table 2.10, entry 8). A similar procedure as in Section 5.2.5(a)(i) was employed. Catalyst **92** (ICP 6.3%, 0.24 g, 78.8 µmol iridium) was loaded onto the stainless steel HPLC column (3 mL) with no sand. A solution of (S)-**103** (0.16 g, 1.6 mmol) and *n*-decane (14.2 mg, 99.8 µmol) in MTBE/ isopropyl alcohol 95:5 (20 mL) was pumped through the catalyst at 50 °C at 0.25 mL min<sup>-1</sup> ( $t_{Res}$  = 12 min). The first RV (RV1) was discarded and the remaining eluent (RV2 to 6) was collected into one single flask. The eluent was sampled (200 µL) by diluting into ethyl acetate (800 µL). The sample was analysed by GC for conversion and chiral GC for determining the ee of **103** after derivatisation with acetic anhydride (10 µL). No conversion or racemisation was observed.

Configuration B was also used for the racemisation of (S)-**103** in flow in isopropyl acetate at 80 °C (Table 2.9, entry 9). Catalyst **92** (ICP 6.3%, 0.32 g, 0.11 mmol iridium) and sand (5.5 g) were mixed and loaded onto the stainless steel HPLC column (4 mL). The column was equilibrated with isopropyl acetate. A solution of (S)-**103** (0.21 g, 2.1 mmol) in isopropyl acetate (20 mL) was pumped through the catalyst at 80 °C at 0.25 mL min<sup>-1</sup> ( $t_{Res}$  = 16 minutes). Each sample (50 µL) from each RV was diluted into ethyl acetate (950 µL) and methanol (100 µL). Benzoyl chloride (10 µL) was added and the samples were analysed by chiral GC (Table 6.11). Conversion was not measured.

RV	ee of <b>103</b> (%)
0	100
1	19
2	20
3	21
4	22
5	21
Average (RV2-5)	21
Drop <sup>[a]</sup>	79

Table 6.11 Results for the racemisation of (S)-**103** in flow at 80 °C in *i*PrOAc ( $t_{Res}$  16 min) using configuration B. <sup>[a]</sup>Drop = RV0 – average (RV2-5)



### 6.2.6. General procedures for reactivation of immobilised SCRAM 92 with hydroiodic acid

Previously used/ reactivated **92** (0.32 g)/ sand (5.5 g) mixture was unloaded into a beaker from the stainless steel HPLC column after its activity was checked *via* the racemisation of (S)-**103** (Section 6.2.7). Aqueous hydroiodic acid at a specific concentration (15 mL) was added and the slurry was stirred at room temperature. After the designated stirring time, isopropyl alcohol/ water 2:1 (v/v) was added until all solid sank and the mixture was decanted. The procedure was repeated until the pH of the decant became neutral and colourless. The solid was further washed with more isopropyl alcohol, decanted and dried in the vacuum oven. The conditions of re-activation were shown in Table 6.12.

[HI (aq)] (M)	Stirring time (h)
0.1	2
0.2	4
0.5	6
1	8
1	24

Table 6.12 Conditions for reactivation of **92**

### 6.2.7. Catalyst activity check of immobilised SCRAM 92 *via* the racemisation of (S)-103 in flow

A similar procedure as in Section 5.2.5(e) was employed using configuration B of the flow racemisation set-up (Fig. 2.20(b) and Fig. 6.26). The reactivated/ deactivated **92**/ sand mixture was loaded onto the stainless steel column (4 mL). The column equilibrated with isopropyl alcohol followed by isopropyl acetate. A solution of (S)-**103** (0.21 g, 2.1 mmol) in isopropyl acetate (20 mL) was pumped through the catalyst at 80 °C at 0.25 mL min<sup>-1</sup> ( $t_{Res} = 16$  minutes). Each sample (50  $\mu$ L) from each RV was diluted into ethyl acetate (950  $\mu$ L) and methanol (100  $\mu$ L). Benzoyl chloride (10  $\mu$ L) was added and the samples were analysed by chiral GC. The catalyst/ sand mixture was unloaded after the reaction, washed with isopropyl alcohol and decanted. The solid was dried in vacuum oven for further reactivation/ deactivation studies.

### 6.2.8. Deactivation of immobilised SCRAM 92 with methylamine in flow

The deactivation procedure was carried out using configuration B of the flow racemisation set-up (Fig. 2.20(b) and Fig. 6.26). Used **92** (0.32 g)/ sand (5.5 g) mixture was loaded onto the stainless steel column (4 mL). The column was equilibrated with isopropyl alcohol at 0.25 mL min<sup>-1</sup> by a syringe pump at 80 °C. A 0.2 M solution of methylamine/ tetrahydrofuran (1.7 M, 6 mL) in isopropyl acetate (44 mL) was pumped through the catalyst at 0.01 mL min<sup>-1</sup> at 80 °C ( $t_{\text{Res}} = 6.7$  hours) for 4 days. The activity of the catalyst was then checked via the racemisation of (S)-**103** in flow using the procedures described in Section 6.2.7.

### 6.2.9. NMR titration of methylamine-bound SCRAM 64 with hydroiodic acid

Catalyst **64** (3.1 mg, 2.7 μmol, 5.3 μmol iridium) and benzene (8.3 mg, 10 μL, 0.1 mmol) were dissolved into *d*<sub>6</sub>-dimethyl sulfoxide (0.64 mL). The sample was analysed by <sup>1</sup>H NMR (500 MHz). Methylamine/ methanol solution (2 M, 53.3 μL, 0.11 mmol) was added and the mixture was shaken for 60 seconds. <sup>1</sup>H NMR was recorded. Aqueous hydroiodic acid (1.5 M) was added as shown in Table 6.13. After each addition, the sample was shaken for 60 seconds and <sup>1</sup>H NMR was recorded.

Total HI (equiv.) <sup>[a]</sup>	Total HI (μmol)	Vol. of HI (aq) added (μL)	Total vol. of HI (aq) (μL)
0	0	0	0
0.5	2.7	1.8	1.8
1	5.4	3.6	1.8
2	10.7	7.1	3.5
5	26.7	17.8	10.7
10	53.3	35.5	17.7
15	80.0	53.3	17.8
20	106.7	71.1	17.8

Table 6.13 Addition of HI (aq, 1.5 M) to **64** in *d*<sub>6</sub>-DMSO (0.64 mL)

### 6.2.10. General procedures for deuterium/ proton exchange of chiral amines by $d_8$ -isopropyl alcohol

Catalyst **64** (29.1 mg, 25.0  $\mu\text{mol}$ ) was added to a microwave tube with a magnetic stirrer. The chiral amine (1 mmol) was dissolved into  $d_8$ -isopropyl alcohol (766  $\mu\text{L}$ ) and  $d_8$ -toluene (306  $\mu\text{L}$ ). The mixture was analysed by  $^1\text{H}$  NMR (300 MHz). Then it was added to **64** and the reaction mixture was heated to 110  $^\circ\text{C}$  by microwave. After each hour of heating, the reaction mixture was cooled down to room temperature and was sampled for  $^1\text{H}$  NMR analysis after which the NMR sample was poured back to the reaction mixture and heated to 110  $^\circ\text{C}$  by microwave again. The heating, cooling and sampling process was repeated for 4 to 6 hours. For amines **39** and **101**, a  $d_6$ -DMSO insert (which was prepared by filling a melting point capillary tube with  $d_6$ -DMSO and sealed at both ends) was placed into the NMR sample for analysis.

### 6.2.11. Attempted racemisation of Rasagiline (*R*)-**109** by microwave

Catalyst **64** (29.2 mg, 25.1  $\mu\text{mol}$ ) was added to a microwave tube with a magnetic stirrer. (*R*)-**109** (0.17 g, 0.99 mmol) and *n*-hexadecane (15.4 mg, 68  $\mu\text{mol}$ ) was dissolved into isopropyl alcohol (766  $\mu\text{L}$ ) and toluene (306  $\mu\text{L}$ ). The mixture was sampled (10  $\mu\text{L}$ ) and diluted into methanol (990  $\mu\text{L}$ ) and was analysed by chiral GC. The solution of (*R*)-**109**/ *n*-hexadecane was then added to **64** and the reaction mixture was heated to 110  $^\circ\text{C}$  by microwave. After each hour of heating, the reaction mixture was cooled down to room temperature and was sampled for chiral GC analysis. The reaction mixture was heated to 110  $^\circ\text{C}$  by microwave again. The heating, cooling and sampling process was repeated for 4 hours. Chiral GC showed about 73% drop in the peak area ratio of (*R*)-**109**/ *n*-hexadecane whilst the racemisation of (*R*)-**109** was not observed.

## 6.3 Resolution-Racemisation-Recycle ( $\text{R}^3$ )

### 6.3.1. Diastereomeric resolution of chiral amines

#### (a) 6,7-Dimethoxy-1-methyl-1,2,3,4-tetrahydroisoquinoline **9** (Table 3.1)

Racemic **9** (0.15 g, 0.72 mmol) and (*S*)-**34** (0.11 g, 0.72 mmol) were both dissolved into ethyl acetate/ alcohol 7:1 (v/v) (4 mL and 1 mL respectively). The solution of **9** was added to the solution of (*S*)-**34** to produce a slurry which was

stirred at room temperature for 6 hours and then filtered. The reaction flask was rinsed with small amount of ML to wash off any residual solid. The solid was dried in air and analysed by  $^1\text{H}$  NMR (in  $\text{CDCl}_3$ , 500 MHz) for de determination.

**(b) 2-Methylpiperidine 103 (Table 3.5)**

Using a similar procedure as for **9** (Section 5.3.1(a)), (*S*)-**34** (0.21 g, 1.4 mmol) was dissolved into the designated solvent and added to *rac*-**103** (0.14 g, 1.4 mmol). Their mixture was seeded with diastereomerically pure (*R*)-**103**-(*S*)-**34** (7.0 mg, 27.9  $\mu\text{mol}$ , 5% w/w) and stirred for 6 hours before filtration. The solid was analysed by  $^1\text{H}$  NMR (in  $\text{CDCl}_3$ , 500 MHz) for de determination.

**(c) N-Methyl- $\alpha$ -methylbenzylamine 39**

**(i) Using (*S*)-34 as resolving acid (Table 3.7)**

Using a similar procedure as for **9** (Section 5.3.1(a)), (*S*)-**34** (0.11 g, 0.72 mmol) was dissolved into the designated solvent (3.7 mL) and added to *rac*-**39** (0.1 g, 0.74 mmol). The mixture was seeded with diastereomerically pure (*R*)-**39**-(*S*)-**34** (5.0 mg, 17.4  $\mu\text{mol}$ , 5% w/w) and stirred for 6 h before filtration. The solid was analysed by  $^1\text{H}$  NMR (in  $\text{CDCl}_3$ , 500 MHz) for de determination.

**(ii) Using (*S,S*)-32 as resolving acid (Table 3.13, entries 1 to 3)**

Using a similar procedure as for **9** (Section 5.3.1(a)), (*S,S*)-**32** (0.14 g, 0.35 mmol) and *rac*-**39** (96.6 mg, 0.70 mmol) were both dissolved into the designated solvent mixture (4 and 1 mL respectively). The solution of (*S,S*)-**32** was added to the solution of **39** and the mixture was stirred at room temperature for 6 h and then filtered. A sample of the isolated solid was dissolved into aqueous  $\text{Na}_2\text{CO}_3$  (10% w/v, 700  $\mu\text{L}$ ) and extracted with ethyl acetate (700  $\mu\text{L}$ ). The ethyl acetate layer was dried by anhydrous  $\text{MgSO}_4$  and filtered through a plug of celite. The sample was reacted with trifluoroacetic anhydride (80  $\mu\text{L}$ ) and analysed by chiral GC for ee determination of the free amine (equivalent to de of the crystals). Similar procedures were employed by changing the concentration of **39** (Table 3.13, entries 4 and 5), equivalence of (*S,S*)-**32** (Table 3.13, entries 6 to 8) and replacing methanol with isopropyl alcohol (Table 3.13, entries 9 and 10). The volume was kept at 5 mL.

Diastereomeric crystallisations of **39** with (*S,S*)-**32** at larger scale (20 mL) were carried out using a similar procedure described above. The reaction was sampled and monitored with time (Fig. 3.24).

#### *Sampling method*

A sample (300  $\mu$ L) was removed and filtered through a syringe filter (0.45  $\mu$ m pore). The filtrate was diluted into ethyl acetate (1.2 mL) and basified with aqueous sodium carbonate solution (10% w/v, 1.5 mL). The ethyl acetate layer was dried by anhydrous  $\text{MgSO}_4$  and filtered by a plug of celite. The sample was analysed by achiral GC and was then reacted with trifluoroacetic anhydride and further analysed by chiral GC. The solid collected in the syringe filter was dissolved into methanol and dried *in vacuo*. The residue was weighed, dissolved into aqueous sodium carbonate solution (10% w/v, 700  $\mu$ L) and extracted with ethyl acetate (700  $\mu$ L). The ethyl acetate layer was treated as described for the filtrate. A sample was also taken prior to the addition of (*S,S*)-**32**. However no filtration was required.

Racemic **39** (0.27 g, 2.0 mmol) and *n*-decane (14.6 mg, 0.1 mmol) were dissolved into ethyl acetate/ methanol 8:2 (20 mL) in a glass CSTR (50 mL) at the designated temperature (Huber-controlled). The mixture was sampled. (*S,S*)-**32** (0.38 g, 0.98 mmol) was added and the mixture was stirred at the designated rate. A slurry was formed and the reaction was sampled after 2 min. The reaction was continuously stirred and sampled throughout the reaction at specific times. After the designated time, the reaction mixture was filtered. The CSTR was rinsed with minimum amount of the ML and the solid was dried in air. The conditions employed were summarised in Table 6.14.

Entry	[1] (M)	(S,S)-32 (equiv.)	T (°C) <sup>[a]</sup>	Stirring rate (rpm)	Stirring time (h)	De (%) <sup>[b]</sup>	Yield (%) <sup>[c]</sup>
1	0.14	0.49	0	300-500	52	6	60
2	0.14	0.49	10	300-500	55	6	64
3	0.14	0.49	25	300-500	30	6	65
4	0.14	0.49	40	300-500	30	9	55
5	0.14	0.49	25	0	52	18	51
6	0.14	0.49	25	100	30	4	69
7	0.14	0.49	25	400	36	4	68
8	0.14	0.49	25	1000	30	1	44 <sup>[d]</sup>
9	0.07	0.49	25	400	36	76	23
10	0.21	0.49	25	400	12	3	76
11	0.14	0.25	25	400	36	83	22
12 <sup>[e]</sup>	0.14	0.49	25	400	30	7	67
13 <sup>[f]</sup>	0.14	0.49	25	400	30	5	71

Table 6.14 Experimental conditions employed in temperature-controlled diastereomeric crystallisation of **39** with (S,S)-**32** with reaction monitoring. <sup>[a]</sup>Temperature was controlled by Huber. <sup>[b]</sup>De corresponds to the ee of the free amine. <sup>[c]</sup>The mass of all samples were included in the calculation of the total yield and any seeds were excluded. <sup>[d]</sup>Some crystals were lost during filtration. <sup>[e]</sup>The reaction was seeded with pure [(S)-**39**]<sub>2</sub>-(S,S)-**32** (5% w/w). <sup>[f]</sup>The reaction was seeded with (S)-**39**-(S,S)-**32**-(R)-**39** (5% w/w)

#### (d) N-Isopropyl- $\alpha$ -methylbenzylamine **101** (Table 3.9)

Using a similar procedure as for **9** (Section 5.3.1(a)), (S)-**34** (93 mg, 0.61 mmol) was dissolved into the designated solvent (6 mL) and added to *rac*-**101** (0.10 g, 0.61 mmol). The mixture was stirred for 6 hours before filtration.

#### (e) $\alpha$ -Methylbenzylamine **42** (Table 3.11)

Using a similar procedure as for **9** (Section 5.3.1(a)), (S)-**34** (0.11 g, 0.70 mmol) was dissolved into the designated solvent (5 mL) and was added to *rac*-**42** (85.7 mg, 0.7 mmol). The mixture was stirred for 6 hours before filtration. A sample of the isolated solid was dissolved into aqueous Na<sub>2</sub>CO<sub>3</sub> (10% w/v, 2 mL) and extracted with ethyl acetate (2 mL). The ethyl acetate layer was dried by anhydrous MgSO<sub>4</sub> and filtered through a plug of celite. The solvent was removed *in vacuo* and the residue was re-dissolved into methanol (1 mL). Triethylamine

(20  $\mu\text{L}$ ) and benzoyl chloride (10  $\mu\text{L}$ ) were added to the sample and was analysed by chiral HPLC for ee determination of the free amine (equivalent to de of the crystals).

**(f) *N,N*-Dimethyl- $\alpha$ -methylbenzylamine **46** (Table 3.15)**

Using a similar procedure as for **9** (Section 5.3.1(a)), (*S,S*)-**32** (0.23 g, 0.67 mmol) and *rac*-**46** (0.1 g, 0.67 mmol) were both dissolved into the designated solvent (3.8 and 1 mL respectively). The solution of (*S,S*)-**32** was added to the solution of **46** and the mixture was stirred at room temperature for 6 hours and then filtered. A small sample of the isolated solid was dissolved into aqueous  $\text{Na}_2\text{CO}_3$  (10% w/v, 1 mL) and extracted with ethyl acetate (1 mL). The ethyl acetate layer was dried by anhydrous  $\text{MgSO}_4$  and filtered through a plug of celite. (*S*)-**34** solution in methanol (0.14 M, 100  $\mu\text{L}$ ) was added and the mixture was sonicated for 5 to 10 minutes. The solvent was removed *in vacuo* and the residue was analysed by  $^1\text{H}$  NMR (in  $\text{CDCl}_3$ , 500 MHz) for ee determination of the free amine (equivalent to de of the crystals).

**6.3.2. General procedures for the diastereomeric resolution of 6,7-dimethoxy-1-methyl-1,2,3,4-tetrahydroisoquinoline **9** with (*S*)-mandelic acid **9** in flow**

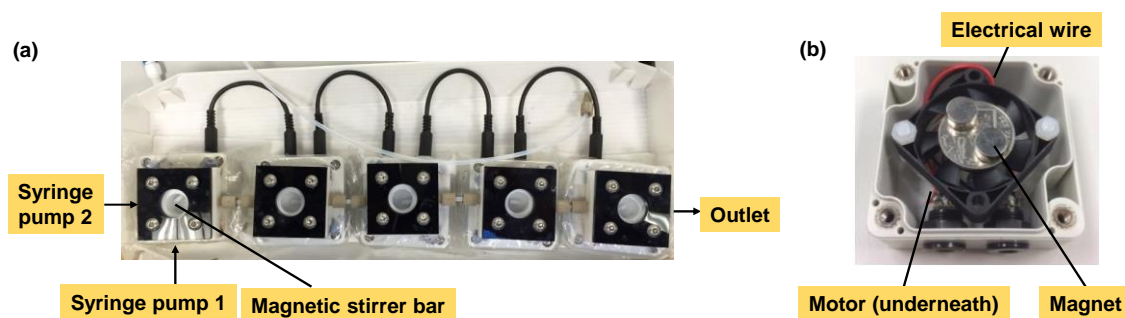


Fig. 6.27 (a) Experimental set-up of the Freactors in series; (b) Inner assembly of the electrical motor beneath each Freactor for stirring

The diastereomeric resolution of *rac*-**9** described in Table 3.2, entry 5 was described as an example. Five Freactors (volume of each = 2 mL) were connected, with the first Freactor having three pots whilst the other four Freactors having two pots (Fig. 6.27). Two syringes (20 mL) filled with ethyl acetate/methanol 7:1 (v/v) were connected to two of the pots of the first Freactor and the

whole set up was held in a vertical orientation with the syringes at the bottom. The Freactors were fully filled with the solvent mixture by pushing the syringes manually. The Freactors were placed onto the magnetic stirrer motors. They were further flushed with the same solvent at a total of  $0.5 \text{ mL min}^{-1}$  ( $0.25 \text{ mL min}^{-1}$  for the solvent from each syringe) to ensure no leakage and air bubbles present in the system. Racemic **9** (3.48 g, 16.8 mmol) and (*S*)-**34** (1.28 g, 8.4 mmol) were dissolved separately into ethyl acetate/ methanol 7:1 (v/v) (60 mL each). The solution of **9** was warmed to about  $40 \text{ }^\circ\text{C}$  with stirring until all solid dissolved and was cooled back to room temperature. The solutions of amine **9** and acid **34** were pumped through the Freactors at  $0.25 \text{ mL min}^{-1}$  each with stirring. The slurry was collected at the outlet of the last Freactor in RVs. After all solutions in the syringes were consumed, the system was flushed with ethyl acetate/ methanol 7:1 (v/v) until all solids were washed out. All collected fractions, including all the washings, were filtered to yield a white powdery solid (1.4 g in total, 24%) with an average de of 91% from  $^1\text{H NMR}$  in  $\text{CDCl}_3$  (500 MHz).

The flow resolution reactions were carried out with different number of Freactors at different flow rates (Table 3.2). The scale of all reactions was based on 12 RVs. In most cases, the reactors were blocked at the middle of the run. When blockage was observed (in which the syringes stopped moving), the pumps were stopped and the system was flushed with ethyl acetate/ methanol 7:1 (v/v) to wash out the solids from the Freactors. The yields were calculated based on the amount of **9** which reacted with **34**.

### 6.3.3. Crystal solubility measurement

Diastereomerically pure crystals prepared as described in Section 6.1 were added to the designated solvents/ solvent mixtures until some remained undissolved. Each slurry was stirred at room temperature overnight and was filtered to yield a saturated solution. A known volume of the filtrate was removed and dried *in vacuo*. The residue was dissolved into  $\text{CDCl}_3$  or  $d_6$ -DMSO, with known amount of external standard added. The sample was analysed by  $^1\text{H NMR}$  and the mass of the crystal present in the NMR sample (hence in the known volume of saturated solution) was calculated by Eqn. 5.2.<sup>186</sup>



$$m_{(X)} = P_{(IS)} \times \frac{MW_{(X)}}{MW_{(IS)}} \times \frac{nH_{(IS)}}{nH_{(X)}} \times \frac{m_{(IS)}}{P_{(X)}} \times \frac{A_{(X)}}{A_{(IS)}} \quad (\text{Eqn. 5.2})$$

Where  $m_{(X)}$  and  $m_{(IS)}$  are the masses of the crystals in the sample and internal standard in mg;  $P_{(X)}$  and  $P_{(IS)}$  are the purities of the crystals and internal standard which were assumed to be 100%;  $MW_{(X)}$  and  $MW_{(IS)}$  are the molecular weights of the crystal and internal standard in  $\text{g mol}^{-1}$ ;  $nH_{(X)}$  and  $nH_{(IS)}$  are the number of protons generating the signals of the crystals and internal standard selected for integration in the  $^1\text{H NMR}$ ;  $A_{(X)}$  and  $A_{(IS)}$  are the integrations of the selected signals correspond to the crystals and internal standard, all respectively.

The solubility (in  $\text{mg mL}^{-1}$ ) was calculated by Eqn. 5.3.

$$\text{Solubility} = \frac{m_{(X)}}{V} \quad (\text{Eqn. 5.3})$$

Where  $V$  is the volume of the saturated solution removed in mL and dried *in vacuo*.

The solubility of various pure diastereomeric salts was determined and summarised in Table 6.15.

Diastereomer	Solvent <sup>[a]</sup>	External standard	Solubility (mg mL <sup>-1</sup> )	Difference (fold) <sup>[b]</sup>
(S)-9-(S)-34	EtOAc/ MeOH 7:1	<i>n</i> -Decane	10.2	4
(R)-9-(S)-34	EtOAc/ MeOH 7:1	<i>n</i> -Decane	2.9	
(S)-9-(S)-34	EtOAc/ <sup>i</sup> PrOH 7:1	<i>n</i> -Decane	3	4
(R)-9-(S)-34	EtOAc/ <sup>i</sup> PrOH 7:1	<i>n</i> -Decane	0.7	
(S)-9-(S)-34	EtOAc/ EtOH 7:1	<i>n</i> -Decane	4.5	3.6
(R)-9-(S)-34	EtOAc/ EtOH 7:1	<i>n</i> -Decane	1.3	
(S)-103-(S)-34	<sup>i</sup> PrOAc	<i>n</i> -Decane	7.5	3
(R)-103-(S)-34	<sup>i</sup> PrOAc	<i>n</i> -Decane	2.4	
(S)-101-(S)-34	EIB <sup>[c]</sup>	Toluene	145.3	484
(R)-101-(S)-34	EIB <sup>[c]</sup>	Toluene	0.3	
(S)-39-(S)-34	<sup>i</sup> PrOAc	<i>n</i> -Decane	25.2	7
(R)-39-(S)-34	<sup>i</sup> PrOAc	<i>n</i> -Decane	3.6	
[(S)-39] <sub>2</sub> -(S,S)-32	EtOAc/ MeOH 9:1	<sup>n</sup> BuOAc	0.5	6
[(R)-39] <sub>2</sub> -(S,S)-32	EtOAc/ MeOH 9:1	<sup>n</sup> BuOAc	3	
[(S)-39] <sub>2</sub> -(S,S)-32	EtOAc/ MeOH 85:15	<sup>n</sup> BuOAc	0.4	23
[(R)-39] <sub>2</sub> -(S,S)-32	EtOAc/ MeOH 85:15	<sup>n</sup> BuOAc	9.3	
[(S)-39] <sub>2</sub> -(S,S)-32	EtOAc/ <sup>i</sup> PrOH 8:2	<sup>n</sup> BuOAc	0.9	4.5
[(R)-39] <sub>2</sub> -(S,S)-32	EtOAc/ <sup>i</sup> PrOH 8:2	<sup>n</sup> BuOAc	0.2	
[(S)-39] <sub>2</sub> -(S,S)-32	EtOAc/ MeOH 8:2	<sup>n</sup> BuOAc	2.3	11
[(R)-39] <sub>2</sub> -(S,S)-32	EtOAc/ MeOH 8:2	<sup>n</sup> BuOAc	24.9	
(S)-46-(S,S)-32 <sup>[d]</sup>	<sup>i</sup> PrOAc/ <sup>i</sup> PrOH 7:3	<sup>n</sup> BuOAc	3.7	4
(R)-46-(S,S)-32 <sup>[d]</sup>	<sup>i</sup> PrOAc/ <sup>i</sup> PrOH 7:3	<sup>n</sup> BuOAc	14.2	
(S)-46-(S,S)-32 <sup>[d]</sup>	<sup>i</sup> PrOAc/ EtOH 7:3	<sup>n</sup> BuOAc	9.5	5
(R)-46-(S,S)-32 <sup>[d]</sup>	<sup>i</sup> PrOAc/ EtOH 7:3	<sup>n</sup> BuOAc	44.1	

Table 6.15 Solubility data of various diastereomeric salts determined by <sup>1</sup>H NMR (500 MHz, 32 scans, relaxation delay = 2.49 s, acquisition time = 2.1825 min). CDCl<sub>3</sub> and d<sub>6</sub>-DMSO were used as the NMR solvents for the salts of (S)-34 and (S,S)-32 respectively. <sup>[a]</sup>The ratios correspond to volume ratios. <sup>[b]</sup>The difference was determined as the solubility ratio of the less soluble salt to the more soluble salt. <sup>[c]</sup>Ethyl isobutyrate. <sup>[d]</sup>NMR acquisition parameters: 64 scans, relaxation delay = 2 s, acquisition time = 3.0672 min

#### 6.3.4. DSC and TGA measurements for the diastereomeric salts of **39** with **(S,S)-32**

The measurements were carried out by T. Howell from School of Chemical and Process Engineering, University of Leeds. Known amounts of diastereopure [(S)-**39**]<sub>2</sub>-(S,S)-**32**, [(R)-**39**]<sub>2</sub>-(S,S)-**32**, a 1:1 mixture of [(S)-**39**]<sub>2</sub>-(S,S)-**32** and [(R)-**39**]<sub>2</sub>-(S,S)-**32**, and the low de crystals from one of the diastereomeric resolution reactions were weighed into separate alumina pans. An empty alumina pan, which acted as a blank, and all four samples were heated under nitrogen from 30 to 200 °C at 5 °C min<sup>-1</sup> in the TGA2 machine. The energy input and weight loss of the samples were monitored.

#### 6.3.5. General procedures for one-pot resolution-racemisation process reaction of *N*-methyl- $\alpha$ -methylbenzylamine **39** with di-*p*-toluoyl-D-tartaric acid **(S,S)-32**

Racemic **39** (0.38 g, 2.8 mmol) and *n*-decane (14.2 mg, 99.8  $\mu$ mol) were dissolved into ethyl acetate/ methanol 8:2 (v/v, 20 mL) in a 50 mL round bottom flask. The mixture was sampled (300  $\mu$ L) and diluted into ethyl acetate (1.2 mL), which was basified with aqueous sodium carbonate solution (10% w/v, 1.5 mL). The organic layer was separated, dried with anhydrous MgSO<sub>4</sub>, filtered through a plug of celite and analysed by achiral GC. Then the sample was derivatised with trifluoroacetic anhydride (60  $\mu$ L) and analysed by chiral GC. **(S,S)-32** (0.53 g, 1.34 mmol) was added to the solution of *rac*-**39**/ *n*-decane and the mixture was stirred at room temperature until it turned cloudy. After 2 minutes, the slurry (300  $\mu$ L) was sampled and filtered through a syringe filter (0.45  $\mu$ m). The filtrate was treated as described above. The solid collected from the syringe filter was dissolved into methanol and dried *in vacuo*. The white solid was weighed and analysed by <sup>1</sup>H NMR in *d*<sub>6</sub>-DMSO (500 MHz). SCRAM **64** or Shvo's catalyst **55** (56.3  $\mu$ mol) was then added and the reaction was sampled at specific times for 55 hours. After the reaction, the mixture was filtered to give a coloured solid. The solid and the filtrate were analysed as described above. The conditions and results were summarised in Table 6.16.

Entry		1	2
Reaction conditions	Catalyst (mg)	64 (65.4)	55 (62)
	(S,S)-32 (g) [mmol, Equiv.]	0.53 [1.34, 0.49]	0.5 [1.26, 0.45]
Results	Crystal colour	Orange	Yellow
	Yield (%)	63	57
	Initial crystal de (%)	72	71
	Final crystal de (%)	2	5
	39 in ML (%)	27	32
	ML ee (%)	16	17

Table 6.16 Reaction conditions and results for the one-pot resolution-racemisation reaction of **39** with (S,S)-**32** using racemisation catalyst **64** or **55**

### 6.3.6. Resolution-Racemisation-Recycle ( $R^3$ ) processes of chiral amines

#### (a) 6,7-Dimethoxy-1-methyl-1,2,3,4-tetrahydroisoquinoline **9**

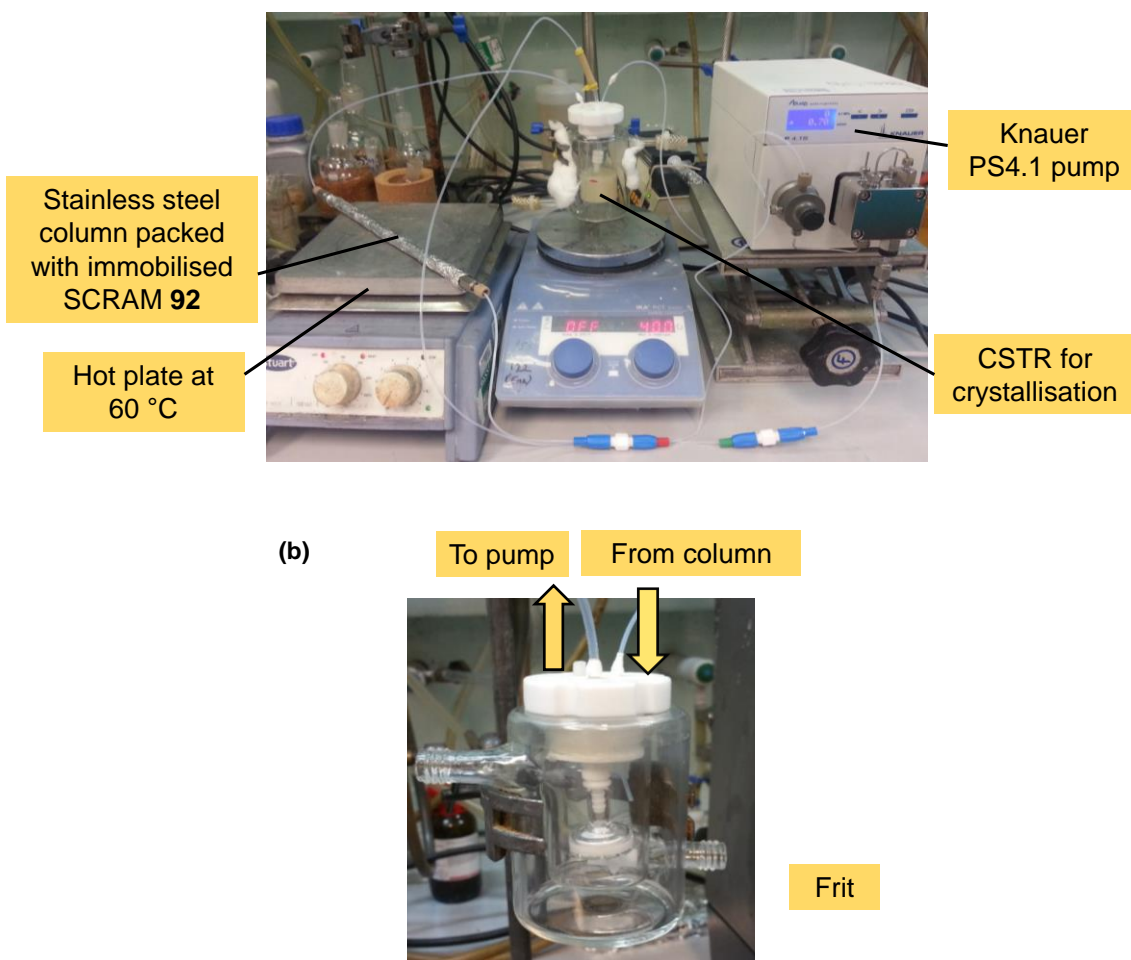


Fig. 6.28(a) Experimental set-up for the  $R^3$  processes of **9**; (b) The frit held in the CSTR and its connection to the pump and the column

The experimental set-up for the R<sup>3</sup> processes of **9** was shown in Fig. 6.28(a). A 50 mL glass CSTR was fitted with a PTFE lid with two ports (3 mm I.D.). A frit was held inside the CSTR and connected to the inlet of a HPLC pump (Knauer PS4.1) *via* a port with PTFE tubing (Fig. 6.28(b)). The outlet of the pump was connected to the inlet of the reactor column and the outlet was fed into the CSTR via another port (Fig. 6.28(b)).

The total reactor volume of the system (RV, 25 mL) was determined by pumping a known volume of reaction solvent from a beaker through the whole set-up until the CSTR was filled with 20 mL solvent. RV equals the difference in the original and the remaining volumes of the solvent in the beaker. Residence times were determined as,

$$\begin{aligned} t_{\text{Res}} (\text{Racemisation}) &= \frac{\text{Volume of packed bed column (mL)}}{\text{Flow rate (mL min}^{-1}\text{)}} \\ &= \frac{4 \text{ mL}}{0.5 \text{ mL min}^{-1}} = 8 \text{ min} \end{aligned}$$

$$\begin{aligned} t_{\text{Res}} (\text{Whole R}^3 \text{ process}) &= \frac{\text{Total volume of R}^3 \text{ system (mL)}}{\text{Flow rate (mL min}^{-1}\text{)}} \\ &= \frac{25 \text{ mL}}{0.5 \text{ mL min}^{-1}} = 50 \text{ min} \end{aligned}$$

#### (i) Sampling method

The reaction was sampled throughout for achiral and chiral HPLC analysis. A sample (200  $\mu\text{L}$ ) was filtered with a syringe filter (0.45  $\mu\text{m}$ ) and diluted into ethyl acetate (800  $\mu\text{L}$ ). It was then basified by equal volume of aqueous sodium carbonate solution (10% w/v, 1 mL). The organic layer was separated and analysed by achiral GC. The solid collected in the filter was dissolved in dichloromethane and the solvent was removed *in vacuo* to give a white solid, which was weighed and dissolved in methanol for chiral HPLC analysis. An initial sample was taken prior to the addition of (*S*)-mandelic acid **34**. Samples were taken after each  $t_{\text{Res}}$  of the process (50 min) for the designated number of cycles.

**(ii) General Procedure A: with slow addition of (S)-34**

A stainless steel HPLC column (4 mL) was packed with immobilised SCRAM **92** (ICP 7.4%, 0.36 g, 0.14 mmol iridium) and was equilibrated with the reaction solvent at 0.5 mL min<sup>-1</sup> at room temperature. Then the column was wrapped with aluminium foil and heated to about 60 °C using a hotplate. In the CSTR, *rac*-**7** (0.58 g, 2.8 mmol) and *n*-hexadecane (22.5 mg, 0.099 mmol) were dissolved in the designated solvent system (20 mL). (S)-**34** (0.21 g, 1.4 mmol) was added to the solution of **9** at the start of the reaction. The mixture slowly turned milky upon stirring at room temperature. After 2 minutes the pump was started (*t* = 0). More (S)-**34** (0.21 g, 1.4 mmol) was dissolved in the reaction solvent (5 mL) and added to the CSTR *via* a syringe pump from cycle 2 onwards. Detailed calculations of the flow rate employed for each cycle was shown in the Appendix (Section 8.4). After the final cycle, the reaction mixture was filtered. The solid was dried in air overnight. Both the solid and the filtrate were analysed as described in the sampling method (i). The column was washed by pumping ethyl acetate/methanol through whilst cooling to room temperature and reused for further experiments without unloading the column. The conditions of the R<sup>3</sup> reaction of **9** with slow addition of (S)-**34** were varied and summarised in Table 3.3.

**(iii) General Procedure B: complete addition of (S)-34 before ML recirculation**

A stainless steel HPLC column (4 mL) was packed with immobilised SCRAM **92** (ICP 7.4%, 0.36 g, 0.14 mmol iridium) and was equilibrated with the reaction solvent at 0.5 mL min<sup>-1</sup> at room temperature. Then the column was wrapped with aluminium foil and heated to about 60 °C using a hotplate. In the CSTR, *rac*-**9** (0.58 g, 2.8 mmol) and *n*-hexadecane (22.5 mg, 0.099 mmol) were dissolved in the reaction solvent (20 mL). Samples were taken as described after each *t*<sub>Res</sub> (50 min) for the designated number of cycles. (S)-**34** (0.42 g, 2.7 mmol) was added into the amine solution and the mixture slowly turned milky upon stirring at room temperature. After 2 minutes the pump was started (*t* = 0). After the final cycle, the reaction mixture was filtered. The solid was dried in air overnight. Both the solid and the filtrate were analysed as described in the sampling method (i). The column was washed by pumping ethyl acetate/methanol through whilst cooling to room temperature and reused for further experiments. The R<sup>3</sup> reaction

conditions of **9** were varied and summarised in Table 3.4. After the last R<sup>3</sup> process of **9**, the racemisation of (*S*)-**9** was carried out in flow to assess the activity of the catalyst (Section 6.3.9).

### (b) 2-Methylpiperidine **103**

A similar procedure as General Procedure B was used. The experimental set-up was modified for amines **103**, **39**, **101** and **46** (Fig. 6.29). The column was heated in an aluminium block by an electrical heating unit. A Jasco pump was used to recirculate the ML. The parameters used for the R<sup>3</sup> processes of **103** were shown in Table 6.17. The reactions were seeded with (*R*)-**103**-(*S*)-**34** (5% w/w) and the slurry was stirred for 10 minutes before recirculation of the ML. The reactions were sampled using similar sampling method described for amine **9** whilst the organic layer was dried with MgSO<sub>4</sub> and filtered through a plug of celite. After the samples were analysed by achiral GC, they were derivatised with acetic anhydride (10 μL) to form the corresponding amide for chiral GC analysis. The final crystals and those from each sample were analysed by <sup>1</sup>H NMR in CDCl<sub>3</sub> (500 MHz). The same packed catalyst was used in all three R<sup>3</sup> processes of **103**. Racemisation of **103** was carried out in flow after each R<sup>3</sup> process to assess the activity of the catalyst (Section 6.2.7).

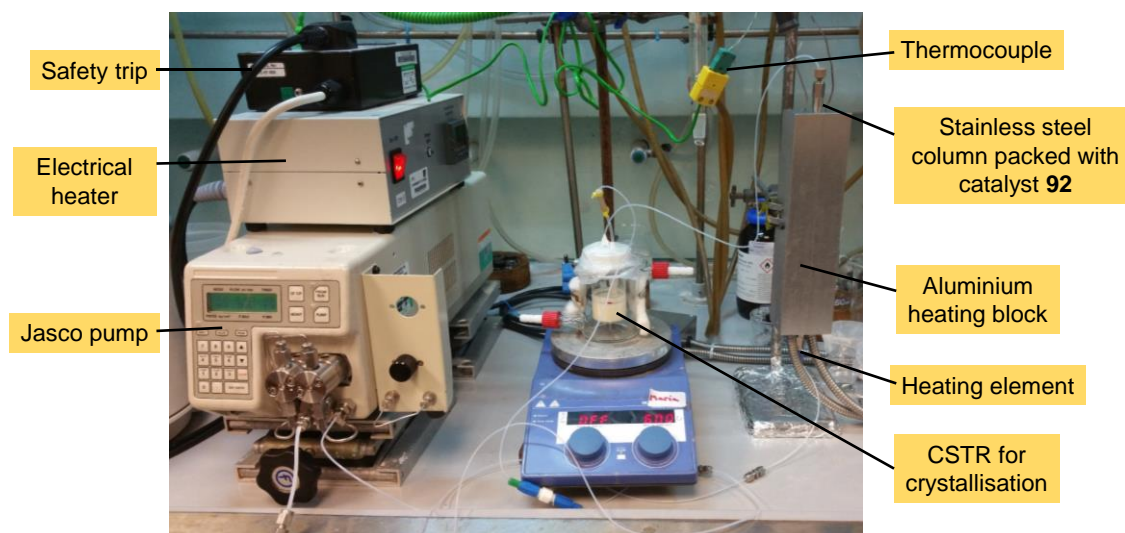


Fig. 6.29 Modified experimental set-up for the R<sup>3</sup> processes of amines **103**, **39**, **101** and **46**

Parameters	Entry		
	1	2	3
<i>rac</i> - <b>103</b> (mmol)	2.8	5	7
Solvent	<sup>i</sup> PrOAc	<sup>i</sup> PrOAc	<sup>i</sup> PrOAc
( <i>S</i> )- <b>34</b> added before ML recirculation (equiv.)	0.9	0.9	0.9
ICP of <b>92</b> (%)	6.3	6.3	6.3
Loading of Ir (mmol%)	7	4	2.8
Internal standard, <i>n</i> -decane (mmol)	0.2	0.4	0.4
Sampling volume (μL)	200	150	150
Volume of diluent in samples, EtOAc (μL)	1800	2850	2850
Racemisation T (°C)	80	80	80
Crystallisation T (°C)	r.t.	r.t.	r.t.
Column volume (mL)	4	4	4
Total RV (mL)	28.5	28.5	28.5
Flow rate (mL min <sup>-1</sup> )	0.25	0.25	0.25
Racemisation t <sub>Res</sub> (min)	16	16	16
Overall t <sub>Res</sub> (min)	114	114	114
No. of cycles	6	16	16
Process time (h)	10	30	30

Table 6.17 Parameters of the R<sup>3</sup> processes of **103**. The entries correspond to those in Table 3.6

**(c) N-Methyl- $\alpha$ -methylbenzylamine 39**

**(i) (*S*)-34 as the resolving acid**

A similar procedure as General Procedure B was used. The catalyst was mixed with sand and was filled into the column. The parameters used were shown in Table 6.18. The reaction was seeded with (*R*)-**39**-(*S*)-**34** (5% w/w) and the slurry was stirred for 10 minutes before recirculation of the ML. The reactions were sampled using similar sampling method described for amine **9** while the organic layer was dried with MgSO<sub>4</sub> and filtered through a plug of celite. After the samples were analysed by achiral GC, they were derivatised with trifluoroacetic anhydride (60 to 80 μL) to form the corresponding amide for chiral GC analysis. The final crystals and those from each sample were analysed by <sup>1</sup>H NMR in CDCl<sub>3</sub> (500 MHz). Fresh immobilised SCRAM **92** was used after each R<sup>3</sup> process.



Racemisation of (S)-**103** was carried out in flow after each R<sup>3</sup> process to assess the activity of the catalyst (Section 6.2.7).

Parameters	Entry	
	1	2
<i>rac</i> - <b>39</b> (mmol)	4	6
Solvent	<sup>i</sup> PrOAc	<sup>i</sup> PrOAc
Additives (equiv.)	-	<b>58</b> (1)
(S)- <b>34</b> added before ML recirculation (equiv.)	0.9	0.9 <sup>[a]</sup>
ICP of <b>92</b> (%)	6.3	7.7
Loading of Ir (mol%)	3.7	3
Internal standard, <i>n</i> -decane (mmol)	0.2	0.4
Sampling volume (μL)	100	75
Volume of diluent, EtOAc (μL)	900	1425
Racemisation T (°C)	80	80
Crystallisation T (°C)	r.t.	12
Column volume (mL)	4	4
Total RV (mL)	28.5	28.5
Flow rate (mL min <sup>-1</sup> )	0.1	0.1
Racemisation t <sub>Res</sub> (min)	40	40
Overall t <sub>Res</sub> (min)	285	285
No. of cycles	40	70
Process time (h)	190	333

Table 6.18 Parameters of the R<sup>3</sup> processes of **39** with (S)-**34**. The entries correspond to those in Table 3.8. <sup>[a]</sup>The slurry of **39**/ (S)-**34** was stirred for 1 h before ML recirculation

## (ii) (S,S)-**32** as the resolving acid

General Procedure B was used for entries 1 and 2 in Table 3.14 and General Procedure A was used for entries 3 and 4 in Table 3.14. The parameters used were summarised in Table 6.19.

Parameters	Entry			
	1	2	3	4
General Procedure	B	B	A	A
<i>rac</i> - <b>39</b> (mmol)	2.8	4.2	4.2	4.2
Co-solvent <sup>[a]</sup>	MeOH	MeOH	MeOH	<i>i</i> PrOH
( <i>S,S</i> )- <b>32</b> added before ML recirculation (Equiv.)	0.49	0.49	0.25	0.25 <sup>[b]</sup>
Rate of ( <i>S,S</i> )- <b>32</b> addition as a 4 mL solution ( $\mu\text{L min}^{-1}$ )	-	-	10 <sup>[c]</sup>	10 <sup>[d]</sup>
ICP of <b>92</b> (%)	7.7	7.7	7.7	7.7
Loading of Ir (mol%)	5	4	4 <sup>[e]</sup>	4
Internal standard, <i>n</i> -decane (mmol)	0.1	0.2	0.2	0.2
Sampling volume ( $\mu\text{L}$ )	150	75	75	75
Volume of diluent, EtOAc ( $\mu\text{L}$ )	750	675	675	675
Racemisation T ( $^{\circ}\text{C}$ )	65	65	65	70
Crystallisation T ( $^{\circ}\text{C}$ )	0	5	12	12
Column volume (mL)	4	4	4	4
Total RV (mL)	28.5	28.5	28.5	28.5
Flow rate ( $\text{mL min}^{-1}$ )	0.1	0.1	0.1	0.1
Racemisation $t_{\text{Res}}$ (min)	40	40	40	40
Overall $t_{\text{Res}}$ (min)	285	285	285	285
No. of cycles	41	10	25	35
Process time (h)	195	48	119	166

Table 6.19 Parameters of the  $R^3$  processes of **39** with (*S,S*)-**32**. The entries correspond to those in Table 3.14. <sup>[a]</sup>All solvent systems contained EtOAc (80% v/v) and alcohol as the co-solvent (20% v/v). <sup>[b]</sup>The slurry of **39**/*S,S*-**32** was stirred for 1 h before ML recirculation. <sup>[c]</sup>The solution of (*S,S*)-**32** was pumped into the CSTR after 5 cycles of recirculation. <sup>[d]</sup>The solution of (*S,S*)-**32** was pumped into the CSTR after 7 cycles of recirculation. <sup>[e]</sup>The catalyst from entry 2 was reused without unloading from the column

The catalyst was mixed with sand and was filled into the column. The slurry of **39**/*S,S*-**32** in the CSTR was stirred for 10 minutes before recirculation of the ML. The reactions were sampled using similar sampling method described for amine **9** while the organic layer was dried with  $\text{MgSO}_4$  and filtered through a plug of celite. After the samples were analysed by achiral GC, they were derivatised with trifluoroacetic anhydride (60 to 80  $\mu\text{L}$ ) to form the corresponding amide for

chiral GC analysis. The final crystals and those from each sample were dissolved into aqueous sodium carbonate solution (10% w/v, 700  $\mu$ L) and extracted with ethyl acetate (700  $\mu$ L). The organic layer was dried by anhydrous  $\text{MgSO}_4$ , filtered through a plug of celite and derivatised with trifluoroacetic anhydride (80  $\mu$ L). The sample was analysed by chiral GC. Fresh immobilised SCRAM **92** was used after each  $\text{R}^3$  process. Racemisation of (S)- **103** was carried out in flow after each  $\text{R}^3$  process to assess the activity of the catalyst (Section 6.2.7). When General Procedure A was used, (S,S)-**32** (0.41 g, 1.1 mmol, 0.25 equiv.) was added into the CSTR as a solution (4 mL reaction solvent) by a syringe pump at 10  $\mu\text{L min}^{-1}$  after 5 or 7 cycles of ML recirculation.

**(d) N-Isopropyl- $\alpha$ -methylbenzylamine 101**

A similar procedure as General Procedure B was used. The catalyst was mixed with sand and was filled into the column. The parameters used were shown in Table 6.20. The slurry containing **101** and (S)-**34** was stirred for 10 minutes before recirculation of the ML. Two separate samples were prepared during each sampling: Both samples (60  $\mu$ L) were filtered and diluted into ethyl acetate (540  $\mu$ L). One sample was basified by aqueous sodium carbonate solution (10% w/w, 600  $\mu$ L) whilst the other sample was basified by aqueous sodium hydroxide solution (0.2 M, 600  $\mu$ L). The organic layers were dried with  $\text{MgSO}_4$  and filtered through a plug of celite. The former sample was for achiral GC analysis. The latter sample was derivatised with trifluoroacetic anhydride (150  $\mu$ L) for chiral GC analysis. The final crystals and those from each sample were analysed by  $^1\text{H}$  NMR in  $\text{CDCl}_3$  (500 MHz). Fresh immobilised SCRAM **92** was used after each  $\text{R}^3$  process. Racemisation of (S)-**103** was carried out after each  $\text{R}^3$  process to assess the activity of the catalyst (Section 6.2.7).

Parameters	Entry		
	1	2	3
<i>rac</i> - <b>101</b> (mmol)	2	2	2
Solvent	EIB <sup>[a]</sup>	<sup>i</sup> PrOAc	EIB <sup>[a]</sup>
( <i>S</i> )- <b>34</b> added before ML recirculation (Equiv.)	0.9	0.9	0.98
ICP of <b>92</b> (%)	6.3	6.3	6.3
Loading of Ir (mol%)	5.3	5.3	5.3
Internal standard, <i>n</i> -decane (mmol)	0.2	0.2	0.2
Sampling volume (μL)	60	60	60
Volume of diluent, EtOAc (μL)	540	540	540
Racemisation T (°C)	80	80	80
Crystallisation T (°C)	r.t.	r.t.	r.t.
Column volume (mL)	4	4	4
Total RV (mL)	28.5	28.5	28.5
Flow rate (mL min <sup>-1</sup> )	0.05	0.05	0.05
Racemisation t <sub>Res</sub> (min)	40	40	40
Overall t <sub>Res</sub> (min)	570	570	570
No. of cycles	11	20	30
Process time (h)	105	190	285

Table 6.20 Parameters of the R<sup>3</sup> processes of **101**. The entries correspond to those in Table 3.10. <sup>[a]</sup>Ethyl isobutyrate

### (e) α-Methylbenzylamine **42**

A similar procedure as General Procedure B was used. The Knauer PS4.1 pump was used while the column was heated in an aluminium block by the electrical heating unit. The parameters used were shown in Table 6.21. The **42**/ (*S*)-**34** slurry was stirred for 10 minutes before recirculation of the ML. The reactions were sampled using similar sampling method described for amine **9** while the organic layer was dried with MgSO<sub>4</sub> and filtered through a plug of celite. After the samples were analysed by achiral GC, the sample was dried *in vacuo* and the residue was re-dissolved into methanol (1 mL). Triethylamine (20 μL) and benzoyl chloride (20 μL) were added and the sample was analysed by chiral HPLC. The same packed catalyst was used in both R<sup>3</sup> processes of **42**.

Parameters	Entry	
	1	2
<i>rac</i> - <b>42</b> (mmol)	2.8	2.8
Solvent	Toluene/ MeOH (5% v/v)	Toluene/ <sup>i</sup> PrOH (20% v/v)
( <i>S</i> )- <b>34</b> added before ML recirculation (Equiv.)	0.8	0.8
ICP of <b>92</b> (%)	7.4	7.4
Loading of Ir (mol%)	5	5
Internal standard, <i>n</i> -decane (mmol)	0.1	0.1
Sampling volume (μL)	400	400
Volume of diluent, EtOAc (μL)	1600	1600
Racemisation T (°C)	100	105
Crystallisation T (°C)	r.t.	r.t.
Column volume (mL)	4	4
Total RV (mL)	25	25
Flow rate (mL min <sup>-1</sup> )	0.25	0.25
Racemisation t <sub>Res</sub> (min)	16	16
Overall t <sub>Res</sub> (min)	100	100
No. of cycles	6	6
Process time (h)	10	10

Table 6.21 Parameters of the R<sup>3</sup> processes of **42**. The entries correspond to those in Table 3.12

(f) ***N,N*-Dimethyl- $\alpha$ -methylbenzylamine **46****

A similar procedure as General Procedure B was used. The catalyst was mixed with sand and was filled into the column. The parameters used were shown in Table 6.22. The slurry containing **46** and (*S,S*)-**32** was stirred for 10 minutes or 1 hour before recirculation of the ML. The reactions were sampled using similar sampling method described for amine **9** while the organic layer was dried with MgSO<sub>4</sub> and filtered through a plug of celite. After the samples were analysed by achiral GC, a solution of (*S*)-**34** (21 mg mL<sup>-1</sup> in methanol, 70 μL) was added and the mixture was sonicated, dried *in vacuo* and analysed by <sup>1</sup>H NMR in CDCl<sub>3</sub> (500 MHz). The final crystals and those from each sample were dissolved into methanol and dried *in vacuo*. The residue was dissolved into aqueous sodium carbonate solution (10% w/v, 700 μL) and extracted with ethyl acetate (700 μL).

The organic layer was dried by anhydrous MgSO<sub>4</sub> and filtered through a plug of celite. A solution of (S)-**34** (21 mg mL<sup>-1</sup> in methanol, 70  $\mu$ L) was added and the mixture was sonicated, dried *in vacuo* and analysed by <sup>1</sup>H NMR in CDCl<sub>3</sub> (500 MHz).

Parameters	Entry	
	1	2
<i>rac</i> - <b>46</b> (mmol)	1.4	1.4
Solvent	<i>i</i> PrOAc/ EtOH (30% by volume)	<i>i</i> PrOAc/ <i>i</i> PrOH (30% by volume)
(S,S)- <b>32</b> added before ML recirculation (Equiv.)	0.9 <sup>[a]</sup>	0.9 <sup>[b]</sup>
ICP of <b>92</b> (%)	7.7	7.7
Loading of Ir (mol%)	5	6
Internal standard, <i>n</i> -decane (mmol)	0.1	0.1
Sampling volume ( $\mu$ L)	150	150
Volume of diluent, EtOAc ( $\mu$ L)	600	600
Racemisation T ( $^{\circ}$ C)	72	80
Crystallisation T ( $^{\circ}$ C)	20	20
Column volume (mL)	4	4
Total RV (mL)	28.5	28.5
Flow rate (mL min <sup>-1</sup> )	0.0333	0.0333
Racemisation t <sub>Res</sub> (min)	120	120
Overall t <sub>Res</sub> (min)	855	855
No. of cycles	17	15
Process time (h)	242	214

Table 6.22 Parameters of the R<sup>3</sup> processes of **46**. The entries correspond to those in Table 3.16. <sup>[a]</sup>The slurry of **46**/ (S,S)-**32** was stirred for 10 min before ML recirculation.

<sup>[b]</sup>The slurry of **46**/ (S,S)-**32** was stirred for 1 h before ML recirculation

### 6.3.7. Attempted racemisation of (S)-**34**

Immobilised SCRAM **92** (91.8 mg, ICP 7.4%, 0.035 mmol Ir) was added to a three-neck round bottom flask under nitrogen. A solution of (S)-**34** (0.10 g, 0.69 mmol) in ethyl acetate/ methanol (7:1 by volume, 5 mL) was charged and the reaction was heated to 60  $^{\circ}$ C for 24 hours. The reaction was sampled (200  $\mu$ L)

before heating and during the reaction. The sample was dried *in vacuo* and the residue was re-dissolved into methanol (1 mL). The samples were analysed by chiral HPLC. No racemisation was observed.

### 6.3.8. Attempted racemisation of triethylammonium (S)-mandelate **34**

Similar procedures as the racemisation of (S)-**34** were employed in that of Et<sub>3</sub>N-(S)-**34**. Et<sub>3</sub>N-(S)-**34** (0.47 g, 1.9 mmol) was dissolved into ethyl acetate/ methanol (7:1 by volume, 13.6 mL). The stock solution (5 mL) was charged into a three-neck round bottom flask containing **92** (91.3 mg, ICP 7.4%, 0.035 mmol). No racemisation was observed after 24 hours of heating to 60 °C but Et<sub>3</sub>N-**126** was suspected of being formed, as observed in both chiral HPLC and <sup>1</sup>H NMR.

### 6.3.9. Catalyst activity check of immobilised SCRAM **92** after the R<sup>3</sup> processes of **9** via the racemisation of (S)-**9** in flow

Configuration B of the flow set-up (Fig. 5.24) was used in assessing the activity of **92** after the R<sup>3</sup> processes of **9**. The stainless steel column packed with **92** (used in the R<sup>3</sup> processes of **9**) was equilibrated by pumping ethyl acetate/ methanol 7:1 (v/v) at 0.5 mL min<sup>-1</sup> and heated to 60 °C. (S)-**9** (0.4 g, 1.9 mmol) was dissolved into ethyl acetate/ methanol 7:1 (v/v, 31 mL). *n*-Hexadecane (25.8 mg, 0.11 mmol) was added to 22.6 mL of the solution of (S)-**9**. The reaction mixture was sampled (200 μL) and diluted into ethyl acetate (800 μL). The reaction mixture was pumped through the column at 0.5 mL min<sup>-1</sup> (*t*<sub>Res</sub> = 8 minutes). The first RV collected (from the first 8 minutes) was discarded and the remaining reaction mixture was collected after passing through the catalyst (cycle 1). The column was flushed with ethyl acetate/ methanol 7:1 (volume, 4 mL). The eluent from cycle 1 was pumped back across as described above and this process was repeated four times (total of 5 cycles). The eluent was sampled as described before pumped through the catalyst again. They were first analysed by GC, then the samples were dried *in vacuo* and re-dissolved into methanol (1 mL) and analysed by chiral HPLC. At the end of the reaction, the column was cooled to room temperature and flushed with ethyl acetate/ methanol 7:1 (v/v) until eluent became colourless.

## 6.4 Alternative racemisation catalysts for chiral amines

### 6.4.1. Racemisation catalyst screening

In the glove box under nitrogen atmosphere, (*R*)-**9** (0.12 g, 0.60 mmol) was dissolved into degassed toluene (12 mL) and was warmed to 50 °C for complete dissolution. Catalysts **A** to **Q** were weighed into 2 mL HPLC vials by Quantos Basic automated powder dispenser (QB5) from Mettler Toledo. Their average mole % were shown in Table 4.1. The vials were placed onto a 48-well aluminum plate. The solution of (*R*)-**9** (500  $\mu$ L, 25  $\mu$ mol) and a stirrer disc were added into each vial. The well plate was heated to 105 °C with stirring at 500 rpm. After 4 and 22 hours, the well plate was removed from the heat. The reaction mixture from each vial (50  $\mu$ L) was removed into a clean 2 mL HPLC vial. Solvent was removed *in vacuo* and methanol (1 mL) was added into each vial. The samples were analysed by chiral SFC. Same procedures were employed for the catalyst screening in isopropyl acetate and chlorobenzene at 80 and 120 °C respectively. Samples were taken after 2 and 20 hours.

### 6.4.2. Racemisation of chiral amines by catalyst **E**

#### (a) 6,7-Dimethoxy-1-methyl-1,2,3,4-tetrahydroisoquinoline **9** (Table 4.3)

##### (i) Glove box (Table 4.3, entry 1):

In the glove box under nitrogen atmosphere, (*R*)-**9** (59.6 mg, 0.29 mmol) and 4,4'-di-*tert*-butylbiphenyl (16.0 mg, 60  $\mu$ mol) were dissolved into degassed toluene (3 mL). A sample (25  $\mu$ L) was removed into a clean 2 mL HPLC vial. The mixture was added to **E** (14.8 mg, 29  $\mu$ mol) and was then heated to 100 °C with stirring at 500 rpm. Samples were taken at specific time intervals for 24 hours. All samples were dried *in vacuo*, re-dissolved into methanol (1 mL), decanted and analysed by chiral SFC. Same procedures were employed with spiking of more **E** (14.5 mg, 29  $\mu$ mol) after 6 hours (Fig. 4.4).

##### (ii) Nitrogen atmosphere outside the glove box (Table 4.3, entry 2):

The stock solution of (*R*)-**9** from Section 1 (3 mL) was added into an Amigo reactor tube containing **E** (15.3 mg, 30  $\mu$ mol). The reaction mixture was degassed and was then heated to 100 °C under nitrogen. The reaction was automatically sampled by the Amigo at specific times for 24 hours by diluting 25  $\mu$ L of reaction



mixture into methanol (500  $\mu\text{L}$ ). All samples collected were dried *in vacuo* and re-dissolved into methanol (1 mL), decanted and analysed by chiral SFC.

**(iii) Air (Table 4.3, entry 3):**

(*R*)-**9** (60.8 mg, 0.29 mmol) was dissolved into undegassed toluene (3 mL) and the solution was added to 4,4'-di-*tert*-butylbiphenyl (15.9 mg, 60  $\mu\text{mol}$ ). A sample (25  $\mu\text{L}$ ) was manually removed and diluted into methanol (500  $\mu\text{L}$ ). The reaction mixture was added into an Amigo reactor tube containing **E** (14.9 mg, 30  $\mu\text{mol}$ ) and was heated to 100 °C in air. The reaction was automatically sampled by the Amigo at specific times for 24 hours by diluting 25  $\mu\text{L}$  of reaction mixture into methanol (500  $\mu\text{L}$ ). All samples collected were dried *in vacuo*, re-dissolved into methanol (1 mL), decanted and analysed by chiral SFC.

**(b) Other substrates (Table 4.4)**

**(i) 2-Methylpiperidine 103 (Table 4.4, entries 1 and 2)**

Inside an atmosbag filled with nitrogen, (*S*)-**103** (72  $\mu\text{L}$ , 0.61 mmol) was dissolved into degassed toluene (6 mL). The solution (3 mL) was added into an ampoule reaction tube containing **E** (15.4 mg, 31  $\mu\text{mol}$ ) and a stirrer bar. The tube was sealed and the reaction was stirred and heated to 105 °C in an oil bath outside the atmosbag. After 24 hours, a reaction sample (40  $\mu\text{L}$ ) was diluted into ethyl acetate (1960  $\mu\text{L}$ ) and filtered through a plug of celite. Benzoyl chloride (10  $\mu\text{L}$ ) was added and analysed by chiral GC. An additional reaction was carried out at the same time with elemental mercury (0.4 mL, 27 mmol) being added into the reaction mixture in the atmosbag prior to heating.

**(ii) *N*-Methyl- $\alpha$ -methylbenzylamine 39 (Table 4.4, entry 3)**

In a glove box under nitrogen atmosphere, **E** (15.6 mg, 31  $\mu\text{mol}$ ) was weighed into an ampoule reaction tube containing dried (*S*)-**39** (44  $\mu\text{L}$ , 0.3 mmol), followed by degassed toluene (3 mL). The reaction tube was sealed and the reaction was stirred and heated to 100 °C in an oil bath outside the glovebox. After 24 hours, a reaction sample (20  $\mu\text{L}$ ) was diluted into ethyl acetate (980  $\mu\text{L}$ ). The reaction sample was first analysed by achiral GC, followed by the addition of trifluoroacetic anhydride (30  $\mu\text{L}$ ). The sample was further analysed by chiral GC.

**(iii)  $\alpha$ -Methylbenzylamine 42 (Table 4.4, entry 4)**

Similar procedures as Section 5.4.2(b)(ii) was employed for the attempted racemisation of (*S*)-**42** with **E**. (*S*)-**42** (39  $\mu$ L, 0.3 mmol) was used. The reaction was sampled after 24 hours by diluting 200  $\mu$ L into methanol (1800  $\mu$ L) which was filtered and analysed by achiral GC and GCMS. Triethylamine (10  $\mu$ L) and benzoyl chloride (5  $\mu$ L) were added and further analysed by chiral HPLC.

**6.4.3. Attempted racemisation/ transfer dehydrogenation of 9 by catalyst K**

**(a) No additional hydride donor; conventional heating (Fig. 4.6)**

The stock solution from Section 1 (3 mL) was added into an Amigo reactor tube containing **K** (5.7 mg, 32  $\mu$ mol). The reaction mixture was degassed and was then heated to 100 °C under nitrogen. The reaction was automatically sampled by the Amigo at specific times for 24 hours by diluting 25  $\mu$ L of reaction sample into methanol (500  $\mu$ L). All samples collected were dried *in vacuo*, re-dissolved into methanol (1 mL), decanted and analysed by chiral SFC.

Similar procedures were employed to carry out the reaction in 1:1 toluene/ alcohol **58**. (*R*)-**9** (89.3 mg, 0.43 mmol) and 4,4'-di-*tert*-butylbiphenyl (15.9 mg, 60  $\mu$ mol) were dissolved into degassed toluene (2.5 mL) and alcohol **58** (1.5 mL) respectively under nitrogen. The reaction mixture was prepared by adding the solution of (*R*)-**9** (1.5 mL) to the solution of 4,4'-di-*tert*-butylbiphenyl. The reaction was manually sampled by diluting 25  $\mu$ L into methanol (500  $\mu$ L). The reaction mixture was charged into an Amigo reactor tube containing **K** (5.5 mg, 30  $\mu$ mol) and proceeded as described above.

**(b) No additional hydride donor; microwave heating (Table 4.5, entry 6)**

A solution of *n*-hexadecane (39.5 mg, 0.17 mmol) in degassed toluene (5.2 mL) was added to (*S*)-**9** (0.11 g, 0.52 mmol) under nitrogen. The mixture was sampled by diluting 30  $\mu$ L into methanol (970  $\mu$ L). The mixture (1.5 mL) was added to a microwave tube containing **K** (2.9 mg, 16  $\mu$ mol). The reaction was stirred and heated by microwave to 165 °C. After 1 hour, the reaction was sampled and filtered through a syringe filter. Both samples were analysed by achiral GC and chiral HPLC.

**(c) Silanes as hydride donor; microwave heating (Table 4.5, entries 3 to 5)**

A stock solution of (*S*)-**9** (0.2 M) was prepared by dissolving (*S*)-**9** (92.9 mg, 0.45 mmol) into degassed toluene (2.24 mL). The stock solution (750  $\mu$ L) and more toluene (450  $\mu$ L) were added to *n*-hexadecane (11.5 mg, 0.051 mmol). The reaction was sampled by diluting 6  $\mu$ L into methanol (194  $\mu$ L). PMHS (310  $\mu$ L, 0.17 mmol) was added. The reaction mixture was added to a microwave tube containing **K** (2.7 mg, 0.015 mmol). The reaction was stirred and heated by microwave to 165 °C. After 1 hour, the reaction was sampled by diluting 30  $\mu$ L into methanol (970  $\mu$ L) and filtered through a plug of celite. Both samples were analysed by achiral GC and chiral HPLC. The above reaction was repeated with phenylsilane and dimethyl(phenyl)silane (Table 6.23).

Entry	Silane (equiv.)	Volume of Silane ( $\mu$ L)	Stock solution of ( <i>S</i> )- <b>9</b> ( $\mu$ L)	Additional toluene ( $\mu$ L)
1	PMHS (1.1)	310	750	450
2	PhSiH <sub>3</sub> (1.5)	28	750	750
3	PhMe <sub>2</sub> SiH (4.5)	103	740	750

Table 6.23 Amount of silanes, (*S*)-**9** and toluene in the attempted racemisation of (*S*)-**9** by **K**

**(d) Hydrogen gas as hydrogen donor; conventional heating (Table 4.5, entry 2)**

(*R*)-**9** (0.105 g, 0.51 mmol) was dissolved into degassed toluene (5 mL). The stock solution of (*R*)-**9** (3 mL, 0.31 mmol of (*R*)-**9**) was added to *n*-hexadecane (68.1 mg, 0.30 mmol). The mixture was sampled by diluting 10  $\mu$ L into methanol (990  $\mu$ L), and was then added to a three-neck round bottom flask containing **K** (11.0 mg, 61  $\mu$ mol) which was initially purged with nitrogen. The system was further purged with hydrogen using a hydrogen balloon for 3 times. The reaction was stirred and heated to reflux by a pre-heat hot plate. The balloon was refilled regularly. The reaction was sampled at specific times and stirred for 8 hours. All samples were analysed by achiral GC and chiral HPLC.

## 7. Reference

1. A. J. Blacker, M. J. Stirling and M. I. Page, *Org. Process Res. Dev.*, 2007, **11**, 642-648.
2. M. Stirling, J. Blacker and M. I. Page, *Tetrahedron Letters*, 2007, **48**, 1247-1250.
3. O. Saidi, A. J. Blacker, M. M. Farah, S. P. Marsden and J. M. J. Williams, *Angew. Chem. Int. Ed.*, 2009, **48**, 7375-7378.
4. L. Rubio-Pérez, F. J. Pérez-Flores, P. Sharma, L. Velasco and A. Cabrera, *Org. Lett.*, 2009, **11**, 265-268.
5. Y. Zhang, C.-S. Lim, D. S. B. Sim, H.-J. Pan and Y. Zhao, *Angew. Chem., Int. Ed.*, 2014, **43**, 1399-1403.
6. *Chiral Amine Synthesis: Methods, Developments and Applications*, Wiley VCH, Weinheim, 2010.
7. L.-C. Sogutoglu, R. R. E. Steendam, H. M. Elias Vlieg and F. P. J. T. Rutjes, *Chem. Soc. Rev.*, 2015, **44**, 6723-6732.
8. I. Myrgorodska, C. Meinert, Z. Martins, L. L. S. d'Hendecourt and U. J. Meierhenrich, *Angew. Chem. Int. Ed.*, 2015, **54**, 1402-1412.
9. R. A. Sheldon, *Chirotechnology: Industrial Synthesis of Optically Active Compounds*, Marcel Dekker, Inc., New York, 1993.
10. N. Chhabra, M. L. Aseri and D. Padmanabhan, *International Journal of Applied and Basic Medical Research*, 2013, **3**, 16-18.
11. J. McConathy and M. J. Owens, *Primary Care Companion J. Clin. Psychiatry*, 2003, **5**, 70-73.
12. S. W. Smith, *Toxicol. Sci.*, 2009, **110**, 4-30.
13. Development of New Stereoisomeric Drugs, <https://www.fda.gov/drugs/guidancecomplianceregulatoryinformation/guidances/ucm122883.htm>, (accessed 30/5, 2017).
14. I. Agranat, H. Caner and J. Caldwell, *Nat. Rev. Drug Discovery*, 2002, **1**, 753-768.
15. H. Lorenz and A. Seidel-Morgenstern, *Angew. Chem. Int. Ed.*, 2014, **53**, 1218-1250.
16. *Progress In Medicinal Chemistry*, Elsevier Science, Amsterdam, 1997.
17. *Preparative Enantioselective Chromatography*, Blackwell Publishing, Oxford, 2005.

18. H. Pfander, *Carotenoids* Birkhäuser Basel 1996.
19. G. K. Friestad and H. Ding, *Angew. Chem. Int. Ed.*, 2001, **40**, 4491-4493.
20. K. R. Lindner, D. P. Bonner and W. H. Koster, *Kirk-Othmer Encyclopedia of Chemical Technology*, John Wiley & Sons, Inc., New York, 4th edn., 2000.
21. D. M. Floyd, A. W. Fritz and C. M. Cimarusti, *J. Org. Chem.*, 1982, **47**, 176-178.
22. H. U. Blaser, *Chem. Rev.*, 1992, **92**, 935-952.
23. G. K. Friestad, *Eur. J. Org. Chem.*, 2005, 3157-3172.
24. P. Zhou, B.-C. Chen and F. A. Davis, *Tetrahedron*, 2004, **60**, 8003–8030.
25. J. A. Ellman, T. D. Owens and T. P. Tang, *Acc. Chem. Res.*, 2002, **35**, 984-995.
26. M. North, *Principles and Applications of Stereochemistry*, Stanley Thornes (Publishers) Ltd., Cheltenham, 1998.
27. A. Johansson, *Contemp. Org. Synth.*, 1995, **2**, 393-407.
28. N. Uematsu, A. Fujii, S. Hashiguchi, T. Ikariya and R. Noyori, *J. Am. Chem. Soc.*, 1996, **118**, 4916-4917.
29. R. Noyori and S. Hashiguchi, *Acc. Chem. Res.*, 1997, **30**, 97-102.
30. G. D. Williams, R. A. Pike, C. E. Wade and M. Wills, *Org. Lett.*, 2003, **5**, 4227-4230.
31. K.-i. Fujita, Y. Enoki and R. Yamaguchi, *Tetrahedron*, 2008, **64**, 1943-1954.
32. O. Saidi, A. J. Blacker, M. M. Farah, S. P. Marsden and J. M. J. Williams, *Chem. Commun.*, 2010, **46**, 1541-1543.
33. P. Fristrup, M. Tursky and R. Madsen, *Org. Biomol. Chem.*, 2012, **10**, 2569-2577.
34. R. Kawahara, K.-i. Fujita and R. Yamaguchi, *J. Am. Chem. Soc.*, 2010, **132**, 15108-15111.
35. K.-i. Fujita, Z. Li, N. Ozekib and R. Yamaguchi, *Tetrahedron Letters*, 2003, **44**, 2687-2690.
36. Z. Wang, K. Ding and Y. Uozumi, *Handbook of Asymmetric Heterogeneous Catalysis*, Wiley-VCH, Weinheim, 2008.
37. D. Zhao and K. Ding, *ACS Catal.*, 2013, **3**, 928-944.
38. S. J. Lucas, B. D. Crossley, A. J. Pettman, A. D. Vassileiou, T. E. O. Screen, A. J. Blacker and P. C. McGowan, *Chem. Commun.*, 2013, **49**, 5562-5564.

39. S. Hussain, F. Leipold, H. Man, E. Wells, S. P. France, K. R. Mulholland, G. Grogan and N. J. Turner, *ChemCatChem*, 2015, **7**, 579 – 583.
40. F. G. Mutti, T. Knaus, N. S. Scrutton, M. Breuer and N. J. Turner, *Science*, 2015, **349**, 1525-1529.
41. H. Pellissier, *Tetrahedron*, 2008, **64**, 1563-1601.
42. H. Pellissier, *Adv. Synth. Catal.*, 2011, **353**, 1613-1666.
43. A. J. Blacker, S. Brown, B. Clique, B. Gourlay, C. E. Headley, S. Ingham, D. Ritson, T. Screen, M. J. Stirling, D. Taylor and G. Thompson, *Org. Process Res. Dev.*, 2009, **13**, 1370-1378.
44. Y. Okamoto, Y. Kawashima and K. Hatada, *J. Am. Chem. Soc.*, 1984, **106**, 5357-5359.
45. V. Šunjić, *Croat. Chem. Acta*, 2009, **82**, 503–530.
46. D.W. Armstrong , T. J. Ward , R. D. Armstrong and T. E. Beesley, *Science*, 1986, **232**, 1132-1135.
47. Y. Xiao, S.-C. Ng, T. T. Y. Tan and Y. Wang, *J. Chromatogr. A*, 2012, **1269**, 52-68.
48. E. S. Cho, J. Y. Sung, J. S. Jin and M. H. Hyun, *J. Sep. Sci.*, 2017, 1-7.
49. L. R. Sousa, G. D. Y. Sogah, D. H. Hoffman and D. J. Cram, *J. Am. Chem. Soc.*, 1978, **100**, 4569-4576.
50. P. S. Z. Gomes, Miriam Zabka, Michal Minceva, Mirjana Rodrigues, Alírio. E., *AIChE J.*, 2009, **56**, 125-142.
51. P. S. Gomes and A. E. Rodrigues, *Chem. Eng. Technol.*, 2012, **35**, 17-34.
52. M. Lämmerhofer, *J. Chromatogr. A*, 2010, **1217**, 814-856.
53. E. Fogassy, M. Nógrádi, D. Kozma, G. Egri, E. Pálovics and V. Kiss, *Org. Biomol. Chem.*, 2006, **4**, 3011-3030.
54. E. Vedejs and M. Jure, *Angew. Chem. Int. Ed.*, 2005, **44**, 3974–4001.
55. J. B. Jones, *Tetrahedron*, 1986, **42**, 3351-3403.
56. G. M. Whitesides and C.-H. Wong, *Angew. Chem., Int. Ed.*, 1985, **24**, 617-638.
57. V. Gotor, R. Brieva and F. Rebolledo, *J. Chem. Soc., Chem. Commun.*, 1988, 957-958.
58. M. B. Höhne, Uwe T., *ChemCatChem*, 2009, **1**, 42-51.
59. G. Asensio, C. Andreu and J. A. Marco, *Tetrahedron Letters*, 1991, **32**, 4197-4198.

60. A. S. de Miranda, L. S. M. Miranda and R. O. M. A. de Souza, *Org. Biomol. Chem.*, 2013, **11**, 3332-3336.
61. D. E. J. E. Robinson and S. D. Bull, *Tetrahedron: Asymmetry*, 2003, **14**, 1407-1446.
62. F. O. Arp and G. C. Fu, *J. Am. Chem. Soc.*, 2006, **128**, 14264-14265.
63. U. T. Strauss, U. Felfer and K. Faber, *Tetrahedron: Asymmetry*, 1999, **10**, 107-117.
64. M. J. Okasinski and M. F. Doherty, *Chem. Eng. Sci.*, 2003, **58**, 1289-1300.
65. Y. Wang and A. M. Chen, *Org. Process Res. Dev.*, 2008, **12**, 282-290.
66. K. Brands and A. Davies, *Chem. Rev.*, 2006, **106**, 2711-2733.
67. J. Vávra, L. Severa, P. Švec, I. Císařová, D. Koval, P. Sázelová, V. Kašička and F. Teplý, *Eur. J. Org. Chem.*, 2012, **2012**, 489-499.
68. S. Srisanga and J. H. t. Horst, *Cryst. Growth Des.*, 2010, **10**, 1808-1812.
69. K. Galan, M. J. Eicke, M. P. Elsner, H. Lorenz and A. Seidel-Morgenstern, *Cryst. Growth Des.*, 2015, **15**, 1808-1818.
70. J. Jacques, A. Collet and S. H. Wilen, *Enantiomers, Racemates and Resolutions*, Krieger, Malabar, 1994.
71. M. Breuer, K. Ditrach, T. Habicher, B. Hauer, M. Keßeler and T. Zelinski, *Angew. Chem., Int. Ed.*, 2004, **43**, 788-824.
72. M. D. Armstrong, *J. Am. Chem. Soc.*, 1951, **73**, 4456-4457.
73. F. C. Ferreira, N. F. Ghazali, U. Cocchini and A. G. Livingston, *Tetrahedron: Asymmetry*, 2006, **17**, 1337-1348.
74. R. N. Samant and S. B. Chandall, *Ind. Eng. Chem. Process Des. Dev.*, 1985, **24**, 426-429.
75. B. Chankvetadze, in *Molecular Biology in Medicinal Chemistry*, eds. T. Dingermann, D. Steinhilber and G. Folkers, Wiley-VCH, Germany, 2004, vol. 21.
76. R. Siedlecka, *Tetrahedron*, 2013, **69**, 6331-6363.
77. P. S. Dragovich, D. E. Murphy, K. Dao, S. H. Kim, L.-S. Li, F. Ruebsam, Z. Sun, C. V. Tran, A. X. Xiang and Y. Zhou, *Tetrahedron: Asymmetry*, 2008, **19**, 2796-2803.
78. J. Blacker and C. E. Headley, in *Green Chemistry in the Pharmaceutical Industry*, eds. P. J. Dunn, A. S. Wells and M. T. Williams, Wiley-VCH, Weinheim, 2010, pp. 269-288.

79. E. J. Ebbers, G. J. A. Ariaans, J. P. M. Houbiers, A. Bruggink and B. Zwanenburg, *Tetrahedron*, 1997, **53**, 9417-9476.
80. F. F. Huerta, A. B. E. Minidis and J.-E. Bäckvall, *Chem. Soc. Rev.*, 2001, **30**, 321-331.
81. S. Takano, A. Kijima, T. Sugihara, S. Satoh and K. Ogasawara, *Chem. Lett.*, 1989, **18**, 87-88.
82. E. R. Bowman, H. McKennis Jr. and B. R. Martin, *Synth. Commun.*, 1982, **12**, 871-879.
83. C. Wolf, *Dynamic Stereochemistry of Chiral Compounds: Principles and Applications*, RSC Publishing, UK, 2008.
84. *United States Pat.*, US5847215A, 1998.
85. S. Escoubet, S. Gastaldi, N. Vanthuyne, G. Gil, D. Siri and M. P. Bertrand, *Eur. J. Org. Chem.*, 2006, 3242–3250.
86. S. p. Escoubet, S. p. Gastaldi, N. Vanthuyne, G. r. Gil, D. Siri and M. I. P. Bertrand, *J. Org. Chem.*, 2006, **71**, 7288-7292.
87. S. p. Gastaldi, S. p. Escoubet, N. Vanthuyne, G. r. Gil and M. I. P. Bertrand, *Org. Lett.*, 2007, **9**, 837-839.
88. M. P. Sibi and P. Renaud, *Radicals in Organic Synthesis Volume 2: Applications*, Wiley VCH, Weinheim, 2001.
89. H.-S. Dang, B. P. Roberts, J. Sekhon and T. M. Smits, *Org. Biomol. Chem.*, 2003, **1**, 1330-1341.
90. S.-I. Murahashi, N. Yoshimura, T. Tsumiyama and T. Kojima, *J. Am. Chem. Soc.*, 1983, **105**, 5002-5011.
91. A. Parvulescu, D. De Vos and P. Jacobs, *Chem. Commun.*, 2005, 5307-5309.
92. A. H. Éll, J. S. M. Samec, C. Brasse and J.-E. Bäckvall, *Chem. Commun.*, 2002, 1144-1145.
93. J. S. M. Samec and J.-E. Bäckvall, *Chem. Eur. J.*, 2002, **8**, 2955-2961.
94. G.-Z. Wang and J.-E. Bäckvall, *J. Chem. Soc. Chem. Commun.*, 1992, 980-982.
95. O. Pámies, A. H. Éll, J. S. M. Samec, N. Hermanns and J.-E. Bäckvall, *Tetrahedron Lett.*, 2002, **43**, 4699–4702.
96. J. Paetzold and J. E. Bäckvall, *J. Am. Chem. Soc.*, 2005, **127**, 17620-17621.



97. M. J. Stirling, J. M. Mwansa, G. Sweeney, A. J. Blacker and M. I. Page, *Org. Biomol. Chem.*, 2016, **14**, 7092–7098.
98. K. Faber, *Chem. - Eur. J.*, 2001, **7**, 5004-5010.
99. N. G. Anderson, *Org. Process Res. Dev.*, 2005, **9**, 800-813.
100. M. T. Reetz and K. Schimossek, *Chimia*, 1996, **50**, 668-669.
101. L. K. Thalén and J.-E. Bäckvall, *Beilstein J. Org. Chem.*, 2010, **6**, 823-829.
102. L. K. Thalén, D. Zhao, J.-B. Sortais, J. Paetzold, C. Hoben and J.-E. Bäckvall, *Chem. Eur. J.*, 2009, **15**, 3403-3410.
103. C.-E. Hoben, L. Kanupp and J.-E. Backvall, *Tetrahedron Letters*, 2008, **49**, 977-979.
104. C.-K. Chen and A. K. Singh, *Org. Process Res. Dev.*, 2001, **5**, 508-513.
105. P. J. Reider, P. Davis, D. L. Hughes and E. J. J. Grabowski, *J. Org. Chem*, 1987, **52**, 955-957.
106. S. Negi, M. Masayuki, M. Mizuno, K. Miyake and N. Minami, *Synthesis*, 1996, 991-996.
107. C. Viedma, *Phys. Rev. Lett.*, 2005, **94**, 065504.
108. C. Viedma, *J. Cryst. Growth*, 2004, **261**, 118-121.
109. W. L. Noorduin, T. Izumi, A. Millemaggi, M. Leeman, H. Meekes, W. J. P. Van Enkevort, R. M. Kellogg, B. Kaptein, E. Vlieg and D. G. Blackmond, *J. Am. Chem. Soc.*, 2008, **130**, 1158-1159.
110. W. L. Noorduin, B. Kaptein, H. Meekes, W. J. P. van Enkevort, R. M. Kellogg and E. Vlieg, *Angew. Chem. Int. Ed.*, 2009, **48**, 4581-4583.
111. M. W. van der Meijden, M. Leeman, E. Gelens, W. L. Noorduin, H. Meekes, W. J. P. van Enkevort, B. Kaptein, E. Vlieg and R. M. Kellogg, *Org. Process Res. Dev.*, 2009, **13**, 1195-1198.
112. W. L. Noorduin, P. van der Asdonk, A. A. C. Bode, H. Meekes, W. J. P. van Enkevort, E. Vlieg, B. Kaptein, M. W. van der Meijden, R. M. Kellogg and G. Deroover, *Org. Process Res. Dev.*, 2010, **14**, 908-911.
113. S. Falß, G. Tomaiuolo, A. Perazzo, P. Hodgson, P. Yaseneva, J. Zakrzewski, S. Guido, A. Lapkin, R. Woodward and R. E. Meadows, *Org. Process Res. Dev.*, 2016, **20**, 558-567.
114. M. R. Chapman, M. H. T. Kwan, G. King, K. E. Jolley, M. Hussain, S. Hussain, I. E. Salama, C. G. Nino, L. A. Thompson, M. E. Bayana, A. D. Clayton, B. N. Nguyen, N. J. Turner, N. Kapur and A. J. Blacker, *Journal*, 2017.

115. S. Lawton, G. Steele and P. Shering, *Org. Process Res. Dev.*, 2009, **13**, 1357-1363.
116. M. E. Kopach, D. J. Roberts, M. D. Johnson, J. M. Groh, J. J. Adler, J. P. Schafer, M. E. Kobierskia and W. G. Tranklea, *Green Chem.*, 2012, **14**, 1524-1536.
117. X. Ni and N. E. Pereira, *AIChE*, 2000, **46**, 37-45.
118. X. Ni and A. Liao, *Cryst. Growth Des.*, 2008, **8**, 2875-2881.
119. C. Ricardo and N. Xiongwe, *Org. Process Res. Dev.*, 2009, **13**, 1080-1087.
120. D. L. Browne, B. J. Deadman, R. Ashe, I. R. Baxendale and S. V. Ley, *Org. Process Res. Dev.*, 2011, **15**, 693-697.
121. Y. Mo and K. F. Jensen, *React. Chem. Eng.*, 2016, **1**, 501-507.
122. R. L. Hartman, J. P. McMullen and K. F. Jensen, *Angew. Chem. Int. Ed.*, 2011, **50**, 7502-7519.
123. F. E. Valera, M. Quaranta, A. Moran, J. Blacker, A. Armstrong, J. T. Cabral and D. G. Blackmond, *Angew. Chem. Int. Ed.*, 2010, **49**, 2478-2485.
124. G. Jas and A. Kirschning, *Chem. Eur. J.*, 2003, **9**, 5708-5723.
125. N. Holmes, G. R. Akien, A. J. Blacker, R. L. Woodward, R. E. Meadows and R. A. Bourne, *React. Chem. Eng.*, 2016, **1**, 366-371.
126. H.-U. Blaser, H.-P. Buser, H.-P. Jalett, B. Pugina and F. Spindler, *Synlett* 1999, 867-868.
127. X. Li, X. Wu, W. Chen, F. E. Hancock, F. King and J. Xiao, *Org. Lett.*, 2004, **6**, 3321-3324.
128. G. Liu, J. Wang, T. Huang, X. Liang, Y. Zhang and H. Li, *J. Mater. Chem.*, 2010, **20**, 1970-1975.
129. A. F. Trindade, P. M. P. Gois and C. A. M. Afonso, *Chem. Rev.*, 2009, **109**, 418-514.
130. N. Haraguchi, K. Tsuru, Y. Arakawa and S. Itsuno, *Org. Biomol. Chem.*, 2009, **7**, 69-75.
131. M. J. Palmer and M. Wills, *Tetrahedron: Asymmetry*, 1999, **10**, 2045-2061.
132. X. Huang and J. Y. Ying, *Chem. Commun.*, 2007, 1825-1827.
133. P.-N. Liu, P.-M. Gu, J.-G. Deng, Y.-Q. Tu and Y.-P. Ma, *Eur. J. Org. Chem.*, 2005, 3221-3227.
134. D. J. Bayston, C. B. Travers and M. E. C. Polywka, *Tetrahedron: Asymmetry*, 1998, **9**, 2015-2018.
135. *Britain Pat.*, WO 2009/093059 A2, 2009.

136. M. J. Stirling, PhD thesis, The University of Huddlesfield, 2007.
137. R. Zhu, Z. Xu, W. Ding, S. Liu, X. Shi and X. Lu, *Chin. J. Chem.*, 2014, **32**, 1039-1048.
138. T. Zweifel and T. Ott, *Angew. Chem. Int. Ed.*, 2008, **47**, 3245-3249.
139. G. J. Sherborne, M. R. Chapman, A. J. Blacker, R. A. Bourne, T. W. Chamberlain, B. D. Crossley, S. J. Lucas, P. C. McGowan, M. A. Newton, T. E. O. Screen, P. Thompson, C. E. Willans and B. N. Nguyen, *J. Am. Chem. Soc.*, 2015, **137**, 4151-4157.
140. C. Davies, Master's report, University of Leeds, 2017.
141. P. Matzel, M. Gand and M. Höhne, *Green Chem.*, 2017, **19**, 385–389.
142. R. Borštnar, M. Repič, M. Kržan, J. Mavri and R. Vianello, *Eur. J. Org. Chem.*, 2011, 6419-6433.
143. C. D. M. Drew, G. T. Knight, D. T. D. Hughes and M. Bush, *Br. J. clin. Pharmacol.*, 1978, **6**, 221-225.
144. *United States Pat.*, US6372931 B1, 2002.
145. *CRC Handbook of Optical Resolutions via Diastereomeric Salt Formation*, CRC Press, Boca Raton, 2001.
146. E. L. Paul, H.-H. Tung and M. Midler, *Powder Technol.*, 2005, **150**, 133-143.
147. C. Tian, L. Gong and E. Meggers, *Chem. Commun.*, 2016, **52**, 4207-4210.
148. V. H. Vu, L.-A. Jouanno, A. Cheignon, T. Roisnel, V. Dorcet, S. Sinbandhit and J.-P. Hurvois, *Eur. J. Org. Chem*, 2013, 5464–5474.
149. M. F. A. Adamo, V. K. Aggarwal and M. A. Sage, *Syn. Commun.*, 1999, **29**, 1747-1756.
150. R. Vardanyan, *Piperidine-Based Drug Discovery*, Elsevier, USA, 2017.
151. H. M. T. B. Herath and N. P. D. Nanayakkara, *J. Heterocyclic Chem.*, 2008, **45**, 129-136.
152. Y. Patel, Master's report, University of Leeds, 2013.
153. P. R. Anandamanoharan, P. W. Cains and A. G. Jones, *Tetrahedron: Asymmetry*, 2006, **17**, 1867-1874.
154. A. W. Ingersoll, S. H. Babcock and F. B. Burns, *J. Am. Chem. Soc.*, 1933, **55**, 411-416.
155. D. G. Blackmond, *Chem. Eur. J.*, 2007, **13**, 10306-10311.
156. A. R. A. Palmans, *Mol. Syst. Des. Eng.*, 2017, **2**, 34-46.
157. *Britain Pat.*, WO2006/046059 A1, 2006.

158. H.-J. Pan, T. W. Ng and Y. Zhao, *Org. Biomol. Chem.*, 2016, **14**, 5490–5493.
159. Y.-Y. Li, S.-L. Yu, W.-Y. Shen and J.-X. Gao, *Acc. Chem. Res.*, 2015, **48**, 2587–2598.
160. K. Junge, B. Wendt, D. Addis, S. Zhou, S. Das, S. Fleischer and M. Beller, *Chem. Eur. J.*, 2011, **17**, 101 – 105.
161. R. D. Patil and S. Adimurthy, *Adv. Synth. Catal.*, 2011, **353**, 1695-1700.
162. A. Martínez-Asencio and M. Yus, *Tetrahedron*, 2011, **67**, 3140-3149.
163. O. Riant, N. Mostefaï and J. Courmarcel, *Synthesis*, 2004, 2943–2958.
164. S. Diez-Gonzalez and S. P. Nolan, *Acc. Chem. Res.*, 2008, **41**, 349-358
165. W. S. Mahoney and J. M. Stryker, *J. Am. Chem. Soc.*, 1989, **111**, 8818-8823.
166. I. Kim, S. Itagaki, X. Jin, K. Yamaguchi and N. Mizuno, *Catal. Sci. Technol.*, 2013, **3**, 2397-2403.
167. D. Amara, I. Felner, I. Nowik and S. Margel, *Colloids and Surfaces A: Physicochem. Eng. Aspects*, 2009, **339**, 106-110.
168. N. Shpaisman, E. R. Bauminger and S. Margel, *Journal of Alloys and Compounds*, 2008, **454**, 89-96.
169. S. L. Yang, C. S. Li and C. H. Cheng, *J. Chem. Soc., Chem. Commun.*, 1987, 1872-1874.
170. K. G. Caulton, M. G. Thomas, B. A. Sosinsky and E. L. Muetterties, *Proc. Nati. Acad. Sci. USA*, 1976, **73**, 4274-4276.
171. C. P. Casey and C. R. Cyr, *J. Am. Chem. Soc.*, 1973, **95**, 2248-2253.
172. M. Greenhalgh, *Iron-Catalysed Hydrofunctionalisation of Alkenes and Alkynes*, Springer, UK, 2006.
173. J. M. Blackwell, E. R. Sonmor, T. Scoccitti and W. E. Piers, *Org. Lett.*, 2000, **2**, 3921-3923.
174. G. M. Sheldrick, *Acta Crystallogr. A*, 2015, **71**, 3-8.
175. G. M. Sheldrick, *Acta Crystallogr. C*, 2015, **71**, 3-8.
176. O. V. Dolomanov, L. J. Bourhis, R. J. Gildea, J. A. K. Howard and H. Puschmann, *J. Appl. Crystallogr.*, 2009, **42**, 339-341.
177. M. Johannes and K.-H. Altmann, *Org. Lett.*, 2012, **14**, 3752-3755.
178. A. Brossi, L. A. Dolan and S. Teitel, *Organic Syntheses Collective Volume 6*, Wiley, USA, 1988.

179. J. Přeč, J. Václavík, P. Šot, J. Pecháček, B. Vilhanová, J. Januščák, K. Syslová, R. Pažout, J. Maixner, J. Zápál, M. Kuzma and P. Kačer, *Catal. Commun.*, 2013, **36**, 67-70.
180. C. Li and J. Xiao, *J. Am. Chem. Soc.*, 2008, **130**, 13208-13209.
181. A. G. Al-Sehemi, R. S. Atkinson and J. Fawcett, *J. Chem. Soc., Perkin Trans. 1*, 2002, 257–274.
182. P. S. Metkar, M. A. Scialdone and K. G. Moloy, *Green Chem.*, 2014, **16**, 4575-4586.
183. V. N. Wakchaure, P. S. J. Kaib, M. Leutzsch and B. List, *Angew. Chem. Int. Ed.*, 2015, **54**, 11852-11856.
184. M. Ezawa, K. Moriyama and H. Togo, *Tetrahedron Letters*, 2015, **56**, 6689-6692.
185. T. d. S. Fonseca, da, M. R. Silva, M. d. C. F. de Oliveira, T. L. G. de Lemos, R. d. A. Marques and M. C. de Mattos, *Appl. Catal., A*, 2015, **492**, 76-82.
186. T. Rundlöf, M. Mathiasson, S. Bekiroglu, B. Hakkarainen, T. Bowden and T. Arvidsson, *J. Pharm. Biomed. Anal.*, 2010, **52**, 645-651.

## 8. Appendix

### 8.1. Proton NMR titration of homogeneous SCRAM 64 with methylamine in $d_6$ -DMSO (Section 2.2.1(b))

#### 8.1.1. NMR integrations, number of Cp\* protons and identification of Ir-MeNH<sub>2</sub> species

The <sup>1</sup>H NMR integrations of dimer **64** and signals A to F upon the titration of **64** with methylamine (2 M in methanol) were shown in Table 1.1. Signals A to C correspond to the Cp\* protons in nearly formed iridium species whilst signals D to F correspond to the CH<sub>3</sub> group of methylamine bound to iridium.

MeNH <sub>2</sub> (equiv.)	I.S.	Dimer (1.87)	A (1.84)	B (1.72)	C (1.62)	D (2.56)	E (2.51)	F (2.45)	Free MeNH <sub>2</sub> (2.24)
0	6	1.1	0	0	0	0	0	0	0
0.5	6	0.75	0.11	0.13	0	0.02	0.06	0	0
1	6	0.53	0.11	0.32	0.02	0.02	0.12	0.01	0
2	6	0.23	0.08	0.61	0.05	0.02	0.24	0.04	0
3	6	0.01	0.02	0.87	0.1	0	0.32	0.07	0.04
4	6	0	0.01	0.75	0.25	0	0.26	0.17	0.13
5	6	0	0	0.66	0.35	0	0.24	0.23	0.23
7.5	6	0	0	0.46	0.56	0	0.18	0.37	0.58
10	6	0	0	0.35	0.68	0	0.14	0.42	0.99
15	6	0	0	0.25	0.8	0	0.1	0.53	1.87
20	6	0	0	0.19	0.84	0	0.06	0.52	2.7
30	6	0	0	0.13	0.89	0	0.06	0.56	4.53
40	6	0	0	0.12	0.9	0	0.04	0.56	5.75

Table 8.1 <sup>1</sup>H NMR integrations of **64**, signals A-F and the CH<sub>3</sub> of free MeNH<sub>2</sub> by titrating SCRAM **64** with MeNH<sub>2</sub> (2 M in MeOH). All integrations were obtained by integrating benzene (internal standard, I.S.) as 6. The value in each bracket corresponds to the chemical shift in ppm

The number of protons corresponded to each signal was summarised in Table 1.2 and was calculated as follows. Before any methylamine was added, the

integration of dimer **64** (1.87 ppm) was 1.1 which corresponds to the 30 protons of the Cp\* ring. Therefore, integration of one proton =  $1.1 \div 30 = 0.0367$ .

Number of protons for each signal = Integration  $\div$  0.0367.

The total number of Cp\* protons from dimer **64**, signals A to C was calculated as the sum of their integrations, which was between 27 to 30, indicating that the signals A to C correspond to newly formed iridium species from **64**.

MeNH <sub>2</sub> (equiv.)	Dimer (1.87)	A (1.84)	B (1.72)	C (1.62)	D (2.56)	E (2.51)	F (2.45)	Total Cp* protons
0	30.0	0.0	0.0	0.0	0.0	0.0	0.0	30
0.5	20.5	3.0	3.5	0.0	0.5	1.6	0.0	27
1	14.5	3.0	8.7	0.5	0.5	3.3	0.3	27
2	6.3	2.2	16.6	1.4	0.5	6.5	1.1	27
3	0.3	0.5	23.7	2.7	0.0	8.7	1.9	27
4	0.0	0.3	20.5	6.8	0.0	7.1	4.6	28
5	0.0	0.0	18.0	9.5	0.0	6.5	6.3	28
7.5	0.0	0.0	12.5	15.3	0.0	4.9	10.1	28
10	0.0	0.0	9.5	18.5	0.0	3.8	11.5	28
15	0.0	0.0	6.8	21.8	0.0	2.7	14.5	29
20	0.0	0.0	5.2	22.9	0.0	1.6	14.2	28
30	0.0	0.0	3.5	24.3	0.0	1.6	15.3	28
40	0.0	0.0	3.3	24.5	0.0	1.1	15.3	28

Table 8.2 Number of protons corresponded to each signal and total number of Cp\* protons

Based on the increasing and decreasing trends of the integrations of signals A to F (Fig. 2.9), signals A to C correlate to signals D to F respectively. To determine the number of methylamine bound to the iridium centre in each of the newly formed species, the ratio of the integrations of A/D, B/E and C/F were calculated at each equivalent of methylamine and an average value was obtained in each case (Table 1.3).

Assuming that species A to C are monomers with only one iridium centre and one Cp\* ring, the number of CH<sub>3</sub> protons in bound CH<sub>3</sub>NH<sub>2</sub> in each species can be

determined as 15/ ratio. The species of A to C were assigned as mono-, di- and tri-methylamine iridium complexes **95**, **96** and **97** respectively (Fig. 8.1).

MeNH <sub>2</sub> (equiv.)	A/D	B/E	C/F
0	-	-	-
0.5	5.5	2.2	-
1	5.5	2.7	2.0
2	4.0	2.5	1.3
3	-	2.7	1.4
4	-	2.9	1.5
5	-	2.8	1.5
7.5	-	2.6	1.5
10	-	2.5	1.6
15	-	2.5	1.5
20	-	3.2	1.6
30	-	2.2	1.6
40	-	3.0	1.6
<b>Average</b>	5.0	2.6	1.6

Table 8.3 Integration ratios of signals A/D, B/E and C/F

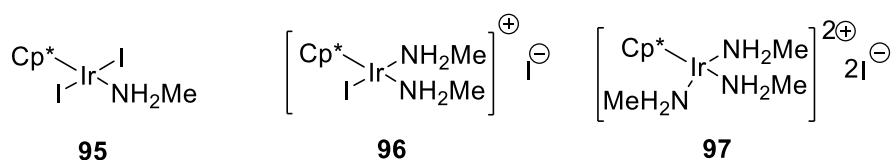


Fig. 8.1 Structures of proposed Ir-MeNH<sub>2</sub> species formed from titrating SCRAM dimer **64** with MeNH<sub>2</sub>

### 8.1.2. Calculations of the concentrations of dimer **64**, **95**, **96** and **97** in the proton NMR titration of dimer **64** with methylamine in d<sub>6</sub>-DMSO

Total reaction volume = volume of MeNH<sub>2</sub> (in MeOH) + volume of IS (benzene) + volume of d<sub>6</sub>-DMSO

Concentration of IS = No. of mole of IS ÷ Total reaction volume

The NMR integration of IS, which corresponds to 6 protons, was set to 6 in every spectrum. So the integration of one proton = 1.



When no MeNH<sub>2</sub> was added, concentration of IS = (0.117 mmol ÷ 0.61 mL) × 1000 = 190.99 mM

NMR integration of **64** = 1.1, which corresponds to 30 protons. Therefore, the concentration of **64** = (1.1 ÷ 30) × 190.99 mM = 7 mM

Similarly when 0.5 equiv. of MeNH<sub>2</sub> was added, concentration of IS = (0.117 mmol ÷ 0.611 mL) × 1000 = 190.57 mM

Concentration of **64** = (0.75 ÷ 30) × 190.57 mM = 4.76 mM

NMR integrations of **95** and **96** are 0.11 and 0.13 respectively, each corresponds to 15 protons. Therefore, concentration of **95** = (0.11 ÷ 15) × 190.57 mM = 1.4 mM; concentration of **96** = (0.13 ÷ 15) × 190.57 mM = 1.65 mM

The concentrations of **64**, **95**, **96** and **97** at different MeNH<sub>2</sub> equivalences were calculated and are shown in Table 8.4.

MeNH <sub>2</sub> (equiv.)	Total MeNH <sub>2</sub> (mM)	Total volume (μL)	IS (mM)	<b>64</b> (mM)	<b>95</b> (mM)	<b>96</b> (mM)	<b>97</b> (mM)	Free MeNH <sub>2</sub> (mM)
0	0.000	0.610	190.99	7.00	0.00	0.00	0.00	0.00
0.5	4.424	0.611	190.57	4.76	1.40	1.65	0.00	0.00
1	8.861	0.613	190.16	3.36	1.39	4.06	0.25	0.00
2	17.610	0.615	189.33	1.45	1.01	7.70	0.63	0.00
3	26.316	0.618	188.52	0.06	0.25	10.93	1.26	2.51
4	35.042	0.621	187.70	0.00	0.13	9.38	3.13	8.13
5	43.372	0.623	186.91	0.00	0.00	8.22	4.36	14.33
7.5	64.516	0.630	184.92	0.00	0.00	5.67	6.90	35.75
10	85.208	0.637	182.98	0.00	0.00	4.27	8.30	60.38
15	125.000	0.650	179.23	0.00	0.00	2.99	9.56	111.72
20	163.172	0.663	175.64	0.00	0.00	2.22	9.84	158.08
30	235.294	0.690	168.84	0.00	0.00	1.46	10.02	254.95
40	301.895	0.717	162.56	0.00	0.00	1.30	9.75	311.57

Table 8.4 Concentrations of benzene internal standard, **64**, **95**, **96**, **97** and free MeNH<sub>2</sub> with increasing equivalence of MeNH<sub>2</sub> added

## 8.2. Proton NMR titration of methylamine-bound iridium complexes with hydroiodic acid in $d_6$ -DMSO (Section 2.4.2)

Similar calculations were performed for the titration of methylamine-bound iridium complexes **95** to **97** with aqueous hydroiodic acid to determine the number of protons corresponded to each signal (Table 8.5), total number of Cp\* protons (Table 8.6) and the integration ratios of Cp\* protons to their corresponding CH<sub>3</sub> protons of bound methylamine (Table 8.7). Based on the ratios of B/E and C/F, signals B and C correspond to the Cp\* protons of di-methylamine and tri-methylamine iridium species **96** and **97** respectively; whilst signals E and F correspond to the respective CH<sub>3</sub> protons of the bound methylamine.

Reagent	Equiv. wrt Ir	I.S.	Dimer (1.89)	B (1.75)	C (1.65)	E (2.54)	F (2.47)	Free MeNH <sub>2</sub> (2.26)
MeNH <sub>2</sub>	0	6	0.78	0	0	0	0	0
	20	6	0	0.1	0.64	0.08	0.44	2.74
HI	0.5	6	0	0.14	0.62	0.08	0.38	2.74
	1	6	0	0.14	0.6	0.1	0.35	2.67
	2	6	0	0.16	0.6	0.1	0.36	2.71
	5	6	0	0.24	0.46	0.16	0.26	2.63
	10	6	0.03	0.24	0.46	0.06	0.3	2.82
	15	6	0.38	0.08	0.35	0.04	0.21	3
	20	6	0.38	0.13	0.29	0.04	0.15	2.94

Table 8.5 <sup>1</sup>H NMR integrations of dimer **64**, signals B, C, E and F, and the CH<sub>3</sub> of free MeNH<sub>2</sub> by adding methylamine (2 M in MeOH, 20 equiv.) to SCRAM **64** followed by titration with HI (aq) (1.5 M). All integrations were obtained by integrating benzene (internal standard, I.S.) as 6. The value in each bracket corresponds to the chemical shift in ppm

Reagent	Equiv. wrt Ir	Dimer (1.89)	B (1.75)	C (1.65)	E (2.54)	F (2.47)	Total Cp* protons
MeNH <sub>2</sub>	0	30.0	0.0	0.0	0.0	0.0	30
	20	0.0	3.8	24.6	3.1	16.9	28
HI	0.5	0.0	5.4	23.8	3.1	14.6	29
	1	0.0	5.4	23.1	3.8	13.5	28
	2	0.0	6.2	23.1	3.8	13.8	29
	5	0.0	9.2	17.7	6.2	10.0	27
	10	1.2	9.2	17.7	2.3	11.5	28
	15	14.6	3.1	13.5	1.5	8.1	31
	20	14.6	5.0	11.2	1.5	5.8	31

Table 8.6 Number of protons corresponded to each signal and total number of Cp\* protons

Reagent	Equiv. wrt Ir	B/E	C/F
MeNH <sub>2</sub>	0	-	-
	20	1.3	1.5
HI	0.5	1.8	1.6
	1	1.4	1.7
	2	1.6	1.7
	5	1.5	1.8
	10	4.0	1.5
	15	2.0	1.7
	20	3.3	1.9
<b>Average</b>		2.1	1.7

Table 8.7 Integration ratios of signals B/E and C/F

### 8.3. Proton NMR spectra for the determination of chiral amine racemisation *via* proton/ deuterium exchange in the presence of SCRAM 64 (Section 2.5.2(b))

#### 8.3.1. *N*-Isopropyl- $\alpha$ -methylbenzylamine 101

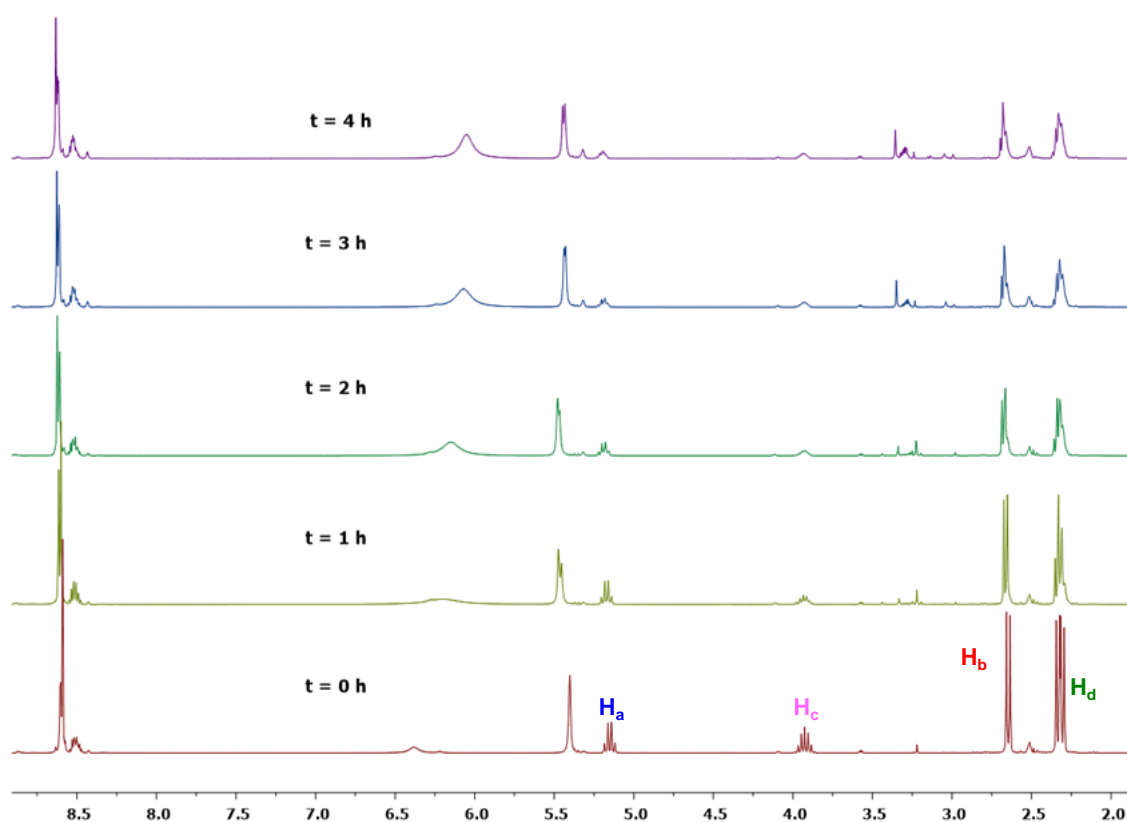
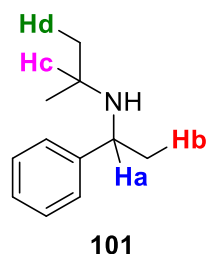


Fig. 8.2  $^1\text{H}$  NMR spectra of  $\text{H}/\text{D}$  exchange of **101** with  $d_8$ -*i*-PrOD in the presence of SCRAM **64**. The spectra were acquired with a  $D_6$ -DMSO insert. At  $t = 0$ ,  $\delta_{\text{H}}$  in ppm (300 MHz,  $d_6$ -DMSO): 8.66-8.56 (m, 4H, aromatics), 8.55-8.42 (m, 1H, aromatics), 5.15 (q,  $J = 6.6$  Hz, 1H,  $\text{H}_a$ ), 3.93 (hept,  $J = 6.3$  Hz, 1H,  $\text{H}_c$ ), 2.65 (d,  $J = 6.6$  Hz, 3H,  $\text{H}_b$ ), 2.32 (dd,  $J = 8.5$  and 6.3 Hz, 6H,  $\text{H}_d$ )<sup>140</sup>

### 8.3.2. *N*-Benzyl- $\alpha$ -methylbenzylamine **107**

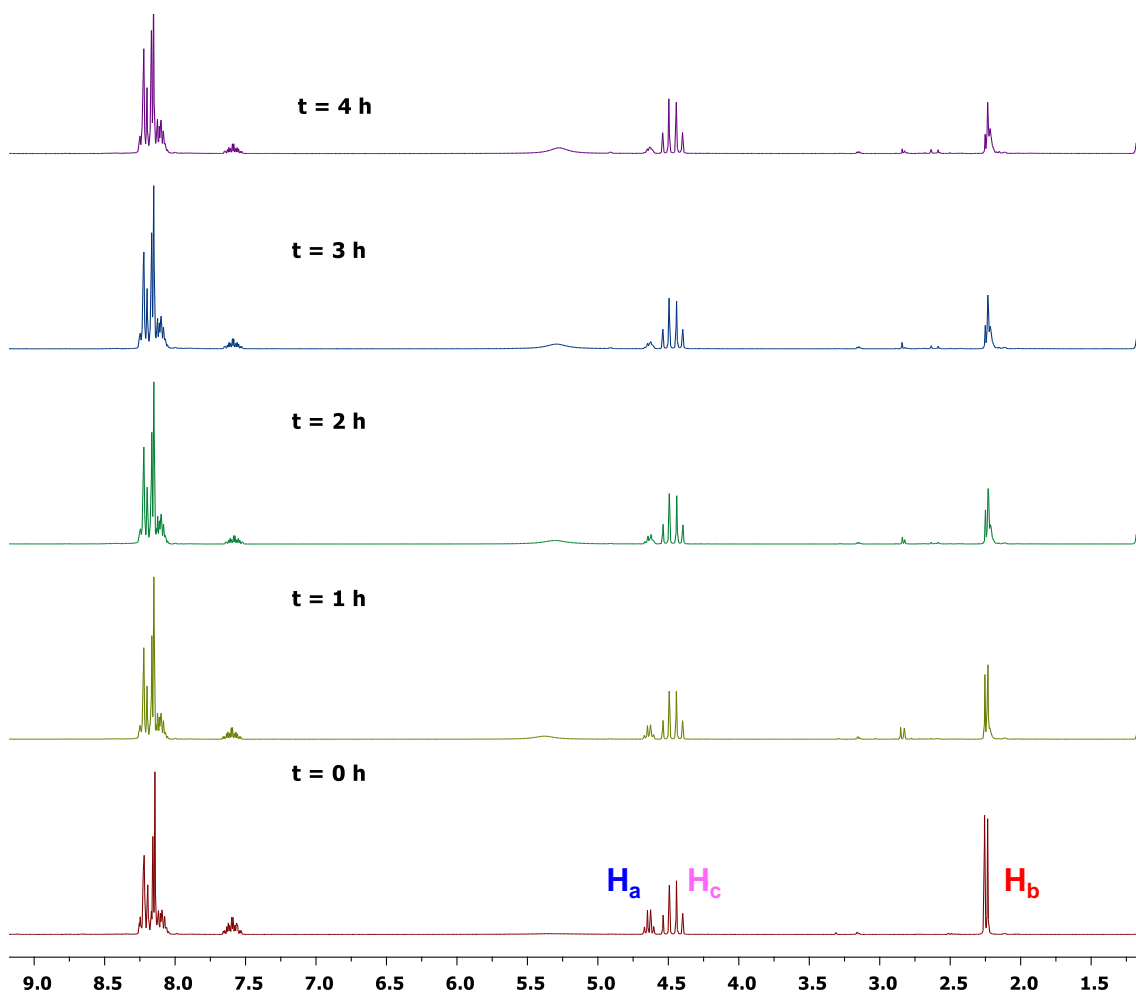
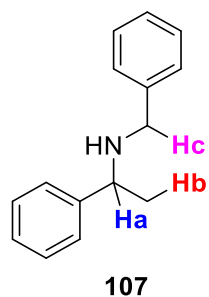


Fig. 8.3 <sup>1</sup>H NMR spectra of H/ D exchange of **107** in *d*<sub>8</sub>-*i*PrOD (with *d*<sub>8</sub>-toluene) in the presence of SCRAM **64**. At *t* = 0,  $\delta_{\text{H}}$  in ppm (300 MHz, *d*<sub>8</sub>-toluene):  $\delta$  8.29-7.96 (m, 10H, aromatics), 4.64 (q, *J* = 6.6 Hz, 1H, H<sub>a</sub>), 4.47 (q, *J* = 13.2 Hz, 2H, H<sub>c</sub>), 2.25 (d, *J* = 6.6 Hz, 3H, H<sub>b</sub>)<sup>140</sup>

### 8.3.3. *N,N*-Dimethyl- $\alpha$ -methylbenzylamine **46**

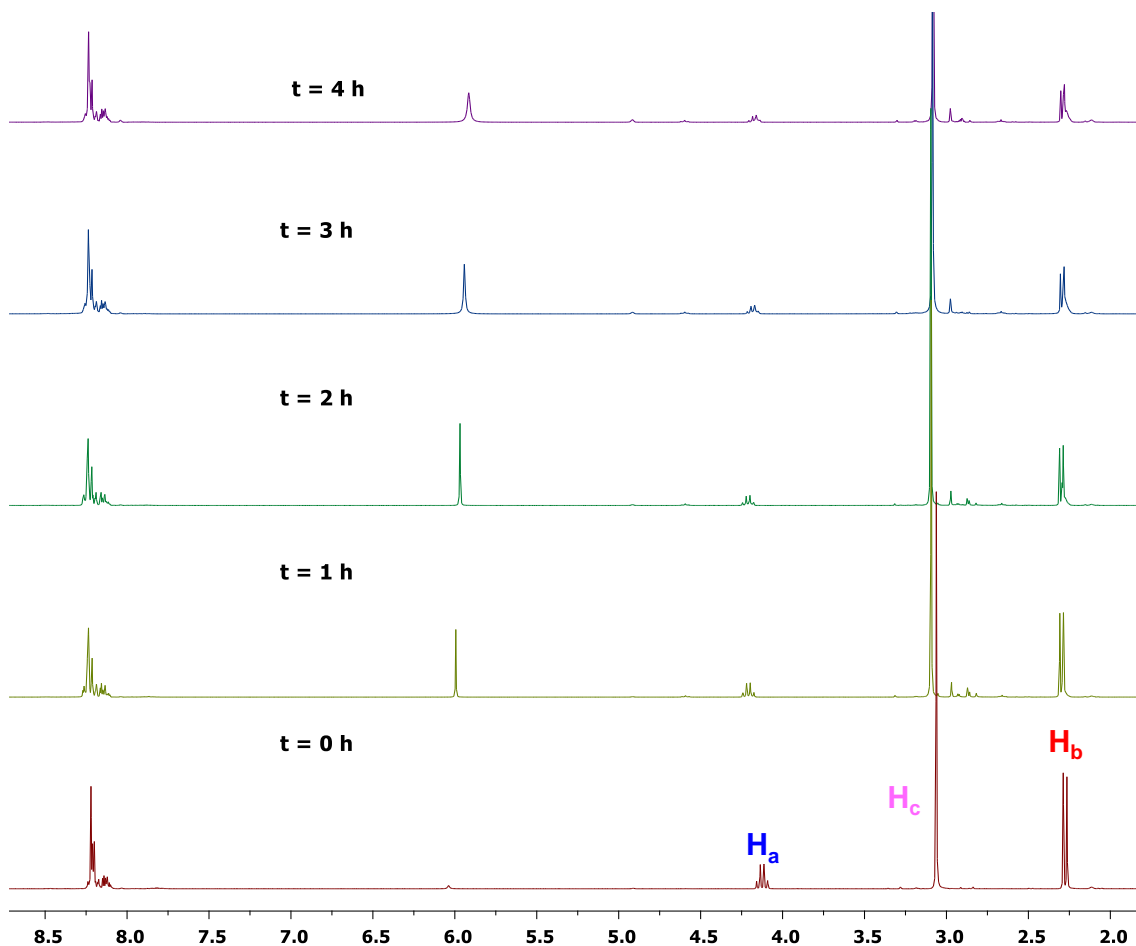
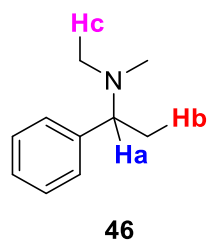
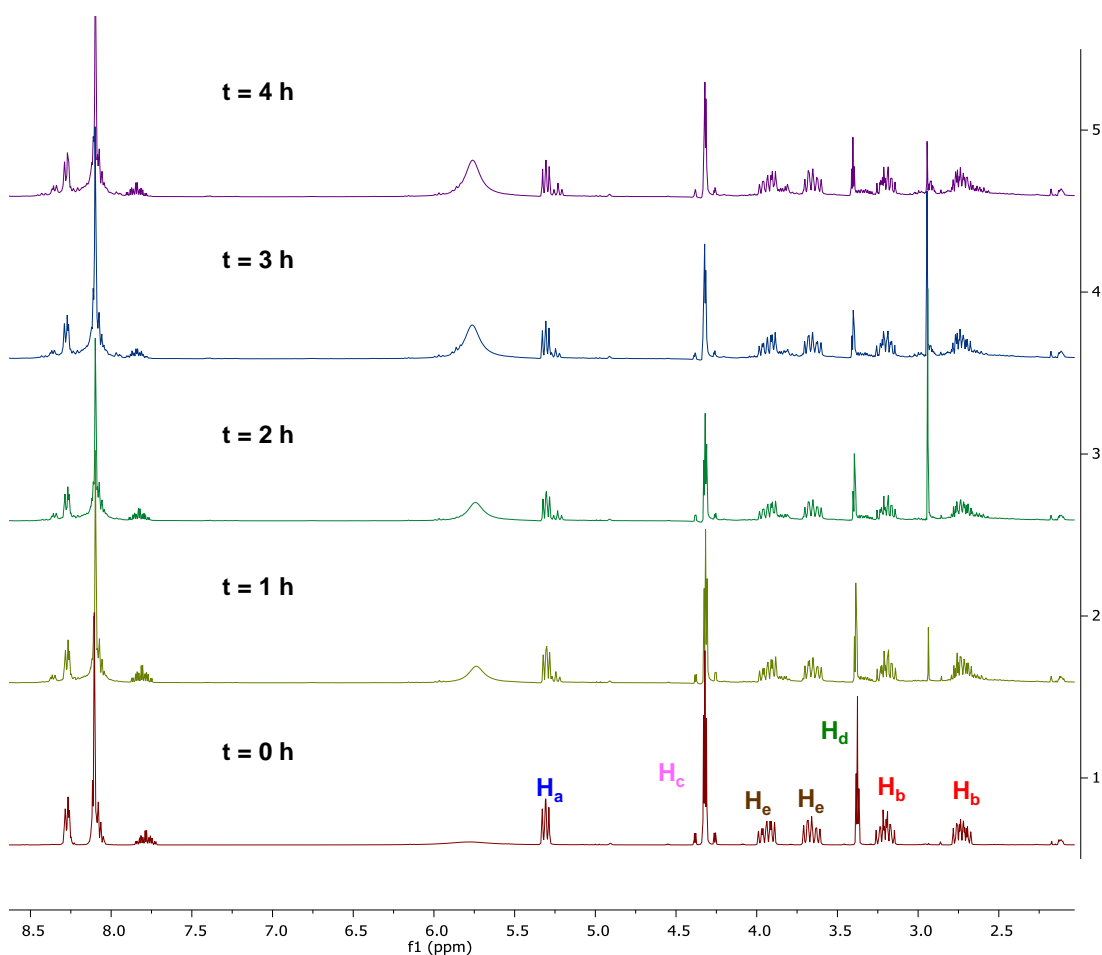
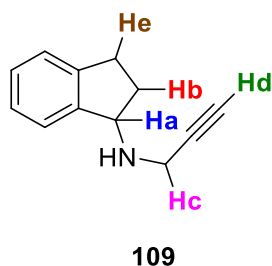


Fig. 8.4  $^1\text{H}$  NMR spectra of  $\text{H}/\text{D}$  exchange of **46** in  $d_8$ - $i$ -PrOD (with  $d_8$ -toluene) in the presence of SCRAM **64**. At  $t = 0$ ,  $\delta_{\text{H}}$  in ppm (300 MHz,  $d_8$ -toluene): 8.27-8.16 (m, 4H, aromatics), 8.16-8.08 (m, 1H, aromatics), 4.12 (q,  $J = 6.7$  Hz, 1H,  $\text{H}_a$ ), 3.06 (s, 6H,  $\text{H}_c$ ), 2.28 (d,  $J = 6.7$  Hz, 3H,  $\text{H}_b$ )

### 8.3.4. Rasagiline (*R*)-109



*Fig. 8.5* <sup>1</sup>H NMR spectra of H/ D exchange of **109** in *d*<sub>8</sub>-*i*-PrOD (with *d*<sub>8</sub>-toluene) in the presence of SCRAM **64**. At *t* = 0,  $\delta_H$  in ppm (300 MHz, *d*<sub>8</sub>-toluene): 8.35-8.17 (m, 1H, aromatics), 8.18-7.97 (m, 3H, aromatics), 5.31 (dd, *J* = 6.5 and 5.6 Hz, 1H, H<sub>a</sub>), 4.32 (ddd, *J* = 19.5, 17.1 and 2.5 Hz, 2H, H<sub>c</sub>), 3.94 (ddd, *J* = 15.1, 8.3 and 5.7 Hz, 1H, H<sub>e</sub>), 3.66 (ddd, *J* = 15.1, 8.3 and 6.3 Hz, 1H, H<sub>e</sub>), 3.38 (t, *J* = 2.5 Hz, 1H, H<sub>d</sub>), 3.29-3.12 (m, 1H, H<sub>b</sub>), 2.80-2.61 (m, 1H, H<sub>b</sub>)

### 8.3.5. *O*-Acetyl-(1*S*,2*R*)-*N*-methylephedrine **111**

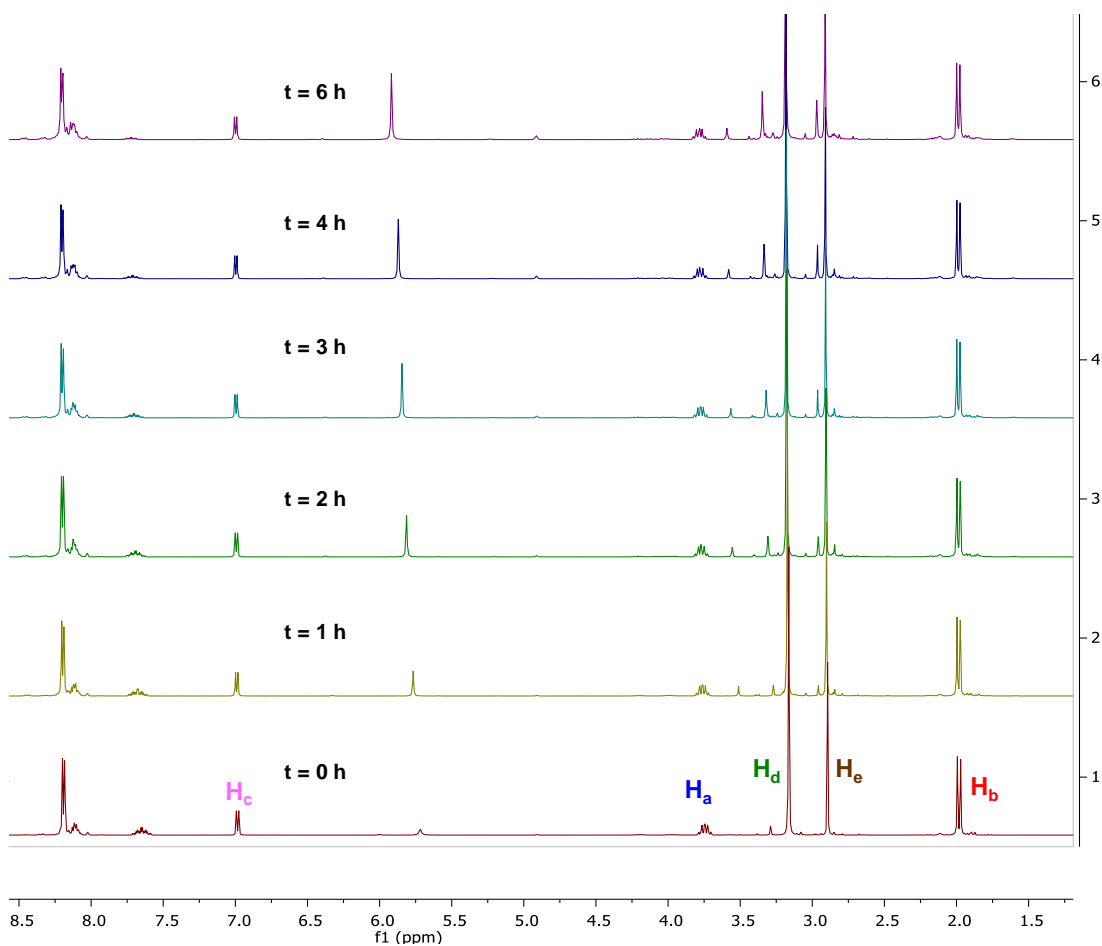
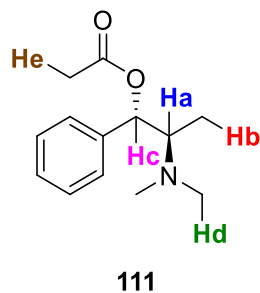


Fig. 8.6 <sup>1</sup>H NMR spectra of H/ D exchange of **111** in *d*<sub>8</sub>-*l*-PrOD (with *d*<sub>8</sub>-toluene) in the presence of SCRAM **64**. At *t* = 0, δ<sub>H</sub> in ppm (300 MHz, *d*<sub>8</sub>-toluene): 8.19 (d, *J* = 4.5 Hz, 4H, aromatics), 8.14-8.06 (m, 1H, aromatics), 6.98 (d, *J* = 5.1 Hz, 1H, H<sub>c</sub>), 3.74 (dd, *J* = 6.9 and 5.1 Hz, 1H, H<sub>a</sub>), 3.16 (s, 6H, H<sub>d</sub>), 2.89 (s, 3H, H<sub>e</sub>), 1.98 (d, *J* = 6.9 Hz, 3H, H<sub>b</sub>)



#### 8.4. Addition of (S)-mandelic acid **34** during the R<sup>3</sup> processes of **9** (Table 3.3)

Due to the unknown effect of (S)-**34** to the activity of immobilised SCRAM **92**, at the early stage of development of the R<sup>3</sup> process of **9**, (S)-**34** was added slowly to the system to minimise its concentration. The result of flow racemisation of the ML from diastereomeric resolution of *rac*-**9** with (S)-**34** using fresh **92** (10 mol% Ir) at 60 °C with a  $t_{Res}$  of 6 minutes showed a drop in ee from 38% to 11% which was > 20% for one pass through the catalyst (Table 2.9, entry 7). The ML was originally enriched with (S)-**9** and the drop in ee by 20% corresponded to 10% increase in the amount of (R)-**9**. Therefore the amount of (S)-**34** added into the system in each cycle should ideally be the same as the amount of (R)-**9** produced. On the other hand, since the concentration of **9** was decreasing with time due to its precipitation with (S)-**34**, the addition rate of (S)-**34** had to be adjusted accordingly so that it was not in excess in any time during the process.

The calculations were shown below using the first R<sup>3</sup> process of **9** with (S)-**34** as an example (Table 3.3, entry 1).

At the start of cycle 1 (after the addition of 0.5 equiv. of (S)-**34**), if 0.5 equiv. of **9** reacted with (S)-**34**, no. of moles of **9** in the system = 2.8 mmol × 0.5 = 1.4 mmol

Since no acid was added during cycle 1, no. of mole of **9** at the start of cycle 2 = 1.4 mmol.

Assume there was 20% drop in ee, increase in the concentration of (R)-**9** in cycle 2 = 10%. Therefore, no. of moles of (R)-**9** produced during cycle 2 = 1.4 mmol × 10% = 0.14 mmol, i.e. (S)-**34** required during cycle 2 = 0.14 mmol.

Since  $t_{Res} = 50$  min, (S)-**34** added per minute during cycle 2 = 0.14 mmol ÷ 50 min =  $2.8 \times 10^{-3}$  mmol min<sup>-1</sup>, which is 0.426 mg min<sup>-1</sup>.

A solution of (S)-**34** was prepared by dissolving 213 mg into 5 mL of reaction solvent (ethyl acetate/ methanol 7:1 v/v), so during cycle 2, rate of addition of (S)-**34** = 0.426 mg min<sup>-1</sup> ÷ (213 mg ÷ 5 mL) = 0.01 mL min<sup>-1</sup>.

At the start of cycle 3, no. of moles of **9** in the system =  $1.4 - 0.14 \text{ mmol} = 1.26 \text{ mmol}$ .

No. of moles of (*R*)-**9** produced during cycle 3 =  $1.26 \text{ mmol} \times 10\% = 0.126 \text{ mmol}$ ,  
i.e. (*S*)-**34** added during cycle 3 =  $0.126 \text{ mmol}$ .

Similar calculations as above were carried out until all of the 0.5 equiv. of (*S*)-**34** was consumed (213 mg). However, more than 20 cycles were required to add all the acid into the system. Therefore, in the first attempt, the process was stopped after 17 cycles, in which about 0.92 equiv. of (*S*)-**34** was added in total. The rates of addition of (*S*)-**34** in each cycle for the first attempt of  $R^3$  of **9** were shown in Table 8.8. The following assumptions were made during the calculations.

- The first 0.5 equiv. of (*S*)-**34** added into the system reacted with 0.5 equiv. of **9**; so only 0.5 equiv. of free **9** was left in the system for racemisation
- All of the (*R*)-**9** reacted with (*S*)-**34** added, so the concentration of **9** dropped by 10% after each cycle
- The catalyst did not lose activity throughout the  $R^3$  process; i.e. ee of the ML dropped by 20% which led to a 10% increase in the concentration of (*R*)-**9** after each cycle
- Constant volume of the system

Cycle	<i>rac</i> - <b>9</b> at the start (mmol)	(S)- <b>34</b> added per cycle (mmol)	(S)- <b>34</b> added per min ( $10^{-3}$ mmol)	(S)- <b>34</b> added per min (mg)	Rate of (S)- <b>34</b> addition ( $\text{mL min}^{-1}$ )
1	1.4	-	-	-	-
2	1.4	0.14	2.8	0.426	0.01
3	1.26	0.126	2.52	0.383	0.009
4	1.134	0.113	2.268	0.345	0.008
5	1.021	0.102	2.041	0.311	0.007
6	0.919	0.092	1.837	0.28	0.007
7	0.827	0.083	1.653	0.252	0.006
8	0.744	0.074	1.488	0.226	0.005
9	0.67	0.067	1.339	0.204	0.005
10	0.603	0.06	1.205	0.183	0.004
11	0.542	0.054	1.085	0.165	0.004
12	0.488	0.049	0.976	0.149	0.003
13	0.439	0.044	0.879	0.134	0.003
14	0.395	0.04	0.791	0.12	0.003
15	0.356	0.036	0.712	0.108	0.003
16	0.32	0.032	0.641	0.097	0.002
17	0.288	0.029	0.576	0.088	0.002

Table 8.8 Addition rate of (S)-**34** in the each cycle in the first attempt of  $R^3$  of **9** with (S)-**34** (Table 3.3, entry 1)

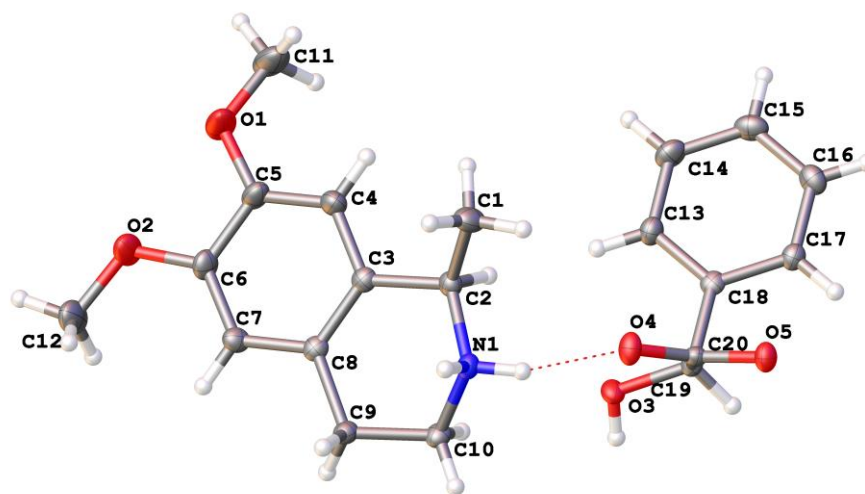
Due to the long cycle time for the process, the rates of addition were increased in each cycle in order to shorten the overall reaction time. The rate of addition in each cycle of the second attempt was increased by 50% while that of the third and fourth attempts were increased by 100% (Table 7.2).

Cycle	Rate of addition of (S)-34 solution (mL min <sup>-1</sup> ) <sup>[a]</sup>			
	Entry 1 <sup>[b]</sup>	Entry 2 <sup>[b]</sup>	Entry 3 <sup>[b]</sup>	Entry 4 <sup>[b]</sup>
1	-	-	-	-
2	0.010	0.015	0.020	0.020
3	0.009	0.014	0.018	0.018
4	0.008	0.012	0.016	0.016
5	0.007	0.011	0.014	0.014
6	0.007	0.011	0.014	0.014
7	0.006	0.009	0.012	0.012
8	0.005	0.008	0.010	0.010
9	0.005	0.008	-	-
10	0.004	0.006	-	-
11	0.004	0.006	-	-
12	0.003	-	-	-
13	0.003	-	-	-
14	0.003	-	-	-
15	0.003	-	-	-
16	0.002	-	-	-
17	0.002	-	-	-
<b>Average rate (mL min<sup>-1</sup>)</b>	0.005	0.010	0.015	0.015
<b>Average rate (mg min<sup>-1</sup>)</b>	0.22	0.43	0.63	0.63
<b>Total added (mg)<sup>[c]</sup></b>	385.5	425.9	426.0 <sup>[d]</sup>	426.4 <sup>[d]</sup>
<b>Equiv. of (S)-34</b>	0.92	1	1	1

Table 8.9 Addition rate of (S)-34 in each cycle in the first four attempts of R<sup>3</sup> processes of 9. <sup>[a]</sup>The solution was prepared by dissolving (S)-34 (0.21 g, 1.4 mmol) into reaction solvent (5 mL), which corresponded to about 42 mg mL<sup>-1</sup>. <sup>[b]</sup>The entries corresponds to those in Table 3.3. <sup>[c]</sup>Total amount of (S)-34 is the sum of the amount added at the beginning of the R<sup>3</sup> process (0.21 g, 0.5 equiv.) and that added during the reaction. <sup>[d]</sup>(S)-34 in the syringe (only 0.5 equiv. in all cases) was completely added into the reaction before the end of the process (cycle 8)

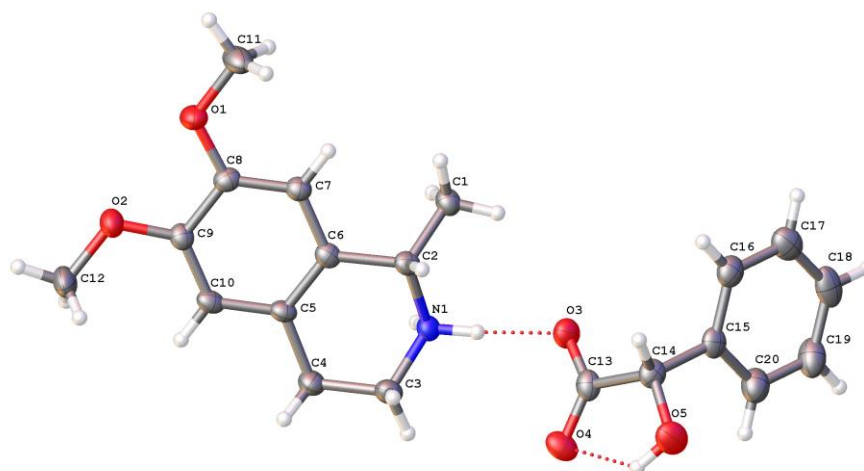
## 8.5. X-ray crystal structure data

### 8.5.1. (*R*)-6,7-dimethoxy-1-methyl-1,2,3,4-tetrahydroisoquinolinium-(*S*)-mandelate (*R*)-9-(*S*)-34



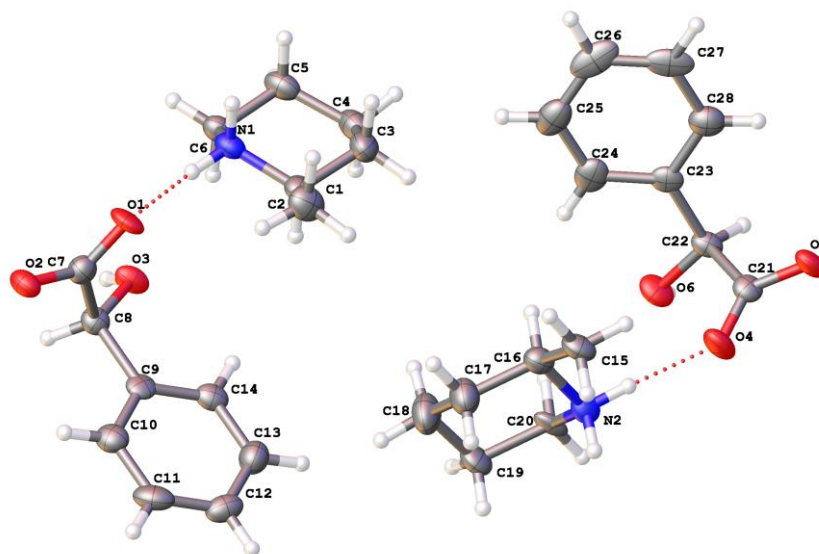
Identification code	MK2_44_Cu
Empirical formula	C <sub>20</sub> H <sub>25</sub> NO <sub>5</sub>
Formula weight	359.41
Temperature/K	120.1(4)
Crystal system	orthorhombic
Space group	P2 <sub>1</sub> 2 <sub>1</sub> 2 <sub>1</sub>
<i>a</i> /Å	7.31725(13)
<i>b</i> /Å	8.39176(15)
<i>c</i> /Å	29.6660(5)
$\alpha$ /°	90
$\beta$ /°	90
$\gamma$ /°	90
Volume/Å <sup>3</sup>	1821.63(6)
<i>Z</i>	4
$\rho_{\text{calc}}$ /cm <sup>3</sup>	1.311
$\mu$ /mm <sup>-1</sup>	0.770
<i>F</i> (000)	768.0
Crystal size/mm <sup>3</sup>	0.11 × 0.07 × 0.03
Radiation	CuK $\alpha$ ( $\lambda$ = 1.54184)
2 $\theta$ range for data collection/°	10.956 to 148.354
Index ranges	-9 ≤ <i>h</i> ≤ 9, -10 ≤ <i>k</i> ≤ 10, -34 ≤ <i>l</i> ≤ 36
Reflections collected	18739
Independent reflections	3698 [ <i>R</i> <sub>int</sub> = 0.0379, <i>R</i> <sub>sigma</sub> = 0.0263]
Data/restraints/parameters	3698/0/239
Goodness-of-fit on <i>F</i> <sup>2</sup>	1.053
Final <i>R</i> indexes [ <i>I</i> ≥ 2 $\sigma$ ( <i>I</i> )]	<i>R</i> <sub>1</sub> = 0.0337, <i>wR</i> <sub>2</sub> = 0.0818
Final <i>R</i> indexes [all data]	<i>R</i> <sub>1</sub> = 0.0368, <i>wR</i> <sub>2</sub> = 0.0838
Largest diff. peak/hole / e Å <sup>-3</sup>	0.44/-0.33
Flack parameter	0.05(7)

**8.5.2. (S)-6,7-dimethoxy-1-methyl-1,2,3,4-tetrahydroisoquinolinium-(S)-mandelate (S)-9-(S)-34**



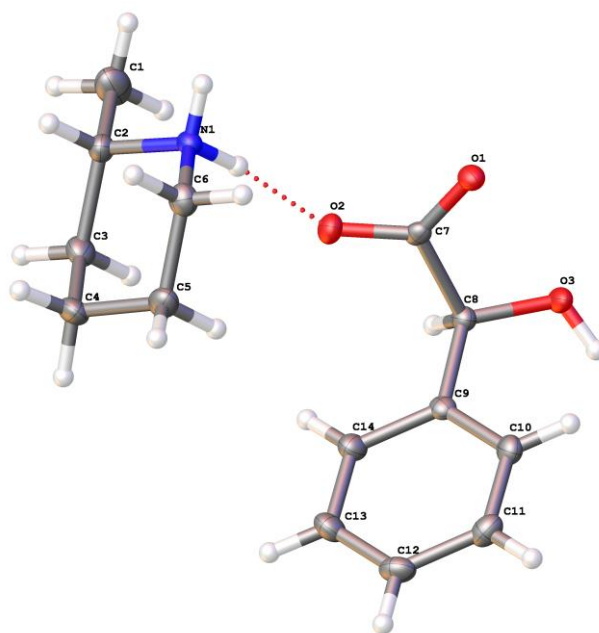
Identification code	MK1_96
Empirical formula	C <sub>20</sub> H <sub>25</sub> NO <sub>5</sub>
Formula weight	359.41
Temperature/K	120.00(16)
Crystal system	orthorhombic
Space group	P2 <sub>1</sub> 2 <sub>1</sub> 2 <sub>1</sub>
a/Å	6.8993(7)
b/Å	8.6813(8)
c/Å	31.049(5)
α/°	90
β/°	90
γ/°	90
Volume/Å <sup>3</sup>	1859.7(4)
Z	4
ρ <sub>calc</sub> /cm <sup>3</sup>	1.284
μ/mm <sup>-1</sup>	0.754
F(000)	768.0
Crystal size/mm <sup>3</sup>	0.16 × 0.06 × 0.03
Radiation	CuKα (λ = 1.54184)
2θ range for data collection/°	10.582 to 149.266
Index ranges	-8 ≤ h ≤ 8, -10 ≤ k ≤ 10, -35 ≤ l ≤ 27
Reflections collected	14223
Independent reflections	3651 [R <sub>int</sub> = 0.0792, R <sub>sigma</sub> = 0.0686]
Data/restraints/parameters	3651/0/250
Goodness-of-fit on F <sup>2</sup>	1.088
Final R indexes [I ≥ 2σ (I)]	R <sub>1</sub> = 0.0573, wR <sub>2</sub> = 0.1235
Final R indexes [all data]	R <sub>1</sub> = 0.0711, wR <sub>2</sub> = 0.1311
Largest diff. peak/hole / e Å <sup>-3</sup>	0.29/-0.24
Flack parameter	0.0(2)

### 8.5.3. (R)-2-Methylpiperidinium-(S)-mandelate (R)-103-(S)-34



Identification code	MK2_142_b
Empirical formula	C <sub>14</sub> H <sub>21</sub> NO <sub>3</sub>
Formula weight	251.32
Temperature/K	120.01(14)
Crystal system	orthorhombic
Space group	P2 <sub>1</sub> 2 <sub>1</sub> 2 <sub>1</sub>
a/Å	7.8229(13)
b/Å	7.9256(12)
c/Å	44.741(17)
α/°	90
β/°	90
γ/°	90
Volume/Å <sup>3</sup>	2774.0(12)
Z	8
ρ <sub>calc</sub> /cm <sup>3</sup>	1.204
μ/mm <sup>-1</sup>	0.680
F(000)	1088.0
Crystal size/mm <sup>3</sup>	0.22 × 0.17 × 0.04
Radiation	CuKα (λ = 1.54184)
2θ range for data collection/°	7.904 to 151.44
Index ranges	-6 ≤ h ≤ 9, -9 ≤ k ≤ 6, -53 ≤ l ≤ 55
Reflections collected	9989
Independent reflections	5451 [R <sub>int</sub> = 0.0695, R <sub>sigma</sub> = 0.1064]
Data/restraints/parameters	5451/0/329
Goodness-of-fit on F <sup>2</sup>	1.130
Final R indexes [I ≥ 2σ (I)]	R <sub>1</sub> = 0.0995, wR <sub>2</sub> = 0.1990
Final R indexes [all data]	R <sub>1</sub> = 0.1196, wR <sub>2</sub> = 0.2125
Largest diff. peak/ hole / e Å <sup>-3</sup>	0.51/-0.36
Flack parameter	0.4(3)

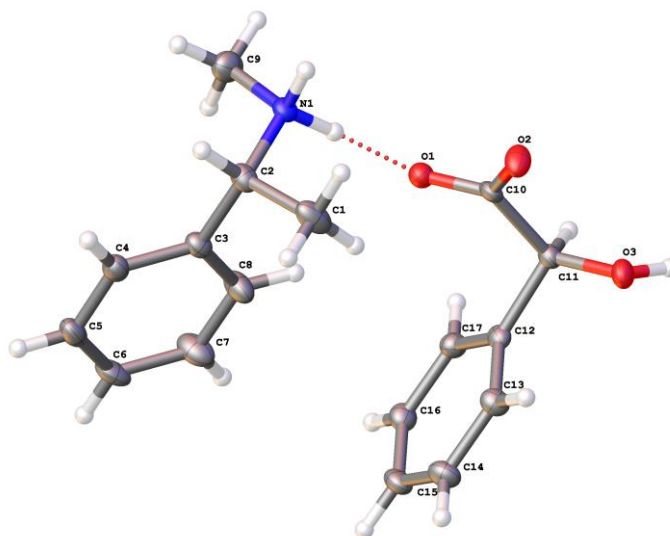
### 8.5.4. (S)-2-Methylpiperidinium-(S)-mandelate (S)-103-(S)-34



Identification code	MK2_140
Empirical formula	C <sub>14</sub> H <sub>21</sub> NO <sub>3</sub>
Formula weight	251.32
Temperature/K	120.2(3)
Crystal system	orthorhombic
Space group	P2 <sub>1</sub> 2 <sub>1</sub> 2 <sub>1</sub>
a/Å	9.66474(13)
b/Å	10.13813(13)
c/Å	14.05560(16)
α/°	90
β/°	90
γ/°	90
Volume/Å <sup>3</sup>	1377.20(3)
Z	4
ρ <sub>calc</sub> /cm <sup>3</sup>	1.212
μ/mm <sup>-1</sup>	0.685
F(000)	544.0
Crystal size/mm <sup>3</sup>	0.43 × 0.08 × 0.06
Radiation	CuKα (λ = 1.54184)
2θ range for data collection/°	10.76 to 147.418
Index ranges	-11 ≤ h ≤ 10, -11 ≤ k ≤ 12, -17 ≤ l ≤ 16
Reflections collected	4981
Independent reflections	2690 [R <sub>int</sub> = 0.0213, R <sub>sigma</sub> = 0.0273]
Data/restraints/parameters	2690/0/176
Goodness-of-fit on F <sup>2</sup>	1.061
Final R indexes [I ≥ 2σ (I)]	R <sub>1</sub> = 0.0258, wR <sub>2</sub> = 0.0669
Final R indexes [all data]	R <sub>1</sub> = 0.0264, wR <sub>2</sub> = 0.0674
Largest diff. peak/hole / e Å <sup>-3</sup>	0.19/-0.14
Flack parameter	-0.01(6)

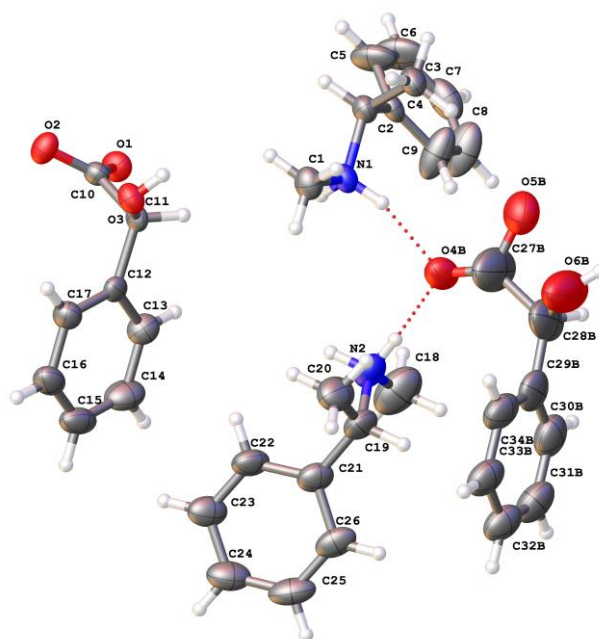


### 8.5.5. (*R*)-*N*-Methyl- $\alpha$ -methylbenzylaminium-(*S*)-mandelate (*R*)-39-(*S*)-34



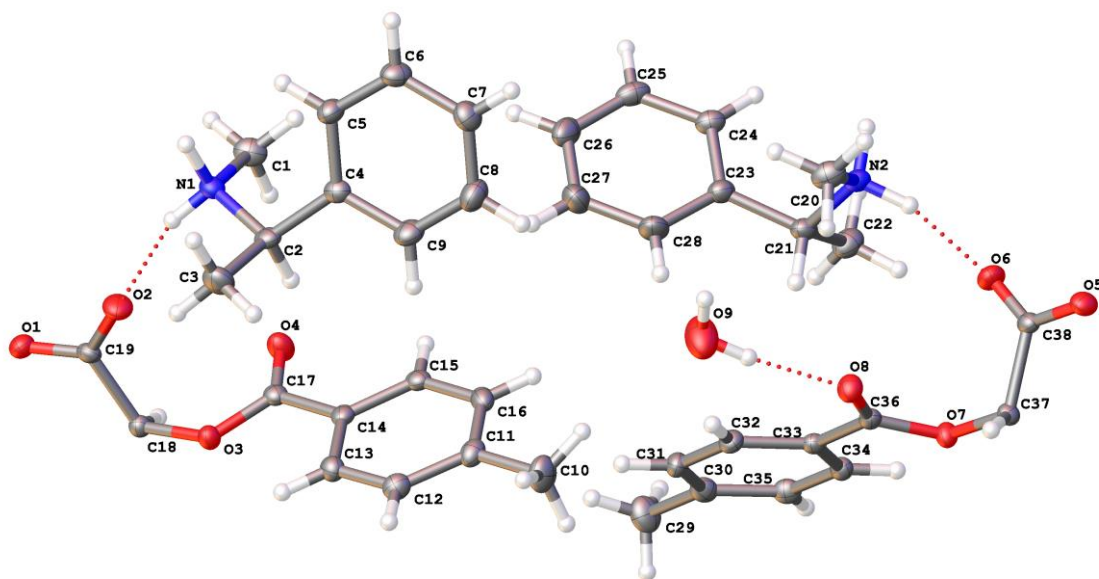
Identification code	MK3_48_R
Empirical formula	C <sub>17</sub> H <sub>21</sub> NO <sub>3</sub>
Formula weight	287.35
Temperature/K	120.0(2)
Crystal system	orthorhombic
Space group	P2 <sub>1</sub> 2 <sub>1</sub> 2 <sub>1</sub>
a/Å	9.56787(11)
b/Å	10.78261(11)
c/Å	15.51044(16)
$\alpha$ /°	90
$\beta$ /°	90
$\gamma$ /°	90
Volume/Å <sup>3</sup>	1600.16(3)
Z	4
$\rho_{\text{calc}}$ /cm <sup>3</sup>	1.193
$\mu$ /mm <sup>-1</sup>	0.657
F(000)	616.0
Crystal size/mm <sup>3</sup>	0.51 × 0.11 × 0.09
Radiation	CuK $\alpha$ ( $\lambda$ = 1.54184)
2 $\theta$ range for data collection/°	9.99 to 147.602
Index ranges	-9 ≤ h ≤ 11, -13 ≤ k ≤ 12, -14 ≤ l ≤ 18
Reflections collected	5701
Independent reflections	3108 [R <sub>int</sub> = 0.0165, R <sub>sigma</sub> = 0.0221]
Data/restraints/parameters	3108/0/204
Goodness-of-fit on F <sup>2</sup>	1.055
Final R indexes [ $ I  \geq 2\sigma(I)$ ]	R <sub>1</sub> = 0.0269, wR <sub>2</sub> = 0.0712
Final R indexes [all data]	R <sub>1</sub> = 0.0275, wR <sub>2</sub> = 0.0716
Largest diff. peak/hole / e Å <sup>-3</sup>	0.20/-0.14
Flack parameter	0.02(6)

### 8.5.6. (S)-N-Methyl- $\alpha$ -methylbenzylaminium-(S)-mandelate (S)-39-(S)-34



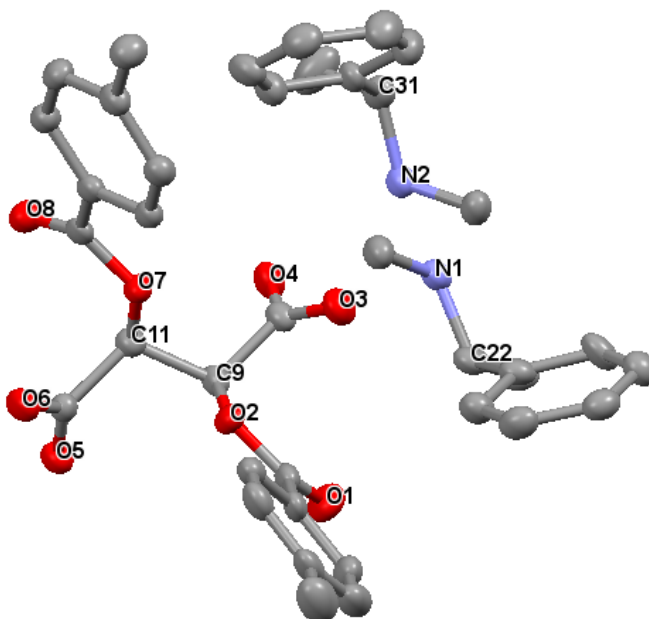
Identification code	MK3_91_S
Empirical formula	C <sub>17</sub> H <sub>21</sub> NO <sub>3</sub>
Formula weight	287.35
Temperature/K	120.02(15)
Crystal system	monoclinic
Space group	P2 <sub>1</sub>
a/Å	14.2947(8)
b/Å	7.2918(3)
c/Å	15.9041(8)
$\alpha$ /°	90
$\beta$ /°	111.819(6)
$\gamma$ /°	90
Volume/Å <sup>3</sup>	1538.99(14)
Z	4
$\rho_{\text{calc}}$ /cm <sup>3</sup>	1.240
$\mu$ /mm <sup>-1</sup>	0.683
F(000)	616.0
Crystal size/mm <sup>3</sup>	0.21 × 0.07 × 0.05
Radiation	CuK $\alpha$ ( $\lambda$ = 1.54184)
2 $\theta$ range for data collection/°	6.66 to 147.822
Index ranges	-17 ≤ h ≤ 15, -8 ≤ k ≤ 8, -19 ≤ l ≤ 18
Reflections collected	11873
Independent reflections	5777 [R <sub>int</sub> = 0.0416, R <sub>sigma</sub> = 0.0528]
Data/restraints/parameters	5777/231/460
Goodness-of-fit on F <sup>2</sup>	1.043
Final R indexes [ $ I  \geq 2\sigma(I)$ ]	R <sub>1</sub> = 0.0692, wR <sub>2</sub> = 0.1654
Final R indexes [all data]	R <sub>1</sub> = 0.0823, wR <sub>2</sub> = 0.1769
Largest diff. peak/hole / e Å <sup>-3</sup>	0.85/-0.31
Flack parameter	-0.19(18)

8.5.7. Di-(*R*)-*N*-Methyl- $\alpha$ -methylbenzylaminium-(*S,S*)-di-*p*-toluoyl-tartrate  
 [(*R*)-39]<sub>2</sub>-(*S,S*)-32



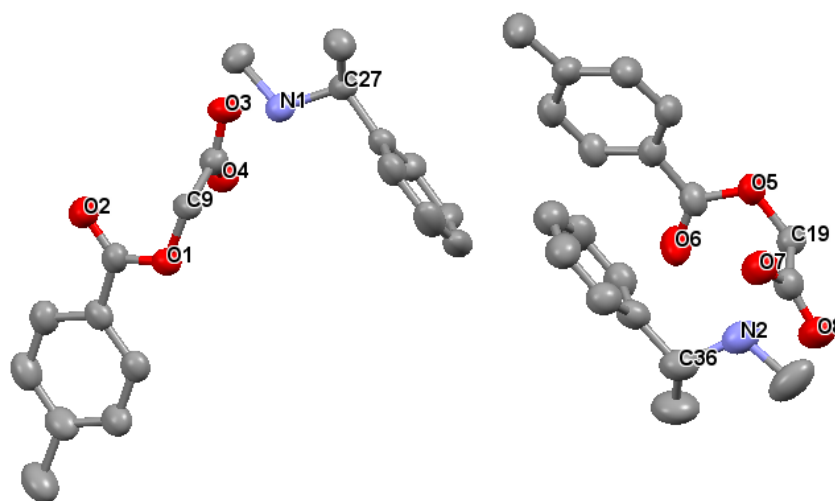
Identification code	MK5_17_R
Empirical formula	C <sub>38</sub> H <sub>44.5</sub> N <sub>2</sub> O <sub>8.25</sub>
Formula weight	661.25
Temperature/K	119.99(11)
Crystal system	monoclinic
Space group	C2
a/Å	18.4711(3)
b/Å	6.93435(8)
c/Å	28.4259(4)
α/°	90
β/°	97.9191(14)
γ/°	90
Volume/Å <sup>3</sup>	3606.21(9)
Z	4
ρ <sub>calc</sub> /cm <sup>3</sup>	1.218
μ/mm <sup>-1</sup>	0.699
F(000)	1410.0
Crystal size/mm <sup>3</sup>	0.37 × 0.12 × 0.05
Radiation	CuKα (λ = 1.54184)
2θ range for data collection/°	9.424 to 147.936
Index ranges	-18 ≤ h ≤ 21, -8 ≤ k ≤ 8, -34 ≤ l ≤ 35
Reflections collected	16665
Independent reflections	6857 [R <sub>int</sub> = 0.0322, R <sub>sigma</sub> = 0.0369]
Data/restraints/parameters	6857/1/467
Goodness-of-fit on F <sup>2</sup>	1.040
Final R indexes [I ≥ 2σ (I)]	R <sub>1</sub> = 0.0325, wR <sub>2</sub> = 0.0770
Final R indexes [all data]	R <sub>1</sub> = 0.0350, wR <sub>2</sub> = 0.0789
Largest diff. peak/hole / e Å <sup>-3</sup>	0.19/-0.17
Flack parameter	0.00(8)

8.5.8 Di-(*S*)-*N*-Methyl- $\alpha$ -methylbenzylaminium-(*S,S*)-di-*p*-toluoyl-tartrate  
 [(*S*)-39]<sub>2</sub>-(*S,S*)-32



Identification code	JRB341_p1
Empirical formula	C <sub>38</sub> H <sub>44</sub> N <sub>2</sub> O <sub>8</sub>
Formula weight	656.75
Temperature/K	100.01(10)
Crystal system	triclinic
Space group	P1
a/Å	8.6142(4)
b/Å	9.8984(5)
c/Å	12.0666(4)
$\alpha$ /°	95.519(3)
$\beta$ /°	105.455(3)
$\gamma$ /°	114.138(5)
Volume/Å <sup>3</sup>	880.00(7)
Z	1
$\rho_{\text{calc}}$ /mg/mm <sup>3</sup>	1.239
$\mu$ /mm <sup>-1</sup>	0.707
F(000)	350.0
Crystal size/mm <sup>3</sup>	0.28 × 0.14 × 0.12
2 $\theta$ range for data collection	7.82 to 133.2°
Index ranges	-10 ≤ h ≤ 10, -11 ≤ k ≤ 11, -14 ≤ l ≤ 14
Reflections collected	15566
Independent reflections	6009[R <sub>int</sub> = 0.0522]
Data/restraints/parameters	6009/3/439
Goodness-of-fit on F <sup>2</sup>	1.066
Final R indexes [I ≥ 2 $\sigma$ (I)]	R <sub>1</sub> = 0.0653, wR <sub>2</sub> = 0.1898
Final R indexes [all data]	R <sub>1</sub> = 0.0706, wR <sub>2</sub> = 0.1968
Largest diff. peak/hole / e Å <sup>-3</sup>	0.69/-0.29
Flack parameter	0.2(2)

**8.5.9 (R,S)-Di-N-Methyl- $\alpha$ -methylbenzylaminium-(S,S)-di-*p*-toluoyl-tartrate  
 [(R)-39]-(S,S)-32-[(S)-39]**

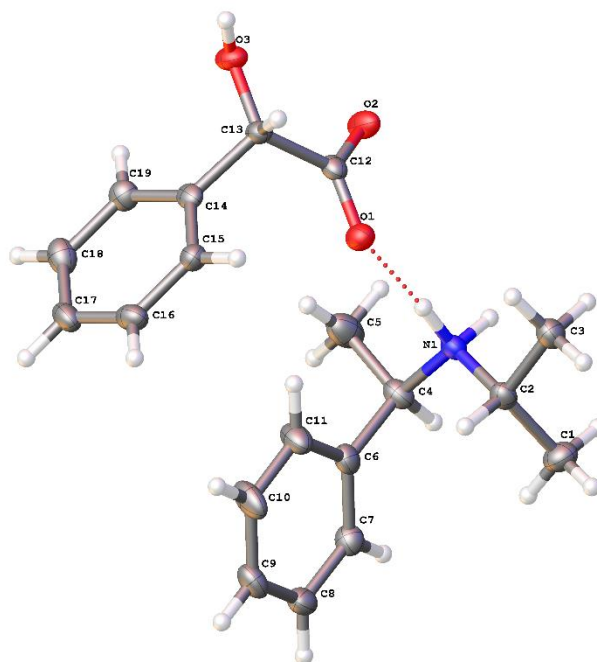


The data was obtained by Dr. Wim Klooster from UK NCS, University of Southampton. The hydrogen atoms are omitted for clarity. Only the chiral carbon, nitrogen and oxygen atoms are labelled.

Identification code	2017ncs0535c
Empirical formula	C <sub>38</sub> H <sub>44</sub> N <sub>2</sub> O <sub>8</sub>
Formula weight	656.75
Temperature/K	100(1)
Crystal system	monoclinic
Space group	C2
<i>a</i> /Å	18.0299(9)
<i>b</i> /Å	8.2271(4)
<i>c</i> /Å	25.1624(14)
$\alpha$ /°	90
$\beta$ /°	106.762(5)
$\gamma$ /°	90
Volume/Å <sup>3</sup>	3573.9(3)
<i>Z</i>	4
$\rho_{\text{calc.}}$ /g cm <sup>-3</sup>	1.221
$\mu$ /mm <sup>-1</sup>	0.697
Crystal size/mm <sup>3</sup>	0.050 × 0.050 × 0.010
Radiation	CuK $\alpha$ ( $\lambda$ = 1.54184)
2 $\theta$ range for data collection	9.84 to 136.49°
Index ranges	-21 ≤ <i>h</i> ≤ 20, -9 ≤ <i>k</i> ≤ 9, -30 ≤ <i>l</i> ≤ 30
Reflections collected	17325
Independent reflections	5566 [ <i>R</i> <sub>int</sub> = 0.0585, <i>R</i> <sub>sigma</sub> = 0.0617]
Data/ restraints/ parameters	5566/1/439
Goodness-of-fit on <i>F</i> <sup>2</sup>	1.048
Final <i>R</i> indexes [ <i>I</i> ≥ 2 $\sigma$ ( <i>I</i> )]	<i>R</i> <sub>1</sub> = 0.0567, <i>wR</i> <sub>2</sub> = 0.1451
Final <i>R</i> indexes [all data]	<i>R</i> <sub>1</sub> = 0.0799, <i>wR</i> <sub>2</sub> = 0.1582
Largest diff. peak/hole / e Å <sup>-3</sup>	0.149/-0.221
Flack Parameter	0.2(2)

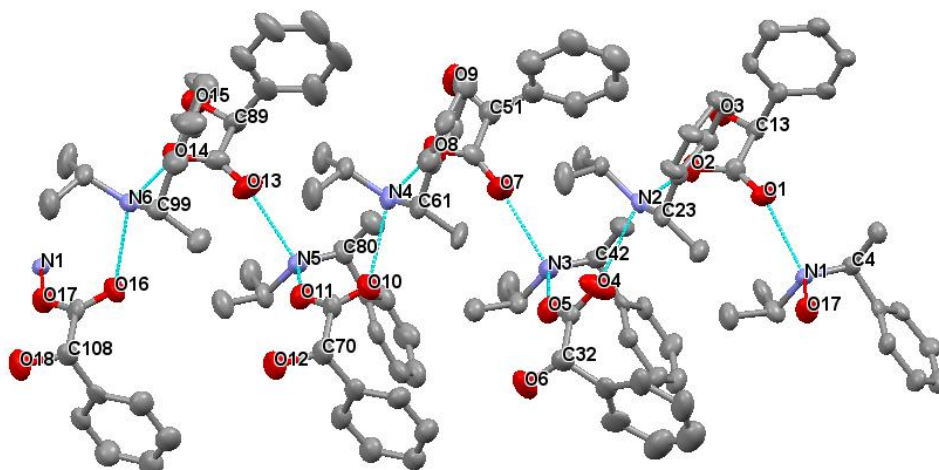
### 8.5.10 (*R*)-*N*-Isopropyl- $\alpha$ -methylbenzylaminium-(*S*)-mandelate (*R*)-101-(*S*)-

34



Identification code	MK5_63
Empirical formula	C <sub>19</sub> H <sub>25</sub> NO <sub>3</sub>
Formula weight	315.40
Temperature/K	120.2(5)
Crystal system	orthorhombic
Space group	P2 <sub>1</sub> 2 <sub>1</sub> 2 <sub>1</sub>
a/Å	9.7444(4)
b/Å	11.3063(6)
c/Å	15.9944(7)
$\alpha$ /°	90
$\beta$ /°	90
$\gamma$ /°	90
Volume/Å <sup>3</sup>	1762.15(14)
Z	4
$\rho_{\text{calc}}$ /cm <sup>3</sup>	1.189
$\mu$ /mm <sup>-1</sup>	0.638
F(000)	680.0
Crystal size/mm <sup>3</sup>	0.47 × 0.03 × 0.02
Radiation	CuK $\alpha$ ( $\lambda$ = 1.54184)
2 $\theta$ range for data collection/°	9.58 to 147.714
Index ranges	-11 ≤ h ≤ 10, -12 ≤ k ≤ 13, -19 ≤ l ≤ 18
Reflections collected	6367
Independent reflections	3435 [R <sub>int</sub> = 0.0476, R <sub>sigma</sub> = 0.0680]
Data/restraints/parameters	3435/0/223
Goodness-of-fit on F <sup>2</sup>	1.004
Final R indexes [ $I \geq 2\sigma(I)$ ]	R <sub>1</sub> = 0.0432, wR <sub>2</sub> = 0.0871
Final R indexes [all data]	R <sub>1</sub> = 0.0608, wR <sub>2</sub> = 0.0951
Largest diff. peak/hole / e Å <sup>-3</sup>	0.16/-0.19
Flack parameter	0.0(2)

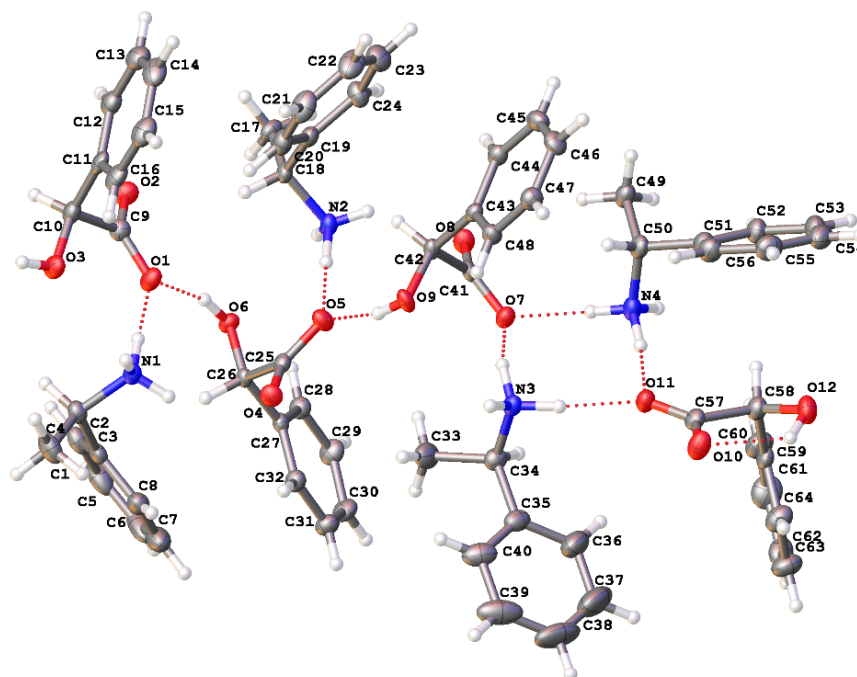
8.5.11 (S)-N-Isopropyl- $\alpha$ -methylbenzylaminium-(S)-mandelate (S)-101-(S)-  
34



The hydrogen atoms are omitted for clarity. Only the chiral carbon, nitrogen and oxygen atoms are labelled.

Identification code	MK5_39_twin1_hklf4
Empirical formula	C <sub>19</sub> H <sub>25</sub> NO <sub>3</sub>
Formula weight	315.40
Temperature/K	120.3(7)
Crystal system	monoclinic
Space group	P2 <sub>1</sub>
a/Å	9.6391(13)
b/Å	24.175(3)
c/Å	22.792(3)
$\alpha$ /°	90
$\beta$ /°	94.282(11)
$\gamma$ /°	90
Volume/Å <sup>3</sup>	5296.3(12)
Z	12
$\rho_{\text{calc}}$ /cm <sup>3</sup>	1.187
$\mu$ /mm <sup>-1</sup>	0.637
F(000)	2040.0
Crystal size/mm <sup>3</sup>	0.19 × 0.09 × 0.07
Radiation	CuK $\alpha$ ( $\lambda$ = 1.54184)
2 $\theta$ range for data collection/°	7.314 to 103.92
Index ranges	-9 ≤ h ≤ 9, -24 ≤ k ≤ 24, -23 ≤ l ≤ 13
Reflections collected	10832
Independent reflections	10832 [R <sub>int</sub> = 0.068, R <sub>sigma</sub> = 0.1455]
Data/restraints/parameters	10832/937/1268
Goodness-of-fit on F <sup>2</sup>	0.924
Final R indexes [ $I \geq 2\sigma(I)$ ]	R <sub>1</sub> = 0.0692, wR <sub>2</sub> = 0.1484
Final R indexes [all data]	R <sub>1</sub> = 0.1421, wR <sub>2</sub> = 0.1688
Largest diff. peak/hole / e Å <sup>-3</sup>	0.25/-0.23
Flack parameter	0.7(4)

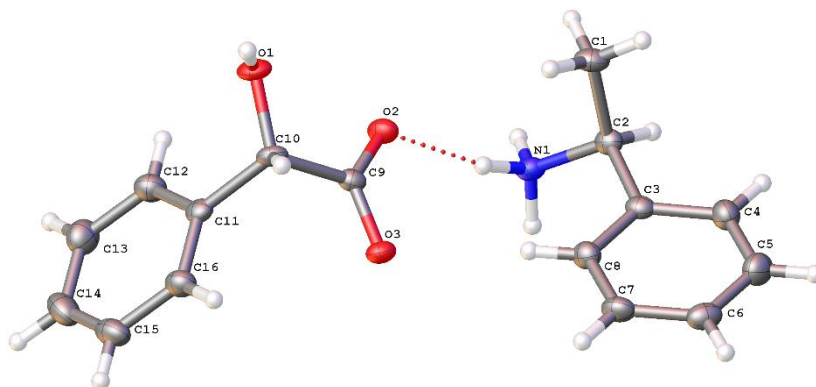
### 8.5.12 (*R*)- $\alpha$ -Methylbenzylaminium-(*S*)-mandelate (*R*)-42-(*S*)-34



Identification code	MK5_11_R_twin1_hklf4
Empirical formula	C <sub>16</sub> H <sub>19</sub> NO <sub>3</sub>
Formula weight	273.32
Temperature/K	120.4(8)
Crystal system	triclinic
Space group	P1
a/Å	6.3960(2)
b/Å	14.8252(5)
c/Å	16.1409(5)
$\alpha$ /°	75.274(3)
$\beta$ /°	82.978(3)
$\gamma$ /°	81.011(3)
Volume/Å <sup>3</sup>	1456.59(8)
Z	4
$\rho_{\text{calc}}$ /cm <sup>3</sup>	1.246
$\mu$ /mm <sup>-1</sup>	0.696
F(000)	584.0
Crystal size/mm <sup>3</sup>	0.16 × 0.13 × 0.06
Radiation	CuK $\alpha$ ( $\lambda$ = 1.54184)
2 $\theta$ range for data collection/°	6.218 to 148.884
Index ranges	-7 ≤ h ≤ 7, -18 ≤ k ≤ 18, -20 ≤ l ≤ 20
Reflections collected	18433
Independent reflections	18433 [R <sub>int</sub> = 0.048, R <sub>sigma</sub> = 0.0614]
Data/restraints/parameters	18433/3/790
Goodness-of-fit on F <sup>2</sup>	0.931
Final R indexes [I >= 2 $\sigma$ (I)]	R <sub>1</sub> = 0.0405, wR <sub>2</sub> = 0.0907
Final R indexes [all data]	R <sub>1</sub> = 0.0558, wR <sub>2</sub> = 0.0956
Largest diff. peak/hole / e Å <sup>-3</sup>	0.18/-0.21
Flack parameter	0.08(10)

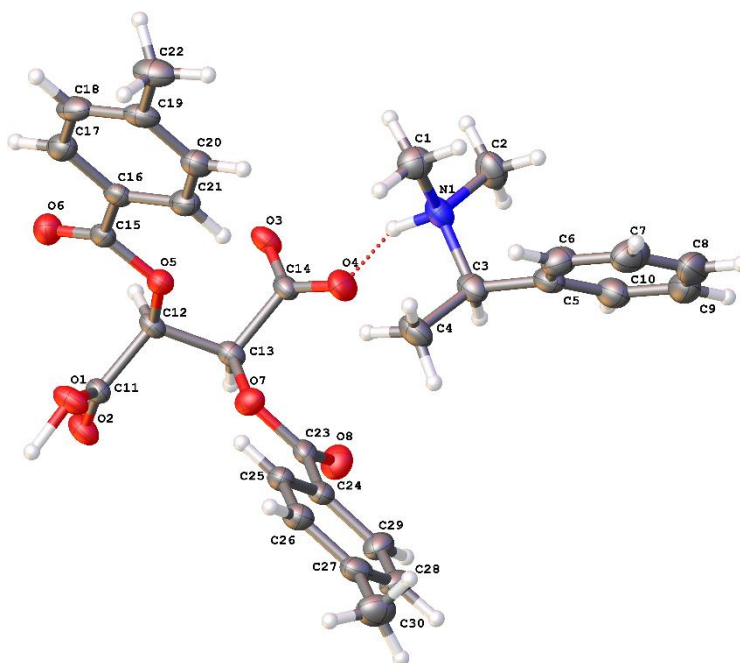


### 8.5.13 (S)- $\alpha$ -Methylbenzylaminium-(S)-mandelate (S)-42-(S)-34



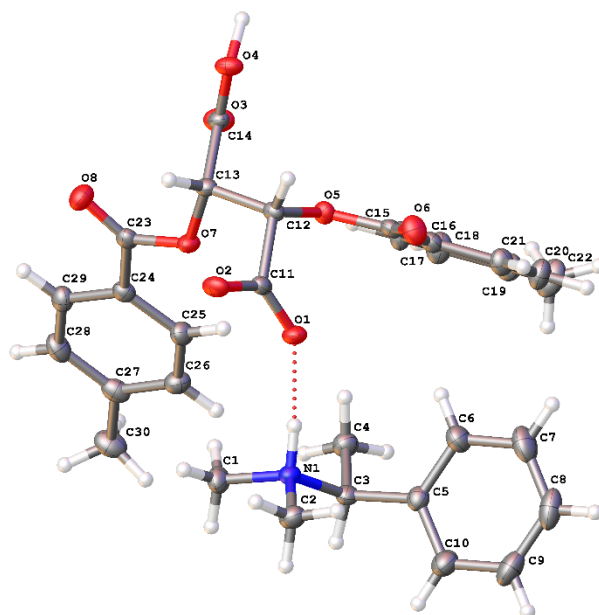
Identification code	MK5_11_S
Empirical formula	C <sub>16</sub> H <sub>19</sub> NO <sub>3</sub>
Formula weight	273.32
Temperature/K	120.00(13)
Crystal system	orthorhombic
Space group	P2 <sub>1</sub> 2 <sub>1</sub> 2 <sub>1</sub>
a/Å	6.8424(4)
b/Å	8.3269(6)
c/Å	25.4596(18)
$\alpha$ /°	90
$\beta$ /°	90
$\gamma$ /°	90
Volume/Å <sup>3</sup>	1450.57(17)
Z	4
$\rho_{\text{calc}}$ /cm <sup>3</sup>	1.252
$\mu$ /mm <sup>-1</sup>	0.699
F(000)	584.0
Crystal size/mm <sup>3</sup>	0.23 × 0.06 × 0.03
Radiation	CuK $\alpha$ ( $\lambda$ = 1.54184)
2 $\theta$ range for data collection/°	6.944 to 147.412
Index ranges	-8 ≤ h ≤ 8, -9 ≤ k ≤ 9, -29 ≤ l ≤ 31
Reflections collected	5088
Independent reflections	2815 [R <sub>int</sub> = 0.0560, R <sub>sigma</sub> = 0.0768]
Data/restraints/parameters	2815/0/198
Goodness-of-fit on F <sup>2</sup>	1.016
Final R indexes [ $I \geq 2\sigma(I)$ ]	R <sub>1</sub> = 0.0469, wR <sub>2</sub> = 0.0931
Final R indexes [all data]	R <sub>1</sub> = 0.0595, wR <sub>2</sub> = 0.0992
Largest diff. peak/hole / e Å <sup>-3</sup>	0.18/-0.22
Flack parameter	-0.2(3)

8.5.14 (*R*)-*N,N*-Dimethyl- $\alpha$ -methylbenzylamine-(*S,S*)-di-*p*-toluoyl-tartrate  
 [(*R*)-46]-(*S,S*)-32



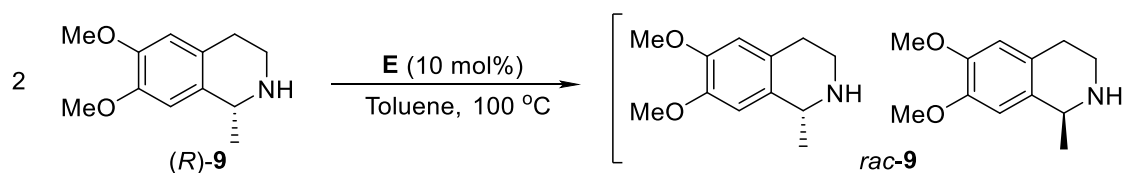
Identification code	MK5_62_R
Empirical formula	C <sub>30</sub> H <sub>33</sub> NO <sub>8</sub>
Formula weight	535.57
Temperature/K	120.3(7)
Crystal system	orthorhombic
Space group	P2 <sub>1</sub> 2 <sub>1</sub> 2 <sub>1</sub>
a/Å	7.7211(4)
b/Å	14.2599(9)
c/Å	26.2847(13)
$\alpha$ /°	90
$\beta$ /°	90
$\gamma$ /°	90
Volume/Å <sup>3</sup>	2894.0(3)
Z	4
$\rho_{\text{calc}}$ /cm <sup>3</sup>	1.229
$\mu$ /mm <sup>-1</sup>	0.736
F(000)	1136.0
Crystal size/mm <sup>3</sup>	0.31 × 0.11 × 0.06
Radiation	CuK $\alpha$ ( $\lambda$ = 1.54184)
2 $\theta$ range for data collection/°	6.726 to 147.838
Index ranges	-6 ≤ h ≤ 9, -17 ≤ k ≤ 16, -32 ≤ l ≤ 31
Reflections collected	16428
Independent reflections	5728 [R <sub>int</sub> = 0.0506, R <sub>sigma</sub> = 0.0546]
Data/restraints/parameters	5728/0/365
Goodness-of-fit on F <sup>2</sup>	1.018
Final R indexes [I ≥ 2 $\sigma$ (I)]	R <sub>1</sub> = 0.0463, wR <sub>2</sub> = 0.0984
Final R indexes [all data]	R <sub>1</sub> = 0.0637, wR <sub>2</sub> = 0.1059
Largest diff. peak/hole / e Å <sup>-3</sup>	0.18/-0.20
Flack parameter	-0.05(17)

8.5.15 (S)-N,N-Dimethyl- $\alpha$ -methylbenzylamine-(S,S)-di-*p*-toluoyl-tartrate  
 [(S)-46]-(S,S)-32



Identification code	MK5_62_S
Empirical formula	C <sub>30</sub> H <sub>33</sub> NO <sub>8</sub>
Formula weight	535.57
Temperature/K	120.01(10)
Crystal system	orthorhombic
Space group	P2 <sub>1</sub> 2 <sub>1</sub> 2 <sub>1</sub>
a/Å	8.82969(14)
b/Å	13.8488(2)
c/Å	23.6449(4)
α/°	90
β/°	90
γ/°	90
Volume/Å <sup>3</sup>	2891.32(8)
Z	4
ρ <sub>calc</sub> /cm <sup>3</sup>	1.230
μ/mm <sup>-1</sup>	0.736
F(000)	1136.0
Crystal size/mm <sup>3</sup>	0.34 × 0.19 × 0.08
Radiation	CuKα (λ = 1.54184)
2θ range for data collection/°	7.398 to 147.594
Index ranges	-10 ≤ h ≤ 10, -12 ≤ k ≤ 16, -22 ≤ l ≤ 28
Reflections collected	10609
Independent reflections	5649 [R <sub>int</sub> = 0.0304, R <sub>sigma</sub> = 0.0399]
Data/restraints/parameters	5649/0/365
Goodness-of-fit on F <sup>2</sup>	1.049
Final R indexes [I > 2σ (I)]	R <sub>1</sub> = 0.0323, wR <sub>2</sub> = 0.0759
Final R indexes [all data]	R <sub>1</sub> = 0.0362, wR <sub>2</sub> = 0.0788
Largest diff. peak/hole / e Å <sup>-3</sup>	0.14/-0.15
Flack parameter	0.11(9)

## 8.6. Calculations of turnover number of $\text{Fe}_3(\text{CO})_{12}$ (Compound **E**) in the racemisation of (*R*)-**9** (Fig. 4.3)



Consider *rac*-**9** as a different species than (*R*)-**9**.

Initial no. of mole of (*R*)-**9** = 0.3 mmol

No. of mole of **E** = 0.03 mmol

After 8 and 24 hours, ee of the system were 55 and 53% respectively. Therefore **E** was virtually fully deactivated after about 8 hours.

Consider at 8 hours, the system contains 77.5% (*R*)-**9** and 22.5% (*S*)-**9** (Eqn. 2.2).

Therefore, no. of mole of *rac*-**9** [(*R*)-**9**-(*S*)-**9**] formed =  $0.3 \times 0.225 = 0.0675$  mmol.

For every mole of *rac*-**9** formed, assume 2 moles of (*R*)-**9** is consumed (one mole is converted to (*S*)-**9**, while the other mole 'combines' with (*S*)-**9** to give *rac*-**9**).

Therefore, no. of moles of (*R*)-**9** converted to *rac*-**9** after 8 hours =  $0.0675 \times 2$  mmol = 0.135 mmol.

No. of mole of active site of **E** =  $3 \times 0.03$  mmol = 0.09 mmol

Turnover number =  $0.135 \text{ mmol} \div 0.09 \text{ mmol} = 1.5 > 1$

Therefore, **E** is still regarded as a catalyst in the racemisation of (*R*)-**9**. However, the high loading (10 mol% **E**, 30% iron) makes it a relatively less efficient catalyst.